Stony Brook University

Towards the Step-wise Synthesis of Molecular Cages:

Potential Components in Single-Electron Transistors

Dissertation Presented

by

Natalie St. Fleur

to

The Graduate School

in Partial Fulfillment of the

Requirements

for the Degree of

Doctor of Philosophy

in

Chemistry

Stony Brook University

August 2013

Stony Brook University

The Graduate School

Natalie St. Fleur

We, the dissertation committee for the above candidate for the

Doctor of Philosophy degree, hereby recommend

acceptance of this dissertation.

Dr. Andreas Mayr – Dissertation Advisor
Professor, Department of Chemistry

Dr. David C. Grills – Dissertation Co-Advisor
Chemist, Chemistry Department, Brookhaven National Laboratory

Dr. Nancy S. Goroff – Chairperson of Defense
Associate Professor, Department of Chemistry

Dr. Stanislaus S. Wong – Third Member
Professor, Department of Chemistry

Dr. Konstantin K. Likharev – Outside Member
Distinguished Professor, Department of Physics and Astronomy

This dissertation is accepted by the Graduate School

Charles Taber
Interim Dean of the Graduate School

Abstract of the Dissertation

Towards the Step-wise Synthesis of Molecular Cages – Potential Components in Single-

Electron Transistors

By

Natalie St. Fleur

Doctor of Philosophy

In

Chemistry

Stony Brook University

2013

Shape-persistent molecular cages with significant internal cavities are very attractive synthetic targets owing to their multifarious applications. We have focused on the design and synthesis of molecular cages that may be used as structural components in single-electron transistors (SETs) designed by K. K. Likharev. This application requires not only shape-persistent cages, but also stable and selectively functionalizable structures with cavities that can host the SET's conducting island. In this vein, we have designed two molecular cages, a triangular prism (**1**) and rhomboid prism (**2**). Both cages consist of oligo-phenyleneethynylene edges and *fac*-[ReL(CO)$_3$(phen')] corner units, where phen' is a 1,10-phenanthroline derivative with coplanar edge substituents at the 4 and 7 positions and L indicates the coordination site for the vertical-edge.

Synthesis of cages **1** and **2** are intended to be achieved by via step-wise synthesis. Most often molecular cages are obtained from suitable building blocks in a single step by self-assembly. Although self-assembly is both a convenient and productive procedure, it is limited to producing structures with a high degree of symmetry. Because we require stable structures that can be functionalized at various specified positions, we elected to use step-wise rather than self-assembly in their construction.

This work addresses the progress made in the construction of **1** and **2**, specifically, the synthesis of a triangular-shaped face and the attempted synthesis of a diamond-shaped face. In addition, our efforts to establish optimal reactions conditions for the connection of two halfprisms by testing Sonogashira cross-coupling reactions of [Re(C≡CR)(CO)$_3$(N^N)] complexes, where N^N is a N,N'-dimethylpiperazine or 1,10-phenanthroline derivative, will be discussed. Finally, in collaboration with Etsuko Fujita and David Grills we have explored redox, optical, and photophysical properties of a series of [ReBr(CO)$_3$(phen')] complexes, which are known for their attractive photophysical and photochemical properties.

Dedication

This work is dedicated to Sheila, Michelle, Jazzmyne, and Grandpa. Thank you all for everything.

Table of Contents

List of Figures

List of Schemes

List of Tables

List of Abbreviations

2D – two dimensional

3D – three dimensional

APT – attached proton test

ATR – Attenuated total reflectance

bpy – 2,2-bipyridine

CI – conducting island

CMOS – complementary metal-oxide semiconductor

CV – cyclic voltammetry

dmpz – N,N'-dimethylpiperazine

DPE – diphenylether

dzn – 1,4-diazine

en – ethylenediamine

EtOH – ethanol

IL – intraligand

LLCT – ligand-to-ligand charge transfer

MeOH – methanol

Mes-phen – 2,9-dimesityl-1,10-phenanthroline

MLCT – metal-to-ligand charge transfer

MOF – metal-organic framework

MOP – metal-organic polymer

MOSFET – metal-oxide semiconductor field effect transistor

phen - 1,10-phenanthroline

phen' – a structural derivative of 1,10-phenanthroline

SBU – secondary building unit

SCE – standard calomel electrode

SET – single-electron transistor

TA – transient absorbance

TBAHFP – tetrabutylammonium hexafluorophosphate

THF – tetrahydrofuran

TIPS – triisopropylsilyl

TMEDA – N,N,N',N'-tetramethylethylenediamine

TMS – trimethylsilyl

TPT – 2,4,6-tri(4'-pyridyl)-1,3,5-triazine

TRIR – time-resolved infrared

Acknowledgments

First and foremost, I would like to thank God. For through Him all things are possible.

I want to thank my advisor Dr. Andreas Mayr; for with his kindness, support, wisdom, and advice I have made it through this process. Thank you for rooting for me. I would also like to show my gratitude to my co-advisor Dr. David Grills whose patience and mentorship, was invaluable to me. To the chair of my committee, Dr. Nancy Goroff, thank you for inspiring me. I would also like to acknowledge the third member of my committee, Dr. Stanislaus Wong and my outside member Dr. Konstantin K. Likharev for all of your support and advice. I would also like to give special acknowledgement toDr. Kathlyn Parker for all of the insightful discussion.

I would like to acknowledge the Stony Brook Department of Chemistry staff: Daniel Cashmar, Heidi Ciolfi, Katherine Hughes, Deborah Stoner-Ma, Lizandia Perez, Michael Teta, and Charmine Yapchin; as well as Nina Maung-Gaona, Kathryne Piazzola, and Toni Sperzel from the Center for Inclusive Education. I am eternally grateful for all of your unending support. To the all of my mentors including: Dr. M. Akhtar, Dr. Frank Fowler, Dr. Etsuko Fujita, Dr. Hanson, Dr. Lauer, Dr. James Marecek, the late Dr. Sheila Morehouse, the late Dr. Michelle Millar, Dr. Susan Oatis, Dr. Troy Wolfskill, Dr. Mike White. I have learned so many invaluable lessons from all of you. Thank you for giving me the opportunity to learn and grow. To my former students, you have all taught me so much and made these years at Stony Brook so much more memorable. A special thanks to Mr. Bannon, who inspired me to pursue a career in chemistry.

Finally to my family and friends, thank you all so much for your love and support. I would not have made it through this process without you. I especially would like to thank my husband Trent Balius, I am so lucky to have you in my life. Thank you for believing in me. To my parents Fritz and Elizabeth St. Fleur, as well as Fredrick Balius and Julie Eiseman, thank you for the love, support, and encouragement. To my sisters Diane and Samanta, my brother Fontaine, and close friends Ivan, Ivan, Lili, Mr. and Mrs. Skeffrey, Olivia, Mary, and Ebony thank you for the love and encouragement. A special thanks to Marie Gelato, I can never repay you for your kindness. Thank you so much for everything. Finally, to Hanna Nekvasil and her daughter Julie, thanks for being so amazing.

Publications

St. Fleur, N.; Hili, C. J.; Mayr, A. Synthesis of alkynyl(tricarbonyl)rhenium complexes containing a lightly coordinated diamine ligand. *Inorg. Chim. Acta.* **2009**, 362, 1571 – 1576.

Mayr, A.; Srisailas, M.; Zhao, Q.; Gao, Y.; Hsieh, H.; Hoshmand-Kochi, M.; St. Fleur, N. Synthesis of oligo(phenyleneethynylene)s containing central pyromellitdiimide or naphthalenediimide groups and bearing terminal isocyanide groups: molecular components for single-electron transistors. *Tetrahedron.* **2007**, 63, 8206 – 8217.

Chapter 1: Introduction

1.1. Single-Electron Transistors

It is well understood that much of the social, economic, and technological progress made since the second half of the 20th century is owing in part to the advances made in the field of electronics. Demands for affordable machines with increasing power, function, and manageability have fueled the drive toward electronic circuits with high component densities and low cost/function ratios. The desire for powerful and affordable electronic circuits in turn has created the need for smaller integratable circuit components including capacitors, resistors, diodes, wires, and transistors.

As the fundamental operational component of all electronic circuits, particular attention has been paid to the low-cost minimization and increased integration of transistors. In this regard, the metal-oxide semiconductor field effect transistor – MOSFET – has been most accommodating. Since the late 1980s MOSFETs and the complementary metal-oxide semiconductor (CMOS) technology used to integrate them have helped sustain the trend known as Moore's law, which predicts the number of components in integrated circuits doubles nearly every two years.[1,2] It has been long understood, however, that the physical limitations and economic inviability associated with the continued shrinkage and closer packing of MOSFETs are inevitable.[3-8] As a result, the ability to produce integrated circuits with higher component densities at the pace established by Moore's law, cannot be maintained unless suitable solutions can be found.[9-29] Although three-dimensional (3D) integration and the use of non-traditional semiconductor materials are being explored as possible short-term solutions, long-term progress will require new innovative transistor technologies that can operate at the nanoscale. One such technology is the single-electron transistor (SET).[14,26,27,29]

SETs are extremely attractive devices with a variety of applications.[29-44] These devices are already in use as supersensitive electrometers.[31,35,37,39,41,42] Additionally, their applications in temperature and dc current standardizations as well as single-electron spectroscopy have been considered.[29] In regards to computing, SETs can perform both voltage-state and charge-state logic operations.[32-34,38,40,43,44]

The SET was designed by K. K. Likharev and D. V. Averin[45] in 1986 and consists of two tunnel junctions, which separate the source and drain electrodes from a small conducting island (CI) that is sandwiched between them. See Figure 1.1. The tunnel junctions may be either a thin insulating layer or vacuum space, which effectively resist the movement of charge carriers from

the source to the CI and from the CI to the drain as dictated by an applied voltage bias. However, if the voltage of the third electrode, known as the gate, is above a certain threshold voltage, an electronic energy level in the CI becomes accessible and the resistance of the tunnel junction drops. With the resistance of the tunnel junctions lowered, a single charge carrier may now tunnel through the tunnel junctions onto and then off of the CI by way of the accessible electronic energy level.[29,46] As with all transistors, the SET switches electrical signals on or off, as well as amplifies or modulates them. However, unlike other transistor models (i.e. field effect or bipolar junction transistors), electrical signals in the SETs are caused by the discrete movement of a single charge carrier, rather than a stream of charge carriers. Therefore, during ideal SET operations only one hole or electron is injected from the source to an unoccupied CI and then from the CI to the drain. To ensure this discrete movement of charge carriers and to prevent unwanted accumulation of charge on the CI, the CI must be extremely small (e.g. a nanocluster or a molecule). For reliable room temperature SET operation the CI's dimensions must be under 1 nm to prevent thermally induced tunneling events.[29,34,46] Unfortunately, at these dimensions it is difficult to position CIs between the two tunnel junctions with the high degree of accuracy and precision required for reliable SETs. As a result, SET fabrication has been quite challenging.
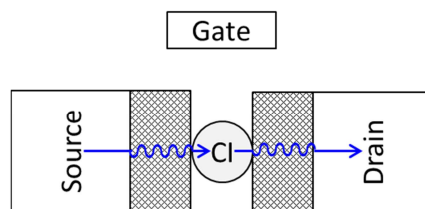
Figure 1. 1: Operation of SET.

The first actual SET device was fabricated in 1987 at AT&T Bell Laboratories by Fulton and Dolan[47] using the suspended mask technique. In the ensuing years, many reports have presented SETs made by a combination of lithography and thin-film deposition methods.[30,34,36,39,48-59] In all of these reports the SETs were presented as individual devices or connected to a small number of other devices in small-scale circuits. For any commercial applications, however, many SETs will need to be integrated into electronic circuits. In order for large-scale integration to be realized, a reliable highly reproducible technique for SET

fabrication must be available. In this vein, our group, in collaboration with K. K. Likharev, has proposed an attractive solution that promises high reproducibility. As shown in Scheme 1.1, this method involves enclosing the CIs in molecular cages either by migration or by trapping, thus forming the cage-CI inclusion complex. This complex can then be chemically anchored onto the surface of the source and/or drain electrodes, thereby positioning the CI between these two electrodes. Since this process avoids direct manipulation of nanosized CIs, it should make SET fabrication less difficult and improve the reproducibility of this process.
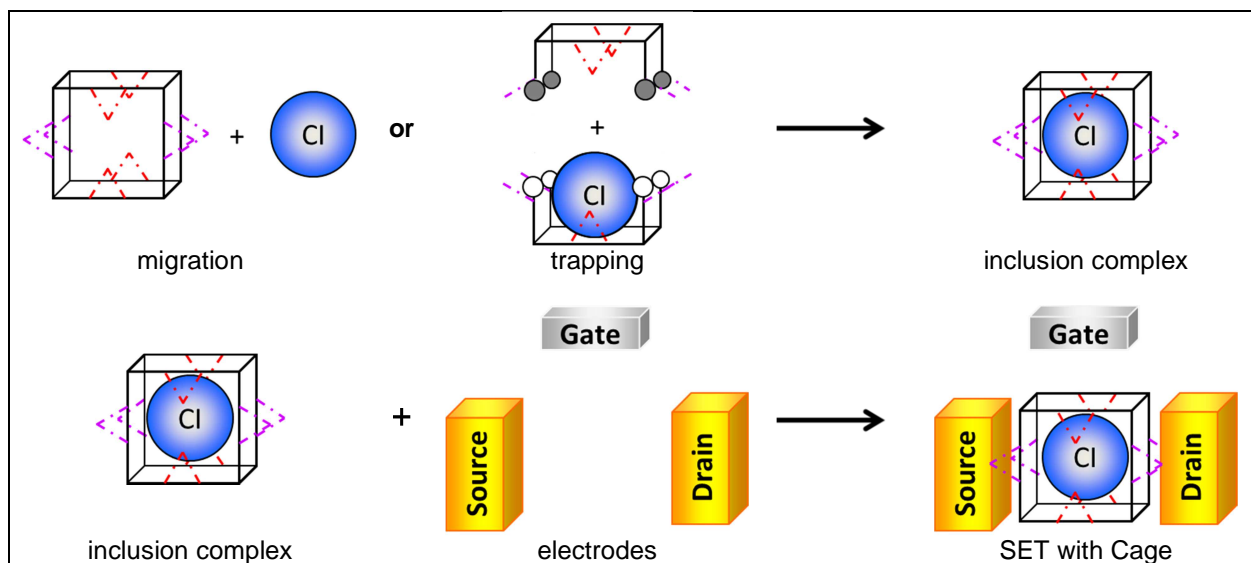
Scheme 1. 1: Cage-assisted fabrication of SET.

In order to produce a stable inclusion complex it may be necessary to append functional groups, indicated by the red-dashed lines in Scheme 1.1, that will stabilize the CI within the cage. The details of the corresponding host-guest chemistry is of course dependent on the identity of the CI. Likewise, functional groups, indicated by the purple-hashed lines in Scheme 1.1, responsible for anchoring the cages onto the surfaces of the electrode would be chosen based on the material of the electrode. Because the CI and electrodes could be of distinct matter, the functional groups used to secure the CI within the cage and tether the cage to the electrodes could be different. For example, a SET consisting of gold source and drain electrodes and a metal-oxide nanocluster for a CI could employ a cage with thiol functional groups on the face and carboxyl functional groups along the edges to anchor the cage and secure the CI, respectively. See the inclusion complex in Scheme 1.1. In order for this procedure to work, the cages must be selectively functionalized

4

during their synthesis. Additionally, the molecular cages will need to be discrete, shape-persistent structures, with a cavity that can accommodate the CI. To this end, we have designed two open-faced polyhedral frameworks: a triangular prism (**1**) and rhomboid prism (**2**) presented in Figure 1.2. This work addresses the progress our group has made toward the stepwise synthesis of these frameworks.

Triangular Prism (1)

Rhomboid Prism (2)
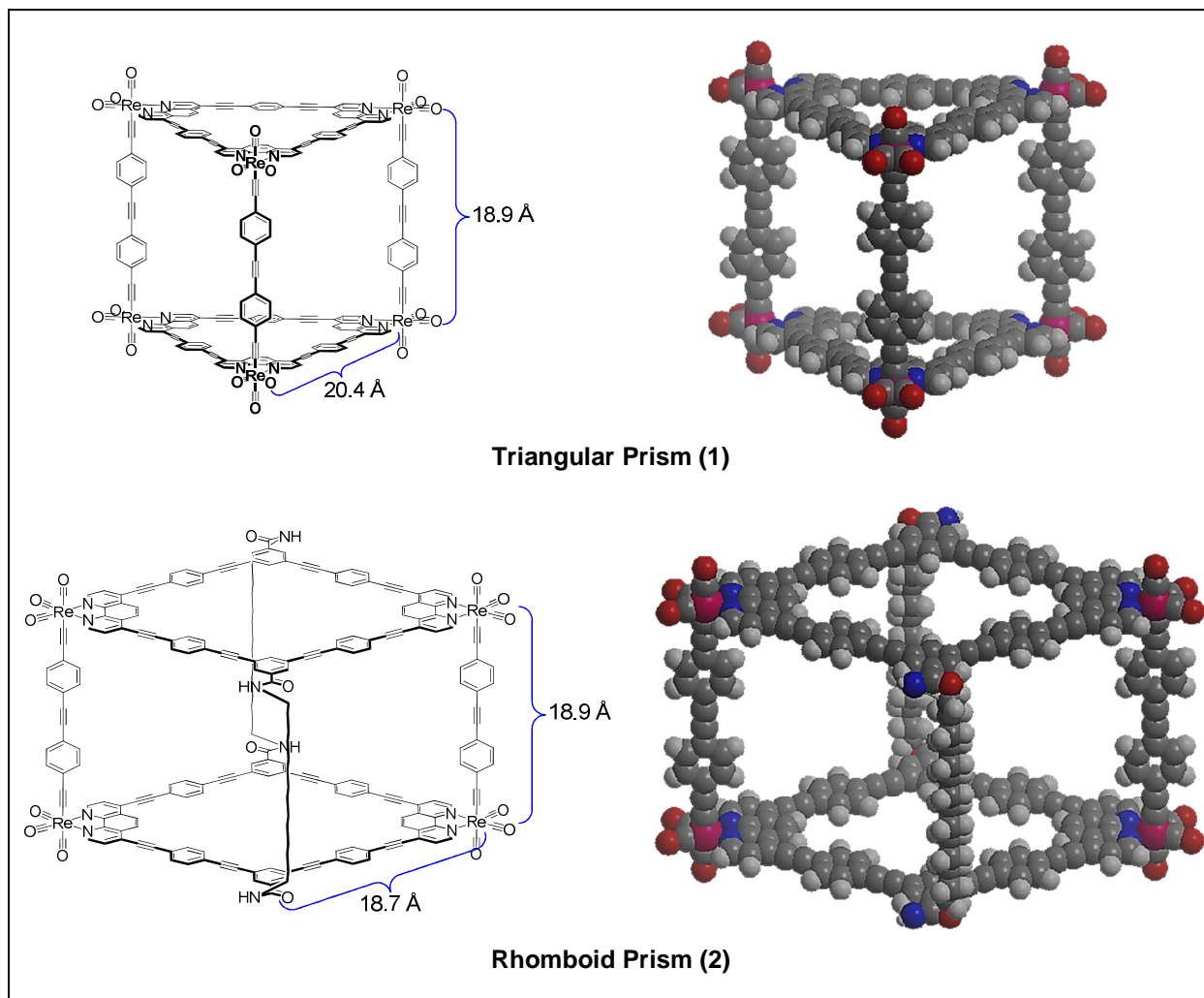
Figure 1. 2: Molecular cages **1** and **2**. Length measurements calculated using Hyperchem 7.5.

1.2. Molecular Cages

The term "molecular cage" describes any compound, complex, network, fragment, or aggregate immediately surrounding an occupied or unoccupied 3D-cavity in any phase(s). Consequently, this label has been aptly applied to micelles, clathrates, zeolites, coordination polymers, cryptands, carcerands, covalent organic frameworks, carboranes, platonic hydrocarbons, fullerenes, and proteins. Considering the volume and diversity of molecular cage structures, it is necessary to restrict our discussion to the abiological shape-persistent systems that are relevant to our work and are of most interest to synthetic chemists. "Shape persistent" refers to structures that retain their shape under normal conditions where no chemical or physical modifications transpire. The skeletal structures of these cages consist of rigid components held together by secure covalent and/or coordinate covalent bonds, rather than by relatively weak van der Waals, π-π stacking, hydrogen bonding, and ionic interactions.

Shape-persistent molecular cages are highly attractive structures with numerous potential applications including heterogeneous catalysis,[60-65] molecular storage,[60,62,65-77] molecular separation,[60,78] chemical sensing,[60,62,79-81] and nanomedicine.[82-88] For example, **MOF-5**, prepared and examined by O. M. Yaghi and M. O'Keeffe, has impressive sorption values for $H_2(g)$,[75] a promising alternative to fossil fuels, as well as for environmentally hazardous chemicals in the vapor phase at 22 °C (e.g. CH_2Cl_2, $CHCl_3$, CCl_4, C_6H_6, and C_6H_{12}).[76] See Figure 1.6c. Likewise, a series of water-soluble trigonal prisms with hydrophobic cavities synthesized and studied by the M. Fujita group (**3a – e** in Figure 1.4a) exhibit many remarkable functions related to their inclusion chemistry. These include performing as size selective chemical sensors[89] and as a regioselective molecular reactor in the nucleophilic substitution of allylic chlorides with a naphthalene substituent.[63] See Figure 1.4a. Like many shape-persistent cages, the conjugated systems used to construct their skeletal structures often lend these cages some interesting photophysical and photochemical properties, as evidenced by the photoinduced electron transfer between adamantane guests in cages **3b** and **3c**.[90,91] Finally, trigonal prism **8**, which consists of cytotoxic arene-ruthenium components, is currently under consideration as an anticancer agent by P.J. Stang's group.[83] See Figure 1.5c.

Considering these aforementioned applications, molecular cages are highly valued synthetic targets. However, their synthesis requires a high degree of organization, and thus can be quite challenging. This is particularly true for more sizable structures with numerous

components. Unsurprisingly, the earliest synthetic cages were relatively small or compact structures. For example adamantane was first synthesized in 1941,[92,93] cubane in 1964,[94] tetra-*tert*-butyltetrahedrane in 1978,[95] dodecahedranes in 1982,[96,97] and trinacrene in 1989[98] by multistep linear covalent synthesis. Because of their tiny and/or inaccessible cavities, these cages have no useful inclusion properties. Nonetheless, their generation by step-wise synthesis represents some of the earliest examples of molecular cage preparation. Because of the high labor cost and low yields, linear step-wise synthesis is not a practical methodology for the preparation of larger cages. In the early 1990's non-linear techniques already in practice in the synthesis of rigid oligomers,[99-102] dendrimers,[103-105] and shape-persistent macrocycles[106-109] were applied to the synthesis of sizable covalent-organic cages.[110-114] Although several impressive structures were obtained in respectable yields by this procedure, these accomplishments, in regards to molecular cage synthesis, were soon overshadowed by the one-step self-assembly of 3D-coordination polymers or metal-organic cages in high or quantitative yields. Owing to the productivity and convenience of this methodology, metal-organic cages, which were initially the only shape-persistent cage targets that could be obtained by self-assembly, have been most popular in the literature. Recently, however, the self-assembly of covalent-organic cages has attracted much attention.

According to Whitesides and Grzybowski,[115,116] self-assembly is an autonomous process whereby pre-programmed components are organized into ordered structures. Under thermodynamically controlled conditions, reversible bond formation between building blocks eventually leads the system to a global energy minimum corresponding to the synthesis of an ordered structure. Although seemingly simple, self-assembly involves complex principles. Consequently, it can be difficult to predict or control the outcome of these reactions. Of course, experimental conditions such as pH, temperature, solvent selection, reactant concentrations, addition rates, and addition order can be optimized for higher product yields. However, the careful selection of building blocks based on their structural, geometrical, and functional features is paramount to successfully obtaining a predetermined structure in both self-assembly and step-wise synthesis. Specifically, it is the distance and angle between the functional groups or coordination sites that serve to connect the building blocks, which determine the dimensions and geometry of the cages and its components. To be clear, the word component refers to a fragment excised from any region of the assembled structure (i.e. edge, joint, corner, or face) and is

distinct from building blocks, which are the reagents used to assemble the cage. Since the components are made up of the building blocks, they share many of the same structural and geometric features. In terms of functionality, however, much depends on the type of cage (i.e. metal-organic or covalent-organic) and the synthetic methodology. Four synthetic methodologies have been used in the synthesis of shape-persistent cages. These include directional-bonding, reticular synthesis, dynamic covalent chemistry, and step-wise synthesis.

1.2.1. Directional-Bonding Synthesis of Metal-Organic Cages

Metal-organic frameworks have been prepared by self-assembly using one of two approaches, directional bonding and reticular synthesis. In both cases, bond formation occurs by reversible coordinate covalent chemistry. Concordantly, building blocks are typically d-block metal complexes and reversibly coordinated rigid organic ligands, such as heterocyclic aromatics or aromatic systems with carboxylate, cyanate, or sulfonate substituents, hence the metal-organic classification. The metal components or acceptors serve as joints (traditionally called nodes) connecting the organic components or donors (traditionally called spacers), which define the edges and/or faces of the cages.

In directional bonding synthesis the arrangement of spacers and nodes are determined by two factors. The first is the arrangement of available binding sites on the metal center of the node. This is dictated by the coordination geometry of the metal center as well as the arrangement of kinetically inert blocking ligands on that center, which "direct" the incoming spacer building block to available coordination site(s) by occluding all other sites. The second factor is the positioning of coordinating atoms in the spacer. As demonstrated in the diagram devised by Stang, select building block combinations in the appropriate ratios are expected to give a particular cage structure. See Figure 1.3. For example, four square planar tritopic spacers with coordinating atoms separated by 120° and six ditopic nodes with available coordination sites at 90° should produce the truncated tetrahedron (or octahedron cage). Indeed, M. Fujita's group successfully synthesized octahedron cages **3a** – **e** in quantitative yields using four equivalents of 2,4,6-tri(4'-pyridyl)-1,3,5-triazine (TPT) spacer and six equivalents of cis-[Pd(L∩L)(ONO$_2$)$_2$] node complexes, where L∩L is a bidentate ligand (e.g. ethylenediamine – en; N,N,N',N'-tetramethylethylenediamine – TMEDA; 2,2-bipyridine – bpy; 1,10-phenanthroline – phen; and 2,9-dimesityl-1,10-phenanthroline – Mes-phen).[63,77,89,117] By

enforcing the cis configuration in the square planar [Pd(L∩L)(ONO$_2$)$_2$] the chelate ligands direct the coordination of the pyridyls in the TPT spacer.

Figure 1. 3: A selection of molecular library subunit combinations and the resulting cage topologies as reported by Stang.[118] The terminal end of each library member represents points of connection in the node (acceptor subunit) and spacer (donor subunit). Reproduced with permission from reference 83. Copyright © 2008, Elsevier.
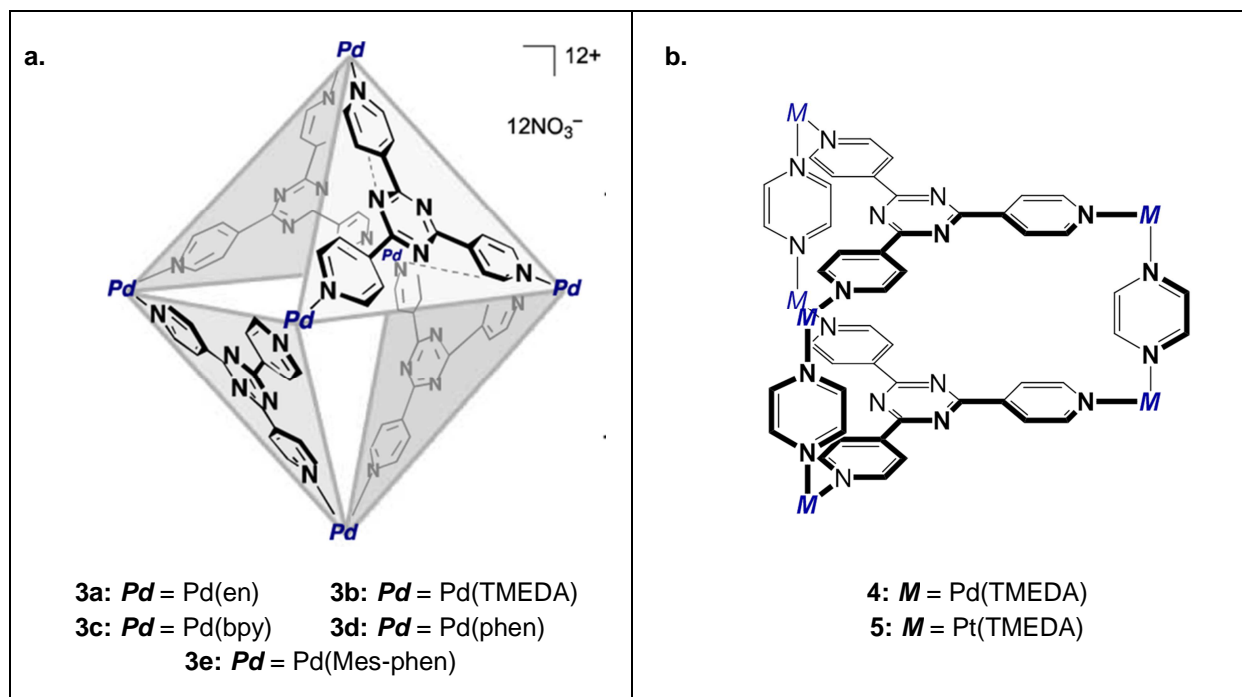
Figure 1. 4: a) Octahedron cages **3a – e**,[89] and b) trigonal prisms **4** and **5**.[119] Figure 1.4a reproduced with permission from reference 83. Copyright © 2013 American Chemical Society

Directional bonding was similarly employed by this same group to generate the closed-face trigonal prisms from two spacers, TPT and 1,4-diazine (dzn), and one node [M(TMEDA)(ONO$_2$)] – where M is Pd (**4**) or Pt (**5**).[73,78] See Figure 1.4b. In addition to the desired products, this one-pot procedure is also expected to produce homocoordinated [M(dzn)]$_4$ macrocycle and octahedron cage byproducts. By using the polycyclic aromatic templates, cages **4** and **5** could be isolated and the byproducts suppressed. In the aqueous environment of the reaction solution, these organic templates aggregate in the cage's hydrophobic cavity sandwiched in between the triazines, which likely stabilizes the cofacial arrangement of the triazine through π-π stacking and facilitates the formation of the trigonal prism. Unfortunately, these templates cannot be removed from the cavity of the Pd cage **4** without destroying the structure.[78] This highlights one of the major drawbacks of template-assisted self-assembly, the inability to remove templates from the structures.

To avoid both use of the template and homocoordinated byproducts, two of the building blocks maybe connected in a pre-assembly step, thus reducing the number of building blocks from three to two. For example, Stang's group produced trigonal prism **8** in 91% yield from 0° ditopic acceptor [(η^5-p-cymene)RuOTf]$_2$(μ-naphthazarin) (**7**) and the D$_{3h}$-symmetric donor 1,3,5-tris(pyridylethynyl)benzene (**6**).[83] See Figure 1.5b. One drawback of this methodology is the increased labor and reduced yields because of the preassembly step.
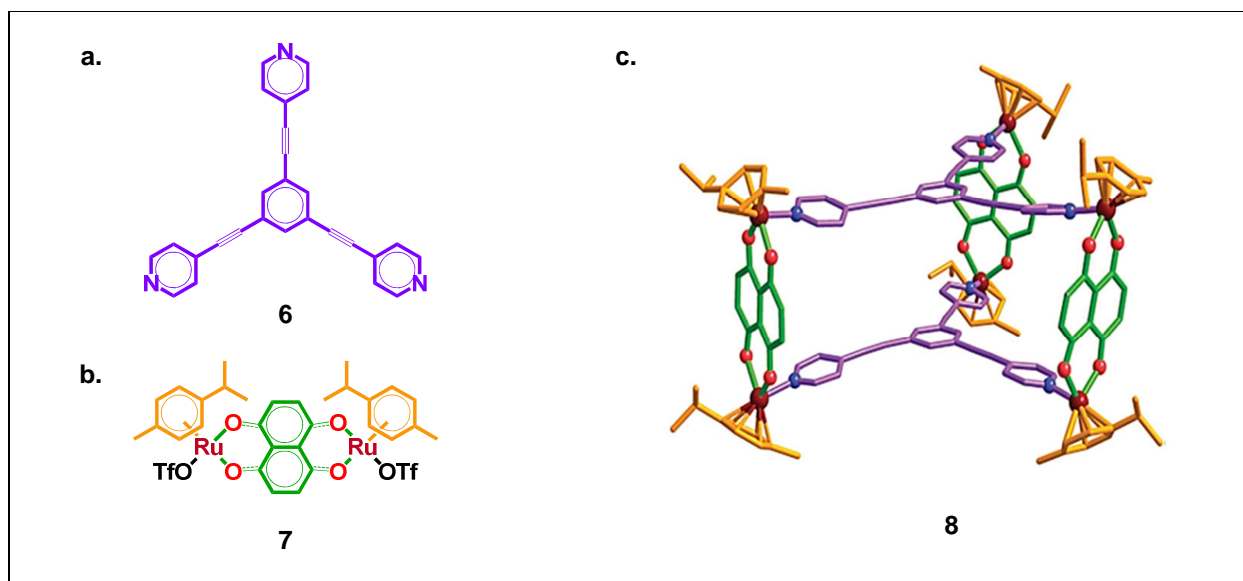
Figure 1. 5: The D$_{3h}$-symmetric tritopic donor (a), and 0° ditopic acceptor (b), subunit building blocks for trigonal prism **8** (c).[83]

1.2.2. Reticular-Synthesis of Metal-Organic Cages

In addition to the directional bonding, metal-organic cages have been synthesized through reticular synthesis.[74,120-131] Unlike in directional bonding synthesis where individual building blocks form a single cage component (i.e. joint or edge), in reticular synthesis multiple building blocks form a single component usually at the joint. This method has been used to produce a host of 3D-metal organic frameworks (MOFs).[129,131] For example **MOF-5** was prepared by O. M. Yaghi and M. O'Keeffe from terephthalate, $Zn(NO_3)_2$, and H_2O_2 by this technique. Additionally, discrete structures called metal-organic polyhedra (MOPs) like **MOP-23** have also been produced using the same techniques. [74,121,122,125-127]

During reticular synthesis the nodes and spacers, which usually contain carboxylate or sulfonate chelating groups, form cluster complexes at joints in the cage. The cage topology is determined by the symmetry of the cluster and the shape of the spacer. Since clusters are formed in situ, there is no way to predict the structure of cages synthesized by reticular synthesis based on the structural and geometrical characteristics of the building blocks. Instead, reticular chemists attempt to predict cage topology based on the point of extensions from the secondary building units (SBUs); a method adopted from zeolite chemistry and developed by Yaghi and O'Keefe.[130]

SBUs are the cluster or spacer components in the cages. Typically, the point of extension in both the inorganic SBU (cluster) or organic SBU (spacer) are select atoms in the chelate. For example, the points of extension in the $[Zn_4(\mu_4\text{-O})(CO_2)_6]$ cluster and terephthalate spacer in **MOF-5** are the carboxylate carbons. Because these carbons are arranged octahedrally in the cluster and linearly in the spacer, these two components combined are expected to produce cubic structures like **MOF-5**.[75] See Figure 1.6. Likewise, **MOP-23**'s truncated cuboctahedron shape can be anticipated by the combination of square planar $[Cu_2(\mu_2\text{-}CO_2)_4]$ cluster and the D_{2h}-symmetric ditopic spacer.[126] See Figure 1.7. The points of extension in both the cluster and spacer are the carbonyl carbons. However, these predictions are based on knowing the cluster's structure and the assumption these clusters will form. In this regard, advances made in crystallography at the end of the last century have been most useful.[120,126,128,130,131]

a.

[Zn₄(μ₄-O)(CO₂)₆]

b.

1,4-benzenedicarboxylate

c.
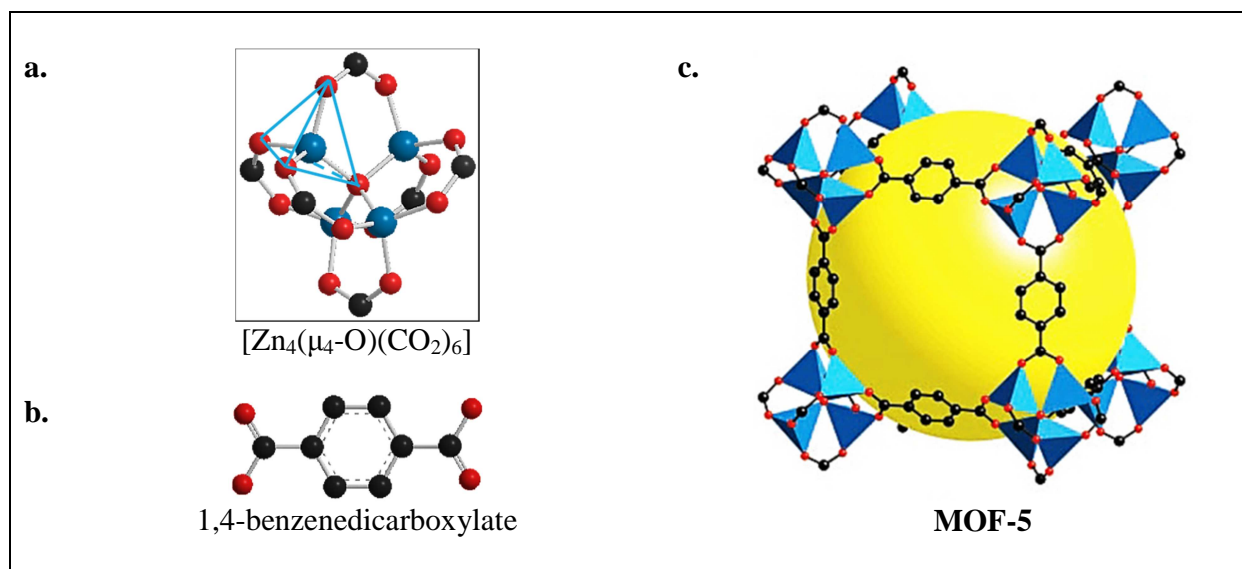
MOF-5

Figure 1. 6: Inorganic (a) and organic (b) SBU for **MOF-5** (c).[76] Reproduce with permission from reference 76. Copyright © 2003 American Association for the Advancement of Science.

a.

[Cu₂(μ₂-CO₂)₄]

b.

2,7-naphtalenedicarboxylate

c.

MOP-23

Truncated Cuboctahedron
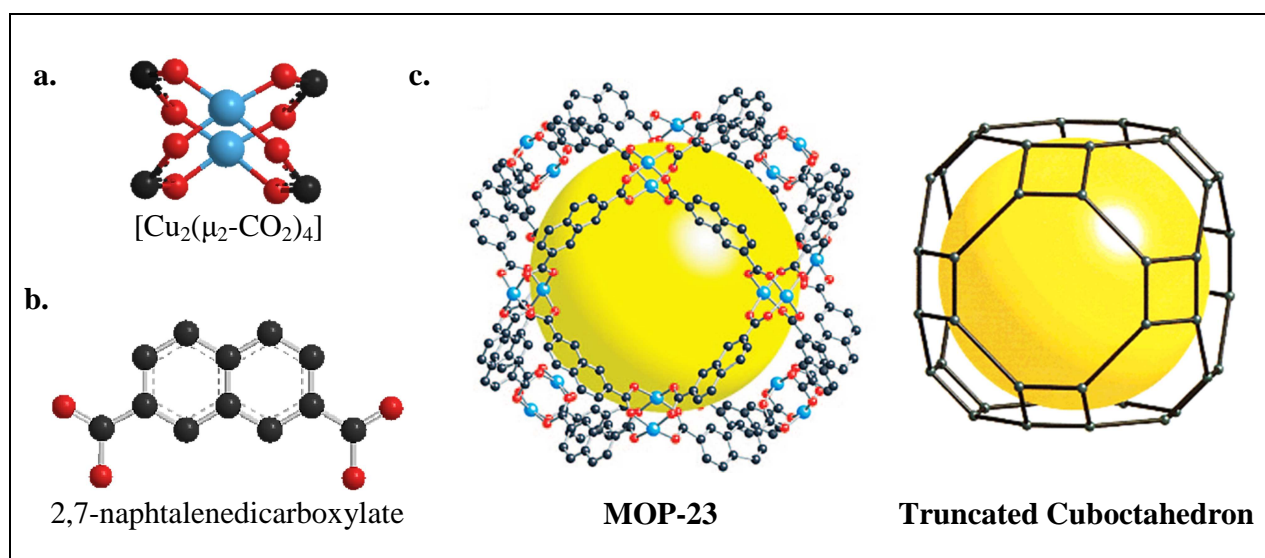
Figure 1. 7: Inorganic (a) and organic (b) SBU for **MOP-23** (c), which is shaped like a truncated cuboctahedron. Reproduced with permission from reference 95. Copyright © 2008 American Chemical Society.[126]

Although designing molecular cages by reticular synthesis is more complicated than by directional bonding, the resulting structures of the former method are typically more sound than those of the latter. The stability of MOFs and MOPs obtained by reticular synthesis is attributed to the SBU cluster, which form far more rigid joints than joints made by inorganic complexes.

12

Consequently, MOFs and MOPs produced by reticular synthesis exhibit desirable characteristics absent in most other metal-organic cages including thermal stability and permanent porosity, which refers to their ability to survive host-guest exchanges.

1.2.3. Synthesis of Covalent Organic Cages via Dynamic Covalent Chemistry

In addition to metal-organic cages, self-assembly has also been useful in the preparation of covalent-organic cages.[67,69,70,72,79,132-136] For example a series of [4+6] adamantoid cages (**11a – d**) with endotopic hydroxy groups were prepared by M. Mastalerz, I. M. Oppel, and coworkers in a one-pot imine condensation from four and six (i.e. [4+6]) equivalents of triptycene triamine (**9**) and the salicyldialdehyde derivatives (**10a – d**), respectively. See Scheme 1.2.[133]

10a: R = CH₃
10b: R = C(CH₃)₃
10c: R = C(C₂H₅)₃
10d: R = C(Ph)₃

11a: R = CH₃ (71%)
11b: R = C(CH₃)₃ (60%)
11c: R = C(C₂H₅)₃ (73%)
11d: R = C(Ph)₃ (52%)
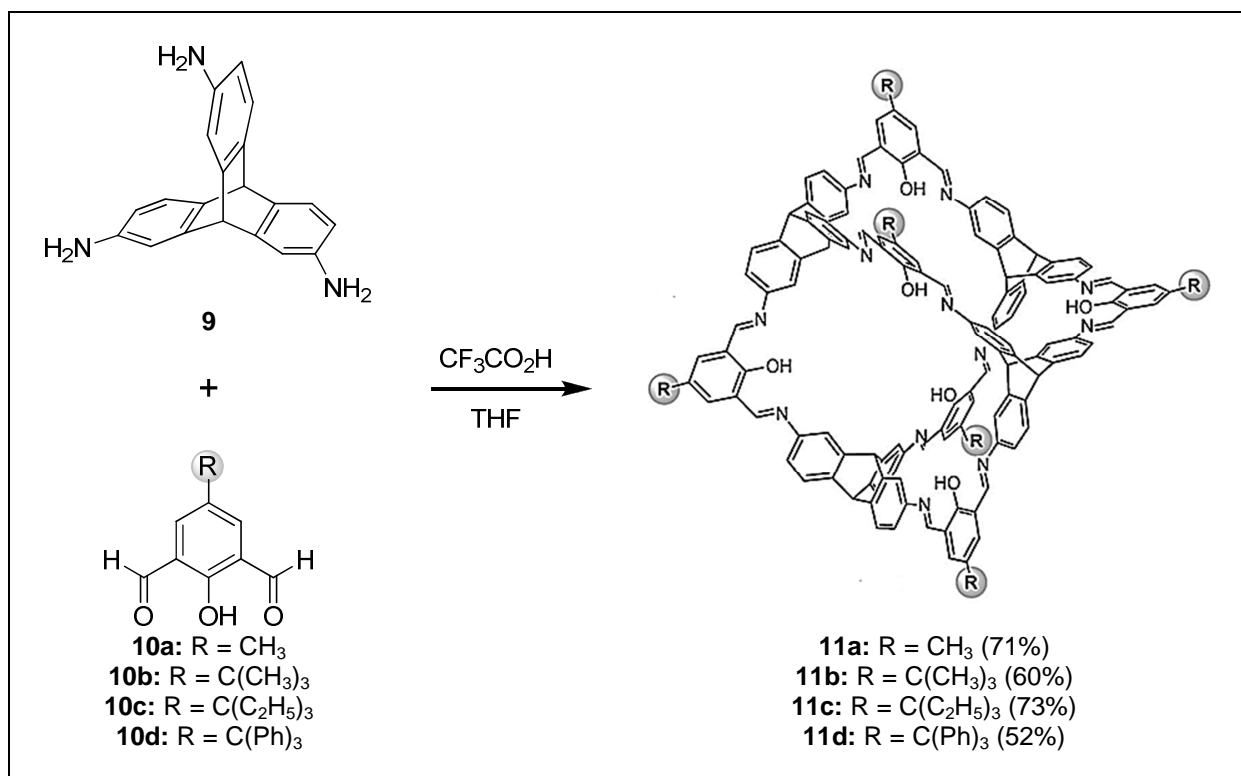
Scheme 1. 2: Synthesis of [4+6] Adamantoid cages **11a – d**. Reproduced with permission from reference 133. Copyright © 2012 John Wiley and Sons Inc.[133]

Similarly other covalent-organic cages have been self-assembled by this group and others using the methodology known as dynamic covalent chemistry. Dynamic covalent chemistry is a branch of dynamic combinatorial chemistry that involves isolating the most thermodynamically stable structure under specific conditions from constituents of the reaction mixture that are in

rapid equilibrium with one another. Because dynamic covalent chemistry requires reactions where equilibrium is established rapidly, covalent-organic cage synthesis is limited to several reactions including the formation of imines, boronic esters, and disulfides, as well as alkene metathesis and transacylation.[137-140] Reagents for these reactions form the building blocks of self-assembled covalent-organic cages. As with metal-organic cages, structural and functional characteristics of these building blocks dictate the topology of the resulting cages and are used in designing predetermined structures.

1.2.4. Step-Wise Synthesis of Covalent Organic Cages

As previously mentioned, self-assembly is a contemporary approach in the synthesis of covalent-organic cages, and until recently most covalent-organic cages were prepared by step-wise synthesis.[92,94-97,110,112-114,141] For example, cubane was synthesized in 1964 through a linear multistep process involving a sequence of nine reactions that afforded the product in 6% yield.[94] The linear synthesis of larger expanded cubane by Diederich and coworkers required eight steps and netted about 1% overall yield.[110] Better results were obtained for the total synthesis of fullerene-C_{60}, and as reported in 2002 required ten steps and yielded 22% of product.[141] In addition to these compact structures, larger covalent organic cages have been prepared by non-linear synthesis. For example Jeffrey S. Moore and coworkers synthesized trigonal prism **17** from fundamental building blocks (i.e. **12** – **15**). See Scheme 1.3. Through a series of alternating coupling and selective demasking reactions, the building blocks were combined to form higher-order building blocks. These higher-order building blocks were then converged into a "branched-sequence" (i.e. **16**) that is patterned to form the cage after the final demasking (i.e. **17**) and intramolecular coupling steps. In total, the synthesis of **17** from the fundamental building blocks required fourteen steps and yielded roughly 20 % of the product.[114] Trigonal prism **21** was produced by Zhang and Chen [142] from fundamental building blocks **18** and **19** in only three steps in an overall percent yield of 33%. See Scheme 1.4. Because the synthesis of **21** occurs through symmetrical coupling reactions, fewer steps are required and yields are slightly higher than those associated with the synthesis of **17**. However, the cages that can be produced by this method are limited to highly symmetric structures.
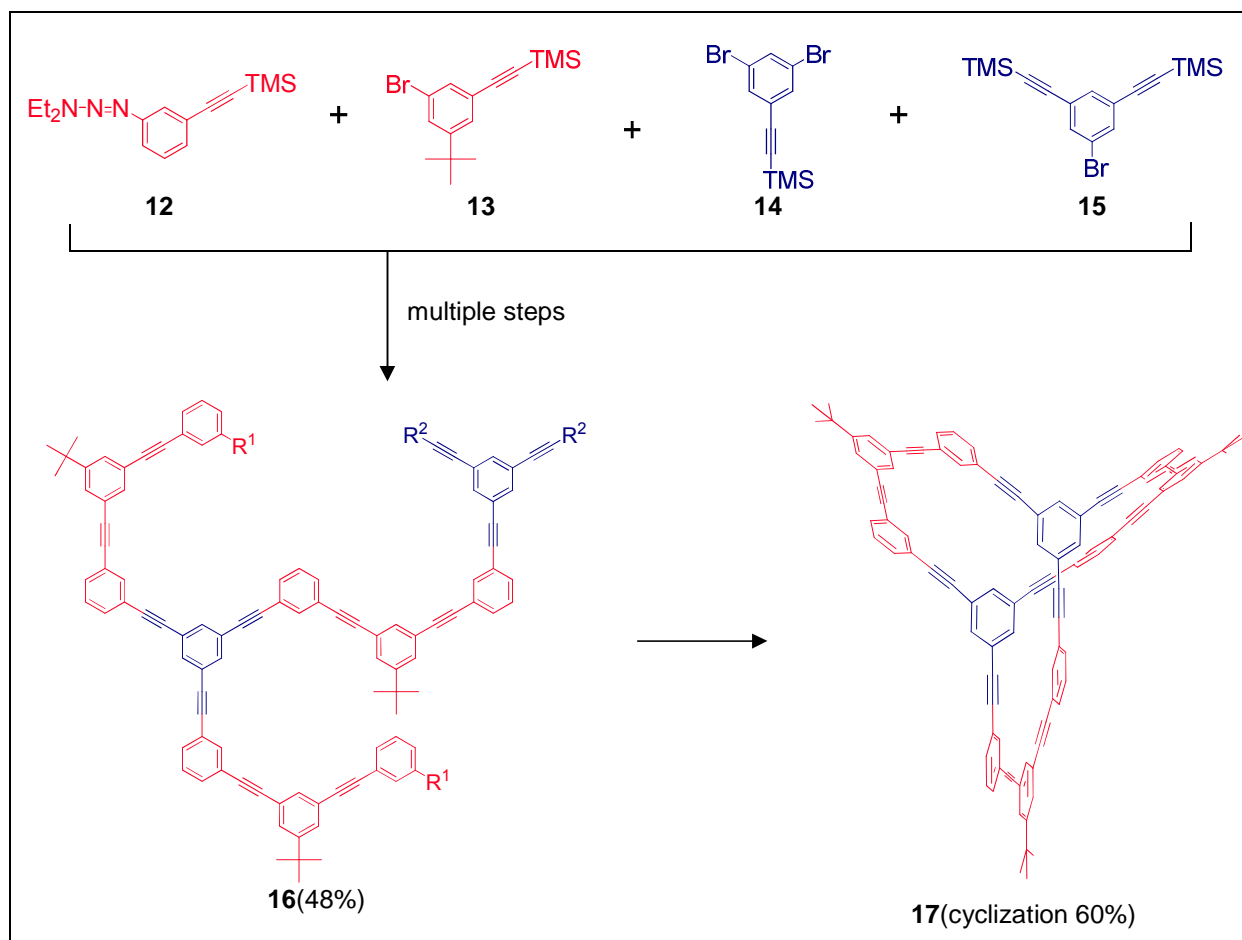
Scheme 1. 3: Step-wise synthesis of trigonal-prism **17**. Key: R^1 = Br; R^2 = H[114]
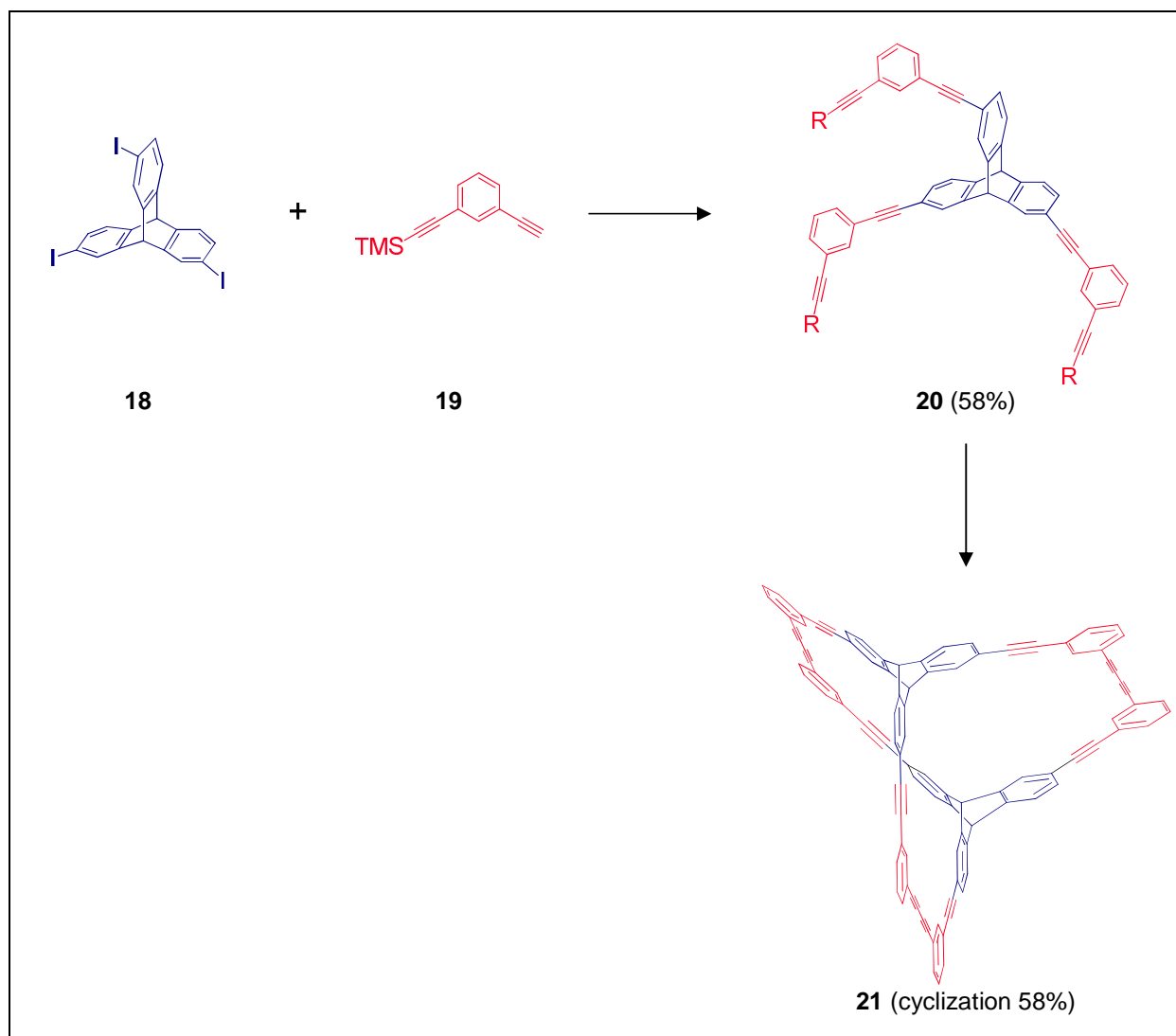
Scheme 1. 4: Synthesis of triangular prism **21**.[142]

1.2.5. Self-Assembly vs. Step-Wise Synthesis

Clearly, there are advantages and disadvantages to all of the above approaches. To summarize, the three self-assembly methods: directional-bonding, reticular synthesis, and dynamic covalent chemistry successfully produce shape-persistent cages in relatively few-steps and high yields, unlike step-wise synthesis. However, of the three self-assembly methods, reticular synthesis is the most reliable method for producing structures with permanent porosity (i.e. survives removal of template or guest exchange). Permanently porous structures can also be afforded via step-wise synthesis. Moreover, step-wise synthesis permits greater control over the arrangement of components than self-assembly. Therefore, one is able to produce structures

with higher asymmetry and more functional complexity. Nevertheless, the high labor cost associated with step-wise synthesis of complex cages is unavoidable, and efforts to reduce the number of steps by employing more symmetric coupling reactions reduce the degree of potential versatility.

Since the method of synthesis has an impact on certain aspects of the cages structure, physical stability, and functionalization, it must be considered seriously when designing cages for a particular purpose. In our case, we require cages that can be selectively functionalized with CI-stabilizing and electrode-anchoring functional groups. Therefore, we elected to use step-wise synthesis. Choosing the method of assembly is just one aspect of the design principles. Equally important are component selection and the synthetic protocol, which will be addressed in the following section.

1.3. Design Principles: Component Selection and Synthetic Protocol

1.3.1. Component Selection and Building Blocks

The selection of cage components requires careful consideration, as the chemical behavior, physical properties, and structural characteristics of the cage are dictated by the component identity and arrangement. In designing functionalizable, shape-persistent, structures with internal cavities suited for hosting the CI, we chose three basic components: oligo-(phenylene ethynylenes) or OPEs for edge components, as well as the *fac*-tricarbonyl(1,10-phenanthroline)rhenium(I) and the benzoate moiety for joint components See Figure 1.8.

OPEs are attractive structural components for molecular cages. These stable rigid materials permit robust shape-persistent structures that can be tailored to different dimensions through highly reliable Sonogashira cross-coupling.[99,100,143,144] Consequently, the cage's volume can be made more suitable to hosting a particular guest such as the CI. Additionally, the 2, 3, 5, and 6 positions of the phenyl rings in the OPE can be functionalized via established aromatic substitution reactions. Therefore, all of the aforedescribed cage requirements can be met by the OPE components alone. The main purpose of the joint components is to connect the linear OPE edges in the appropriate orientations to achieve the desired 3D-geometry.

The *fac*-tricarbonyl(1,10-phenanthroline)rhenium(I) joint connects a pair of coplanar OPE edges, which extend from the 4 and 7 positions of the 1,10-phenanthroline ligand at approximately 60° degree angles, as well as a vertical edge that coordinates directly to the
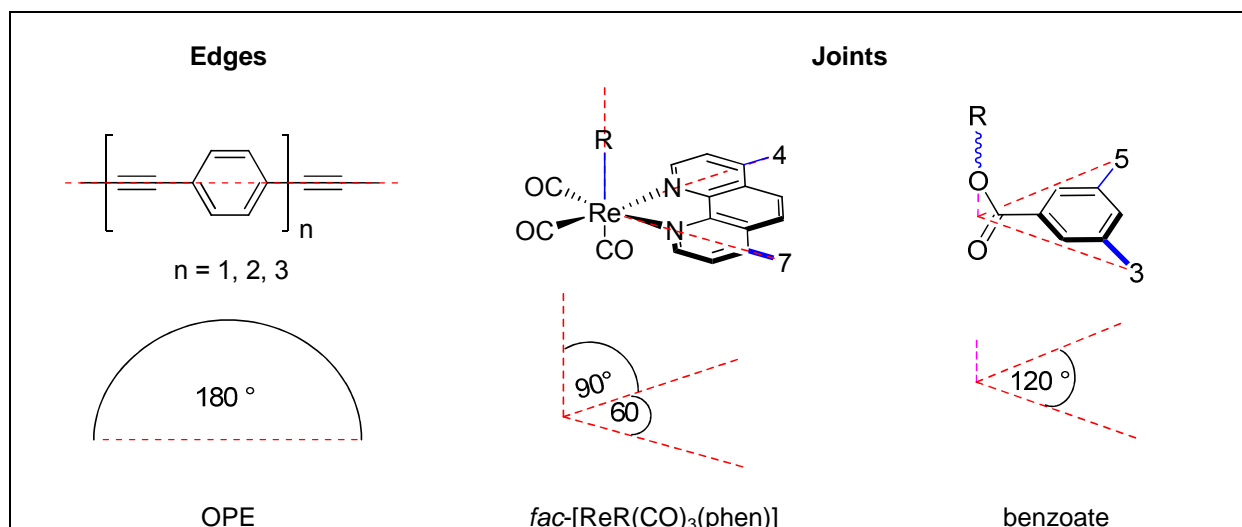
Figure 1. 8: Framework components. The dashed red lines are used to show fixed angles. The dashed magenta lines are used to show angles that are not fixed.

rhenium center. It should be noted that, the facial arrangement of the carbonyls in these rhenium moieties is essential, as these 3D architectures cannot be formed with the alternative meridional geometry. Fortunately, in the absence of very bulky ligands (e.g. triphenylphosphine ligands in *mer*-tricarbonylchloro-bis(triphenylphosphine)rhenium(I)) the facial conformation of rhenium tricarbonyl complexes is most preferred because it avoids the transoidal arrangement of competing π-accepting carbonyl ligands.

The three OPE edges connected to the *fac*-tricarbonyl(1,10-phenanthroline)rhenium(I) joint form the *fac*-[Re(C≡CR)(CO)₃(phen')] 3D-corner component in these cages. The dihedral angle between alkynyl ligand (i.e. the vertical edge) and the phenanthroline ligand connecting the two coplanar edges (i.e. phen') is expected to be about 90°. The crystal structures of *fac*-[Re(C≡CR)(CO)₃(phen')] complex **22** reported V. Yam's group and presented in Figure 1.9 supports the anticipated geometry for the corner component.[145] The dihedral angle between the alkynyl and phenanthroline ligands is found to be about 85° (i.e. very close to the ideal 90°).
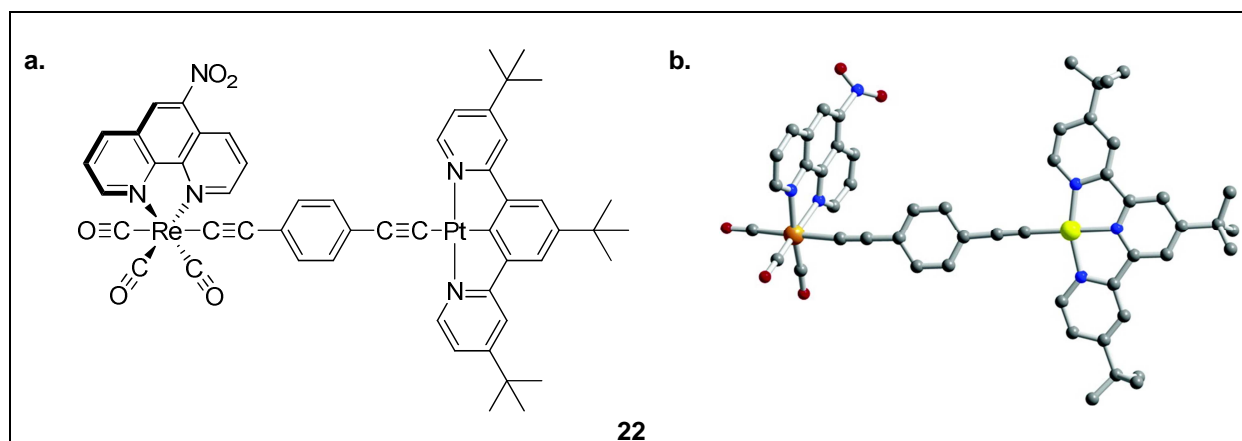
Figure 1. 9: The (a) structural formula and (b) crystal structure of **22**.[145]

In addition to the geometric contributions of the [Re(C≡CR)(CO)₃(phen')] corner component to the structure of the cages, these complexes may also provide these cages with some interesting redox properties. Indeed, Re(C≡CR)(CO)₃(phen')] complexes are known to be redox active.[146-149] For example, the alkynyl ligand and rhenium center in complex **23** gets oxidized at +0.99 V and +1.79 V vs. SCE, respectively, while the diimine gets reduced at –1.52 V vs. SCE in acetonitrile.[146] Because there are six redox active [Re(C≡CR)(CO)₃(phen')] corner components in cage **1** and four in cage **2** connected in a conjugated system, the redox chemistry of these cages is expected to contain more redox couples at more favorable potentials than observed in **23**.[147-149] During the operation of the SET, cages **1** and **2** may become oxidized or reduced by the drain or source electrodes. There are two concerns raised by the electrodes oxidizing or reducing the cages. Firstly, the charged cages, particularly the oxidized cages, could be unstable and decompose; thus destroying the device. The oxidation of complex **23** was irreversible due to the loss of the alkynyl ligand.[146] Since the entropic cost associated with ligand dissociation in these cages would be significant and the charges should be delocalized over rather extensive conjugated systems, decomposition is unlikely. The second concern is whether the redox activity of the cages will interfere with the transfer of charge carriers between the CI and electrodes. If the drain or source electrode sends the charge carrier to the cage rather than the CI, the charge carrier must be transferred to the CI from the oxidized or reduced cage. Since the cages have multiple redox active [Re(C≡CR)(CO)₃(phen)] centers and the oxidized and reduced cages are expected to be relatively stable due to charge delocalization, the cages may

need to accumulate a significant amount of charge before transferring the charge carrier to the CI.

23
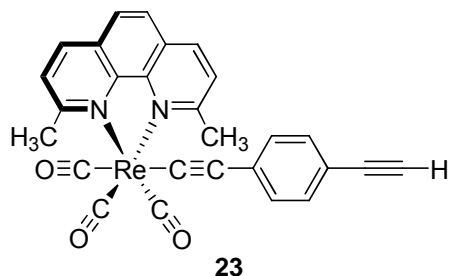
Figure 1. 10: Complex **23**.Sss[146]

The second joint component, the benzoate moiety, is only present in cage **2**. Unlike the rhenium joint, the benzoate joint is not essential for construction of 3D-shape-persistent structures since the edge orthogonal to the diamond face (**35**) extends from a flexible ester group. However, the coplanar edges that are attached to the 3 and 5 positions in the benzoate are affixed at roughly 120° angles, and thus contribute to shape-persistence in 2D. The diamond face of cage **2** (**35**), as well as the triangular face of cage **1** (**32**) are expected to be planar structures with D_{2h}- and D_{3h}-symmetry, respectively. See Scheme 1.5. The anticipated planar geometry of macrocycles **32** and **35** is supported by crystal structure of the OPE-conjugated macrocycle **24**, which shows all the aromatic rings to be coplanar and the macrocycle almost perfectly flat.[150] See Figure 1.11. Although our structures contain bulky hexyl groups that could render coplanarity of aromatic rings sterically unfavorable, the ^{1}H and ^{13}C NMR spectra of **32** supports a D_{3h}-symmetric structure; suggesting the hexylated benzene rings rotate freely around the sp^{2}-sp carbon-carbon bond. See Figure AC4.17 and AC4.18.
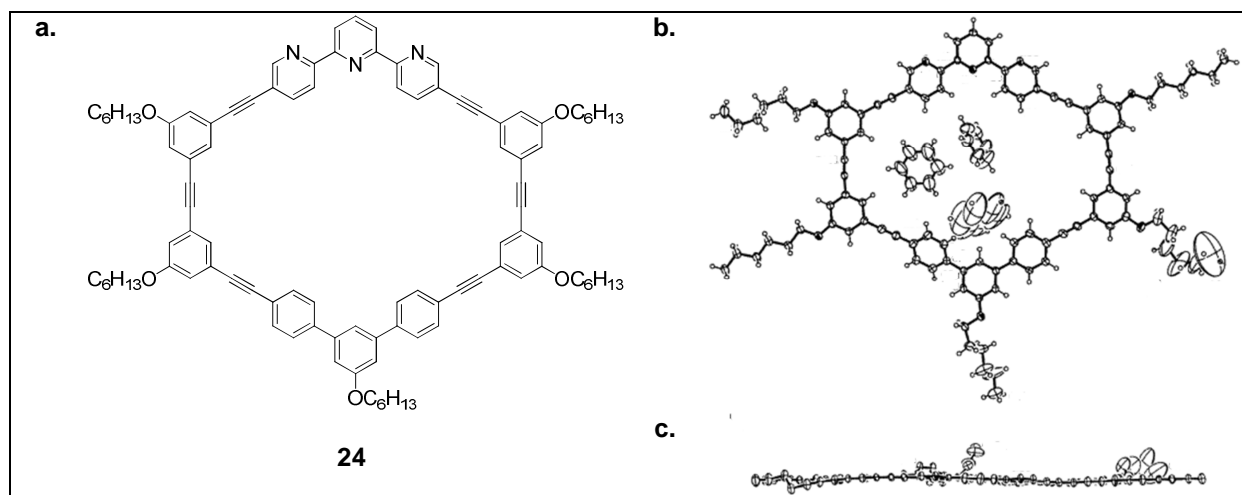
Figure 1. 11: The a) structural formula and the b) front-view and c) side-view of the crystal structure of **24**.[150]
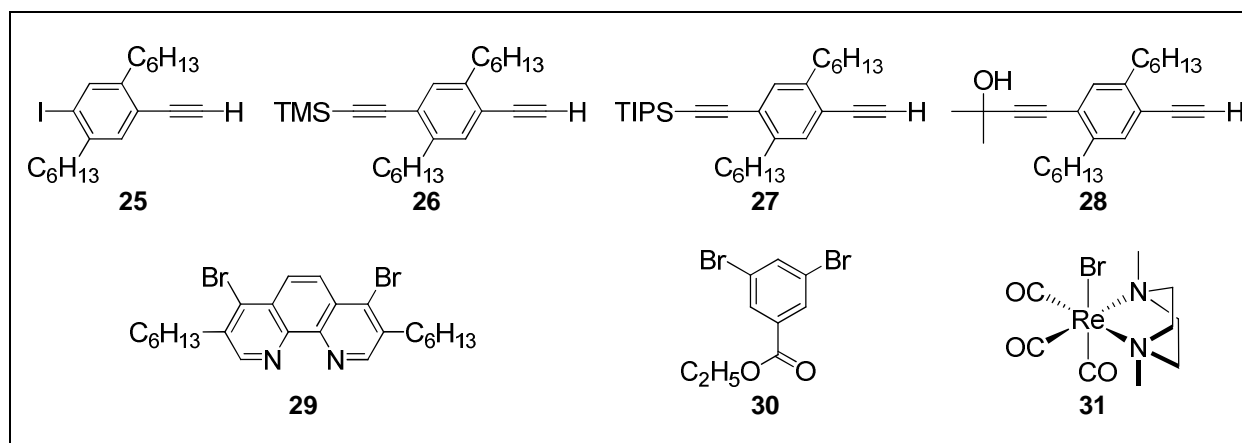
Figure 1. 12: Fundamental or primary Building Blocks **25 – 31**.

1.3.2. Synthetic Protocol

The OPE edge as well as the rhenium and benzoate joint components can be assembled into the cages in a three-stage bottom-up approach outlined in Scheme 1.5. This synthetic protocol uses several fundamental building blocks **25 – 29**, which are depicted in Figure 1.12. During the first stage, complementary vertical-edges **33** and **34** are synthesized from **31** and the alkynyl silver derivatives of **25** and **27**, respectively. The details of this synthesis are discussed in Chapter 2 of this document. In addition to the vertical-edges, triangular face **32** and diamond
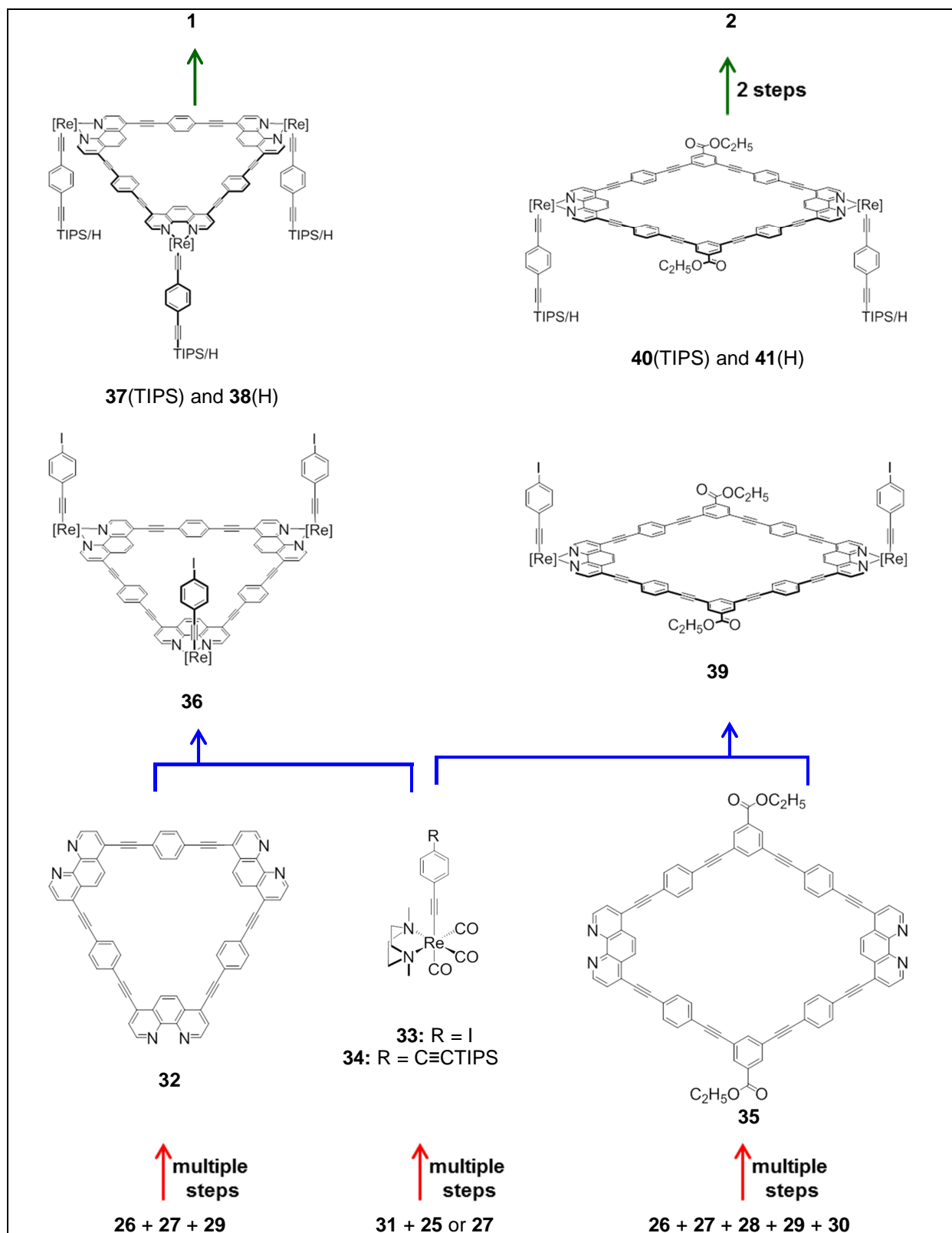
Scheme 1. 5: Synthetic protocol of **1** and **2**. [Re] = *fac*-Re(CO)₃. Hexyl groups omitted for clarity.

face **35** are synthesized from organic building blocks **26** – **30** during the first stage of the synthetic protocol. Both **32** and **35** are organic shape-persistent macrocycles, which makes them valuable and challenging targets in their own right. Efforts toward their step-wise synthesis are addressed in Chapter 4 of this document.

In the second stage of the cage synthesis, vertical-edges **33** and **34** are inserted into the phenanthroline corners of the triangular (i.e. **32**) and diamond (i.e. **35**) faces by substitution of the N,N'-dimethylpiperazine (dmpz) ligands to produce a pair of complementary half prisms for each cage (i.e. **36** and **37** for **1** and **39** and **40** for **2**). The group terminating the vertical-edge of a member of the half-prism pair is either a sp^2-iodide (i.e. **36** and **39**) or a triisopropylsilyl or TIPS-masked acetylene (i.e. **37** and **40**). Desilylation of the TIPS group in **37** and **40** should produce **38** and **41**, respectively. Therefore, **36** and **38** as well as **39** and **41** form complementary reagents in a Sonogashira cross-coupling reaction that should produce **1** and an open form of **2**, respectively. This coupling occurs during the third and final stage of the protocol. To complete the synthesis of cage **2**, two auxiliary vertical-edges can be inserted into the open rhomboid prism. Likely, the open rhomboid prism will be closed by amidation of the ester group using two diamines (i.e. $NH_2(CH_2)_nNH_2$), as the auxiliary vertical edges.

According to this protocol, both cages **1** and **2** should be obtainable through this step-wise approach. However overall yields are expected to be low. As with all multistep processes, the inevitable loss of product after each reaction step can be significant. In addition, competing diastereomeric or oligomeric byproducts will reduce productivity at each stage of the procedure. For example, loss of product during the first stage to oligomerization in the cyclization reaction used to form macrocycles **32** and **35** is quite problematic. Likewise, during the final stage, coupling of the half-prisms will generate oligomers in addition to the cages. See Scheme 1.6. In both cases the propensity of the reaction to form oligomers may be lowered by optimizing reaction conditions (e.g. dilute conditions and using a template) in favor of cyclization and cage formation.

Generation of diastereomers during the synthesis of half-prisms **36**, **37**, **39**, and **40** in the second stage of synthetic protocol is also expected to lower product yields. Since vertical-edges point to the same or opposite sides of the triangular and diamond face, both syn- and anti-addition products are possible. The probability of adding all three vertical-edges to the same side of the triangular face to produce **36** or **37** is only one in four or 25 %. See Scheme 1.7a. A 50%

probability of producing the desired half-prism could be obtained for **39** and **40**, since fewer vertical-edges are added. See Scheme 1.7b. Indeed, if all four vertical-edges were to be added, as seen in the synthesis of square prism in Scheme 1.7c, the chances of syn-addition product is only one in eight or 12.5%. Despite the potential for oligomerization of the open rhomboid prism in the final step in the synthesis of **2**, yields are still anticipated to be higher than that of the square prism, since the flexible benzoate edge should be able to bend into a conformation that will promote cage formation. Moreover, oligomers that are generated may be self-corrected through reversible transacylation reactions that would be used to make the flexible edges. Therefore, under highly dilute conditions the potential for oligomerization in the final step in the synthesis of cage **2** can be greatly reduced by using these flexible edges. The flexibility of the benzoate edges may have a negative impact on the structural integrity of **2**. However, the benefit of higher overall product yields outweigh any suspected reduction in cage robustness.
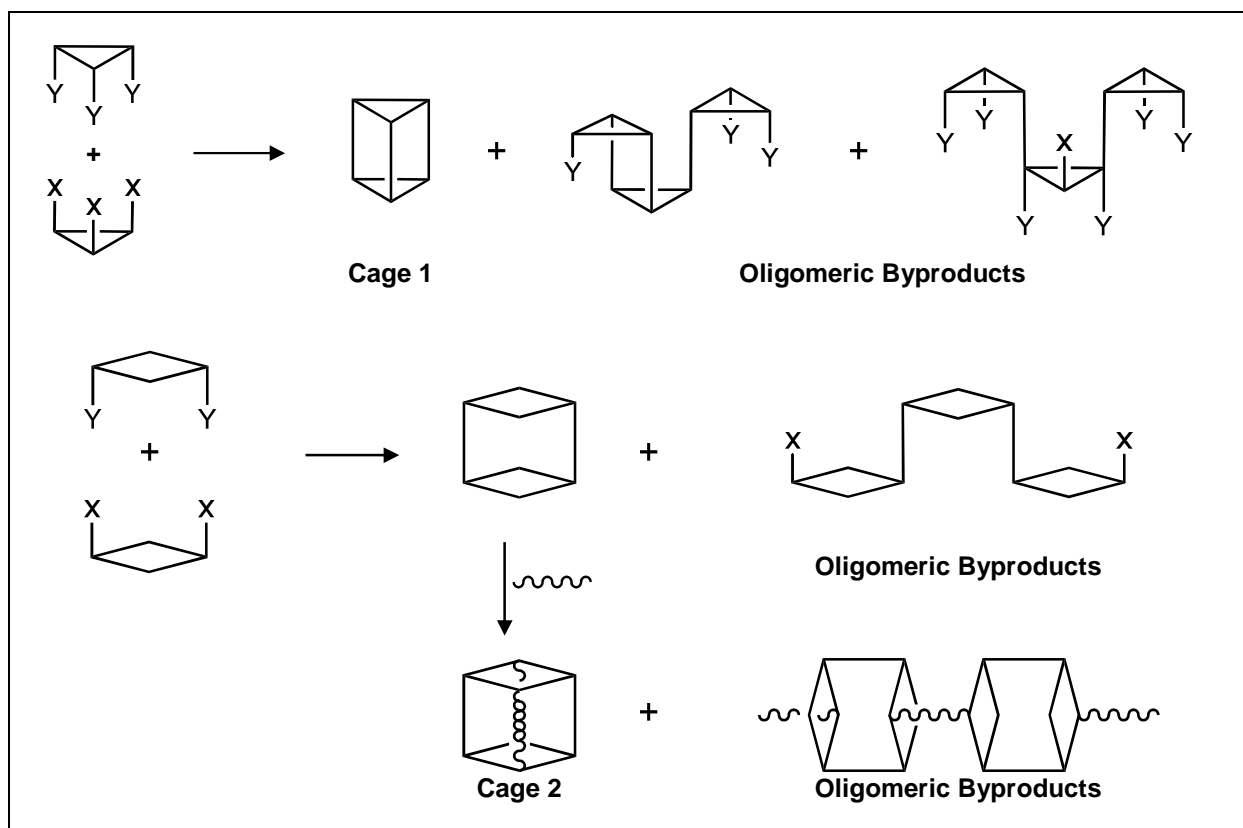
Scheme 1. 6: Oligomeric byproducts predicted for the synthesis of **1** and **2**.
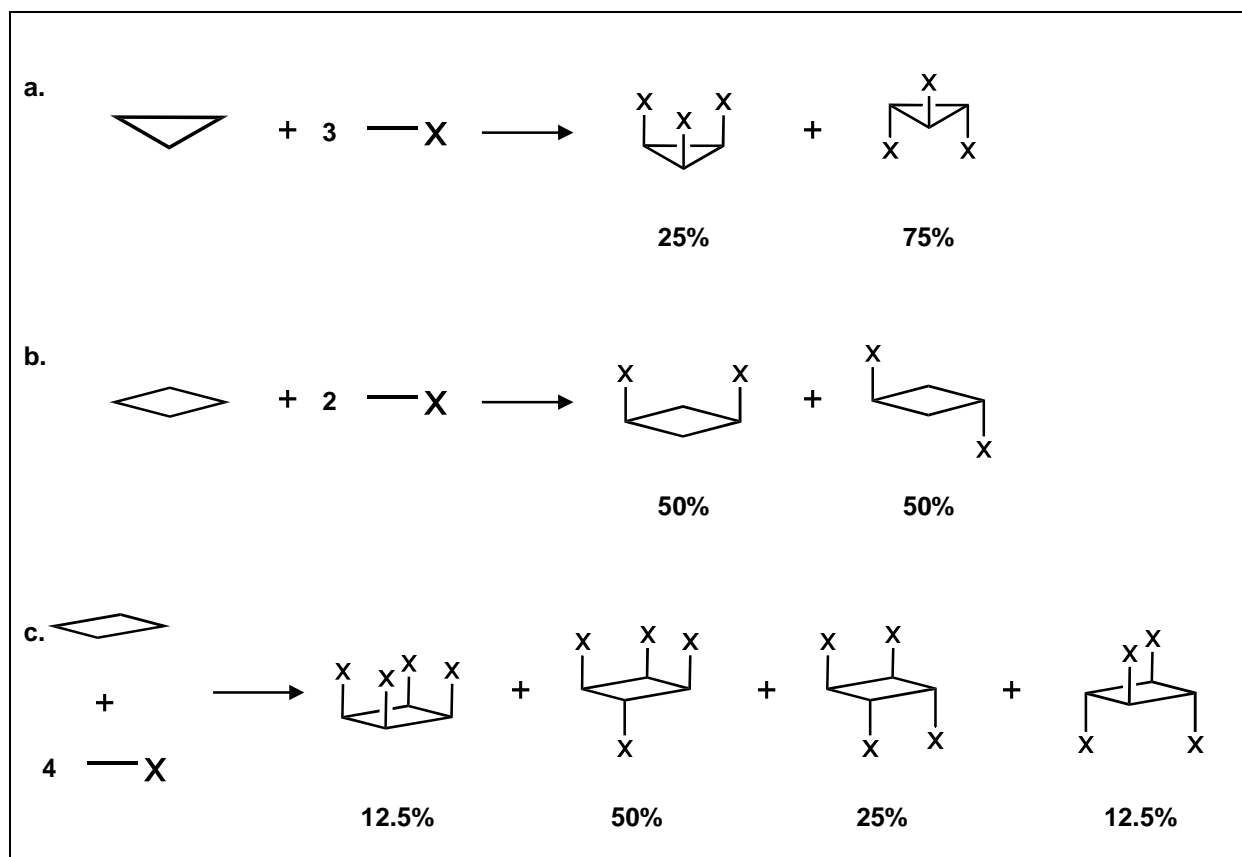
Scheme 1. 7: Diastereomeric syn- and anti- product distribution predicted for a) half-prism of **1** (i.e. **36** and **37**); b) half-prism of **2** (i.e. **39** and **40**); as well as half-prism of a rectangular prism.

1.4. Synthesis and Characterization of Fundamental Building Blocks

The fundamental building blocks depicted in Figure 1.12 form the basis of the bottom-up synthesis of cages **1** and **2** as presented in Scheme 1.5. These seven compounds are essential starting materials, in that all other building blocks used during the cages' synthesis can be generated from compounds **25 – 31**. The phenanthroline and benzoate corner components are constructed from building block compounds **29** and **30**, respectively. Likewise compounds **25 – 28** are building materials for all of the OPE edge-components. Finally, the *fac*-tricarbonylrhenium(I) moities found in the and *fac*-tricarbonyl(1,10-phenanthroline)rhenium(I) joint-component are incorporated into the cages through building block complex **31**. There are key chemical functionalities located at the appropriate positions in these compounds that serve as points of connections during the synthesis of the cages. The terminal sp carbons in compounds **25 – 28** can couple to the halogenated-sp^2 carbons in compounds **25**, **29**, and **30**. The bromine and N,N'-dimethylpiperazine ligands in complex **31** maybe substituted by alkynyl (i.e. **25 – 27**)

25

and 1,10-phenanthrolne ligands (i.e. **29**), respectively. Although the details of these reactions are addressed in subsequent chapters, it was important to note the chemical features of these fundamental building blocks as they relate to the construction of the cages.

Because the fundamental building blocks form the basis of the cages' synthesis, significant quantities of these compounds are required. Fortunately, all of the fundamental building blocks were synthesized by established reliable procedures, which are are summarized in Schemes 1.8 – 1.10. The synthesis of the 4,7-dibromo-3,8-dihexyl-1,10-phenanthroline (**29**) was accomplished according to the known procedure from 1,3-diaminobenzene and ethyl 2-(hydroxymethylene)octanoate. See equation 1 in Scheme 1.8. The benzoate corner compound ethyl 3,5-dibromobenzoate (**30**) was synthesized from 3,5-dibromobenzoic acid through the 3,5-dibromobenzoyl chloride as shown in equation 2 in Scheme 1.8. Although this compound may be purchased through commercial sources, it is more economical and convenient to synthesize **30** as it expensive and has limited commercial availability. The rhenium complex was synthesized from dirhenium decacarbonyl following bromination by oxidative addition and substitution of carbonyl ligands by dmpz as reported in our publication.[151]
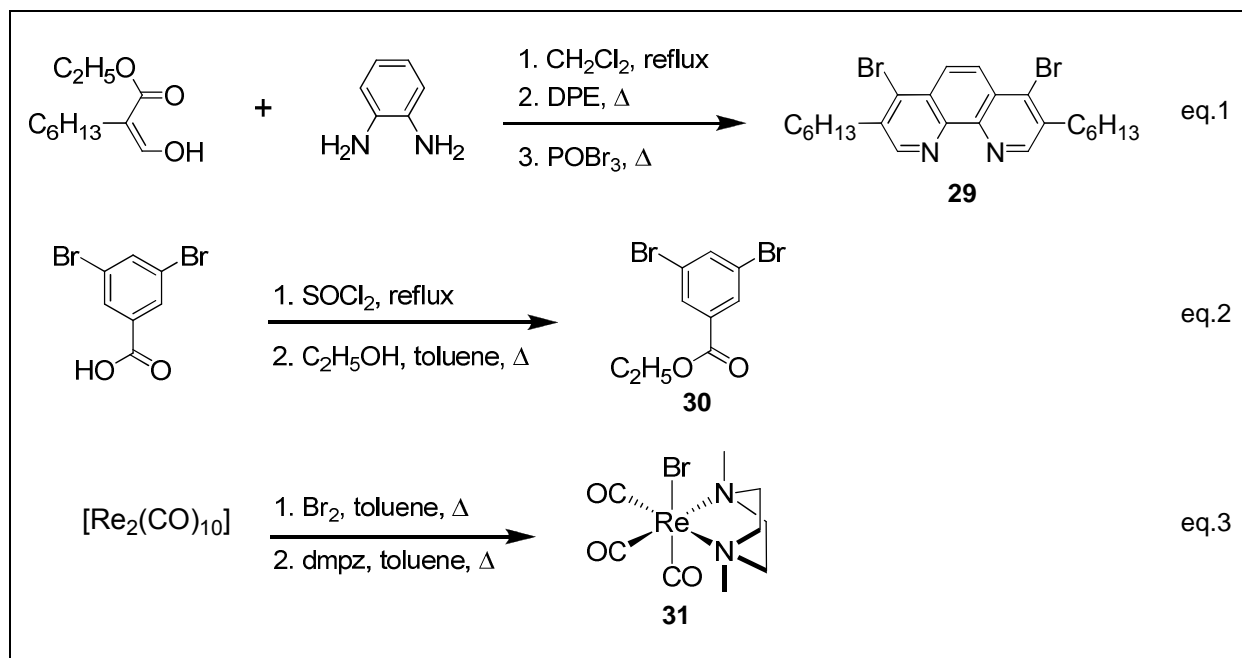
Scheme 1. 8: Synthesis of Fundamental building blocks **29**,[152] **30**,[153] and **31**.[151]

The remaining four fundamental building blocks, compounds **25** – **28** were prepared from 1,4-dihexyl-2,5-diiodobenzene (**42**) by Sonogashira cross-coupling and selective deprotection of masked acetylenes as shown in Schemes 1.9 and 1.10, respectively. Selective deprotection of acetylene is a valuable technique that has been used in the synthesis of dendrimers,[103-105] rigid oligomers,[99-102] as well as shape-persistent macrocycles[106-109] and molecular cages.[110-114] By employing a variety of protecting groups with different reactivities, one is able to control which acetylene will undergo coupling at a particular step. We employed three different protecting groups: trimethylsilyl (TMS), triisopropylsilyl (TIPS), and isopropanol-2-yl ($C(CH_3)_2OH$),. The conditions of their deprotection reactions are summarized in Figure 1.13. Removal of the propargyl alcohol requires hydroxide or hydride base and high temperatures, usually achieved by refluxing in toluene. Both trialkylsilyl groups may be removed by reduction with fluoride. In addition, desilylation of TMS protected acetylenes is achievable in hydroxide or carbonate solutions, but not for TIPS protected acetylenes.

The synthesis of compound **25** from **42** was achieved via two parallel pathways. The first is a known procedure that involves Sonogashira cross-coupling of 1 equivalent of **42** and 1.3 equivalents of trimethylsilylacetylene to produce **43** in 50 % yield relative to **42**. Desilylation of **41** by NaOH in a solvent mixture of CH_2Cl_2 and CH_3OH produced **23** in 89 % yield. In the second procedure **25** was synthesized in 99% yield by removal of the propargyl alcohol in compound **45**; the latter compound was synthesized in 51 % yield from 1 equivalent of **42** and 1.1 equivlants of 2-methyl-3-butyn-2-ol. In both pathways, a fraction of the starting material was recovered and the dicoupled byproducts (i.e. **44** and **46**) were produced. Although the starting material, the monocoupled product, and dicoupled product were separable via column chromatography the separation in the latter procedure was much cleaner. This is owing to the larger differences between the retention factor (R_f) values of **42**, **45**, and **46** as compared to the differences between R_f values of **42**, **43**, and **44**. The easier separation coupled with the cheaper cost of 2-methyl-3-butyn-2-ol relative to trimethylsilylacetylene makes the synthesis of **25** through **45** a more advantageous method.

Unlike fundamental building block **25**, which was attainable by two pathways, compound **26** could only be produced via a single pathway: the selective deprotection of the propargyl alcohol in compound **48** by NaH in refluxing dried toluene. Alternatively NaOH may be used as a base instead of NaH. However, NaOH is hydroscopic and may introduce water into the

reaction, which may result in the the desilylation of the TMS. The deprotection of the C(CH$_3$)$_2$OH-masked acetylene in **48** produced compound **26** in 94 % yield. The synthesis of compound **48** (86 %) was achieved by the coupling of trimethylsilylacetylene and **45**. Analogously compounds **47** (92 %) and **49** (95 %) were produced by the coupling of triisopropylsilylacetylene to **43** and **45**, respectively. Both compounds **47** and **49** were used to produce fundamental building block **27** through selective deprotection. By employing the same conditions used to remove the propargyl alcohol in **48** to compound **49** we were able to produce fundamental building block **27** in 91 % yield. The removal of the TMS group in **47** by reaction with KOH generated compound **27** in 93 % yield. Although fluoride solutions may also cleave the TMS, it is indiscrimenitory toward trialkylsily-masked acetylenes and would result in the loss of a TIPS group as well, if present.

The final fundamental building block, **28**, was prepared from **48** in 88 % yield and **49** in 93 % yield by selective deprotection of TMS and TIPS masked acetylenes, respectively, with N(C$_4$H$_9$)$_4$F. Alternatively, **28** may be synthesized from **46** by removal of a single propargyl alcohol. However, this procedure is non-selective and deprotection of one of (i.e. synthesis of **28**) or both of (i.e. synthesis of 1,4-diethynyl-2,5-dihxylbenzene) the masked-acetylenes in **46** does occur; these products being produced in 45% and 19% yields, respectively. Although the latter procedure (i.e. non-selective deprotection of **46**) is attractive because it makes use of the byproduct produced during the synthesis of **45**, it is not as productive as the former method (i.e. selective deprotection of **48** or **49**). Consequently, it is more preferable to produce compound **28** from **48** or **49**, rather than from **46**.

All products were characterized by ^{1}H NMR. In addition, previously unreported compounds (**27**, **28** and **45** – **46**, **48** – **49**) were fully characterized by ^{13}C NMR, FTIR, and EIMS. Both ^{1}H and ^{13}C NMR spectroscopy are particularly useful indicators of which functional groups terminate the ethynylene; the protecting groups resonating at distinct frequencies from each other and the acetylenic protons. In addition the phenyl protons and to a lesser extent the benzyl protons (i.e. methylene protons adjacent to the phenyl group) are sensitive to the electronic environment created by the non-hexyl substituents on the phenyl group. Therefore, the ^{1}H and ^{13}C NMR spectra of these compounds, their parents, and derivatives are easily distinguished from one another.
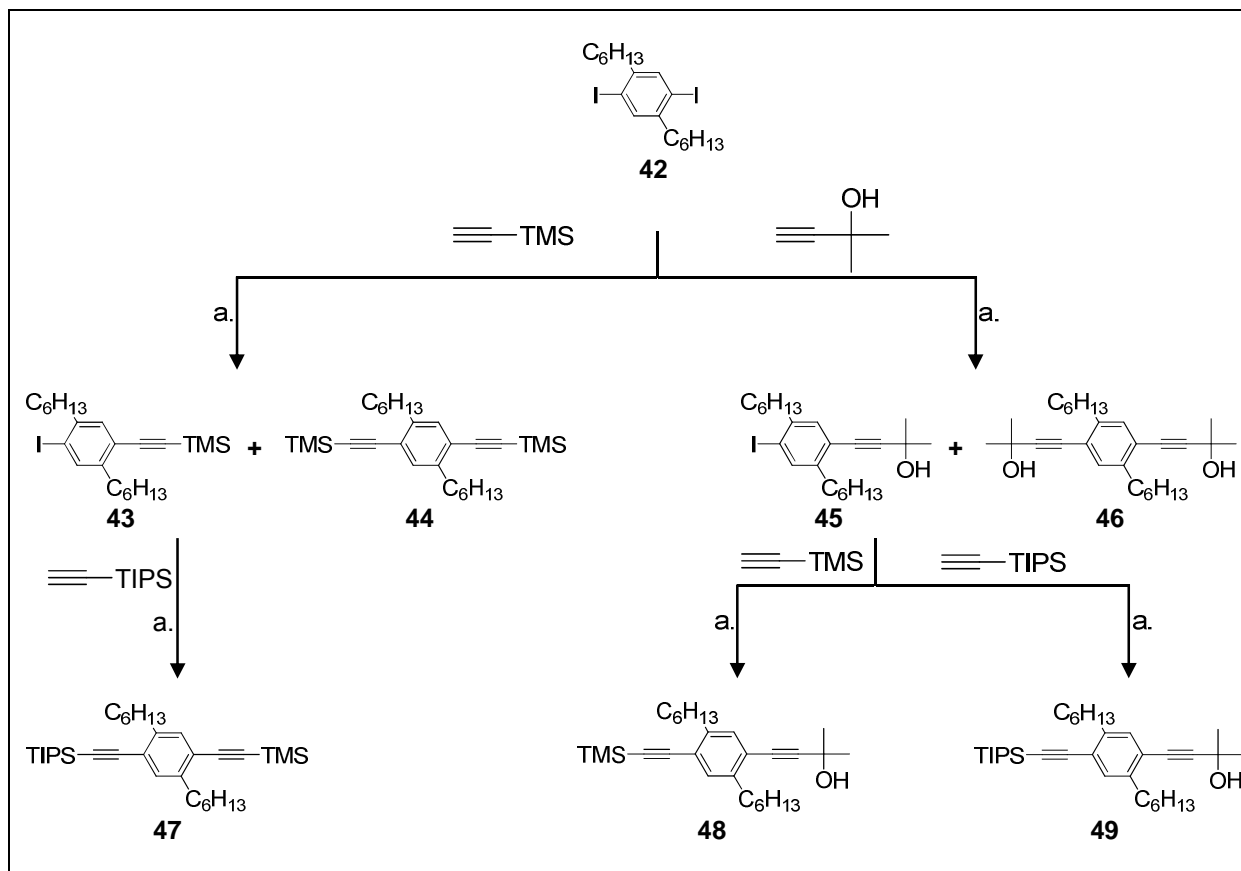
Scheme 1. 9: Synthesis of compounds **47 – 49**. Key: a. Pd(PPh$_3$)$_4$, CuI, NEt$_3$, toluene.
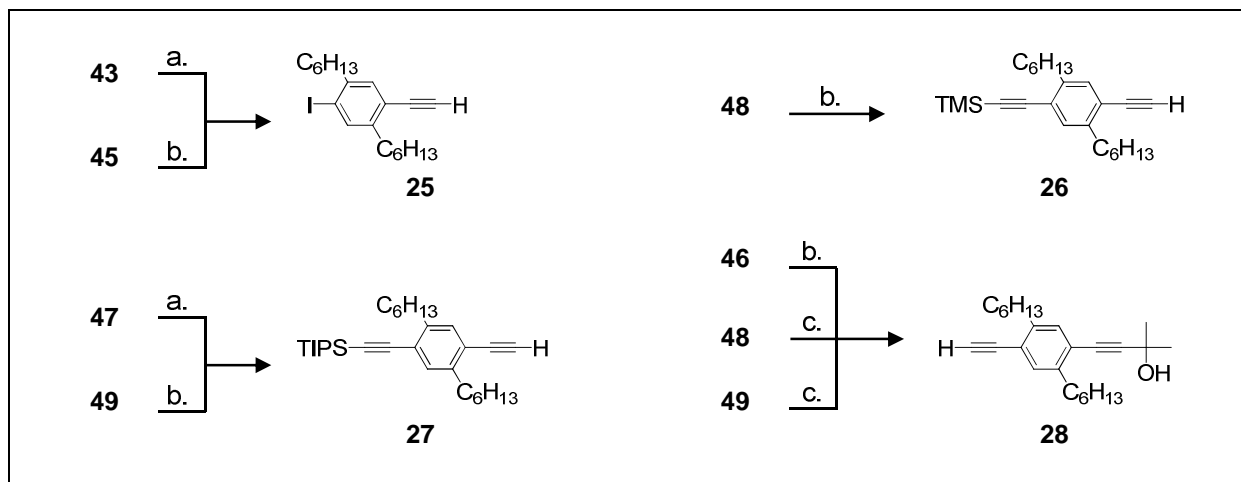
Scheme 1. 10: Synthesis of 1° building blocks **25 – 28** by selective deprotection of masked acetylenes in compounds **43, 45, 47 – 49**. Key: a. NaOH or KOH, CH$_2$Cl$_2$, and CH$_3$OH or C$_2$H$_5$OH; b. NaH, toluene, reflux; c. N(Bu)$_4$F, THF, CH$_2$Cl$_2$.

Figure 1. 13: Conditions for de rotecting TMS, TIPS, and C(CH$_3$)$_2$OH masked acetylenes.
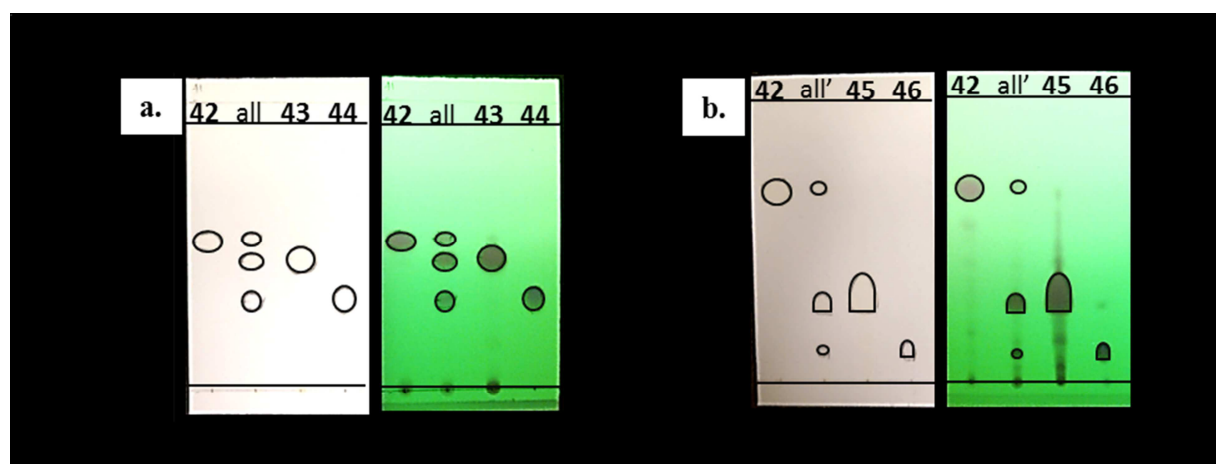
Figure 1. 14: Thin-layer chromatography TLC plate of compounds **42 – 46** under ambient light and fluorescing under UV lamp. Key: a. solvent hexanes, compounds **42**, all (**42 – 44**), **43**, and **44**; b. solvent 3:1 hexane/ethyl acetate v/v, compounds **42**, all' (**42, 45, 46**), **45**, and **46**.

The ^{1}H NMR of compound **47** contains two sizable singlets one at 1.14 ppm and the other near 0.00 ppm, which correspond to protons in the TMS and TIPS groups, respectively. These functional groups are also evidenced in the ^{13}C NMR spectra of **47**, which features a peak at 0.0 ppm appointed to the TMS as well as peaks at 18.7 and 11.4 ppm, that are respectively assigned to the methyl and methine carbons of the TIPS group. The carbons in TIPS protected ethynyl group resonate at 105.7 and 95.2 ppm, while the acetylenic carbons adjacent to the TMS group resonate at 104.0 and 98.7 ppm. Because the electronic environments created by the triisopropylsilylethynyl and trimethylsilylethynyl groups are similar, the two phenyl protons resonate at nearly the same frequencies (i.e. 7.25 and 7.24 ppm); the corresponding peaks are two overlapping singlets (apparent doublets – appd). Likewise, there is significant overlap of peaks corresponding to the two pairs of benzyl protons, which resonate between 2.74 – 2.66 ppm. Similarly, peaks for the two pairs of benzyl protons in **27** also overlap in the ^{1}HNMR spectra. However, the chemical shift difference between the two phenyl protons is sufficient so that the peaks appear as two separate singlets at 7.28 and 7.27 ppm. The existence of the singlet near 3.28 ppm, assigned to the acetylenic proton, as well as the absence of the singlet near 0.00 ppm in the ^{1}H NMR and ^{13}C NMR spectras of compound **27** are evidence of the successful deprotection of the TMS-masked acetylene in compound **47**. Because the ^{13}C NMR experiment was recorded with ^{1}H and ^{13}C coupling, the doublet at 81.3 ppm and the singlet at 82.5 could be asigned to the protonated carbon and the carbon attached to the phenyl group, respectively, in the terminal alkyne.

The characteristic features observed in the ^{1}H NMR spectra of compound **45** include the singlet peaks found at 1.81 and 1.62 ppm in the ^{1}H NMR of **45**, which are assigned to the hydroxyl and methyl protons in the $C(CH_3)_2OH$ protecting group, respectively. The chemical shift of the methyl protons in the propargyl alcohol coincide with the range of peaks assigned to methylene protons adjacent to the benzyl group in compounds. Consequently, both the methyl and methylene protons peaks are reported to be a complicated multiplet (ie. comp). In the ^{13}C NMR the methyl carbons in the $C(CH_3)_2OH$ protecting group resonate near 31.5 ppm and the quaternary carbon at 65.7 ppm. The acetylenic carbons in compound **45** resonate near 97.8 and 80.4 ppm.

The ^{1}H NMR spectra of compound **45** shows the two phenyl protons resonate at very distinct frequencies, 7.62 and 7.19 ppm, as a result of the distinct electronic environments

31

imposed on by the iodo and ethynylene substituents. This large difference between the chemical shifts of the phenyl protons is not observed in the ^{1}H NMR spectra of compounds **48** and **49**, because these compounds contain two ethynyl substituents. Unremarkably, the ^{1}H and ^{13}C NMR spectra of these two compounds are similar, save for the features associated with their different trialkylsilyl groups.

The ^{1}H and ^{13}C NMR spectra of compounds **26** and **27**, produced by the selective deprotection of the $C(CH_3)_2OH$-masked acetylene in **48** and **49**, respectively, are unsurprisingly similar. The product of desilylation of **48** and **49** (i.e compound **28**) features the acetylenic proton near 3.27 ppm, while the peaks associated with trialkylsilyl groups are missing as expected. As with compound **26** the ^{13}C NMR spectra of compound **28** was recorded with ^{1}H-^{13}C coupling in order to assign the peaks near 81 ppm, which could be attributed sp carbons in the terminal acetylene or 2-methyl-3-butyn-2-ol-4-yl groups. The doublet at 81.3 ppm was thus assigned to $\equiv$C–H carbon and the singlet at 80.8 ppm assigned to one of the sp carbons in the $C\equiv C$–$C(CH_3)_2OH$ group.

In addition to ^{1}H and ^{13}C NMR spectroscopy, vibrational spectroscopy is also useful in characterizing which ethynyls are present in these compounds. The IR spectra were recorded with neat samples (i.e. ATR) and in KBr. Although the neat samples produce spectra with sharper bands, particularly for the C–H stretch vibrations, than those seen in the spectra obtained from the KBr pellet, the $C\equiv C$ stretch for the $C(CH_3)_2OH$–masked acetylenes were very weak in ATR . Fortunately, these bands were apparent, albeit weakly, in the IR spectra obtained from the KBr pellets and found between $2228 - 2221$ cm^{-1}. More indicative of these group is the broad OH stretch found between $3346 - 3249$ cm^{-1}. In compound **28** the OH stretch and $\equiv$C–H stretch band, which is found at 3312 cm^{-1}, merge in the IR spectra in both media (i.e. neat and KBr). In all of the fundamental building blocks (i.e. compounds **25 – 28**, the $\equiv$C–H appears near 3312 with a shoulder near 3297 cm^{-1}. The $C\equiv C$ stretching frequencies for TMS and TIPS masked acetylenes appear around 2151 and 2147 cm^{-1}, respectively.

1.5. Conclusions

Sizable, shape-persistent molecular cages, like the two prisms we present here, are highly valuable synthetic targets. Recognizably, the step-wise synthesis of cages **1** and **2** is an ambitious undertaking. However, this synthetic methodology was elected to ensure the features necessary for these cages to be used as components in SETs.

Although we have not yet synthesized cages **1** and **2**, we have been able to produce most of their components and building blocks. Some of these species possess interesting properties with applications in other fields or are useful starting materials for other structures. For example, the electrochemistry and select photophysical properties of the [ReR(CO)$_3$(phen')] joint component was explored through a series [ReBr(CO)$_3$(phen')] complexes; and the results discussed in Chapter 2. The study of these properties in complexes similar to the joint component in our cages, allows us to predict the electrochemical behavior and photophysical character of cages **1** and **2**. In Chapter 3, both the synthesis and Sonogashira cross-coupling of the [Re(C≡CR)(CO)$_3$(phen')] corner component are addressed. These reactions are relevant to the synthesis and coupling of the half-prisms building blocks (i.e. **36** – **41**), which occurs during the second and third stage of the step-wise synthesis of these cages. See Scheme 1.5. The final chapter, Chapter 4, addresses the synthesis of triangular face (**32**) and diamond faces (**35**) of cages **1** and **2**, respectively.

1.6. Experimental

1.6.1. General Remarks

Commercially available reagents and solvents were obtained from reputable chemical distributers. When necessary, toluene, triethylamine, and dichloromethane were dried using established procedures under an inert atmosphere of nitrogen. All compounds were synthesized under a nitrogen environment using standard Schlenk techniques and purified via chromatography using Silica gel (45–60 μm). The ^{1}H NMR spectra were recorded at 400 MHz using Varian Gemini 2300 spectrometer, and the ^{13}C NMR spectra were recorded at 400 MHz using Varian Inova 400 spectrometer. The specific magnetic field frequency is indicated below in the individual descriptions of the results. The chemical shifts were calibrated relative to accepted resonance frequency of the NMR solvent, CDCl$_3$. FTIR spectra were recorded using Nicolet iS10 without suspending medium or with a KBr pellet. Samples for mass spectrometry

were submitted to the Stony Brook University Mass Spectrometry Facility where electron ionization mass spectra (EI-MS) were obtained on a Thermo DSQII and analyzed by Xcalibur software.

1.7.2. Conditions for deprotecting masked acetylenes

Deprotecting acetylenes masked by $C(CH_3)_2OH$ protecting group: To a Schlenk flask charged with a solution containing the compound with a $C(CH_3)_2OH$-masked acetylene dissolved in dried toluene was added NaH (60% in mineral oil) The flask was evacuated and back filled with nitrogen gas three times before being fitted with a condenser attached to a bubbler and submerged in an oil bath heated to 140 °C. The contents were stirred until the reaction was complete, as signaled by the gas no longer effervescing into the bubbler; this usually takes about one hour. When the reaction was complete, the hot solution was filtered through a short layer of silica over a fritted disk to remove the unreacted base. The silica was rinsed with hexanes while periodically scratching the top layer of silica with spatula to avoid blockage by a fine precipitate. The filtrate was collected and the solvent removed from the reaction by rotovaporation and then dried under vacuum before the residue was purified via column chromatography.[153,154]

Deprotecting acetylenes masked by TMS protecting group: To a solution containing the compound with a TMS-masked acetylene dissolved in dichloromethane was added a large excess of KOH or NaOH (alternatively CO_3^{2-} salt may be used) in CH_3OH or C_2H_5OH. The reaction was monitored by TLC and the contents were stirred until the reaction is complete; usually this takes between two to three hours. Next, the solution was washed with distilled water in a separatory funnel and the organic layer collected. If the aqueous and organic phases did not separate, a HCl solution (enough to neutralize the amount of KOH used in the reaction) was mixed with contents in the separatory funnel before reattempting separation. Additional product was recovered from the aqueous solution by two more extraction with dichloromethane. All three organic extractions were combined and then dried over anhydrous $MgSO_4$, which was filtered from the solution before the solvent was removed from the solution via rotovaporation. The residue was dried under vacuum before the product purified using column chromoatography.[100]

Deprotecting acetylenes masked by TMS or TIPS protecting group: To a solution containing the compound with a TMS- or TIPS-masked acetylene dissolved in a mixture of THF and

dichloromethane was added wet NBu$_4$F. It is important to note NBu$_4$F is fairly hydroscopic, absorbing moisture from the air, and was clearly wet before being weighed for the reaction. Therefore, the actual mass of NBu$_4$F used was less than was recorded. The reaction was monitored by TLC and the contents were stirred until the reaction complete; usually this takes between half-hour to one hour. Next the solution was diluted with dichloromethane before it was neutralized by a saturated solution of NaHCO$_3$ (aq) in a separatory funnel. After neutralization the organic layer was collected along with two additional fractions. All three organic extractions were combined and then dried over anhydrous MgSO$_4$. After filtering the solution through a fritted disk to remove the MgSO$_4$, solvent was removed from the filtered solution via rotovaporation. The residue was dried under vacuum before the product was purified using column chromoatography.[99,155]

1.7.3. Synthesis of Primary Building Blocks.
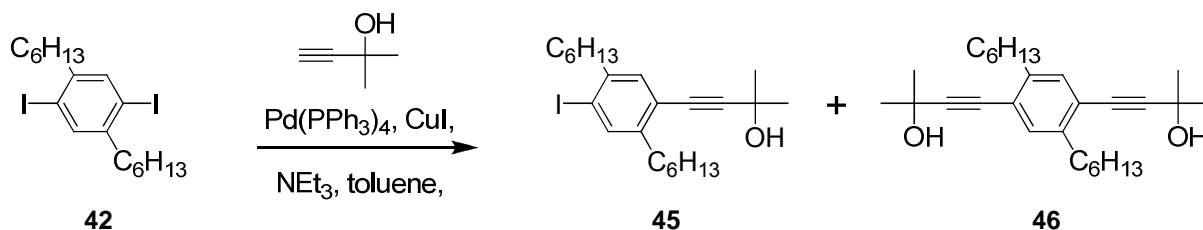
4-(4-iodo-2,5-dihexylphenyl)-2-methyl-3-butyn-2-ol (45).[156,157] To a solution containing 22.080 g (44.3 mmol) of **42** and 1 g (0.9 mmol) of PdP(Ph$_3$)$_4$ dissolved in 100 mL of toluene and 50 mL of NEt$_3$ under a N$_2$ atmosphere was added in succession 4.8 mL (4.17 g, 49.5 mmol) of 2-methyl-3-butyn-2-ol followed by 0.5 g (3 mmol) CuI. The contents were allowed to stir for 20 hours at room temperature before the reaction solution was filtered through a fritted disk under negative pressure. The filtrate was collected and the solvent was removed via rotoevaporation and then dried under vacuum resulting in a heterogeneous mixture of a yellow viscous oil and a white solid. To this crude product mixture was added a warm mixture of 10:1 hexanes/ethyl acetate v/v, which dissolved the oil. The suspension was added onto a silca column and the products purified via chromatography. The first eluted fraction contained 2.897 g (5.81 mmol, 13% recovered) of **42**. The second eluted fraction contained **45** and the third a mixture of **45** and **46**. Products **45** and **46** from the third fraction were separated by additional column

chromatography using 2:1 hexanes/dichloromethane v/v and pure dichloromenthane as the eluent, respectively. This nets a total of 10.326 g (22.70mmol, 59%) of **45** and 5.753 g (14.0 mmol, 36%) of **46**.

43: ^{1}H NMR (300 MHz, CDCl$_3$) δ 7.62 (s, 1H), 7.19 (s, 1H), 2.65 – 2.58 (m, 4H), 1.81 (bs, 1H), 1.70 – 1.49 (comp, 10H), 1.44 – 1.20 (m, 12H), 0.98 – 0.82 (m, 6H); ^{13}C NMR (400 MHz, CDCl$_3$) δ 144.0, 142.7, 139.4, 132.3, 122.1, 100.8, 97.8, 80.4, 65.7, 40.2. 33.8, 31.7, 31.6, 31.5, 30.5, 30.2, 29.2, 29.0, 22.6, 14.1; IR (KBr) 3346, 2957, 2925, 2857, 2221, 2150; IR (neat) 3334, 2954, 2924, 2856 cm^{-1}; MS (EI) m/z, Calcd for C$_{23}$H$_{35}$IO 454.17 [M$^+$], found 454.1 [M$^+$]. R$_f$ = 0.32 (3:1, v/v , hexanes/ethyl acetate).

44: ^{1}H NMR (400 MHz, CDCl$_3$) δ 7.20 (s, 2H), 2.65 (t, J^3 = 7.8 Hz, 4H), 2.01 (s, 2H), 1.63 – 1.55 (comp, 16H), 1.38 – 1.28 (m, 12H), 0.90 – 0.87 (m, 6H); ^{13}C NMR (400 MHz, CDCl$_3$) δ 142.1, 132.3, 121.9, 98.1, 80.9, 65.7, 34.0, 31.8, 31.5, 30.5, 29.2, 22.6, 14.1; IR(KBr) 3270, 2980, 2956, 2927, 2858, 2222 cm^{-1}; IR (neat) 3249, 2980, 2955, 2926, 2857, 2223* cm^{-1}; R$_f$ = 0.14 (3:1, v/v , hexanes/ethyl acetate).
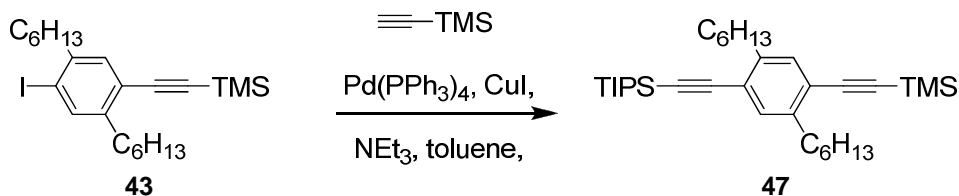
1,4-dihexyl-2-triisopropylsilylethynyl-5-trimethylsilylethynylbenzene (47). To a solution containing 1.799 g (3.84 mmol) of **43**[158] and 0.080 g (0.07 mmol) of Pd(PPh$_3$)$_4$ in 55 mL of NEt$_3$ and 20 mL of toluene was added 1.1 mL of triisopropyl acetylene (0.9 g, 5 mmol) and 0.040 g (2.1 mmol) of CuI along with an additional 20 mL of toluene. The reaction mixture was stirred for 14 hours before the solvent was removed via rotoevaporation. The oily residue was purified via column chromatography using hexanes as the eluent to afford 1.851 g (3.5 mmol, 92 %) of **47**. ^{1}H NMR (300 MHz, CDCl$_3$) δ 7.25 (appd, 2H), 2.74 – 2.66 (m, 4H), 1.65 – 1.55 (m, 4H), 1.41 – 1.24 (m, 12H), 1.14 (s, 21H), 0.95 – 0.84 (m, 6H), 0.25 (s, 9H); ^{13}C NMR (400 MHz, CDCl$_3$) δ 142.7, 142.5, 132.8, 132.4, 123.0, 122.4, 105.7, 104.0, 98.7, 95.2, 34.4, 34.2, 31.8, 31.7, 30.9, 30.7, 29.4, 22.7, 22.6, 18.7, 14.1, 11.4, 0.0; IR (KBr) 2958, 2942, 2927, 2865, 2152,

2063 cm^{-1}; IR (neat) 2956, 2941, 2926, 2864, 2151, 2063, 2032 cm^{-1}; MS (EI) *m/z*, Calcd for C$_{34}$H$_{58}$Si$_2$ 5 522.41 [M$^+$], found 522.4 [M$^+$]; R$_f$ = 0.53 (hexanes)..
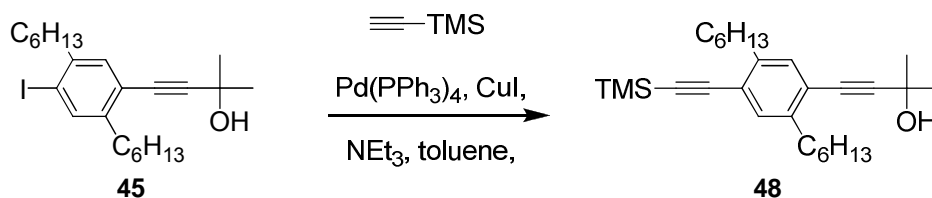
4-(4-trimethylsilylethynyl-2,5-dihexylphenyl)-2-methyl-3-butyn-2-ol (48).[156]   To a solution containing 1.845 g (4.06 mmol) of 4-(4-iodo-2,5-dihexylphenyl)-2-methyl-3-butyn-2-ol **45** and 0.428 g (0.370) of Pd(PPh$_3$)$_4$ dissolved in 25 mL of toluene and 25 mL of NEt$_3$ under nitrogen was added 0.80 mL (0.556 g, 5.66 mmol) of trimethylsilylacetylene and 0.200 g (1.04 mmol) of CuI. The reaction was stirred for 48 hours before filtering the solution through a fritted disk with negative pressure. Solvent was removed from the brown filtrate via rotovaporation and dried under vacuum. The product was purified by column chromatography on silica gel using toluene and toluene/ethyl acetate (20:1, v/v), to afford 1.489 g (3.50 mmol, 86%) of the product as a amber-colored oil. ^{1}H NMR (300 MHz, CDCl$_3$) δ 7.24 (s, 1H), 7.20 (s, 1H), 2.66 (appq, *J*^{3} = 8.1 Hz, 4H), 2.02 (bs, 1H), 1.65 – 1.54 (comp, 10H), 1.36 – 1.26 (m, 12H), 0.91 – 0.84 (m, 6H), 0.25 (s, 1H); ^{13}C NMR (400 MHz, CDCl$_3$) δ 142.7, 142.1, 132.4, 132.2, 122.4, 122.1, 103.9, 98.7, 98.2, 81.0, 65.7, 34.1, 34.0, 31.8, 31.7, 31.5, 30.6, 29.2, 22.6, 14.1, -0.0; IR (KBr); 3289, 2960, 2927, 2857, 2228, 2151 cm^{-1}; IR (neat) 3283, 2958, 2924, 2856, 2228, 2151 cm^{-1}; MS (EI) *m/z*, Calcd for C$_{28}$H$_{44}$OSi 424.32 [M$^+$], found 424.4 [M$^+$]; R$_f$ = 0.35 (3:1, v/v , hexanes/ethyl acetate)..
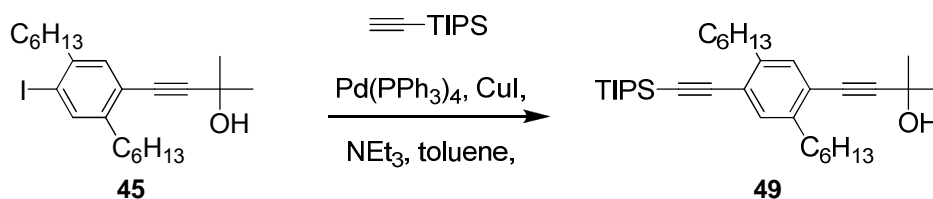
4-(4-triisopropylsilylethynyl-2,5-dihexylphenyl)-2-methyl-3-butyn-2-ol (49).[156]

Compound **49** was prepared in the same way as compound **48** using 2.071 g (4.56 mmol) of 4-(4-iodo-2,5-dihexylphenyl)-2-methyl-3-butyn-2-ol **45**, 1.4 mL (1.1 g, 6.3. mmol) of triisopropylacetylene, 0.5 g (0.4 mmol) of Pd(PPh$_3$)$_4$, 0.25 g (1 mmol) of CuI, in 25 mL of toluene and 25 mL of NEt$_3$. Following the previously described work up and purification procedures, compound **49** was obtained in 2.211 g (4.34 mmol, 95%). ^{1}H NMR (300 MHz, CDCl$_3$) δ 7.25 (s, 1H), 7.20 (s, 1H), 2.74 – 2.63 (m, 4H), 1.88 (bs, 1H), 1.66 – 1.55 (comp, 12H), 1.40 – 1.25 (m, 12H), 1.13 (s, 21H), 0.93 – 0.84 (m, 6H); ^{13}C NMR (400 MHz, CDCl$_3$) δ 142.5, 142.1, 132.8, 132.2, 122.8, 121.9, 105.6, 98.1, 95.0, 81.0, 65.7, 34.3, 34.1, 31.8, 31.8, 31.5, 30.8, 30.6, 29.3, 22.6, 18.7, 14.1, 11.4; IR (KBr) 3345, 2957, 2930, 2864, 2224, 2147 cm^{-1}; IR (neat) 3334, 2955, 2926, 2863, 2227, 2147 cm^{-1}; MS (EI) m/z, Calcd for C$_{34}$H$_{56}$OSi 508.41 [M$^+$], found 508.4 [M$^+$]; R$_f$ = 0.36 (3:1, v/v , hexanes/ethyl acetate)..

1-ethynyl-2,5-dihexyl-4-iodobenzene (25).
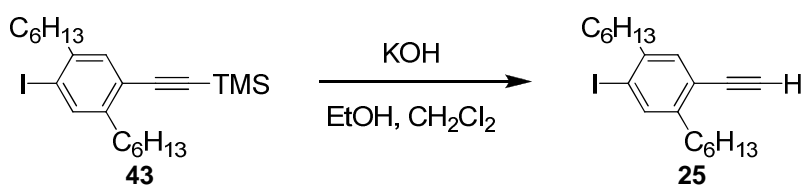
Compound **25** was prepared from **43** according to the procedure for the deprotection of TMS-masked acetylene using 5.713 g (12.2 mmol) of **43** in 300 mL of dichloromethane and 3.5 g (62 mmol) of KOH in 300 mL EtOH. After the contents were stirred for three hours the reaction was subjected to the normal work up procedure (i.e. washing to remove KOH, drying organic solution with MgSO$_4$, filtering the solution to remove MgSO$_4$, and removing solvent via rotavaporation and drying under vacuum) described above. Because the aqueous and organic

phases did not separate during the initial washing 80 mL of a 3M solution of HCl was added to separatory funnel neutralize the base. After the reaction contents were washed and the solvent removed, the product was purified via column chromatography on silica gel using hexanes as eluent, to afford 4.337 g (10.9 mmol, 89%) of **25** as a faint-pink-colored oil.
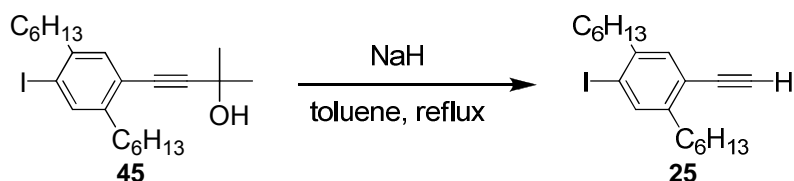
Compound **25** was prepared from **45** according to the procedure for the deprotection of $C(CH_3)_2OH$ -masked acetylene using 3.686 g (8.11 mmol) of **45**, 0.4 g (mmol) of NaH (60% in mineral oil), in 100 mL of dried toluene. The solution was stirred under refluxed for 1.5 hours before being subjected to the normal work up as described above. The crude product was purified via column chromatography on silica gel using hexanes as eluent, to afford 3.195 g (8.06 mmol, 99%) of **25**.

In both cases the product was confirmed by ^{1}H and ^{13}C NMR.[159].

^{1}H NMR (300 MHz, CDCl$_3$) 7.64 (s, 1H), 7.26 (s, 1H + solvent), 3.25 (s, 1H), 2.64 (appquint, 4H), 1.64 – 1.50 (m, 4H), 1.42 – 1.25 (comp, 12 H), 0.94 – 0.80 (m, 6H); ^{13}C NMR (400 MHz, CDCl$_3$) 144.6, 142.7, 139.4, 132.9, 132.9, 121.6, 101.5, 81.9, 81.1 (d), 40.1, 33.5, 31.6, 31.6, 30.5, 30.1, 29.1, 29.0, 22.6, 14.1.
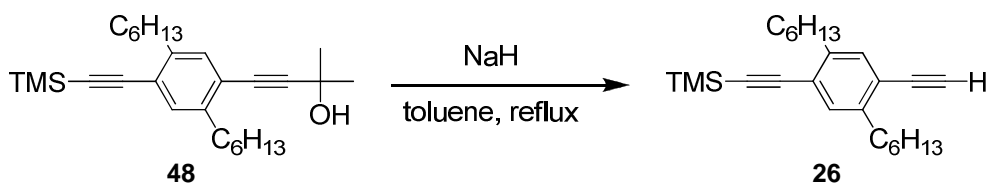
1-ethynyl-2,5-dihexyl-4-trimethylsilylethynylbenzene (26).[156]

Compound **26** was prepared from **48** according to the procedure for the deprotection of $C(CH_3)_2OH$ -masked acetylene using 1.112 g (2.62 mmol) of **48** and 0.125 g (3.1 mmol) of NaH (60 % in mineral oil) in 30 mL dried toluene. The solution was stirred under reflux for 1 hour before being subjected to the normal work up as described above. The crude product was

purified by column chromatography on silica gel using pure hexanes to afford 0.899 g (2.45 mmol, 94%) of **26**. ^{1}H NMR (300 MHz, CDCl$_3$) δ 7.28 (appd, 2H), 3.28 (s, 1H), 2.73 – 2.68 (m, 4H), 1.66 – 1.56 (m, 4H), 1.40 – 1.27 (m, 12H), 0.92 – 0.88 (m, 6H), 0.27 (s, 9H); ^{13}C NMR (400 MHz, CDCl$_3$) δ 142.7, 142.6, 133.0, 132.9, 132.5, 132.4, 122.9, 121.6, 103.8, 99.0, 82.4, 81.4, 81.4, 34.1, 33.8, 31.7, 31.7, 30.5, 30.5, 29.2, 29.1, 22.6, 22.6, 14.1, -0.0; IR (KBr) 3314, 3298, 2958, 2928, 2858, 2152, 2104 cm^{-1}; IR (neat) 3314, 3297, 2956, 2925, 2857, 2152, 2103 cm^{-1}; MS (EI) *m/z*, Calcd for C$_{25}$H$_{38}$Si 366.27 [M$^+$], found 366.2 [M$^+$]; R$_f$ = 0.52 (hexanes).

1-ethynyl-2,5-dihexyl-4-triisopropylsilylethynylbenzene (27).
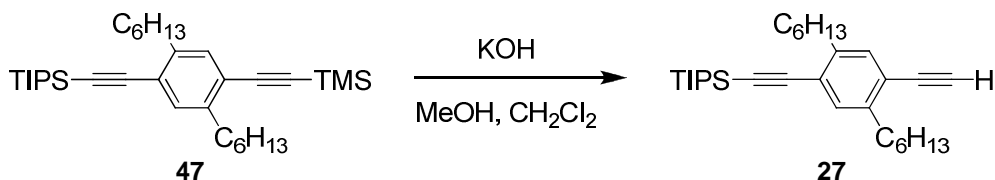
Compound **27** was prepared from **47** according to the procedure for the deprotection of TMS masked acetylene using 1.888 g (3.61 mmol) of **47** dissolved in 125 mL of CH$_2$Cl$_2$ and 54 g (962 mmol) KOH dissolved in 200 mL of MeOH. The solution was stirred for 4 hours before being subjected to the normal work up as described above. The crude product was purified via column chromatography on silica gel using hexanes as eluent, to afford to afford 1.515 g (3.36 mmol, 93% yield) of **27**.
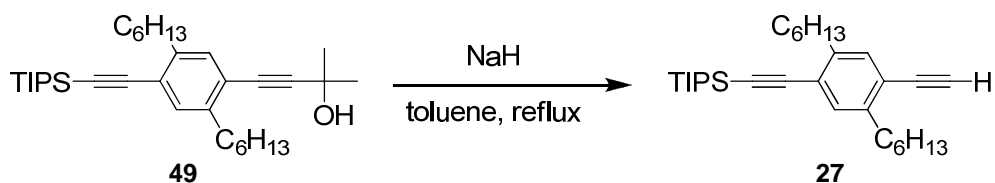
Compound **27** was prepared from **49** according to the procedure for the deprotection of C(CH$_3$)$_2$OH -masked acetylene using 1.267 g (2.49 mmol) of **49** and 0.175 g (4.38 mmol) of NaH (60 % in mineral oil) in 50 mL dried toluene. The solution was stirred under reflux for 1 hour before being subjected to the normal work up as described above. The crude product was

40

purified by column chromatography on silica gel using pure hexanes to afford 1.018 g (2.26 mmol, 91%) **27**.

In both cases the product was confirmed by ^{1}H and ^{13}C NMR data.[99]

^{1}H NMR (300 MHz, CDCl$_3$) δ 7.27 (appd, 2H), 3.28 (s, 1H), 2.75 – 2.68 (m, 4H), 1.66 – 1.56 (m, 4H), 1.39 – 1.26 (m, 12H), 1.14 (s, 21H), 0.94 – 0.86 (m, 6H); ^{13}C NMR (400 MHz, CDCl$_3$) δ 142.7, 142.5, 133.0 (d), 132.9 (d), 123.3, 121.4, 105.5, 95.3, 82.5, 81.3(d), 34.4, 33.9, 31.9. 31.7, 30.9, 30.6, 29.4, 29.2, 22.7, 22.6, 18.7, 14.1, 11.41 R$_f$ = 0.50 (hexanes)..

4-(4-ethynyl-2,5-dihexylphenyl)-2-methyl-3-butyn-2-ol (28).
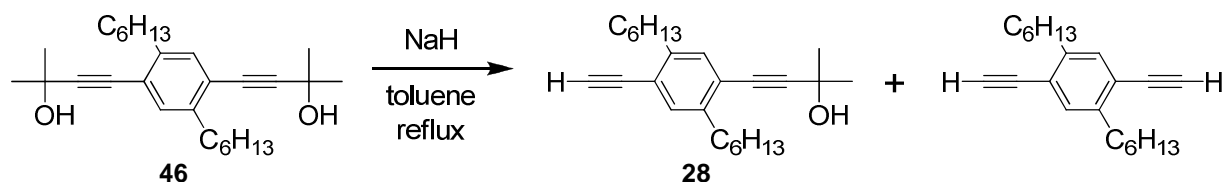
Compound **28** was prepared from **46** according to the procedure for the deprotection of C(CH$_3$)$_2$OH -masked acetylene using 2.810 g (mmol) and 0.235 g of NaH (60% in mineral oil) in 200 mL of dried toluene. The solution was stirred under reflux for 2 hours before being subjected to the normal work up as described above. The crude product, which contained 1,4-di(ethynyl)-2,5-di(*n*-hexyl)benzene, **28**, and recovered **46**, was dissolved in warm hexanes and then purified by column chromatography on silica gel. First 0.297 g (1.01 mmol, 19 %) of the 1,4-di(ethynyl)-2,5-di(*n*-hexyl)benzene byproduct elueted from the column with pure hexane as eluent. Next 0.846 g (2.40 mmol, 45 %) of compound **28** eluted from the column with hexanes/ethyl acetate (1:1, v/v) as the eluent. Finally 0.632 g (1.54 mmol) of reagent **46** was recovered from the column with hexanes/ethyl acetate (1:1, v/v) as eluent.
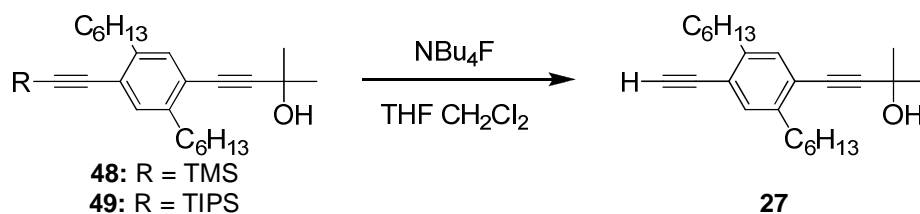
Compound **28** was prepared from **48** according to the procedure for the deprotection of TMS- or TIPS- masked acetylene using 0.647 g (1.52 mmol) of **48** and 1.253 g (4.79 mmol) of wet N(Bu)$_4$F. dissolved in 50 mL of a CH$_2$Cl$_2$/THF (1:1, v/v) solvent mixture. The solution was stirred for 30 minutes before being subjected to the normal work up as described above. The crude product was purified by column chromatography on silica gel using ethyl acetate/hexane (1:5, v/v) as eluent to afford 0.472 g (1.34 mmol, 88 % yield) of **28**.

Compound **28** was prepared from **49** according to the procedure for the deprotection of TMS- or TIPS- masked acetylene using 0.836 g (1.64 mmol) of **49** and 2.9 g (11 mmol) of wet N(Bu)$_4$F dissolved in 26 mL of a CH$_2$Cl$_2$/THF (1:1, v/v) solvent mixture. The solution was stirred for 45 minutes before being subjected to the normal work up as described above. The crude product was purified by column chromatography on silica using CH$_2$Cl$_2$/Hexanes (1:4 to 2:1, v/v) as eluent to afford 0.537 g (1.52 mmol, 93 % yield)

^{1}H NMR (300 MHz, CDCl$_3$) δ 7.27 (s, 1H), 7.22 (s, 1H), 3.27 (s, 1H), 2.72 – 2.63 (m, 4H), 2.03 (bs, 1H), 1.65 – 1.55 (comp, 10H), 1.39 – 1.27 (m, 12H), 0.90 – 0.86 (m, 6H); ^{13}C NMR (400 MHz, CDCl$_3$) δ 142.7, 142.1, 132.9 (d), 132.3 (d), 122.5, 121.4, 98.3, 82.4, 81.3 (d), 80.8, 65.7, 34.0, 33.8, 31.7, 31.6, 31.5, 30.5, 30.4, 29.2, 29.1, 22.6, 22.6, 14.0; IR (KBr) 3370, 3312, 3296, 2978, 2956, 2928, 2858, 2219, 2102 cm^{-1}; IR (neat) 3312, 3296, 3020, 2956, 2928, 2858, 2200, 2102 cm^{-1}; MS (EI) m/z, Calcd for C$_{25}$H$_{36}$O 352.28 [M$^+$], found 352.3 [M$^+$]; R$_f$ = 0.35 (3:1, v/v , hexanes/ethyl acetate)..

1.7. References

(1)   Deal, B.; Talbot, J.: Principia Moore. *Electrochem. Soc. Interface* **1997**, *6*, 18-23.
(2)   Moore, G. E.: Cramming More Components Onto Integrated Circuits. *Proceedings of the IEEE* **1998**, *86*, 82-85.

(3)   Dodd, P. E.; Shaneyfelt, M. R.; Schwank, J. R.; Felix, J. A.: Current and future challenges in radiation effects on CMOS electronics. *IEEE Trans. Nucl. Sci.* **2010**, *57*, 1747-1763.

(4)   Lundstrom, M.: Applied Physics: Moore's law forever? *Science (Washington, DC, U. S.)* **2003**, *299*, 210-211.

(5)   Marsh, G.: Moore's law at the extremes. *Mater. Today (Oxford, U. K.)* **2003**, *6*, 28-33.

(6)   Nuzzo, R. G.: The future of electronics manufacturing is revealed in the fine print. *Proc. Natl. Acad. Sci. U. S. A.* **2001**, *98*, 4827-4829.

(7)   Peercy, P. S.: The drive to miniaturization. *Nature (London)* **2000**, *406*, 1023-1026.

(8)   Weldon, M. K.; Queeney, K. T.; Eng, J., Jr.; Raghavachari, K.; Chabal, Y. J.: The surface science of semiconductor processing. Gate oxides in the ever-shrinking transistor. *Surf. Sci.* **2002**, *500*, 859-878.

(9)   Thomas, S. G.; Tomasini, P.; Bauer, M.; Vyne, B.; Zhang, Y.; Givens, M.; Devrajan, J.; Koester, S.; Lauer, I.: Enabling Moore's Law beyond CMOS technologies through heteroepitaxy. *Thin Solid Films* **2010**, *518*, S53-S56.

(10)   Thayne, I. G.; Hill, R. J. W.; Holland, M. C.; Li, X.; Zhou, H.; MacIntyre, D. S.; Thoms, S.; Kalna, K.; Stanley, C. R.; Asenov, A.; Droopad, R.; Passlack, M.: Review of current status of III-V MOSFETs. *ECS Trans.* **2009**, *19*, 275-286.

(11)   Liang, D.; Bowers, J. E.: Photonic integration: Si or InP substrates? *Electron. Lett.* **2009**, 10-13.

(12)   French, R. H.; Tran, H. V.: Immersion lithography: photomask and wafer-level materials. *Annu. Rev. Mater. Res.* **2009**, *39*, 93-126.

(13)   Emtsev, K. V.; Bostwick, A.; Horn, K.; Jobst, J.; Kellogg, G. L.; Ley, L.; McChesney, J. L.; Ohta, T.; Reshanov, S. A.; Roehrl, J.; Rotenberg, E.; Schmid, A. K.; Waldmann, D.; Weber, H. B.; Seyller, T.: Towards wafer-size graphene layers by atmospheric pressure graphitization of silicon carbide. *Nat. Mater.* **2009**, *8*, 203-207.

(14)   Wickenden, D. K.: Semiconductor devices: Moore marches on. *Johns Hopkins APL Tech. Dig.* **2008**, *28*, 30-39.

(15)   Toh, E.-H.; Wang, G. H.; Chan, L.; Sylvester, D.; Heng, C.-H.; Samudra, G. S.; Yeo, Y.-C.: Device design and scalability of a double-gate tunneling field-effect transistor with silicon-germanium source. *Jpn. J. Appl. Phys.* **2008**, *47*, 2593-2597.

(16)   Schlom, D. G.; Guha, S.; Datta, S.: Gate oxides beyond SiO_2. *MRS Bull.* **2008**, *33*, 1017-1025.

(17)   Kaminow, I. P.: Optical integrated circuits: a personal perspective. *J. Lightwave Technol.* **2008**, *26*, 994-1004.

(18)   Ferry, D. K.: Quo vadis nanoelectronics? *Phys. Status Solidi C* **2008**, *5*, 17-22.

(19)   Renugopalakrishnan, V.; Khizroev, S.; Anand, H.; Li, P.; Lindvold, L.: Future memory storage technology: protein-based memory devices may facilitate surpassing Moore's law. *IEEE Trans. Magn.* **2007**, *43*, 773-775.

(20)   Moers, J.: Turning the world vertical: MOSFETs with current flow perpendicular to the wafer surface. *Appl. Phys. A: Mater. Sci. Process.* **2007**, *87*, 531-537.

(21)   Datta, S.: III-V field-effect transistors for low power digital logic applications. *Microelectron. Eng.* **2007**, *84*, 2133-2137.

(22)   Jackson, T. N.: Organic Semiconductors: Beyond Moore's Law. *Nat. Mater.* **2005**, *4*, 581-582.

(23)   Graham, A. P.; Duesberg, G. S.; Seidel, R. V.; Liebau, M.; Unger, E.; Pamler, W.; Kreupl, F.; Hoenlein, W.: Carbon nanotubes for microelectronics? *Small* **2005**, *1*, 382-390.

(24)   Bez, R.: Innovative technologies for high density non-volatile semiconductor memories. *Microelectron. Eng.* **2005**, *80*, 249-255.

(25)   Kim, H.; McIntyre, P. C.; On, C. C.; Saraswat, K. C.; Stemmer, S.: Engineering chemically abrupt high-k metal oxide/silicon interfaces using an oxygen-gettering metal overlayer. *J. Appl. Phys.* **2004**, *96*, 3467-3472.

(26)   Flood, A. H.; Stoddardt, J. F.; Steuerman, D. W.; Heath, J. R.: Whence molecular electronics? *Science (Washington, DC, U. S.)* **2004**, *306*, 2055-2056.

(27)   Likharev, K.: Hybrid semiconductor - molecular nanoelectronics. *Ind. Phys.* **2003**, *9*, 20-23.

(28)   Huff, H. R.; Hou, A.; Lim, C.; Kim, Y.; Barnett, J.; Bersuker, G.; Brown, G. A.; Young, C. D.; Zeitzoff, P. M.; Gutt, J.; Lysaght, P.; Gardner, M. I.; Murto, R. W.: High-k gate stacks for planar, scaled CMOS integrated circuits. *Microelectron. Eng.* **2003**, *69*, 152-167.

(29)   Likharev, K. K.: Single-electron devices and their applications. *Proc. IEEE* **1999**, *87*, 606-632.

(30)   Maeda, K.; Okabayashi, N.; Kano, S.; Takeshita, S.; Tanaka, D.; Sakamoto, M.; Teranishi, T.; Majima, Y.: Logic operations of chemically assembled single-electron transistor. *ACS Nano* **2012**, *6*, 2798-2803.

(31)   Podd, G. J.; Angus, S. J.; Williams, D. A.; Ferguson, A. J.: Charge sensing in intrinsic silicon quantum dots. *Appl. Phys. Lett.* **2010**, *96*, 082104/1-082104/3.

(32)   Ono, Y.; Inokawa, H.; Takahashi, Y.; Nishiguchi, K.; Fujiwara, A.: Single-Electron Transistor and its Logic Application. In *Nanotechnology*; Wiley-VCH Verlag GmbH & Co. KGaA, 2010.

(33)   Silva, L. M.; Guimaraes, J. G.: Performance analysis of single-electron NAND gates. *ECS Trans.* **2009**, *23*, 311-318.

(34)   Beaumont, A.; Dubuc, C.; Beauvais, J.; Drouin, D.: Room temperature single-electron transistor featuring gate-enhanced ON-state current. *IEEE Electron Device Lett.* **2009**, *30*, 766-768.

(35)   Brenning, H. T. A.; Kubatkin, S. E.; Erts, D.; Kafanov, S. G.; Bauch, T.; Delsing, P.: A Single Electron Transistor on an Atomic Force Microscope Probe. *Nano Lett.* **2006**, *6*, 937-941.

(36)   Jan, Y.-R.; Hu, M., Jr.; Chiou, S.-C.; Yang, S.-C.: Manufacturing method for sub-micrometer t-shaped double time gate etchings. National Central University, Taiwan . 2005; pp 12 pp.

(37)   Glasson, P.; Papageorgiou, G.; Harrabi, K.; Rees, D. G.; Antonov, V.; Collin, E.; Fozooni, P.; Frayne, P. G.; Mukharsky, Y.; Lea, M. J.: Trapping single electrons on liquid helium. *J. Phys. Chem. Solids* **2005**, *66*, 1539-1543.

(38)   Uchida, K.; Koga, J.; Ohba, R.; Toriumi, A.: Programmable single-electron transistor logic for future low-power intelligent LSI: proposal and room-temperature operation. *IEEE Trans. Electron Devices* **2003**, *50*, 1623-1630.

(39)   Papageorgiou, G.; Mukharsky, Y.; Harrabi, K.; Glasson, P.; Fozooni, P.; Frayne, P. G.; Collin, E.; Lea, M. J.: Detecting electrons on helium with a single-electron transistor (SET). *Physica E (Amsterdam, Neth.)* **2003**, *18*, 179-181.

(40)   Kim, D. H.; Sung, S.-K.; Kim, K. R.; Lee, J. D.; Park, B.-G.; Choi, B. H.; Hwang, S. W.; Ahn, D.: Silicon single-electron transistors with sidewall depletion gates and their application to dynamic single-electron transistor logic. *IEEE Trans. Electron Devices* **2002**, *49*, 627-635.

(41)   Devoret, M. H.; Schoelkopf, R. J.: Amplifying quantum signals with the single-electron transistor. *Nature (London)* **2000**, *406*, 1039-1046.

(42)   Schoelkopf, R. J.; Wahlgren, P.; Kozhevnikov, A. A.; Delsing, P.; Prober, D. E.: The radio-frequency single-electron transistor (RF-SET): a fast and ultrasensitive electrometer. *Science (Washington, D. C.)* **1998**, *280*, 1238-1242.

(43)   Chen, R. H.; Korotkov, A. N.; Likharev, K. K.: Single-electron transistor logic. *Appl. Phys. Lett.* **1996**, *68*, 1954-6.

(44)   Korotkov, A. N.; Chen, R. H.; Likharev, K. K.: Possible performance of capacitively coupled single-electron transistors in digital circuits. *J. Appl. Phys.* **1995**, *78*, 2520-2530.

(45)   Averin, D. V.; Likharev, K. K.: Coulomb blockade of single-electron tunneling, and coherent oscillations in small tunnel junctions. *J Low Temp Phys* **1986**, *62*, 345-373.

(46)   Averin, D. V.; Likharev, K. K.: Single-electronics - recent developments. *Springer Ser. Electron. Photonics* **1992**, *31*, 3-12.

(47)   Fulton, T. A.; Dolan, G. J.: Observation of single-electron charging effects in small tunnel junctions. *Physical Review Letters* **1987**, *59*, 109-112.

(48)   Roche, B.; Voisin, B.; Jehl, X.; Wacquez, R.; Sanquer, M.; Vinet, M.; Deshpande, V.; Previtali, B.: A tunable, dual mode field-effect or single electron transistor. *arXiv.org, e-Print Arch., Condens. Matter* **2012**, 1-4, arXiv:1201.3760v1 [cond-mat.mes-hall].

(49)   Azuma, Y.; Suzuki, S.; Maeda, K.; Okabayashi, N.; Tanaka, D.; Sakamoto, M.; Teranishi, T.; Buitelaar, M. R.; Smith, C. G.; Majima, Y.: Nanoparticle single-electron transistor with metal-bridged top-gate and nanogap electrodes. *Appl. Phys. Lett.* **2011**, *99*, 073109/1-073109/3.

(50)   Yamaguchi, H.; Terui, T.; Noguchi, Y.; Ueda, R.; Nasu, K.; Otomo, A.; Matsuda, K.: A photoresponsive single electron transistor prepared from oligothiophene molecules and gold nanoparticles in a nanogap electrode. *Appl. Phys. Lett.* **2010**, *96*, 103117/1-103117/3.

(51)   Shin, S. J.; Jung, C. S.; Park, B. J.; Yoon, T. K.; Lee, J. J.; Kim, S. J.; Choi, J. B.; Takahashi, Y.; Hasko, D. G.: Si-based ultrasmall multiswitching single-electron transistor operating at room-temperature. *Appl. Phys. Lett.* **2010**, *97*, 103101/1-103101/3.

(52)   Moriya, R.; Kobayashi, H.; Shibata, K.; Masubuchi, S.; Hirakawa, K.; Ishida, S.; Arakawa, Y.; Machida, T.: Fabrication of single-electron transistor composed of a self-assembled quantum dot and nanogap electrode by atomic force microscope local oxidation. *Appl. Phys. Express* **2010**, *3*, 035001/1-035001/3.

(53)   Ihn, T.; Guttinger, J.; Molitor, F.; Schnez, S.; Schurtenberger, E.; Jacobsen, A.; Hellmuller, S.; Frey, T.; Drroer, S.; Stampfer, C.; Ensslin, K.: Graphene single-electron transistors. *Mater. Today (Oxford, U. K.)* **2010**, *13*, 44-50.

(54)   Gustafsson, D.; Bauch, T.; Nawaz, S.; Mumtaz, M.; Signorello, G.; Lombardi, F.: Low capacitance HTS junctions for single electron transistors. *Phys. C (Amsterdam, Neth.)* **2010**, *470*, S188-S190.

(55)   Paraoanu, G. S.; Halvari, A. M.: Suspended single-electron transistors: fabrication and measurement. *Appl. Phys. Lett.* **2005**, *86*, 093101/1-093101/3.

(56)	Saitoh, M.; Hiramoto, T.: Observation of current staircase due to large quantum level spacing in a silicon single-electron transistor with low parasitic series resistance. *J. Appl. Phys.* **2002**, *91*, 6725-6728.

(57)	Park, H.; Lim, A. K. L.; Alivisatos, A. P.; Park, J.; McEuen, P. L.: Fabrication of metallic electrodes with nanometer separation by electromigration. *Appl. Phys. Lett.* **1999**, *75*, 301-303.

(58)	Ji, L.; Dresselhaus, P. D.; Han, S.; Lin, K.; Zheng, W.; Lukens, J. E.: Fabrication and characterization of single-electron transistors and traps. *J. Vac. Sci. Technol., B* **1994**, *12*, 3619-22.

(59)	Fujisawa, T.; Hirayama, Y.; Tarucha, S.: AlGaAs/InGaAs/GaAs single electron transistors fabricated by Ga focused ion beam implantation. *Appl. Phys. Lett.* **1994**, *64*, 2250-2.

(60)	Betard, A.; Fischer, R. A.: Metal-Organic Framework Thin Films: From Fundamentals to Applications. *Chem. Rev. (Washington, DC, U. S.)* **2012**, *112*, 1055-1083.

(61)	Corma, A.; Garcia, H.; Llabres, i. X. F. X.: Engineering Metal Organic Frameworks for Heterogeneous Catalysis. *Chem. Rev. (Washington, DC, U. S.)* **2010**, *110*, 4606-4655.

(62)	Janiak, C.: Engineering coordination polymers towards applications. *Dalton Trans.* **2003**, 2781-2804.

(63)	Kohyama, Y.; Murase, T.; Fujita, M.: A self-assembled cage as a non-covalent protective group: regioselectivity control in the nucleophilic substitution of aryl-substituted allylic chlorides. *Chemical Communications* **2012**, *48*, 7811-7813.

(64)	Lee, J. Y.; Farha, O. K.; Roberts, J.; Scheidt, K. A.; Nguyen, S. B. T.; Hupp, J. T.: Metal-organic framework materials as catalysts. *Chem. Soc. Rev.* **2009**, *38*, 1450-1459.

(65)	Yoshizawa, M.; Klosterman, J. K.; Fujita, M.: Functional Molecular Flasks: New Properties and Reactions within Discrete, Self-Assembled Hosts. *Angew. Chem., Int. Ed.* **2009**, *48*, 3418-3438.

(66)	Takezawa, H.; Murase, T.; Fujita, M.: Temporary and Permanent Trapping of the Metastable Twisted Conformer of an Overcrowded Chromic Alkene via Encapsulation. *J. Am. Chem. Soc.* **2012**, *134*, 17420-17423.

(67)	Schneider, M. W.; Oppel, I. M.; Mastalerz, M.: Exo-Functionalized Shape-Persistent [2+3] Cage Compounds: Influence of Molecular Rigidity on Formation and Permanent Porosity. *Chem.--Eur. J.* **2012**, *18*, 4156-4160, S4156/1-S4156/20.

(68)	Zheng, S.-T.; Wu, T.; Irfanoglu, B.; Zuo, F.; Feng, P.; Bu, X.: Multicomponent Self-Assembly of a Nested Co24@Co48 Metal-Organic Polyhedral Framework. *Angew. Chem., Int. Ed.* **2011**, *50*, 8034-8037.

(69)	Sumida, K.; Hill, M. R.; Horike, S.; Dailly, A.; Long, J. R.: Synthesis and Hydrogen Storage Properties of Be12(OH)12(1,3,5-benzenetribenzoate)4. *J. Am. Chem. Soc.* **2009**, *131*, 15120-15121.

(70)	Hunt, J. R.; Doonan, C. J.; LeVangie, J. D.; Cote, A. P.; Yaghi, O. M.: Reticular Synthesis of Covalent Organic Borosilicate Frameworks. *J. Am. Chem. Soc.* **2008**, *130*, 11872-11873.

(71)	Dinca, M.; Long, J. R.: Hydrogen storage in microporous metal-organic frameworks with exposed metal sites. *Angew. Chem., Int. Ed.* **2008**, *47*, 6766-6779.

(72)	El-Kaderi, H. M.; Hunt, J. R.; Mendoza-Cortes, J. L.; Cote, A. P.; Taylor, R. E.; O'Keeffe, M.; Yaghi, O. M.: Designed Synthesis of 3D Covalent Organic Frameworks. *Science (Washington, DC, U. S.)* **2007**, *316*, 268-272.

(73)   Yoshizawa, M.; Nakagawa, J.; Kumazawa, K.; Nagao, M.; Kawano, M.; Ozeki, T.; Fujita, M.: Discrete stacking of large aromatic molecules within organic-pillared coordination cages. *Angew. Chem., Int. Ed.* **2005**, *44*, 1810-1813.

(74)   Sudik, A. C.; Millward, A. R.; Ockwig, N. W.; Cote, A. P.; Kim, J.; Yaghi, O. M.: Design, Synthesis, Structure, and Gas (N2, Ar, CO2, CH4, and H2) Sorption Properties of Porous Metal-Organic Tetrahedral and Heterocuboidal Polyhedra. *J. Am. Chem. Soc.* **2005**, *127*, 7110-7118.

(75)   Rosi, N. L.; Eckert, J.; Eddaoudi, M.; Vodak, D. T.; Kim, J.; O'Keeffe, M.; Yaghi, O. M.: Hydrogen Storage in Microporous Metal-Organic Frameworks. *Science (Washington, DC, U. S.)* **2003**, *300*, 1127-1130.

(76)   Li, H.; Eddaoudi, M.; O'Keeffe, M.; Yaghi, O. M.: Design and synthesis of an exceptionally stable and highly porous metal-organic framework. *Nature* **1999**, *402*, 276-279.

(77)   Fujita, M.; Oguro, D.; Miyazawa, M.; Oka, H.; Yamaguchi, K.; Ogura, K.: Self-assembly of ten molecules into a nanometer-sized organic host frameworks. *Nature (London)* **1995**, *378*, 469-71.

(78)   Kumazawa, K.; Biradha, K.; Kusukawa, T.; Okano, T.; Fujita, M.: Multicomponent assembly of a pyrazine-pillared coordination cage that selectively binds planar guests by intercalation. *Angew. Chem., Int. Ed.* **2003**, *42*, 3909-3913.

(79)   Wang, M.-X.: Nitrogen and Oxygen Bridged Calixaromatics: Synthesis, Structure, Functionalization, and Molecular Recognition. *Acc. Chem. Res.* **2012**, *45*, 182-195.

(80)   Kreno, L. E.; Leong, K.; Farha, O. K.; Allendorf, M.; Van, D. R. P.; Hupp, J. T.: Metal-Organic Framework Materials as Chemical Sensors. *Chem. Rev. (Washington, DC, U. S.)* **2012**, *112*, 1105-1125.

(81)   Wang, M.; Vajpayee, V.; Shanmugaraju, S.; Zheng, Y.-R.; Zhao, Z.; Kim, H.; Mukherjee, P. S.; Chi, K.-W.; Stang, P. J.: Coordination-Driven Self-Assembly of M3L2 Trigonal Cages from Preorganized Metalloligands Incorporating Octahedral Metal Centers and Fluorescent Detection of Nitroaromatics. *Inorg. Chem.* **2011**, *50*, 1506-1512.

(82)   Wanka, L.; Iqbal, K.; Schreiner, P. R.: The Lipophilic Bullet Hits the Targets: Medicinal Chemistry of Adamantane Derivatives. *Chem. Rev. (Washington, DC, U. S.)* **2013**, Ahead of Print.

(83)   Vajpayee, V.; Yang, Y. J.; Kang, S. C.; Kim, H.; Kim, I. S.; Wang, M.; Stang, P. J.; Chi, K.-W.: Hexanuclear self-assembled arene-ruthenium nano-prismatic cages: potential anticancer agents. *Chemical Communications* **2011**, *47*, 5184-5186.

(84)   Anilkumar, P.; Lu, F.; Cao, L.; Luo, P. G.; Liu, J. H.; Sahu, S.; Tackett, K. N., II; Wang, Y.; Sun, Y. P.: Fullerenes for applications in biology and medicine. *Curr. Med. Chem.* **2011**, *18*, 2045-2059.

(85)   Lamoureux, G.; Artavia, G.: Use of the adamantane structure in medicinal chemistry. *Curr. Med. Chem.* **2010**, *17*, 2967-2978.

(86)   Kim, B. Y. S.; Rutka, J. T.; Chan, W. C. W.: Nanomedicine. *N. Engl. J. Med.* **2010**, *363*, 2434-2443.

(87)   Chawla, P.; Chawla, V.; Maheshwari, R.; Saraf, S. A.; Saraf, S. K.: Fullerenes: from carbon to nanomedicine. *Mini-Rev. Med. Chem.* **2010**, *10*, 662-677.

(88)   Mahkam, M.: New terpolymers as hydrogels for oral protein delivery application. *J. Drug Targeting* **2009**, *17*, 29-35.

(89)   Fang, Y.; Murase, T.; Sato, S.; Fujita, M.: Noncovalent Tailoring of the Binding Pocket of Self-Assembled Cages by Remote Bulky Ancillary Groups. *Journal of the American Chemical Society* **2013**, *135*, 613-615.

(90)   Furutani, Y.; Kandori, H.; Kawano, M.; Nakabayashi, K.; Yoshizawa, M.; Fujita, M.: In Situ Spectroscopic, Electrochemical, and Theoretical Studies of the Photoinduced Host-Guest Electron Transfer that Precedes Unusual Host-Mediated Alkane Photooxidation. *J. Am. Chem. Soc.* **2009**, *131*, 4764-4768.

(91)   Yoshizawa, M.; Miyagi, S.; Kawano, M.; Ishiguro, K.; Fujita, M.: Alkane Oxidation via Photochemical Excitation of a Self-Assembled Molecular Cage. *J. Am. Chem. Soc.* **2004**, *126*, 9172-9173.

(92)   Prelog, V.; Seiwerth, R.: New method for the preparation of adamantane. *Ber. Dtsch. Chem. Ges. B* **1941**, *74B*, 1769-72.

(93)   Prelog, V.; Seiwerth, R.: Synthesis of adamantane. *Ber. Dtsch. Chem. Ges. B* **1941**, *74B*, 1644-8.

(94)   Eaton, P. E.; Cole, T. W.: Cubane. *Journal of the American Chemical Society* **1964**, *86*, 3157-3158.

(95)   Maier, G.; Pfriem, S.; Schäfer, U.; Matusch, R.: Tetra-tert-butyltetrahedrane. *Angewandte Chemie International Edition in English* **1978**, *17*, 520-521.

(96)   Ternansky, R. J.; Balogh, D. W.; Paquette, L. A.: Dodecahedrane. *Journal of the American Chemical Society* **1982**, *104*, 4503-4504.

(97)   Paquette, L. A.; Ternansky, R. J.; Balogh, D. W.: A strategy for the synthesis of monosubstituted dodecahedrane and the isolation of an isododecahedrane. *Journal of the American Chemical Society* **1982**, *104*, 4502-4503.

(98)   Ashton, P. R.; Isaacs, N. S.; Kohnke, F. H.; D'Alcontres, G. S.; Stoddart, J. F.: Trinacrene – a Product of Structure-Directed Synthesis. *Angewandte Chemie International Edition in English* **1989**, *28*, 1261-1263.

(99)   Kukula, H.; Veit, S.; Godt, A.: Synthesis of monodisperse oligo(para-phenyleneethynylene)s using orthogonal protecting groups with different polarity for terminal acetylene units. *Eur. J. Org. Chem.* **1999**, 277-286.

(100)   Lavastre, O.; Ollivier, L.; Dixneuf, P.; Sibandhit, S.: Sequential catalytic synthesis of rod-like conjugated polyynes. *Tetrahedron* **1996**, *52*, 5495-504.

(101)   Schumm, J. S.; Pearson, D. L.; Tour, J. M.: Synthesis of linear conjugated oligomers with an iterative divergent/convergent method to the doubling of monomer purity: rapid access to a 128-Å length potentially conductive molecular wire. *Angew. Chem.* **1994**, *106*, 1445-8.

(102)   Grubbs, R. H.; Kratz, D.: Highly unsaturated oligomeric hydrocarbons: α-(phenylethynyl)-ω-phenylpoly [1,2-phenylene(2,1-ethynediyl)]. *Chem. Ber.* **1993**, *126*, 149-57.

(103)   Moore, J. S.: Shape-persistent molecular architectures of nanoscale dimension. *Acc. Chem. Res.* **1997**, *30*, 402-413.

(104)   Xu, Z.; Moore, J. S.: Design and synthesis of a convergent and directional molecular antenna. *Acta Polym.* **1994**, *45*, 83-7.

(105)   Moore, J. S.; Xu, Z.: Synthesis of rigid dendritic macromolecules: enlarging the repeat unit size as a function of generation, permitting growth to continue. *Macromolecules* **1991**, *24*, 5893-4.

(106)   Zhang, J.; Pesak, D. J.; Ludwick, J. L.; Moore, J. S.: Geometrically-Controlled and Site-Specifically-Functionalized Phenylacetylene Macrocycles. *Journal of the American Chemical Society* **1994**, *116*, 4227-4239.

(107)   Zhang, J.; Moore, J. S.: Nanoarchitectures. 6. Liquid Crystals Based on Shape-Persistent Macrocyclic Mesogens. *Journal of the American Chemical Society* **1994**, *116*, 2655-2656.

(108)   Zhang, J.; Moore, J. S.; Xu, Z.; Aguirre, R. A.: Nanoarchitectures. 1. Controlled synthesis of phenylacetylene sequences. *Journal of the American Chemical Society* **1992**, *114*, 2273-2274.

(109)   Moore, J. S.; Zhang, J.: Efficient Synthesis of Nanoscale Macrocyclic Hydrocarbons. *Angewandte Chemie International Edition in English* **1992**, *31*, 922-924.

(110)   Manini, P.; Amrein, W.; Gramlich, V.; Diederich, F.: Expanded cubane: Synthesis of a cage compound with a C56 core by acetylenic scaffolding and gas-phase transformations into fullerenes. *Angew. Chem., Int. Ed.* **2002**, *41*, 4339-4343.

(111)   Tobe, Y.; Nakagawa, N.; Naemura, K.; Wakabayashi, T.; Shida, T.; Achiba, Y.: [16.16.16](1,3,5)Cyclophanetetracosayne (C60H6): A Precursor to C60 Fullerene. *J. Am. Chem. Soc.* **1998**, *120*, 4544-4545.

(112)   Rubin, Y.; Parker, T. C.; Pastor, S. J.; Jalisatgi, S.; Boulle, C.; Wilkins, C. L.: Acetylenic cyclophanes as fullerene precursors: formation of C60H6 and C60 by laser desorption mass spectrometry of C60H6(CO)12. *Angew. Chem., Int. Ed.* **1998**, *37*, 1226-1229.

(113)   Wu, Z.; Moore, J. S.: A freely hinged macrotricycle with a molecular cavity. *Angew. Chem., Int. Ed. Engl.* **1996**, *35*, 297-9.

(114)   Wu, Z.; Lee, S.; Moore, J. S.: Synthesis of three-dimensional nanoscaffolding. *J. Am. Chem. Soc.* **1992**, *114*, 8730-2.

(115)   Whitesides, G. M.; Grzybowski, B.: Self-Assembly at All Scales. *Science* **2002**, *295*, 2418-2421.

(116)   Whitesides, G. M.; Boncheva, M.: Beyond molecules: Self-assembly of mesoscopic and macroscopic components. *Proceedings of the National Academy of Sciences* **2002**, *99*, 4769-4774.

(117)   Ibukuro, F.; Kusukawa, T.; Fujita, M.: A Thermally Switchable Molecular Lock. Guest-Templated Synthesis of a Kinetically Stable Nanosized Cage. *J. Am. Chem. Soc.* **1998**, *120*, 8561-8562.

(118)   Northrop, B. H.; Chercka, D.; Stang, P. J.: Carbon-rich supramolecular metallacycles and metallacages. *Tetrahedron* **2008**, *64*, 11495-11503.

(119)   Kumazawa, K.; Biradha, K.; Kusukawa, T.; Okano, T.; Fujita, M.: Multicomponent Assembly of a Pyrazine-Pillared Coordination Cage That Selectively Binds Planar Guests by Intercalation. *Angewandte Chemie International Edition* **2003**, *42*, 3909-3913.

(120)   Koeberl, M.; Cokoja, M.; Herrmann, W. A.; Kuehn, F. E.: From molecules to materials: Molecular paddle-wheel synthons of macromolecules, cage compounds and metal-organic frameworks. *Dalton Trans.* **2011**, *40*, 6834-6859.

(121)   Jung, H.; Moon, D.; Chun, H.: Non-framework coordination polymers with tunable bimodal porosities based on inter-connected metal-organic polyhedra. *Bull. Korean Chem. Soc.* **2011**, *32*, 2489-2492.

(122)   Alkordi, M. H.; Belof, J. L.; Rivera, E.; Wojtas, L.; Eddaoudi, M.: Insight into the construction of metal-organic polyhedra: metal-organic cubes as a case study. *Chem. Sci.* **2011**, *2*, 1695-1705.

(123)   Farha, O. K.; Hupp, J. T.: Rational Design, Synthesis, Purification, and Activation of Metal-Organic Framework Materials. *Acc. Chem. Res.* **2010**, *43*, 1166-1175.

(124)   Perry, J. J. I. V.; Perman, J. A.; Zaworotko, M. J.: Design and synthesis of metal-organic frameworks using metal-organic polyhedra as supermolecular building blocks. *Chem. Soc. Rev.* **2009**, *38*, 1400-1417.

(125)   Tranchemontagne, D. J.; Ni, Z.; O'Keeffe, M.; Yaghi, O. M.: Reticular chemistry of metal-organic polyhedra. *Angew. Chem., Int. Ed.* **2008**, *47*, 5136-5147.

(126)   Furukawa, H.; Kim, J.; Ockwig, N. W.; O'Keeffe, M.; Yaghi, O. M.: Control of Vertex Geometry, Structure Dimensionality, Functionality, and Pore Metrics in the Reticular Synthesis of Crystalline Metal-Organic Frameworks and Polyhedra. *J. Am. Chem. Soc.* **2008**, *130*, 11650-11661.

(127)   Brant, J. A.; Liu, Y.; Sava, D. F.; Beauchamp, D.; Eddaoudi, M.: Single-metal-ion-based molecular building blocks (MBBs) approach to the design and synthesis of metal-organic assemblies. *J. Mol. Struct.* **2006**, *796*, 160-164.

(128)   Rowsell, J. L. C.; Yaghi, O. M.: Metal-organic frameworks: a new class of porous materials. *Microporous Mesoporous Mater.* **2004**, *73*, 3-14.

(129)   Yaghi, O. M.; O'Keeffe, M.; Ockwig, N. W.; Chae, H. K.; Eddaoudi, M.; Kim, J.: Reticular synthesis and the design of new materials. *Nature* **2003**, *423*, 705-714.

(130)   Kim, J.; Chen, B.; Reineke, T. M.; Li, H.; Eddaoudi, M.; Moler, D. B.; O'Keeffe, M.; Yaghi, O. M.: Assembly of Metal-Organic Frameworks from Large Organic and Inorganic Secondary Building Units: New Examples and Simplifying Principles for Complex Structures. *J. Am. Chem. Soc.* **2001**, *123*, 8239-8247.

(131)   Eddaoudi, M.; Moler, D. B.; Li, H.; Chen, B.; Reineke, T. M.; O'Keeffe, M.; Yaghi, O. M.: Modular Chemistry: Secondary Building Units as a Basis for the Design of Highly Porous and Robust Metal–Organic Carboxylate Frameworks. *Accounts of Chemical Research* **2001**, *34*, 319-330.

(132)   Acharyya, K.; Mukherjee, S.; Mukherjee, P. S.: Molecular Marriage through Partner Preferences in Covalent Cage Formation and Cage-to-Cage Transformation. *J. Am. Chem. Soc.* **2013**, *135*, 554-557.

(133)   Schneider, M. W.; Oppel, I. M.; Ott, H.; Lechner, L. G.; Hauswald, H.-J. S.; Stoll, R.; Mastalerz, M.: Periphery-substituted [4+6] salicylbisimine cage compounds with exceptionally high surface areas: influence of the molecular structure on nitrogen sorption properties. *Chemistry* **2012**, *18*, 836-47.

(134)   Mastalerz, M.: Shape-Persistent Organic Cage Compounds by Dynamic Covalent Bond Formation. *Angew. Chem., Int. Ed.* **2010**, *49*, 5042-5053.

(135)   Uribe-Romo, F. J.; Hunt, J. R.; Furukawa, H.; Kloeck, C.; O'Keeffe, M.; Yaghi, O. M.: A Crystalline Imine-Linked 3-D Porous Covalent Organic Framework. *J. Am. Chem. Soc.* **2009**, *131*, 4570-4571.

(136)   Liu, Y.; Liu, X.; Warmuth, R.: Multicomponent dynamic covalent assembly of a rhombicuboctahedral nanocapsule. *Chem.--Eur. J.* **2007**, *13*, 8953-8959.

(137)   Shomura, R.; Higashibayashi, S.; Sakurai, H.; Matsushita, Y.; Sato, A.; Higuchi, M.: Chiral phenylazomethine cage. *Tetrahedron Lett.* **2012**, *53*, 783-785.

(138)   Belowich, M. E.; Stoddart, J. F.: Dynamic imine chemistry. *Chem. Soc. Rev.* **2012**, *41*, 2003-2024.

(139)   Corbett, P. T.; Leclaire, J.; Vial, L.; West, K. R.; Wietor, J.-L.; Sanders, J. K. M.; Otto, S.: Dynamic Combinatorial Chemistry. *Chem. Rev. (Washington, DC, U. S.)* **2006**, *106*, 3652-3711.

(140)   Lehn, J.-M.: Dynamic combinatorial chemistry and virtual combinatorial libraries. *Chem.--Eur. J.* **1999**, *5*, 2455-2463.

(141)   Scott, L. T.; Boorum, M. M.; McMahon, B. J.; Hagen, S.; Mack, J.; Blank, J.; Wegner, H.; de, M. A.: A rational chemical synthesis of C60. *Science (Washington, DC, U. S.)* **2002**, *295*, 1500-1503.

(142)   Zhang, C.; Chen, C.-F.: Synthesis and Structure of A Triptycene-Based Nanosized Molecular Cage. *J. Org. Chem.* **2007**, *72*, 9339-9341.

(143)   Chinchilla, R.; Najera, C.: Recent advances in Sonogashira reactions. *Chem. Soc. Rev.* **2011**, *40*, 5084-5121.

(144)   Nagy, A.; Novak, Z.; Kotschy, A.: Sequential and domino Sonogashira coupling: Efficient tools for the synthesis of diarylalkynes. *J. Organomet. Chem.* **2005**, *690*, 4453-4461.

(145)   Lam, S. C.-F.; Yam, V. W.-W.; Wong, K. M.-C.; Cheng, E. C.-C.; Zhu, N.: Synthesis and Characterization of Luminescent Rhenium(I)–Platinum(II) Polypyridine Bichromophoric Alkynyl-Bridged Molecular Rods. *Organometallics* **2005**, *24*, 4298-4305.

(146)   Chung, W.-K.; Wong, K. M.-C.; Lam, W. H.; Zhu, X.; Zhu, N.; Kwok, H.-S.; Yam, V. W.-W.: Syntheses, photophysical, electroluminescence and computational studies of rhenium(i) diimine triarylamine-containing alkynyl complexes. *New Journal of Chemistry* **2013**, *37*, 1753-1767.

(147)   Bhattacharya, D.; Chang, C.-H.; Cheng, Y.-H.; Lai, L.-L.; Lu, H.-Y.; Lin, C.-Y.; Lu, K.-L.: Multielectron Redox Chemistry of a Neutral, NIR-Active, Indigo-Pillared ReI-Based Triangular Metalloprism. *Chemistry – A European Journal* **2012**, *18*, 5275-5283.

(148)   Dinolfo, P. H.; Coropceanu, V.; Brédas, J.-L.; Hupp, J. T.: A New Class of Mixed-Valence Systems with Orbitally Degenerate Organic Redox Centers. Examples Based on Hexa-Rhenium Molecular Prisms. *Journal of the American Chemical Society* **2006**, *128*, 12592-12593.

(149)   Sun, S.-S.; Lees, A. J.: Self-Assembly Triangular and Square Rhenium(I) Tricarbonyl Complexes: A Comprehensive Study of Their Preparation, Electrochemistry, Photophysics, Photochemistry, and Host-Guest Properties. *J. Am. Chem. Soc.* **2000**, *122*, 8956-8967.

(150)   Grave, C.; Lentz, D.; Schäfer, A.; Samorì, P.; Rabe, J. P.; Franke, P.; Schlüter, A. D.: Shape-Persistant Macrocycles with Terpyridine Units: Synthesis, Characterization, and Structure in the Crystal. *Journal of the American Chemical Society* **2003**, *125*, 6907-6918.

(151)   St. Fleur, N.; Craig, H. J.; Mayr, A.: Synthesis of alkynyl(tricarbonyl)rhenium complexes containing a lightly coordinated diamine ligand. *Inorg. Chim. Acta* **2009**, *362*, 1571-1576.

(152)   Schmittel, M.; Ammon, H.: A short synthetic route to novel, highly soluble 3,8-dialkyl-4,7-dibromo-1,10-phenanthrolines. *Synlett* **1997**, 1096-1098.

(153)   Shinohara, K. i.; Aoki, T.; Kaneko, T.; Oikawa, E.: Syntheses and enantioselective recognition of chiral poly(phenyleneethynylene)s bearing bulky optically active menthyl groups. *Polymer* **2000**, *42*, 351-355.

(154)   Havens, S. J.; Hergenrother, P. M.: Synthesis of arylacetylenes by the sodium hydride catalyzed cleavage of 4-aryl-2-methyl-3-butyn-2-ols. *J. Org. Chem.* **1985**, *50*, 1763-5.

(155)   Nierengarten, J.-F.; Gu, T.; Hadziioannou, G.; Tsamouras, D.; Krasnikov, V.: A new iterative approach for the synthesis of oligo(phenyleneethynediyl) derivatives and its application for the preparation of fullerene-oligo(phenyleneethynediyl) conjugates as active photovoltaic materials. *Helv. Chim. Acta* **2004**, *87*, 2948-2966.

(156)   Rodriguez, J. G.; Tejedor, J. L.; La, P. T.; Diaz, C.: Synthesis of conjugated 2,7-bis(trimethylsilylethynyl)-(phenylethynyl)nfluoren-9-one and 9-(p-methoxyphenyl)-9-methyl derivatives: optical properties. *Tetrahedron* **2006**, *62*, 3355-3361.

(157)   Khatyr, A.; Ziessel, R.: Synthesis of Soluble Bis-terpyridine Ligands Bearing Ethynylene-Phenylene Spacers. *J. Org. Chem.* **2000**, *65*, 3126-3134.

(158)   Francke, V.; Mangel, T.; Muellen, K.: Synthesis of α,ω-Difunctionalized Oligo- and Poly(p-phenyleneethynylene)s. *Macromolecules* **1998**, *31*, 2447-2453.

(159)   Kovalev, A. I.; Takeuchi, K.; Asai, M.; Ueda, M.; Rusanov, A. L.: Selective cross-coupling of 1-ethynyl-4-iodobenzenes with activated arylacetylenes. *Russ. Chem. Bull.* **2004**, *53*, 1749-1754.

Chapter 2: Influence of Increasingly Conjugated Substituents at the 4 and 7 Positions of 1,10-Phenanthroline Ligands on the Properties of [ReBr(CO)$_3$(phen')] Complexes

2.1. Introduction

The *fac*-[ReL(CO)$_3$(phen')] species, which serves as the corner-joint component in our polyhedral frameworks, is an example of the highly desirable class of rhenium(I) α-diimine complexes. Such compounds are renowned for their stability, excited state chemistry, and tunable luminescence; three qualities that make them applicable to chemical sensing,[160-173] luminescent labeling,[174-179] photocatalysis,[180-188] photosensitization,[189-193] optoelectronic and structural material components,[194-199] as well as molecular machines.[200-202]

In collaboration with Etsuko Fujita and David Grills at BNL, we have studied a series of three *fac*-[ReBr(CO)$_3$(phen')] complexes, which could serve as potential photocatalysts for the reduction of CO$_2$. The phen' ligands in these species are 4,7-disubstituted-3,8-dihexyl-1,10-phenanthroline derivatives. The substituents at the 4 and 7 positions are conjugated moieties whose conjugation increases as the series progresses from compounds **50** to **52**. The three [ReBr(CO)$_3$(phen')] complexes are identified as follows: **50**, with phen' = **53** = 3,8-di-*n*-hexyl-4,7-bis(triisopropylsilylethynyl)-1,10-phenanthroline; **51**, with phen' = **54** = 3,8-di-*n*-hexyl-4,7-bis(phenylethynyl)-1,10-phenanthroline; and **52**, with phen' = **55** = 3,8-di-*n*-hexyl-4,7-bis(triisopropylsilyl-2',5'-di-*n*-hexylphenyl)ethynyl)-1,10-phenanthroline. See Figure 2.1. The influence of the extended conjugation in these complexes has been explored through the results of optical, vibrational, and electrochemical experiments.

2.1.1. *fac*-ReBr(CO)$_3$(phen') Excited State Chemistry

The rising levels of atmospheric CO$_2$ as well as the impending shortage of fossil fuel resources have created a demand for alternative energy solutions. One possibility is to utilize CO$_2$ as a carbon feedstock for the production of organic compounds.[203-208] Unfortunately, CO$_2$, the most oxidized state of carbon, is very stable as is evidenced by the standard reduction potential for the 1e$^-$ and 2e$^-$ reduction of CO$_2$. Proton-coupled 2e$^-$ CO$_2$ reduction reactions are energetically more favorable, and so are the preferred pathways for many CO$_2$ reduction. Despite this favorability, proton coupled reactions are also energetically uphill. See Figure 2.2.[209] In addition CO$_2$ is kinetically inert, owing to the geometric transformation that accompanies reduction of linear CO$_2$ to bent CO$_2^{\bullet-}$ and CO$_2^{2-}$. To overcome both the thermodynamic and kinetic barriers associated with the reduction of CO$_2$, this process requires an energy source and catalyst. Moreover, the energy supplied must be renewable if this process is to be considered a

viable solution to the aforementioned social issues. In light of these considerations, photocatalytic reduction of CO_2 seems a very agreeable option.
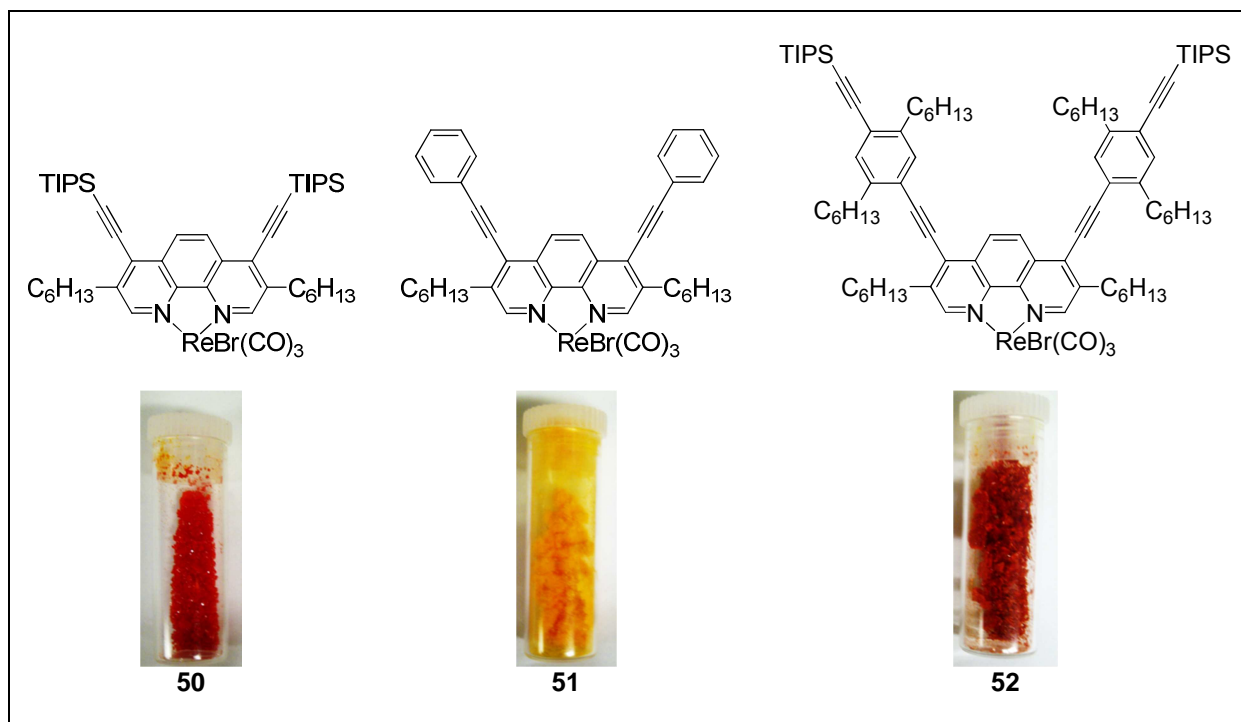
Figure 2. 1: Complexes **50** – **52**.
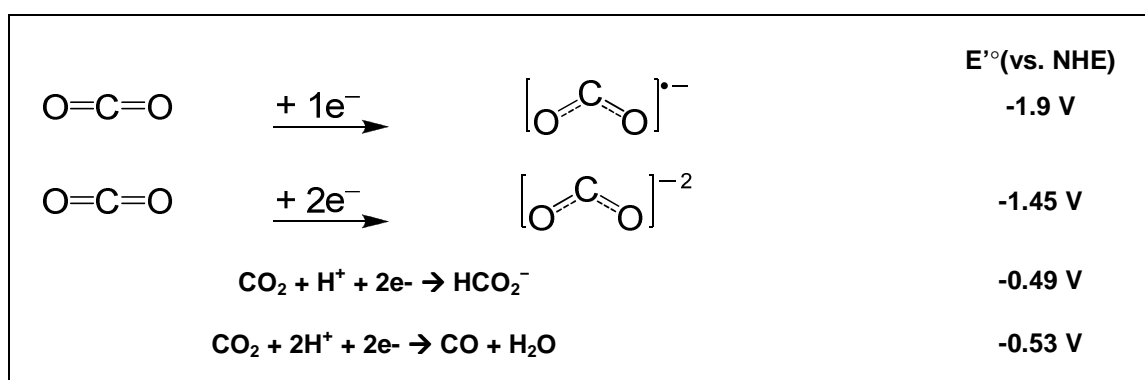
Figure 2. 2: Standard reduction potentials for one and two electron reduction of CO_2 at pH 7.

[$ReL(CO)_3(\alpha\text{-diimine})$]^n complexes, such as [$ReBr(CO)_3(phen)$] have been studied in the photocatalytic reduction of CO_2 since the mid-1980's, the dominant product of which is CO.[210]

Although carbon monoxide cannot be used directly as a fuel source, it can be used to produce methanol or hydrocarbons via the Fisher-Tropsch process:

n CO + (2n+1) H$_2$ → C$_n$H$_{2n+2}$ + n H$_2$O.[211-216] Therefore, reduction of CO_2 by [ReL(CO)$_3$(α-diimine)] photocatalysts could be a useful alternative energy resource.

As photocatalysts, [ReL(CO)$_3$(α-diimine)]^n complexes act as chromophores that effectively convert light into the electrochemical potential of a redox active charge separated excited state, [Re^{II}L(CO)$_3$(α-diimine$^{\bullet-}$)]^n, following absorption events.[210] Oxidative quenching of the excited state produces [Re^{II}L(CO)$_3$(α-diimine)]$^{n+1}$. Analogously, reductive quenching of the excited state generates the [Re^{I}L(CO)$_3$(α-diimine$^{\bullet-}$)]$^{n-1}$, which is an attractive reducing agent in photocatalytic CO_2 reduction.[180,182-188] Of course, the oxidized [Re^{II}L(CO)$_3$(α-diimine)]$^{n+1}$ and reduced [Re^{I}L(CO)$_3$(α-diimine$^{\bullet-}$)]$^{n-1}$ complexes can be generated electrochemically. However, the redox potentials of the ground state species are lower than the redox potentials of the corresponding excited states by the energy difference between the thermally relaxed ground and excited states (E$_{0-0}$).[209] Therefore, reduction of the excited state is much more favorable than the reduction of the ground state. In addition to their redox capabilities, the excited states of these complexes are also prone to triplet energy quenching, particularly by O$_2$.[163,167,172,210] These chemical reactions are what lend the [ReL(CO)$_3$(α-diimine)]^n complexes many of their aforementioned applications.

2.1.2. Photophysical Properties of the MLCT Excited State and Ground State Electrochemistry

The [ReL(CO)$_3$(α-diimine)]^n excited state involved in the CO_2 reduction process is the metal-to-ligand charge-transfer (MLCT) state. Incidentally, only complexes whose lowest energy MLCT excited states absorb in the visible region, as revealed through absorption spectroscopy and theoretical calculations, are considered for photocatalysis using visible light. Other excited states, including those corresponding to intraligand (IL) and ligand-to-ligand charge-transfer (LLCT) transitions, are also featured in the UV-Vis spectra of these complexes, but often at higher frequencies.[217-219] In some cases, the LLCT absorptions are coincident with the MLCT absorptions. Being generally non-emissive and short lived, the LLCT transition can have measurable impact on the emission lifetime.

The ^{1}MLCT state originates from the d$\pi \rightarrow \pi^*$ transition of an electron in a rhenium-localized dπ orbital to an unoccupied low-lying diimine-π^* orbital. Consequently, the rhenium center is oxidized and the diimine reduced, creating the charge-separated state, [Re^{II}L(CO)$_3$(α-diimine$^{\bullet-}$)]^n. The MLCT absorption band is generally found between 340 and 500 nm and is highly solvent dependent, demonstrating negative solvatochromism – decreasing with increasing solvent polarity.[209,210,220] Rapid and efficient intersystem crossing generates the ^{3}MLCT. Owing to the spin-forbidden nature of the ^{3}MLCT emission ($\Delta S \neq 0$), the ^{3}MLCT is sufficiently long-lived (emission lifetime, $\tau \sim 25$ ns – 2.5 μs) and therefore available to participate in subsequent bimolecular redox reactions.[209]

The excess charge in the one-electron oxidized or reduced species is localized on the rhenium center or diimine, respectively. The vibrational stretching frequencies of the carbonyl ligands, which engage in metal-to-ligand π-back-bonding, can be used to qualify the relative electron density on the rhenium in the excited state, oxidized, and reduced species. The excited and oxidized species, having lost electron density at the Re center, have weaker back-bonding interactions than the neutral ground state species. This is manifested in the vibrational spectra as an increase in the C$\equiv$O stretching frequencies. In regard to the reduced species, the frequencies of the C$\equiv$O stretching vibrations decrease by about 30 cm^{-1} relative to the neutral ground state complexes, due to stronger σ-donation by the (diimine$^{\bullet-}$) ligand.[209] Because the ν(C$\equiv$O) stretching vibrations are intensely IR active and the ground, excited, reduced, and oxidized species have distinct ν(C$\equiv$O) stretching frequencies, it is possible to monitor the formation and structural character of the latter three states by time-resolved infrared (TRIR) spectroscopy.[221-226]

The electrochemistry of the ground state, as revealed by cyclic voltammetry experiments in room temperature solutions, generally include two reduction potentials and an oxidation potential within the normal sweep range ($\sim$ –2 to +2 V). First reduction potentials are usually reversible and correspond to the formation of the one-electron reduced species [Re^{I}L(CO)$_3$(α-diimine$^{\bullet-}$)]$^{n-1}$. As is evident from the chemical formula, the added electron is localized on the diimine ligand. The fate of the second electron in the two-electron reduced species is dependent on the identity of the auxiliary ligand, L. For [Re^I(CN)(CO)$_3$(α-diimine)] complexes, the second reduction is also diimine based and reversible. Contrastingly, the second reduction in [Re^{I}X(CO)$_3$(α-diimine)] complexes, where X = Cl or Br, is irreversible and localized in rhenium orbitals. These differences may be owing to the relative energies of the unoccupied rhenium-

centered dσ* orbitals, which are expected to be higher in cyano than halo complexes because of the relative ligand field strength. [223,227-229] As a result, the dσ* orbitals in [Re^{I}X(CO)$_3$(α-diimine)] complexes may be more accessible to the additional electron added in the second reduction than in [Re^{I}CN(CO)$_3$(α-diimine)].

In the absence of quenchers, photo-excited [ReL(CO)$_3$(diimine)]^n complexes generally luminesce. Although emission is often dominated by depopulation of the MLCT, it is important to note emission can also originate simultaneously or predominately from the intraligand (IL) excited state formed from the diimine centered π–π* transition.[220,230-234] Strictly IL emission is distinct from MLCT emission as it is usually observed at higher wavelengths and features vibrational structure; whereas the MLCT is generally broad and featurless.[233,235] Contributions from the IL radiative decay to the MLCT assigned emission observed in these complexes are dependent on the relative energies of the MLCT and IL transitions. In cases where these transitions have similar energies (e.g. complexes with highly conjugated diimines or at cryogenic temperatures) both IL and MLCT emission will contribute to the observed broad-band emission.[220] The result of this combined emission is a longer emission lifetime. The emission profiles for the MLCT excited states are usually broad and centered between 520 – 650 nm. Unlike the MLCT absorption maxima, emission from this excited state is not generally solvent dependent.[209,220] Furthermore, emission maxima are consistent even when irradiated by different excitation energy.

The MLCT absorption and emission energies, emission lifetime, as well as the ground state electrochemistry of the [ReL(CO)$_3$(α-diimine)]^n complexes are tunable through modification of the diimine.[236-242] In general, modifications that stabilize the excited or added electron in the excited or reduced species, respectively, are expected to lower the energy of the MLCT and improve the favorability of the first or second reduction. These modifications include introduction of electron withdrawing group(s) or extending the area of conjugation in the diimine. According to the energy gap law, a larger λ_{MLCT} should increase the rate of non-radiative decay and ultimately lead to a shorter emission lifetime. [243] Although this law often holds, it fails for cases where the increase in λ_{MLCT} is the result of increased delocalization of the unpaired electron in the diimine. Tunability can also be achieved by modifying the auxiliary L ligand, which affects the electron density at the Re nucleus. However, the trend is not as

conspicuous as trends associated with diimine modification, since one must consider changes in the overall oxidation state of the complex, as well as differences in the HOMO character.[227]

2.1.3. Mechanism of CO_2 reduction.

Photocatalyzed CO_2 reduction is usually coupled to proton or hydroxide transfer because of the more favorable reduction potential.[209,244] See Figure 2.2. Details of the mechanism are not well understood since the mechanism is complex, highly dependent on the reaction environment, and involves many species some of which require further confirmation.[245-247] Despite this uncertainty, the involvement of a CO_2-bridge rheninum dimer species $[Re^0(CO)_3(\alpha\text{-}diimine)]_2(CO)_2$ as outlined in Scheme 2.1 seems to be of key importance to the mechanism. This dimer is believed to be generated from the reductively quenched species $[Re^IX(CO)_3(\alpha\text{-}diimine^{\bullet-})]^-$ during the photochemical reduction of CO_2 by $[ReX(CO)_3(\alpha\text{-}diimine)]$ catalysts in coordinating solvents and in the presence of a sacrificial electron donor, such as triethanolamine. Elimination of the halide followed by coordination of the solvent (S) produces the 19 e^- ligand localized radical species $[R^IeS(CO)_3(\alpha\text{-}diimine^{\bullet-})]$, which in the presence of CO_2 can generate the $[Re^0(CO)_3(\alpha\text{-}diimine)]_2(CO)_2$ dimer. Since this dimerization step involves a shift from a ligand localized radical intermediate to a rhenium centered radical, this process is unfavorable and often slow. However, once formed the insertion of a second CO_2 molecule into the $[Re^0(CO)_3(\alpha\text{-}diimine)]_2(CO)_2$ followed by rearrangement of the complex leads to the elimination of CO.[246,248] See Scheme 2.1. Much of the empirical evidence for the involvement of the CO_2-bridged dimer was performed and reported by Sullivan et. al. in 1985[249] and Hayashi et. al. in 2003.[248] In these reports, the CO_2 bridged dimer was, respectively, proposed and observed by ^1H, ^{13}C, FTIR, and GC characterization. Recent theoretical studies reported by E. Fujita and J. T. Muckerman in 2004[247] and the same authors in collaboration with J. Agarwal and H. F. Schaefer in 2012[246] supports this mechanism and provides insight into the kinetics of the dimerization step as well as structures of the involved intermediates and transition states.[246]

Owing to the key role played by the CO_2-bridged dimer in the photocatalytic reduction of CO_2, measures that promote the formation of said species should improve the efficiency of the photocatalytic system in the reduction of CO_2. Potentially, this can be accomplished by introducing a physical link connecting the two $[ReL(CO)_3(diimine)]$ complexes at the diimine, thereby reducing the entropic cost associated with dimerization while leaving the rhenium core

intact. Such a linkage must offer sufficient rigidity and flexibility to allow coordination and insertion of the first and second CO_2 and elimination of CO, while keeping the two rhenium centers in the resulting dinuclear species in close proximity.

$$2\ [ReX(CO)_3(\alpha\text{-diimine})] \xrightarrow{h\upsilon} 2\ [Re^{II}X(CO)_3(\alpha\text{-diimine}^{\bullet-})]^*$$

with $2\ D \longrightarrow 2\ D^+$

$$2\ [Re^{I}X(CO)_3(\alpha\text{-diimine}^{\bullet-})]^-$$

with $2\ S \longrightarrow 2\ X^-$

$$2\ S + [Re^{0}(CO)_3(\alpha\text{-diimine})]_2 \underset{h\upsilon}{\rightleftharpoons} 2\ [Re^{I}S(CO)_3(\alpha\text{-diimine}^{\bullet-})]$$

CO_2

$2\ S$

CO_2

$$[Re^{I}(CO)_3(\alpha\text{-diimine})]_2(CO_2) \rightleftharpoons [Re^{I}(CO)_3(\alpha\text{-diimine})]_2(CO_3) + CO$$

$$2\ [Re^{I}(CO)_3(\alpha\text{-diimine})]^+ + CO_3^{2-}$$
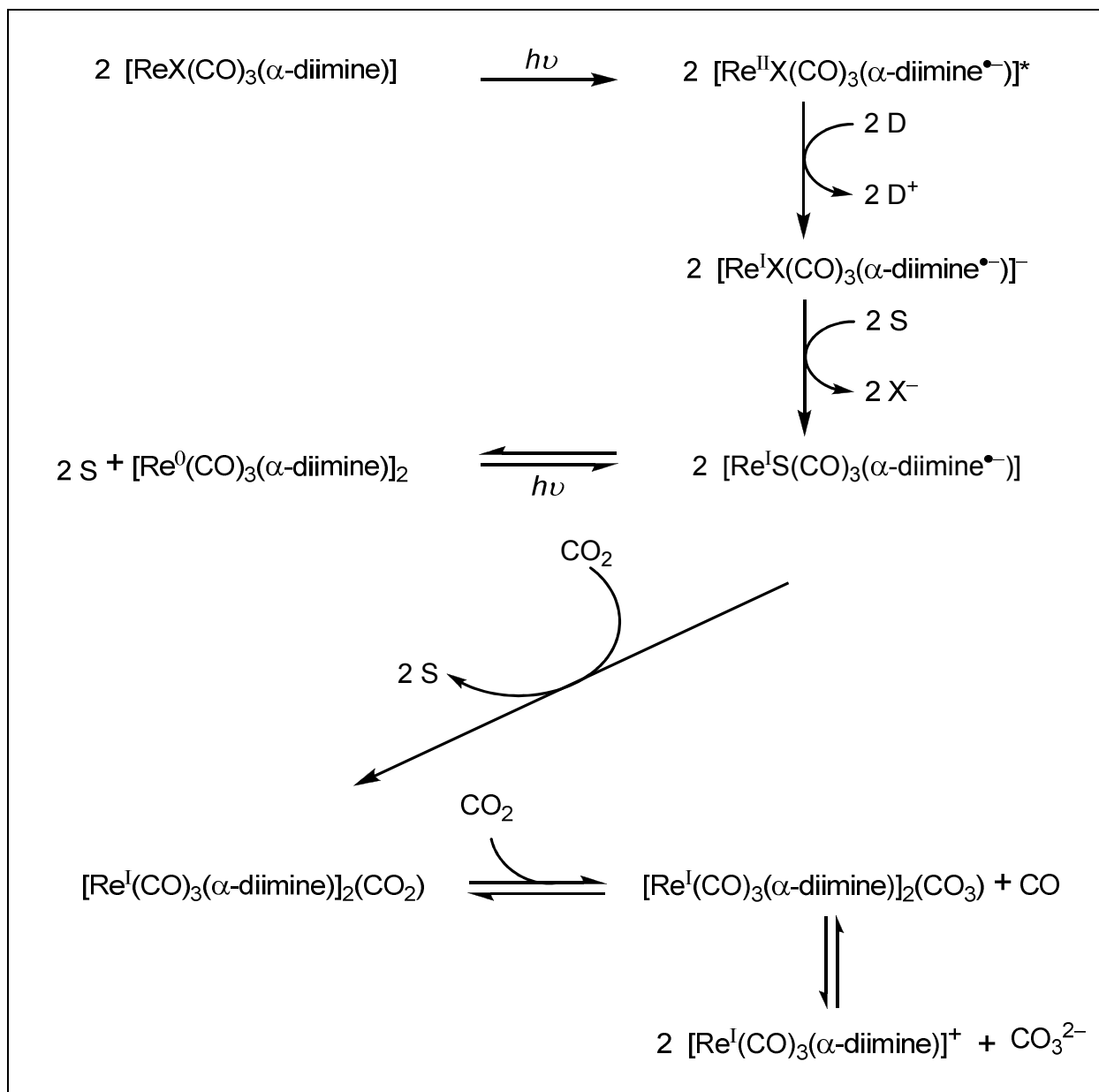
Scheme 2. 1: Proposed photocatalytic reduction of CO_2 by $[ReX(CO)_3(\alpha\text{-diimine})]$ in the presence of a sacrificial electron donor (D). [246,248]

60

In this vein, we initially proposed two species, **[ReBr(CO)$_3$(clip1)]** and **[ReBr(CO)$_3$(clip2)]**, each containing two rhenium centers connected through a clip made from two phenanthrolines linked to an anthracene by an ethynylene or para-bisethynylenebenzene. See Figure 2.3. During the course of our investigations, however, the energetically minimized structure of the CO$_2$-bridged dimer [Re(CO)$_3$(bpy)]$_2$(CO$_2$) was determined to be, as described by the authors of the 2012 theoretical study, "skewed 'trans'."[246,247] The trans refers to the relative orientation of the diimine ligands, while the "skewed" denotes the non-parallel geometric arrangement of the two bipyridyl ligands.[247] An impression of this structure is presented in Figure 2.4. As is evident from this image, the orientation of the diimines in this skewed "trans" structure is opposite to the orientation seen in our proposed clipped dimer. Therefore, our phenanthroline-based clip design is not ideal. In the interim, however, we began investigating what influence the systematic extension of the diimine conjugation through alternate additions of ethynylene and phenyl moieties at the 4 and 7 positions of the phenanthroline ligand would have on the excited state properties and ground state electrochemistry of the [ReBr(CO)$_3$(phen')] complexes.

Previously, photophysical properties were reported for a collection of [Ru(phen')(bpy)$_2$]$^{2+}$ complexes, where phen' is a 1,10-phenanthroline derivative with ethynylphenyl, trimethylsilylethynyl, and 3-ethynyl-1,10-phenanthroline substituents at the 3, 5, 4, and/or 7 positions of the phen' ligand.[250] Their investigation, confirmed the superiority of the 4 and 7 position of the phenanthroline for affecting measurable influences on the excited state properties.[251] They also discovered emission from two MLCT excited states, one involving phen'-centered π^* orbital and the other a bpy-centered π^* orbital, in violation of Kasha's rule. However, a clear pattern describing the influence of increased conjugation was not evident in the more complicated [Ru(diimine)$_3$]$^{2+}$ systems, and no mention was made of the electrochemistry of their complexes. In the examination of our complexes, a clear relationship emerges between phenanthroline conjugation and photophysical and electrochemical properties of the [ReBr(CO)$_3$(phen')] complexes, which are presented in this document. In addition, results of time-resolved spectroscopic experiments including transient absorbance (TA) and TRIR are briefly addressed. A detailed discussion of the transient experiments is not presented here, as this author made no significant contribution to these experiments, but is planned for an upcoming publication.
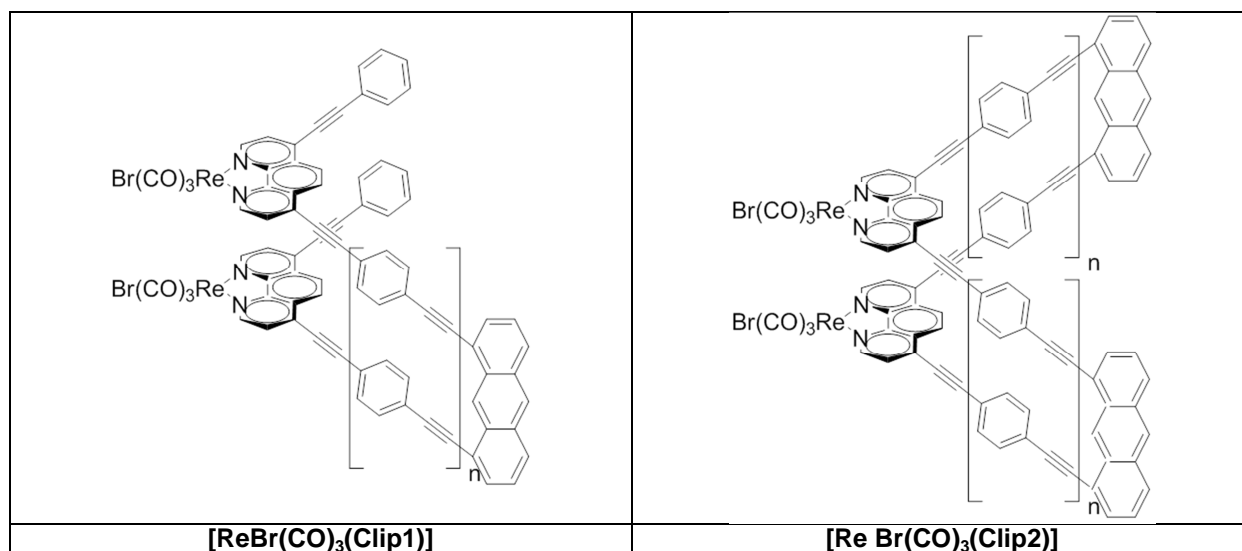
Figure 2. 3: [**ReBr(CO)₃(Clip1)**] and [**ReBr(CO)₃(Clip2)**], which may potentially facilitate the formation of the Re-dimer an important intermediate in the photoreduction of CO_2.
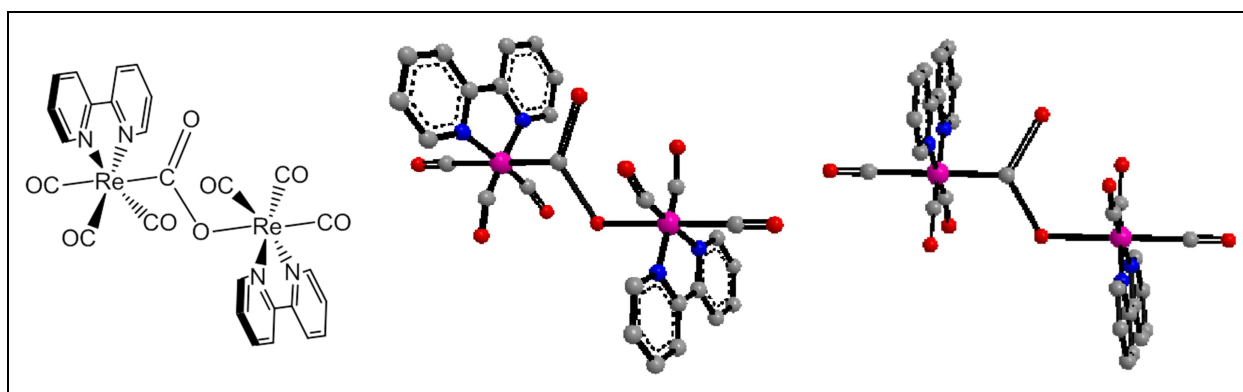
Figure 2. 4: Three representations of the "skewed trans" structure found to be the minimized conformer for the CO_2-bridge rhenium dimer.[246]

2.2. Results and Discussion

2.2.1. Synthesis and Characterization

Rhenium phenanthroline complexes **50** – **52** could be produced via two general methods: ligand substitution, pathways 1 and 2 in Scheme 2.3; or Sonogashira cross-coupling pathway 3 in Scheme 2.3. Carbonyl or diamine substitution in [ReBr(CO)₅] or [ReBr(CO)₃(N,N'-dimethylpiperazine)] (**31**) by the phenanthroline ligand (**53** – **55**) via the established method[236,252,253] or our published procedure[151], respectively, gives expectedly good yields. Ligands **53** – **55** were synthesized, according to the known procedure, namely the Sonogashira

cross-coupling of the 4,7-dibromo-3,8-dihexyl-1,10-phenanthroline (**29**) and the appropriate acetylene.[152,254] See Scheme 2.2. Alternatively, complexes **50** – **52** may be prepared via Sonogashira cross-coupling of [ReBr(CO)$_3$(4,7-dibromo-3,8-dihexyl-1,10-phenanthroline)] (**59**).[250] See Scheme 2.3. Unfortunately, this latter reaction produces [ReI(CO)$_3$(phen')] byproducts because of halide substitution of the desired product and/or starting material when the CuI cocatalysis used. [ReI(CO)$_3$(phen')] complexes are generally not considered for photocatalysis due to the large contribution of the LLCT states.[255]
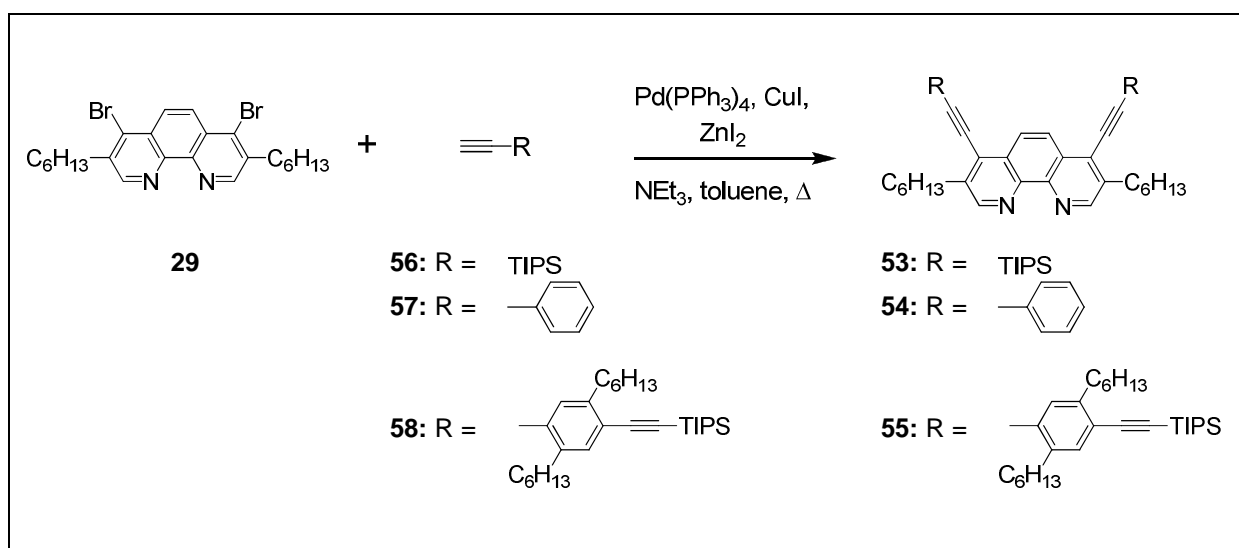
Scheme 2. 2: Synthesis of Ligands **53** – **55**. a. Pd(PPh$_3$)$_4$, CuI, ZnI$_2$, Toluene, NEt$_3$, 85 °C – 100 °C.[254]

Despite this drawback, synthesis of **50** – **52** by Sonogashira cross-coupling of the appropriate alkyne to complex **59** is still attractive. The synthesis of ligands **53** – **55** by Sonogashira cross-coupling requires an enhancement of the electrophilicity of sp^2-halide at the 4 and 7 positions on the phenanthroline, which are para to the heteroatom. Usually this is accomplished by an excess of CuI or the addition of stoichiometric amounts of ZnI$_2$, which coordinate to the heteroatoms of the phenanthroline. During work up, the metals must be removed by washing with a solution of KCN.[254] Owing to the toxicity of cyanide solutions, it is beneficial to employ procedures that obviate their use. Since the phenanthroline nitrogen atoms in **59** are already coordinated to the rhenium center, synthesis of **50** – **52** via Sonogashira coupling of complex **59** rather than from the free ligands **53** – **55**, does not require the use of excess Cu$^+$ or the addition of Zn^{2+} and as a consequence KCN solutions.[250] In addition, it is more convenient to purify the colorful rhenium

phenanthroline complexes via column chromatography than their respective ligands, as un-coordinated phenanthroline compounds have lower R_f values, longer retention times, and elute as tailing colorless fractions. Because the R_f values of the bromo and iodo complexes are quite distinct, with the iodo complexes eluting first, the iodo byproduct can be separated during purification. The complexes can be distinguished by small but measurable differences in the $C\equiv O$ stretch and the ^{13}C nuclear frequencies in the FTIR and NMR spectra, respectively.
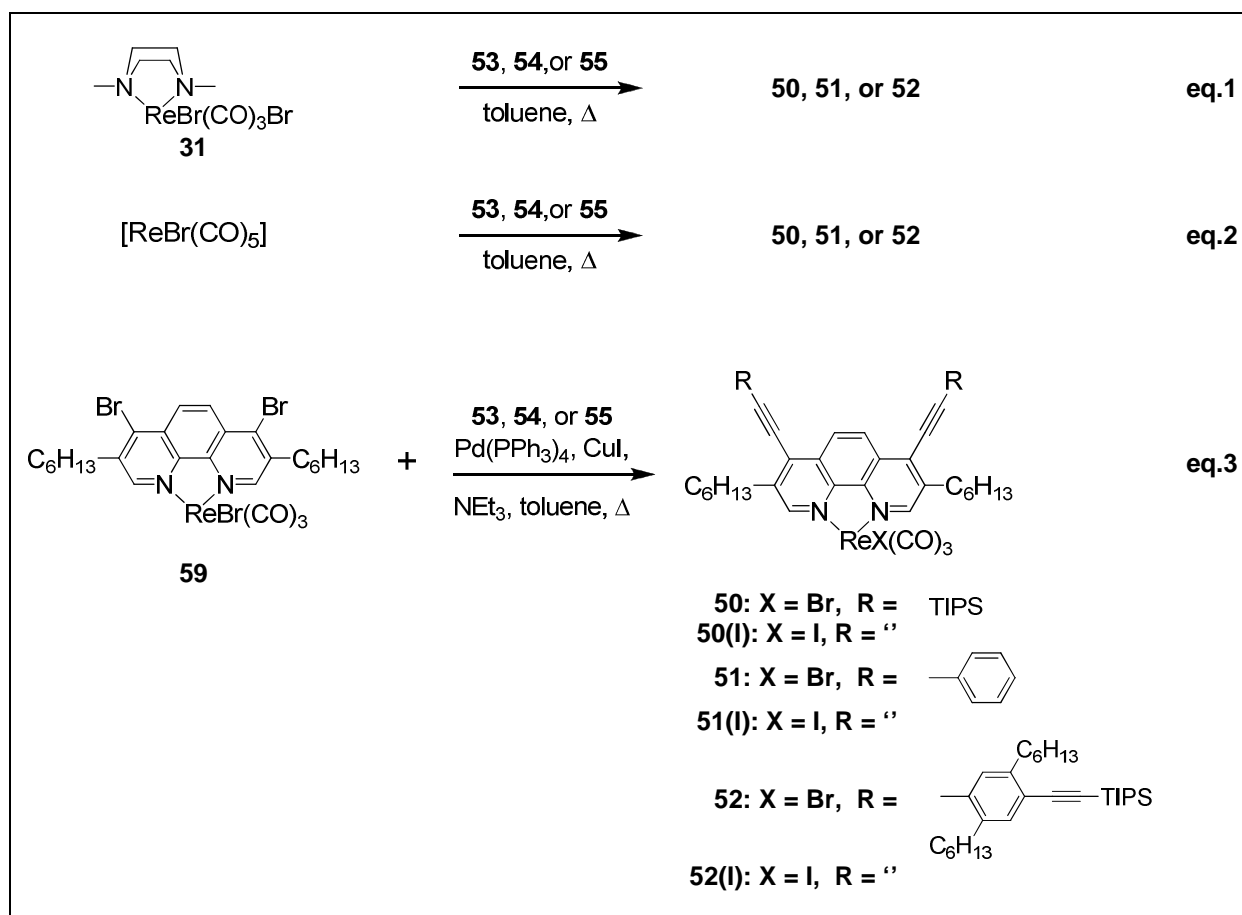
Scheme 2. 3: Synthesis of compounds **50 – 52**. Key: a. Toluene, 85 °C b. Pd(PPh$_3$)$_4$, CuI, Toluene, NEt$_3$, 85 °C. eq.1[151], eq. 2[236,252,253], eq.3[250].

All compounds were purified via column chromatography. The yellow, orange, and red ReBr(CO)$_3$(phen') complexes were further purified via two-solvent recrystallization by the careful addition of a layer of hexanes over a solution of each complex dissolved in dichloromethane. Complexes **50 – 52** were fully characterized through ^{1}H NMR, ^{13}C NMR, FTIR, and elemental analysis. The ^{1}H resonance frequencies for the isochronous nuclei pairs at

positions 2 & 9 and 5 & 6 on the phenanthroline, the two pairs of methylene protons adjacent to the phenanthroline (i.e. picolinyl protons), as well as the phenyl protons in complexes **50** – **52** and free ligand **53** – **55** are listed in Table 2.1. The chemical shift values for protons at the 2 & 9 and 5 & 6 positions are found to be between 9.02 – 9.20 ppm and 8.03 – 8.49 ppm, respectively. Relative to their respective free ligands, the nuclear frequencies in **50** and **52** resonate downfield, with the most pronounced difference being observed for the protons at the 2 & 9 positions ($\Delta\delta$ = 0.16 ppm for **53** and complex **50**; $\Delta\delta$ = 0.13 ppm for **55** and complex **52**).

Because of deshielding effects, the chemical shifts are expected to increase with increasing conjugation in this series. These deshielding effects are evident in the ^{1}H NMR of the free ligands, where the lowest and highest resonance frequencies are observed for the phenanthroline and picolinyl protons in **53** and **55**, respectively. The resonance frequencies of the phenanthroline are also expected to shift downfield following coordination to the transition metal, due to the electron donating role of the ligand. However, the resonance frequencies of the phenanthroline protons in **51** are surprisingly low, particularly at the 5 & 6 positions, and are found upfield of **50** ($\Delta\delta$ = 0.13 ppm) and **54** ($\Delta\delta$ = 0.03 ppm). On the other hand, the chemical shift values of the phenyl protons in **51** seem remarkably high; especially when considering the fact the resonance frequencies of the phenyl protons in complex **52** are only slightly downfield of those in **55** ($\Delta\delta$ ~ 0.01 ppm), but the phenyl protons in complex **51** are found significantly downfield of its respective ligand ($\Delta\delta$ ~ 0.1 ppm). See Table 2.1. Thus, the phenanthroline protons in complex **51** appear to be more shielded than anticipated, and the phenyl protons more deshielded. This suggests, the phenyl group in complex **51** loses electron density to the phenanthroline through the π-system. However, it is unclear why this phenomenon is not observed in complex **52** or why the phenanthroline protons in **54** are not shielded. We reason the phenyl groups in both **51** and **54** can adopt a coplanar arrangement, which provides a resonance pathway for π-electrons to move from the phenyl to phenanthroline in both species. However, the bulky hexyl substituents in **52** and **55** may make such an arrangement in these compounds unfavorable, thus preventing such a pathway. In complex **51** the [ReBr(CO)$_3$] substrate may help draw electron density from the phenyl into the phenanthroline, while in **54** this impetus does not exist. Therefore, the fact the phenyl protons in **54** are downfield of the phenyl protons in **55** may simply be owing to increased delocalization in the former because of the suspected coplanar arrangement of the π-orbitals. See Figure 2.6. In order to explore this line of reasoning, it would

be quite useful to have a crystal structure of these complexes **51**. Unfortunately, crystals for this complex could not be obtained.

Another interesting feature of the ^{1}H NMR spectrum of **51** is the two sets of 2H-integrated multiplets at 3.08 and 2.60 ppm corresponding to the picolinyl protons. Generally, the resonance frequencies of all four of the picolinyl protons appear as a single multiplet centered around 3.1 ppm, as is evidenced in the ^{1}H NMR spectra for **50** and **52** as well as **53 – 55**. To determine whether the two pairs of protons resonating at median frequencies of 3.08 and 2.06 ppm in **51** are bound to the same or different methylene carbons, we performed a 2D COSY experiment. See Figure AC2.21 in the Appendix. The results of this experiment clearly show the two proton pairs are coupled, suggesting a geminal relationship between them. These protons are also coupled to a set of four protons located upfield that appear to be a pair of overlapping multiplets centered near 1.76 and 1.67 ppm. These multiplets are assigned to the methylene protons adjacent to the picolinyl group. Although their chemical shift difference is much smaller than those observed for the picolinyl protons, these protons, as with the picolinyl protons, are usually found to be isochronous in **50**, **52**, and **53 – 55**. Owing to the diastereotopic relationship between the geminal proton pairs in the methylene groups (see Figure 2.5), geminal-anisochronicity is not wholly unexpected. The chemical differences between the bromo and carbonyl ligands "above" and "below" the plane of phenanthroline ligand may induce an anisotropy in the circulation of the π-electrons, and this effect may be enhanced by conjugation with the attached phenylethynylene group.[256-258] Although long-range anisotropic effects are rare, they do occur.[257,259,260] Since the picolinyl and its adjacent methylene are most proximal to the 4,7-disubtituted-1,10-phenanthroline, they experience the greatest anisotropic effects generated by the 4,7-disubtituted-1,10-phenanthroline. Why these same anisotropic effects are not evident in the ^{1}H NMR of **52** or **54** is however perplexing. Again we speculate the unique features in the ^{1}H NMR of **51** may be owing to the ability of the non-hexylated phenyl groups to adopt a coplanar arrangement with the phenanthroline and the influence of the coordinated [ReBr(CO)$_3$] substrate on the phenanthroline-based molecular orbitals. Since the coplanar arrangement may be unfavorable in **52** and the free ligand (**54**) is not coordinated to the substrate, geminal-anisochronicity is not evident in their ^{1}H NMR. See Figure 2.6. This arrangement may also explain some of the unique physical characteristics of complex **51**. For example **51** crystalizes as fine, light, yellow-orange particles, whereas **50** and **52** crystalize into

larger denser, red-orange and red particles, respectively. See Figure 2.1. Additionally, **51** is far less soluble in CH_2Cl_2 and chloroform than **50** or **52**. Again, crystal structures of complexes **50** – **52** would be needed to substantiate whether the coplanarity of the phenyl groups in **51** is different from that in **50** or **52**.

Skewed-top View 51   **3D-Side View of 51**
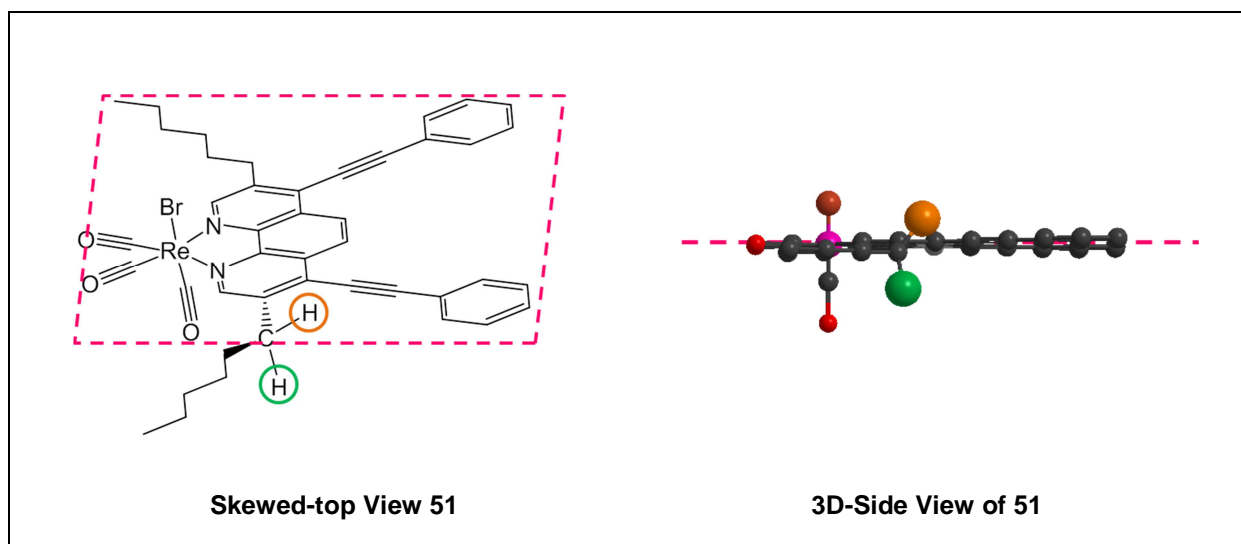
Figure 2. 5: Diastereotopic Relationship Between Geminal Methylene Protons. The chemical environments above the and below the plane of the phenanthroline ligand (indicated by magenta dashed-lines) are distinct. When the hydrogen, in orange, is above the plane it is closer to the bromine. When the hydrogen, in green, is below the plane it is closer to the axial carbonyl ligand.

51   **52**   **52 (potentially unfavorable)**
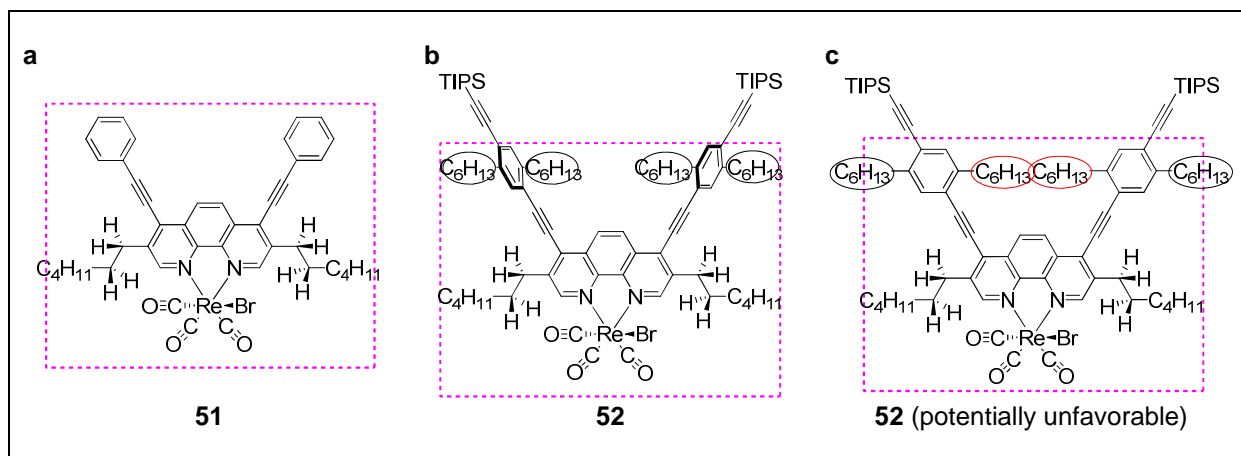
Figure 2. 6: a) the coplanar arrangement of phenyl and phenanthroline rings in complex **51**; b) the non-coplanar arrangement of phenyl and phenanthroline rings in complex avoids steric clash of hexyl groups in complex **52**; c) steric clash of hexyl groups in potentially unfavorable

coplanar arrangement of phenyl and phenanthroline rings in complex **52**. Magenta dashed-box represents the plane of the phenanthroline ring.
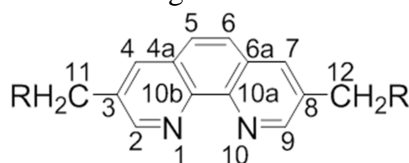
Figure 2. 7: Phenanthroline ligand numbering scheme used for **Table 2.1** and **Table 2.2**.

Table 2. 1: ^{1}H (300 MHz, CDCl$_3$)

#	phenanthroline 2 & 9	5 & 6	picolinyl[a]	phenyl[a]	#	phenanthroline 2 & 9	5 & 6	picolinyl[a]	phenyl[a]
50	9.17	8.39	3.10		**53**	9.01	8.35	3.05	
51	9.02	8.03	3.08, 2.60	7.80, 7.56	**54**	9.05	8.43	3.10	7.69, 7.45
52	9.20	8.48	3.16	7.49, 7.41	**55**	9.07	8.45	3.13	7.48, 7.39

a. The median frequency for multiplets and triplets are reported for simplicity.

Table 2. 2: ^{13}C (400 MHz, CDCl$_3$) phenanthroline nuclei

			[Re(phen')(CO)$_3$Br]			
#	2 & 9	10a & 10b	4 & 7	3 & 8 or 4a & 6a	5 & 6	picolinyl
50	153.2	145.3	142.7	130.6, 130.4	126.1	33.2
51	152.7	145.3	141.6	130.7, 129.9	126.2	32.8
52	153.1	145.5	143.2	131.0, 130.1	126.0	33.0
			Ligands			
53	151.2	144.2	139.4	127.9, 127.9	125.1	32.9
54	151.2	144.4	138.9	127.9, 127.6	125.0	32.6
55	151.3	144.5	138.7	128.1, 127.6	125.0	32.6

The ^{13}C resonance frequencies for complexes **50** – **52** and ligands **53** – **55** were determined and tentatively assigned based on information available in the literature[254,261] and the

results of attached proton test (APT) experiments. APT analysis was useful in discerning between carbon atoms at the 4 & 7 position on the phenanthroline and the hexylated phenyl carbons, as well as between non-hexylated phenyl carbons and carbons at the 3 & 8 and 4a & 6a positions on the phenanthroline. However, isochronous pairs 3 & 8 and 4a & 6a, both being tertiary sp^2 carbons, are indistinguishable by APT experiments and so listed together as 3 & 8 / 4a & 6a. These results are presented in Table 2.2. It is worth noting the ^{13}C assignments for the phenanthroline carbons 5 & 6, 4a & 6a, and the phenyl carbons ortho to the ethynylene groups differ from those reported in the reference for **54**.[254] To clarify, the coupling pattern results from the ^{1}H -coupled ^{13}C NMR experiment reported by the authors were not consistent with the number of attached protons we discovered in our APT experiments. They observed a singlet at 131.8 and two doublets at 127.6 and 125.0, which they attributed to the 4a & 6a, 5 & 6, and aforementioned phenyl carbons, respectively. On other hand, we found nuclei at the above frequencies to have +, −, + phases in our APT experiments suggesting the number of attached protons to be 1, 0, and 1, respectively. Because carbons at 4a & 6a are not protonated, we assigned the chemical shift at 127.6 to this pair. The resonance frequency at 125.0 ppm was matched to phenanthroline carbons 5 & 6 based on the persistence of this chemical shift in all three ligands

The ^{13}C chemical shifts for the phenanthroline nuclei are quite typical and invariant in [ReBr(CO)$_3$(phen')] complexes **50 – 52** with respect to the degree of conjugation in the phenanthroline ligand. See Table 2.2. The isochronous phenanthroline carbon pairs at the 2 & 9; 10$_a$ & 10$_b$; 4 & 7; 3 & 8/4a & 6a; and 5 & 6 positions as well as the phenanthroline-adjacent CH$_2$ are found near: 153, 145, 142, 131/130, 126, and 33 ppm, respectively in all three complexes. In the free ligands **53 – 55**, these nuclei resonate slightly upfield of the corresponding rhenium complex, as anticipated,[261] and are found near: 151, 144, 139, 128/128, 125, and 33 ppm, respectively. The carbon nuclei of the phenyl rings in **51**, **52**, **54**, and **55** are listed in Table 2.3. The non-hexylated carbons ortho or meta to the ethynylene groups resonate near between 129 – 133 ppm, while the hexylated carbons resonate around 142 ppm. The remaining phenyl carbons resonate between 121 – 129 ppm. Interestingly, there is significant downfield shift of all phenyl carbons in **51** relative to **54** ($\Delta\delta \sim$ 4ppm), which is not observed in **52** relative to **55**. This shielding is consistent with our earlier assessment, namely electron

density in the phenyl groups shifts into the phenanthroline in the ground state of complex **51**. *Vide supra.*

The acetylenic carbon resonance frequencies are found in the anticipated region between 80 – 120 ppm and listed in Table 2.3.[254] The chemical shifts for the equatorial and axial carbonyl carbons for all three rhenium complexes are found near 197 and 190, respectively. See Table 2.4. This suggests the extended conjugation in the phenanthroline has no significant influence on the electron density at the rhenium center, which is in agreement with the $C\equiv O$ stretch vibrational frequencies. The three stretching modes – A'(1), A'', and A'(2) – commonly expressed in the FTIR spectra of *fac*-rhenium tricarbonyl complexes have vibrational frequencies near 2020, 1920, and 1900 cm^{-1}, respectively in KBr media.[227] See Table 2.5. The most notable differences exist in the A'(2) stretching mode, which increases incrementally 5 cm^{-1} in the series from **50** – **52**. The A'' stretching mode in **52** is also distinct from **50** and **51**. The reference complex, ReBr(CO)$_3$(phen) share similar frequencies for the symmetric stretching modes A'(1) and A'(2) but is quite distinct for the asymmetric stretch ($\tilde{v}_{C\equiv O}$ = 2016, 1932, 1901 cm^{-1}). In dichloromethane solutions, the $C\equiv O$ stretching frequencies for **50** – **52** and the reference are nearly identical, being found near 2021, 1920, and 1900 cm^{-1} for the complexes and at 2021, 1921, 1896 cm^{-1} for the reference. The vibrational spectra also feature $C\equiv C$ stretches for all three complexes and their respective ligands. The ethynylene group adjacent to the phenanthroline has a small but measurable difference, while the farthest ethynylene is the same in **55** as in **52**.

Table 2. 3: ^{13}C (400 MHz, CDCl$_3$) phenyl and acetylenic nuclei.

Phenyl ^{13}C Resonances δ(ppm)			
#	**Phenyl Resonances**	**#**	**Phenyl Resonances**
51	132.6, 130.6, 128.9, 126.2	**54**	131.8, 129.2, 128.6, 122.5
52	142.6, 141.9, 133.3, 133.0, 125.1, 120.5	**55**	142.9, 142.2, 133.1, 132.8, 124.0, 121.7

Acetylenic ^{13}C Resonances δ(ppm)			
#	^{13}**C (C≡C)**	**#**	^{13}**C (C≡C)**

50	111.9, 99.0	53	105.7, 100.8
51	107.3, 82.8	54	102.2, 83.8
52	106.3, 105.1, 97.4 86.7	55	105.4, 101.4, 96.1, 88.2

Table 2. 4: ^{13}C (400 MHz, CDCl$_3$) carbonyl carbon

#	^{13}C (C≡O)$_{eq}$	^{13}C (C≡O)$_{ax}$
50	196.7	188.8
51	197.2	189.1
52	196.8	189.1

Table 2. 5: Select vibrational stretching frequencies from FTIR

Select FTIR frequencies in cm^{-1}					
#	$\tilde{v}_{C≡O}$, KBr	$\tilde{v}_{C≡O}$, CH$_2$Cl$_2$	$\tilde{v}_{C≡C}$, KBr	L#	$\tilde{v}_{C≡C}$, KBr
50	2020, 1917, 1885	2023, 1923, 1901	2146	53	2146
51	2017, 1918, 1890	2022, 1920, 1900	2201	54	2210
52	2020, 1926, 1905	2022, 1922, 1900	2192, 2148	55	2199, 2147

2.2.2. Electrochemical Properties

Reduction and oxidation potentials have been obtained from cyclic voltammetry (CV) experiments for compounds **50** – **52** in dichloromethane solution containing 0.1 M Tetrabutylammonium hexafluorophosphate (TBAHFP). The results were compared with redox potentials obtained under the same conditions for the reference complex [ReBr(CO)$_3$(phen)]. A composite of voltammograms for all three complexes and the reference is given in Figure 2.8, and the redox potentials, recorded at 100 mV/s sweep rates and at ambient temperatures, are summarized in Table 2.6. Dichloromethane was elected as the solvent because compounds **50** – **52** had limited solubility in more preferable solvents, including acetonitrile and dimethylformamide. The low solubility of compounds **50** – **52** in more polar media is likely due

to the presence of the large lipophilic hexyl substituents on the phenanthroline ligand. Unfortunately, dichloromethane becomes increasingly redox active at voltages below −1.5 V and above 1.3 V. Consequently, the potential sweep range was generally limited between

Table 2. 6: First reduction and oxidation potentials for complexes **50 – 52** and reference vs. Fc^+/Fc^a at 100 mV/s scan rates. [ReBr(CO)$_3$(phen')] equals 0.4 mM in 0.1 M TBAHFP/CH$_2$Cl$_2$ for all experiments except where noted.

Compound	Red. 1	Red. 2	Ox. 1
	$E_{1/2}(\Delta E_p)$	E_{pc}	E_{pa}
[ReBr(CO)$_3$(phen)]	-1.83(88)	----	+0.97
50	-1.70(70)	----	+0.95
51	-1.67(72)	-1.87	+0.98
52	-1.66(72)[b]	-1.89[b]	+1.0[c]

a. The Fc^+/Fc redox couple in CH$_2$Cl$_2$ was set to 0 V.
b. [**52**] = 0.2 mM.
c. Data recorded for the cathodic potential and the anodic potential was obtained during separate experiments. The unreferenced $E_{1/2\ red}$ measured in both experiments are found to be 1374 and 1376 mV, respectively.

+1300 mV and −1500 mV during the experiments, which is inclusive of the one-electron reduction and oxidation for all complexes under investigation. Redox potentials were measured using Ag/AgNO$_3$ as the reference electrode and ferrocenium/ferrocene as an internal standard.[262]

The one-electron reduction of the rhenium complexes is a quasi-reversible process. According to Table 2.6, the first reduction potentials increase as the series progress toward increasing phenanthroline conjugation, with [ReBr(CO)$_3$(phen)] and **52** having the lowest and highest E_{red}, respectively. These results are consistent with previous findings, and is expected as the electron in the one-electron reduced species, [ReBr(CO)$_3$(phen$^{\bullet-}$)]$^-$ is delocalized over an increasingly large area. Moreover, since the electron extra electron in the reduced species is added into a π^* orbital the energy of π^* orbitals decreases with an increase in conjugation, the reduction potentials are expected to increase with the increase in conjugation. The most

72

pronounced increase in E_{red} occurs between [ReBr(CO)$_3$(phen)] and **50**, the differences in their potentials being roughly 130 mV. The large difference in the reduction potentials of **50** and **51** is not likely due to the presence of the hexyl groups. Indeed, substitution by an alkyl group is expected to decrease the reduction potential. For example the $\Delta E^{red}_{1/2}$ = $E^{red}_{1/2}$ [Re(py)(CO)$_3$(Me$_4$phen)]$^+$ – $E^{red}_{1/2}$ [Re(py)(CO)$_3$(phen)]$^+$ = –45 mV, where phen is 1,10-phenanthroline and Me$_4$phen is 3.4,7,8-tetramethyl-1,10-phenanthroline, as reported by Wallace et. al.[241] Between **50** and **51**, there is a modest increase of about 30 mV and between **51** and **52** a 10 mV difference. The second reduction potentials also demonstrate a modest increase (~ 20 mV) between **51** and **52**. Unfortunately, second reduction potentials could not be obtained for **50** and the reference complexes, as these processes occur at voltages greater than the cathodic switching potential. The second reduction potentials for **51** and **52** were found to be –1.87 and –1.89 V, respectively, when measured against the ferrocenium/ferrocene couple.
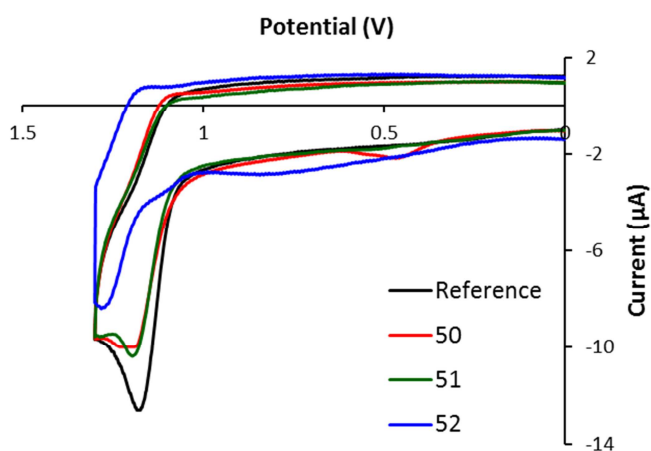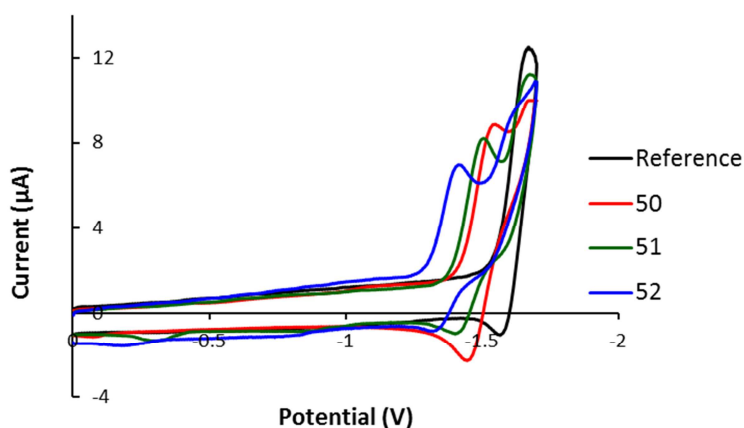
Figure 2. 8: Cyclic Voltammograms of complexes **50** – **52** and the [ReBr(CO)$_3$(phen)] reference in dichloromethane vs. Fc$^+$/Fc^a at 100 mV/s scan rates.

The oxidation process is chemically irreversible at a sweep rate of 100 mV/s, as is evident by the irregularities between the shape of the anodic and cathodic waves. Unlike the reduction potentials, increasing the area of delocalization in the diimine has no discernible influence on E$_{pa}$ values for oxidation. Since oxidation has been shown to be a rhenium-centered process, the fact the conjugation of the diimine ligand has little effect on oxidation potentials is unsurprising. -Therefore, oxidation potentials should not be significantly affected by the diimine ligand.

2.2.3. Electronic Absorption and Emission Properties

The absorption spectra of complexes **50** – **52** and the reference complex [ReBr(CO)$_3$(phen)] were obtained in dichloromethane solutions. The UV-Vis spectra feature sharp bands between 260 and 380 nm and a broad band or shoulder devoid of vibrational character between 380 and 420 nm. Based on the shapes and energies of these bands, they are tentatively assigned to the π—π* and MLCT transitions, respectively. See Figure 2.9. Additional features in the UV region of the absorbance spectra of complex **52**, including an intense band at 284 nm with a shoulder at ~ 272 nm and a series of three closely spaced bands at 302, 316, and 324 nm, are likely the result of electronic transitions of orbitals centered on the bis-ethynylphenyl moiety.[263-265] The assignment of these bands to the bis-ethynylpheyl moiety is supported by the observation of these bands in the electronic absorbance spectra of heteroleptic [Ru(L3)(bpy)$_2$]$^{2+}$, complex **60**, in CH$_2$Cl$_2$. See Figure 2.10. The λ_{MLCT} and $\lambda_{\pi—\pi*}$ and their corresponding molar absorptivity are compiled in Table 2.7. As is evident from the data, both λ_{MLCT} and $\lambda_{\pi—\pi*}$, as well as ε_{MLCT}, increase with phenanthroline conjugation. These results are consistent with previous reports that showed a red-shift in the MLCT and π–π* transitions as a result of the decreased π*- LUMO energy of complexes with higher conjugated diimine ligands. Interestingly, the energy difference between the π—π* and MLCT transitions becomes smaller as the series progresses, so much so that the MLCT transition in **52** appears as a shoulder on the more intense π—π* band. Therefore, emission from both the MLCT and IL excited states is possible in **52**.
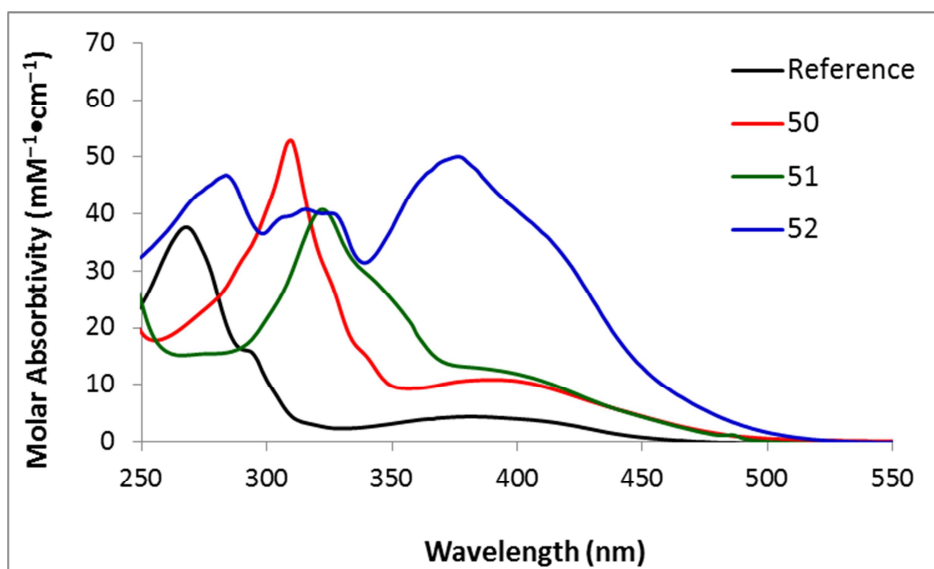
Figure 2. 9: Electronic Absorbance spectra of complexes **50 – 52** and [ReBr(CO)$_3$(phen)] in dichloromethane.
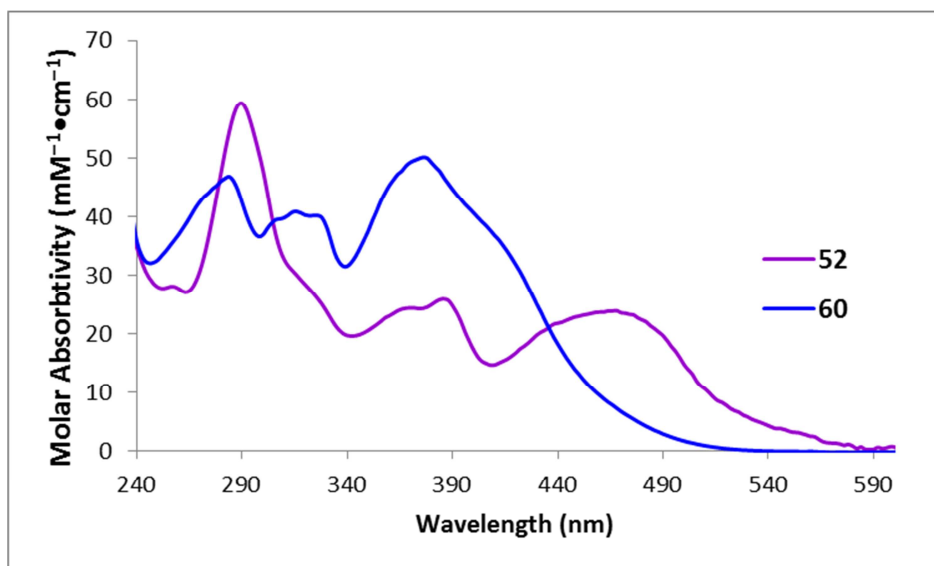
Figure 2. 10: Electronic Absorbance spectra of complexes **52** and **60** in dichloromethane.

Unlike the MLCT absorption energies, the energy of emission changed very little with conjugation, and all complexes display a single broad emission band centered between 642 – 648 nm following excitation into the MLCT state. See Figure 2.11. Similar results were seen in the series of [Ru(phen')(bpy)$_2$]$^{2+}$ complexes investigated by Glazer et. al., where the emission maxima of bis-(2,2'-bipyridine)(4-trimethylsilylethynyl-1,10-phenanthroline)ruthenium(II) and bis-(2,2'-bipyridine)(4-phenylethynyl-1,10-phenanthroline)ruthenium(II) were reported to be

660 nm.[250]   Compared to the reference, however, the emission energies of **50** – **52** were significantly red shifted by about 40 nm. This suggests that in the emissive state, the excited electron is not located in orbitals with significant character from the phenanthroline substituents beyond the first ethynyl group attached to the 1,10-phenanthroline ligand in these complexes.

Table 2. 7: Absorption, Emission, and Excitation Data.

Compound	$\lambda_{\pi-\pi^*}$ (nm)	ε (1/cm•mM)	λ_{MLCT} (nm)	ε (1/cm•mM)	λ_{em} (nm)	Stokes Shift (nm)
[ReBr(CO)₃(phen)]	268	35.7	380	4.541	606	226
50	310	51.3	390	10.4	648	258
51	322	43. 2	400(sh)	12.6	642	242
52	374	50.3	420(sh)	31.8	646	226
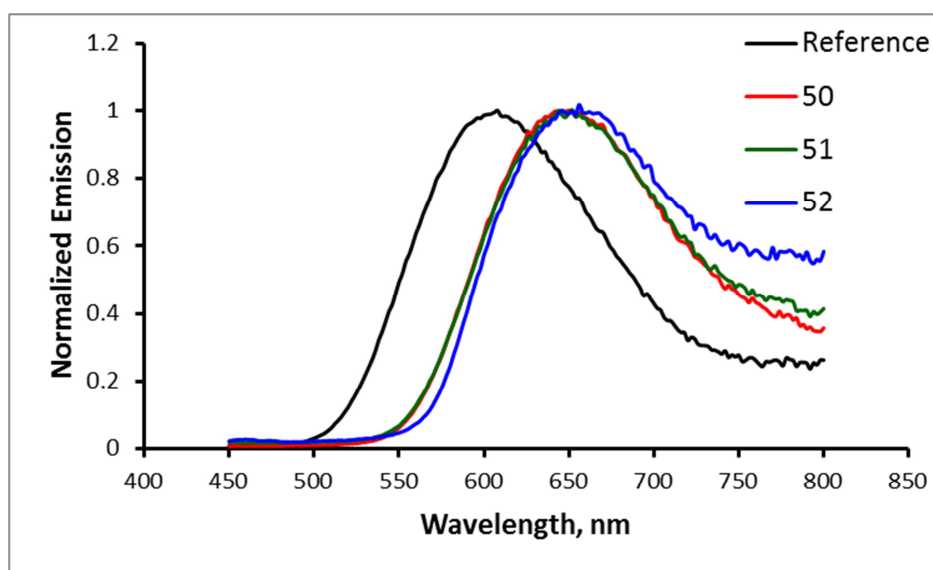
Figure 2. 11: Corrected Emission Spectra for Complexes **50** – **52** and reference.

Overlays of the emission and MLCT band from the absorption spectra reveal the anticipated mirror-image phenomena for complex **50** as well as the reference, which confirms the emissive radiation is MLCT in origin. See Figure 2.12. For complex **51** and **52** the emergence

76

of the π–π* band at frequencies close to the MLCT in the absorption spectra precludes the observation of this phenomena. Although, luminescence in **51** and **52** are also assumed to originate from the ^{3}MLCT, contributions from the ^{3}IL excited state cannot be excluded, especially for complex **52** where the π–π* and MLCT transition energies are so close. The gradual decrease in the stokes shift values for **50** – **52**, as estimated by the differences in the λ_{MLCT} and λ_{em} with diimine conjugation, attests to an increase in vibrational modes available in the excited and/or ground states of the more conjugated complexes.
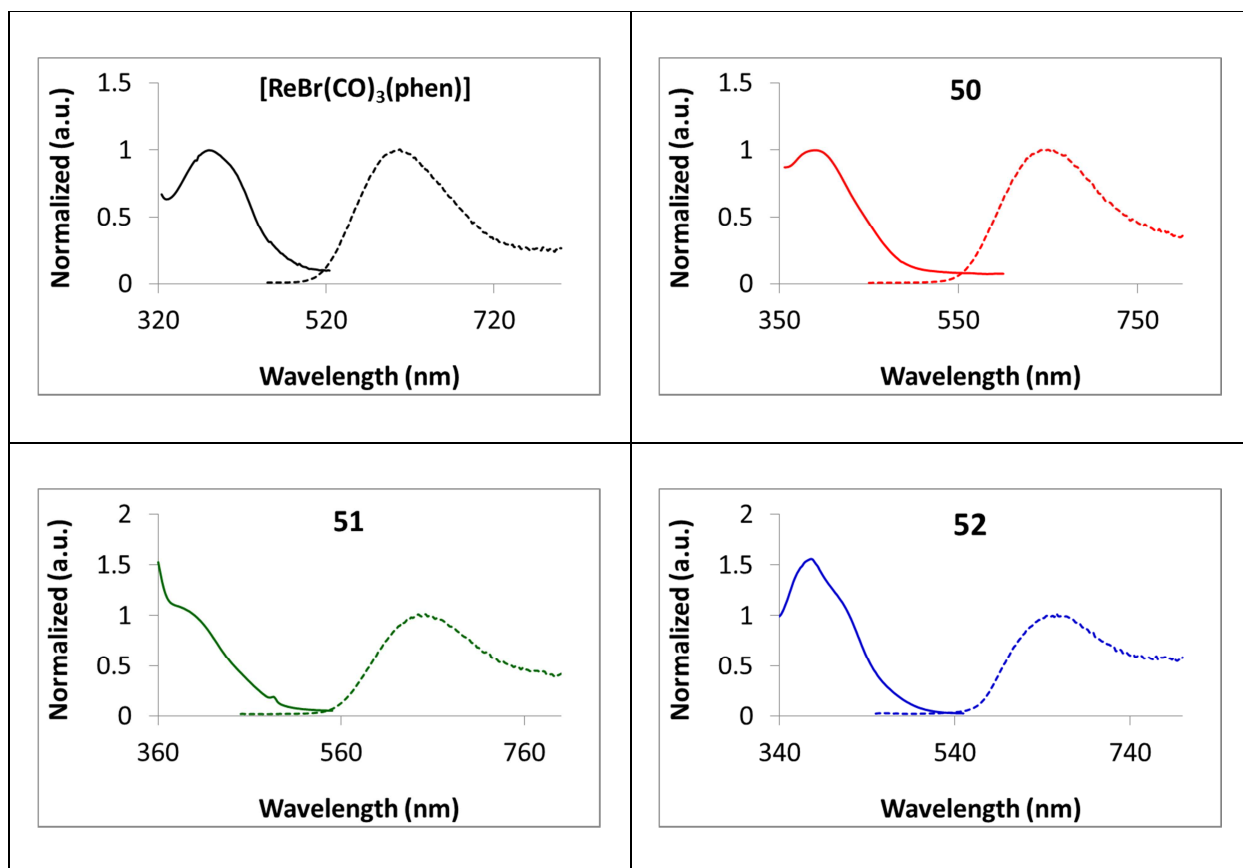
Figure 2. 12: Overlay of Absorbance and Corrected Emission Spectra for Complexes **50** – **52** and reference in CH_2Cl_2 solutions. See **Table 2.7**.

The emission data are summarized in Table 2.7. Overlays of the excitation and absorption spectra are presented in Figure 2.13 and are found to be nearly superimposable for complexes **50** – **52** in the MLCT region of the spectra, with greatest overlap in **50** and least overlap in **52**. This suggests the emitting excited states are mostly MLCT in character.
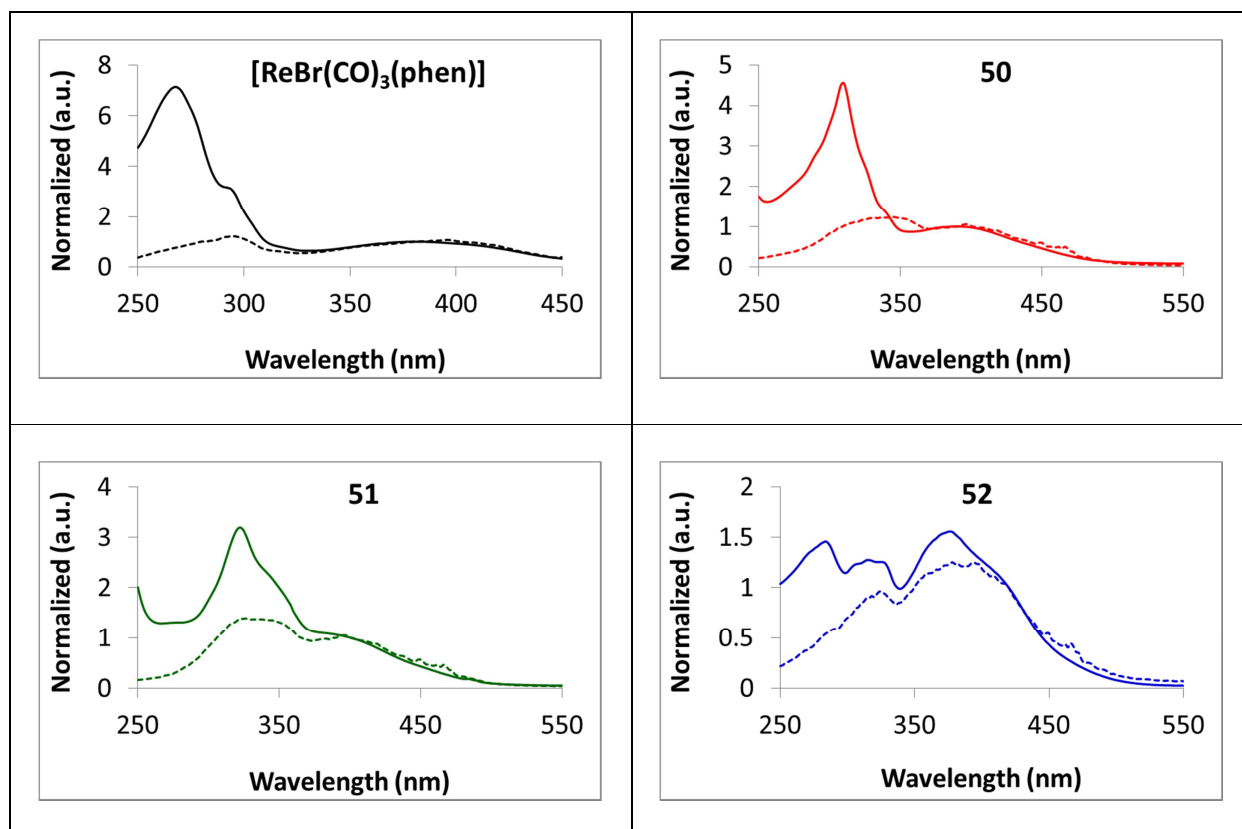
Figure 2. 13: Overlay of Absorbance (—) and Excitation (---) spectra for reference and **50** – **52** recorded in CH₂Cl₂ solutions. All complexes were monitored at the wavelength of their maximum emission for the excitation spectra. See **Table 2.7**.

2.3. Comments on Transient Spectra

In addition to the steady state spectroscopies, David Grills of the Etsuko Fujita group, performed transient studies on the three complexes. The results of these experiments are to be presented in an upcoming paper, but a cursory discussion will be provided here as it helps clarify some unresolved questions.

The pump-probe TA experiments were performed in dichloromethane without quencher and the samples were excited by near UV-irradiation at the wavelength specified. TA spectra after excitation in the near UV display the typical bleach of the MLCT and π–π* with transient growths at higher wavelengths. In the least conjugated complex, **50**, however, a broad and intense band with λ_max near 510 nm overlays with the MLCT bleach near 390 nm. The broadness of the 510 nm transient may be partially attributed to the dichloromethane solvent media,[223,224] but this does not explain the structural details and intensity. See Figure 2.12. A

similar situation is observed in the most conjugated complex, **52**, but in this case both the π–π* and MLCT bleach is hidden by the transient at 640 nm. This transient is just as intense and broad as that seen in **50**, but with fewer structural features. TA spectra recorded in toluene for several oligo(phenylethynylene) species also reveal transients in this same region.[266,267] Therefore, it seems likely the unusual features in the TA of complexes **50** – **52** are due to transients associated with the substituents. Processing the decay kinetics by single exponential fitting produces excited-state lifetimes of 2 and 3 μs, respectively, for **50** and **52**. These values are significantly longer than the chloride derivative of the reference, $[ReCl(CO)_3(phen)]$, which was determined to have a 0.3 μs emission lifetime in dichloromethane.[268]

Structural details of the excited states were elucidated by TRIR experiments without quencher. As expected, the spectra display bleaching of the three C≡O stretch bands with transients appearing at higher frequencies due to the oxidation of the Re(I) center in the MLCT. Owing to dichloromethane solvent effects, which typically broaden and reduce the intensity of the vibrational transients, the A'' and A'(2) vibrational modes of the excited state transient bands are not well resolved and appear as a single broad band for all three complexes and the reference.[224] Surprisingly, for complexes **50** – **52** an additional transient appears in the same region (between 1920 – 2000 cm^{-1}) as the as the A'' and A'(2) C≡O excited state vibrations. Because of the intensity of this band, the shape of the vibrational frequency in that region cannot be attributed to solvent effects. Therefore, we assumed this additional growth could result from C≡C vibrations of the excited state complexes. The C≡C stretching frequencies typically appear between 2200 and 2100 cm^{-1} in the ground state FTIR spectra for these complexes. The large shift (~150 cm^{-1}) of the ν(C≡C) stretch to lower frequencies, has been previously observed in oligo(phenylethynylene) species and suggests the electron in the excited species is delocalized on the conjugated substituents of the phenanthroline.[266,267,269] To confirm the assignment of features in the TRIR of complexes **50** – **52** were due to the C≡C stretch, TRIR experiments were performed on $[Ru(L3)(bpy)_2]^{2+}$ complex (**60**), since this complex lacks carbonyl groups. Therefore, any growths in the active region of the IR spectra can be attributed to the C≡C stretches of **55**. Since thee TRIR spectra of complex **60** also features broad bands centered at 1980 cm^{-1}, which is in the same range as those seen in complex **52**, we are confident these bands are owing to C≡C stretching vibrations of the excited state species. Furthermore, the TRIR

spectrum of these complexes strongly suggest delocalization of the excited electrons extends to the conjugated substituents.
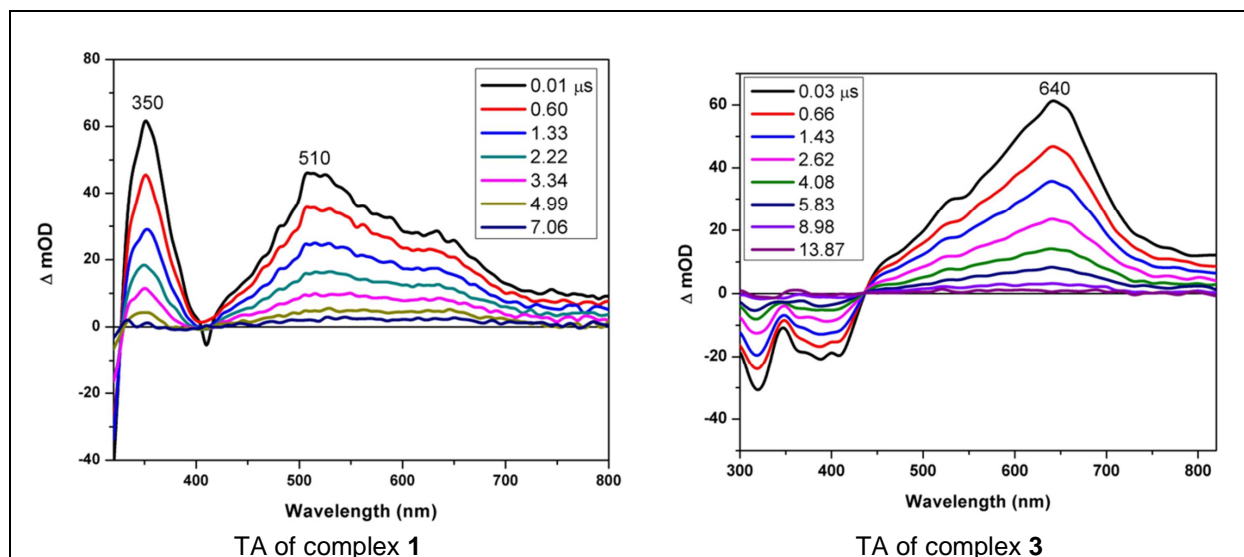
Figure 2. 14: Transient Absorbance (TA) Spectra of complex **50** (λ_{ex} = 410 nm) and **52** (λ_{ex} = 355 nm) in CH_2Cl_2. These images were used with permission from David Grills.

2.4. Conclusions and Future Work

The investigations of the redox and photophysical properties of the series of [ReBr(CO)$_3$(phen')] complexes presented here, where phen' is a 1,10-phenanthroline with increasingly conjugated π-systems attached at the 4 and 7 positions of the phenanthroline, produced interesting result. The relatively low resonance frequencies (i.e. shielded) of the phenanthroline protons in complex **51** and the geminal-anisochronicity of the two pairs of methylene protons in the hexyl chain nearest the phenanthroline, as well as the unique physical characteristics of this complex, have been tentatively attributed to the coplanar arrangement of its phenyl and phenanthroline rings and electronic contributions from the [ReBr(CO)$_3$] substrate. The hexyl groups in complex **52** may make this arrangement less favorable in **52**. However, crystal structures of these complexes would be necessary to determine the validity of this supposition.

The increased conjugation in the phenanthroline ligand in these complexes has an obvious influence on the ground state redox chemistry, and the energies of the MLCT and π-π* transitions, as well as the emission energies complexes **50** – **52**. In regards to the redox

chemistry the first reduction potential becomes increasingly positive with the extended conjugation. This trend may also hold true for the two-electron reduction process, however second reduction potentials could only be confidently measured for complexes **51** and **52**, due to the limited potential sweep range. We attribute the ease of reduction step(s) to an increase in the area of delocalization available to the additional electron in the phenanthroline ligands of the $1e^-$ reduced species and the reduction of the π^* orbital energies. It is important to note, the relatively low ground state reduction potentials for the $1\ e^-$ reduction of complexes **50** – **52** could preclude the use of these or similarly conjugated complexes as CO_2 reduction catalysts. To explore this concern further, electrochemical measurements can be repeated under CO_2 atmosphere to test for CO_2 reduction.[270-272]

Energies of the electronic absorptions are also influenced by the conjugation shifting toward the red for both the MLCT and $^*\pi$–π transitions. Relative to the reference complex, the emission energies of complexes **50** – **52** are also red shifted. However, among the three complexes the emission energy was largely invariant. The emission source is dominated by a phosphorescing ^{3}MLCT state, but we believe there are contributions from the ^{3}IL excited states as well. To further explore the nature of the radiative decay in these species, emission studies could be repeated for rigid solutions at cryogenic temperatures (i.e. 77 K). Low temperature emission results will also allow us to calculate the thermally induced stokes shift ΔE_s, which is quantified by the differences in the room temperature and cryogenic emission energies. Finally, quantum yields and rate constants from non-radiative and radiative decay would also be useful.

2.5. Experimental

2.5.1. General Information

Commercially available reagents and solvents were obtained from reputable chemical distributers. When necessary, toluene, triethylamine, and dichloromethane were dried using established procedures under an inert atmosphere of nitrogen or argon. All compounds were synthesized under a nitrogen environment using standard Schlenk techniques and purified via chromatography using silica gel (45–60 lm). The ^{1}H NMR spectra were recorded using Varian Gemini 2300 or Brucker NMR spectrometers at 300 MHz 400 MHz, respectively. The ^{13}C NMR spectra were recorded using a Varian Inova 400 spectrometer at 400 MHz. The specific magnetic field frequencies are indicated below in the individual procedures. The chemical shifts

were calibrated relative to the accepted resonance frequency of the NMR solvent, $CDCl_3$. FTIR measurements were recorded using Nicolet is10 spectrometer. Elemental analyses were performed by Quantitative Technologies Inc.

Cyclic voltammograms (CV) were acquired using a BAS 100B potentiostat and analyzed by BASi BAS 100W software © 1992-2000. CV experiments were performed under an inert atmosphere by bubbling Ar through solutions of the complexes and 0.1 M Tetrabutylammonium hexafluorophosphate (TBAHFP) in dichloromethane. Owing to the volatility of the solvent, the Ar was passed through dichloromethane reservoir before entering the cell chamber. Despite this precaution, a small amount of solvent evaporated from the chamber. Therefore, the actual concentrations of the complexes are higher than calculated. Polished platinum, Ag/0.01 M $AgNO_3$ (0.1 M TBAHFP in CH_2Cl_2), and glassy carbon were employed as auxiliary, reference, and working electrodes, respectively. Generally, voltammograms were recorded between −1700 to +1300 mV sweep range at 100 mV/s scan rates, and potentials are referenced against the ferrocenium/ferrocene couple.

Steady state UV-Vis spectra were obtained for 10^{-5} M solutions of the complexes in dichloromethane using a HP 8452A diode array spectrophotometer. Emission spectra were obtained for 10^{-5} M solutions of the complexes in dichloromethane following excitation into the MLCT band; using a Photon Technology International steady-state fluorescence spectrometer. Transient absorption experiments were performed using either a Continuum Powerlite 7010 pulsed Nd:YAG laser (6 ns pule width) or an Opotek Vibrant LD 355 II tunable, pulsed OPO laser (5 ns pulse width) as the excitation source. A pulsed xenon lamp was used as the probe light source. Transient absorption kinetic decay traces were obtained by passing the probe light through a monochromator (ISA model DH10) after the sample and onto a Hamamatsu R928 photomultiplier tube detector, the signal from which was digitized by a Tektronix DPO 4032 digital oscilloscope. Degassed CH_2Cl_2 solutions of complexes **50**, **51**, and **52** were excited at either 355, 410, or 425 nm. Kinetic profiles were analyzed via exponential decay fits using WaveMetrics Igor Pro 6 software. Time-resolved infrared (TRIR) experiments were performed using the same pulsed lasers as the excitation source, and a Bruker IFS 66/S time-resolved step-scan FTIR spectrometer. TRIR spectra were typically acquired with 4 cm-1 spectral resolution and 16 or 32 averages..

2.5.2. Synthesis

Ligands **53** – **55** were synthesized via procedures adapted from the literature.[152,254] Generally, this involved combining one equivalent of 4,7-dibromo-3,8-dihexyl-1,10-phenanthroline (**29**) and a small excess of ZnI_2 in mixture of dried toluene and dried triethylamine under an inert N_2 atmosphere at elevated temperatures. When the ZnI_2 was completely or mostly dissolved, the appropriate acetylene was added followed by the $Pd(PPh_3)_4$ and CuI catalysts. The resulting mixture was stirred for at least two days before the solvent was removed via rotovaporation. The crude product was redissolved in CH_2Cl_2 and washed with at least ten equivalents of KCN in aqueous solution. The organic phase, which was collected in three extractions with CH_2Cl_2, was combined and washed with distilled H_2O before being dried over anhydrous $MgSO_4$(s). Removal of CH_2Cl_2 solvent via rotovaporation preceded purification via column chromatography. Previously unreported ligands **53** and **55** were fully characterized by ^{1}H NMR, ^{13}C NMR, FTIR, and Elemental Analysis. *Vide Supra*.

The [ReBr(CO)$_3$(phen')]complexes **50** – **52** were synthesized via one of two methods: **Methods A** and **B**. The first method, **Method A** is the procedure developed in our lab for the synthesis of [ReBr(CO)$_3$(phen)] complexes and involves stirring a mixture [ReBr(CO)$_3$(dmpz)] and the appropriate phenanthroline ligand in dried toluene at elevated temperatures under an inert atmosphere for several hours.[151] The second method, **Method B** involves the coupling of [ReBr(CO)$_3$(3,8-dihexyl-4,7-dibromo-1,10-phenantroline)] (**59**) and the appropriate acetylene under Sonogashira cross-coupling conditions.[250] During Sonogashira cross-coupling reaction complex **59** and the appropriate acetylene were combined in 30 mL of dried toluene and 15 mL of dried NEt$_3$. The contents were stirred in an oil bath heated to 80 °C under N_2 atmosphere. After **59** dissolved, $Pd(PPh_3)_4$ followed by CuI were added to the reaction solution and the contents stirred for an additional eight hours before the solution was allowed to cool to room temperature and filtered. Solvent from the filtered solution was removed by rotovaporation. The residue was then dried under vacuum. The crude product was then purified on a silica gel column chromatography. Reference complex [ReBr(CO)$_3$(1,10-phenanthroline)] was prepared in 91 % yield according to **Method A**.
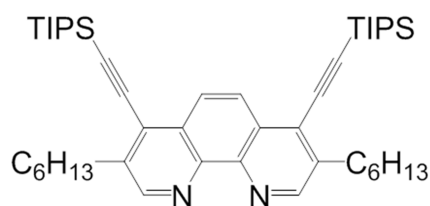
3,8-dihexyl-4,7-bis(triisopropylsilylethynyl)-1,10-phenanthroline (53): **53** was prepared using 0.506 g (0.99 mmol) of **29**, 0.8 mL (0.7 g, 3.6 mmol) of triisopropylacetylene, 0.352 g (1.10 mmol) ZnI$_2$, 0.060 g (0.05 mmol) of Pd(PPh$_3$)$_4$, 0.025 g (mmol) CuI, which was stirred for 78 hours in a 75 °C oil bath. The product mixture was subjected to the general work up procedure before purification by column chromatography using a 9:1 (v/v) mixture of hexane and ethyl acetate, which afforded 0.520 g (0.73 mmol, 73 %) of **53**. ^{1}H NMR (300 MHz, CDCl$_3$) δ 9.01 (s, 2H), 8.35 (s, 2H), 3.05 (t, J^3 = 7.8 Hz, 4H), 1.81 – 1.71 (m, 4H), 1.48 – 1.15 (comp, 54H), 0.89 – 0.84 (m, 6H); ^{13}C NMR (400 MHz, CDCl$_3$) 151.2, 144.2, 139.4, 127.9, 127.9, 125.1, 105.6, 100.7, 32.9, 31.7, 30.8, 29.3, 22.6, 18.7, 14.0, 11.3; IR (neat): 2925, 2941, 2982, 2864, 2147; Anal. Calc. for C$_{46}$H$_{72}$N$_2$Si$_2$: C, 77.90; H, 10.23; N, 3.95. Found: C, 76.57; H, 10.66; N, 3.67%.
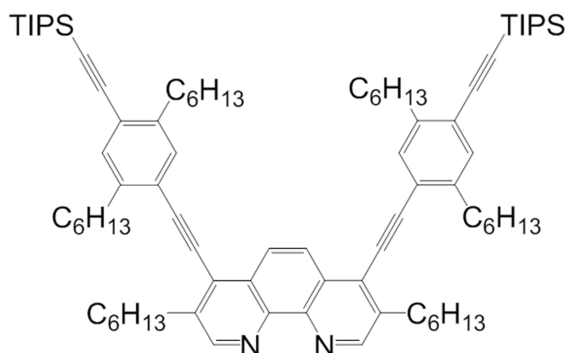
3,8-dihexyl-4,7-bis(4-triisopropylsilyl-2,5-dihexylphenyl)ethynyl)-1,10-phenanthroline (55): **55** was prepared using 0.794 g (1.57 mmol) of **29**, 1.800 g (3.99 mmol) of 4-triisopropylsilyl-2,5-dihexylphenylacetylene, 0.578 g (1.81 mmol) ZnI$_2$, 0.200 g (0.173 mmol) Pd(PPh$_3$)$_4$, 0.104 g (0.546 mmol) of CuI, and stirred for 3 days in 30 mL of NEt$_3$ at 95 °C under N$_2$. The product mixture was subjected to the general work up procedure using 1.361 g (20.90 mmol) KCN dissolved in 125 mL of water. Purification by column chromatography using a 10:1 (v/v) mixture of toluene and ethyl acetate afforded 1.878 g (1.51 mmol, 96%) of **55**. ^{1}H NMR (300

MHz, CDCl$_3$) δ 9.07 (s, 2H), 8.45 (s, 2H), 7.48 (s, 2H), 7.39 (s, 2H), 3.13 (t, J^3 = 7.8 Hz, 4H), 2.92 (t, J^3 = 8.0 Hz, 4H), 2.82 (t, J^3 = 8.0 Hz, 4H), 1.89 – 1.64 (comp, 12H), 1.50 – 1.27 (comp, 36H), 1.16 (s, 42H), 0.91 – 0.85 (m, 12H), 0.83 – 0.78 (m, 6H) ^{13}C NMR (400 MHz, CDCl$_3$) δ 151.3 (d), 144.5, 142.9, 142.2, 138.7, 133.1 (d), 132.8 (d), 128.1, 127.6, 125.0, 124.0, 121.7, 105.4, 101.4, 96.1, 88.2, 34.5, 34.4, 32.7, 31.8, 31.7, 30.9, 30.9, 30.7, 29.4, 29.3, 29.2, 22.6, 22.6, 22.6, 18.7, 14.1, 14.0, 14.0, 11.4; IR (neat): 2954, 2924, 2859, 2201, 2147; Anal. Calc. for C$_{86}$H$_{128}$N$_2$Si$_2$: C, 82.89; H, 10.35; N, 2.25. Found: C, 82.44; H, 10.70; N, 2.21%.
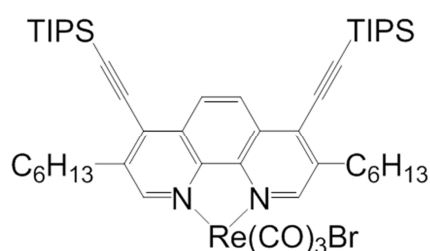
[ReBr(CO)$_3$(3,8-dihexyl-4,7-bis(triisopropylsilylethynyl)-1,10-phenantroline)] (50): **50** was prepared via **Method B** using 0.428 g (0.500 mmol) of **59** and 0.400 g (2.19 mmol) triisopropylsilylacetylene. The crude product was purified via column chromatography using a 9:1 (v/v) mixture of hexane and CH$_2$Cl$_2$. The red-orange ReI(CO)$_3$(3,8-dihexyl-4,7-bis(triisopropylsilylethynyl)-1,10-phenantroline) byproduct **50(I)** elutes before the orange target complex **50**. Both 0.366 g (0.345 mmol, 69%) of **50** and 0.009 mg (0.008 mmol) **50(I)** were recrystallized from CH$_2$Cl$_2$ and hexane.

50. ^{1}H NMR (400 MHz, CDCl$_3$) δ 9.17 (s, 2H), 8.39 (d, 2H, J = 0.48 Hz), 3.17 – 3.03 (m, 4H), 1.87 – 1.79 (m, 4H), 1.54 – 1.46 (m, 4H), 1.39 – 1.35 (comp, 8H), 1.24 (m, 42H), 0.94 – 0.90 (m, 6H); ^{13}C NMR (400 MHz, CDCl$_3$) δ 196.8, 188.9, 153.2, 145.3, 142.7, 130.6, 130.4, 126.1, 111.9, 99.0, 33.2, 31.6, 30.7, 29.5, 22.6, 18.7, 18.6, 14.0, 11.5, 11.3; IR (neat): 2942, 2928, 2865, 2160, 2017, 1912, 1880; Anal. Calc. for C$_{49}$H$_{72}$BrN$_2$O$_3$ReSi$_2$: C, 55.55; H, 6.85; N, 2.64. Found: C, 55.59; H, 7.02; N, 2.55%.

50(I): ^{1}H NMR (400 MHz, CDCl$_3$) δ 9.21 (s, 2H), 8.40 (s, 2H), 3.16 – 3.04 (m, 4H), 1.87 – 1.79 (m, 4H), 1.53 – 1.46 (m, 4H), 1.40 – 1.35 (comp, 8H), 1.24 (m, 42H), 0.93 – 0.90 (m, 6H); ^{13}C NMR (400 MHz, CDCl$_3$) δ 196.2, 188.3, 153.4, 145.2, 142.6, 130.5, 126.1, 111.9, 99.0, 33.2, 31.6, 30.7, 29.5, 22.6, 18.7, 14.0, 11.3; IR (neat): 2942, 2927, 2864, 2151, 2018, 1917, 1884;

Anal. Calc. for $C_{49}H_{72}IN_2O_3ReSi_2$: C, 53.19; H, 6.56; N, 2.53. Found: C, 53.27; H, 6.91; N, 2.51%.
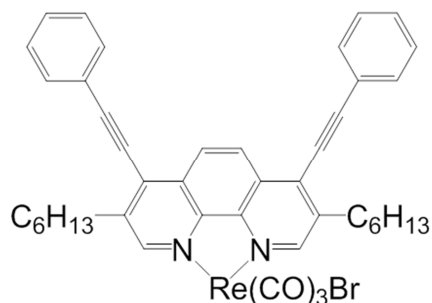
[ReBr(CO)₃(3,8-dihexyl-4,7-bis(phenylethynyl)-1,10-phenantroline)] (51): **51** was prepared via **Method A** using 0.200 g (0.492 mmol) of ReBr(CO)₅ and 0.300 g (0.547 mmol) of **54** dissolved in 30 mL toluene. The solution was stirred in an oil bath heated to 80 °C for 20 hours. After removal of the solvent via rotovaporation the product was dissolved in CH_2Cl_2/hexane (1:1 v/v) and then filtered through a 5 cm plug of silica gel. After removal of the solvent the product was recrystallized from CH_2Cl_2 and hexane to afford 0.182 g (0.202 mmol, 41%) of yellow-orange crystals of **51**. ^{1}H NMR (400 MHz, CDCl₃) δ 9.02 (s, 2H), 8.04 (s, 2H), 7.81 – 7.79 (comp, 4H), 7.57 – 7.55 (comp, 6H), 3.12 – 3.05 (m, 2H), 2.66 – 2.58 (m, 2H), 1.80 – 1.61 (m, 4H), (1.46 – 1.34 (m, 12H), 0.93 – 0.90 (m, 6H); ^{13}C NMR (400 MHz, CDCl₃) δ 197.1, 189.1, 152.7, 145.3, 141.6, 132.6, 130.7, 130.6, 129.9, 128.9, 126.2, 121.4, 107.3, 82.8, 32.8, 31.8, 31.5, 30.1, 29.3, 22.6, 14.0; IR (neat): 3055, 2950, 2927, 2856, 2200(overtone 2160), 2015, 1938, 1910, 1890, 1876; Anal. Calc. for $C_{43}H_{40}BrN_2O_3Re$: C, 57.45; H, 4.49; N, 3.12. Found: C, 57.94; H, 4.26; N, 2.91%.
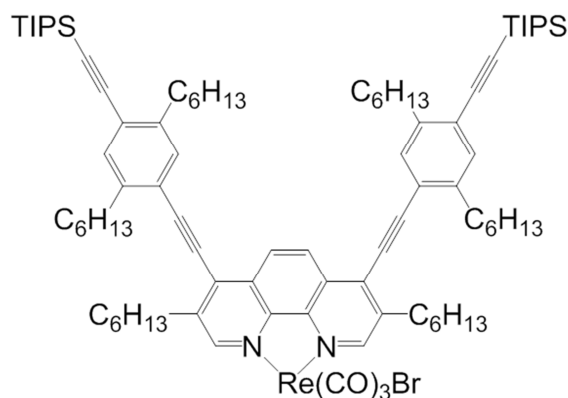
[ReBr(CO)₃(3,8-dihexyl-4,7-bis(triisopropylsilyl-2,5-dihexylphenyl)ethynyl)-1,10-phenantroline)] (52): **52** was prepared via **Method B** using 0.428 g (0.500 mmol) of **59** and 0.189 g (0.420 mmol) 4-triisopropylsilyl-2,5-dihexylphenylacetylene. Since only 0.84 equivalents of the acetylene was reacted with one equivalent of the **59**, the reaction expectedly produced the monocoupled products ReBr(CO)₃(3,8-dihexyl-4-bromo-7-(4-triisopropylsilyl-2,5-dihexylphenyl)ethynyl)-1,10-phenantroline) and ReI(CO)₃(3,8-dihexyl-4-bromo-7-(4-triisopropylsilyl-2,5-dihexylphenyl)ethynyl)-1,10-phenantroline) – **52'** – in addition to product (**52**) and anticipated iodo byproduct ReI(CO)₃(3,8-dihexyl-4,7-bis(triisopropylsilylethynyl)-1,10-phenantroline) – **52(I)**. The crude product mixture was resolved via column chromatography using hexane/ethyl acetate (9:1 v/v) as the eluent. Owing to the limited solubility of the products in the eluent solvent, 250 mL of the warm hexane ethyl acetate mixture was added to crude product in several portions before the combined extracts were applied to the column. Iodo complexes ReI(CO)₃(3,8-dihexyl-4-bromo-7-(4-triisopropylsilyl-2,5-dihexylphenyl)ethynyl)-1,10-phenantroline) and ReI(CO)₃(3,8-dihexyl-4,7-bis(triisopropylsilylethynyl)-1,10-phenantroline), eluted before the corresponding bromo complexes. Residues of the individual product fractions were next recrystallized from CH_2Cl_2 and hexane. This afforded 0.133 g (0.109 mmol, 22%) of the orange monocoupled product and 0.089 mg (0.056 mmol, 11%) of the red-orange complex **52**. Only a few mg each of the red-orange iodo complexes were recovered from the mother liquor.

52: ^{1}H NMR (400 MHz, CDCl₃) δ 9.20 (s, 2H), 8.48 (s, 2H), 7.49 (s, 2H), 7.41 (s, 2H), 3.24 – 3.10 (m, 4H), 2.91 (t, J^3 = 7.8 Hz, 4H), 2.83 (t, J^3 = 8.0 Hz, 4H), 1.94 – 1.86 (m, 4H), 1.79 – 1.66 (comp, 8H), 1.58 – 1.28 (m, 42H + H₂O)[273], 1.18 (s, 42H), 0.93 – 0.88 (m, 12H), 0.85 – 0.82 (m, 6H); ^{13}C NMR (400 MHz, CDCl₃) δ 196.8, 189.1, 153.1, 145.5, 143.2, 142.6, 141.9, 133.3, 133.0, 131.0, 130.1, 126.0, 125.1, 120.5, 106.3, 105.1, 97.2, 86.7, 34.5, 33.0, 31.8, 31.8, 31.6, 31.0, 30.9, 30.5, 29.5, 29.4, 29.4, 22.7, 22.6, 22.6, 18.7, 14.1, 14.1, 14.0, 11.4; IR (neat): 2955, 2926, 2861, 2192, 2149, 2018, 1924, 1899 cm^{-1}; Anal. Calc. for $C_{89}H_{128}BrN_2O_3ReSi_2$: C, 66.97; H, 8.08; N, 1.75. Found: C, 67.04; H, 8.53; N, 1.67%.

52(I): ^{1}H NMR (400 MHz, CDCl₃) δ 9.24 (s, 2H), 8.48 (s, 2H), 7.48 (s, 2H), 7.41 (s, 2H), 3.22 – 3.10 (m, 4H), 2.91 (t, J^3 = 8.0 Hz, 4H), 2.83 (t, J^3 = 7.8 Hz, 4H), 1.94 – 1.86 (m, 4H), 1.79 – 1.66 (comp, 8H), 1.57 – 1.26 (m, 42H + H₂O)[273], 1.18 (s, 42H), 0.93 – 0.88 (m, 12H), 0.85 – 0.82 (m, 6H); ^{13}C NMR (400 MHz, CDCl₃) δ 196.3, 193.3, 153.3, 145.4, 143.1, 142.6, 141.8,

133.3, 133.1, 130.8, 130.1, 126.0, 125.1, 120.5, 106.3, 105.1, 97.2, 86.8, 34.5, 33.0, 31.8, 31.8, 31.6, 31.0, 30.9, 30.5, 29.4, 29.4, 22.7, 22.6, 22.6, 22.6, 18.7, 14.1, 14.1, 14.0, 11.4; IR (neat): 2954, 2927, 2861, 2191, 2149, 2018, 1926, 1901 cm^{-1}; Anal. Calc. for $C_{89}H_{128}IN_2O_3ReSi_2$: C, 65.05; H, 7.85; N, 1.70. Found: C, 64.38; H, 7.44; N, 1.49%..

52': ^{1}H NMR (400 MHz, CDCl$_3$) δ 9.21 (s, 1H), 9.10 (s, 1H), 8.51 (d, J^3 = 9.2 Hz, 1H), 8.40 (d, J^3 = 9.2 Hz, 1H), 7.48 (s, 1H), 7.41 (s, 1H), 3.24 – 3.03 (m, 4H), 2.91 (t, J^3 = 7.8 Hz, 2H), 2.84 (t, J^3 = 8.2 Hz, 2H), 1.94 – 1.66 (m, 8H), 1.58 – 1.30 (comp, 24H + H$_2$O)[273], 1.18 (s, 21H), 0.96 – 0.87 (m, 12H); ^{13}C NMR (400 MHz, CDCl$_3$) δ 196.6, 196.6, 188.8, 153.5, 153.1, 146.0, 145.0, 143.2, 142.7, 142.2, 141.3, 133.3, 133.1, 131.1, 130.5, 130.1, 126.9, 126.8, 125.3, 120.3, 106.8, 105.0, 97.3, 86.6, 34.8, 34.5, 34.5, 33.0, 31.8, 31.6, 31.4, 31.1, 30.4, 30.5, 29.5, 29.5, 29.4, 29.4, 29.2, 22.7, 22.7, 22.6, 22.6, 18.7, 14.1, 14.1, 14.0, 14.0, 11.3; IR (neat): 2954, 2927, 2860, 2190, 2148, 2017, 1918, 1894 cm^{-1}; Anal. Calc. for $C_{58}H_{79}Br_2N_2O_3ReSi$: C, 56.80; H, 6.49; N, 2.28. Found: C, 56.80; H, 6.10; N, 2.13%.
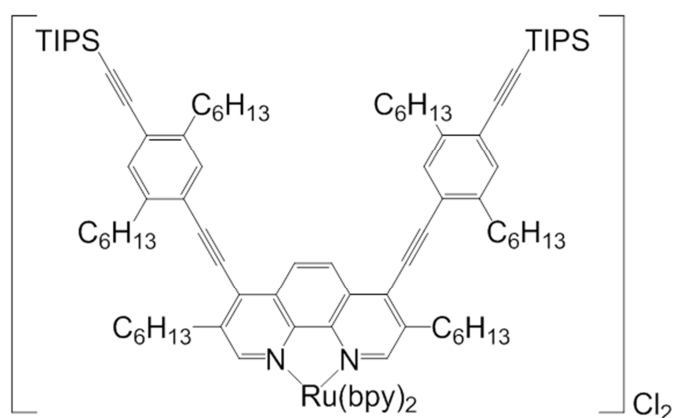
[Ru(2,2'-bipyridine)(3,8-dihexyl-4,7-bis(triisopropylsilyl-2,5-dihexylphenyl)ethynyl)-1,10-phenantroline)]Cl$_2$ 60: Complex **60** was prepared according to the established procedure[274] using 0.147 g (0.282 mmol) of Ru(2,2'-bipyridine)$_2$Cl$_2$•H$_2$O dissolved in 30 mL of ethanol and 0.234 g (0.188 mmol) of **29** dissolved in 15 mL of toluene. The two solutions were combined and refluxed for several hours before being gradually cooled to room temperature. The solvent was removed via rotovaporation, and the residue dried under vacuum. The product was recrystallized from THF solution, which afforded 0.203 g (0.117 mmol, 62 %) of **60**. ^{1}H NMR (400 MHz, CDCl$_3$) δ 9.23 (appt, 4H) 8.56 (s, 2H), 8.20 (m, 4H), 7.96 – 7.92 (comp, 4H), 7.48 – 7.43 (comp, 4H), 7.38 (s, 2H), 3.06 – 2.98 (m, 4H), 2.88 (t, J^3 = 7.8 Hz, 4H), 2.80 ((t, J^3 = 8.0

Hz, 4H), 1.77 – 1.58 (comp, 12H), 1.35 – 1.19 (m, 36H), 1.16 (s, 42H), 0.91 – 0.76 (comp, 18H) ; ^{13}C NMR (400 MHz, CDCl$_3$) δ 156.9, 156.8, 151.8, 151.5, 150.8, 149.1, 146.0, 143.1, 142.5, 142.4, 139.0, 138.7, 137.3, 134.9, 133.3, 133.0, 129.9, 129.7, 128.2, 127.7, 126.6, 126.0, 125.8, 125.3, 120.8, 120.2, 113.8, 107.0, 104.9, 97.4, 86.5, 34.4, 34.3, 31.7, 31.7, 31.4, 30.9, 30.8, 29.8, 29.6, 29.3, 29.2, 29.0, 22.6, 22.5, 18.6, 14.0, 14.0, 11.3

2.6. References

(151)   St. Fleur, N.; Craig, H. J.; Mayr, A.: Synthesis of alkynyl(tricarbonyl)rhenium complexes containing a lightly coordinated diamine ligand. *Inorg. Chim. Acta* **2009**, *362*, 1571-1576.

(152)   Schmittel, M.; Ammon, H.: A short synthetic route to novel, highly soluble 3,8-dialkyl-4,7-dibromo-1,10-phenanthrolines. *Synlett* **1997**, 1096-1098.

(160)   Li, M.-J.; Liu, X.; Nie, M.-J.; Wu, Z.-Z.; Yi, C.-Q.; Chen, G.-N.: New Rhenium(I) Complexes: Synthesis, Photophysics, Cytotoxicity, and Functionalization of Gold Nanoparticles for Sensing of Esterase. *Organometallics* **2012**, *31*, 4459-4466.

(161)   Odago, M. O.; Hoffman, A. E.; Carpenter, R. L.; Tse, D. C. T.; Sun, S.-S.; Lees, A. J.: Thioamide, urea and thiourea bridged rhenium(I) complexes as luminescent anion receptors. *Inorg. Chim. Acta* **2011**, *374*, 558-565.

(162)   Ng, C.-O.; Lai, S.-W.; Feng, H.; Yiu, S.-M.; Ko, C.-C.: Luminescent rhenium(I) complexes with acetylamino- and trifluoroacetylamino-containing phenanthroline ligands: Anion-sensing study. *Dalton Trans.* **2011**, *40*, 10020-10028.

(163)   Liu, Y.; Li, B.; Cong, Y.; Zhang, L.; Fan, D.; Shi, L.: Optical oxygen sensing materials based on a novel dirhenium(I) complex assembled in mesoporous silica. *J. Lumin.* **2011**, *131*, 781-785.

(164)   Louie, M.-W.; Liu, H.-W.; Lam, M. H.-C.; Lau, T.-C.; Lo, K. K.-W.: Novel Luminescent Tricarbonylrhenium(I) Polypyridine Tyramine-Derived Dipicolylamine Complexes as Sensors for Zinc(II) and Cadmium(II) Ions. *Organometallics* **2009**, *28*, 4297-4307.

(165)   Patrocinio, A. O. T.; Murakami, I. N. Y.: Photoswitches and Luminescent Rigidity Sensors Based on fac-[Re(CO)3(Me4phen)(L)]+. *Inorg. Chem. (Washington, DC, U. S.)* **2008**, *47*, 10851-10857.

(166)   Li, M.-J.; Ko, C.-C.; Duan, G.-P.; Zhu, N.; Yam, V. W.-W.: Functionalized rhenium(I) complexes with crown ether pendants derived from 1,10-phenanthroline: selective sensing for metal ions. *Organometallics* **2007**, *26*, 6091-6098.

(167)   Huynh, L.; Wang, Z.; Yang, J.; Stoeva, V.; Lough, A.; Manners, I.; Winnik, M. A.: Evaluation of Phosphorescent Rhenium and Iridium Complexes in Polythionylphosphazene Films for Oxygen Sensor Applications. *Chem. Mater.* **2005**, *17*, 4765-4773.

(168)   Higgins, B.; DeGraff, B. A.; Demas, J. N.: Luminescent Transition Metal Complexes as Sensors: Structural Effects on pH Response. *Inorg. Chem.* **2005**, *44*, 6662-6669.

(169)   Beer, P. D.; Timoshenko, V.; Maestri, M.; Passaniti, P.; Balzani, V.: Anion recognition and luminescent sensing by new ruthenium(II) and rhenium(I) bipyridyl calix[4]diquinone receptors. *Chem. Commun. (Cambridge)* **1999**, 1755-1756.

(170)   Lees, A. J.: Organometallic complexes as luminescence probes in monitoring thermal and photochemical polymerizations. *Coord. Chem. Rev.* **1998**, *177*, 3-35.

(171)   Zipp, A. P.; Sacksteder, L.; Streich, J.; Cook, A.; Demas, J. N.; DeGraff, B. A.: Luminescence of rhenium(I) complexes with highly sterically hindered α-diimine ligands. *Inorg. Chem.* **1993**, *32*, 5629-32.

(172)   Sacksteder, L.; Demas, J. N.; DeGraff, B. A.: Design of oxygen sensors based on quenching of luminescent metal complexes: Effect of ligand size on heterogeneity. *Anal. Chem.* **1993**, *65*, 3480-3.

(173)   MacQueen, D. B.; Schanze, K. S.: Cation-controlled photophysics in a rhenium(I) fluoroionophore. *J. Am. Chem. Soc.* **1991**, *113*, 6108-10.

(174)   Balasingham, R. G.; Thorp-Greenwood, F. L.; Williams, C. F.; Coogan, M. P.; Pope, S. J. A.: Biologically Compatible, Phosphorescent Dimetallic Rhenium Complexes Linked through Functionalized Alkyl Chains: Syntheses, Spectroscopic Properties, and Applications in Imaging Microscopy. *Inorg. Chem. (Washington, DC, U. S.)* **2012**, *51*, 1419-1426.

(175)   Olmon, E. D.; Hill, M. G.; Barton, J. K.: Using Metal Complex Reduced States to Monitor the Oxidation of DNA. *Inorg. Chem. (Washington, DC, U. S.)* **2011**, *50*, 12034-12044.

(176)   Louie, M.-W.; Fong, T. T.-H.; Lo, K. K.-W.: Luminescent Rhenium(I) Polypyridine Fluorous Complexes as Novel Trifunctional Biological Probes. *Inorg. Chem. (Washington, DC, U. S.)* **2011**, *50*, 9465-9471.

(177)   Lo, K. K.-W.; Zhang, K. Y.; Li, S. P.-Y.: Recent Exploitation of Luminescent Rhenium(I) Tricarbonyl Polypyridine Complexes as Biomolecular and Cellular Probes. *Eur. J. Inorg. Chem.* **2011**, *2011*, 3551-3568.

(178)   Brueckmann, N. E.; Koegel, S.; Hamacher, A.; Kassack, M. U.; Kunz, P. C.: Fluorescent Polylactides with Rhenium(bisimine) Cores for Tumour Diagnostics. *Eur. J. Inorg. Chem.* **2010**, 5063-5068.

(179)   Lo, K. K.-W.; Louie, M.-W.; Sze, K.-S.; Lau, J. S.-Y.: Rhenium(I) Polypyridine Biotin Isothiocyanate Complexes as the First Luminescent Biotinylation Reagents: Synthesis, Photophysical Properties, Biological Labeling, Cytotoxicity, and Imaging Studies. *Inorg. Chem. (Washington, DC, U. S.)* **2008**, *47*, 602-611.

(180)   Dubois, K. D.; Petushkov, A.; Garcia, C. E.; Larsen, S. C.; Li, G.: Adsorption and Photochemical Properties of a Molecular CO2 Reduction Catalyst in Hierarchical Mesoporous ZSM-5: An In Situ FTIR Study. *J. Phys. Chem. Lett.* **2012**, *3*, 486-492.

(181)   Yui, T.; Tamaki, Y.; Sekizawa, K.; Ishitani, O.: Photocatalytic reduction of CO2: from molecules to semiconductors. *Top. Curr. Chem.* **2011**, *303*, 151-184.

(182)   Takeda, H.; Ohashi, M.; Tani, T.; Ishitani, O.; Inagaki, S.: Enhanced Photocatalysis of Rhenium(I) Complex by Light-Harvesting Periodic Mesoporous Organosilica. *Inorg. Chem. (Washington, DC, U. S.)* **2010**, *49*, 4554-4559.

(183)   Takeda, H.; Koike, K.; Inoue, H.; Ishitani, O.: Development of an Efficient Photocatalytic System for CO2 Reduction Using Rhenium(I) Complexes Based on Mechanistic Studies. *J. Am. Chem. Soc.* **2008**, *130*, 2023-2031.

(184)   Sato, S.; Koike, K.; Inoue, H.; Ishitani, O.: Highly efficient supramolecular photocatalysts for CO2 reduction using visible light. *Photochem. Photobiol. Sci.* **2007**, *6*, 454-461.

(185)   Hori, H.; Ishihara, J.; Koike, K.; Takeuchi, K.; Ibusuki, T.; Ishitani, O.: Photocatalytic reduction of carbon dioxide using [fac-Re(bpy)(CO)3(4-Xpy)]+ (Xpy = pyridine derivatives). *J. Photochem. Photobiol., A* **1999**, *120*, 119-124.

(186)   Koike, K.; Hori, H.; Ishizuka, M.; Westwell, J. R.; Takeuchi, K.; Ibusuki, T.; Enjouji, K.; Konno, H.; Sakamoto, K.; Ishitani, O.: Key Process of the Photocatalytic Reduction of CO2 Using [Re(4,4'-X2-bipyridine)(CO)3PR3]+ (X = CH3, H, CF3; PR3 = Phosphorus Ligands): Dark Reaction of the One-Electron-Reduced Complexes with CO2. *Organometallics* **1997**, *16*, 5724-5729.

(187)   Hori, H.; Johnson, F. P. A.; Koike, K.; Ishitani, O.; Ibusuki, T.: Efficient photocatalytic CO2 reduction using [Re(bpy)(CO)3{P(OEt)3}]. *J. Photochem. Photobiol., A* **1996**, *96*, 171-174.

(188)   Hawecker, J.; Lehn, J. M.; Ziessel, R.: Efficient photochemical reduction of carbon dioxide to carbon monoxide by visible light irradiation of systems containing bipyridyl(halo)(tricarbonyl)rhenium or tris(bipyridyl)ruthenium dication-cobalt dication combinations as homogeneous catalysts. *J. Chem. Soc., Chem. Commun.* **1983**, 536-8.

(189)   Jiang, W.; Liu, J.; Li, C.: Photochemical hydrogen evolution catalyzed by trimetallic [Re-Fe] complexes. *Inorg. Chem. Commun.* **2012**, *16*, 81-85.

(190)   Probst, B.; Guttentag, M.; Rodenberg, A.; Hamm, P.; Alberto, R.: Photocatalytic H2 Production from Water with Rhenium and Cobalt Complexes. *Inorg. Chem. (Washington, DC, U. S.)* **2011**, *50*, 3404-3412.

(191)   Wang, H.-Y.; Wang, W.-G.; Si, G.; Wang, F.; Tung, C.-H.; Wu, L.-Z.: Photocatalytic Hydrogen Evolution from Rhenium(I) Complexes to [FeFe] Hydrogenase Mimics in Aqueous SDS Micellar Systems: A Biomimetic Pathway. *Langmuir* **2010**, *26*, 9766-9771.

(192)   Probst, B.; Kolano, C.; Hamm, P.; Alberto, R.: An Efficient Homogeneous Intermolecular Rhenium-Based Photocatalytic System for the Production of H2. *Inorg. Chem. (Washington, DC, U. S.)* **2009**, *48*, 1836-1843.

(193)   Fihri, A.; Artero, V.; Pereira, A.; Fontecave, M.: Efficient H2-producing photocatalytic systems based on cyclometalated iridium- and tricarbonylrhenium-diimine photosensitizers and cobaloxime catalysts. *Dalton Trans.* **2008**, 5567-5569.

(194)   Lam, S.-T.; Wang, G.; Yam, V. W.-W.: Luminescent Metallogels of Alkynylrhenium(I) Tricarbonyl Diimine Complexes. *Organometallics* **2008**, *27*, 4545-4548.

(195)   Lam, S.-T.; Yam, V. W.-W.: Synthesis, characterisation and photophysical study of alkynylrhenium(I) tricarbonyl diimine complexes and their metal-ion coordination-assisted metallogelation properties. *Chem.--Eur. J.* **2010**, *16*, 11588-11593, S11588/1-S11588/5.

(196)   Liu, X.; Xia, H.; Gao, W.; Wu, Q.; Fan, X.; Mu, Y.; Ma, C.: New rhenium(I) complexes with substituted diimine ligands for highly efficient phosphorescent devices fabricated by a solution process. *J. Mater. Chem.* **2012**, *22*, 3485-3492.

(197)   Lundin, N. J.; Blackman, A. G.; Gordon, K. C.; Officer, D. L.: Synthesis and characterization of a multicomponent rhenium(I) complex for application as an OLED dopant. *Angew. Chem., Int. Ed.* **2006**, *45*, 2582-2584.

(198)   Wong, K. M.-C.; Lam, S. C.-F.; Ko, C.-C.; Zhu, N.; Yam, V. W.-W.; Roue, S.; Lapinte, C.; Fathallah, S.; Costuas, K.; Kahlal, S.; Halet, J.-F.: Electroswitchable Photoluminescence Activity: Synthesis, Spectroscopy, Electrochemistry, Photophysics, and X-ray Crystal and Electronic Structures of [Re(bpy)(CO)3(C≡C-C6H4-C≡C)Fe(C5Me5)(dppe)][PF6]n (n = 0, 1). *Inorg. Chem.* **2003**, *42*, 7086-7097.

(199)   Yam, V. W.-W.; Lau, V. C.-Y.; Cheung, K.-K.: Synthesis and Photophysics of Luminescent Rhenium(I) Acetylides-Precursors for Organometallic Rigid-Rod Materials. X-ray Crystal Structures of [Re(tBu2bpy)(CO)3(tBuC≡C)] and [Re(tBu2bpy)(CO)3Cl]. *Organometallics* **1995**, *14*, 2749-53.

91

(200)   Frin, K. P. M.; Zanoni, K. P. S.; Murakami, I. N. Y.: Optomechanical trans-to-cis and cis-to-trans isomerization and unusual photophysical behavior of fac-[Re(CO)3(phen)(CNstpy)]+. *Inorg. Chem. Commun.* **2012**, *20*, 105-107.

(201)   Angelos, S.; Yang, Y.-W.; Khashab, N. M.; Stoddart, J. F.; Zink, J. I.: Dual-Controlled Nanoparticles Exhibiting AND Logic. *J. Am. Chem. Soc.* **2009**, *131*, 11344-11346.

(202)   Ashton, P. R.; Balzani, V.; Kocian, O.; Prodi, L.; Spencer, N.; Stoddart, J. F.: A Light-Fueled "Piston Cylinder" Molecular-Level Machine. *J. Am. Chem. Soc.* **1998**, *120*, 11190-11191.

(203)   Cokoja, M.; Bruckmeier, C.; Rieger, B.; Herrmann, W. A.; Kuehn, F. E.: Transformation of Carbon Dioxide with Homogeneous Transition-Metal Catalysts: A Molecular Solution to a Global Challenge? *Angew. Chem., Int. Ed.* **2011**, *50*, 8510-8537.

(204)   Olah, G. A.: Beyond oil and gas: The methanol economy. *Angew. Chem., Int. Ed.* **2005**, *44*, 2636-2639.

(205)   Olah, G. A.; Goeppert, A.; Prakash, G. K. S.: Chemical Recycling of Carbon Dioxide to Methanol and Dimethyl Ether: From Greenhouse Gas to Renewable, Environmentally Carbon Neutral Fuels and Synthetic Hydrocarbons. *J. Org. Chem.* **2009**, *74*, 487-498.

(206)   Olah, G. A.; Prakash, G. K. S.; Goeppert, A.: Anthropogenic chemical carbon cycle for a sustainable future. *J Am Chem Soc* **2011**, *133*, 12881-98.

(207)   Sakakura, T.; Choi, J.-C.; Yasuda, H.: Transformation of Carbon Dioxide. *Chem. Rev. (Washington, DC, U. S.)* **2007**, *107*, 2365-2387.

(208)   Usubharatana, P.; McMartin, D.; Veawab, A.; Tontiwachwuthikul, P.: Photocatalytic Process for CO2 Emission Reduction from Industrial Flue Gas Streams. *Ind. Eng. Chem. Res.* **2006**, *45*, 2558-2568.

(209)   Fujita, E.; Brunschwig, B. S.: Homogeneous redox catalysis in CO2 fixation. Wiley-VCH Verlag GmbH, 2001; Vol. 4; pp 88-126.

(210)   Wrighton, M.; Morse, D. L.: Nature of the lowest excited state in tricarbonylchloro-1,10-phenanthrolinerhenium(I) and related complexes. *J. Amer. Chem. Soc.* **1974**, *96*, 998-1003.

(211)   Zaman, S.; Smith, K. J.: A Review of Molybdenum Catalysts for Synthesis Gas Conversion to Alcohols: Catalysts, Mechanisms and Kinetics. *Catal. Rev.: Sci. Eng.* **2012**, *54*, 41-132.

(212)   Khodakov, A. Y.; Chu, W.; Fongarland, P.: Advances in the Development of Novel Cobalt Fischer-Tropsch Catalysts for Synthesis of Long-Chain Hydrocarbons and Clean Fuels. *Chem. Rev. (Washington, DC, U. S.)* **2007**, *107*, 1692-1744.

(213)   Petrus, L.; Noordermeer, M. A.: Biomass to biofuels, a chemical perspective. *Green Chem.* **2006**, *8*, 861-867.

(214)   Maitlis, P. M.: Fischer-Tropsch, organometallics, and other friends. *J. Organomet. Chem.* **2004**, *689*, 4366-4374.

(215)   Van, d. L. G. P.; Beenackers, A. A. C. M.: Kinetics and selectivity of the Fischer-Tropsch synthesis: a literature review. *Catal. Rev. - Sci. Eng.* **1999**, *41*, 255-318.

(216)   Maitlis, P. M.; Quyoum, R.; Long, H. C.; Turner, M. L.: Towards a chemical understanding of the Fischer-Tropsch reaction: alkene formation. *Appl. Catal., A* **1999**, *186*, 363-374.

(217)   Kumar, A.; Sun, S.-S.; Lees, A. J.: Photophysics and photochemistry of organometallic rhenium diimine complexes. *Top. Organomet. Chem.* **2010**, *29*, 1-35.

(218) Long, C.: Photophysics of CO loss from simple metal carbonyl complexes. *Top. Organomet. Chem.* **2010**, *29*, 37-71.

(219) Vlcek, A., Jr.: Ultrafast excited-state processes in Re(I) carbonyl-diimine complexes: from excitation to photochemistry. *Top. Organomet. Chem.* **2010**, *29*, 73-114.

(220) Stufkens, D. J.: The remarkable properties of α-diimine rhenium tricarbonyl complexes in their metal-to-ligand charge-transfer (MLCT) excited states. *Comments Inorg. Chem.* **1992**, *13*, 359-85.

(221) El, N. A.; Consani, C.; Blanco-Rodriguez, A. M.; Lancaster, K. M.; Braem, O.; Cannizzo, A.; Towrie, M.; Clark, I. P.; Zalis, S.; Chergui, M.; Vlcek, A.: Ultrafast Excited-State Dynamics of Rhenium(I) Photosensitizers [Re(Cl)(CO)3(N,N)] and [Re(imidazole)(CO)3(N,N)]+: Diimine Effects. *Inorg. Chem. (Washington, DC, U. S.)* **2011**, *50*, 2932-2943.

(222) Blanco-Rodriguez, A. M.; Busby, M.; Gradinaru, C.; Crane, B. R.; Di, B. A. J.; Matousek, P.; Towrie, M.; Leigh, B. S.; Richards, J. H.; Vlcek, A., Jr.; Gray, H. B.: Excited-state dynamics of structurally characterized [ReI(CO)3(phen)(HisX)]+ (X = 83, 109) Pseudomonas aeruginosa azurins in aqueous solution. *J. Am. Chem. Soc.* **2006**, *128*, 4365-4370.

(223) Pomestchenko, I. E.; Polyansky, D. E.; Castellano, F. N.: Influence of a Gold(I)-Acetylide Subunit on the Photophysics of Re(Phen)(CO)3Cl. *Inorg. Chem.* **2005**, *44*, 3412-3421.

(224) Gabrielsson, A.; Matousek, P.; Towrie, M.; Hartl, F.; Zalis, S.; Vlcek, A., Jr.: Excited States of Nitro-Polypyridine Metal Complexes and Their Ultrafast Decay. Time-Resolved IR Absorption, Spectroelectrochemistry, and TD-DFT Calculations of fac-[Re(Cl)(CO)3(5-Nitro-1,10-phenanthroline)]. *J. Phys. Chem. A* **2005**, *109*, 6147-6153.

(225) Busby, M.; Matousek, P.; Towrie, M.; Clark, I. P.; Motevalli, M.; Hartl, F.; Vlcek, A., Jr.: Rhenium-to-Benzoylpyridine and Rhenium-to-Bipyridine MLCT Excited States of fac-[Re(Cl)(4-benzoylpyridine)2(CO)3] and fac-[Re(4-benzoylpyridine)(CO)3(bpy)]+: A Time-Resolved Spectroscopic and Spectroelectrochemical Study. *Inorg. Chem.* **2004**, *43*, 4523-4530.

(226) Dattelbaum, D. M.; Omberg, K. M.; Schoonover, J. R.; Martin, R. L.; Meyer, T. J.: Application of Time-Resolved Infrared Spectroscopy to Electronic Structure in Metal-to-Ligand Charge-Transfer Excited States. *Inorg. Chem.* **2002**, *41*, 6071-6079.

(227) Kurz, P.; Probst, B.; Spingler, B.; Alberto, R.: Ligand variations in [ReX(diimine)(CO)3] complexes: effects on photocatalytic CO2 reduction. *Eur. J. Inorg. Chem.* **2006**, 2966-2974.

(228) Yamamoto, Y.; Shiotsuka, M.; Onaka, S.: Luminescent rhenium(I)-gold(I) hetero organometallics linked by ethynylphenanthrolines. *J. Organomet. Chem.* **2004**, *689*, 2905-2911.

(229) Paolucci, F.; Marcaccio, M.; Paradisi, C.; Roffia, S.; Bignozzi, C. A.; Amatore, C.: Dynamics of the Electrochemical Behavior of Diimine Tricarbonyl Rhenium(I) Complexes in Strictly Aprotic Media. *J. Phys. Chem. B* **1998**, *102*, 4759-4769.

(230) Chen, Y.; Liu, W.; Jin, J.-S.; Liu, B.; Zou, Z.-G.; Zuo, J.-L.; You, X.-Z.: Rhenium(I) tricarbonyl complexes with bispyridine ligands attached to sulfur-rich core: Syntheses, structures and properties. *J. Organomet. Chem.* **2009**, *694*, 763-770.

(231) Tsubaki, H.; Sugawara, A.; Takeda, H.; Gholamkhass, B.; Koike, K.; Ishitani, O.: Photocatalytic reduction of CO2 using cis,trans-[Re(dmbpy)(CO)2(PR3)(PR'3)]+ (dmbpy = 4,4'-dimethyl-2,2'-bipyridine). *Res. Chem. Intermed.* **2007**, *33*, 37-48.

(232)   Baba, A. I.; Shaw, J. R.; Simon, J. A.; Thummel, R. P.; Schmehl, R. H.: The photophysical behavior of d6 complexes having nearly isoenergetic MLCT and ligand localized excited states. *Coord. Chem. Rev.* **1998**, *171*, 43-59.

(233)   Shaw, J. R.; Schmehl, R. H.: Photophysical properties of rhenium(I) diimine complexes: observation of room-temperature intraligand phosphorescence. *J. Am. Chem. Soc.* **1991**, *113*, 389-94.

(234)   Fredericks, S. M.; Luong, J. C.; Wrighton, M. S.: Multiple emissions from rhenium(I) complexes: intraligand and charge-transfer emission from substituted metal carbonyl cations. *J. Am. Chem. Soc.* **1979**, *101*, 7415-17.

(235)   Barigelletti, F.; Ventura, B.; Collin, J.-P.; Kayhanian, R.; Gaviña, P.; Sauvage, J.-P.: Electrochemical and Spectroscopic Properties of Cyclometallated and Non-Cyclometallated Ruthenium(II) Complexes Containing Sterically Hindering Ligands of the Phenanthroline and Terpyridine Families. *European Journal of Inorganic Chemistry* **2000**, *2000*, 113-119.

(236)   Si, Z.; Li, X.; Li, X.; Zhang, H.: Synthesis, photophysical properties, and theoretical studies on pyrrole-containing bromo Re(I) complex. *J. Organomet. Chem.* **2009**, *694*, 3742-3748.

(237)   Thomas, K. R. J.; Lin, J. T.; Lin, H.-M.; Chang, C.-P.; Chuen, C.-H.: Ruthenium and Rhenium Complexes of Fluorene-Based Bipyridine Ligands: Synthesis, Spectra, and Electrochemistry. *Organometallics* **2001**, *20*, 557-563.

(238)   Damrauer, N. H.; Boussie, T. R.; Devenney, M.; McCusker, J. K.: Effects of Intraligand Electron Delocalization, Steric Tuning, and Excited-State Vibronic Coupling on the Photophysics of Aryl-Substituted Bipyridyl Complexes of Ru(II). *J. Am. Chem. Soc.* **1997**, *119*, 8253-8268.

(239)   Treadway, J. A.; Loeb, B.; Lopez, R.; Anderson, P. A.; Keene, F. R.; Meyer, T. J.: Effect of Delocalization and Rigidity in the Acceptor Ligand on MLCT Excited-State Decay. *Inorg. Chem.* **1996**, *35*, 2242-6.

(240)   Strouse, G. F.; Schoonover, J. R.; Duesing, R.; Boyde, S.; Jones, W. E., Jr.; Meyer, T. J.: Influence Of Electronic Delocalization In Metal-to-Ligand Charge Transfer Excited States. *Inorg. Chem.* **1995**, *34*, 473-87.

(241)   Wallace, L.; Rillema, D. P.: Photophysical properties of rhenium(I) tricarbonyl complexes containing alkyl- and aryl-substituted phenanthrolines as ligands. *Inorg. Chem.* **1993**, *32*, 3836-43.

(242)   Worl, L. A.; Duesing, R.; Chen, P.; Della, C. L.; Meyer, T. J.: Photophysical properties of polypyridyl carbonyl complexes of rhenium(I). *J. Chem. Soc., Dalton Trans.* **1991**, 849-58.

(243)   Englman, R.; Jortner, J.: Energy gap law for radiationless transitions in large molecules. *Mol. Phys.* **1970**, *18*, 145-64.

(244)   Alstrum-Acevedo, J. H.; Brennaman, M. K.; Meyer, T. J.: Chemical Approaches to Artificial Photosynthesis. 2. *Inorg. Chem.* **2005**, *44*, 6802-6827.

(245)   Agarwal, J.; Sanders, B. C.; Fujita, E.; Schaefer, I. I. I. H. F.; Harrop, T. C.; Muckerman, J. T.: Exploring the intermediates of photochemical CO2 reduction: reaction of Re(dmb)(CO)3 COOH with CO2. *Chem. Commun. (Cambridge, U. K.)* **2012**, *48*, 6797-6799.

(246)   Agarwal, J.; Fujita, E.; Schaefer, H. F.; Muckerman, J. T.: Mechanisms for CO Production from CO2 Using Reduced Rhenium Tricarbonyl Catalysts. *J. Am. Chem. Soc.* **2012**, *134*, 5180-5186.

(247)   Fujita, E.; Muckerman, J. T.: Why Is Re-Re Bond Formation/Cleavage in [Re(bpy)(CO)3]2 Different from That in [Re(CO)5]2? Experimental and Theoretical Studies on the Dimers and Fragments. *Inorg. Chem.* **2004**, *43*, 7636-7647.

(248)   Hayashi, Y.; Kita, S.; Brunschwig, B. S.; Fujita, E.: Involvement of a Binuclear Species with the Re-C(O)O-Re Moiety in CO2 Reduction Catalyzed by Tricarbonyl Rhenium(I) Complexes with Diimine Ligands: Strikingly Slow Formation of the Re-Re and Re-C(O)O-Re Species from Re(dmb)(CO)3S (dmb = 4,4'-Dimethyl-2,2'-bipyridine, S = Solvent). *J. Am. Chem. Soc.* **2003**, *125*, 11976-11987.

(249)   Sullivan, B. P.; Bolinger, C. M.; Conrad, D.; Vining, W. J.; Meyer, T. J.: One- and two-electron pathways in the electrocatalytic reduction of carbon dioxide by fac-(2,2'-bipyridine)tricarbonylchlororhenium. *J. Chem. Soc., Chem. Commun.* **1985**, 1414-16.

(250)   Glazer, E. C.; Magde, D.; Tor, Y.: Ruthenium Complexes That Break the Rules: Structural Features Controlling Dual Emission. *J. Am. Chem. Soc.* **2007**, *129*, 8544-8551.

(251)   Miller, M. T.; Karpishin, T. B.: Phenylethynyl Substituent Effects on the Photophysics and Electrochemistry of [Cu(dpp)2]+ (dpp = 2,9-Diphenyl-1,10-phenanthroline). *Inorg. Chem.* **1999**, *38*, 5246-5249.

(252)   Morse, D. L.; Wrighton, M. S.: Reaction of pentacarbonylmanganese(-I) and rhenium(-I) with metal carbonyl halide derivatives. *J. Organomet. Chem.* **1977**, *125*, 71-7.

(253)   Wagner, J. R.; Hendricker, D. G.: Coordination of manganese(I) and rhenium(I) carbonyls with nitrogen heterocyclic ligands. *J. Inorg. Nucl. Chem.* **1975**, *37*, 1375-9.

(254)   Schmittel, M.; Ammon, H.: A short synthetic route to 4,7-dihalogenated 1,10-phenanthrolines with additional groups in 3,8-position. Soluble precursors for macrocyclic oligophenanthrolines. *Eur. J. Org. Chem.* **1998**, 785-792.

(255)   Schutte, M.; Kemp, G.; Visser, H. G.; Roodt, A.: Tuning the Reactivity in Classic Low-Spin d6 Rhenium(I) Tricarbonyl Radiopharmaceutical Synthon by Selective Bidentate Ligand Variation (L,L'-Bid; L,L'= N,N', N,O, and O,O' Donor Atom Sets) in fac-[Re(CO)3(L,L'-Bid)(MeOH)]n Complexes. *Inorg. Chem. (Washington, DC, U. S.)* **2011**, *50*, 12486-12498.

(256)   Haefelinger, G.; Knapp, W.; Zuschneid, T.; Dietrich, F. P.: Vinyl or isopropenyl substituents as experimental and theoretical probes for diamagnetic anisotropies of aromatic hydrocarbons. *J. Phys. Org. Chem.* **2005**, *18*, 800-817.

(257)   Viglione, R. G.; Zanasi, R.; Lazzeretti, P.: Are Ring Currents Still Useful to Rationalize the Benzene Proton Magnetic Shielding? *Org. Lett.* **2004**, *6*, 2265-2267.

(258)   Klein, A.; Kaim, W.; Waldhor, E.; Hausen, H.-D.: Different orbital occupation by an added single electron in 1,10-phenanthroline and its 3,4,7,8-tetramethyl derivative. Evidence from electron paramagnetic resonance spectroscopy of the anion radicals and of their dimesitylplatinum(II) complexes. X-Ray molecular structure of dimesityl(1,10-phenanthroline)platinum(II). *Journal of the Chemical Society, Perkin Transactions 2* **1995**, 2121-2126.

(259)   Cotton, F. A.; Daniels, L. M.; Lei, P.; Murillo, C. A.; Wang, X.: Di- and trinuclear complexes with the mono- and dianion of 2,6-bis(phenylamino)pyridine: high-field displacement of chemical shifts due to the magnetic anisotropy of quadruple bonds. *Inorg Chem* **2001**, *40*, 2778-84.

(260)   Tan, Z. F.; Liu, C. Y.; Li, Z.; Meng, M.; Weng, N. S.: Abnormally Long-Range Diamagnetic Anisotropy Induced by Cyclic dδ-pπ π Conjugation within a Six-Membered Dimolybdenum/Chalcogen Ring. *Inorg. Chem. (Washington, DC, U. S.)* **2012**, *51*, 2212-2221.

(261)   Cook, M. J.; Lewis, A. P.; McAuliffe, G. S. G.: Luminescent metal complexes. 4 - carbon-13 NMR spectra of the tris chelates of substituted 2,2'-bipyridyls and 1,10-phenanthrolines with ruthenium(II) and osmium(II). *Org. Magn. Reson.* **1984**, *22*, 388-94.

(262)   Smith, T. J., Stevenson, Keith J.: Reference Electrodes. In *Handbook of Electrochemistry*; 1st ed.; Zoski, C. G., Ed.; Elsevier: Kidlington, Oxford OX5 IGB, UK, 2007; pp 73 - 102.

(263)   Swager, T. M.; Gil, C. J.; Wrighton, M. S.: Fluorescence Studies of Poly(p-phenyleneethynylene)s: The Effect of Anthracene Substitution. *J. Phys. Chem.* **1995**, *99*, 4886-93.

(264)   Ziener, U.; Godt, A.: Synthesis and Characterization of Monodisperse Oligo(phenyleneethynylene)s. *J. Org. Chem.* **1997**, *62*, 6137-6143.

(265)   James, P. V.; Yoosaf, K.; Kumar, J.; Thomas, K. G.; Listorti, A.; Accorsi, G.; Armaroli, N.: Tunable photophysical properties of phenyleneethynylene based bipyridine ligands. *Photochem. Photobiol. Sci.* **2009**, *8*, 1432-1440.

(266)   Sudeep, P. K.; James, P. V.; Thomas, K. G.; Kamat, P. V.: Singlet and Triplet Excited-State Interactions and Photochemical Reactivity of Phenyleneethynylene Oligomers. *J. Phys. Chem. A* **2006**, *110*, 5642-5649.

(267)   Matsunaga, Y.; Takechi, K.; Akasaka, T.; Ramesh, A. R.; James, P. V.; Thomas, K. G.; Kamat, P. V.: Excited-State and Photoelectrochemical Behavior of Pyrene-Linked Phenyleneethynylene Oligomer. *J. Phys. Chem. B* **2008**, *112*, 14539-14547.

(268)   Kalyanasundaram, K.: Luminescence and redox reactions of the metal-to-ligand charge-transfer excited state of tricarbonylchloro(polypyridyl)rhenium(I) complexes. *J. Chem. Soc., Faraday Trans. 2* **1986**, *82*, 2401-15.

(269)   Polyansky, D. E.; Danilov, E. O.; Voskresensky, S. V.; Rodgers, M. A. J.; Neckers, D. C.: Delocalization of Free Electron Density through Phenylene-Ethynylene: Structural Changes Studied by Time-Resolved Infrared Spectroscopy. *J. Am. Chem. Soc.* **2005**, *127*, 13452-13453.

(270)   Portenkirchner, E.; Oppelt, K.; Ulbricht, C.; Egbe, D. A. M.; Neugebauer, H.; Knör, G.; Sariciftci, N. S.: Electrocatalytic and photocatalytic reduction of carbon dioxide to carbon monoxide using the alkynyl-substituted rhenium(I) complex (5,5′-bisphenylethynyl-2,2′-bipyridyl)Re(CO)3Cl. *Journal of Organometallic Chemistry* **2012**, *716*, 19-25.

(271)   Hawecker, J.; Lehn, J. M.; Ziessel, R.: Photochemical and electrochemical reduction of carbon dioxide to carbon monoxide mediated by (2,2'-bipyridine)tricarbonylchlororhenium(I) and related complexes as homogeneous catalysts. *Helv. Chim. Acta* **1986**, *69*, 1990-2012.

(272)   Hawecker, J.; Lehn, J.-M.; Ziessel, R.: Electrocatalytic reduction of carbon dioxide mediated by Re(bipy)(CO)3Cl (bipy = 2,2[prime or minute]-bipyridine). *Journal of the Chemical Society, Chemical Communications* **1984**, 328-330.

(273)   Gottlieb, H. E.; Kotlyar, V.; Nudelman, A.: NMR Chemical Shifts of Common Laboratory Solvents as Trace Impurities. *The Journal of Organic Chemistry* **1997**, *62*, 7512-7515.

(274)   Crosby, G. A.; Elfring, W. H.: Excited states of mixed ligand chelates of ruthenium(II) and rhodium(III). *The Journal of Physical Chemistry* **1976**, *80*, 2206-2211.

Chapter 3: Synthesis and Characterization of Alkynyl Silver and Alkynyl Rhenium Complexes

3.1. Introduction

The synthesis and Sonogashira cross-coupling of alkynyl rhenium complexes with the general formula [Re(C≡CR)(CO)$_3$(N^N)], where N^N is a N,N'-dimethylpiperazine (dmpz) or a structural derivative of 1,10-phenanthroline (phen') ligand, are essential steps in the construction of molecular cages **1** and **2** (see Figure 3.1), as described in Chapter 1 (see Chapter 1 Scheme 1.5). Specifically [Re(C≡CR)(CO)$_3$(dmpz)] complexes **33** and **34**, which were previously determined to be excellent candidates for vertical-edge building blocks,[275] will be synthesized and then each will be inserted into the 1,10-phenanthroline corners within the prisms faces. This dmpz → phen' ligand substitution reaction will produce the complementary half-prism pairs for cage **1** (i.e. **36** and **38**), as well as for \ cage **2** (i.e. **39** and **41**). See Figure 3.2. Each of the half-prisms will contain, through the ligand substitution reaction, [Re(C≡CR)(CO)$_3$(phen')] moities in which the R group is terminated by an iodinated sp^2-hybridized carbon (i.e. half-prisms **36** and **39**) or acetylene (i.e. half-prisms **38** and **41**) functionalities. In the final stages of the cages' synthesis these two pairs of half-prisms will be coupled at their [Re(C≡CR)(CO)$_3$(phen')] moieties via Sonogashira cross-coupling. To summarize, the alkynyl rhenium chemistry that is required for the synthesis of cages **1** and **2** includes: 1) the synthesis of [Re(C≡CR)(CO)$_3$(dmpz)] complexes (i.e. **33** and **34**); 2) the synthesis of [Re(C≡CR)(CO)$_3$(phen')] species (i.e. **36**, **38**, **39**, **41**) via ligand substitution of the dmpz ligands in **33** and **34**; and 3) the Sonogashira cross-coupling of these [Re(C≡CR)(CO)$_3$(phen')] species. In this vein, we sought a reliable and productive procedure for the synthesis of the alkynyl rheniums, specifically for vertical edge building block complexes **33** and **34**, as well as optimal conditions for the ligand substitution and Sonogashira cross-coupling reactions. Herein I present the contributions I made toward this endeavor.
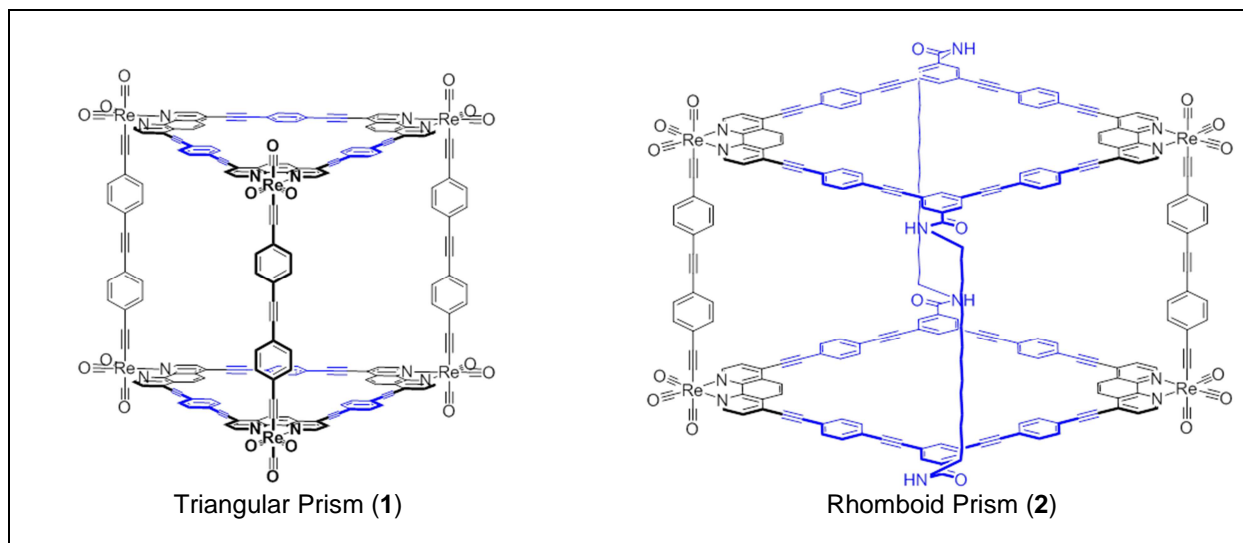
Figure 3. 1: Molecular Cages **1** and **2**.
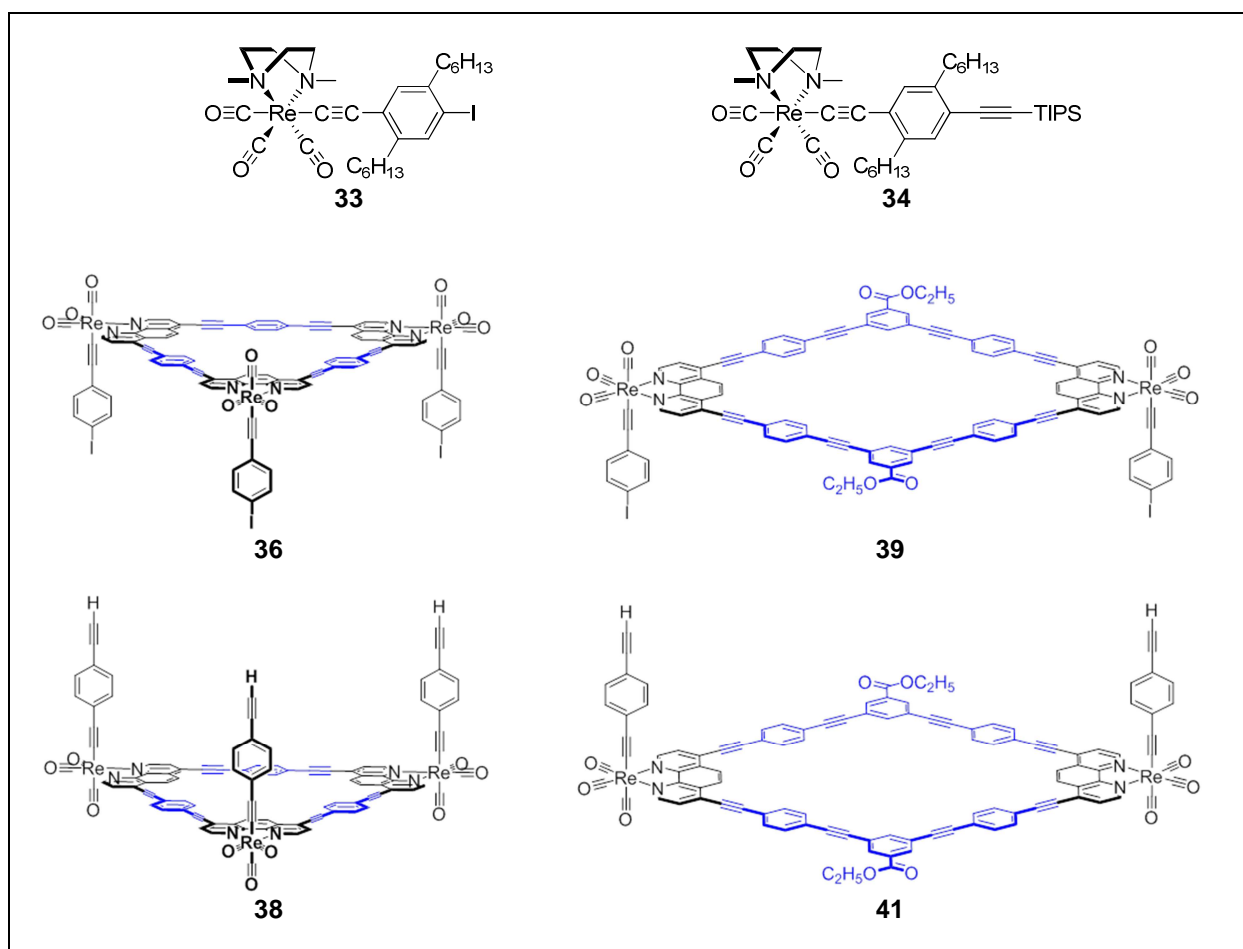
Figure 3. 2: Vertical edge building blocks **33** and **34**, and half-prisms **36**, **38**, **39**, **41**.

3.1.1. Synthesis of [Re(C≡CR)(CO)$_3$(dmpz)] complexes from [AgC≡CR] via Transmetallation

Alkynyl rhenium(I) species are attractive complexes targeted for their potential use in a molecular electronics as molecular wires[276,277] and in non-linear optics.[276,278-285] Owing to these applications, the synthesis of alkynyl rhenium complexes is a worthy albeit challenging endeavor. Some of the earliest alkynyl rhenium(I) compounds were synthesized via transmetallation of alkynyl lithium and copper reagents and rhenium(I) substrates, [ReCl(CO)$_5$][286] and [ReCl(CO)$_3$(PPh$_3$)$_2$].[287] Unfortunately, yields for these transmetallation reactions were invariably low. More reasonable yields (40 – 45%) were obtained by Vivian Yam's group, which reported synthesis of a series of [Re(C≡CR)(CO)$_3$(^{t}Bu$_2$bpy)] from the reaction of [LiC≡CR] and [ReCl(CO)$_3$(^{t}Bu$_2$bpy)], where ^{t}Bu$_2$bpy is 4,4'-di-*tert*-butyl-2,2'-bipyridine.[288] In the early 1980's, Gladysz's group produced [(η^5-C$_5$H$_5$)Re(C≡CR)(NO)(PPh$_3$)] via the reduction of rhenium acyl complexes, [(η^5-C$_5$H$_5$)Re(C(O)CH$_2$R)(NO)(PPh$_3$)]$^+$, followed by deprotonation of rhenium vinylidene [(η^5-C$_5$H$_5$)Re(=C=CHR)(NO)(PPh$_3$)]$^+$.[289] In 1992 this same group employed a similar strategy to generate [(η^5-C$_5$H$_5$)Re(C≡CCH$_3$)(NO)(PPh$_3$)] in 77% yield by producing the vinylidene from [(η^5-C$_5$H$_5$)Re(CH$_3$)(NO)(PPh$_3$)]$^+$BF$_4^-$ and propyne in the presence of acidic HBF$_4$·OEt$_2$.[290] The homodinuclear complex [(CO)$_5$Re–C≡C–Re(CO)$_5$] was produced in 64% yields from [ReFBF$_3$(CO)$_5$] and trimethylsilylacetylene by Appel et. al..[291] It is clear from these examples that the starting materials are active rhenium substrates with available coordination sites and/or alkynyls with enhanced Lewis basicity.

Perhaps the first notable advancement in the synthesis of alkynyl rhenium is the "one-pot" method developed by Vivian Yam's group.[279,283,292,293] This procedure was used to produce [Re(C≡CR)(CO)$_3$(^{t}Bu$_2$bpy)] complexes in 30 – 59 % yield from [ReCl(CO)$_3$(^{t}Bu$_2$bpy)] and the respective alkyne, in the presence of stoichiometric amounts of AgOTf. It seems the interactions between the Ag$^+$ and the alkyne and/or the in situ formation of [Re(OTf)(CO)$_3$(^{t}Bu$_2$bpy)] intermediates may drive this reaction forward. Unfortunately, the success of this reaction is highly dependent on the identity of the rhenium substrate and alkyne. For example, in the absence of electron donating groups on the bipyridyl ligand, this procedure failed to produce the rhenium alkynyl in substantial yields. In 2007, a similar reaction was reported by Gardinier and coworkers, using Tl(PF$_6$) instead of AgOTf to produce a series of [Re(C≡CR)(CO)$_3$(bpy')] from the bromo precursor [ReBr(CO)$_3$(bpy')] and aryl alkynes. Using this method, the authors

obtained yields between 30 – 81%, which were consistently greater than those obtained by the silver-assisted method. The authors suggests the electrochemical degradation pathway, viable with AgOTf, is inactive with electrochemically inert thallium.[294]

Owing to the promising results of the one-pot methodology and the fact our [Re(C≡CR)(CO)$_3$(dmpz)] targets are similar to the [Re(C≡CR)(CO)$_3$(bpy')] complexes Yam and Gardinier made via the aforementioned Ag- and Tl-mediated reactions, we attempted to synthesize model complex [Re(C≡CC$_6$H$_5$)(CO)$_3$(dmpz)] (**64**) from [ReBr(CO)$_3$(dmpz)] (**28**) and phenylacetylene using these two methods. Unfortunately, both procedures failed to produce much if any of the product. However, we did find success with the transmetallation reaction developed by our group and presented in Scheme 3.1.[151] Using this procedure, **64** was produced in 55% yield from **28** and phenylalkynyl silver (**63**), which were stirred in the presence of free dmpz ligand for three hours in a heated toluene solution. In addition to the formation of the alkynyl rhenium, the reaction also generates AgBr precipitate as a byproduct. It is believed the precipitation of the silver halide in our procedure and in Yam's one-pot alkynyl rhenium synthesis serves as the thermodynamic driving force for these reactions by enhancing the Lewis basicity of the alkynyl and assisting in the decoordination of the halide ligand from the rhenium(I) center. However, unlike in the one-pot method where the silver likely enhances the Lewis basicity of the alkynyl by coordinating to it in situ, in our transmetallation reaction the alkynyl silver is prepared ex situ and used as a reagent.

28: X = Br	55 %	eq.1
61: X = Cl	50 %	eq.2
62: X = I	65 %	eq.3
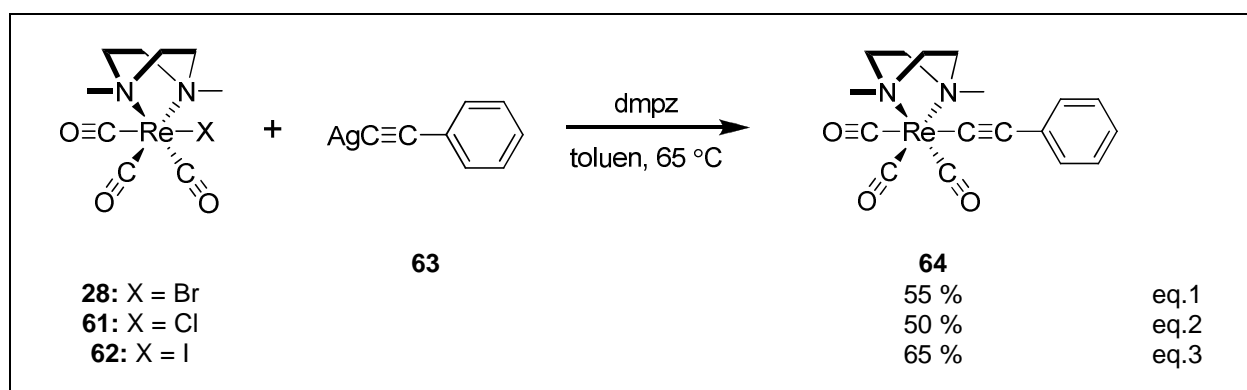
Scheme 3. 1: Synthesis of complex **64** via transmetallation from [ReX(CO)$_3$(dmpz)] complexes **28**, **61**, and **62**.

In addition to synthesizing **64** from [ReBr(CO)$_3$(dmpz)] (**28**), **64** was also produced from [ReCl(CO)$_3$(dmpz)] (**61**) and [ReI(CO)$_3$(dmpz)] (**62**) and in 50% and 65% yields, respectively.

See Scheme 3.1. The fact the chloro and iodo complexes produce **64** in the lowest and highest yields, respectively, is consistent with our belief that the reaction is facilitated by the halogenophilic behavior of the silver ion. According to Pearson's Hard and Soft Acid Base theory, the softest halide (i.e. I) should form the strongest interactions with the soft silver(I) cation, while the hardest halide (i.e. Cl) should form the weakest interactions.[295,296] Therefore, it is reasonable to suggest the silver ion may assist the reaction in two ways: driving the reaction forward through the precipitation of AgX as well as facilitating the cleavage of the Re–X bond.

Following the promising results obtained for the transmetallation synthesis of model complex **64**, we next attempted to synthesize the vertical edge buildings via this procedure. To this end, J. Craig Hili, a former member of our group, synthesized complex **33** from **28** and alkynyl silver **65**. See Scheme 3.2. Unfortunately, this reaction proved to be far less fruitful than expected, with **33** obtained in 25% yield, a little more than half the yield obtained for the synthesis of **64**. Since one of our aims, which was mentioned in the introduction section of this chapter, is to find a reliable and productive synthesis for complexes **33** and **34**, these results needed further improvement.
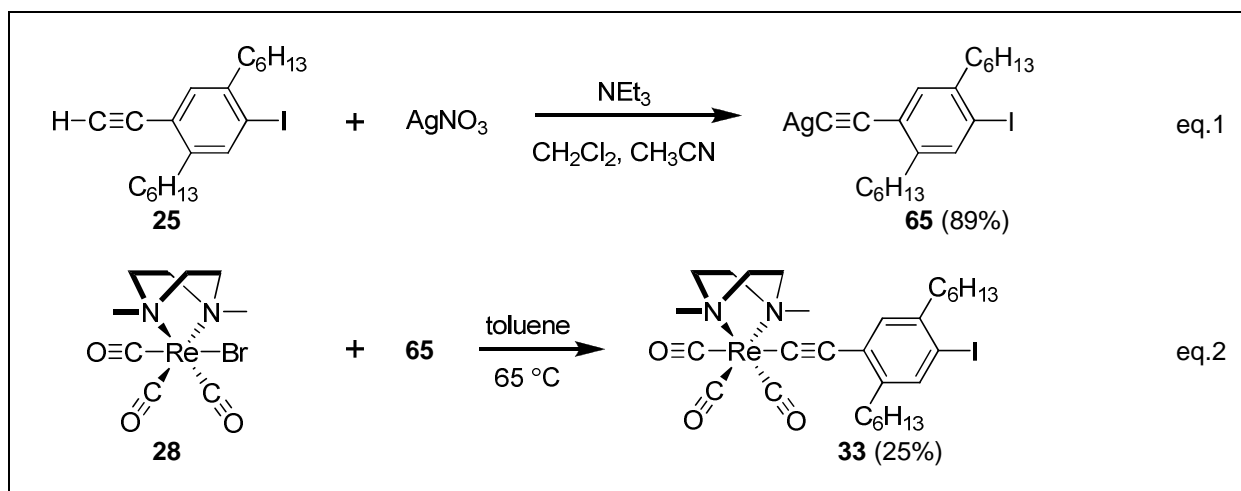
Scheme 3. 2: Synthesis of vertical edge building block complex **33** and its alkynyl silver **65** as reported by Hili.[275]

In an effort to understand why complex **33** was not produced in higher yields by transmetallation, I tried generating both vertical edge building blocks **33** and **34**. The first step in producing these species is of course synthesizing their respective alkynyl silvers. Surprisingly, the synthesis of complexes **65** and **66** proved to be extremely challenging. See Figure 3.4.

Unlike the phenylalkynyl silver (**63**), which immediately precipitates as a white powder from a basic solution of Ag^+ and phenylacetylene, **65** and **66** did not readily precipitate from their respective reaction solutions. Furthermore, the substance Hili was able to isolate from the synthesis of **65** and that he subsequently used to generate complex **33** was not a pristine powder but an oily gummy mass. Based on the crude appearance of this alkynyl silver we began to suspect the poor result for the synthesis of **33** was due to impurities in **65** and not the conditions of the transmetallation reaction. Therefore, we focused on finding better conditions to synthesize our alkynyl silvers.

3.1.2. Synthesis of alkynyl silvers.

Alkynyl silver complexes have been known since the latter half of the 19th century. Nevertheless, only recently has attention been given to their preparation as a result of waxing interests in the luminescent properties of their double salts and their synthetic utility.[297-306] These complexes have been reportedly synthesized via transmetallation of monovalent silver salts (AgL) with more electropositive metal alkynyls (e.g. Li or K)[307,308] as well as by electro-oxidation of alkynes on a silver anode.[309] The most established method for their preparation, however, is the metallation of terminal alkynes by AgL salt in a basic solution. See Scheme 3.3. In 2006 Patrick Pale's group expanded this metallation procedure and synthesized alkynyl silvers from trimethylsilylated alkynes and $AgNO_3$ or AgOTf salts.[310] Unlike the previous method, this reaction does not require a base. Under these conditions alkynyl silvers with base sensitive groups, (e.g. epoxides) or an acetylenic alcohol, which is susceptible to cyclization using $AgNO_3$ or AgOTf, could be produced. The researchers suggest the trimethylsilyl group is eliminated by Lewis base attack from the AgL anion. Yields for this procedure were reported to be comparable or better than those obtained from the former metallation process.

Method A: Y = H, Lewis Base (LB) = amine
Method B: Y = TMS, LB = silver salt anion
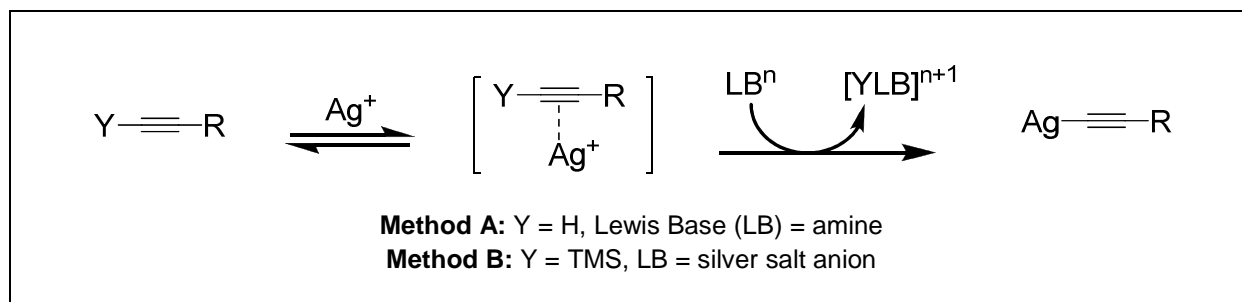
Scheme 3. 3: Metallation reaction A and B.

Both metallation reactions are believed to follow the pathway presented in Scheme 3.3. According to this mechanism, coordination of the monovalent silver cation to the alkyne activates the terminal group for attack by a Lewis base, which then cleaves the terminal group from the alkyne resulting in the alkynyl silver. In non-coordinating solvents, the alkynyl silvers will precipitate from solution by arranging themselves into a coordination polymer network, a representation of which is provided in Figure 3.3. The formation of this polymeric network and the subsequent precipitation of these complexes from solution play three key roles in the synthesis of alkynyl silvers. The precipitation of the product serves both as a convenient indicator that the reaction is complete. In addition, the formation of the precipitate helps drives the reaction toward completion. Finally, the polymeric network stabilizes the alkynyl silver, protecting it from destruction by oxidation and hydrolyzation of which other organosilver complexes and metal alkynyls are less resistant. Therefore, it seems the successful synthesis and isolation of alkynyl silvers depends on the ability of the reaction environment to facilitate network polymerization and precipitation of the alkynyl silvers, while maintaining the solvation of all other species in solution. For alkynyl silvers **65** and **66**, achieving these two criteria was quite challenging since their hexyl groups renders these complexes particularly lipophilic. Owing to their lipophilicity, **65** and **66** are soluble in many of same solvents as their parent alkyne (i.e. **25** and **27**, respectively). Consequently, we struggled to find suitable solvents for the preparation of hexylated alkynyl silvers. Hili's approach to this problem was to use a large volume of dichloromethane and acetonitrile to dissolve the alkyne and AgNO$_3$, respectively.
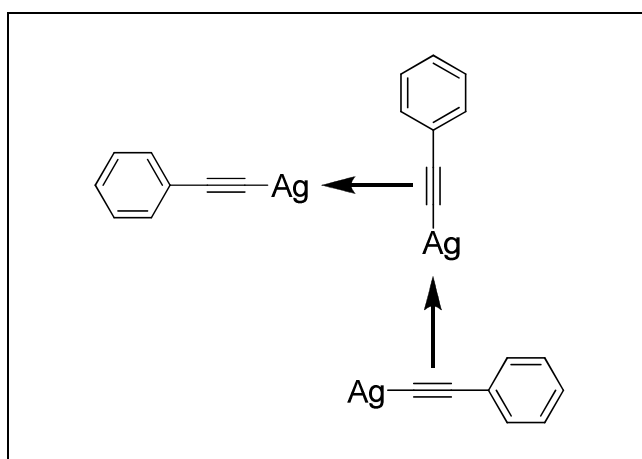
Figure 3. 3: Representation of the polymeric network of alkynyl silvers.
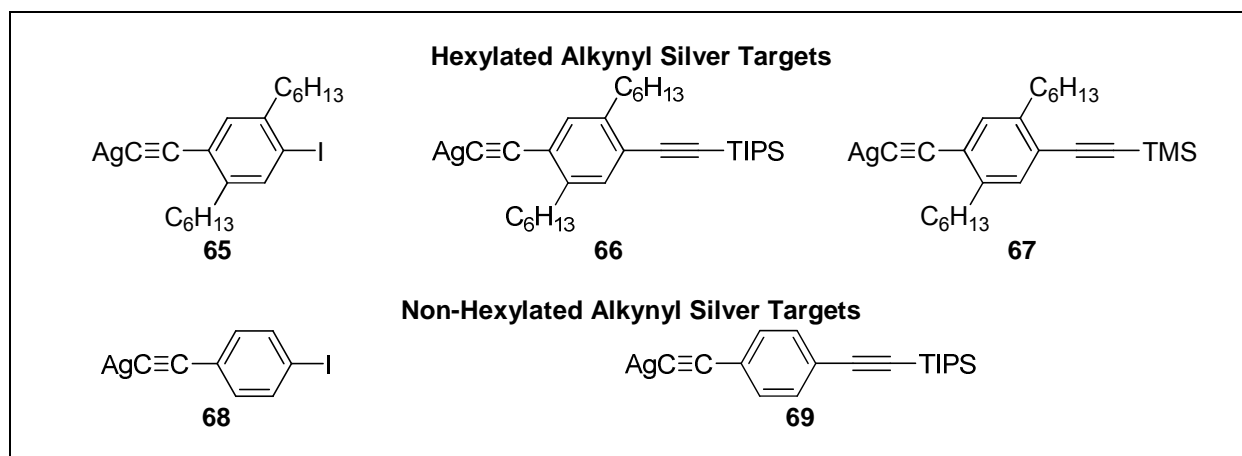
Figure 3. 4: Alkynyl silver targets **65 – 69**.

The resulting solution along with the necessary base, was stirred for 24 hours, which is significantly longer than the time usually required for this reaction. Presumably, this time is necessary because the solution's large volume may impede the synthesis of the alkynyl silver complexes and the assembly of the polymeric network. In order to isolate the product, which is dispersed in the solution as a fine colloid, Hili reduced the solvent volume by rotary evaporation. Since dichloromethane is more volatile, it evaporated first resulting in a solution that contains mostly acetonitrile as solvent. Because complex **65** is insoluble in acetonitrile but soluble in dichloromethane, Hili presumed this step caused the "precipitation" of the product from the solution.[275] However, it is more likely the reduction of the solvent volume allows the suspended precipitate (i.e. **65**) to aggregate into a single large solid mass. On the other hand, the removal of the dichloromethane from solution does appear to have a negative effect on the reaction. This aggregation appears to cause the segregation of organic substances, such as the parent alkyne (i.e. **25**) and perhaps an unidentified byproduct of **25**, from the solution. These oily organic substances, which are not soluble or miscible in acetonitrile, become trapped in the polymeric network of **65** as it aggregates into a larger mass. Consequently, the gummy mass Hili isolated from this procedure has an oily sheen and does not appear to be pristine like alkynyl silver **63**. In my own experience with this procedure, I found it impossible to maintain the miscibility of these organic substances while trying to isolate pure **65**. Therefore, I tried alternative reaction solutions and found three reliable conditions for the synthesis and isolation of alkynyl silvers **65** and **66**, as well as **67** without impurities. See Figure 3.4. The absence of impurities was

confirmed by FTIR, and ^{1}H and ^{13}C NMR characterization as well as by the successful synthesis of their respective [Re(C≡CR)(CO)$_3$(dmpz)] complexes.

3.1.2. Interesting results for the synthesis of ^{13}C-labeled [Re(C≡CR)(CO)$_3$(phen)] complexes via ligand substitution

In addition to establishing a reputable procedure for producing [Re(C≡CR)(CO)$_3$(dmpz)] complexes **33** and **34**, our goals include optimizing conditions for the synthesis of [Re(C≡CR)(CO)$_3$(phen')] complexes via ligand substitution. Fortunately, these complexes were readily and consistently produced in respectable yields (65 – 95 %) by combining [Re(C≡CR)(CO)$_3$(dmpz)] and the free (phen') ligand in a heated toluene solution. Additionally, these complexes may be generated in decent yields from alkynyl silvers and [ReBr(CO)$_3$(phen')] complexes.

In an effort to determine chemical shift assignments for the alkynyl carbons in the Re–C$_1$≡C$_2$ bond I synthesized isotopically labeled phenyl alkynyl silver [Ag^{13}C≡CC$_6$H$_5$] (**70**) and used it to produce isotopically labeled [Re(^{13}C≡CC$_6$H$_5$)(CO)$_3$(dmpz)] (**71**). Subsequently I employed **71** in the ligand substitution reaction to generate [Re(^{13}C≡CC$_6$H$_5$)(CO)$_3$(4,7-dibromo-3,8-dihexyl-1,10-phenanthroline)] (**72**). See Scheme 3.4. The ^{13}C NMR spectra of **71** clearly shows a single intense peak at 132 ppm, which is consistent with a single ^{13}C-labeled carbon. See Figure 3.5a. Based on these results we were able to assign the peaks at 132 ppm and 103 ppm to the C$_1$ and C$_2$, respectively. On the other hand, peak assignments for these same carbons in complex **72** were not so straight forward as the ^{13}C NMR spectrum features two intense peaks, one at 124 ppm and the other 105 ppm. See Figure 3.5b. These results were quite remarkable, since we expect to find one large peak as seen in the ^{13}C NMR spectra of **71**. The fact that both C$_1$ and C$_2$ are isotopically labeled carbons are present in the NMR sample of complex **72** synthesized from **71** suggests the formation of isomer [Re(C≡^{13}CC$_6$H$_5$)(CO)$_3$(4,7-dibromo-3,8-dihexyl-1,10-phenanthroline)] (**72'**). Moreover, their peak integrations suggest both isomers (i.e. **72** and **72'**) are present in equal abundance. When **72** was prepared by transmetallation only the peak at 124 ppm was found to have a strong signal, which permitted confident peak assignments for C$_1$ (i.e. 124 ppm) and C$_2$ (i.e. 105 ppm). See Figure 3.5c.
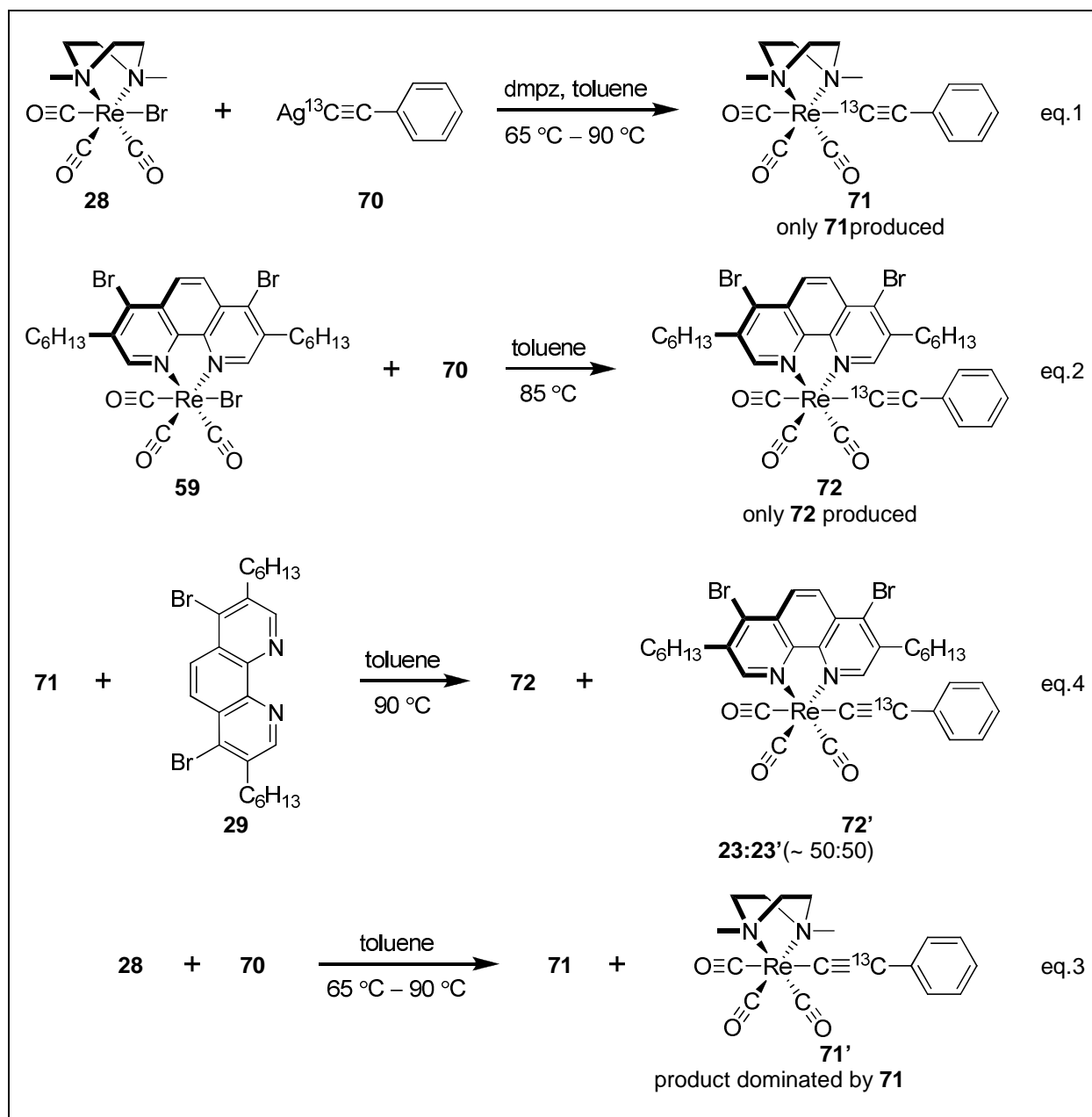
Scheme 3. 4: Synthesis of isotopically labeled alkynyl rhenium complexes **71** and **72**.
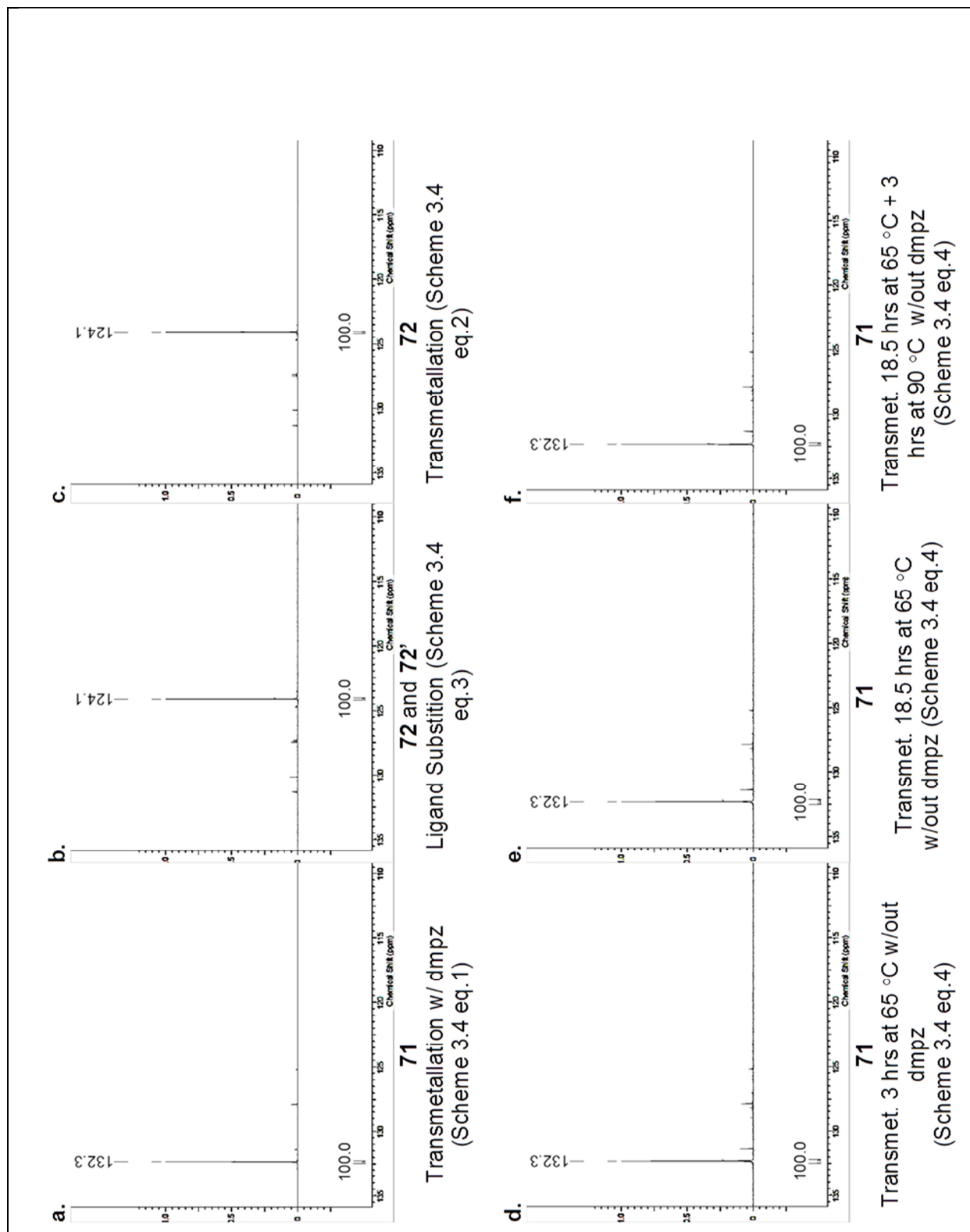
Figure 3. 5: ^{13}C NMR of products obtained in the reactions shown in Scheme 3.4.

Initially it was presumed isomer **72'** was generated through a π-coordinated alkynyl rhenium species as a result of the formation of coordinatively unsaturated Re species following decoordination of the dmpz ligand. See Scheme 3.5 and Scheme 3.6. Unlike diimine ligands such as bpy and phen, whose coordination to certain d^6 metal centers is strengthened by metal-to-ligand π-backbonding, the dmpz ligand is relatively labile and may be expected to decoordinate from the Re^I in solution. In one aspect this lability is beneficial, as it facilitates the ligand substitution reaction – i.e. [Re(C≡CR)(CO)$_3$(dmpz)] → [Re(C≡CR)(CO)$_3$(phen')]. On the other hand, coordinatively unsaturated Re^I complexes are not particularly stable and π-coordinated alkynyl rhenium species may form as a result. See Scheme 3.5. Since the phen' ligand in complex **59** and **72** is not expected to decoordinate from the Re^I centers, we speculate π-coordinated alkynyl rhenium species will not form during the transmetallation reaction of **59** and **63**; thus this reaction fails to produce **72'**. On the other hand, decoordination of the dmpz ligand complex **71**, the starting complex used in the ligand substitution reaction to produce **72**, may lead to the π-coordinated alkynyl rhenium species, which ultimately produces **72'**.
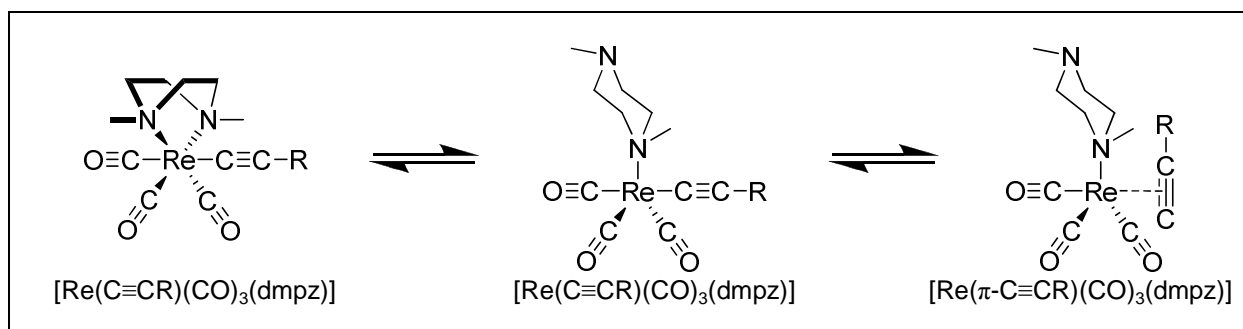
Scheme 3. 5: Formationof π-coordinated alkynyl rhenium following the decoordination of dmpz ligand.

Furthermore, we reasoned isomer **71'** was not formed when complex **28** was used to produce **71** via transmetallation, owing to the presence of free dmpz ligand in the solution, which should prevent the formation of coordinatively unsaturated species. However, when we repeated the reaction for the synthesis of **71** in the absence of dmpz, the ^{13}C NMR spectra of the product did not show any evidence of **71'** even after the reaction was stirred for 18.5 hours at 65 °C and then for an additional 3 hours at 90 °C (i.e. the temperature of the ligand substitution reaction). Currently, it is unclear what pathway may lead to the formation of isomer **72'**. However, it appears the isomers are only generated in the ligand substitution reaction not the transmetallation

reaction. Thus it appears that decoordination of the dmpz does not leads to potentially troublesome π-coordinated alkynyl rhenium.
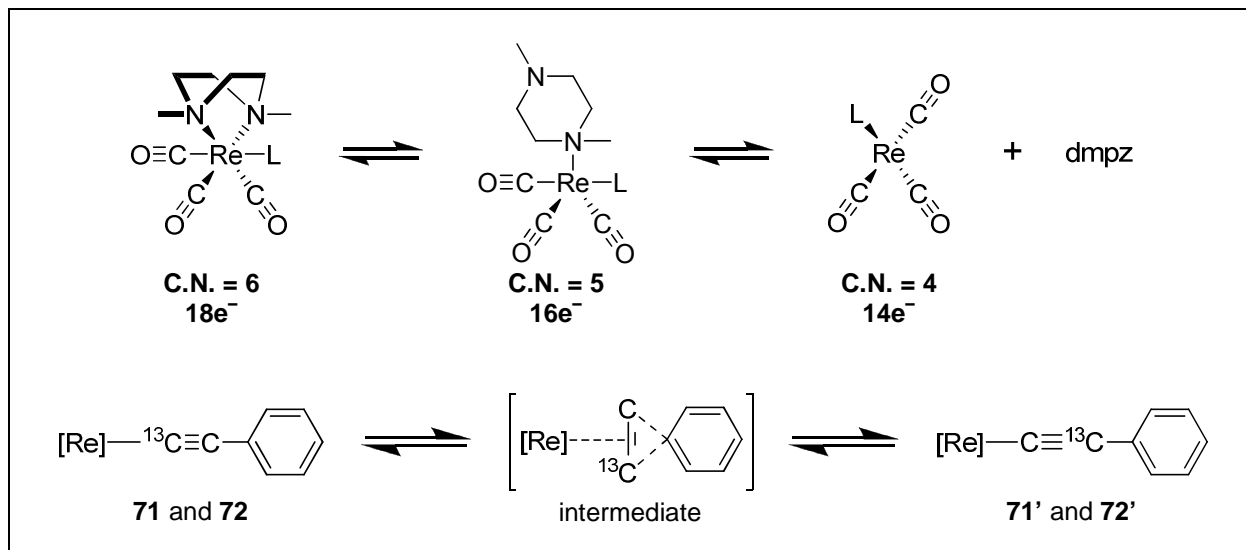
Scheme 3. 6: Possible intermediate that forms isotopically labeled isomers [Re] = [Re(CO)$_3$(dmpz)] **71'** and [Re] = [Re(CO)$_3$(phen')] **72'**.

3.1.3. Sonogashira Cross coupling of [Re(C≡CR)(CO)$_3$(N^N)] complexes

The final goal of the work presented in this chapter is to establish conditions for the Sonogashira cross-coupling of the half-prism by coupling [Re(C≡CR)(CO)$_3$(phen)] complexes. During Sonogashira coupling reactions an sp^2-hybridized carbon functionalized with a halide or triflate substituent couples to an sp-hybridized carbon in an acetylene following activation by a Pd^0-catayst and Cu^1 cocatalyst, respectively. Both the Pd- and Cu-catalytic cycles have been discussed at length, so their details will not be addressed here.[143] However, it should be noted that electron-poor halogenated or triflated sp^2 carbons are generally more reactive than electron-rich ones, because of their more favorable reactivity in the oxidative addition step in the Pd-catalyzed cycle. Likewise, iodinated and triflated sp^2 carbons perform better in the oxidative addition step than Br and Cl. Therefore reactions with brominated and particularly chlorinated species must often be heated and usually take longer to affect products. Moreover, the competing homocoupling pathway, possible through the Cu-cocatalysts, necessitates anaerobic conditions for this reaction. Finally, base is usually required to remove the acidic acetylenic protons. The ammonium salt byproduct of this acid-base chemistry sometimes precipitates from

110

the reaction solution, of course depending on the type and volume of solvent used, thus serving as a useful indicator of the reactions progress.

We have employed Sonogashira cross-coupling throughout the synthesis of the organic macrocycles we wish to use as our prisms' faces. Therefore, we are familiar with many of the characteristic nuances of this reaction. Despite this familiarity, we were unsure how our organometallic complexes would perform under those conditions. Promising results were obtained early in our studies by Hili who successfully coupled trimethylsilylacetylene to **33** thus producing **73** in 90% yield. I later repeated this reaction with triisopropylsilylacetylene and produced **34** in 96% yield. See Scheme 3.7. However, the coupling of these half-prisms involve [Re(C≡CR)(CO)$_3$(phen')] rather than [Re(C≡CR)(CO)$_3$(dmpz)] moieties. Therefore, it was important to consider any possible effects the[Re(CO)$_3$(phen)] substrate may have on the chemistry of the coupling reaction. To this end we performed some preliminary investigations of the Sonogashira cross-coupling of [Re(C≡CR)(CO)$_3$(phen)] complexes **79** and **81** and these intial results will be discussed.
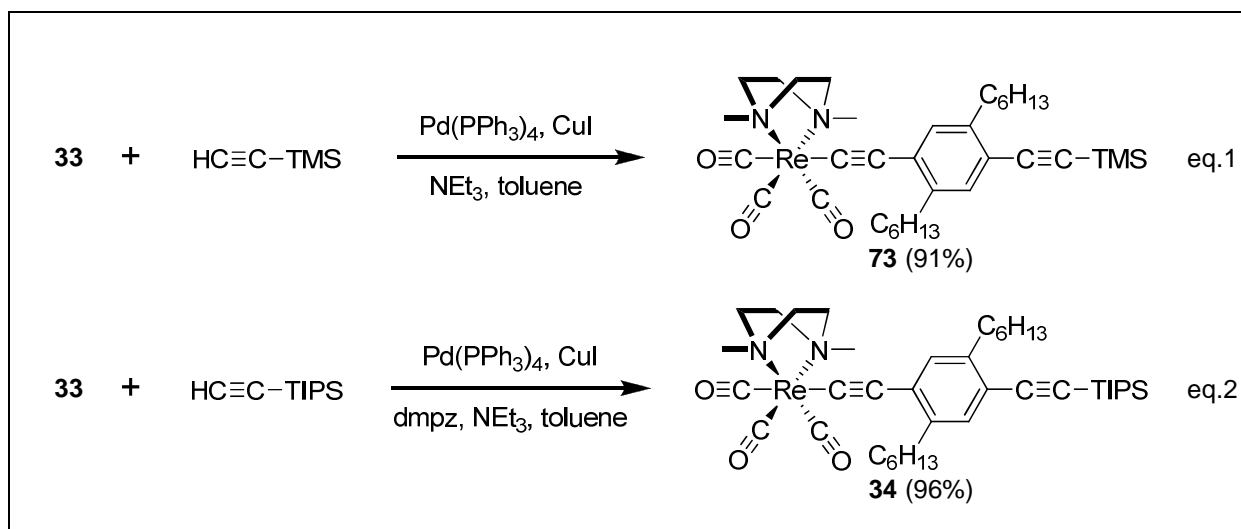
Scheme 3. 7: Sonogashira cross-coupling of complex **3**.

3.2. Results and Discussion

3.2.1. Synthesis and characterization of alkynyl silvers without hexyl substituents and their respective alkynyl rheniums

The lipophilicity caused by the hexyl groups in complexes **65 – 67** have been blamed for impeding coordination polymerizaiton and precipitation of these alkynyls silvers in acetonitrile. The justification for this assessment has been provided in the introduction section of this chapter. However, it is important that we rule out any effects the iodo and triisopropylsilylethynyl substituents may have on the synthesis of alkynyl silvers and on the synthesis of subsequently formed alkynyl rhenium. Therefore, before further exploring suitable reaction conditions for the hexylated alkynyls I first generated their non-hexylated analogs (i.e. **68** and **69**). See Figure 3.4 and Scheme 3.8. These complexes precipitated immediately as an off-white powdery solids from the acetonitrile solution containing their parent alkyne, $AgNO_3$, and NEt_3 in much the same way as phenylalkynyl silver (**63**). Both **68** and **69** were isolated effortlessly via filtration and then characterized by FTIR. The FTIR spectra for these alkynyl silver complexes are void of the H–C$\equiv$ stretching frequency near 3400 cm^{-1}, which confirms both samples are free of their respective parent alkynes. The C$\equiv$C stretching frequencies for the argentated alkynyl in **68** and **69** are found at 2034 and 2019 cm^{-1}, respectively. As expected, these vibrational frequencies are lower in energy than the C$\equiv$C stretching frequency of the terminal alkyne in **74** and **75**, which are

57: R = H	**63:** R = H (91%)	**64:** R = H (55%) overall yield = 50% eq.1
74: R = I	**68:** R = I (87%)	**76:** R = I (52%) overall yield = 45% eq.2
75: R = C$\equiv$CTIPS	**69:** R = C$\equiv$CTIPS (95%)	**77:** R = C$\equiv$CTIPS (54 %) overall yield = 51% eq.3
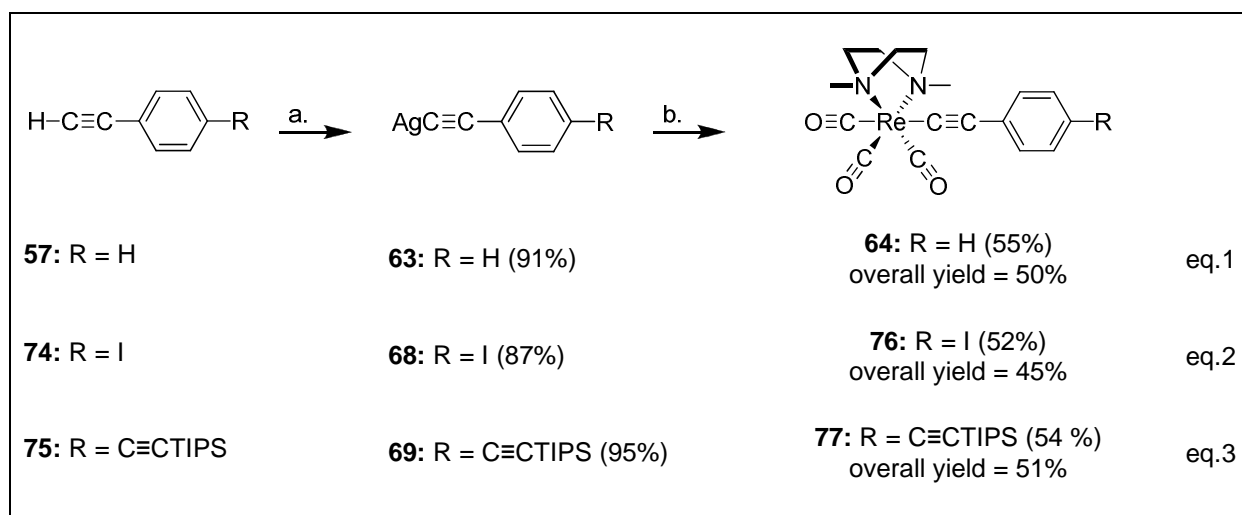
Scheme 3. 8: Synthesis of non-hexylated alkynyl silvers (**63**, **68**, and **69**) and alkynyl rhenium complexes (**64**, **76**, and **77**).

found at 2103 cm^{-1} and 2110, respectively. In addition to the C≡C stretch in the AgC≡C bond, the FTIR spectra of complex **69** also features a C≡C stretching vibration corresponding the triisopropylsilylated alkyne at 2152 cm^{-1}, which is nearly the same as the same SiC≡C stretching vibration in **27** (i.e. 2151 cm^{-1}). Following the satisfactory results of the FTIR characterization, alkynyl silvers **68** and **69** were used to make **76** in 52% and **77** in 54% yields, respectively. The alkynyl rhenium complexes were fully characterized by ^{1}H NMR, ^{13}C NMR, FTIR, and elemental analysis as previously discussed.[151] The yields for the alkynyl silver and alkynyl rhenium complexes are comparable to those obtained for **63** and model complex **64**, respectively. Therefore, it may be concluded that the iodo substituent in alkynyl silvers **65** and **68**, as well as the trialkylsilylethynyl substituents in **66**, **67**, and **69**, do not negatively influence either the synthesis of alkynyl silver or alkynyl rhenium complexes. Moreover, based on these results we were confident we could produce **33**, **34**, and **73** in decent yields by the transmetallation reaction if we employ the right conditions for the synthesis of alkynyl silver **65 – 67**.

3.2.2. Synthesis and characterization of alkynyl silvers with hexyl substituents and their respective alkynyl rhenium complexes.

The hexylated alkynyl silvers were prepared by three methods shown in Scheme 3.9. In the first method, Method A, **65**, **66**, and **67** precipitate from a solution of AgNO$_3$ in a solvent mixture containing acetonitrile, dichloromethane, and ethanol in 78, 90, and 82% yields respectively. These conditions are similar to the previously described method used by Hili in that acetonitrile and dichloromethane are used to dissolve the silver salt and alkyne, respectively. However, unlike the previous method where the alkyne and possible organic byproducts do not maintain miscibility in the reaction solution, the ethanol helps keep both the organic and inorganic reagents solvated and only the alkynyl silver product precipitates from the solution. The precipitates were isolated as dense brown, orange, and yellow spongy solids. See Figure 3.6. In each case, the purity of the product was confirmed by FTIR. The FTIR spectra for these complexes are unremarkable. As observed in the FTIR spectra of **68** and **69**, argentation of the terminal alkyne results in a decrease in the C≡C stretch frequency of the terminal alkyne. On the other hand, the C≡C stretch of the trialkylsilylated alkynes in complexes **66** and **67** is virtually the same as in **27** and **26**, respectively. Finally, the absence of the H–C≡ stretching band between 3600 – 3400 cm^{-1} suggests our alkynyl silver complexes are free of the alkyne reagents.

Following their characterization, all three alkynyl silvers (i.e. **65** – **67**) were used to produce their corresponding alkynyl rhenium complexes (i.e. **33**, **34**, **73**) in 69, 58, and 42% respectively. These results further confirm the purity of the alkynyl silver produced by Method A.

Method A

H–C≡C–(aryl, C$_6$H$_{13}$, C$_6$H$_{13}$)–R + AgNO$_3$ $\xrightarrow[\text{CH}_2\text{Cl}_2,\ \text{CH}_3\text{CN},\ \text{EtOH}]{\text{NEt}_3}$ AgC≡C–(aryl, C$_6$H$_{13}$, C$_6$H$_{13}$)–R

25: R = I

27: R = C≡CTIPS

26: R = C≡CTMS

65: R = I (78%) eq.1
66: R = C≡CTIPS (90%) eq.2
67: R = C≡CTMS (82%) eq.3

Method B

H–C≡C–(aryl, C$_6$H$_{13}$, C$_6$H$_{13}$)–R + AgOTf $\xrightarrow[\text{acetone, EtOH}]{\text{NEt}_3}$ AgC≡C–(aryl, C$_6$H$_{13}$, C$_6$H$_{13}$)–R

25: R = I

26: R = C≡CTMS

65: R = I (102%) eq.4
67: R = C≡CTMS (63%) eq.5

Method C

H–C≡C–(aryl, C$_6$H$_{13}$, C$_6$H$_{13}$)–R + AgNO$_3$ $\xrightarrow[\text{acetone, CH}_3\text{CN}]{\text{NEt}_3}$ AgC≡C–(aryl, C$_6$H$_{13}$, C$_6$H$_{13}$)–R

25: R = I

27: R = C≡CTIPS

26: R = C≡CTMS

65: R = I (99%) eq.6
66: R = C≡CTIPS (93%) eq.7
67: R = C≡CTMS (90%) eq.8

Scheme 3. 9: Synthesis of hexylated alkynyl Silvers Methods A – C.

114
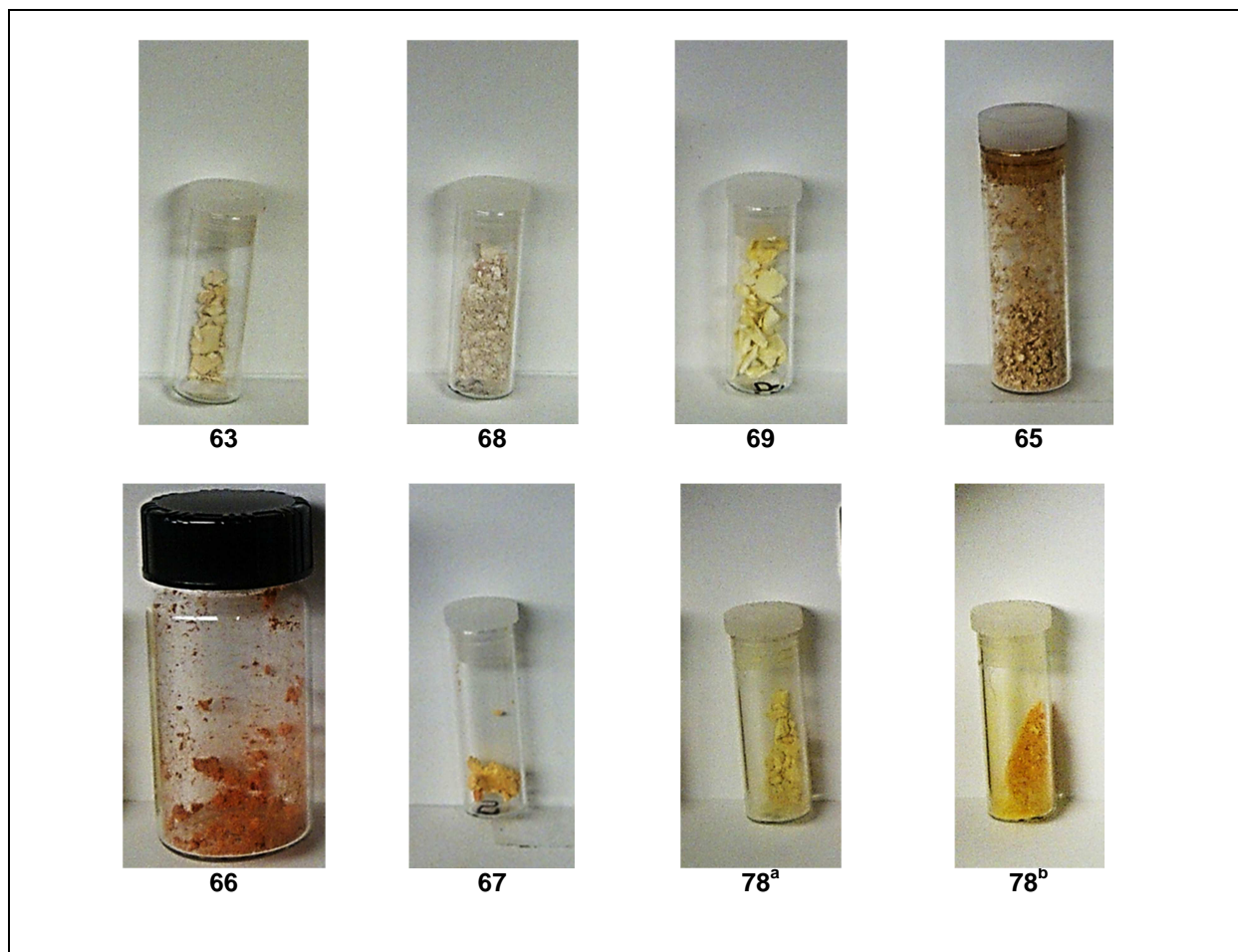
Figure 3. 6: Alkynyls silvers and the unidentified powder **78** that a) precipitates form the reaction of AgOTf in acetone and b) recovered from the supernatant after reducing the solvent volume.

Although alkynyl silvers **65**, **66**, and **67** can be cleanly isolated by Method A, it is not an effortless process. The success of this method is highly dependent on the concentration of the alkyne, which range from 0.010 – 0.016 M, and on using at least 5- to 10-fold molar excess of NEt$_3$. Moreover, the solution must consist of nearly equal parts dichloromethane and acetonitrile and at least two-and-half times as much ethanol by volume. If this latter condition is altered, the reaction fails and only the viscous oil is produced. In some instances, the reaction can be salvaged and the miscibility of the organic species can be re-established by adjusting the solvent mixture, but it is not guaranteed. In an effort to avoid the tricky solvent adjustments, we sought a more reliable method that uses a single solvent. Because a common solvent that dissolves both AgNO$_3$ and the alkyne could not be found, we decided to use the more lipophilic silver salt

AgOTf. Interestingly, when we combined the AgOTf, NEt$_3$, and the alkynes in acetone alkyne **25** decomposes immediately and alkyne **27** produces a viscous oil. Surprisingly, under these conditions alkyne **26** produces a powdery yellow precipitate (**78**) that was insoluble in most solvents. See Figure 3.6. This product, which was initially thought to be **67**, failed to produce the corresponding rhenium alkynyl complex **73**. Furthermore, the FTIR features two bands at 3307 and 2013 cm^{-1}, which are consistent with a terminal alkyne. Moreover, the absence of the C≡CTMS stretching frequency at 2152 cm^{-1} suggest the TMS group is attacked by the triflate, possibly producing 4-ethynyl-2,5-dihexylphenylethynyl silver complexes.[310] In their 2006 publication Vitérisi et. al. reports AgOTf salts generate 1-hexynylsilver from 1-trimethylsilyl-1-hexyne in protic solvents (e.g. alcohol) only.[310] Therefore, we repeated the reactions with a 1:1 acetone to ethanol solvent mixture. Through this method, known as Method B, alkynyl silvers **65** and **67**, were successfully produced. Although complex **66** was not synthesized through Method B, we anticipate it should give similar results to **65** and **67**. The major advantage of Method B over Method A is that the former is far more forgiving in regards to reagent concentrations and solvent ratios, since both AgOTf and the alkyne are soluble in acetone, and ethanol is used to prevent the silver salt from destroying the alkyne. Following FTIR characterization of these complexes, alkynyl silver **67** was used to produce **73** in 28% yield. In this case, the lower yields maybe owing to some unknown impurities.

Alkynyl silvers **65** – **67** were produced by one final method, Method C. in 99, 93, and 90% yields, respectively, as confirmed by FTIR. According to this process, the hexylated alkynyl silvers are produced using AgNO$_3$ and a 1:1 acetone to acetonitrile solvent mixture. Unlike Method B, in which acetone is a common solvent dissolving both the alkyne and the silver salt equally well, there is no common solvent in Method C. Therefore, like Method A the solvent ratios are important to the outcome of the reaction. In addition alkynyl silver **67** generated by Method C was employed in the transmetallation procedure to produce **73** in 79% yields.

In addition to the IR spectra, we were able to obtain ^{1}H and ^{13}C NMR spectra for these lipophilic complexes; this characterization was made possible by their solubility in typical NMR solvents, such as CDCl$_3$. NMR spectroscopy is not a common method for characterizing alkynyl silvers, owing to their insolubilities. However, Pale's group was able to characterize 1-hexynyl silver by ^{1}H, and ^{13}C NMR spectroscopy in in CDCl$_3$.[311] They observed the proton and carbon
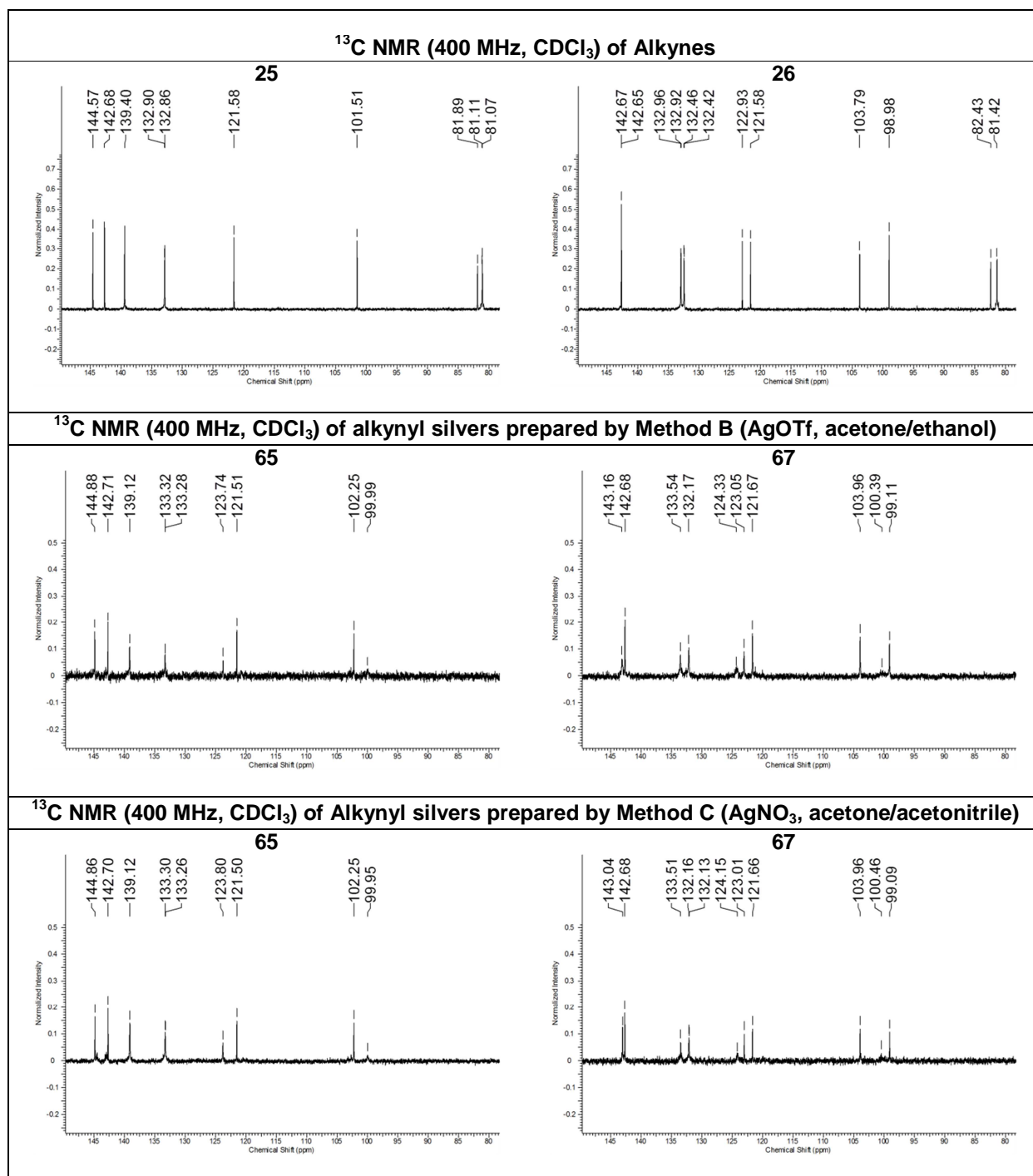
Figure 3. 7: A comparison of the ^{13}C NMR spectra of alkynes **25** and **26** with the ^{13}C NMR spectra of alkynyl silvers **65** and **67** obtained by Method B and C.

resonance frequencies of the alkynyl silvers to be downfield of the corresponding nuclei in the parent alkyne. This difference was most notable for C^2 in the $AgC^1{\equiv}C^2$ and $HC^1{\equiv}C^2$ bonds, which resonates at 129.9 ppm in 1-hexynyl silver and at 84.7 ppm in 1-hexyne. The resonance frequencies for the C^1 carbons in these bonds are also significantly different, resonating at 80.2 ppm and 68.1 ppm in the alkynyl silver and 1-hexyne, respectively. Similar differences are observed in the chemical shift of our complexes and their corresponding alkyne, with the sp-hybridized carbons in the $AgC^1{\equiv}C^2$ resonating near 100 ppm (C^1) and 124 ppm (C^2) in complexes **65 – 67**, and near 81 ppm (C^1) and 82 ppm (C^2) in compounds **25**, **26**, and **27**. See Figure 3.7.

3.2.3. Sonogashira Cross-coupling reaction.

The [Re(C≡CR)(CO)$_3$(phen)] complexes **79** and **81** were prepared in order to determine whether these complexes would couple under Sonogashira conditions. Complex **79** was synthesized in 76% yield from 3 and 1,10-phenanthroline by ligand substitution. See Scheme 3.10 eq.1. This complex was characterized by ^{1}H and ^{13}C NMR before being used to produce complex **80** by Sonogashira cross-coupling. The yields for this reaction was remarkably low (20%). See Scheme 3.10 eq.2. However the low yields were attributed to the instability of these complexes on silica gel columns during column chromatography. This attribution was based on the observation that the orange-red color of the product gradually fades during chromatography. Owing to the poor results of the previous reaction, we next attempted to produce **80** via ligand substitution from **73** and 1,10-phenanthroline. Unlike in other the coupling reactions, the products of this reaction can be obtained in sufficient purity by crystallization rather than chromatography. Through this process we were able to obtain **80** in 98% yields. This product was characterized by ^{1}H NMR. Scheme 3.10 eq.2.

Desilylation of complex **80** with KOH produced complex **81** in 83% yield. Again this complex was characterized by ^{1}H NMR. Finally, we tried to couple complexes **79** and **81**. Unfortunately, we were unable to isolate **82** by column chromatography. Again this may be owing to the fact these complexes are unstable on the column. Moreover, the complexes are not very soluble. In order to increase their solubility it may be best to repeat this reaction with hexylated 1,10-phenanthroline ligands. Of course, the 4,7-dibromo-3,8-dihexyl-1,10-phenanthroline ligand (**29**) could not be used because it also possesses sp^2-halide, the carbon of

118

which is active under Sonogashira coupling. Since we have already prepared these ligands and their corresponding complexes as discussed in Chapter 2, the synthesis of complexes **83 – 86** should be fairly straight forward.
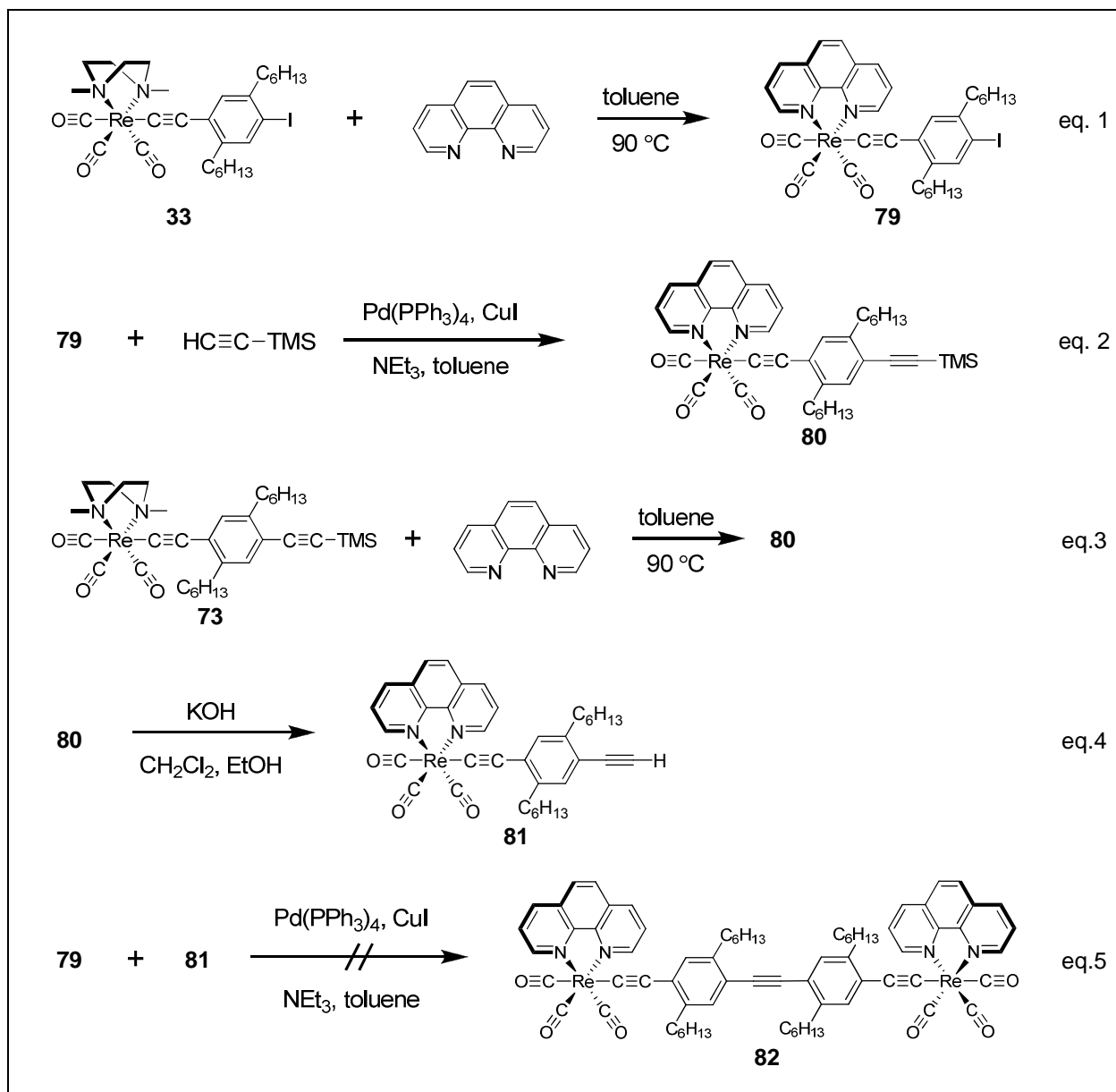
Scheme 3. 10: Synthesis and Sonogashira cross-coupling of [Re(C≡CR)(CO)$_3$(phen)] complexes **79** and **81**.

119
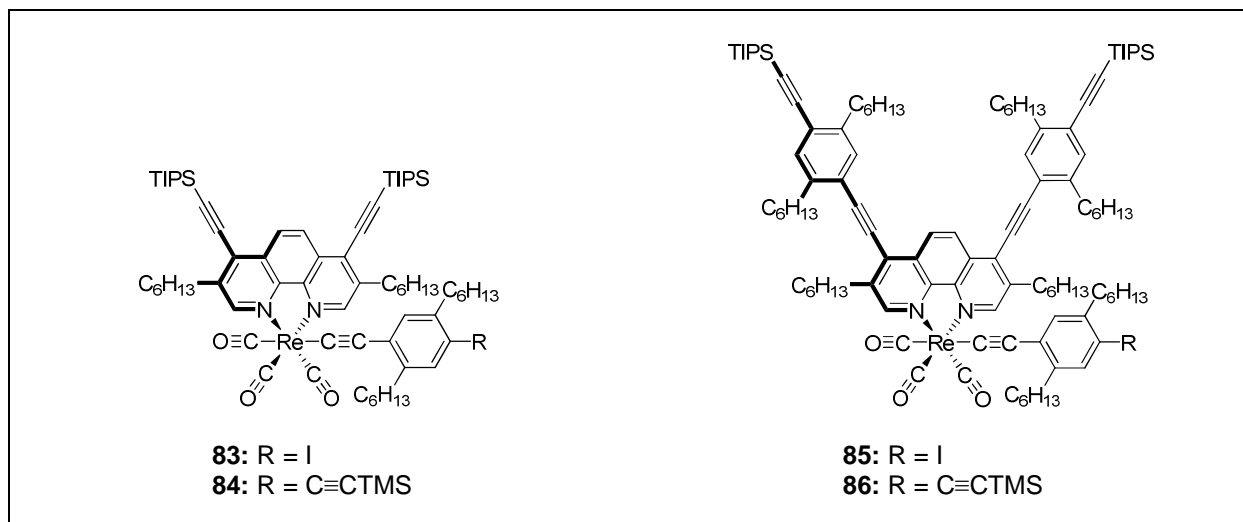
Figure 3. 8: New potential [Re(C≡CR)(CO)$_3$(phen')] complexes for Sonogashira cross-coupling **83 – 86**.

3.3. Conclusions and Future Work.

We have shown three methods for the synthesis of lipophilic alkynyl silvers **65 – 67**. All three methods employ solvent conditions that maintains miscibility of all reagents and permits precipitation of the alkynyl silver complex with decent purity. The purity of these complexes was confirmed by FTIR and supported by ^{1}H and ^{13}C NMR characterization methods. Further, these alkynyl silvers produced their corresponding alkynyl rhenium complexes in decent yields. The low yields obtained for successfully used to synthesize their respective alkynyl rhenium complexes. We have also performed Sonogashira cross-coupling reaction [Re(C≡CR)(CO)$_3$(phen')] complexes **79** and **81**. Unfortunately, this reaction failed and should be repeated with more lipophilic complexes **83 – 86**.

3.4. Experimental

3.4.1. General Information

Commercially available reagents and solvents were obtained from reputable chemical distributers. When necessary, toluene, triethylamine, and dichloromethane were dried using established procedures under an inert atmosphere of nitrogen. All compounds were synthesized under a nitrogen environment using standard Schlenk techniques and purified via chromatography using Silica gel (45–60 μm). The ^{1}H NMR spectra were recorded at 400 MHz using Varian Gemini 2300 spectrometer, and the ^{13}C NMR spectra were recorded at 400 MHz

using Varian Inova 400 spectrometer. The specific magnetic field frequency is indicated below in the individual descriptions of the results. The chemical shifts were calibrated relative to accepted resonance frequency of the NMR solvent, CDCl$_3$. FTIR spectra were recorded using Nicolet iS10 without suspending medium.

3.4.2. Synthesis of Alkynyl Silvers
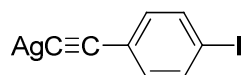
[Ag(CC-4-I-C$_6$H$_4$)] (68): To a solution containing 0.420 g (2.47 mmol) of AgNO$_3$ in 30 mL of acetonitrile was added under low-light conditions a solution containing 0.515 g (2.26 mmol) of 4-iodophenylacetylenen (**74**) and 5 mL (3.64 g, 36.0 mmol) of NEt$_3$ in 30 mL of acetonitrile. The contents were stirred in darkness for 24 h at room temperature. The white precipitate was filtered off, washed four times with ethanol, and dried under vacuum. Yield: 0.657 g (1.96 mmol), 87%. IR (KBr) 2033 (w) cm^{-1}.
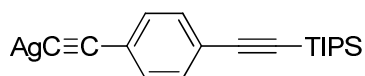
[Ag(CC-4-i-Pr$_3$SiCC-C$_6$H$_4$)] (69): This compound was synthesized in a procedure analogous to that for **68** from a solution of 2.545 g (9.01 mmol) of 4-(triisopropysilyllethynyl) phenylacetylene (**75**) and 3.5 mL (2.55 g, 25.2 mmol) of NEt$_3$ in 110 mL of acetonitrile and a solution of 1.559 g (9.18 mmol) of AgNO$_3$ in 40 mL of acetonitrile. Pale yellow solid. Yield: 3.329 g (8.55 mmol), 95%. IR (KBr) 2152 (m), 2019 (w) cm^{-1}.
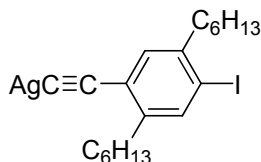
[Ag(CC-2,5-di-n-hexyl-4-I-C$_6$H$_2$)] (65): This complex was synthesized
Method A: To a solution containing .620 g (3.65 mmol) of AgNO$_3$ in 50 mL of acetonitrile and 50 mL of ethanol was added a solution of 1.222 g (3.31 mmol) of 2,5-dihexyl-4-iodophenylacetylene (**25**) and 5 mL (3.64 g, 36.0 mmol) of NEt$_3$ in 50 mL of dichloromethane

and 75 mL of ethanol. The mixture is stirred for 20 h in darkness. The light yellow precipitate is filtered from the solution and washed three times with 25 mL of acetonitrile followed by two rinsings with 25 mL ethanol. Yield: 1.325 g (2.63 mmol, 78%). IR (KBr) 2020 (w) cm^{-1}.

Method B: To a solution containing 0.266 g (0.671 mmol) 2,5-dihexyl-4-iodophenylacetylene (**25**) dissolved in 10 mL acetone and 10 mL of EtOH was added 0.195 g (0.759 mmol) of AgOTf dissolved in 5 mL of acetone and 5 mL of EtOH followed by 0.275 g (2.72 mmol) of NEt_3 in 5 mL of acetone and 5 mL of EtOH. The contents were stirred in the darkness for thirty minutes. The precipitate is filtered from the solution and washed two times with 20 mL of acetone followed by two rinsing with 20 mL of ethanol. Yield: 0.343 g (0.682 mmol, 102 %).

Method C: To a solution containing 0.399 g (1.01 mmol) 2,5-dihexyl-4-iodophenylacetylene (**25**) dissolved in 15 mL of acetone and 15 mL of acetonitrile was added 0.185 g (1.09 mmol) of $AgNO_3$ dissolved in 21 mL of acetonitrile and 7 mL of acetone followed by 0.394 g (3.89 mmol) of NEt_3 in 4 mL acetonitrile and 3 mL of acetone. The contents were stirred in darkness for 30 min. The precipitate is filtered from the solution and washed two times with 20 mL of acetonitrile followed by two rinsing with ethanol. Yield: 0.503 g (1.00 mmol, 99%).
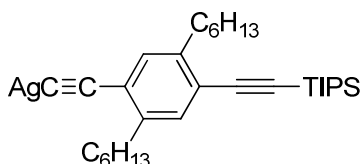
[Ag(CC-2,5-di-*n*-hexyl-4-*i*-Pr₃SiCC-C₆H₂)] (66):

Method A: To a solution containing 0.524 g (3.08 mmol) of $AgNO_3$ dissolved in 10 mL of a acetonitrile and 50 mL of ethanol was added 1.251 g (2.77 mmol) of 2,5-dihexyl-4-(triisopropylsilylethynyl)phenylacetylene (**27**) and 4 mL (3 g, 30 mmol) of NEt_3 dissolved in 50 mL of dichloromethane and 100 mL of ethanol. The solution turns cloudy immediately, and after 10 minutes an oily substance at the bottom of the flask was observed. Therefore, 50 mL of ethanol followed by 25 mL of acetonitrile was added to the reaction solution and the contents stirred for an additional 16 hours in darkness. The precipitate is filtered from the solution and washed two times with 25 mL of acetonitrile followed by two rinsing with 25 mL of ethanol. Yield: 1.397 g (2.51 mmol, 90%). IR (KBr): 2145 (m), 2018 (w) cm^{-1}.

Method C: To a solution containg 0.270 g (0.599 mmol) of 2,5-dihexyl-4-(triisopropylsilylethynyl)phenylacetylene (**27**) dissovled in 8 mL of acetone and 8 mL of

acetonitrile was added 0.112 g (0.659 mmol) $AgNO_3$ dissolved in 2 mL of acetonitrile and 2 mL of acetone followed by 0.255 g (2.52 mmol) NEt_3. The contents were stirred in darkness for 30 minutes. The precipitate is filtered from the solution and washed two times with 20 mL of acetonitrile followed by two rinsing with 20 mL of ethanol. Yield: 0.312 g (0.559 mmol, 93%).

[Ag(CC-2,5-di-*n*-hexyl-4-Me₃SiCC-C₆H₂)] (67):

Method A: To a solution containg 0.315 g (1.85 mmol) $AgNO_3$ dissolved in 25 mL of acetonitrile and 25 mL of ethanol is added 0.718 g (1.96 mmol) of 2,5-dihexyl-4-(trimethylsilylethynyl)phenylacetylene (**26**) and 3 mL (2.2 g, 22 mmol) of NEt_3 dissolved in 30 mL dichloromethane and 80 mL of ethanol. The contents were stirred for 3 hours before being placed in the freezer for three days. The precipitate is filtered from the solution and washed two times with 20 mL of acetonitrile followed by two rinsing with 20 mL of ethanol. Yield: 0.767 g (1.62 mmol, 82%). IR (KBr): 2150 (m), 2016 (w) cm^{-1}.

Method B-1: To a solution containing 0.328 g (0.895 mmol) 2,5-dihexyl-4-(trimethylsilylethynyl)phenylacetylene (**26**) dissolved in 15 mL of acetone and 15 mL of ethanol was added 0.284 g (1.11 mmol) of AgOTf dissolved in 3 mL acetone and 3 mL of ethanol followed by 0.657 g (6.49 mmol) NEt_3. The contents were stirred in darkness for 30 minutes. The precipitate is filtered from the solution and washed two times with 20 mL of acetone followed by two rinsing with 20 mL of ethanol. Yield: 0.341 g (0.568 mmol, 63%).

Method B-2: To a solution containing 0.201 g (0.548 mmol) of 2,5-dihexyl-4-(trimethylsilylethynyl)phenylacetylene (**26**) dissolved in 15 mL acetone and 15 mL of ethanol was added 0.175 g (0.681 mmol) of AgOTf in 5 mL of acetone and 5 mL ethanol followed by 0.255 g (2.52 mmol) of NEt_3. The contents were stirred in darkness for 30 minutes. The precipitate is filtered from the solution and washed two times with 20 mL of acetone followed by two rinsing with 20 mL of ethanol. Yield: 0.192 g (0.405 mmol, 74%).

Method C-1: To a solution containing 0.433 g (1.18 mmol) 2,5-dihexyl-4-(trimethylsilylethynyl)phenylacetylene (**26**) dissolved in 25 mL of acetone and 20 mL of acetonitrile was added 0.240 g (1.67 mmol) of $AgNO_3$ dissolved in 5 mL acetonitrile followed

by 0.905 g (1.25 mmol) NEt₃. The contents were stirred in darkness for 30 minutes.   The precipitate is filtered from the solution and washed two times with 20 mL of acetonitrile followed by two rinsing with 20 mL of ethanol.   Yield: 0.341 g (0.720 mmol, 61%).
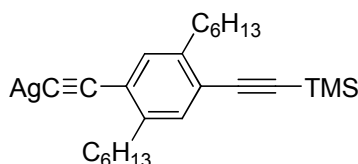
Method C-2: To a solution containing 0.201 g (0.548 mmol) of 2,5-dihexyl-4-(trimethylsilylethynyl)phenylacetylene (**26**) dissolved in 15 of mL acetone and 15 mL of acetonitrile was added 0.115 g (0.677 mmol) of AgNO₃ dissolved in 3 mL of acetone and 3 mL acetonitrile followed by 0.259 g (2.56 mmol) of NEt₃. Yield: 0.233 g (0.492 mmol, 90 %).
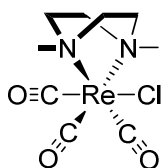
[ReCl(CO)₃(dmpz)] (61): A mixture containing 0.399 (1.10 mmo) of [ReCl(CO)₅], 0.256 g (2.24 mmol) of N,N'-dimethylpiperazine, and 70 mL of toluene was stirred in a flask equipped with a gas outlet at 85 °C for 2 h. The reaction mixture was stirred for an additional 2 h at 65 °C before cooling to room temperature. The white solid was filtered off, washed with toluene and hexane, and dried under vacuum. Yield: 0.308 g (0.734 mmol ,67%). ^{1}H NMR (300 MHz, CDCl₃) δ 4.10–4.03 (m, 2H), 3.72–3.61 (m, 2H), 3.15–3.09 (m, 2H), 2.97 (s, 6H), 2.38–2.32 (m, 2H); ^{13}C NMR (400 MHz, CDCl₃) δ 194.9, 190.9, 63.1, 56.8, 49.7; IR (CH₂Cl₂) 2027 (s), 1922 (s), 1879 (s) cm^{-1}; Anal. Calc. for C₉H₁₄ClN₂O₃Re: C, 25.74; H, 3.36; N, 6.67. Found: C, 25.49; H, 3.12; N, 6.56%.
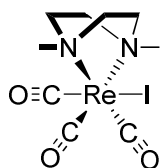
[ReI(CO)₃(dmpz)] (62):

From 28: A mixture containing 1.2 g (2.5 mmol) of [ReBr(CO)₃(dmpz)] (**28**), 2 g (6.2 mmol) of zinc iodide, 0.5 mL (0.6 g, 5 mmol) of N,N'-dimethylpiperazine and 60 mL of toluene was heated to 65 °C for 4 h. The solvent was removed under vacuum. The residue was extracted with dichloromethane. The combined extracts were filtered. The solvent was removed and the residue washed with cold hexane. Colorless crystalline solid. Yield: 1.2 g (2.3 mmol, 92%).

From 61: A solution containing 0.382 g (0.910 mmol) of [ReCl(CO)$_3$(dmpz)] (**61**), 0.285 g (1.90 mmol) of sodium iodide, and 0.1 mL (0.117 g, 1.03 mmol) of N,N'-dimethylpiperazine dissolve in 50 mL of THF was refluxed for 1.5 h. The solvent was removed under vacuum. The product was extracted with methylene chloride. The combined extracts were filtered, and the solvent was removed under vacuum. Crystallization from methylene chloride/hexane afforded a colorless solid. Yield: 0.459 g (0.898 mmol, 99%).

^{1}H NMR (300 MHz, CDCl$_3$) δ 4.30–4.23 (m, 2H), 3.77–3.70 (m, 2H), 3.34–3.26 (m, 2H), 3.04 (s, 6H), 2.80–2.71 (m, 2H); ^{13}C NMR (400 MHz, CDCl$_3$) δ 194.0, 190.2, 63.2, 60.4, 49.8; IR (CH$_2$Cl$_2$) 2026 (s), 1924 (s), 1883 (s) cm^{-1}; Anal. Calc. for C$_9$H$_{14}$IN$_2$O$_3$Re: C, 21.14; H, 2.76; N, 5.48. Found: C, 21.17; H, 2.61; N, 5.45%.
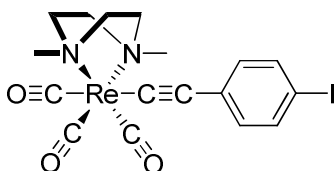
Complex 76: A solution containing 0.564 g (1.68 mmol) of **68**, 0.874 g (1.88 mmol) of **28**, and 0.1 mL (0.085 g, 0.75 mmol) of N,N'-dimethylpiperazine in 25 mL of toluene was stirred in darkness for 3 h at 70 °C. The solution was allowed to cool to room temperature and filtered. The solvent was evaporated under vacuum. The residue was purified by column chromatography, using a mixture of hexane/ethyl acetate (3/2, v/v) as the eluent. Recrystallization from ethyl acetate/hexane afforded pale yellow crystals. Yield: 0.538 g (0.880 mmol), 52%. ^{1}H NMR (300 MHz, CDCl$_3$) δ 7.50 (d, J^3 = 9 Hz, 2H), 7.06 (d, J^3 = 9 Hz, 2H), 4.28 (m, 2H), 3.59 (m, 2H), 3.15 (m, 2H), 3.01 (s, 6H), 2.55 (m, 2H); ^{13}C NMR (400 MHz, CDCl$_3$) δ 196.0, 195.4, 136.9, 134.8, 133.2, 127.3, 102.1, 89.8, 64.2, 60.0, 50.1; IR (CH$_2$Cl$_2$) 2086 (w), 2009 (s), 1906 (s), 1885 (s) cm^{-1}; Anal. Calc. for C$_{17}$H$_{18}$IN$_2$O$_3$Re: C, 33.39; H, 2.97; N, 4.58. Found: C, 33.13; H, 2.86; N, 4.52%.

O≡C—Re—C≡C—〈benzene ring〉—≡—TIPS
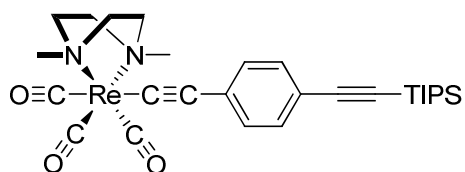
Complex 77: This compound was synthesized following a procedure analogous to that for compound **76**, starting from 0.948 g (2.43 mmol) of **69**, 1.231 g (2.651 mmol) of **28**, and 0.1 mL (0.0852 g, 0.746 mmol) of N,N'-dimethylpiperazine in 50 mL of toluene. Pale yellow solid. Yield: 0.867 g (1.30 mmol), 54%. ^{1}H NMR (300 MHz, CDCl$_3$) δ 7.30 (d, J^3 = 8 Hz, 2H), 7.23 (d, J^3 = 8 Hz, 2H), 4.28 (m, 2H), 3.57 (m, 2H), 3.13 (m, 2H), 3.01 (s, 6H), 2.53 (m, 2H), 1.12 (s, 21H); ^{13}C NMR (400 MHz, CDCl$_3$) δ 196.0, 195.4, 135.9, 131.6, 131.1, 127.9, 119.9, 107.5, 103.2, 90.8, 64.2, 59.9, 50.1, 18.6, 11.3; IR (CH$_2$Cl$_2$) 2150 (m), 2084 (w), 2010 (s), 1910 (s), 1883 (s) cm^{-1}; Anal. Calc. for C$_{28}$H$_{39}$N$_2$O$_3$ReSi: C, 50.50; H, 5.90; N, 4.21. Found: C, 50.24; H, 5.74; N, 4.21%.

C$_6$H$_{13}$

O≡C—Re—C≡C—〈benzene ring〉—I

C$_6$H$_{13}$
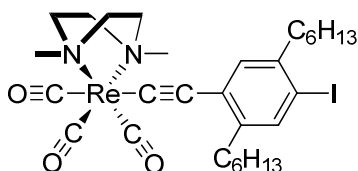
Complex 33: This complex was prepared following the procedure described for **76**, using 0.434 g (0.935 mmol) of **28**, 0.2 mL (0.235 g, 2.06 mmol) of N,N'-dimethylpiperazine, 50 mL of toluene, and 0.383 g (0.801 mmol) of **65** obtained via Method A. The product was purified by column chromatography on silica gel using methylene chloride/hexane (1:1, v/v) as the eluent. This afforded a pale yellow solid. Yield: 0.369 g (59%). ^{1}H NMR (300 MHz, CDCl$_3$) δ 7.53 (s, 1H), 7.12 (s, 1H), 4.31 (m, 2H), 3.59 (m, 2H), 3.13 (m, 2H), 3.02 (s, 6H), 2.72 (t, 2H), 2.56 (m, 4H), 1.64 (m, 2H), 1.50 (m, 2H), 1.32 (m, 12H), 0.88 (m, 6H); ^{13}C NMR (400 MHz, CDCl$_3$) δ 196.1, 195.6, 143.8, 142.0, 138.8, 137.0, 132.3, 127.2, 101.0, 96.5, 64.1, 60.0, 50.1, 40.2, 34.4, 31.8, 31.7, 30.6, 30.4, 29.4, 29.1, 22.7, 22.6, 14.1, 14.1; IR (CH$_2$Cl$_2$) 2078 (w), 2008 (s), 1906 (s), 1883 (s) cm^{-1}; Anal. Calc. for C$_{29}$H$_{42}$IN$_2$O$_3$Re: C, 44.67; H, 5.43; N, 3.59. Found: C, 44.88; H, 5.42; N, 3.53%.
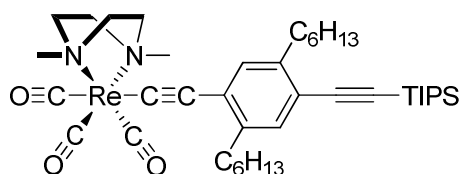
Complex 34: This compound was synthesized following a procedure analogous to that for complex **76**, 1.315 g (2.83 mmol) **28**, 1.397 (2.51 mmol) of **66** obtained via Method A, 0.2 mL (0.2 g, 1.4 mmol) of dmpz, and 45 mL of dried toluene. Yield:1.208 g (1.45mmol, 58%).
^{1}H NMR (300 MHz, CDCl$_3$) δ 7.19 (s, 1H), 7.11 (s, 1H), 4.30 (m, 2H), 3.56 (m, 2H), 3.10 (m, 2H), 3.01 (s, 6H), 2.75 (m, 2H), 2.51 (m, 2H), 1.64 (m, 4H), 1.32 (m, 12H), 1.14 (s, 21H), 0.88 (m, 6H); ^{13}C NMR (400 MHz, CDCl$_3$) δ 196.2, 195.6, 142.1, 141.5, 138.0, 132.5, 131.9, 127.3, 119.3, 106.6, 102.0, 93.2, 64.1, 60.0, 50.1, 34.7, 34.5, 31.9, 31.8, 31.1 30.8, 29.5, 29.5, 22.7, 22.6, 18.7, 14.1, 14.1, 11.3; IR (CH$_2$Cl$_2$) 2143 (m), 2081 (w), 2008 (s), 1906 (s), 1882 (s) cm^{-1}; Anal. Calc. for C$_{40}$H$_{63}$N$_2$O$_3$ReSi: C, 57.59; H, 7.61; N, 3.36. Found: C, 57.48; H, 7.62; N, 3.38%.
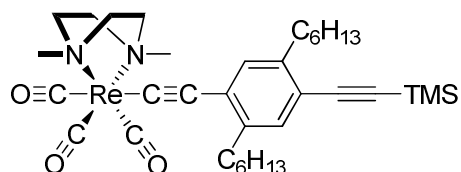
Complex 73:

Using 67 from Method A: A warm solution prepared from 0.509 g (1.10 mmol) of **28**, 0.303 g (2.65 mmol) of dmpz, and 75 mL of dried toluene heated to 75 °C was added to a Schlenk flask containing 0.487 g (1.03 mmol) of **67** obtained via Method A. The reaction flask was evacuated and backfilled with nitrogen gas twice before being submerged in oil bath at 75 °C. The contents were heated and stirred for 3 hours. The solvent was removed under vacuum. The product was purified by column chromatography on silica gel using initially using hexane/ethyl acetate (4:1, v/v) and later hexane/ethyl acetate (2:1, v/v) as the eluent to afford 0.327 g (0.436 mmol, 42%).

Using 17 from Method B-1: This procedure is analogous to the one above except 0.424 g (0.913 mmol) **28**, 0.269 g (0.568 mmol) of **67** obtained via Method B-1, 30 mL dried tolune, and 0.347 g (3.04 mmol) of dmpz were used. Yield: 0.119 (0.159 mmol, 28%).

Using 67 from Method C: This procedure is analogous to the one above except 0.428 g (0.922 mmol) of **28**, and 0.341 g (0.720 mmol) of **67** obtained via Method C-1, 30 mL of dried toluene, and 0.370 g (3.24 mmol) of dmpz. Yield: 0.428 g (0.571 mmol, 79%)

^{1}H NMR (300 MHz, CDCl$_3$) δ d 7.18 (s, 1H), 7.10 (s, 1H), 4.33–4.31 (m, 2H), 3.60–3.56 (m, 2H), 3.15–3.12 (m, 2H), 3.02 (s, 6H), 2.77–2.74 (m, 2H), 2.71–2.63 (m, 2H), 2.56–2.52 (m, 2H), 1.67–1.57 (m, 4H), 1.36–1.26 (m, 12H), 0.91–0.85 (m, 6H), 0.26–0.21 (s, 9H); ^{13}C NMR (400 MHz, CDCl$_3$) δ d 196.1, 195.7, 142.4, 141.6, 138.1, 132.2, 132.00, 127.4, 118.9, 105.0, 102.1, 97.1, 64.2, 60.1, 50.2, 34.7, 34.3, 31.9, 31.8, 30.8, 30.6, 29.5, 29.4, 22.7, 14.1, 0.1; IR (CH$_2$Cl$_2$) 2143 (m), 2080 (w), 2008 (s), 1906 (s), 1883 (s) cm^{-1}.
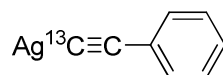
Complex 70: This complex was prepared by adopting the literature procedures[312,313] using 0.199 g (1.93 mmol) of 1-^{13}C-phenylacetylene, 0.400 g (2.355 mmol) of AgNO$_3$, 0.8 mL (0.58 g, 5.7 mmol) of NEt$_3$ and 21 mL of acetonitrile. Yield: 0.340 g (1.62 mmol, 84%).
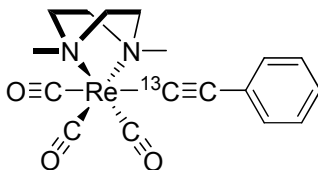
Complex 71:

Prepared with dmpz: This complex was prepared according to our published procedure[151] using 0.340 g (1.62 mmol) of **70**, 0.882 g (1.90 mmol) of **28**, 0.4 mL (0.34 g, 3.0 mmol) of dmpz , and 45 mL of toluene. The solution was stirred for 3.5 h, during which the temperature gradually increased from 65 °C to 90 °C. Following the normal work up procedure affords the product in 0.548 g 1.13 (mmol, 70%) of **71**.

Prepared without dmpz: This complex was prepared according to the procedure reported by Hili[275] using 0.110 g (0.524 mmol) **70**, 0.202 g (0.435 mmol) of **28**, and 25 mL of dried toluene. 3 – 5 mL portions of the solution was removed after 3 h of stirring at 65 °C, after 18.5 h of stirring at 65 °C, after an additional 3 hr of stirring at 90 °C. For each of these portions the solvent was removed by vacuum and then ^{1}H and ^{13}C NMR spectra recorded at 400 MHz in CDCl$_3$.

128
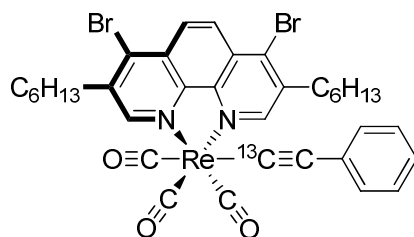
Prepared from 59 by transmetallation: This complex was prepared by adopting our published procedure[151] using 0.205 g (0.976 mmol) of **70**, 0.900 g (1.05 mmol) of **59**, in 50 mL of toluene. The contents were stirred at 85 °C for 3 hours before being purified by column chromatography using toluene:hexanes (1:1, v/v) as eluent. Crystallization from a toluene/hexanes afforded the product in 0.458 g (0.521 mmol, 53%)

Prepared from 71 by ligand substitution: This complex was prepared by adopting our published procedure[151] using 0.100 g (0.206 mmol) of **71**, 0.111 g (0.219 mmol) of **29**, and 45 mL of toluene. The contents were stirred at 90 °C for 18 hours before being purifed by column chromatography using toluene:hexanes (1:1, v/v) as eluent to afford 0.144 g (0.164 mmol, 80%) of **72** and **72'** 1:1.
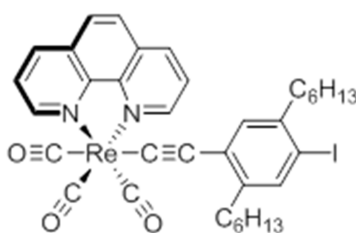
Complex 79: This complex was prepared by adopting our published procedure[151] using 0.516 g (0.662 mmol) of **33**, 0.204 g (1.13 mmol) of 1,10-phenanthroline, and 40 mL of toluene. The contents were stirred at 95 °C for 12 h before the removed. . Crystallization from toluene/hexanes afforded the product in 0.428 g (0.506 mmol, 76%). ^{1}H NMR (400 MHz, CDCl$_3$) δ ; ^{13}C NMR (400 MHz, CDCl$_3$) δ 197.7, 192.1, 153.5, 153.4, 145.7, 141.4, 136.3, 136.3, 136.2, 133.1, 130.1, 127.5, 126.9, 126.8, 104.8, 89.4, 34.7, 31.4, 29.5, 29.1, 22.5, 14.0.
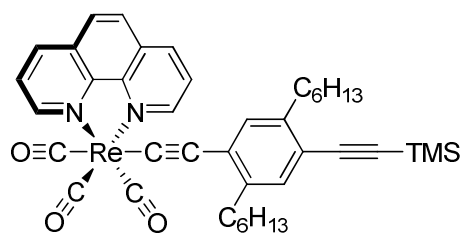
Prepared from by Sonogashira cross-coupling: A Schlenk flask containing 0.415 g (0.490 mmol) of **79** in 100 mL of toluene and 20 mL of NEt$_3$ was evacuated and back filled with nitrogen gas three times before 0.257 g (0.222 mmol) Pd(PPh$_3$)$_4$, 0.586 g (5.97 mmol) of trimethylsilylacetylene, and 0.186 (0.977 mmol) of CuI were added. The flask was submerged in an oil bath at 85 °C for 10 minutes to dissolve all of the reagents before placing the flask in another oil bath set at 65 °C. The contents were stirred for 3h before the solvent removed under vacuum. The product was purified via column chromatography using toluene/ethyl acetate (4:1 v/v) to afford 0.080 g (0.10 mmol, 20%) of **80**.

Prepared from by ligand substitution: This complex was prepared by adopting our published procedure[151] using 0.327 g (0.435 mmol) of **73**, 0.083 g (0.461 mmol) of 1,10-phenanthroline, and 70 mL of toluene. The contents were stirred at 85 °C for 3 h, before the solvent removed under vacuum. Crystalization from toluene/hexanes affords 0.347 g (0.425 mmol, 98%) of **35**.
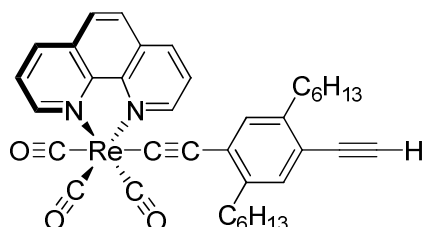
Complex 81: To a solution containing 0.347 g (0.425 mmol) of **80** dissolved in 50 mL of dichloromethane and 100 mL of ethanol is added 4.407 g (78.5 mmol) of KOH in 20 mL of water. The contents we stirred for 2 h before the solution was washed with 100 mL of distilled water. Afterwards the organic phase was separated from the aqueous phase and collected. Two subsequent extractions of the organic substance from the aqueous solution were carried out using dichloromethane. The combine collected organic solutions was dried over anhydrous MgSO$_4$ and the solvent removed via rotoevaporation and dried under vacuum. The product was purified via column chromatography using a short column of silica and toluene as an eluent to afford 0.265 g (0.356 mmol, 83%).

3.5. References

(143)   Chinchilla, R.; Najera, C.: Recent advances in Sonogashira reactions. *Chem. Soc. Rev.* **2011**, *40*, 5084-5121.

(151)   St. Fleur, N.; Craig, H. J.; Mayr, A.: Synthesis of alkynyl(tricarbonyl)rhenium complexes containing a lightly coordinated diamine ligand. *Inorg. Chim. Acta* **2009**, *362*, 1571-1576.

(275)   Hili, J. C.: Bis-isocyanide rhenium acetylide complexes for the stepwise assembly of molecular cages. 2006.

(276)   Lam, S. C.-F.; Yam, V. W.-W.; Wong, K. M.-C.; Cheng, E. C.-C.; Zhu, N.: Synthesis and Characterization of Luminescent Rhenium(I)-Platinum(II) Polypyridine Bichromophoric Alkynyl-Bridged Molecular Rods. *Organometallics* **2005**, *24*, 4298-4305.

(277)   Dembinski, R.; Bartik, T.; Bartik, B.; Jaeger, M.; Gladysz, J. A.: Toward Metal-Capped One-Dimensional Carbon Allotropes: Wirelike C6-C20 Polyynediyl Chains That Span Two Redox-Active (η5-C5Me5)Re(NO)(PPh3) Endgroups. *J. Am. Chem. Soc.* **2000**, *122*, 810-822.

(278)   Chong, S. H.-F.; Lam, S. C.-F.; Yam, V. W.-W.; Zhu, N.; Cheung, K.-K.; Fathallah, S.; Costuas, K.; Halet, J.-F.: Luminescent Heterometallic Branched Alkynyl Complexes of Rhenium(I)-Palladium(II): Potential Building Blocks for Heterometallic Metallodendrimers. *Organometallics* **2004**, *23*, 4924-4933.

(279)   Yam, V. W.-W.; Wong, K. M.-C.; Chong, S. H.-F.; Lau, V. C.-Y.; Lam, S. C.-F.; Zhang, L.; Cheung, K.-K.: Synthesis, electrochemistry and structural characterization of luminescent rhenium(I) monoynyl complexes and their homo- and hetero-metallic binuclear complexes. *J. Organomet. Chem.* **2003**, *670*, 205-220.

(280)   Wong, K. M.-C.; Lam, S. C.-F.; Ko, C.-C.; Zhu, N.; Yam, V. W.-W.; Roue, S.; Lapinte, C.; Fathallah, S.; Costuas, K.; Kahlal, S.; Halet, J.-F.: Electroswitchable Photoluminescence Activity: Synthesis, Spectroscopy, Electrochemistry, Photophysics, and X-ray Crystal and Electronic Structures of [Re(bpy)(CO)3(C≡C-C6H4-C≡C)Fe(C5Me5)(dppe)][PF6]n (n = 0, 1). *Inorg. Chem.* **2003**, *42*, 7086-7097.

(281)   Yam, V. W.-W.: Luminescent carbon-rich rhenium(i) complexes. *Chem. Commun. (Cambridge, U. K.)* **2001**, 789-796.

(282)   Yam, V. W.-W.; Kam-Wing, L. K.; Man-Chung, W. K.: Luminescent polynuclear metal acetylides. *J. Organomet. Chem.* **1999**, *578*, 3-30.

(283)   Yam, V. W.-W.; Chong, S. H.-F.; Cheung, K.-K.: Synthesis and luminescence behavior of rhenium(I) diynyl complexes. X-Ray crystal structures of [Re(CO)3(tBu2bpy)(C≡C-C≡CH)] and [Re(CO)3(tBu2bpy)(C≡C-C≡CPh)]. *Chem. Commun. (Cambridge)* **1998**, 2121-2122.

(284)   Yam, V. W.-W.; Lau, V. C.-Y.; Cheung, K.-K.: Luminescent Rhenium(I) Carbon Wires: Synthesis, Photophysics, and Electrochemistry. X-ray Crystal Structure of [Re(tBu2bpy)(CO)3(C≡CC≡C)Re(tBu2bpy)(CO)3]. *Organometallics* **1996**, *15*, 1740-4.

(285)   Yam, V. W.-W.; Lau, V. C.-Y.; Cheung, K.-K.: Synthesis and Photophysics of Luminescent Rhenium(I) Acetylides-Precursors for Organometallic Rigid-Rod Materials. X-ray Crystal Structures of [Re(tBu2bpy)(CO)3(tBuC≡C)] and [Re(tBu2bpy)(CO)3Cl]. *Organometallics* **1995**, *14*, 2749-53.

(286)   Bruce, M. I.; Harbourne, D. A.; Waugh, F.; Stone, F. G. A.: Some transition-metal acetylides. *Journal of the Chemical Society A: Inorganic, Physical, Theoretical* **1968**, *0*, 356-359.

(287)   Salah, O. M. A.; Bruce, M. I.: New Group IB metal chemistry. Part 6. Reactions of copper(I) acetylides with chloro([small eta]-cyclopentadienyl)bis(triphenylphosphine)ruthenium and cis-tricarbonylchlorobis(triphenylphosphine)rhenium. *Journal of the Chemical Society, Dalton Transactions* **1975**, *0*, 2311-2315.

(288)   Yam, V. W.-W.; Lau, V. C.-Y.; Cheung, K.-K.: Synthesis and Photophysics of Luminescent Rhenium(I) Acetylides-Precursors for Organometallic Rigid-Rod Materials. X-ray Crystal Structures of [Re(tBu2bpy)(CO)3(tBuC.tplbond.C)] and [Re(tBu2bpy)(CO)3Cl]. *Organometallics* **1995**, *14*, 2749-2753.

(289)   Wong, A.; Gladysz, J. A.: Syntheses and reactions of rhenium vinylidene and acetylide complexes. Unprecedented chirality transfer through a C.tplbond.C triple bond. *Journal of the American Chemical Society* **1982**, *104*, 4948-4950.

(290)   Ramsden, J. A.; Weng, W.; Gladysz, J. A.: Deprotonation of rhenium terminal acetylide complexes (.eta.5-C5R5)Re(NO)(PPh3)(C.tplbond.CH): generation and reactivity of rhenium/lithium C2 complexes. *Organometallics* **1992**, *11*, 3635-3645.

(291)   Appel, M.; Heidrich, J.; Beck, W.: Metallorganische Lewis-Säuren, XXXII1) σ,π-Ethinid- und σ,σ-Ethindid-verbrückte Rheniumcarbonyle, [(OC)5Re(μ-η1,η2-C☐CH)Re(CO)5]+ BF–4 und (OC)5Re–C☐C–Re(CO)5. *Chemische Berichte* **1987**, *120*, 1087-1089.

(292)   Chong, S. H.-F.; Lam, S. C.-F.; Yam, V. W.-W.; Zhu, N.; Cheung, K.-K.; Fathallah, S.; Costuas, K.; Halet, J.-F.: Luminescent Heterometallic Branched Alkynyl Complexes of Rhenium(I)−Palladium(II): Potential Building Blocks for Heterometallic Metallodendrimers. *Organometallics* **2004**, *23*, 4924-4933.

(293)   Yam, V. W.-W.: Luminescent carbon-rich rhenium() complexes. *Chemical Communications* **2001**, *0*, 789-796.

(294)   Liddle, B. J.; Lindeman, S. V.; Reger, D. L.; Gardinier, J. R.: A Thallium Mediated Route to σ-Arylalkynyl Complexes of Bipyridyltricarbonylrhenium(I). *Inorganic Chemistry* **2007**, *46*, 8484-8486.

(295)   Pearson, R. G.: Hard and soft acids and bases, HSAB, part 1: Fundamental principles. *Journal of Chemical Education* **1968**, *45*, 581.

(296)   Pearson, R. G.: Hard and soft acids and bases, HSAB, part II: Underlying theories. *Journal of Chemical Education* **1968**, *45*, 643.

(297)   Proietti, S. I.; Andemarian, F.; Khairallah, G. N.; Wan, Y. S.; Quach, T.; Tsegay, S.; Williams, C. M.; O'Hair, R. A. J.; Donnelly, P. S.; Williams, S. J.: Copper(I)-catalyzed cycloaddition of silver acetylides and azides: Incorporation of volatile acetylenes into the triazole core. *Org. Biomol. Chem.* **2011**, *9*, 6082-6088.

(298)   Yamamoto, Y.: Silver-Catalyzed Csp-H and Csp-Si Bond Transformations and Related Processes. *Chem. Rev. (Washington, DC, U. S.)* **2008**, *108*, 3199-3222.

(299)   Weibel, J.-M.; Blanc, A.; Pale, P.: Ag-Mediated Reactions: Coupling and Heterocyclization Reactions. *Chem. Rev. (Washington, DC, U. S.)* **2008**, *108*, 3149-3173.

(300)   Halbes-Letinois, U.; Weibel, J.-M.; Pale, P.: The organic chemistry of silver acetylides. *Chem. Soc. Rev.* **2007**, *36*, 759-769.

(301)   Pouwer, R. H.; Williams, C. M.; Raine, A. L.; Harper, J. B.: "One-step" alkynylation of adamantyl iodide with silver(I) acetylides. *Org. Lett.* **2005**, *7*, 1323-1325.

(302)　Carpita, A.; Mannocci, L.; Rossi, R.: Silver(I)-catalyzed protiodesilylation of 1-(trimethylsilyl)-1-alkynes. *Eur. J. Org. Chem.* **2005**, 1859-1864.

(303)　Shahi, S. P.; Koide, K.: Alkynylation: A mild method for the preparation of γ-hydroxy-α,β-acetylenic esters. *Angew. Chem., Int. Ed.* **2004**, *43*, 2525-2527.

(304)　Dillinger, S.; Bertus, P.; Pale, P.: First Evidence for the Use of Organosilver Compounds in Pd-Catalyzed Coupling Reactions; A Mechanistic Rationale for the Pd/Ag-Catalyzed Enyne Synthesis? *Org. Lett.* **2001**, *3*, 1661-1664.

(305)　Agawa, T.; Miller, S. I.: Reaction of silver acetylide with acylpyridinium salts: N-benzoyl-2-phenylethynyl-1,2-dihydropyridine. *J. Am. Chem. Soc.* **1961**, *83*, 449-53.

(306)　Davis, R. B.; Scheiber, D. H.: The preparation of acetylenic ketones using soluble silver acetylides. *J. Am. Chem. Soc.* **1956**, *78*, 1675-8.

(307)　Zhao, L.; Mak, T. C. W.: Silver(I) 1,3-Butadiynediide and Two Related Silver(I) Double Salts Containing the C42- Dianion. *J. Am. Chem. Soc.* **2004**, *126*, 6852-6853.

(308)　Brasse, C.; Raithby, P. R.; Rennie, M.-A.; Russell, C. A.; Steiner, A.; Wright, D. S.: Structural Variation in Silver Acetylide Complexes: Syntheses and x-ray Structure Determinations of [Ph3PAgC≡CPh]4·3.5THF and [Me3PAgC≡CSiMe3]∞. *Organometallics* **1996**, *15*, 639-44.

(309)　Mitsudo, K.; Shiraga, T.; Mizukawa, J.-i.; Suga, S.; Tanaka, H.: Electrochemical generation of silver acetylides from terminal alkynes with a Ag anode and integration into sequential Pd-catalyzed coupling with arylboronic acids. *Chem. Commun. (Cambridge, U. K.)* **2010**, *46*, 9256-9258.

(310)　Viterisi, A.; Orsini, A.; Weibel, J.-M.; Pale, P.: A mild access to silver acetylides from trimethylsilyl acetylenes. *Tetrahedron Lett.* **2006**, *47*, 2779-2781.

(311)　Letinois-Halbes, U.; Pale, P.; Berger, S.: Ag NMR as a Tool for Mechanistic Studies of Ag-Catalyzed Reactions: Evidence for in Situ Formation of Alkyn-1-yl Silver from Alkynes and Silver Salts. *J. Org. Chem.* **2005**, *70*, 9185-9190.

(312)　Teo, B. K.; Xu, Y. H.; Zhong, B. Y.; He, Y. K.; Chen, H. Y.; Qian, W.; Deng, Y. J.; Zou, Y. H.: A Comparative Study of Third-Order Nonlinear Optical Properties of Silver Phenylacetylide and Related Compounds via Ultrafast Optical Kerr Effect Measurements. *Inorganic Chemistry* **2001**, *40*, 6794-6801.

(313)　Davis, R. B.; Scheiber, D. H.: The Preparation of Acetylenic Ketones Using Soluble Silver Acetylides. *Journal of the American Chemical Society* **1956**, *78*, 1675-1678.

Chapter 4: Synthesis of Triangular and Diamond Face

4.1. Introduction:

4.1.1. Synthesis of Shape Persistent Macrocycles Uni- and Multi-step Techniques

In our quest to construct the trigonal and rhomboid prisms discussed in the introductory chapter of this document, we first sought to synthesize the prisms' faces. Both the triangular (**32**) and diamond face (**35**) shown in Figure 4.1, are examples of highly sought after shape-persistent macrocycles. The well-defined dimensions and sizable cavities (on the order of nanometers) make these types of macrocycles ideal components for higher architectural structures[314-319] as well as chemical hosts.[320-327] Furthermore, the rigid unsaturated and conjugated materials generally used to construct these compounds, lend some of them interesting optical and electronic properties[320,321,328-332] often distinct from their corresponding acyclic form.[321,328,330,331,333] A number of reviews have been published summarizing their applications and the advances made toward their assembly.[319,334-343] Included in some of the reviews are examples of 2D metal organic frameworks (MOFs). Although MOFs are popular and highly attractive, only organic macrocycles whose backbones are made solely of classical covalent bonds will be considered henceforth, as these macrocycles most closely resemble our two targets in regards to chemical structure and assembly.

The synthesis of shape-persistent macrocycles is quite challenging. Because these structures are rigid, the corresponding building blocks must be rigid, so aromatic rings and unsaturated hydrocarbon chains are often employed for their construction. Owing to the inflexibility of these building materials, angles apparent in the final structure are generally featured in the building blocks, since they cannot easily be formed during coupling or ring closing events. Often angles are introduced into these shape-persistent macrocyclic systems by selectively functionalized aromatic and polycyclic aromatic compounds. Another consequence of using rigid building blocks, coupled with the generally unforgiving nature of covalent bonds, is purely covalent shape-persistent macrocycles are difficult to produce in significant yields. Unlike in supramolecular structures, where bonds can be broken and rearranged so that in the end the most thermodynamically favored products prevail, during covalent synthesis of these macrocycles, bonds once formed are rarely broken. The most notable exception to this being metathesis reactions[139,334,344-347] and imine condensations.[324,348-350] Therefore, kinetically favored oligomeric and polymeric byproducts persist. Considerable theoretical and empirical evidence suggests high dilution conditions ($\leq 10^{-3}$ M) are kinetically more favorable to cyclization than

dilute ($\leq 10^{-1}$ M) or non-dilute ($> 10^{-1}$ M) conditions.[351,352] The influence of solution concentration on the kinetics of the cyclization and chain growth reactions, is attributed to the differences in the molecularity of these reactions which are uni- and bimolecular, respectively.[353] The rates of bimolecular reactions are expected to decrease with a decrease in reactant concentrations. On the other hand, the rate constants of unimolecular reactions are unaffected by reactant concentrations, since the local concentrations of the reactive environment is theoretically the same. Therefore, dilute, particularly highly dilute environments, improves the favorability of cyclization by slowing the rate of the oligomerization/polymerization reactions more than the rate of cyclization.
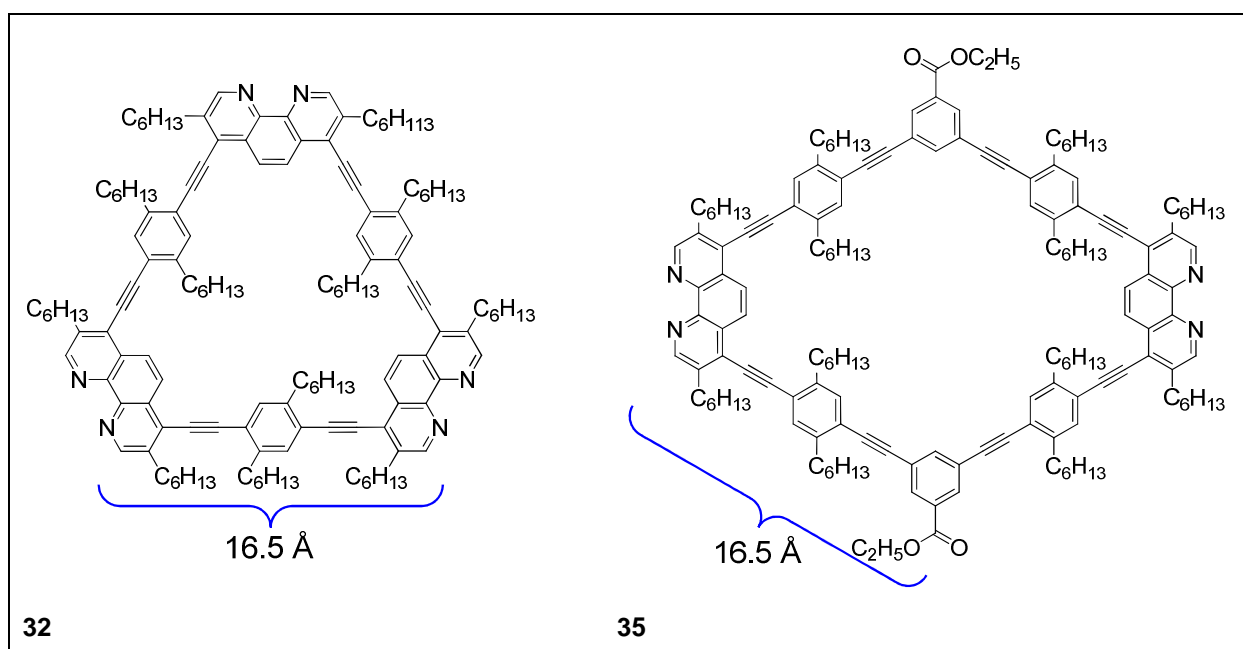
Figure 4. 1: Triangular (**32**) and Diamond (**35**) Faces.

To achieve these high dilution conditions there are two useful approaches, batch-wise or constant flow synthesis. During constant flow, a solution containing one or all of the reactants is added drop-wise into a solution containing the remaining reagents. Because only a very small amount of the reactants are added slowly and gradually into a relatively large volume of reaction solution, the concentration of reactant(s) remain(s) low. The addition rate is a key factor in the final product distribution.[351] To control this rate special equipment such as automated addition funnels, chemical injectors, and syringe pumps are often employed. Alternatively, all of the

136

reactants can be added simultaneously to a very large volume of solvent, as is done during batch-wise synthesis. Although the batch-wise approach does not require special equipment, it suffers from requiring a very large volume of solvent, which increase the reaction times. See Figure 4.2.

Reactants →

All Reagents →

Batch-wise High Dilution Synthesis

Remaining Reagents →

Continous Flow High Dilution Synthesis
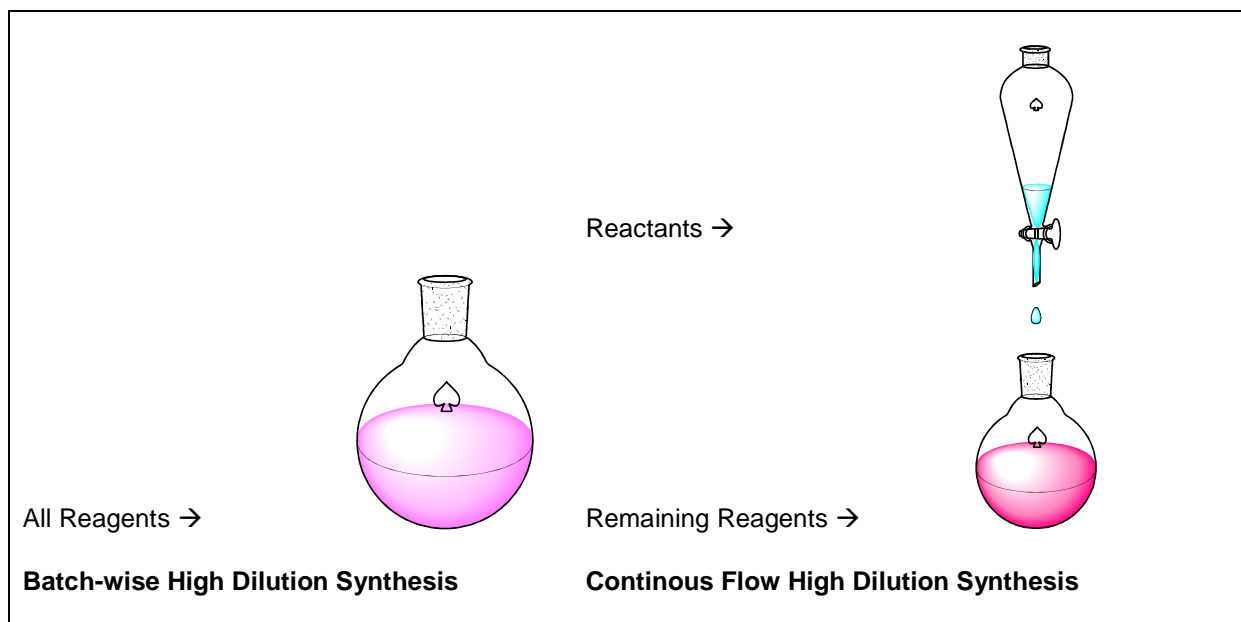
Figure 4. 2: Batch-wise vs. Continuous Flow Synthesis

Shape-persistent macrocycles have been produced via three general methods: intramolecular cyclizations,[106,109,354-357] as well as one-pot,[334,347,358-360] and multistep intermolecular[316,320-322,327,328,331-333,361-365] cyclizations. These three classifications are distinguished by the number of steps preceding and the number of species involved in the annulation reaction of an individual macrocycle. In the intramolecular process, cyclization involves a single acyclic precursor, which is produced from building components through at least one coupling reaction. Contrastingly, for the one-pot intermolecular cyclization multiple building blocks are coupled in a single step. Finally, the multistep intermolecular cyclization involves coupling of two or more higher-ordered building components that were synthesized from basic building blocks. All three methods have been employed with varying degrees of success and there are clear advantages and disadvantages to them. On the one hand, one-pot intermolecular reaction is attractive because it is the least labor intensive. On the other hand, it is easier to control the design and size of the macrocycle using the intramolecular process. Moreover, under dilute or highly dilute conditions, yields for the intramolecular reaction are

137

often higher than an analogous intermolecular reaction under similar conditions. The multistep intermolecular cyclization generally shares benefits and deficits of the two former cyclization classifications, requiring fewer steps than the intramolecular but generating higher yields than the one-pot intramolecular cyclization. Of course, these remarks are very general and depend on the size, shape, complexity, and number of distinct components of the macrocycle.

A comparison between the one-pot intermolecular and intramolecular cyclization is often illustrated by juxtaposing the work of Staab[366] and Moore[106] in the synthesis of phenylacetylene macrocyclic hexamers **88**[366] and **93**,[106] which were produced through intermolecular and intramolecular cyclizations, respectively. As is evident in Scheme 4.1, the one-pot-synthesis Staab employed to produce the highly symmetric macrocycle **88** from its corresponding monomer (**87**) is by far the most convenient; cyclization is accomplished after one coupling procedure rather than after the four coupling reactions needed to produce **93** from compounds **89**, **90**, and **91**. On the other hand, the intramolecular reaction developed by Moore can be used to produce a greater variety of more complex macrocycles at significantly higher yields, with **93** and **88** produced in 37 % and 4.6 % yield, respectively. It is clear from these examples the overall yields of the intermolecular reaction is quite low but the work required for the intramolecular procedure is significantly greater. Therefore, implementing methods that maximize productivity while minimizing labor expense is of key importance in the synthesis of macrocycles.

The productivity of one-pot intermolecular cyclization reactions have been improved by using extrinsic or intrinsic templates. For example, the one-pot synthesis of foldamers **97** in 69 % and **98** in 84 % yield from dilute solutions of their corresponding monomers was governed by exotopic H-bond interactions.[360] See Scheme 4.2. Likewise, endotopic H-bonding assists in the production of macrocycles **100a** in 46 % and **100b** in 6% yield from 0.1M solutions of 3-amino-2-methoxybenzoic acid (**99**) at 25 °C. When reaction temperature is increased to 40 °C, the overall yield increased to 90%. Unfortunately, at these elevated temperatures there was no predominant product and all three products, **100a**, **100b**, and **100c** were reportedly obtained in 42%, 33%, and 16% yields, respectively, relative to the monomer.[358] See Scheme 4.3. The mixture of products generated during the synthesis of **100** highlights one of the previously mentioned drawbacks of intermolecular synthesis that may not be corrected by using templates.

87: $R^1 = R^2 = H$

88: $R^1 = R^2 = H$ (4.6%)
93: R^1 CO_2CH_3; $R^2 = C(CH_3)_3$ (cyclization 73%; overall 37%)

pyridine
Δ, reflux

$Pd(dba)_2$, CuI
PPh_3, NEt_3

92 (51%)

multiple
steps

89   +   3   **90**   +   2   **91**
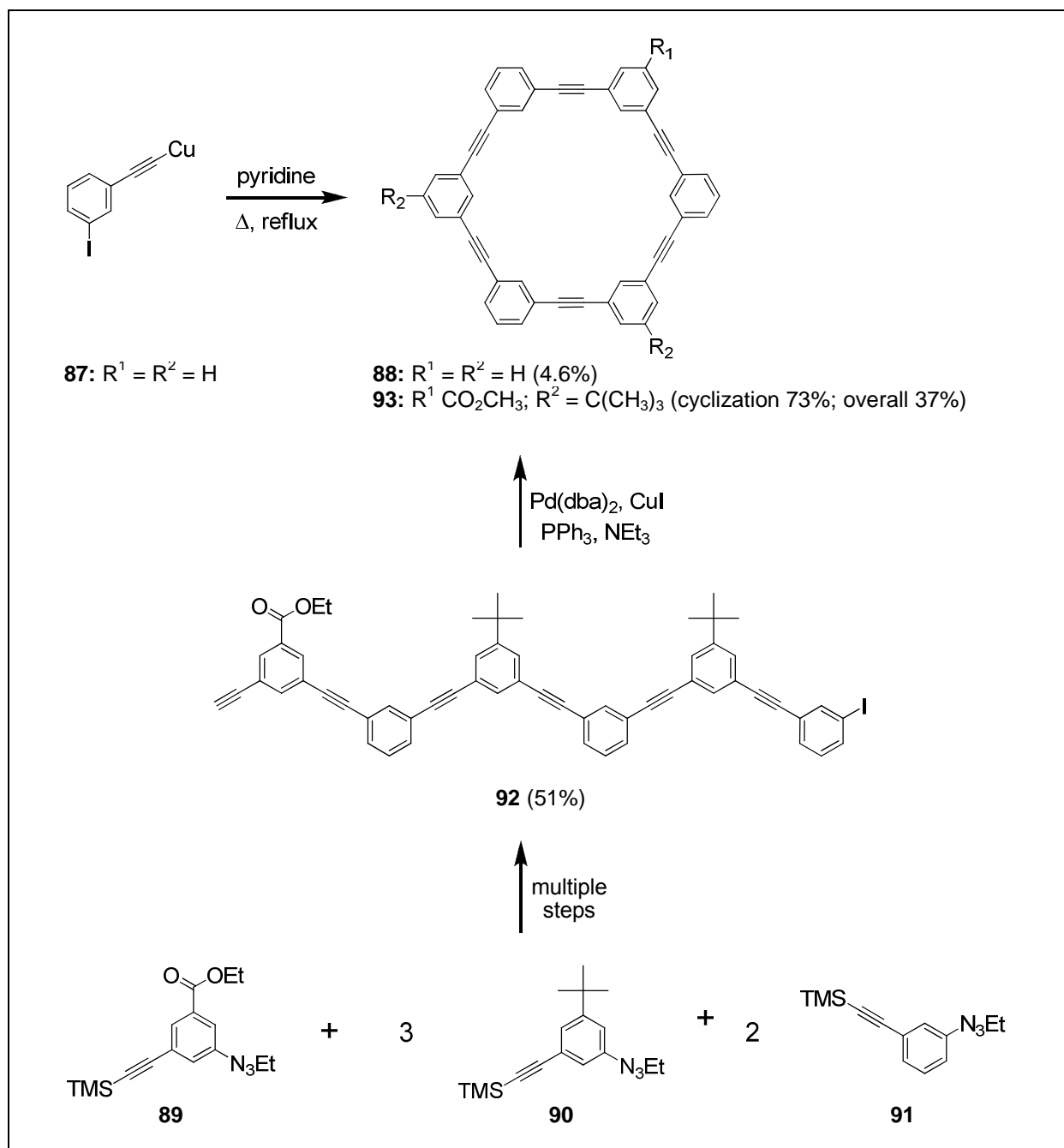
Scheme 4. 1: Synthesis of macrocycles **88** by Staab[366] and **93** by Moore[106] via intermolecular and intramolecular cyclization reactions, respectively.

139
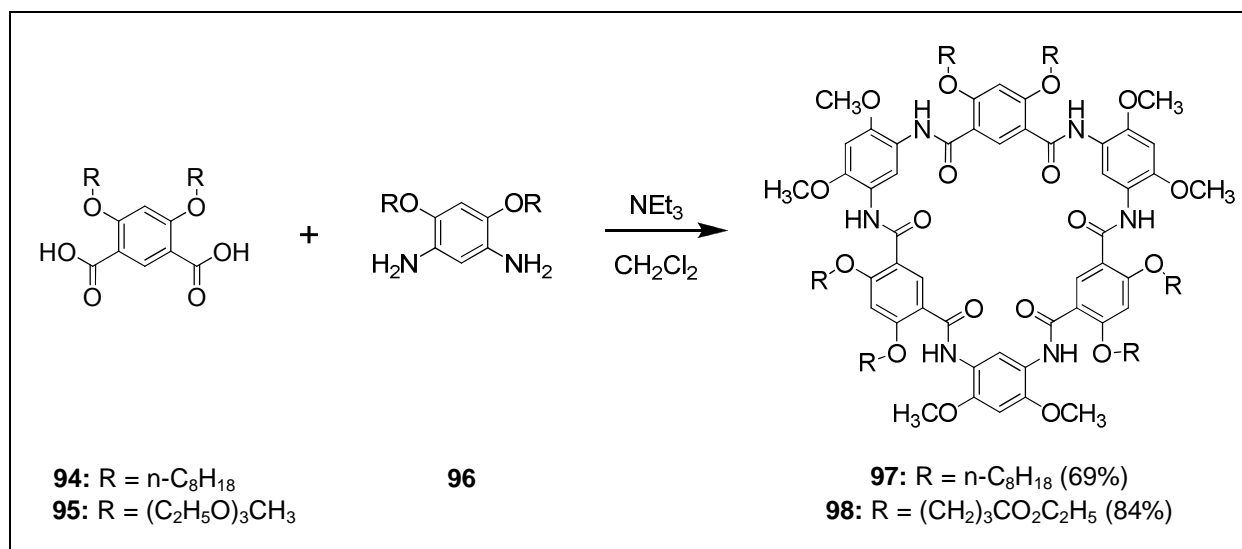
Scheme 4. 2: Synthesis of macrocycles **97** and **98** assisted by the intrinsic exotopic H-bond template.[360]
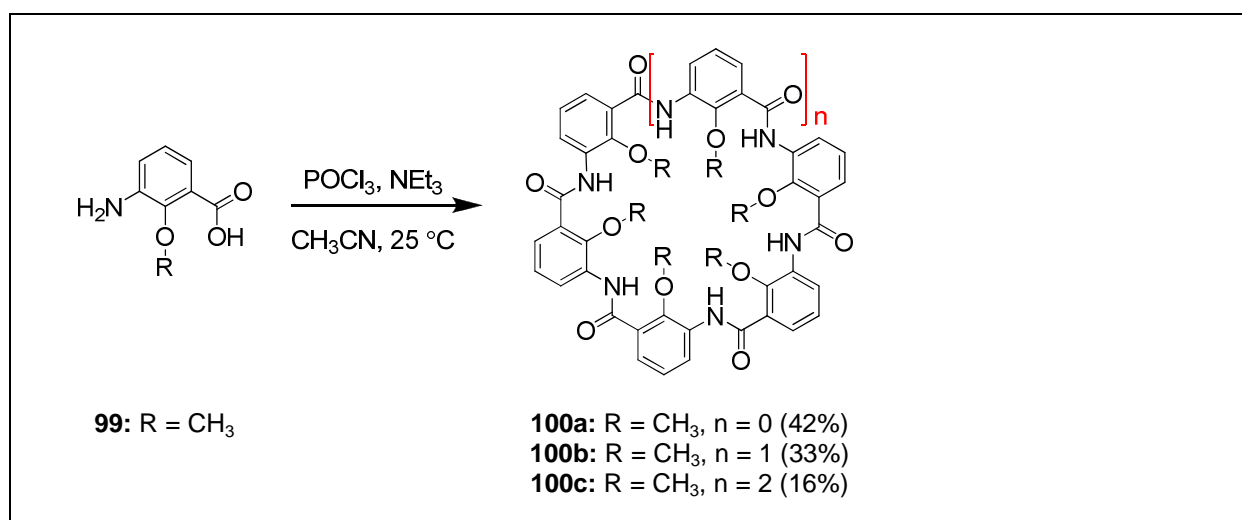
Scheme 4. 3: Synthesis of macrocycles **100** aided by the intrinsic endotopic H-bond template.[358]

Indeed, it is more difficult to control or predict the size, shape, and the arrangement of monomers in the products synthesized via one-pot intermolecular cyclizations. Therefore, in cases where macrocyclic targets lack a high degree of symmetry or when a specific size is desired, the two multi-step processes are preferred. In order to be considered viable, however, multi-step processes must be designed to minimize the number of required steps while maximizing productivity.

140

4.1.2 Rational Design

Two approaches have been considered for minimizing the labor expense of the multistep processes. The first is solid-support synthesis, during which the acyclic precursor is grown off of a solid support in a step-wise fashion and then released upon cyclization. Because the intermediate products are purified by washing away byproducts and unused starting materials between reactions rather than by time-consuming and product reducing chromatography, solid-support synthesis reduces the amount of work required and optimizes product recovery from the intermediary steps. Although this method has been used in the preparation of polymers and non-rigid macrocycles in high yields, it has rarely if ever been used successfully to synthesize shape-persistent macrocycles. For example, Tour attempted to synthesize cyclic phenylacetylenes by solid-phase synthesis but could not isolate the desired product, which was presumed to be lost to catenation of the macrocycle and resin.[342] Another issue with solid phase synthesis is that potential targets are limited to those with an acyclic precursor that is sufficiently flexible so that its free terminus can fold toward the tethered end during the cyclization step. Since acyclic precursors of most shape-persistent macrocycles are non-flexible, solid support synthesis is not an advantageous method for their construction.[367]

The second, more practical approach is to optimize coupling yields by employing reliable reactions and reduce labor costs by limiting the number of distinct component targets and/or the coupling reactions that are performed prior to cyclization. This methodology requires rational design of an efficient multi-step synthesis, as is demonstrated in the elegantly designed synthesis of macrocycle **106** by Höger's group.[368] See Scheme 4.4 and Figure 4.3. The assembly of **106** involved construction of the symmetric higher-order building component **103** (91 % yield) from basic building blocks **101** and **102** in a single step. Formation of **105** requires three of these components, which were tethered to a 1, 3, 5-benzenetricarboxylic acid anchor by breakable ester bonds producing **105** (73% overall yield) prior to intramolecular cyclization. Finally, the macrocycle's cavity is emptied after the anchor is released in a single reduction reaction, producing **106** in 94% yield. Owing to the arrangement and proximity of the anchored building blocks, the formation of **106** is highly efficient, as is made apparent when comparing the 94% yield for the intramolecular cyclization of **106** with the 54% yield for the intermolecular cyclization of **107**.[369] See Figure 4.3. Despite the additional steps required for fastening and
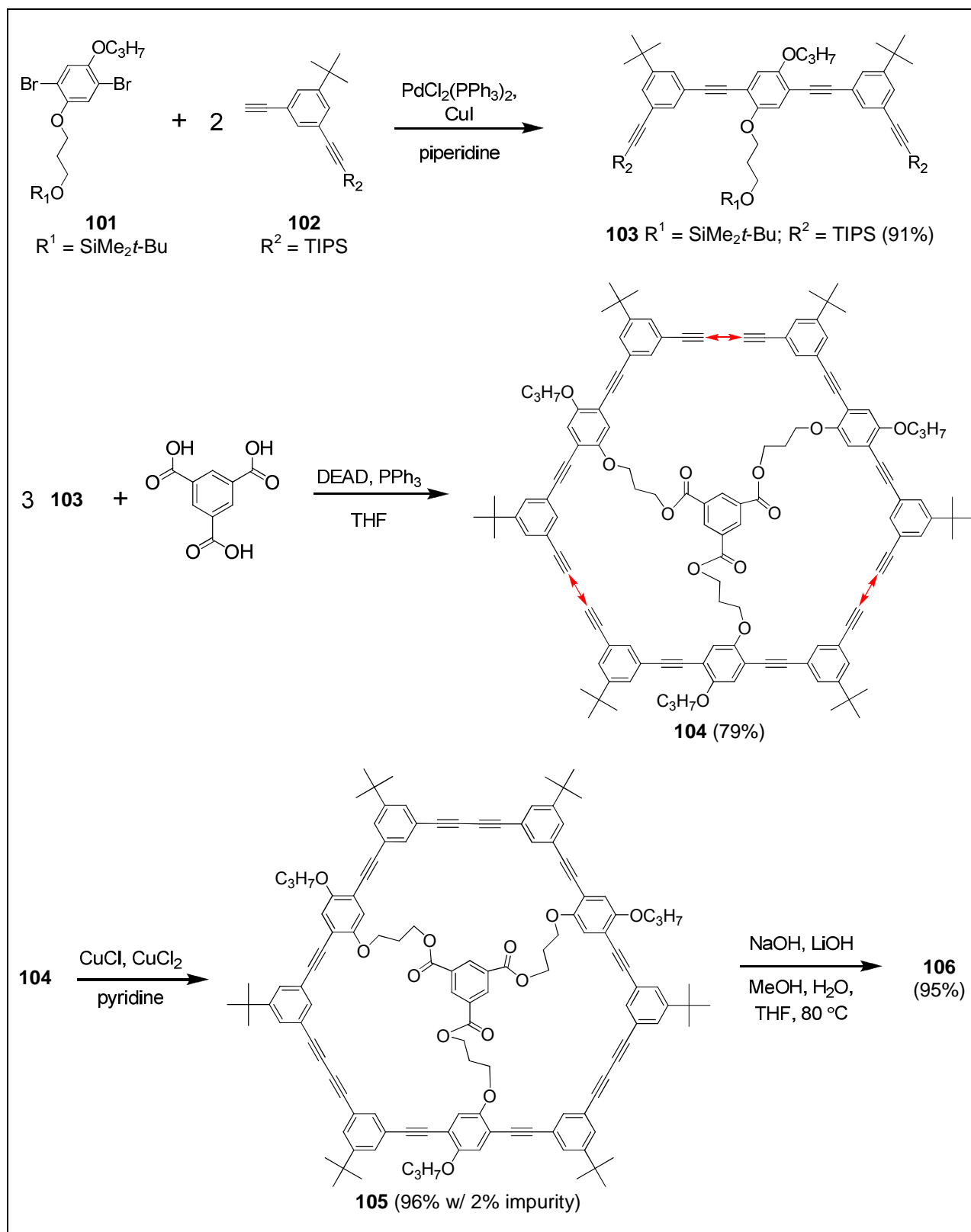
Scheme 4. 4: Synthesis of macrocycle **106** and its precursor **105**.[368]
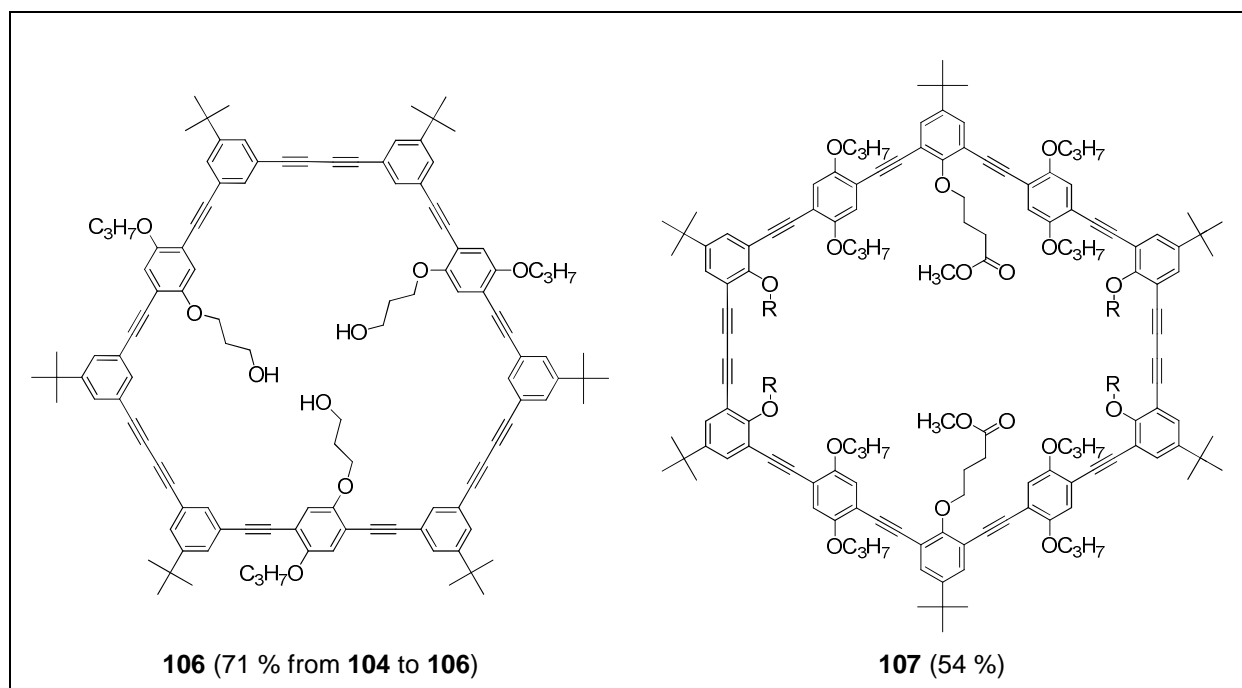
Figure 4. 3: Macrocycles **106**[368] and **107**[369]. Percent yields listed correspond to the cyclization reaction.

unfastening the anchor, this procedure limits the number of coupling reactions to two. Because, the work up required for the anchor binding condensation and anchor releasing hydration reactions are much less burdensome than the work up required for the organic coupling reactions, the overall procedure is less arduous than an alternative step-by-step method. Moreover, the overall yield of the reaction calculated relative to basic building block **101** is roughly 60%, which is impressive for shape-persistent macrocycles.

The synthesis of macrocycle **111** as reported by Schmittel and Ammon is another example of an efficient multistep synthesis.[370] See Scheme 4.5. According to their procedure the coupling of the basic building blocks **75** and **29** followed by deprotection of the acetylene produces the higher order building component **108** in an overall yield of 84 %. This species along with the basic building block **109** is then used to produce component **110**. To avoid oligomeric byproducts the authors used a ten-fold excess of the "capping" building block (i.e. **109**) isolating **110** in 84% yield. Finally coupling of **110** and **108** generates macrocycle **111** in 16% yield.

143
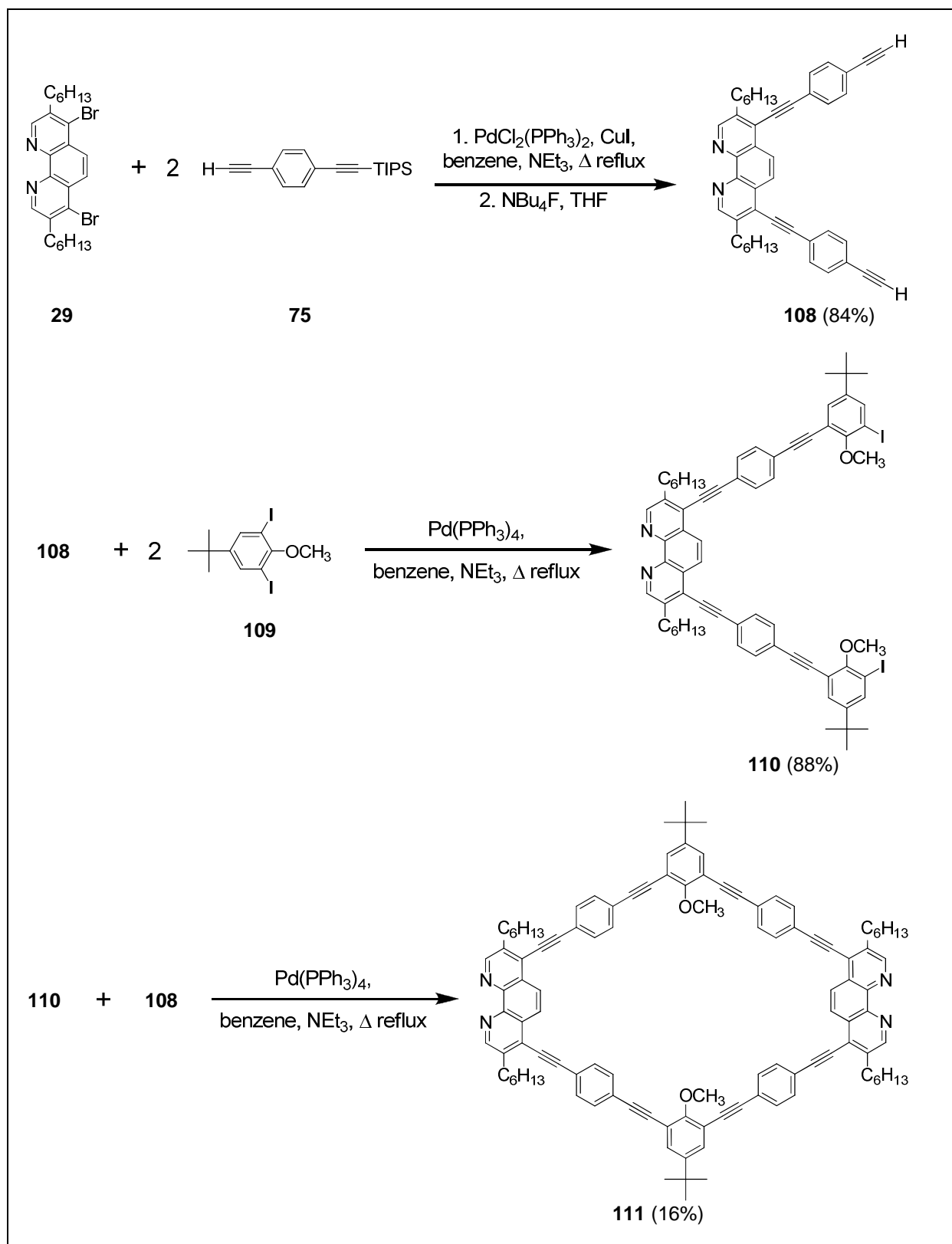
Scheme 4. 5: Synthesis of Macrocycle **111** by Schmittel and Ammon.[318,370]

As is obvious in their relative yields the anchor-assisted intermolecular cyclization of **106** is more productive than the intermolecular cyclization of **111**. However, closer inspection of the two procedures reveals some general commonalities in the pre-cyclization steps. For example, all components were produced from a few basic building blocks and assembled using non-linear synthetic techniques of convergence. Moreover, the symmetric couplings used to generate the higher order components reduce the number of required coupling reactions. Yields of these reactions are consistently high when the capping building block is used in excess. Therefore, the synthetic design implemented to construct both **106** and **111** is advantageous with respect to the linear synthesis employed by Moore. In regard to our aims, we also intended to implement rational design to construct our prisms' faces with several fundamental building block compounds, which are illustrated in Figure 4.4 and include: 4,7-dibromo-3,8-dihexyl-1,10-phenanthroline (**29**) and ethyl-3,5-dibrombenzoate (**30**), as well as edge components 1-ethynyl-2,5-dihexyl-4-trimethylsilylethynylbenzene (**26**).; 1-ethynyl-2,5-dihexyl-4-triisopropylsilylethynylbenzene (**27**); and 4-(4-ethynyl-2,5-dihexylphenyl)-2-methyl-3-butyn-2-ol (**28**). These building blocks were assembled using a pattern of selective acetylene deprotection and reliably established Sonogashira cross-coupling mechanism.

Corners

29
Corner for Triangle Face (**32**) and Diamond Face (**35**)

30
Corner for Diamond Face (**2**)

Edges

26: R = TMS
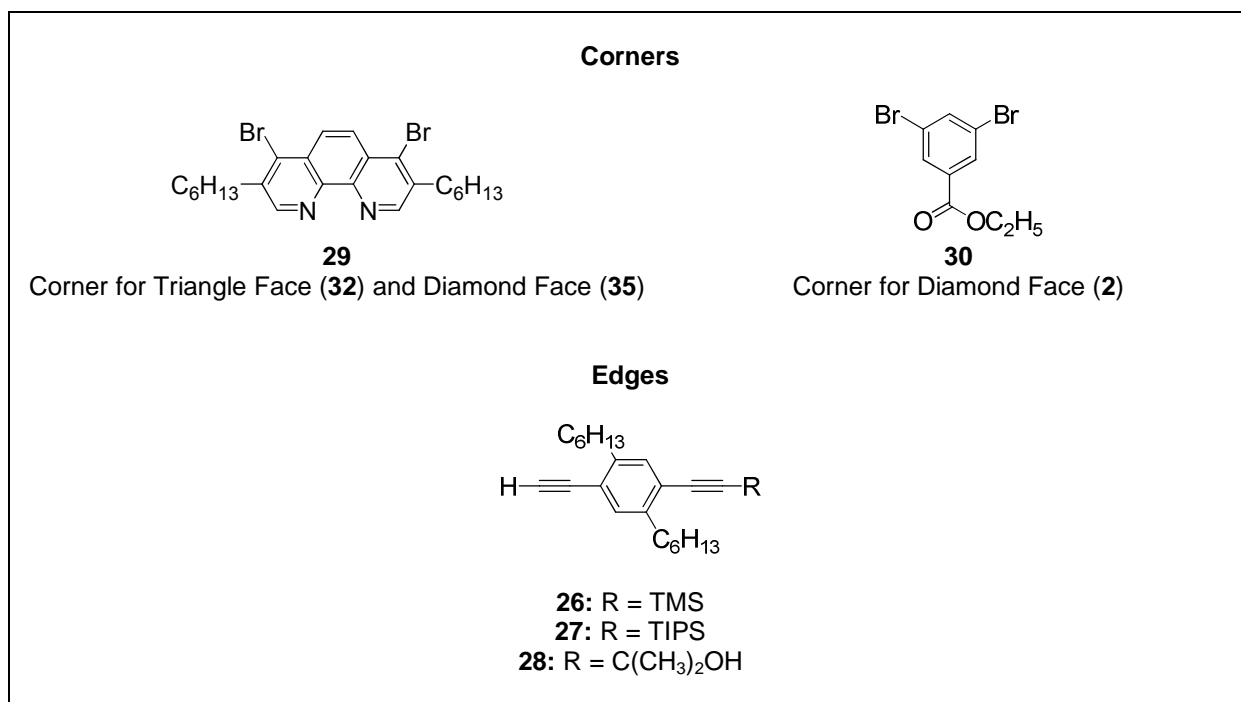**27:** R = TIPS
28: R = C(CH$_3$)$_2$OH

Figure 4. 4: Fundamental or 1°-building blocks for **32** and **35**.

Of course there are many potential pathways that can be used to generate macrocycles shape-persistent macrocycles from a select set of building blocks materials. These pathways will differ in both the number of steps and overall product yields. In keeping with our goal of creating and employing a rationally design pathway with maximal product yields through the minimal number of reaction steps, it is important to establish a clear procedure tabulating how many steps were used to produce a particular product via a specific pathway. To this end, the building blocks and macrocycles have been classified by degree designations (i.e. 1°, 2°, 3°, 4° - read as first degree, second degree, third degree, fourth degree ect.) that quantify the number of unique coupling that were used to produce that building block or macrocycle. Other reactions, such as deprotection reactions are neglected in the count.

Coupling Examples		**Description**
		General Example
a. $\quad$ A $+$ B $\longrightarrow$ C $\quad$ 1° $\quad$ 2° $\qquad$ 3°		Degree designations are usually determined as the sum of the degree designations of the reagents in the coupling reaction.
		Exceptions
b. $\quad$ 2A $+$ B $\longrightarrow$ D $\quad$ 1° $\quad$ 2° $\qquad$ 3°		Degree designations ignore the reaction stoichiometry.
c. $\qquad\qquad$ 2B $\longrightarrow$ E $\qquad\qquad$ 2° $\qquad$ 3°		For homocoupling reactions simply add 1° to the degree designation of the building block, again ignoring stoichiometry.
d. step 1 $\quad$ 2A $+$ F $\longrightarrow$ G $\qquad$ 1° $\quad$ 1° $\qquad$ 2°		Building block reagents used more than once during a sequence of steps are counted as 1° in subsequent coupling reactions (e.g. G in step 3).
$\quad$ step 2 $\quad$ G $+$ H $\longrightarrow$ I $\qquad$ 2° $\quad$ 1° $\qquad$ 3°		
$\quad$ step 3 $\quad$ I $+$ G $\longrightarrow$ I $\qquad$ 3° $\quad$ 2° $\qquad$ 4°		

Figure 4. 5: Description of the degree designations used.

The most fundamental building blocks are given 1° designations. See Figure 4.4. In general the designation for higher-order building blocks are calculated as a sum of the degree designation of its reagent building blocks, ignoring stoichiometry. See Figure 4.5 a and b. To avoid over counting by adding the degree designation for a building blocks used multiple times throughout

the synthesis of a single end product each time that building block is used, repeat building blocks are added as 1° after the first time they are counted as a reagent. This exception applies to a reagent that appears in the same reaction (i.e. homocoupling) or in different steps in a multistep process. See Figure 4.5 c and d. The degree designations are a convenient way of comparing procedures based on the number of coupling steps and will be employed for the remainder of this chapter to describe both the building blocks and macrocycles.

4.2. Results and Discussion

4.2.1. Synthesis and Characterization of Triangular Face:

The synthesis of triangular face **32** was attempted via intramolecular cyclization as shown in Schemes 4.6 – 4.8. Potentially, **32** could be generated in fewer steps by the one-pot and multistep intermolecular cyclization procedures shown in Scheme 4.9a and b, respectively. Through the one-pot method, compound **32** may be produced as a 3° macrocycle from the intermolecular cyclization of 2° building block **121**. See Scheme 4.9a. However, as with the synthesis of **88** by Staab (see Scheme 4.1), the synthesis of **32** via the one-pot procedure is expected to generate very little product due to competing oligomerization reactions. On the other hand, higher yields are expected for the intermolecular cyclization of 3° building block **123** and 1° building block **124** (see Scheme 4.9b), which is similar to the synthesis of **111** by Schmittel and Ammon (see Scheme 4.5). See Scheme 4.9a. By this procedure **32** could be generated as a 4° macrocycle. Unfortunately, previous experience has shown, compound **124** is not a reliable coupling agent under the conditions needed for this reaction; conditions that will be described below. Although both intermolecular cyclization procedures are attractive as convenient methods for obtaining **32** in relatively few steps, it will be difficult to isolate any significant amount of product from the oligomeric byproducts produced during these reactions, since 1,10-phenanthroline compounds have low R_f values and long retention times. Therefore, the oligomers and the macrocycle are not expected to separate on the chromatography column. Indeed, isolation of **123** from the crude product proved unsuccessful after several attempts by column chromatography. Therefore, the most reasonable route toward **32** is the intramolecular synthesis shown in Schemes 4.6 – 4.8. According to this procedure, the acyclic precursor is produced from two 2° building blocks, **112** and **114**, as well as 1°, and 3° building blocks **29** and

147

116, respectively. Even though this method is not labor saving, we have been able to synthesize **32** via this route.
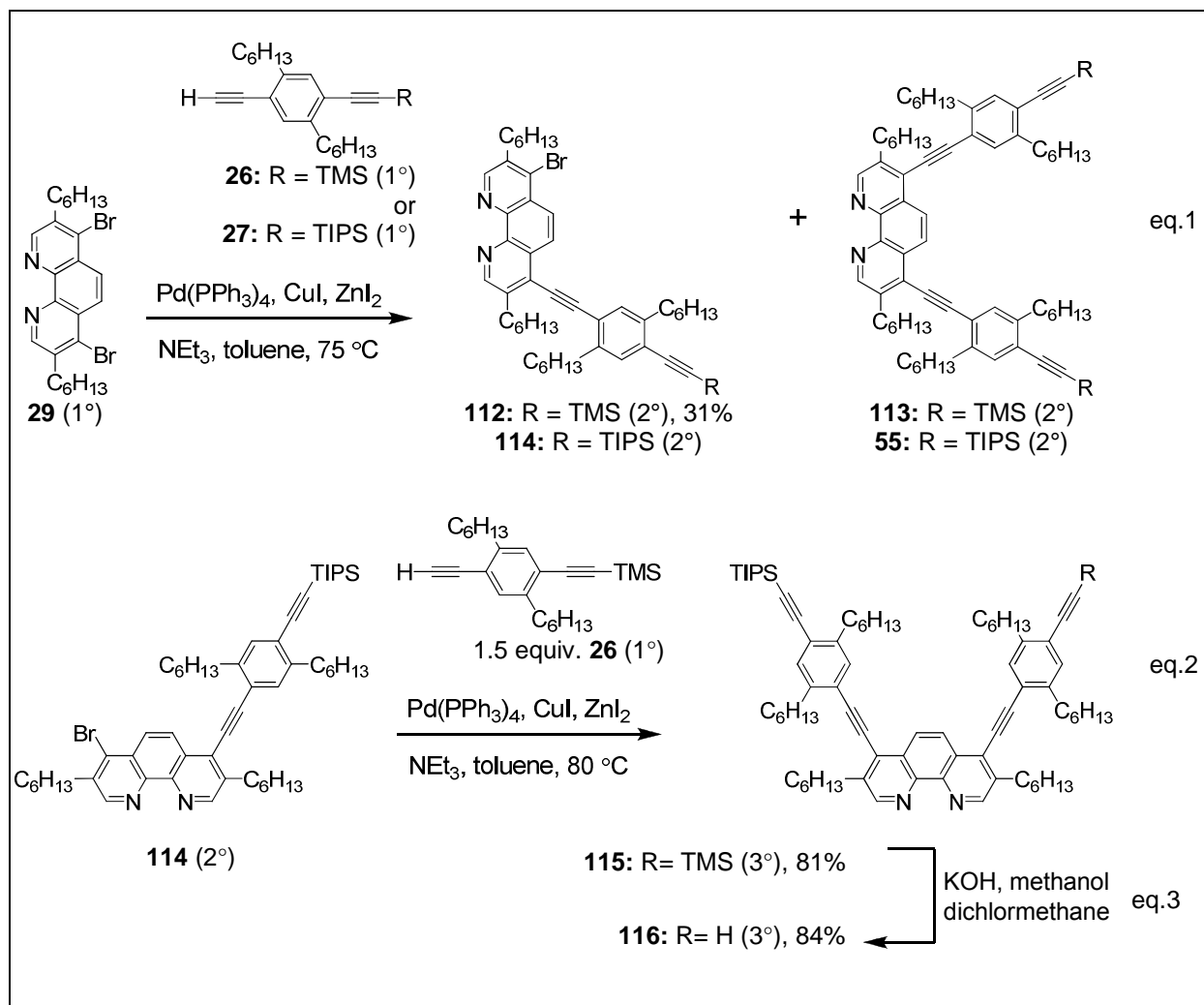
Scheme 4. 6: Synthesis of 2° building blocks **112** and **114** as well as 3° building block **116** for triangular face **32**.
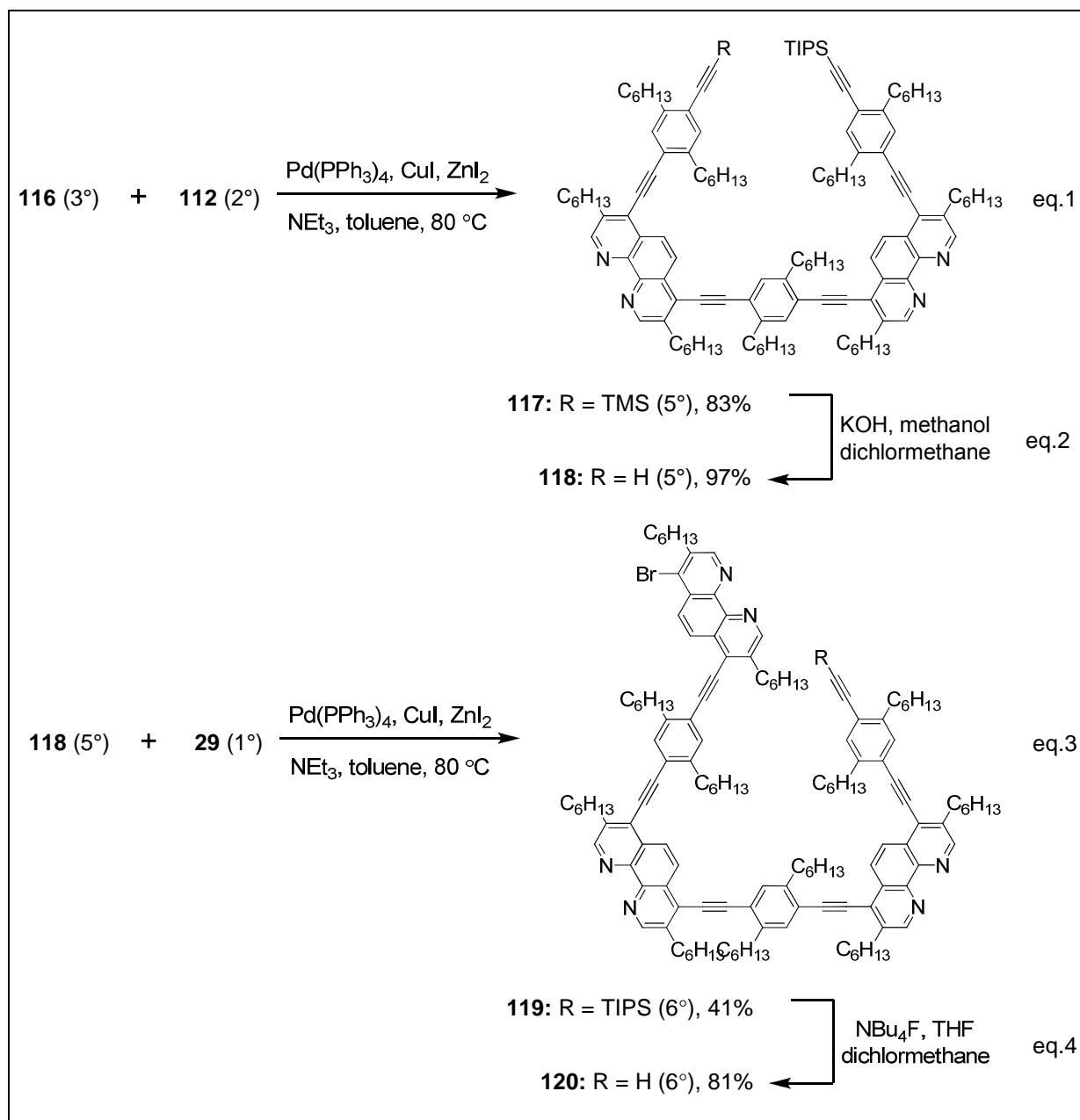
Scheme 4. 7: Synthesis of the 6° acyclic precursor (**120**) of diamond face **32**.
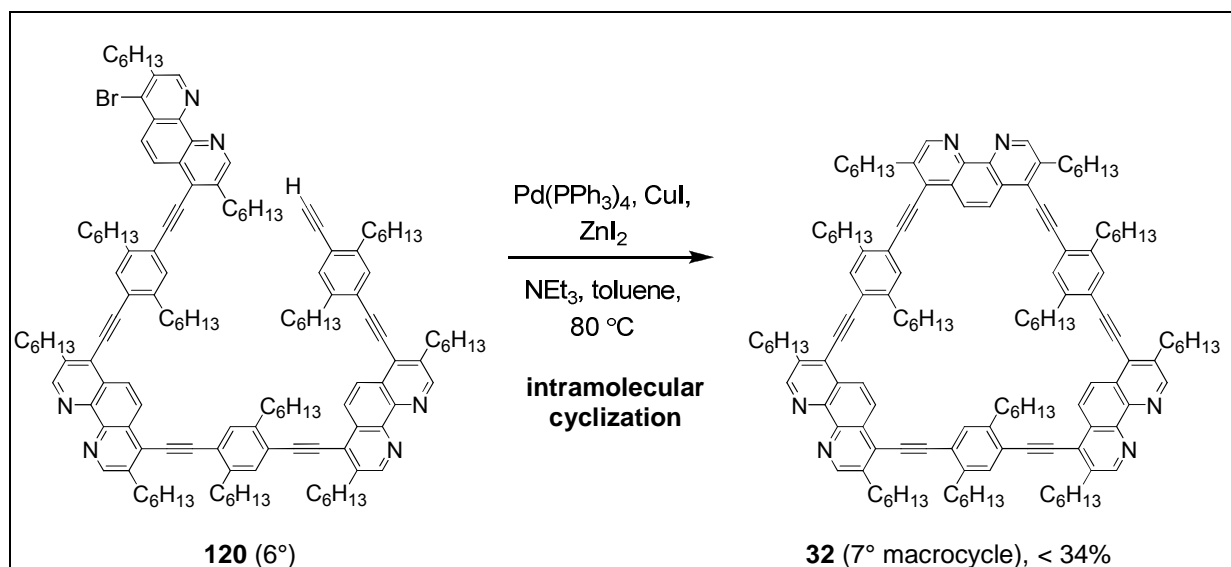
Scheme 4. 8: Synthesis of triangular face **32** via intramolecular cyclization of 7° acyclic precursor **120**.

The first targets in the intramolecular cyclization procedure are 2° building blocks **112** and **114**. These 2° building blocks were synthesized via two analogous reactions from 1° building blocks **29** and **26** or **27**, respectively via Sonogashira cross-coupling. Because brominated sp^2-carbons para to the nitrogen in pyridine rings are not particularly reactive in the Pd-catalytic cycle of the Sonogashira coupling, this reaction required elevated reaction temperatures ($\geq 70°$ C), prolonged reaction times (≥ 48 hrs.), as well as the addition of ZnI_2 or the use of excess CuI co-catalyst in the reaction mixture. This latter condition most likely results in zinc (II) or Cu (I) phenanthroline complexes that may facilitate coupling to **29** in two ways. Firstly, the phenanthroline ring in the d^{10} metal complexes is expected to be more electrophilic than the free phenanthroline. The increased electrophilicity of the phenanthroline may facilitate the oxidative addition step during the Pd-catalytic cycle of Sonogashira coupling. Secondly, formation of the zinc and copper phenanthroline complexes may be beneficial for the copper catalytic cycle since free phenanthroline may consume the Cu^+ ions necessary for the Cu-catalytic cycle catalysts through coordination. Indeed in the absence of ZnI_2 or excess CuI, yields for these coupling reactions were invariably low. Employing these conditions and one molar equivalent each of **29** and **26** or **27**, we were able to isolate 2° building blocks **112** and **114** in roughly 30% yield. In addition to the desired products, these reactions also produce byproducts **113** and **55**, which were not isolated.

150
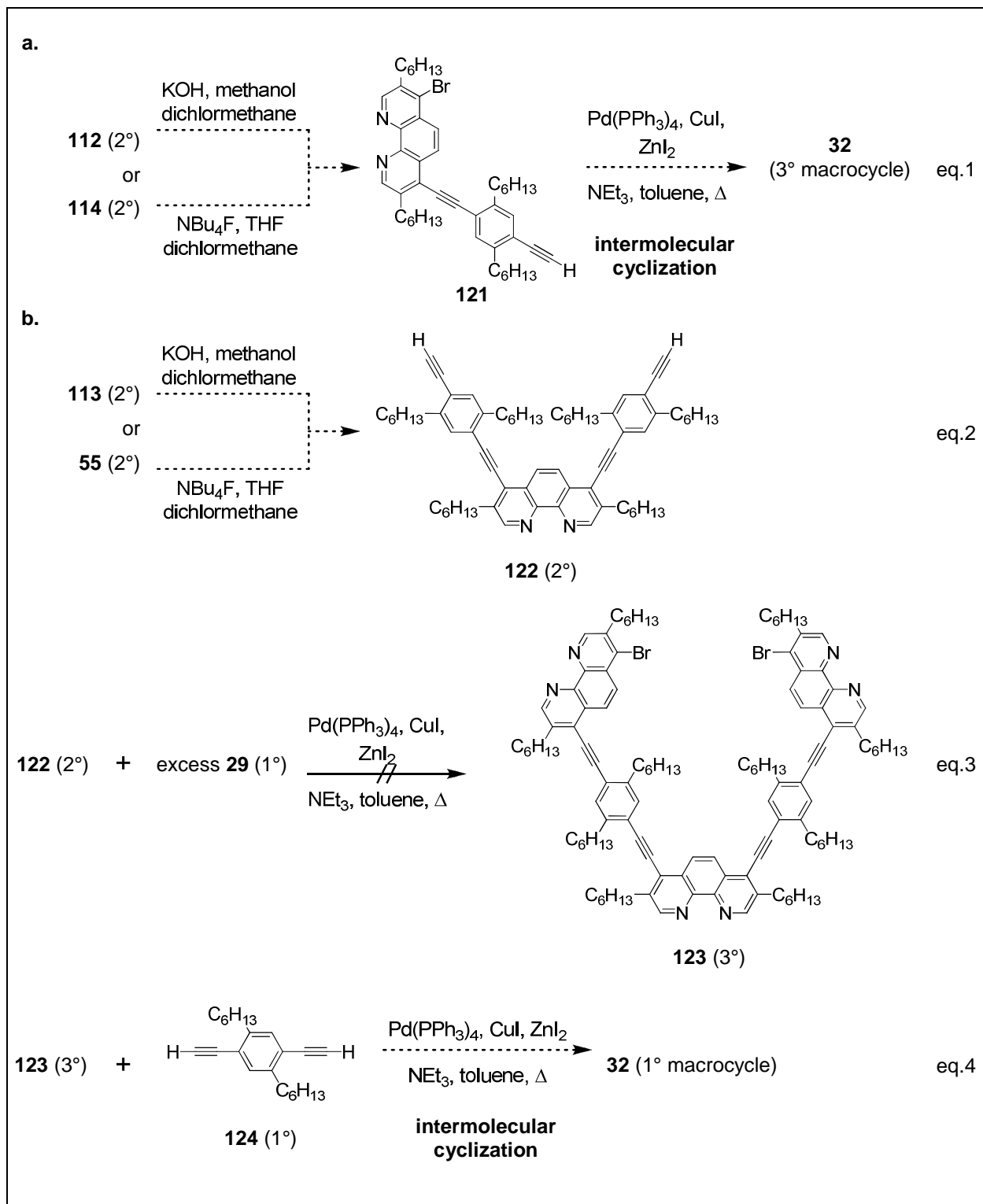
Scheme 4. 9: Proposed intermolecular cyclization pathways: a. one-pot synthesis from **121**; and b. multistep synthesis.

151

Compounds **112** and **114** were easily identified by the chemical shift values for several notable protons in their ^{1}H NMR spectra. See Table 4.1. ^{1}H NMR spectroscopy is a particularly convenient method for characterizing these compounds, as their proton signal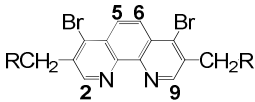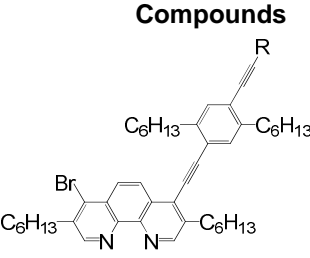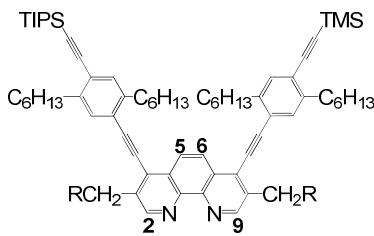s are straightforward to assign; especially in the aromatic region, where complications caused by second order or virtual coupling effects are absent, and where the phenyl and the two types of phenanthroline protons resonate at very distinct frequencies. As a result, the aromatic region can be analyzed by simple first-order techniques. The ^{1}H NMR spectra of 3,8-dihexyl-4-bromo-7-(4-trimethylsilylethynyl-2,5-di-n-hexylphenylethynyl)-1,10-phenanthroline (**112**) and 3,8-dihexyl-4-bromo-7-(4-triisopropylsilylethynyl-2,5-di-n-hexylphenylethynyl)-1,10-phenanthroline (**114**) are alike and only distinguishable by the trialkylsilyl proton peaks. Both spectra feature singlets at, 8.91 and 9.05 ppm, which correspond to protons at the 2 and 9 positions, as well the AB doublet peaks centered near 8.30 and 8.41 ppm assigned to protons at the 5 and 6 positions. The two pairs of methylene protons adjacent to the phenanthroline (i.e. picolinyl protons) also resonate at distinct frequencies, with those closest to the bromine substituent resonating near 3.01 ppm and the remaining pair resonating near 3.10 ppm. These assignments were determined by comparing the chemical shifts of **112** and **114** with 3,8-dihexyl-4,7-dibromo-1,10-phenanthroline (**29**) and 3,8-dihexyl-4,7-bis(4-triisopropylsilylethynyl-2,5-di-n-hexylphenylethynyl)-1,10-phenanthroline (**55**). As evident in Table 4.1, the identities of the substituents at the 4 and 7 positions of the phenanthroline have a pronounced influence on the chemical shifts of both the phenanthroline and the adjacent methylene (i.e. picolinyl) protons. Apparently, protons nearest the bromine substituent are less deshielded than those nearest the alkyne substituent. The phenyl protons and methylene protons adjacent to the phenyl (i.e. benzyl protons) in **112** also resonate at frequencies nearly equivalent to those in **114**. Indeed, the only significant distinguishing spectral features are the trialkylsilyl protons peaks; the TMS peak resonating at 0.28 ppm in **112** and the TIPS resonating at 1.15 ppm in **114**. Likewise, the ^{13}C NMR spectra of **112** and **114** are quite similar. Both contain twelve phenanthroline (δ = 151.5, 151.2, 145.4, 144.0, 138.9, 137.7, 134.7, 128.1, 127.8, 127.5, 125.7, 125.7 ppm) and six phenyl ($\delta \approx$ 143.0, 142.2, 133.0, 132.7, 123.7, 121.7 ppm) peaks, which resonate at identical or nearly identical frequencies. In addition, there are four alkynyl carbon peaks. The two carbons in the alkyne bond linking the phenanthroline and benzyl groups resonate near 101.6 ppm and 88.0 in both compounds. On the other hand, the terminal alkynyl carbons resonate near 103.6 and 99.8

ppm in **112** and near 105.3 and 96.2 ppm in **114**. These chemical shifts are nearly identical to those observed in the ^{13}C NMR spectra of **26** (δ = 103.8 and 99.0 ppm) and **27** (δ = 105.5 and 95.3 ppm). Finally, the trimethylsilyl carbons in **112** (δ = –0.1 ppm) and the triisopropylsilyl carbons in **114** (δ = 18.7 and 11.3 ppm) resonate at their anticipated frequencies.

Table 4. 1: ^{1}H NMR Data of Select Protons in Phenanthroline Compound **29**, **112**, **114**, and **55**

δ (ppm)	**29**	**112:** R = TMS or **114:** R = TIPS	**55**
2, 9	8.89	8.91, 9.05	9.07
5, 6	8.24	8.30, 8.41	8.44
picolinyl	2.99	3.01, 3.10	3.13

The next step in the construction of **32** via the intramolecular cyclization pathway is to generate 3° building block **115**. See Scheme 4.6. Compound **115** may be synthesized by coupling **112** and **27**. This approach is attractive, since it eliminates the need for compound **114**, and thus macrocycle **32** could be achieved as a 6° rather than a 7° macrocycle. Nevertheless, compound **115** was produced in 81% yield by coupling **114** and an excess of **26** under the previously described Sonogashira cross-coupling conditions.

The ^{1}H NMR and ^{13}C NMR spectra of **115** feature fewer peaks than the corresponding spectra of the actual and potential parent compounds **114** and **112**. This is owing to the fact the chemical environments created by the substituents at the 4 and 7 positions of the phenanthroline are similar in **115** and distinct in, **112** and **114**. Consequently, all protons and many carbons related by the local C_2- symmetry element, which bisects the C_5–C_6 and C_{10a}–C_{10b} carbon-carbon bonds, resonate at frequencies indistinguishable in the spectra. See Figure 4.6a. Therefore the two singlets assigned to protons at the 2 and 9 positions as well as the AB doublet assigned to protons at the 5 and 6 positions, which are characteristic of monocoupled products that have a single bromine substituent at the 4 position of the phenanthroline (i.e. **112** and **114**), is absent in

153

the ^{1}H NMR spectra **115**. Instead, there are only two singlets in the phenanthroline region of the spectra at 9.07 ppm and 8.44 ppm, which correspond to the protons ortho and para to the nitrogen in the phenanthroline. See Table 4.1. Likewise, there is only one triplet, centered at 3.13 ppm for the picolinyl protons in **115**. Similarly, most carbons related by a local pseudo symmetry operation, save for a pair of carbons at the 3 and 8 or at the 4a and 6a positions, are isochronous at 400 MHz of **115**; hence there are only seven phenanthroline carbon peaks in the ^{13}C NMR spectra (i.e. δ = 151.2, 144.5, 138.7, 128.1, 128.0, 127.6, 125.0 ppm). On the other hand, all twelve of the phenyl peaks (δ = 143.1, 142.9, 142.2, 142.1, 133.1, 132.7, 132.7, 132.7, 124.0, 123.4, 121.9, 121.7 ppm) as well as all eight alkynyl peaks (δ =105.4, 103.6, 101.4, 101.3, 99.7, 96.1, 88.2, 88.2) resonate at distinct frequencies. The chemical shift values for the phenyl and alkynyl carbons are consistent with resonance frequencies of the corresponding carbons in **112** and **114**. See Figure 4.6a.
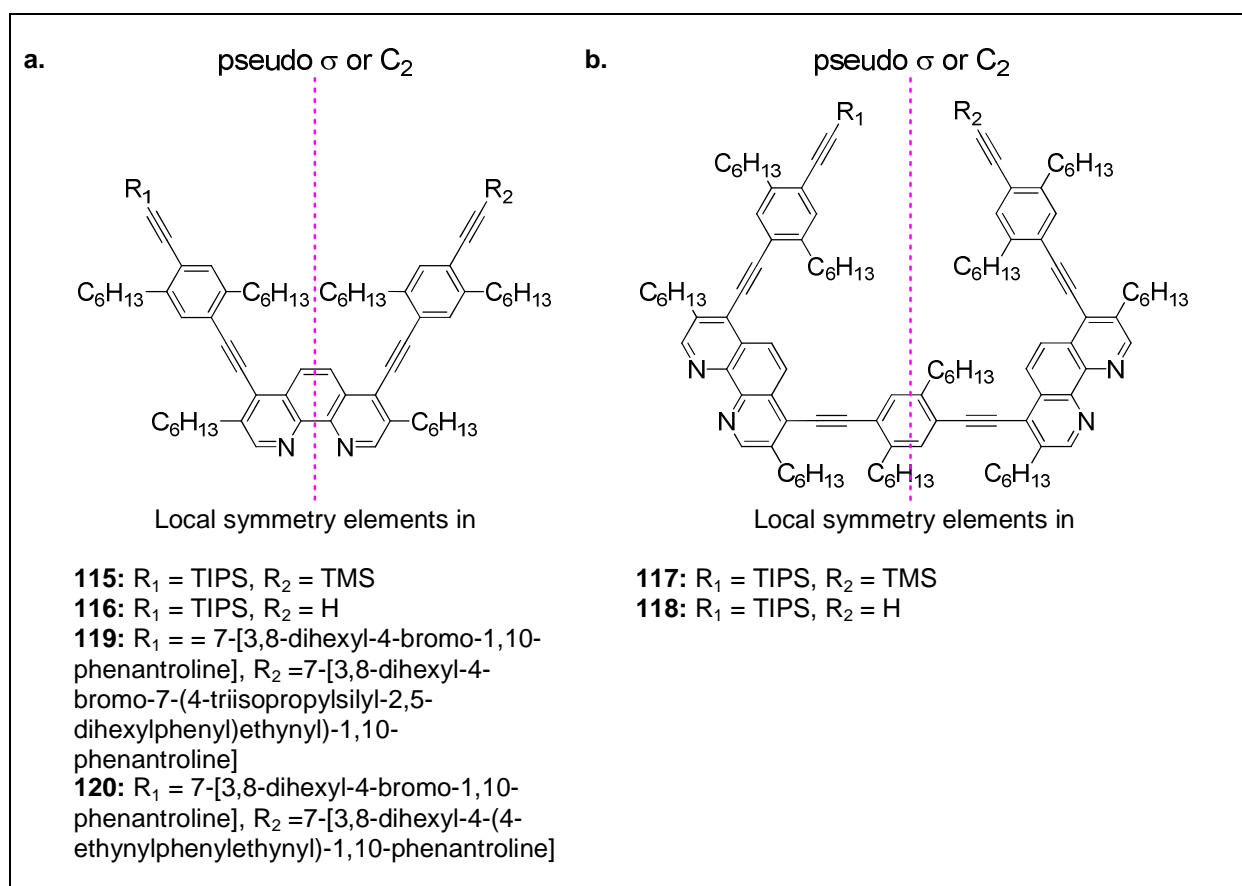

Figure 4. 6: Local pseudo-symmetrs element in compounds **115 – 120**.

The TMS group in building block **115** was next selectively removed in order to generate 3° building block **116** in 84 % yield. The success of the desilylation reaction was confirmed by the absence of a TMS carbon peak at −0.1 ppm and proton peak at 0.28 ppm in the ^{13}C NMR and ^{1}H NMR spectra, respectively, of **116**, as well as the absence of the trimethylsilylated alkynyl carbon signals at 103.6 and 99.7 ppm. Concurrently the existence of the acetylenic proton at 3.36 ppm in the ^{1}H NMR spectra of **116**, as well as the acetylenic carbons at 88.2 and 88.3 ppm in the ^{13}C NMR spectra confirm the formation of the terminal alkyne.

The 3° building block **116** is next coupled to 2° building block **112** to produce the 5° building block **117** in 83% yield. The selective deprotection of the TMS-masked acetylene in the **117** then produces compound **118** in 97% yield. The number of peaks in the ^{1}H NMR and ^{13}C NMR spectra of **117** are fewer than the number of protons and carbons, respectively. Again we attribute this to the existence of a local C_2-symmetry element that bisects the C_2–C_3 and C_5–C_6 carbon-carbon bonds in the benzene of the internal 1,4-di(ethynylene)-2,5-di(n-hexyl)benzene moiety. See Figure 4.6b. Therefore, the isochronicity of the protons and carbons related by this symmetry element is not surprising. The ^{13}C NMR spectra of **117** displays thirteen phenanthroline (δ = 151.3, 151.3, 144.5, 144.5, 138.8, 138.7, 128.1, 128.1, 127.9, 127.7, 127.6, 125.1, 124.9 ppm) and thirteen phenyl carbon peaks,(δ = 143.1, 142.9, 142.6, 142.2, 142.1, 133.1, 133.1, 132.7, 124.0, 124.0, 123.0, 121.8, 121.6 ppm) as well as ten alkynyl peaks (δ = 105.3, 103.6, 101.4, 101.4, 101.0, 99.7, 96.2, 88.8, 88.2, 88.1 ppm). The ^{1}H NMR spectra of **117** features three phenanthroline peaks, two closesly spaced singlets at 9.10 and 9.08 ppm assigned to protons ortho to the nitrogen and a singlet at 8.47 ppm assigned to protons on the central phenanthroline rings, as well as a single multiplet assigned to the picolinyl protons. There are also four singlets at 7.60, 7.48, 7.47, and 7.39 ppm assigned to the phenyl protons and three multiplets centered near 3.02, 2.92, and 2.80 ppm assigned to benzyl protons. Based on the presumption that the phenanthroline group is expected to have a stronger deshielding effect on the phenyl protons than the ethynyl group, the highest frequency phenyl and benzyl protons signals are tentatively assigned to those on the internal 1,4-di(ethynylene)-2,5-di(n-hexyl)benzene moiety, while the lowest frequency peaks assigned to protons farthest away from the phenanthroline on the terminal 1-ethynyl-2,5-dihexyl-4-trialkylsilylethynylbenzene moieties. Deshielding through the conjugated π-system may also explain why the chemical shifts of the phenanthroline, phenyl, picolinyl, and benzyl protons in **117** resonate at a slightly higher

frequency (downfield) than in **115** or **116**. Remarkably, resonance effects appear to have no apparent influence on the carbon signals. The ^{1}H NMR and ^{13}C NMR spectra of **118** is similar to **117**'s save for the anticipated differences associated with the desilylation of the TMS group. Moreover the electronic environments created by the terminal 1-ethynyl-2,5-dihexyl-4-triisopropylsilylethynylbenzene and 1,4-ethynyl-2,5-dihexylbenzene substituents in **118** are a little more distinct than the environments created by the two -ethynyl-2,5-dihexyl-4-trialkylsilylethynylbenzene substituents in **117**. Consequently the ^{1}H NMR and ^{13}C NMR for compound **118** feature one additional peak in both the phenanthroline and phenyl regions of the spectrum than is seen in the corresponding spectrum from **117**.

The final two steps before cyclization in the intramolecular pathway involves the coupling of 5° building block **118** and 1° building block **29** to generate 6° building block **119** in 41% yield. This was followed by desilylation of the TIPS protected acetylene produced the acyclic precursor **120** in 81% yields. The ^{1}H NMR spectra of compounds **119** and **120** feature the AB doublet centered near 8.47 and 8.35 ppm assigned to protons on the 5' and 6' position of the monobrominated phenanthroline moiety. The signals for the lower frequency doublets in both **119** and **120** are coincident with peaks near 8.50 ppm that assigned to other phenanthroline protons. See Figure 4.7. However, these doublets were verified through coupling constants and through the integration of the combined peaks. As previously mentioned this splitting pattern, which was also observed in the ^{1}H NMR spectra of **112** and **114**, is characteristic of a monobrominated phenanthroline. Many of the protons and carbons associated with the interior phenanthroline and phenyl groups in **119** and **120** related by the local C_2-symmetry element seen in Figure 4.6a are found to be isochronous in the ^{1}H NMR and ^{13}CNMR.
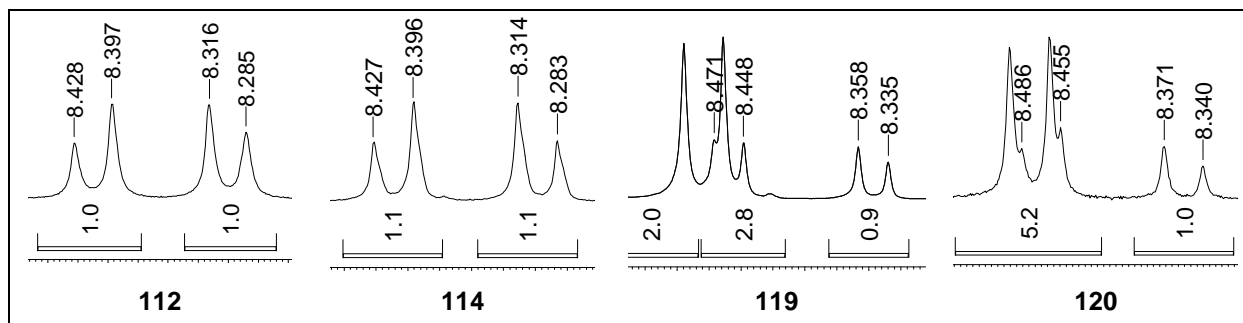

Figure 4. 7: Close up of AB doublets in mono-brominated phenanthroline species **112**, **114**, **119**, and **120**.

The final step in the intramolecular cyclization pathway involves coupling of the brominated carbon to the terminal alkyne in **120**. Although we were able to produce **32** (< 34%) through this intramolecular cyclization using high dilution batch-wise synthesis, we have so far been unable to isolate a significant amount of this macrocycle from its oligomeric byproducts for full characterization. However, we were able to obtain the ^{1}H and ^{13}C NMR spectra of the cleanest sample obtained after crude product was subjected to several chromatography procedures. The ^{1}H NMR spectra for **32** features three singlets at 9.12, 8.55, and 7.64 ppm, which are assigned to phenanthroline protons in the 2,9 and 5,6 positions and the phenyl protons, respectively. There are also two sets of overlapping virtual triplets centered at 3.18 and 3.08 ppm, which are assigned to the picolinyl and benzyl protons. The integrations for each of the aromatic proton peaks and the combined integration for the two triplets are 6 and 24, respectively, which is consistent with macrocycle **32**. There are nine peaks in the aromatic region of the ^{13}C NMR spectra, six of these are assigned to the phenanthroline carbons (δ = 151.3, 144.3, 138.9, 127.9, 127.7, 125.1 ppm) and the remaining three to the phenyl carbons (δ = 142.7, 133.2, 123.0 ppm). Additionally, there are two acetylenic carbons peaks at 101.2 and 88.9 ppm. As seen in Figure 4.9, both the ^{1}H and ^{13}C NMR spectra of **32** present far fewer peaks than its acyclic precursor **120**, which is consistent with the high degree of symmetry in the macrocycle (i.e. D$_{3h}$-symmetric). In addition, the AB doublets centered around 8.47 and 8.36 ppm, indicative of protons at the 5 and 6 positions in a monobrominated phenanthroline, as well as the acetylene proton at 3.30 ppm in the ^{1}H NMR spectrum of **120** are completely absent in the spectrum of **1**, which supports the coupling of the brominated carbon and terminal acetylene groups in **120**.
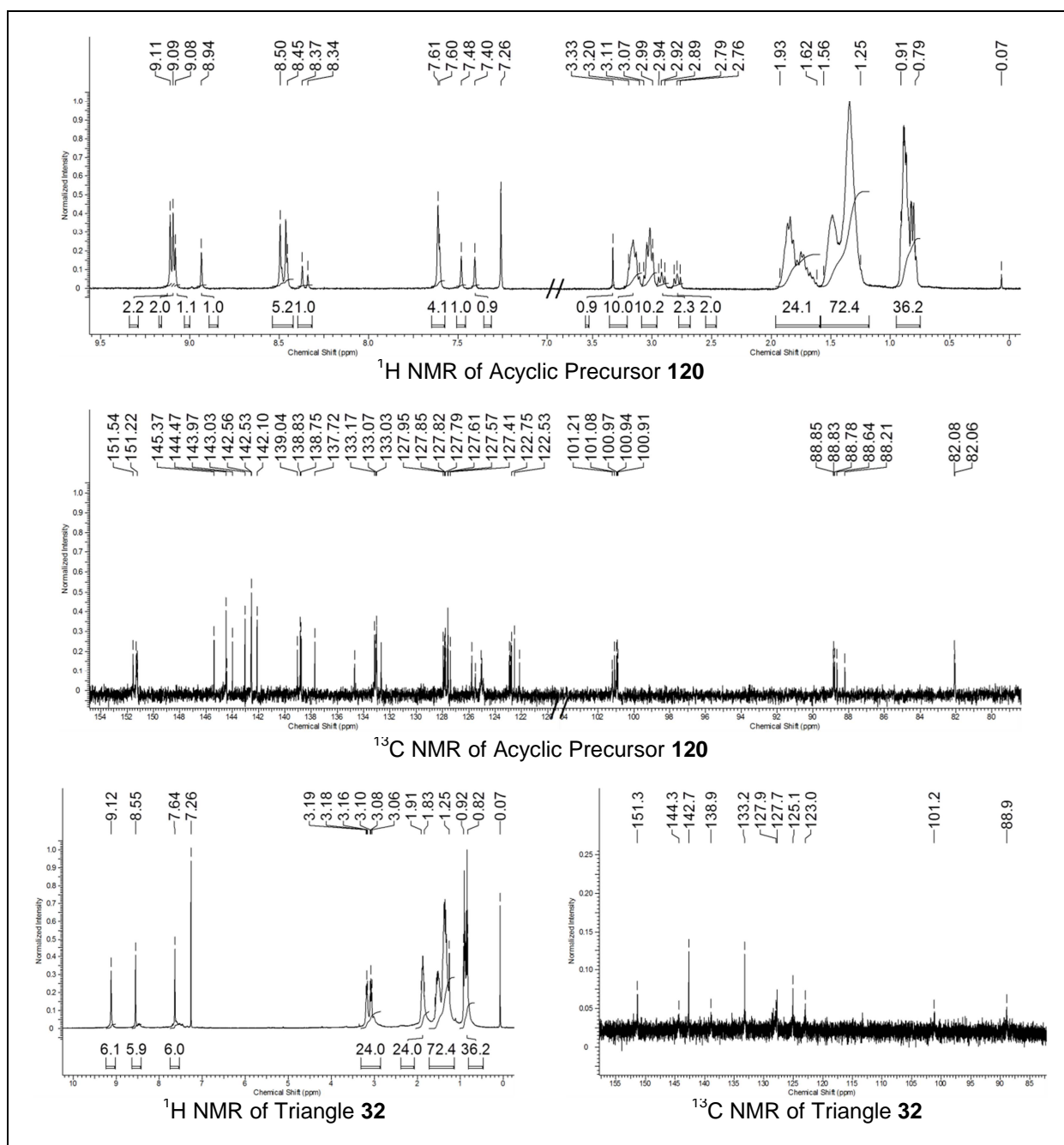
Figure 4. 8: ^{1}H and ^{13}C NMR of **120** and **32** in CDCl$_3$ at 400 MHz

158

4.2.2. Attempted Synthesis of Diamond Face (35) and Characterization of Building Blocks

Attempts to synthesize diamond face (**35**) proved unsuccessful. This was surprising in light of the fact both macrocycle **35** and **111** share the same chemical backbone, so should be attainable through parallel pathways. However, when we endeavored to assemble **35** via a multistep intermolecular cyclization pathway (see Scheme 4.10) that is analogous to the one used in the synthesis of **111** (see Scheme 4.5) we were unable to isolate any product. The first two steps in the intermolecular cyclization pathway is the synthesis of 2° building block **55** by coupling 1° building blocks **29** and **27**, followed by desilylation of the TIPS groups to produce 2° building block **122**. Relative to **29**, overall yields for the synthesis of **122** was high (95%). Alternatively, **122** could be generated from 2° building block **113**. However, since **55** was also being employed by us as a ligand in the [ReBr(CO)$_3$(phen')] complex **52** discussed in Chapter 2 it was already available. The ^{1}H and ^{13}C NMR characterization for compound **55** has been discussed in Chapter 2, so will not be repeated here. The ^{1}H NMR spectra of **122** features five singlets at 9.07, 8.44, 7.48, 7.41, and 3.36 ppm. The first two peaks (in order of decreasing resonance frequencies) are of course assigned to the phenanthroline protons, the next two to the phenyl protons, and the last to the acetylene proton. The two triplets at 3.13 and 2.92 ppm are assigned to the picolinyl and benzyl protons, respectively. The ^{13}C NMR spectra for **122** recorded with ^{13}C and ^{1}H coupling, features five singlets and one doublet peaks corresponding to the phenanthroline carbons (δ = 151.2 (d), 144.5, 138.7, 127.9, 127.6, 125.0 ppm) and four singlets and two doublets corresponding to the phenyl carbons (δ = 143.1, 142.1, 133.2 (d), 132.7 (d), 122.5, 122.2 ppm). There are also three singlets carbons at 101.1, 88.3, 82.1 ppm and one doublet at 82.0 ppm for the acetylenic carbons. Both the ^{1}H and ^{13}C NMR spectra for **122** are for the most part unremarkable and consistent with characterizations previously performed on related phenanthroline compounds. However, the phenanthroline carbon peak at 125.0 ppm assigned to carbons 5 and 6 is expected to be a doublet due to carbon and hydrogen coupling.

The next step in the intermolecular cyclization pathway 1° building block **30** is coupled to 2° building block **122** producing 3° building block **125** in a 76 % yield. To prevent oligomerization an eight-fold excess of **30** was used. The phenanthroline, phenyl, picolinyl, and benzyl proton peaks in the ^{1}H NMR spectra of compound **125** are similar to, being only slightly downfield of, the corresponding peaks in its parent compound **122**. The three sets of triplets centered at 8.14, 8.12, and 7.83 ppm are assigned to the two benzoate protons ortho to the ester

and the single proton para to the ester, respectively. The triplet-splitting pattern in these protons is an effect of long range coupling, hence the small coupling constants (J ~ 1.7 Hz). The quartet at 4.41 ppm is assigned to the methylene protons in the ester group. The methyl protons of the ester group resonate at frequencies that are coincident to the methylene protons nearest to the methyl group in the hexyl chain. Nevertheless, the triplet for the ester's methyl protons is clearly visible in the spectra and the coupling constant matches that of the quartet for the ester's methylene protons ($J^3 = 7.7$ Hz), thus confirming their assignments.

The ^{13}C NMR spectra of **125** also clearly shows evidence of the ester group in the benzoate with the peaks at 164.6, 61.7, and 14.2 ppm assigned to the carbonyl, methylene, and methyl carbons, respectively. As with the ^{1}H NMR the phenanthroline and phenyl carbon signals in the ^{13}C NMR spectra of **125** are similar to those in **122**. However, the phenyl carbons of the benzoate group resonate at similar frequencies as the phenanthroline and phenyl carbons. Consequently, the eighteen aromatic carbon signals were not assigned, but are assumed to correspond to six unique phenanthroline, phenyl, and benzoate carbons.

The next and final step in the synthesis shown in Scheme 4.10 is to combine 3° building block **125** and 2° building block **122** to produce **35** as a 4° macrocycle. Because building block **122** was used as a reagent in a previous step in this process, we add 1° to the degree designation of building block **125** rather than add the 2° assigned to **122** to determine the degree of the macrocycle product. See Figure 4.5d. The result of the coupling reaction was unfortunate as only oligomeric products could be isolated despite using high dilution conditions (total molar concentration of reagent building blocks ~ 9 x10^{-4} M). Although, oligomeric products were anticipated, we expected to produce macrocycle **2** as well. The failure toproduce macrocycle **35** via the multistep intermolecular procedure may be owing in part to our use of batch-wise synthesis to create the highly dilute conditions during cyclization. Although the batch-wise method has been proven effective for intramolecular cyclization of shape persistent macrocycles, it is rarely used in intermolecular cyclization. In fact, Schmittel and coworkers employed continous flow technique during the synthesis of **111** using an injection pump to gradually add 20 mL of a 17 mM solution of **110** and **108** to a solution containing one equivalent of Pd(PPh$_3$)$_4$ catalysts in 80 mL of solvent over a 32 hour period. See Scheme 4.5.
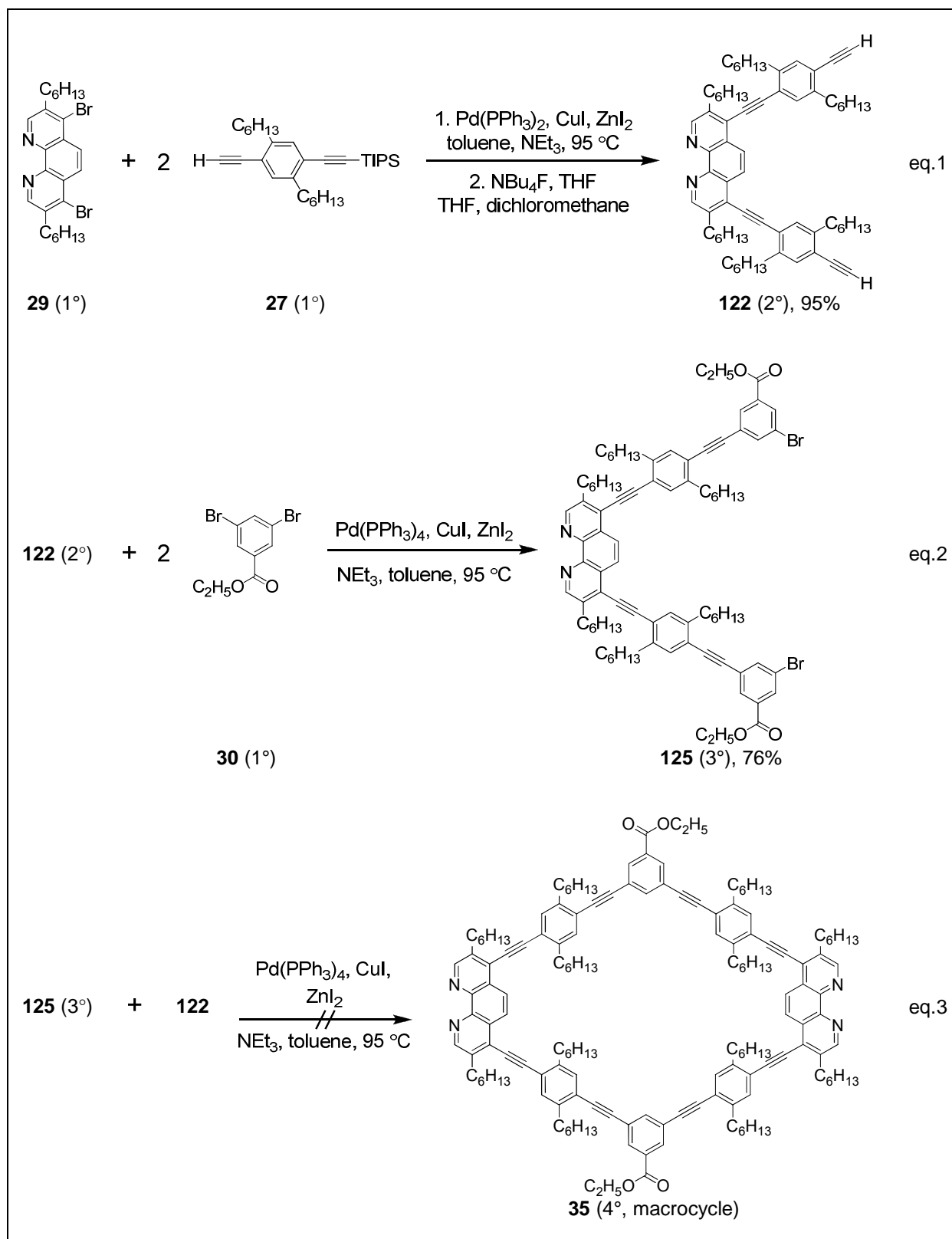
Scheme 4. 10: Synthesis of macrocycle **35** by multistep intermolecular cyclization.

Without the benefit of an automated chemical feeder tool, we were not equipped to perform controlled continuous addition experiments. Therefore, we must consider an intramolecular cyclization route, which requires an acyclic precursor. To this end, we pursued the strategy presented in Scheme 4.11 – 4.13. The first steps in Scheme 4.11 is the synthesis of 3° building blocks **128** and **129**, which were produced in 84 % and 72 % yields, respectively, from common parent 2° building block **126**. The ^{1}HNMR spectra of compounds **128** and **129**, are expectedly similar, being distinguishable only by their trialkylsilyl proton signals. Both spectra feature a doublet centered at 8.12 ppm and a triplet centered near 7.79 ppm, which are assigned to benzoate protons ortho and para to the ester, respectively. This splitting pattern is attributed to the local-C_2 symmetry element that bisects C1 and C4 in the benzoate ring. The hydroxyl and methyl protons of the propargyl alcohols resonate near 2.0 and 1.7 ppm, respectively. The methine carbon of the propargyl alcohol resonates near 65 ppm in the ^{13}C NMR. The IR spectra for both compounds contain a broad band at 3436 cm^{-1} assigned to the OH stretch and a sharp peak at 1727 cm^{-1} assigned to the carbonyl stretch.

The next step in the synthesis is removal of the isopropylalcohol protecting group in **128** and **129** to produce **130** (90 %) and **131** (67 %), respectively. As mentioned in the introduction chapter of this document, removal of the propargyl alcohol via retro-Favorskii requires harsh conditions. As a result, both the trialkylsilyl and ester groups are susceptible. Therefore, care was taken to minimize the exposure of our compounds to these conditions and remove moisture and air. Deprotection of the propargyl alcohol-masked acetylenes in **128** and **129** has the expected impact on the ^{1}H NMR spectra of **130** and **131**, respectively. The most notable is the absence of methyl and hydroxyl protons of the propargyl alcohol group and the correlating presence of the acetylene proton at 3.32 ppm. Similarly, the ^{13}C NMR spectra of **129** and **130** are void of the methine alcohol carbon at 65 ppm, but feature peaks at 81.7 ppm, which are assigned to a terminal alkyne. The removal of the propargyl alcohol was further confirmed by the FTIR spectra, which lacks the broad OH band at 3436 cm^{-1}, but displays the H–C≡ stretching vibration band at 3311 cm^{-1}.
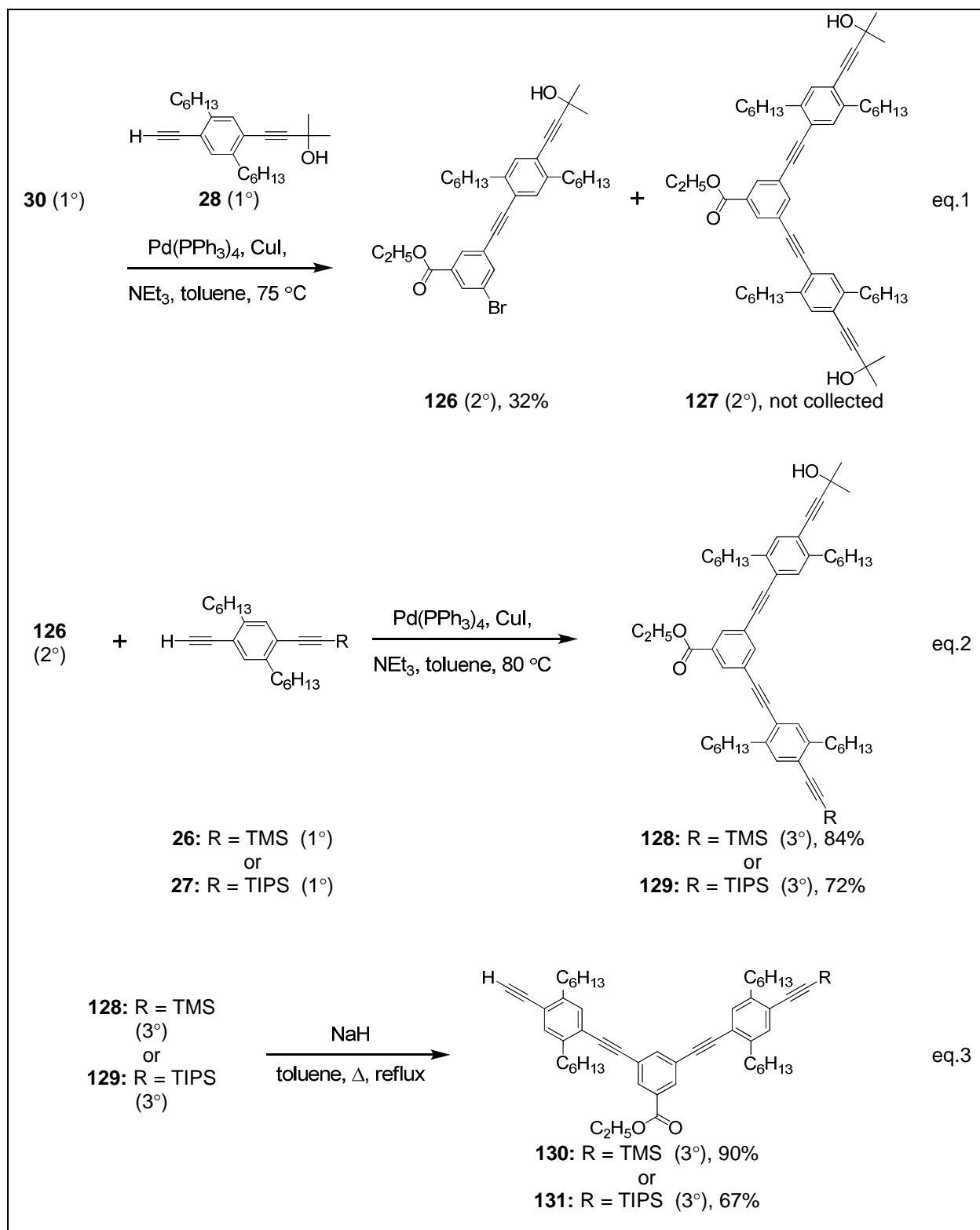
Scheme 4. 11: Synthesis of 3° building blocks **130** and **131** during the multistep intramolecular cyclization procedure for the synthesis of **35**.
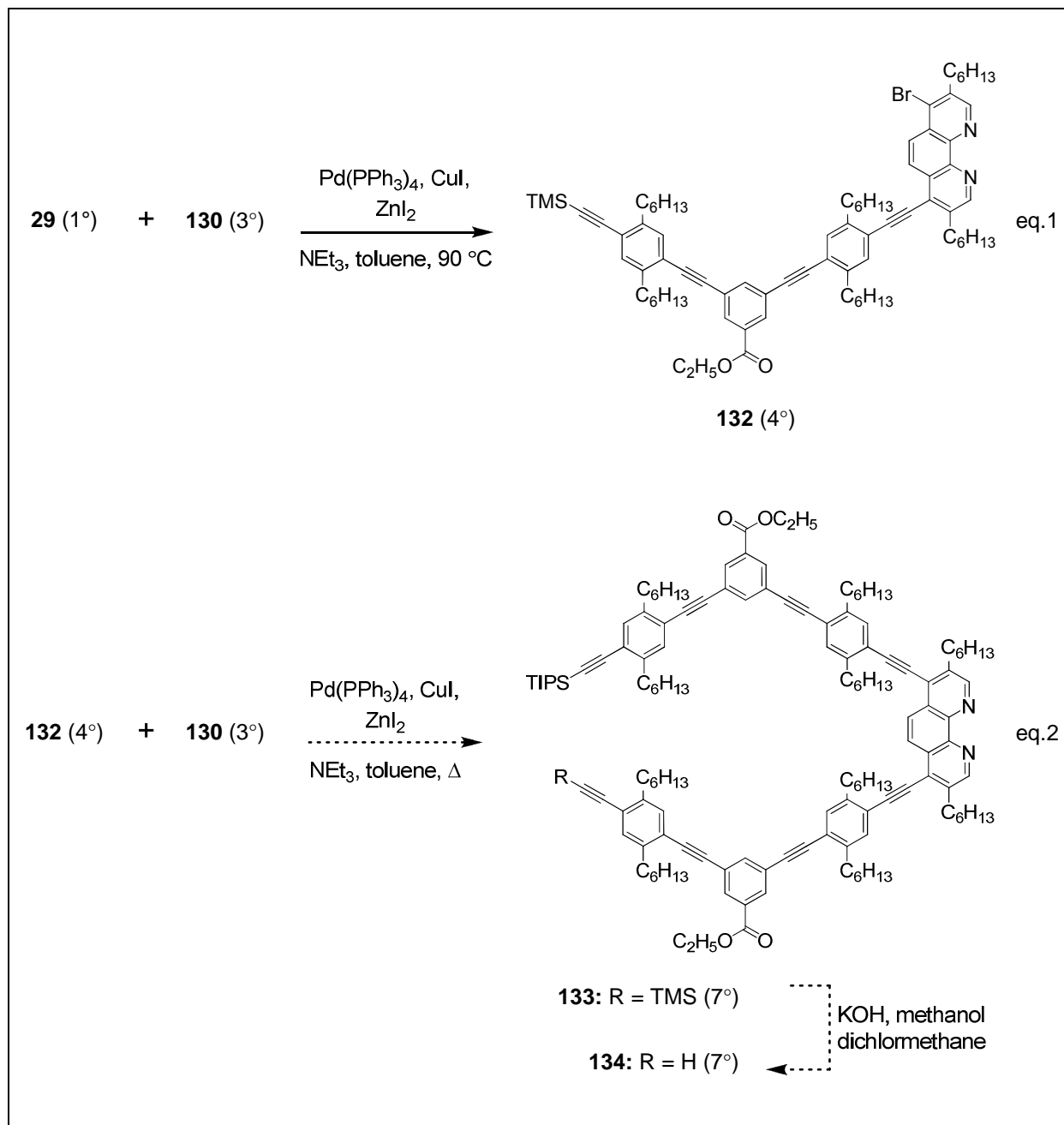
Scheme 4. 12: Synthesis of 7° building block **134** for diamond face **35**.
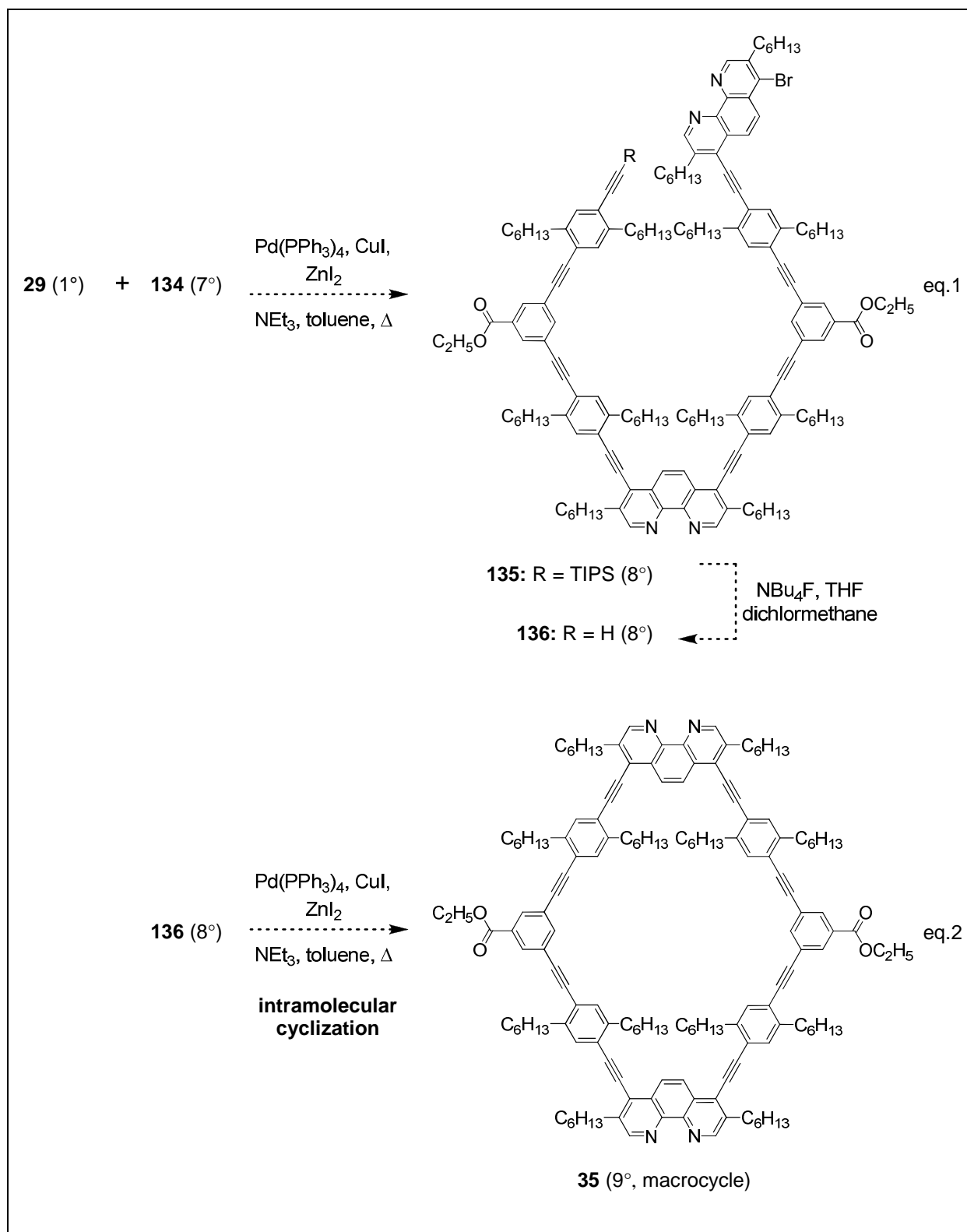
Scheme 4. 13: Synthesis of diamond face **35** from 8° acyclic precursor **136**.

The final steps involves the synthesis of **35** from **29**, **130**, and **131**. This portion of the synthesis is presented in Schemes 4.12 – 4.13 and starts with the coupling of **130** and 1° building block **29**, to produce **132**. The final two steps before cyclization involve the coupling of **132** and **131** to form **133**. Removal of the TMS group to produce **134** followed by cross-coupling with an excess of **29**, should produce the TIPS protected acyclic precursor **135**. See Scheme 4.12. Finally, reduction of the masked acetylene to form **135** and intramolecular cyclization step would be expected to produce **35**.

4.3. Conclusions and Future Work:

The synthesis of shape-persistent macrocycles is a challenging task. Two key considerations that must be taken into account when designing the synthetic protocol for these structures is the expected productivity of the cyclization step and the number of steps required by a particular pathway. Quite often, pathways that are expected to produce high yields of the macrocycle during the cyclization step requires multiple pre-cyclization steps, which significantly reduce the overall yields. In our case, we have attempted to make macrocycles **32** and **35** to serve as components in our cages (i.e. **1** and **2**). Therefore, we sought the most productive pathways. Unfortunately, yields for macrocycle **32** synthesized through the intramolecular cyclization route presented in Schemes 4.6 – 4.8 were quite low. More regrettably, the attempted synthesis of diamond face **35** by the intermolecular cyclizations presented in Scheme 4.10 failed to produce any product. Since these macrocycles are to be used in the synthesis of cages **1** and **2** improving the yields of **32** and **35** is imperative. Currently we are attempting to synthesize diamond face 35 by the synthetic pathway presented in Scheme 4.11 – 4.13. We are also in the process of synthesizing more of the triangular prism.

4.4. Experimental

4.4.1. General Methods:

Primary building block 4,7-dibromo-3,8-dihexyl-1,10-phenanthroline (**23**) was prepared following the published procedure. Synthesis of primary building blocks blocks was addressed in Chapter 1.   Each macrocycle several different nominal pathways are proposed that are distinguished by the number of reaction steps. Since the yield and controllability of the overall reaction are related to the number of reaction steps, it was important to devise a way to account for the number of steps when comparing different pathways.   In this vein, we have adopted degree designations, which quantify the number of unique coupling reactions used to produce that building block starting with fundamental or 1° building blocks **23 – 29**. See Scheme 1.6. Degree designations for higher ordered building blocks is equal to the sum of the degree designations of the reactants coupled to make said building block. To avoid double counting stoichiometry is ignored and any reactant that was used in a previous step is considered a 1° building block in the current step. Finally, deprotection reactions are ignored since they are generally high yielding. In this way the degree of each building block whether 1° 2° 3° etc. is equal to one plus the total number of unique coupling reactions used to make that building block.   Oligomers in synthesis

. Synthesis of secondary building block = 3,8-di-*n*-hexyl-4,7-bis(2,5-di-*n*-hexyl-4-triisopropylethynylene-1-ethynylbenzene)-1,10-phenanthroline (**42**) was previously described in Chapter 2 of this document. Commercially available reagents and solvents were obtained from reputable chemical distributers. When necessary, toluene and triethylamine were dried using established procedures under an inert atmosphere of nitrogen. All other solvents were used as is. Moisture- and air- sensitive Sonogashira-cross-coupling and retro-Favorskii reactions were performed under a nitrogen environment using standard Schlenk techniques and dried solvents. All compounds were purified via chromatography using Silica gel (45–60 lm). ^{1}H NMR experiments were conducted using Varian Gemini 2300 (300 MHz) or xxx instruments. ^{13}C NMR experiments were conducted using Varian Inova (400 MHz) or or xxx instruments. Both ^{1}H and ^{13}C NMR spectra were recorded in CDCl$_3$ solutions, which was used as the lock and reference. All NMR data were processed by ACD/NMR Processor Academic Edition, version 12.01, Advanced Chemistry Development, Inc., Toronto, ON, Canada, www.acdlabs.com, 2012.

FTIR measurements were recorded using. Elemental analyses were performed by Quantitative Technologies Inc.

4.4.2. Synthesis of Triangle

A detaile general procedure for Songashira Coupling with 3,8-dihexyl-1,10-phenanthroline derivatives:

A flask charged with all starting materials and about one equivalent of ZnI_2 for every mole of phenanthroline moiety dissolved in a in toluene and NEt3 mixture was evacuated and back filled with nitrogen three times. While the nitrogen connection remained open the flask containing the contents were next submerged in a an oil bath set at 80 °C to dissolve all the ZnI_2 and form the Zn(phen) complex. Upon formation of this complex the color of the solution changes from yellow to orange or orange/red. To this reaction mixture was added $Pd(PPh_3)_4$ followed by CuI, by which time the color of the reaction solution becomes a brick red or dark brown. After each addition the flask was evacuated and back filled with nitrogen to re-established an inert atmosphere. The contents were generally stirred overnight, roughly 18 hours at 80 °C. Afterwards the solution allowed to cool to room temperature before the $HNEt_3I$ byproduct was filtered onto a fritted disk under reduced pressure. Solvent was then removed via rotoevaporation and the brown liquid dried under vacuum before being re-dissolved in 75 mL of methylene chloride and washed with a 0.010 M KCN solution. Upon washing with KCN the solution becomes a bright yellow color. The combined organic phases of the first washing followed by two additional extractions were drived over anhydrous $MgSO_4$. The $MgSO_4$ was filtered onto a fritted disk washed several times with dichloromethane and the filtrate collected. Solvent removal by rotovaportation and further drying under vacuum usually produced a yellow oil. The crude product mixture was next purified via column chromatography on silica gel.
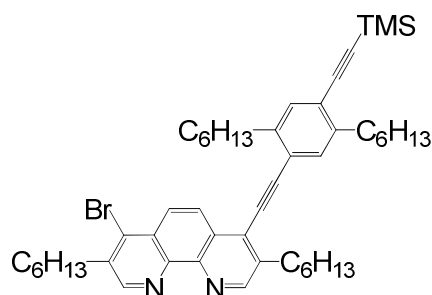
Compound 112: To a solution containing 0.506 g (1.00 mmol) of **29**, 0.367 (1.00 mmol) g of **26**, 0.160 g (0.50 mmol) of ZnI$_2$ in 10 mL of NEt$_3$ and 20 mL of toluene at 75 °C is added 0.030 g (0.026 mmol) of Pd(Ph$_3$)$_4$ followed by 0.015 g (0.079 mmol) of CuI. The resulting mixture was stirred at 75 °C for 48 hrs before removing the solvent via rotoevaporation. Next the crude substance was redissolved in 30 mL dichloromethane and the solution was washed with 10 mL 0.8 M KCN solution. Afterwards the organic phase was separated from the aqueous phase and collected. Two subsequent extractions of the organic substance from the aqueous solution were carried out using small amounts of dichloromethane. The combine collected organic solutions was dried over anhydrous MgSO$_4$ and the solvent removed via rotoevaporation and dried under vacuum. The crude yellow product was purified via flash chromatography using hexane/ethyl acetate (5:1, v/v), which afforded 0.248 g (0.313 mmol, 31 %) of **112**. ^{1}H NMR (300 MHz, CDCl$_3$) δ 9.05 (s, 1H), 8.91 (s, 1H), 8.41 (d, J^3 = 9.3 Hz, 1H), 8.30 (d, J = 9.3 Hz, 1H), 7.44 (s, 1H), 7.37 (s, 1H), 3.10 (t, J = 7.7 Hz, 2H), 3.01 (t, J = 7.7 Hz, 2H), 2.89 (t, J = 7.8 Hz, 2H), 2.77 (t, J = 7.7 Hz, 2H), 1.88-1.63 (m, 8H), 1.51-1.24 (m, 24H), 0.ss-0.80 (m, 12H), 0.28 (s, 9H); ^{13}C NMR (400 MHz, CDCl$_3$) δ 151.5, 151.2, 145.4, 144.0, 143.1, 142.2, 138.9, 137.7, 134.7, 132.8, 132.7, 128.1, 127.8, 127.5, 125.7, 125.7, 123.7, 121.7, 103.6, 101.6, 99.8, 88.0, 34.5, 34.4, 34.2, 32.7, 31.8, 31.7, 31.7, 31.6, 30.9, 30.7, 30.6, 29.8, 29.4, 29.3, 29.2, 29.0, 22.6, 22.6, 22.6, 22.6, 14.1, 14.1, 14.0, 14.0, -0.1; IR (neat): 2955, 2923, 2855, 2201, 2150 cm^{-1}; Anal. Calc. for C$_{49}$H$_{67}$BrN$_2$Si: C, 74.30; H, 8.53; N, 3.54. Found: C, 73.50; H, 7.78; N, 3.37%.
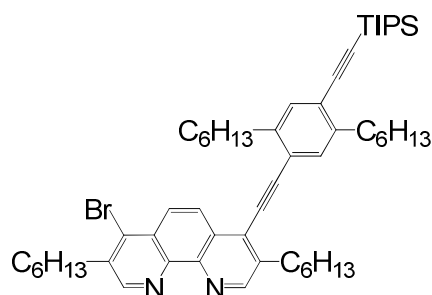
Compound 114: ^{1}H NMR (300 MHz, CDCl$_3$) δ 9.05 (s, 1H), 8.91 (s, 1H), 8.41 (d, J^3 = 9.3 Hz, 1H), 8.30 (d, J^3 = 9.3 Hz, 1H), 7.44 (s, 1H), 7.37 (s, 1H), 3.10 (t, J^3 = 7.8 Hz, 2H), 3.01 (t, J^3 = 7.5 Hz, 2H), 2.90 (t, J^3 = 8.0 Hz, 2H), 2.81 (t, J^3 = 8.0 Hz, 2H), 1.87 – 1.62 (comp, 8H), 1.52 – 1.22 (comp, 24H), 1.15 (s, 24H), 0.94 – 0.80 (comp, 12H); ^{13}C NMR (400 MHz, CDCl$_3$) δ 151.5, 151.1, 145.4, 144.0, 142.9, 142.2, 138.9, 137.6, 134.7, 133.1, 132.8, 128.1, 127.8, 127.4, 125.7, 125.7, 124.0, 121.5, 105.3, 101.7, 96.2, 88.0, 34.4, 32.7, 31.8, 31.7, 31.6, 31.0, 30.9, 30.7, 29.8, 29.4, 29.4, 29.2, 29.0, 22.7, 22.6, 22.6, 22.6, 18.7, 14.1, 14.0, 11.3; IR (neat): 2955, 2924, 2856, 2197, 2145 cm^{-1}; Anal. Calc. for C$_{55}$H$_{79}$BrN$_2$Si: C, 75.39; H, 9.09; N, 3.20. Found: C, 75.29; H, 8.63; N, 2.96%
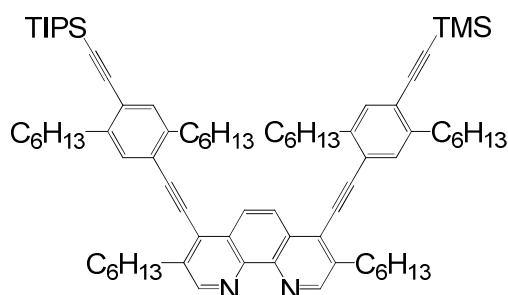
Compound 115: To a solution containing 1.377 g (1.57 mmol) of **114**, 0.865 g (2.36 mmol) of **26**, and 0.632 g (1.98 mmol) of ZnI$_2$ dissolved in 20 mL of NEt$_3$ and 20 mL of toluene at 80 °C under an inert N$_2$ atmosphere was added 0.285 g (0.247 mmol) of Pd(Ph$_3$)$_4$ followed by 0.180 g (0.945 mmol) of CuI. The resulting mixture was stirred at 80 °C overnight (approximately 18 hours) before gradually cooling to room temperature. The cooled solution was filtered through a plug of cellulose atop a glass frit. The filtrate solution was collected and the solvent removed via rotoevaporation. Next the crude substance was redissolved in 75 mL of dichloromethane and the solution was washed with 75 mL 0.1 M KCN solution. Afterwards the organic phase was

170

separated from the aqueous phase and collected.   Two subsequent extractions of the organic substance from the aqueous solution were carried out using dichloromethane.   The combine collected organic solutions was dried over anhydrous MgSO$_4$ and the solvent removed via rotoevaporation and dried under vacuum.   The crude yellow product was purified via flash chromatography using hexane/ethyl acetate (4:1 v/v), which afforded 1.470 g (1.27 mmol) of **115** in 81%. IR (KBr, cm^{-1}) 2197 (vw), 2147 (m) v(C≡C). ^{1}H NMR (300 MHz, CDCl$_3$) δ 9.07 (s, 2H), 8.44 (s, 2H), 7.47 (s, 2H), 7.38 (s, 2H), 3.13 (t, J^3 = 7.7 Hz, 4H), 2.94 – 2.89 (m, 4H), 2.84 – 2.76 (m, 4H), 1.89 – 1.64 (comp, 12H), 1.53 – 1.22 (comp, 36H), 1.16 (s, 21H), 0.96 – 0.76 (comp, 18H), 0.28 (s, 9H); ^{13}C NMR (400 MHz, CDCl$_3$) δ 151.2, 144.5, 143.1, 142.9, 142.2, 142.1, 138.7, 133.1, 132.7, 132.7, 132.7, 128.1, 128.0, 127.6, 125.0, 124.0, 123.4, 121.9, 121.7, 105.4, 103.6, 101.4, 101.3, 99.7, 96.1, 88.2, 88.2, 34.5, 34.4, 34.3, 34.2, 32.7, 31.8, 31.7, 31.7, 31.0, 30.9, 30.8, 30.7, 30.7, 29.4, 29.3, 29.2, 29.2, 22.6, 22.6, 22.6, 22.6, 18.7, 14.1, 14.0, 11.3, -0.1; IR (neat): 2955, 2925, 2857, 2199, 2148 cm^{-1}; Anal. Calc. for C$_{80}$H$_{116}$N$_2$Si$_2$: C, 82.69; H, 10.06; N, 2.41. Found: C, 82.32; H, 10.35; N, 2.32%.
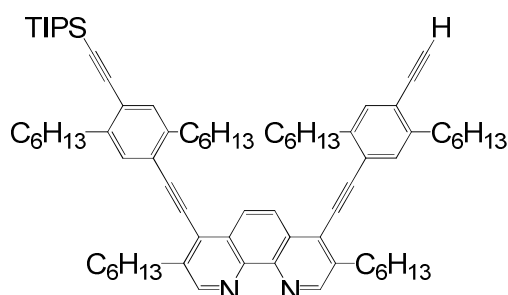
Compound 116: To a solution containing 1.470 g (1.27 mmol) of **115** dissolved in 25 mL of dichloromethane was added 0.463 g (8.25 mmol) KOH dissolved in 15 mL of methanol. The contents were stirred at room temperature for two hours and then washed with 100 mL of distilled water. Afterwards the organic phase was separated from the aqueous phase and collected. Two subsequent extractions of the organic substance from the aqueous solution were carried out using dichloromethane. The combine collected organic solutions was dried over anhydrous MgSO$_4$ and the solvent removed via rotoevaporation and dried under vacuum, which afforded 1.168 g (1.07 mmol) of **116** in 84 % yield. IR (KBr, cm^{-1}) 3312 (m) v(CC–H); 2198 (w), 2147 (m) v(CC). ^{1}H NMR (300 MHz, CDCl$_3$) δ 9.07 (s, 2H), 8.44 (s, 2H), 7.48 (appd, 2H), 7.41 (s, 1H), 7.39 (s, 1H), 3.36 (s, 1H), 3.13 (t, J^3 = 7.8 Hz, 4H), 2.92 (t, J^3 = 7.8 Hz, 4H), 2.84 –

2.77 (m, 4H), 1.89 – 1.63 (m, 12H), 1.54 – 1.23 (m, 36H), 1.16 (s, 21H), 0.97 – 0.75 (m, 18H); ^{13}C NMR (400 MHz, CDCl$_3$) δ 151.2, 144.4, 143.1, 142.9, 142.2, 138.7, 138.7, 133.2, 133.1, 132.8, 132.7, 128.1, 128.0, 127.6, 125.1, 125.0, 124.0, 122.5, 122.2, 121.7, 105.4, 101.4, 101.1, 96.1, 88.3, 88.1, 82.2, 82.0, 34.5, 34.4, 34.3, 33.9, 32.7, 31.8, 31.7, 31.6, 31.0, 30.9, 30.8, 30.7, 30.6, 29.4, 29.3, 29.2, 29.2, 29.1, 22.6, 22.6, 22.6, 22.6, 18.7, 14.1, 14.0, 14.0, 11.3; ; IR (neat): 3310, 3169, 2954, 2925, 2857, 2201, 2149, 2091, 2035 cm^{-1}; Anal. Calc. for C$_{77}$H$_{108}$N$_2$Si: C, 84.86; H, 9.99; N, 2.57. Found: C, 84.02; H, 9.81; N, 2.32%
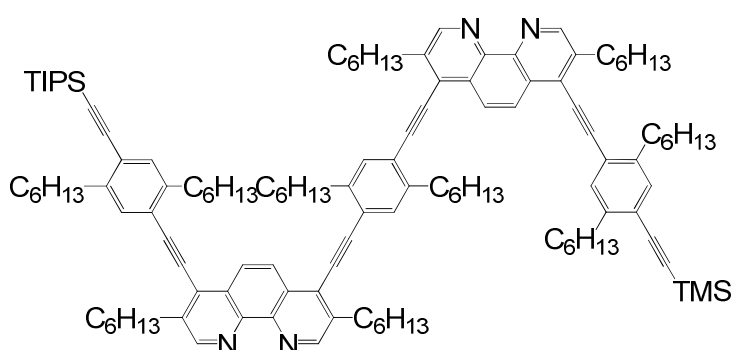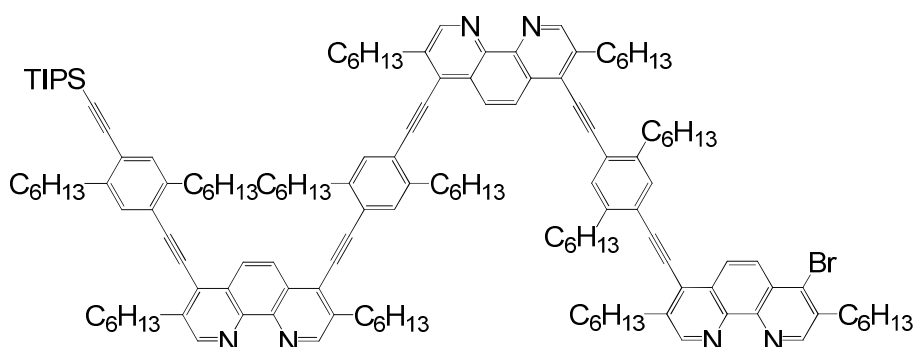

Compound 117 To a solution containing 1.090 g (1.00 mmol) **116**, 1.2 g (1.5 mmol) of **112**, and 0.958 g (3.00 mmol) of ZnI$_2$ dissolved in 20 mL toluene and 20 mL of NEt$_3$ at 80 °C under an inert N$_2$ atmosphere was added 0.150 g (0.130 mmol) Pd(Ph$_3$)$_4$ followed by 0.050 g (0.263 mmol) of CuI. The resulting mixture was stirred overnight at 80 °C before the solution was gradually cooled to room temperature. The cooled reaction solution was filtered through a plug of cellulose atop a glass frit. The filtrate solution was collected and the solvent removed via rotoevaporation. Next the crude substance was redissolved in 75 mL dichloromethane and the solution was washed with 75 mL of a 0.1 M KCN solution. Afterwards the organic phase was separated from the aqueous phase and collected. Two subsequent extractions of the organic substance from the aqueous solution were carried out using dichloromethane. The combine collected organic solutions was dried over anhydrous MgSO$_4$ and the solvent removed via rotoevaporation and dried under vacuum. The crude yellow product was purified via flash chromatography using hexane/ethyl acetate (3:2, v/v) mixture initially. The solvent polarity was increased to hexanes and ethyl acetate (1:1, v/v) as the eluent, which afforded 1.486 g (0.825 mmol) **117** in 83% yield. IR (KBr, cm^{-1}) 2201 (w), 2148 (m) ν(CC).). ^{1}H NMR (300 MHz, CDCl$_3$) δ 9.10 (s, 2H), 9.08 (s, 2H), 8.47 (s, 4H), 7.60 (s, 2H), 7.48 (s, 1H), 7.47 (s, 1H), 7.39 (s,

2H), 3.19-3.11 (m, 8H), 3.02 (t, J = 7.8 Hz, 4H), 2.95-2.88 (m, 4H), 2.84-2.76 (m, 4H), 1.94-1.63 (m, 20H), 1.56-1.23 (m, 60H), 1.16 (s, 21H), 0.95-0.76 (m, 30H), 0.28 (s, 9H); ^{13}C NMR (400 MHz, CDCl$_3$) δ 151.3, 151.3, 144.5, 144.5, 143.1, 142.9, 142.6, 142.2, 142.1, 138.8, 138.7, 133.1, 133.1, 132.7, 128.1, 128.1, 127.9, 127.7, 127.6, 125.1, 124.9, 124.0, 124.0, 123.0, 121.8, 121.6, 105.3, 103.6, 101.4, 101.4, 101.0, 99.7, 96.2, 88.8, 88.2, 88.1, 34.5, 34.4, 34.3, 34.2, 32.7, 31.8, 31.7, 31.7, 31.0, 30.9, 30.8, 30.8, 30.7, 30.6, 29.4, 29.3, 29.3, 29.3, 29.2, 29.2, 29.2, 22.6, 22.6, 22.6, 18.7, 14.1, 14.0, 14.0, 11.3, -0.1; IR (neat): 3015, 2955, 2924, 2856, 2200, 2149, 2037 cm^{-1}; Anal. Calc. for C$_{126}$H$_{174}$N$_4$Si$_2$: C, 84.03; H, 9.74; N, 3.11. Found: C, 83.70; H, 9.75; N, 2.95%
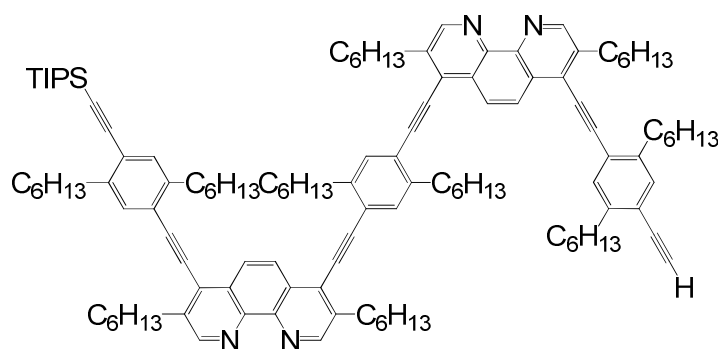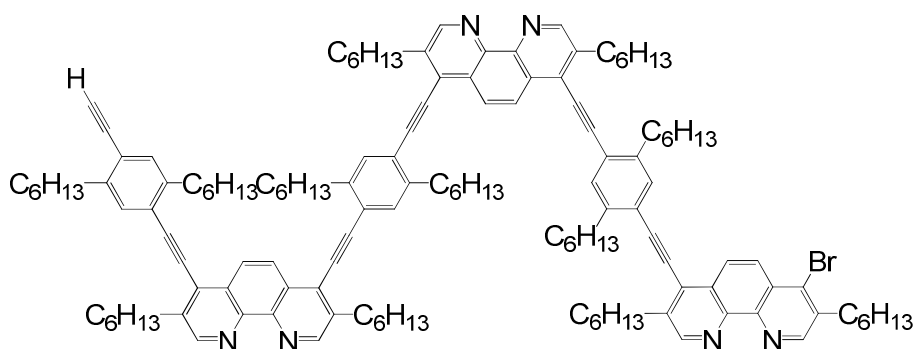

Compound 118: To a solution containing 0.426 g (0.237 mmol) of **117** dissolved in 25 mL of dichloromethane was added 1.4 g (25 mmol) of KOH dissolved in 15 mL of methanol. The resulting mixture was stirred for two hours at room temperature and then diluted with 25 mL of dichloromethane and washed with distilled water. Afterwards the organic phase was separated from the aqueous phase and collected. Two subsequent extractions of the organic substance from the aqueous solution were carried out using dichloromethane. The combine collected organic solutions was dried over anhydrous MgSO$_4$ and the solvent removed via rotoevaporation and dried under vacuum. After drying the substance under vacuum purification was performed via flash chromatography using hexane/ethyl acetate (3:1, v/v), which afforded 0.398 g (0.230 mmol) of **118** in 97 % yield. IR (KBr, cm^{-1}) 3313 (m) ν(CC–H); 2204 (w), 2150 (w) ν(CC). ^{1}H NMR (300 MHz, CDCl$_3$) δ 9.10 (s, 2H), 9.09 (s, 1H), 9.09 (s, 1H), 8.47 (s, 4H), 7.60 (s, 2H), 7.49 (s, 1H), 7.48 (s, 1H), 7.42 (s, 1H), 7.39 (s, 1H), 3.36 (s, 1H), 3.21-309 (m, 8H), 3.01 (t, J = 7.8 Hz, 4H), 2.93 (t, J = 7.8 Hz, 4H), 2.84-2.78 (m, 4H), 1.92-1.64 (m, 20H), 1.54-1.23 (m, 60H), 1.16 (s, 21H), 0.92-0.78 (m, 30H); ^{13}C NMR (400 MHz, CDCl$_3$) δ 151.3, 144.6, 144.5,

143.1, 142.9, 142.6, 142.2, 138.8, 133.3, 133.2, 133.1, 132.8, 128.1, 128.0, 127.9, 127.9, 127.7, 127.6, 125.2, 125.1, 125.0, 124.9, 124.0, 123.0, 122.9, 122.6, 122.2, 121.7, 105.4, 101.5, 101.1, 101.0, 101.0, 99.8, 96.2, 88.9, 88.3, 88.2, 82.2, 82.0, 34.5, 34.4, 34.3, 32.8, 31.8, 31.7, 30.9, 30.8, 30.7, 30.6, 29.7, 29.4, 29.2, 29.2, 22.6, 22.6, 22.6, 18.7, 14.1, 14.0, 11.4; IR (neat): 3313, 3165, 2954, 2924, 2855, 2201, 2147, 2103, 2030 cm^{-1}; Anal. Calc. for $C_{123}H_{166}N_4Si$: C, 85.46; H, 9.68; N, 3.24. Found: C, 85.21; H, 9.57; N, 3.03%

**Compound 119:** To a solution containing 1.5 g (3.0 mmol) of **29** and 1.596 g (5.00 mmol) ZnI_2 dissolved in 65 mL of toluene under an inert N_2 atmosphere was added a 0.761 g (0.440 mmol) of **118** dissolved in 61 mL of NEt$_3$ followed by 0.250 g (0.216 mmol) Pd(PPh$_3$)$_4$, and finally 0.100 g (0.525 mmol) of CuI. While the nitrogen connection remained open the flask containing the contents were submerged in a an oil bath set at 80 °C. The nitrogen connection was closed after thermal equilbrium established and the contents stirred stirred overnight before the solvent removed via rotoevaporation. Following the evaporation of the solvent, the solution was redissolved in 75 mL of dichloromethane and washed with 75 mL of a 0.1 M KCN solution. Afterwards the organic phase was separated from the aqueous phase and collected. Two subsequent extractions of the organic substance from the aqueous solution were carried out using dichloromethane. The combine collected organic solutions was dried over anhydrous MgSO$_4$ and the solvent removed via rotoevaporation and dried under vacuum. The crude yellow product was purified via flash chromatography using initially hexane/ethyl acetate (3:1, v/v) mixture. The solvent polarity was increased to pure ethyl acetate, followed by ethyl acetate/methanol (9:1, v/v), which afforded 0.387 g (0.180 mmol) of **119** in 41% yield. IR (KBr, cm^{-1}) 2199 (m), 2149 (w) ν(CC). ^{1}H NMR (400 MHz, CDCl$_3$) δ 9.11 (s, 2H), 9.10 (s, 2H), 9.09 (s, 1H), 9.08 (s, 1H), 8.93 (s, 1H), 8.50 (s, 2H), 8.47-8.45 (m, 3H), 8.35 (d, J = 9.2 Hz, 1H), 7.62 (s, 3H), 7.60 (s, 1H),

7.47 (s, 1H), 7.37 (s, 1H), 3.19-3.11 (m, 10H), 3.05-3.00 (m, 10H), 2.92 (t, J = 7.8 Hz, 2H), 2.81 (t, J = 7.8 Hz, 2H), 1.92-1.64 (m, 24H), 1.56-1.22 (m, 72H), 1.13 (s, 21H), 0.91-0.78 (m, 36H); ^{13}C NMR (400 MHz, CDCl$_3$) δ 151.6, 151.3, 151.2, 145.4, 144.5, 144.4, 144.0, 142.8, 142.6, 142.6, 142.1, 139.1, 138.9, 138.8, 137.8, 134.7, 133.1, 133.1, 132.7, 128.1, 127.9, 127.9, 127.8, 127.8, 127.6, 127.4, 125.8, 125.2, 125.1, 124.0, 123.0, 122.9, 122.8, 122.8, 121.6, 105.3, 101.5, 101.2, 101.0, 101.0, 100.9, 96.2, 88.9, 88.8, 88.7, 88.1, 34.5, 34.5, 34.4, 32.7, 31.8, 31.8, 31.7, 31.6, 31.0, 30.9, 30.9, 30.7, 30.7, 29.8, 29.4, 29.3, 29.3, 29.2, 29.0, 22.7, 22.6, 22.6, 18.6, 14.1, 14.0, 11.3; IR (neat): 2954, 2925, 2856, 2198, 2162, 2147 cm^{-1}; Anal. Calc. for C$_{147}$H$_{195}$BrN$_6$Si: C, 81.96; H, 9.12; N, 3.90. Found: C, 80.87; H, 8.73; N, 3.75%.

Compound 120: To a solution containing 0.337 g (0.156 mmol) of **119** dissolved in 25 mL of dichloromethane was added 0.25g (0.96 mmol) N(n-Bu)$_4$F dissolved in 5 mL of THF. The resulting mixture stirred for two hours. The color of the solution immediately transitions from yellow to orange to amber. The reaction solutions were diluted with dichloromethane and then washed with a saturated NaHCO$_3$ solution. The organic phases were separated, collected, and then dried over anhydrous MgSO$_4$ and the solvent removed via rotoevaporation and dried under vacuum. The crude yellow product was purified via flash chromatography using dichloromethane/ethyl acetate (1:1, v/v) as the eluent initially. The solvent polarity was increased to pure ethyl acetate, followed by ethyl acetate/methanol (30:1, v/v) and ethyl acetate/methanol (20:1, v/v), which afforded 0.254 g (0.127 mmol) of **120** 81 % yield. IR (KBr, cm^{-1}) 3311 (w) ν(CC–H); 2198 (w) ν(CC). ^{1}H NMR (300 MHz, CDCl$_3$) δ 9.11 (s, 2H), 9.10 (s, 2H), 9.08 (s, 1H), 8.94 (s, 1H), 8.50-8.46 (m, 5H), 8.36 (d, J = 9.3 Hz, 1H), 7.61 (s, 3H), 7.60 (s, 1H), 7.48 (s, 1H), 7.41 (s, 1H), 3.33 (s, 1H), 3.20-3.11 (m, 10H), 3.07-2.99 (m, 10H), 2.92 (t, J = 7.8 Hz, 2H), 2.79 (t, J = 7.7 Hz, 2H), 1.93-1.62 (m, 24H), 1.56-1.25 (m, 72H), 0.91-0.79 (m,

175

36H); ^{13}C NMR (400 MHz, CDCl$_3$) δ 151.5, 151.3, 151.2, 145.4, 144.5, 144.4, 144.0, 143.0, 142.6, 142.5, 142.1, 139.0, 138.8, 138.8, 137.7, 134.7, 133.2, 133.1, 133.0, 132.7, 128.0, 127.9, 127.9, 127.8, 127.8, 127.8, 127.6, 127.6, 127.4, 125.8, 125.5, 125.1, 125.0, 122.9, 122.9, 122.8, 122.8, 122.5, 122.2, 101.2, 101.1, 101.0, 100.9, 100.9, 88.8, 88.8, 88.6, 88.2, 82.1, 77.3, 77.2, 77.0, 76.7, 34.5, 34.4, 34.3, 33.9, 32.7, 31.8, 31.7, 31.7, 31.6, 31.5, 31.0, 30.9, 30.7, 30.7, 30.5, 29.7, 29.4, 29.3, 29.2, 29.2, 29.1, 29.0, 22.7, 22.6, 22.5, 14.0; IR (neat): 3310, 3162, 3016, 2954, 2924, 2855, 2198, 2161, 2090, 2030 cm^{-1}; Anal. Calc. for C$_{138}$H$_{175}$BrN$_6$: C, 82.96; H, 8.83; N, 4.21. Found: C, 81.72; H, 8.75; N, 4.04%
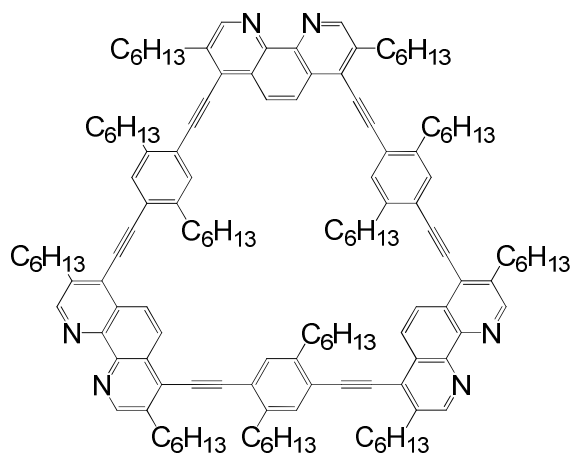
Triangular Face 32: To a solution containing 0.099 g (0.0496 mmol) of **120** and 0.050 g (0.157 mmol) of ZnI$_2$ dissolved in 75 mL of NEt$_3$ and 100 mL of toluene under an inert N$_2$ atmosphere was added 0.500 g (0.433 mmol) Pd(PPh$_3$)$_4$ followed by 0.150 g (0.788 mmol) of CuI. While the nitrogen connection remained open the flask containing the contents were submerged in a an oil bath set at 80 °C. The nitrogen connection was closed after thermal equilbrium established. The reaction was monitored by ^{1}H NMR after 2 and 6 hours by extracting 12mL of reaction mixture each time. After eight hours the reaction was stopped and the solvent removed via rotoevaporation and dried under vacuuum. The resulting brown substance was redissolved in 100 mL of dichloromethane and washed with 400 mL of 0.25 M KCN solution. Afterwards the organic phase was separated from the aqueous phase and collected. Two subsequent extractions of the organic substance from the aqueous solution were carried out using dichloromethane. The combine collected organic solutions was dried over anhydrous MgSO$_4$ and the solvent removed

via rotoevaporation and dried under vacuum. After drying the substance under vacuum purification was attempted by column chromatography using initially dichloromethane/ethyl acetate (1:1, v/v) as the elutant. The solvent polarity was increased to pure ethyl acetate, followed by ethyl acetate/methanol (30:1, v/v) and ethyl acetate/ethanol (20:1, v/v). This afforded a mixture of possible desired product as well as oligomeric byproducts (0.033 mg, < 0.017 mmol because contaminated, < 34% because contaminated). Total integration matches! ^{1}H NMR (400 MHz, CDCl$_3$) 9.12 (s, 6H), 8.55 (s, 6H), 7.64 (s, 6H), 3.19 – 3.06 (comp, 24H), 1.91 – 1.83 (comp, 24H), 1.59 – 1.25 (comp, 72H), 0.92 – 0.82 (comp, 36H), 0.07* greese ^{13}C NMR (400 MHz, CDCl$_3$) 151.3, 144.3, 142.7, 138.9, 133.2, 127.9, 127.7, 125.1, 123.0, 101.2, 88.9, 34.6, 32.8, 31.8, 31.8, 30.9, 30.8, 29.7, 29.4, 29.3, 29.3, 22.7, 14.1, 1.00 * greese; IR (neat): 2955, 2925, 2855, 2198, 2162, 2019, 1979 cm^{-1}.

4.4.3. Synthesis of Diamond
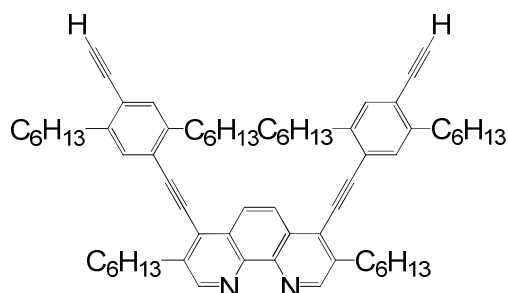
Compound 122: To a solution containing 0.736g (0.591 mmol) of **55** in 25 mL of dichloromethane is added 1.949 g (7.5 mmol) N(Bu)$_4$F in 25 mL of THF. The contents are stirred at room temperature for 45 minutes and then washed with 200 mL of a saturated NaHCO$_3$ solution. Two subsequent extractions of the organic substance from the aqueous solution were carried out using dichloromethane. The combine collected organic solutions was dried over anhydrous MgSO$_4$ and the solvent removed via rotoevaporation and dried under vacuum. The crude brown product was purified via flash chromatography using dichloromethane as eluent, initially. The solvent polarity was increased to dichloromethane/ethyl acetate (10:1, v/v), which afforded 0.547g (0.586 mmol) **122** in 99% yield. ^{1}H NMR (300 MHz, CDCl$_3$) δ 9.07 (s, 2H), 8.44 (s, 2H), 7.48 (s, 2H), 7.41 (s, 2H), 3.36 (s, 2H), 3.13 (t, 4H, $J^3 = 7.2$ Hz), 2.92 (t, 4H, $J^3 = 7.8$ Hz), 2.80 (t, 4H, $J^3 = 7.8$ Hz), 1.89 – 1.62 (comp, 12H), 1.46 – 1.23 (comp, 36H), 0.92 –

0.77 (m, 18H); ^{13}C NMR (400 MHz, CDCl$_3$) δ 151.2 (d), 144.5, 143.1, 142.1, 138.7, 133.2 (d), 132.7(d), 127.9, 127.6, 125.0, 122.5, 122.2, 101.1, 88.3, 82.1, 82.0 (d),
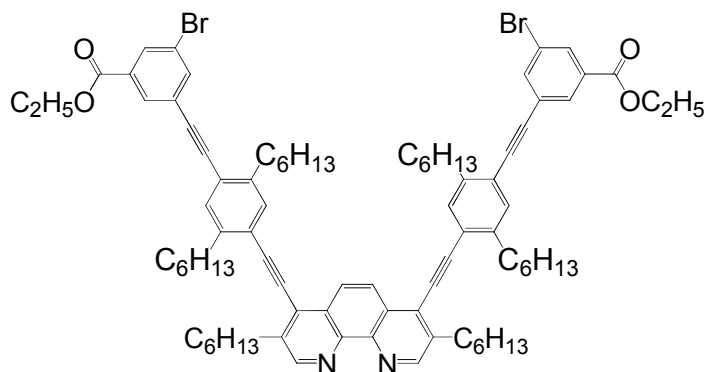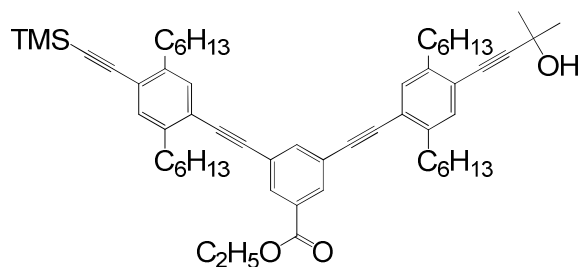

Compound 125: To a solution containing 2.264 g (7.35 mmol) of **30**, 0.434 g (0.46 mmol) of **122**, 0.160 g (mmol) of ZnI$_2$ dissolved in 120 mL was added 0.791 g (0.68 mmol) Pd(PPh$_3$)$_4$ followed by 0.647 g (3.40 mmol) of CuI and the contents stirred under N$_2$ atmosphere for 3days at 95 °C. mass 0.487 yield 76%. ^1H NMR (300 MHz, CDCl$_3$) δ 9.08 (s, 2H), 8.46 (s, 2H), 8.14 (t, J^4 = 1.8 Hz, 2H), 8.12 (t, J^4 = 1.7 Hz, 2H), 7.83 (t, J^4 = 1.7 Hz, 2H), 7.53 (s, 2H), 7.46 (s, 2H), 4.41 (q, 4H, J^3 = 7.0 Hz), 3.14 (t, J^3 = 8.0 Hz, 4H), 2.95 (t, J^3 = 7.7 Hz, 4H), 2.86 (t, 4H, J^3 = 7.7 Hz), 1.93 – 1.61 (comp, 12H), 1.53 – 1.21 (comp, 39H), 0.91 – 0.79 (comp, 18H); ^{13}C NMR (400 MHz, CDCl$_3$) δ 165.0, 151.2, 144.9, 143.5, 139.6, 138.5, 137.9, 134.9, 133.5, 132.3, 131.4, 127.9, 127.6, 127.4, 126.1, 125.4, 124.4, 122.9, 102.6, 100.7, 96.9, 84.8, 65.8, 34.5, 32.6, 31.6, 31.5, 31.4, 31.3, 30.6, 29.7, 29.1, 29.0, 28.6, 25.6. 22.5, 22.5, 14.0, 14.0, -0.2. IR (neat): 3071, 2954, 2924, 2854, 2206, 2156, 2022, 1968, 1724 cm^{-1}; Anal. Calc. for C$_{86}$H$_{102}$Br$_2$N$_2$O$_4$: C, 74.44; H, 7.41; N, 2.02. Found: C, 71.57; H, 7.41; N, 1.90%
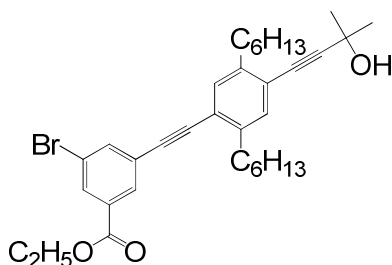

Compound 126: To a solution containing 0.749 g (2.43 mmol) of **30**, 0.350 g, (0.303 mmol) of Pd(Ph$_3$)$_4$, and 0.489 g, (1.39 mmol) **28**, and dissolved in 150 mL of NEt$_3$ at 75 °C under an inert

N$_2$ atmosphere was added 0.175 g (0.919 mmol) of CuI. The resulting mixture stirred at 75 °C for eighteen hours before the reaction solution was cooled and filtered through a 1.5 inch plug of silica atop a glass frit. The solvent was removed from the filtrate by rotoevaporation and the brown residue was dried under vacuum. The crude substance was purified via column chromatography initially using toluene as eluent to recover 0.428 g (1.39 mmol) of **30**. The solvent polarity was increased to toluene/ethyl acetate (20:1, v/v) as the eluent, which afforded 0.449 g, (0.776 mmol) of **126** in 32 % yield. A small sample of the product was further purified for characterization via column chromatography using dichloromethane/hexanes (1:1, v/v) as eluent to remove and remaining catalyst. ^{1}H NMR (300 MHz, CDCl$_3$) δ 8.13 – 8.11 (m, 1H), 8.09 – 8.08 (m, 1H), 7.81 – 7.79 (m, 1H), 7.32 (s, 1H), 7.25 (s, 1H), 4.40 (q, J^3 = 7.1 Hz, 2H), 2.75 – 2.69 (m, 4H), 2.10 (bs, 1H), 1.71 – 1.55 (comp, 10H), 1.43 – 1.25 (comp, 15H), 0.91 – 0.85 (m, 6H); ^{13}C NMR (400 MHz, CDCl$_3$) δ 164.6, 142.4, 142.3, 137.8, 132.4, 132.0, 131.0, 125.7, 122.7, 122.2, 121.6, 98.6, 91.2, 90.6, 80.8, 65.7, 61.6, 34.0, 31.7, 31.7, 31.5, 30.6, 30.5, 29.2, 29.1, 22.6, 14.2, 14.1; IR (neat): 3432, 3074, 2977, 2955, 2926, 2856, 2210, 1726 cm^{-1}.


Compound 128: To a solution containing 1.080 g (1.86 mmol) of **126** and 0.848 g (2.31 mmol) of **26** in and 0.300 g (0.260 mmol) Pd(Ph$_3$)$_4$, dissolved in 100 mL of NEt$_3$ at 80 °C under an inert N$_2$ atmosphere was added and 0.150 g (0.788 mmol) CuI. The resulting mixture was stirred at 80 °C for 24 hours before the reaction solution was filtered through a 1.5 inch plug of silica atop a glass frit. Following the removal of the solvent from the filtrate via rotoevaporation the brown substance was dried under vacuum and then purified via flash chromatography using hexanes/ethyl acetate (4:1 v/v), which afforded 1.260 g (1.46 mmol) of **128** in 84% yield A small sample of the product was further purified for characterization via column chromatography using dichloromethane/hexanes (1:1, v/v) as eluent to remove and remaining catalyst. ^{1}H NMR (300 MHz, CDCl$_3$) δ 8.12 (appd, J^4 = 1.8 Hz, 2H), 7.79 (t, J^4 = 1.8 Hz, 1H), 7.33 (s, 2H), 7.31 (s, 1H), 7.27 (s, 1H), 4.42 (q, J^3 = 7.1 Hz, 2H), 2.80 – 2.68 (m, 8H), 2.07 (bs, 1H), 1.72 – 1.58 (comp,

14H), 1.45 – 1.24 (comp, 27H), 0.92 – 0.85 (m, 12H), 0.27 (s, 9H); ^{13}C NMR (400 MHz, CDCl$_3$) δ 165.3,142.8, 142.4, 142.3, 142.3, 137.7, 134.0, 133.9, 132.6, 132.4, 131.9, 131.3, 129.7, 128.6, 128.5, 124.3, 122.9, 122.5, 122.0, 121.9, 103.8, 99.2, 98.5, 92.0, 91.9, 89.9, 89.8, 80.9, 65.7, 61.4, 34.1, 34.1, 34.0, 31.8, 31.7, 31.5, 30.6, 30.5, 29.3, 29.2, 29.2, 22.6, 22.6, 14.3, 14.1, -0.0; IR (neat): 3436, 2955, 2926, 2856, 2211, 2149, 1727 cm^{-1}.
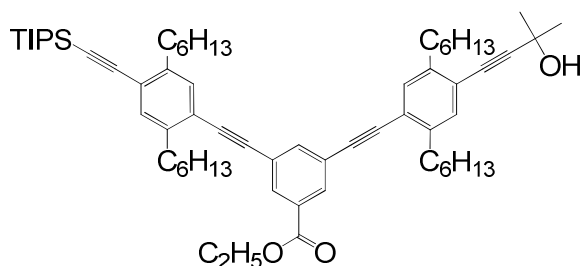
Compound 129: This procedure was analgous to that used to produce **128** except 1.08 g (1.86 mmol) of **126**, 1.050 g (2.33 mmol) of **27**, 0.300 g, (0.260 mmol)Pd(Ph$_3$)$_4$, 25 mL of NEt$_3$, and 0.158g (0.830 mmol) of CuI used instead. The crude brown product was purified via flash chromatography using hexane/ethyl acetate (4:1, v/v). The yellow oil was further purified by flash chromatography using hexane/dichloromethane (4:1 v/v) as eluent intitialy. The solvent polarity was increased to hexane/dichloromethane (2:1 v/v), which afforded 1.261 g (1.33 mmol) of **129** 72 %. ^{1}H NMR (300 MHz, CDCl$_3$) δ 8.12 (appd, J^4 = 1.5 Hz, 2H), 7.80 (t, J^4 = 1.5 Hz, 1H), 7.34 (s, 2H), 7.32 (s, 1H), 7.27 (s, 1H), 4.42 (q, J^3 = 7.1 Hz, 2H), 2.81 – 2.68 (m, 8H), 1.88 (bs, 1H), 1.74 – 1.57 (comp, 14H), 1.45 – 1.24 (comp, 27H), 1.15 (s, 21H), 0.92 – 0.85 (m, 12H); ^{13}C NMR (400 MHz, CDCl$_3$) δ 165.3, 142.6, 142.3, 142.3, 142.3, 137.7, 133.0, 132.4, 131.9, 131.2, 124.3, 124.3, 123.3, 122.5, 121.9, 121.8, 105.5, 98.5, 95.6, 91.9, 91.9, 89.9, 89.8, 80.9, 65.7, 61.4, 34.4, 34.1, 34.1, 34.0, 31.8, 31.8, 31.7, 31.5, 30.8, 30.7, 30.6, 30.5, 29.3, 29.2, 29.2, 22.6, 22.6, 18.7, 14.3, 14.1, 11.4; IR (neat): 3311, 2954, 2925, 2856, 2210, 2146, 2103, 2025, 1727 cm^{-1}..

TMS—≡— C$_6$H$_{13}$ C$_6$H$_{13}$ —H

C$_6$H$_{13}$ C$_6$H$_{13}$

C$_2$H$_5$O   O
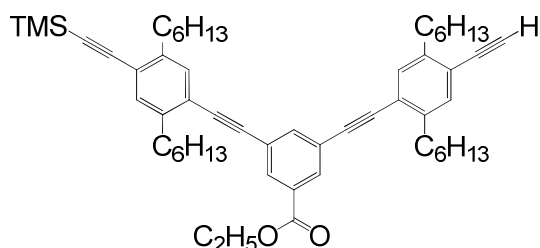
Compond 130: A flask charged with 0.264 g (0.305 mmol) of **128** 0.015 g (0.375 mmol) of NaH (60% in mineral oil) dissolved in 20 mL of toluene was refluxed for 50 minutes under an inert N$_2$ atmosphere. The hot light yellow solution was filtered through a 1.5 inch plug of silica atop a glass frit. The light yellow solution was rinsed from the silica with additional toluene. After removing the solvent via rotoevaporation and drying the light brown oil under vacuum the product was characterized by ^{1}H NMR and found to be sufficiently pure. Therefore no further purification performed and 0.222 g (0.275 mmol) of **130** was obtained in 90% yield. ^{1}H NMR (400 MHz, CDCl$_3$) δ 8.14 (appd, J^4 = 1.2 Hz, 2H), 7.81 (t, J^4 = 1.2 Hz, 1H), 7.37 (s, 1H), 7.35 (s, 2H), 7.33 (s, 1H), 4.43 (q, J^3 = 7.2 Hz, 2H), 3.32 (s, 1H), 2.82 – 2.72 (m, 8H), 1.73 – 1.59 (m, 8H), 1.45 – 1.27 (comp, 27H), 0.93 – 0.87 (m, 12H), 0.28 (s, 9H); ^{13}C NMR (400 MHz, CDCl$_3$) δ 165.2, 142.8, 142.3, 142.3, 137.8, 133.1, 133.0, 132.6, 132.5, 132.4, 132.4, 132.0, 131.8, 131.3, 124.3, 124.3, 123.0, 122.4, 122.0, 121.9, 103.9, 99.2, 92.1, 92.0, 89.9, 89.7, 82.4, 81.7, 81.6, 61.4, 34.2, 34.1, 34.0, 33.8, 31.7, 31.7, 30.6, 30.6, 30.6, 30.4, 29.7, 29.3, 29.2, 29.1, 29.1, 22.6, 22.6, 14.3, 14.2, 14.1, -0.0; IR (neat): 3310, 2955, 2925, 2856, 2210, 2149, 2102, 1727 cm^{-1}.

TIPS—≡— C$_6$H$_{13}$ C$_6$H$_{13}$ —H

C$_6$H$_{13}$ C$_6$H$_{13}$

C$_2$H$_5$O   O
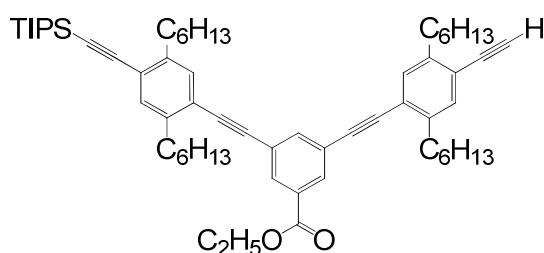
Compound 131: This procedure was analgous to that used to produce **130** except 0.294 g (mmol) of **129**, 0.040g (mmol) of NaH, in 50 mL of dried toluene and contents stirred for 1 hour. Yield: 0.185 g (mmol) 67% yield. ^{1}H NMR (300 MHz, CDCl$_3$) δ 8.13 (appd, J^4 = 1.5 Hz, 2H), 7.81 (t, J^4 = 1.5 Hz, 1H), 7.36 (s, 1H), 7.36 (s, 2H), 7.32 (s, 1H), 4.42 (q, J^3 = 7.2 Hz, 2H), 3.32 (s, 1H), 2.82 – 2.73 (m, 8H), 1.74 – 1.60 (m, 8H), 1.46 – 1.26 (comp, 27H), 1.15 (s, 21H), 0.92 – 0.85 (m, 12H); ^{13}C NMR (400 MHz, CDCl$_3$) δ 165.2, 142.8, 142.6, 142.3, 137.7, 133.1, 133.1,

133.0, 132.4, 131.9, 131.9, 131.3, 124.4, 124.3, 123.4, 122.4, 122.0, 121.9, 105.6, 95.6, 92.1, 92.0, 90.0, 89.7, 82.4, 81.7, 61.4, 34.4, 34.1, 34.0, 33.9, 31.8, 31.7, 31.7, 30.8, 30.8, 30.6, 30.4, 29.7, 29.4, 29.2, 29.2, 29.1, 22.6, 22.6, 18.7, 14.3, 14.1, 11.4, 1.0* (grease); IR (neat): 3311, 2954, 2925, 2858, 2210, 2146, 1727 cm^{-1}.
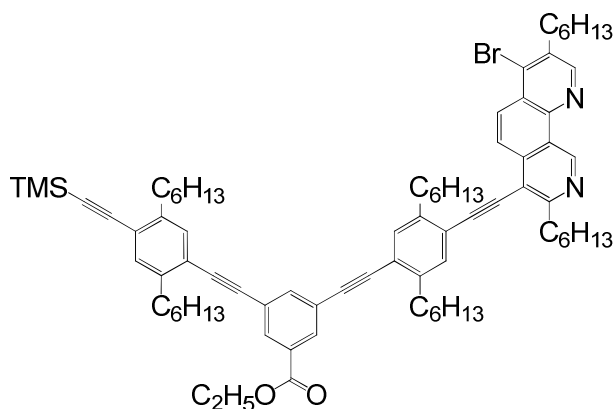
Compound 132: To a solution containing 0.999 g (1.97 mmol) of **29**, 0.653 g (2.05 mmol) of ZnI$_2$ dissolved in 50 mL of toluene under an inert N$_2$ atmosphere was added 0.289 g (0.250 mmol) Pd(Ph$_3$)$_4$, followed by 0.277 g, (0.343 mmol) **130** dissolved in 50 mL of NEt$_3$ and finally 0.156 g (0.819 mmol) CuI. Next the reaction flask was submerged in an oil bath at 90 °C and the resulting mixture stirred at 90 °C for twenty four hours before removing the solvent via rotoevaporation. Next the crude substance was dissolved with dichloromethane and the solution was washed with KCN solution. Afterwards the organic phase was separated from the aqueous phase and collected. Two subsequent extractions of the organic substance from the aqueous solution were carried out using dichloromethane. The collected organic solutions were combined, and then dried over anhydrous MgSO$_4$ before the solvent was removed via rotoevaporation. After drying the substance under vacuum purification was attempted via column chromatography using initially toluene/ethyl acetate (20:1 v/v). The solvent polarity was increased to toluene/ethyl acetate (10:1, v/v) as the eluent, which afforded 0.484 g of product contaminated with starting material. A second purification via column chromatography was performed on the impure sample and an impure sample from a previous experiment using toluene/ethyl acetate (20:3, v/v), which afforded 0.388 g in total. ^{1}H NMR (300 MHz, CDCl$_3$) δ 9.08 (s, 1 H), 8.93 (s, 1 H), 8.46 (d, J^3 = 9.3 Hz, 1H), 8.34 (d, J^3 = 9.3 Hz, 1H), 8.16 – 8.13 (m, 2H), 7.82 (t, J^4 = 1.8 Hz, 1H), 7.52 (s, 1H), 7.47 (s, 1H), 7.34 (s, 1H), 7.32 (s, 1H), 4.43 (q, J^3 =

7.1 Hz, 2H), 3.14 (t, J^3 = 7.7 Hz, 2H), 3.04 (t, J^3 = 7.7 Hz, 2H), 2.96 (t, J^3 = 7.8 Hz, 2H), 2.88 (t, J^3 = 7.7 Hz, 2H), 2.81 – 2.70 (m, 4H), 1.90 – 1.59 (comp, 12H), 1.49 – 1.23 (comp, 39H), 0.92 – 0.85 (comp, 18H), 0.27 (s, 9H); ^{13}C NMR (400 MHz, CDCl$_3$) δ 165.1, 151.5, 151.1, 145.4, 144.0, 142.8, 142.7, 142.3, 142.2, 138.9, 137.7, 137.6, 134.7, 132.9, 132.6, 132.5, 132.4, 132.3, 132.0, 131.9, 131.3, 128.0, 127.8, 127.4, 125.7, 125.6, 124.3, 124.1, 123.1. 122.9, 122.1, 121.9, 103.8, 101.5, 99.2, 92.7, 91.9, 90.0, 89.6, 88.3, 61.4, 34.4, 34.4, 34.1, 34.1, 34.0, 32.7, 31.8, 31.7, 31.5, 30.8, 30.6, 30.6, 30.5, 29.7, 29.3, 29.2, 29.1, 29.0, 22.6, 22.6, 22.5, 14.2, 14.0, 14.0, -0.1; IR (neat): 2954, 2924, 2855, 2205, 2149, 2019, 1979, 1726 cm^{-1}.

4.6. References

(106)   Zhang, J.; Pesak, D. J.; Ludwick, J. L.; Moore, J. S.: Geometrically-Controlled and Site-Specifically-Functionalized Phenylacetylene Macrocycles. *Journal of the American Chemical Society* **1994**, *116*, 4227-4239.

(109)   Moore, J. S.; Zhang, J.: Efficient Synthesis of Nanoscale Macrocyclic Hydrocarbons. *Angewandte Chemie International Edition in English* **1992**, *31*, 922-924.

(139)   Corbett, P. T.; Leclaire, J.; Vial, L.; West, K. R.; Wietor, J.-L.; Sanders, J. K. M.; Otto, S.: Dynamic Combinatorial Chemistry. *Chem. Rev. (Washington, DC, U. S.)* **2006**, *106*, 3652-3711.

(314)   Xu, X.-N.; Wang, L.; Wang, G.-T.; Lin, J.-B.; Li, G.-Y.; Jiang, X.-K.; Li, Z.-T.: Hydrogen-Bonding-Mediated Dynamic Covalent Synthesis of Macrocycles and Capsules: New Receptors for Aliphatic Ammonium Ions and the Formation of Pseudo[3]rotaxanes. *Chem.--Eur. J.* **2009**, *15*, 5763-5774, S5763/1-S5763/10.

(315)   Schmittel, M.; Kalsani, V.; Michel, C.; Mal, P.; Ammon, H.; Jäckel, F.; Rabe, J. P.: Towards Nanotubular Structures with Large Voids: Dynamic Heteroleptic Oligophenanthroline Metallonanoscaffolds and their Solution-State Properties. *Chemistry – A European Journal* **2007**, *13*, 6223-6237.

(316)   Cheng, X.; Heyen, A. V.; Mamdouh, W.; Uji-i, H.; De, S. F.; Hoeger, S.; De, F. S.: Synthesis and Adsorption of Shape-Persistent Macrocycles Containing Polycyclic Aromatic Hydrocarbons in the Rigid Framework. *Langmuir* **2007**, *23*, 1281-1286.

(317)   Couet, J.; Biesalski, M.: Conjugating self-assembling rigid rings to flexible polymer coils for the design of organic nanotubes. *Soft Matter* **2006**, *2*, 1005-1014.

(318)   Kalsani, V.; Ammon, H.; Jaeckel, F.; Rabe, J. P.; Schmittel, M.: Synthesis and self-assembly of a rigid exotopic bisphenanthroline macrocycle: Surface patterning and a supramolecular nanobasket. *Chem.--Eur. J.* **2004**, *10*, 5481-5492.

(319)   Hoeger, S.: Shape-persistent macrocycles: from molecules to materials. *Chem.--Eur. J.* **2004**, *10*, 1320-1329.

(320)   Matsui, K.; Segawa, Y.; Itami, K.: Synthesis and Properties of Cycloparaphenylene-2,5-pyridylidene: A Nitrogen-Containing Carbon Nanoring. *Org. Lett.* **2012**, *14*, 1888-1891.

(321)   Leu, W. C. W.; Fritz, A. E.; Digianantonio, K. M.; Hartley, C. S.: Push-Pull Macrocycles: Donor-Acceptor Compounds with Paired Linearly Conjugated or Cross-Conjugated Pathways. *J. Org. Chem.* **2012**, *77*, 2285-2298.

(322)   Abe, H.; Chida, Y.; Kurokawa, H.; Inouye, M.: Selective Binding of D2h-Symmetrical, Acetylene-Linked Pyridine/Pyridone Macrocycles to Maltoside. *J. Org. Chem.* **2011**, *76*, 3366-3371.

(323)   Qin, B.; Ren, C.; Ye, R.; Sun, C.; Chiad, K.; Chen, X.; Li, Z.; Xue, F.; Su, H.; Chass, G. A.; Zeng, H.: Persistently Folded Circular Aromatic Amide Pentamers Containing Modularly Tunable Cation-Binding Cavities with High Ion Selectivity. *J. Am. Chem. Soc.* **2010**, *132*, 9564-9566.

(324)   Jiang, J.; MacLachlan, M. J.: Unsymmetrical Triangular Schiff Base Macrocycles with Cone Conformations. *Org. Lett.* **2010**, *12*, 1020-1023.

(325)   Sanford, A. R.; Yuan, L.; Feng, W.; Yamato, K.; Flowers, R. A.; Gong, B.: Cyclic aromatic oligoamides as highly selective receptors for the guanidinium ion. *Chemical Communications* **2005**, 4720-4722.

(326)   Kawase, T.; Tanaka, K.; Seirai, Y.; Shiono, N.; Oda, M.: Complexation of Carbon Nanorings with Fullerenes: Supramolecular Dynamics and Structural Tuning for a Fullerene Sensor. *Angewandte Chemie International Edition* **2003**, *42*, 5597-5600.

(327)   Baxter, P. N. W.: Synthesis and fluorescence ion-sensory properties of the first dehydropyridoannulene-type cyclophane with enforced exotopic metal ion binding sites. *Chem.-- Eur. J.* **2003**, *9*, 2531-2541.

(328)   Chen, P.; Jäkle, F.: Highly Luminescent, Electron-Deficient Bora-cyclophanes. *Journal of the American Chemical Society* **2011**, *133*, 20142-20145.

(329)   Zhu, Y.-Y.; Li, C.; Li, G.-Y.; Jiang, X.-K.; Li, Z.-T.: Hydrogen-Bonded Aryl Amide Macrocycles: Synthesis, Single-Crystal Structures, and Stacking Interactions with Fullerenes and Coronene. *J. Org. Chem.* **2008**, *73*, 1745-1751.

(330)   Nakamura, Y.; Aratani, N.; Osuka, A.: Cyclic porphyrin arrays as artificial photosynthetic antenna: synthesis and excitation energy transfer. *Chemical Society Reviews* **2007**, *36*, 831-845.

(331)   Zhao, T.; Liu, Z.; Song, Y.; Xu, W.; Zhang, D.; Zhu, D.: Novel Diethynylcarbazole Macrocycles: Synthesis and Optoelectronic Properties. *J. Org. Chem.* **2006**, *71*, 7422-7432.

(332)   Sun, S.-S.; Lees, A. J.: Synthesis and Photophysical Properties of Dinuclear Organometallic Rhenium(I) Diimine Complexes Linked by Pyridine-Containing Macrocyclic Phenylacetylene Ligands. *Organometallics* **2001**, *20*, 2353-2358.

(333)   Nakao, K.; Nishimura, M.; Tamachi, T.; Kuwatani, Y.; Miyasaka, H.; Nishinaga, T.; Iyoda, M.: Giant Macrocycles Composed of Thiophene, Acetylene, and Ethylene Building Blocks. *J. Am. Chem. Soc.* **2006**, *128*, 16740-16747.

(334)   Gross, D. E.; Zang, L.; Moore, J. S.: Arylene-ethynylene macrocycles: privileged shape-persistent building blocks for organic materials. *Pure Appl. Chem.* **2012**, *84*, 869-878.

(335)   Iyoda, M.; Yamakawa, J.; Rahman, M. J.: Conjugated Macrocycles: Concepts and Applications. *Angew. Chem., Int. Ed.* **2011**, *50*, 10522-10553.

(336)   Hoeger, S.: Shape-persistent rings and wheels. *Pure Appl. Chem.* **2010**, *82*, 821-830.

(337)   Diederich, F.; Kivala, M.: All-Carbon Scaffolds by Rational Design. *Adv. Mater. (Weinheim, Ger.)* **2010**, *22*, 803-812.

(338)   Tykwinski, R. R.; Gholami, M.; Eisler, S.; Zhao, Y.; Melin, F.; Echegoyen, L.: Expanded radialenes: modular synthesis and properties of cross-conjugated enyne macrocycles. *Pure Appl. Chem.* **2008**, *80*, 621-637.

(339)   Zhang, W.; Moore, J. S.: Shape-persistent macrocycles: structures and synthetic approaches from arylene and ethynylene building blocks. *Angew. Chem., Int. Ed.* **2006**, *45*, 4416-4439.

(340)   Hoeger, S.: Shape-persistent phenylene-acetylene macrocycles: Large rings-low yield? *Angew. Chem., Int. Ed.* **2005**, *44*, 3806-3808.

(341)   Zhao, D.; Moore, J. S.: Shape-persistent arylene ethynylene macrocycles: syntheses and supramolecular chemistry. *Chem. Commun. (Cambridge, U. K.)* **2003**, 807-818.

(342)   Grave, C.; Schluter, A. D.: Shape-persistent, nano-sized macrocycles. *Eur. J. Org. Chem.* **2002**, 3075-3098.

(343)   Hoger, S.: Highly efficient methods for the preparation of shape-persistent macrocyclics. *J. Polym. Sci., Part A: Polym. Chem.* **1999**, *37*, 2685-2698.

(344)   Sisco, S. W.; Moore, J. S.: Directional Cyclooligomers via Alkyne Metathesis. *Journal of the American Chemical Society* **2012**, *134*, 9114-9117.

(345)   Zhang, W.; Moore, J. S.: Alkyne metathesis: catalysts and synthetic applications. *Adv. Synth. Catal.* **2007**, *349*, 93-120.

(346)   Zhang, W.; Moore, J. S.: Arylene Ethynylene Macrocycles Prepared by Precipitation-Driven Alkyne Metathesis. *J. Am. Chem. Soc.* **2004**, *126*, 12796.

(347)   Ge, P.-H.; Fu, W.; Herrmann, W. A.; Herdtweck, E.; Campana, C.; Adams, R. D.; Bunz, U. H. F.: Structural characterization of a cyclohexameric meta-phenyleneethynylene made by alkyne metathesis with in situ catalysts. *Angew. Chem., Int. Ed.* **2000**, *39*, 3607-3610.

(348)   Guieu, S.; Crane, A. K.; MacLachlan, M. J.: Campestarenes: novel shape-persistent Schiff base macrocycles with 5-fold symmetry. *Chem. Commun. (Cambridge, U. K.)* **2011**, *47*, 1169-1171.

(349)   Shopsowitz, K. E.; Edwards, D.; Gallant, A. J.; MacLachlan, M. J.: Highly substituted Schiff base macrocycles via hexasubstituted benzene: a convenient double Duff formylation of catechol derivatives. *Tetrahedron* **2009**, *65*, 8113-8119.

(350)   Korich, A. L.; Hughes, T. S.: Arylene Imine Macrocycles of C3h and C3 Symmetry from Reductive Imination of Nitroformylarenes. *Organic Letters* **2008**, *10*, 5405-5408.

(351)   Fastrez, J.: Macrocyclization versus polymerization in polycondensation reactions under high-dilution conditions: a theoretical study. *J. Phys. Chem.* **1989**, *93*, 2635-42.

(352)   Ercolani, G.; Mandolini, L.; Mencarelli, P.: Kinetic treatment of irreversible cyclooligomerization of bifunctional chains and its relevance to the synthesis of many-membered rings. *Macromolecules* **1988**, *21*, 1241-6.

(353)   Brouard, M.: *Reaction Dynamics*; Oxford University Press Inc.: New York, 1998.

(354)   Datar, A.; Gross, D. E.; Balakrishnan, K.; Yang, X.; Moore, J. S.; Zang, L.: Ultrafine nanofibers fabricated from an arylene-ethynylene macrocyclic molecule using surface assisted self-assembly. *Chem. Commun. (Cambridge, U. K.)* **2012**, *48*, 8904-8906.

(355)   Feng, W.; Yamato, K.; Yang, L.; Ferguson, J. S.; Zhong, L.; Zou, S.; Yuan, L.; Zeng, X. C.; Gong, B.: Efficient Kinetic Macrocyclization. *J. Am. Chem. Soc.* **2009**, *131*, 2629-2637.

(356)   Seo, S. H.; Jones, T. V.; Seyler, H.; Peters, J. O.; Kim, T. H.; Chang, J. Y.; Tew, G. N.: Liquid Crystalline Order from ortho-Phenylene Ethynylene Macrocycles. *J. Am. Chem. Soc.* **2006**, *128*, 9264-9265.

(357)   Nomoto, A.; Sonoda, M.; Yamaguchi, Y.; Ichikawa, T.; Hirose, K.; Tobe, Y.: A Clue to Elusive Macrocycles: Unusually Facile, Spontaneous Polymerization of a Hexagonal Diethynylbenzene Macrocycle. *J. Org. Chem.* **2006**, *71*, 401-404.

(358)   Liu, Y.; Qin, B.; Zeng, H.: POCl$_3$-mediated H-bonding-directed one-pot synthesis of macrocyclic pentamers, strained hexamers and highly strained heptamers. *SCIENCE CHINA Chemistry* **2012**, *55*, 55-63.

(359)   Norouzi-Arasi, H.; Pisula, W.; Mavrinskiy, A.; Feng, X.; Müllen, K.: Synthesis and Self-Assembly of Macrocyclic Mesogens Based on 1,10-Phenanthroline. *Chemistry – An Asian Journal* **2011**, *6*, 367-371.

(360)   Yuan, L.; Feng, W.; Yamato, K.; Sanford, A. R.; Xu, D.; Guo, H.; Gong, B.: Highly Efficient, One-Step Macrocyclizations Assisted by the Folding and Preorganization of Precursor Oligomers. *Journal of the American Chemical Society* **2004**, *126*, 11120-11121.

(361)   Wettach, H.; Hoeger, S.; Chaudhuri, D.; Lupton, J. M.; Liu, F.; Lupton, E. M.; Tretiak, S.; Wang, G.; Li, M.; De, F. S.; Fischer, S.; Foerster, S.: Synthesis and properties of a triphenylene-butadiynylene macrocycle. *J. Mater. Chem.* **2011**, *21*, 1404-1415.

(362)   Kaleta, J. i.; Mazal, C.: A Triangular Macrocycle Altering Planar and Bulky Sections in Its Molecular Backbone. *Organic Letters* **2011**, *13*, 1326-1329.

(363)   Chen, S.; Yan, Q.; Li, T.; Zhao, D.: Arylene Ethynylene Macrocycles with Intramolecular π-π Stacking. *Org. Lett.* **2010**, *12*, 4784-4787.

(364)   Opris, D. M.; Franke, P.; Schlueter, A. D.: Shape-persistent macrocycles with bipyridine units: progress in accessibility and widening of applicability. *Eur. J. Org. Chem.* **2005**, 822-837.

(365)   Lehmann, U.; Schluter, A. D.: A shape-persistent macrocycle with two opposing 2,2':6',2"-terpyridine units. *Eur. J. Org. Chem.* **2000**, 3483-3487.

(366)   Staab, H. A.; Neunhoeffer, K.: [2.2.2.2.2.2]Metacyclophane-1,9,17,25,33,41-hexayne from m-iodophenylacetylene by sixfold Stephens-Castro coupling. *Synthesis* **1974**, 424.

(367)   Shortell, D. B.; Palmer, L. C.; Tour, J. M.: Solid-phase approaches toward cyclic oligomers. *Tetrahedron* **2001**, *57*, 9055-9065.

(368)   Höger, S.; Meckenstock, A.-D.; Pellen, H.: High-Yield Macrocyclization via Glaser Coupling of Temporary Covalent Templated Bisacetylenes. *The Journal of Organic Chemistry* **1997**, *62*, 4556-4557.

(369)   Fischer, M.; Höger, S.: Synthesis of a shape-persistent macrocycle with intraannular carboxylic acid groups. *Tetrahedron* **2003**, *59*, 9441-9446.

(370)   Schmittel, M.; Ammon, H.: Preparation of a rigid macrocycle with two exotopic phenanthroline binding sites. *Synlett* **1999**, 750-752.

Bibliography

(1)   Deal, B.; Talbot, J.: Principia Moore. *Electrochem. Soc. Interface* **1997**, *6*, 18-23.

(2)   Moore, G. E.: Cramming More Components Onto Integrated Circuits. *Proceedings of the IEEE* **1998**, *86*, 82-85.

(3)   Dodd, P. E.; Shaneyfelt, M. R.; Schwank, J. R.; Felix, J. A.: Current and future challenges in radiation effects on CMOS electronics. *IEEE Trans. Nucl. Sci.* **2010**, *57*, 1747-1763.

(4)   Lundstrom, M.: Applied Physics: Moore's law forever? *Science (Washington, DC, U. S.)* **2003**, *299*, 210-211.

(5)   Marsh, G.: Moore's law at the extremes. *Mater. Today (Oxford, U. K.)* **2003**, *6*, 28-33.

(6)   Nuzzo, R. G.: The future of electronics manufacturing is revealed in the fine print. *Proc. Natl. Acad. Sci. U. S. A.* **2001**, *98*, 4827-4829.

(7)   Peercy, P. S.: The drive to miniaturization. *Nature (London)* **2000**, *406*, 1023-1026.

(8)   Weldon, M. K.; Queeney, K. T.; Eng, J., Jr.; Raghavachari, K.; Chabal, Y. J.: The surface science of semiconductor processing. Gate oxides in the ever-shrinking transistor. *Surf. Sci.* **2002**, *500*, 859-878.

(9)   Thomas, S. G.; Tomasini, P.; Bauer, M.; Vyne, B.; Zhang, Y.; Givens, M.; Devrajan, J.; Koester, S.; Lauer, I.: Enabling Moore's Law beyond CMOS technologies through heteroepitaxy. *Thin Solid Films* **2010**, *518*, S53-S56.

(10)   Thayne, I. G.; Hill, R. J. W.; Holland, M. C.; Li, X.; Zhou, H.; MacIntyre, D. S.; Thoms, S.; Kalna, K.; Stanley, C. R.; Asenov, A.; Droopad, R.; Passlack, M.: Review of current status of III-V MOSFETs. *ECS Trans.* **2009**, *19*, 275-286.

(11)   Liang, D.; Bowers, J. E.: Photonic integration: Si or InP substrates? *Electron. Lett.* **2009**, 10-13.

(12)   French, R. H.; Tran, H. V.: Immersion lithography: photomask and wafer-level materials. *Annu. Rev. Mater. Res.* **2009**, *39*, 93-126.

(13)   Emtsev, K. V.; Bostwick, A.; Horn, K.; Jobst, J.; Kellogg, G. L.; Ley, L.; McChesney, J. L.; Ohta, T.; Reshanov, S. A.; Roehrl, J.; Rotenberg, E.; Schmid, A. K.; Waldmann, D.; Weber, H. B.; Seyller, T.: Towards wafer-size graphene layers by atmospheric pressure graphitization of silicon carbide. *Nat. Mater.* **2009**, *8*, 203-207.

(14)   Wickenden, D. K.: Semiconductor devices: Moore marches on. *Johns Hopkins APL Tech. Dig.* **2008**, *28*, 30-39.

(15)   Toh, E.-H.; Wang, G. H.; Chan, L.; Sylvester, D.; Heng, C.-H.; Samudra, G. S.; Yeo, Y.-C.: Device design and scalability of a double-gate tunneling field-effect transistor with silicon-germanium source. *Jpn. J. Appl. Phys.* **2008**, *47*, 2593-2597.

(16)   Schlom, D. G.; Guha, S.; Datta, S.: Gate oxides beyond SiO2. *MRS Bull.* **2008**, *33*, 1017-1025.

(17)   Kaminow, I. P.: Optical integrated circuits: a personal perspective. *J. Lightwave Technol.* **2008**, *26*, 994-1004.

(18)   Ferry, D. K.: Quo vadis nanoelectronics? *Phys. Status Solidi C* **2008**, *5*, 17-22.

(19)   Renugopalakrishnan, V.; Khizroev, S.; Anand, H.; Li, P.; Lindvold, L.: Future memory storage technology: protein-based memory devices may facilitate surpassing Moore's law. *IEEE Trans. Magn.* **2007**, *43*, 773-775.

(20)   Moers, J.: Turning the world vertical: MOSFETs with current flow perpendicular to the wafer surface. *Appl. Phys. A: Mater. Sci. Process.* **2007**, *87*, 531-537.

(21)   Datta, S.: III-V field-effect transistors for low power digital logic applications. *Microelectron. Eng.* **2007**, *84*, 2133-2137.

(22)   Jackson, T. N.: Organic Semiconductors: Beyond Moore's Law. *Nat. Mater.* **2005**, *4*, 581-582.

(23)   Graham, A. P.; Duesberg, G. S.; Seidel, R. V.; Liebau, M.; Unger, E.; Pamler, W.; Kreupl, F.; Hoenlein, W.: Carbon nanotubes for microelectronics? *Small* **2005**, *1*, 382-390.

(24)   Bez, R.: Innovative technologies for high density non-volatile semiconductor memories. *Microelectron. Eng.* **2005**, *80*, 249-255.

(25)   Kim, H.; McIntyre, P. C.; On, C. C.; Saraswat, K. C.; Stemmer, S.: Engineering chemically abrupt high-k metal oxide/silicon interfaces using an oxygen-gettering metal overlayer. *J. Appl. Phys.* **2004**, *96*, 3467-3472.

(26)   Flood, A. H.; Stoddardt, J. F.; Steuerman, D. W.; Heath, J. R.: Whence molecular electronics? *Science (Washington, DC, U. S.)* **2004**, *306*, 2055-2056.

(27)   Likharev, K.: Hybrid semiconductor - molecular nanoelectronics. *Ind. Phys.* **2003**, *9*, 20-23.

(28)   Huff, H. R.; Hou, A.; Lim, C.; Kim, Y.; Barnett, J.; Bersuker, G.; Brown, G. A.; Young, C. D.; Zeitzoff, P. M.; Gutt, J.; Lysaght, P.; Gardner, M. I.; Murto, R. W.: High-k gate stacks for planar, scaled CMOS integrated circuits. *Microelectron. Eng.* **2003**, *69*, 152-167.

(29)   Likharev, K. K.: Single-electron devices and their applications. *Proc. IEEE* **1999**, *87*, 606-632.

(30)   Maeda, K.; Okabayashi, N.; Kano, S.; Takeshita, S.; Tanaka, D.; Sakamoto, M.; Teranishi, T.; Majima, Y.: Logic operations of chemically assembled single-electron transistor. *ACS Nano* **2012**, *6*, 2798-2803.

(31)   Podd, G. J.; Angus, S. J.; Williams, D. A.; Ferguson, A. J.: Charge sensing in intrinsic silicon quantum dots. *Appl. Phys. Lett.* **2010**, *96*, 082104/1-082104/3.

(32)   Ono, Y.; Inokawa, H.; Takahashi, Y.; Nishiguchi, K.; Fujiwara, A.: Single-Electron Transistor and its Logic Application. In *Nanotechnology*; Wiley-VCH Verlag GmbH & Co. KGaA, 2010.

(33)   Silva, L. M.; Guimaraes, J. G.: Performance analysis of single-electron NAND gates. *ECS Trans.* **2009**, *23*, 311-318.

(34)   Beaumont, A.; Dubuc, C.; Beauvais, J.; Drouin, D.: Room temperature single-electron transistor featuring gate-enhanced ON-state current. *IEEE Electron Device Lett.* **2009**, *30*, 766-768.

(35)   Brenning, H. T. A.; Kubatkin, S. E.; Erts, D.; Kafanov, S. G.; Bauch, T.; Delsing, P.: A Single Electron Transistor on an Atomic Force Microscope Probe. *Nano Lett.* **2006**, *6*, 937-941.

(36)   Jan, Y.-R.; Hu, M., Jr.; Chiou, S.-C.; Yang, S.-C.: Manufacturing method for sub-micrometer t-shaped double time gate etchings. National Central University, Taiwan . 2005; pp 12 pp.

(37)   Glasson, P.; Papageorgiou, G.; Harrabi, K.; Rees, D. G.; Antonov, V.; Collin, E.; Fozooni, P.; Frayne, P. G.; Mukharsky, Y.; Lea, M. J.: Trapping single electrons on liquid helium. *J. Phys. Chem. Solids* **2005**, *66*, 1539-1543.

(38)   Uchida, K.; Koga, J.; Ohba, R.; Toriumi, A.: Programmable single-electron transistor logic for future low-power intelligent LSI: proposal and room-temperature operation. *IEEE Trans. Electron Devices* **2003**, *50*, 1623-1630.

(39)   Papageorgiou, G.; Mukharsky, Y.; Harrabi, K.; Glasson, P.; Fozooni, P.; Frayne, P. G.; Collin, E.; Lea, M. J.: Detecting electrons on helium with a single-electron transistor (SET). *Physica E (Amsterdam, Neth.)* **2003**, *18*, 179-181.

(40)   Kim, D. H.; Sung, S.-K.; Kim, K. R.; Lee, J. D.; Park, B.-G.; Choi, B. H.; Hwang, S. W.; Ahn, D.: Silicon single-electron transistors with sidewall depletion gates and their application to dynamic single-electron transistor logic. *IEEE Trans. Electron Devices* **2002**, *49*, 627-635.

(41)   Devoret, M. H.; Schoelkopf, R. J.: Amplifying quantum signals with the single-electron transistor. *Nature (London)* **2000**, *406*, 1039-1046.

(42)   Schoelkopf, R. J.; Wahlgren, P.; Kozhevnikov, A. A.; Delsing, P.; Prober, D. E.: The radio-frequency single-electron transistor (RF-SET): a fast and ultrasensitive electrometer. *Science (Washington, D. C.)* **1998**, *280*, 1238-1242.

(43)   Chen, R. H.; Korotkov, A. N.; Likharev, K. K.: Single-electron transistor logic. *Appl. Phys. Lett.* **1996**, *68*, 1954-6.

(44)   Korotkov, A. N.; Chen, R. H.; Likharev, K. K.: Possible performance of capacitively coupled single-electron transistors in digital circuits. *J. Appl. Phys.* **1995**, *78*, 2520-2530.

(45)   Averin, D. V.; Likharev, K. K.: Coulomb blockade of single-electron tunneling, and coherent oscillations in small tunnel junctions. *J Low Temp Phys* **1986**, *62*, 345-373.

(46)   Averin, D. V.; Likharev, K. K.: Single-electronics - recent developments. *Springer Ser. Electron. Photonics* **1992**, *31*, 3-12.

(47)   Fulton, T. A.; Dolan, G. J.: Observation of single-electron charging effects in small tunnel junctions. *Physical Review Letters* **1987**, *59*, 109-112.

(48)   Roche, B.; Voisin, B.; Jehl, X.; Wacquez, R.; Sanquer, M.; Vinet, M.; Deshpande, V.; Previtali, B.: A tunable, dual mode field-effect or single electron transistor. *arXiv.org, e-Print Arch., Condens. Matter* **2012**, 1-4, arXiv:1201.3760v1 [cond-mat.mes-hall].

(49)   Azuma, Y.; Suzuki, S.; Maeda, K.; Okabayashi, N.; Tanaka, D.; Sakamoto, M.; Teranishi, T.; Buitelaar, M. R.; Smith, C. G.; Majima, Y.: Nanoparticle single-electron transistor with metal-bridged top-gate and nanogap electrodes. *Appl. Phys. Lett.* **2011**, *99*, 073109/1-073109/3.

(50)   Yamaguchi, H.; Terui, T.; Noguchi, Y.; Ueda, R.; Nasu, K.; Otomo, A.; Matsuda, K.: A photoresponsive single electron transistor prepared from oligothiophene molecules and gold nanoparticles in a nanogap electrode. *Appl. Phys. Lett.* **2010**, *96*, 103117/1-103117/3.

(51)   Shin, S. J.; Jung, C. S.; Park, B. J.; Yoon, T. K.; Lee, J. J.; Kim, S. J.; Choi, J. B.; Takahashi, Y.; Hasko, D. G.: Si-based ultrasmall multiswitching single-electron transistor operating at room-temperature. *Appl. Phys. Lett.* **2010**, *97*, 103101/1-103101/3.

(52)   Moriya, R.; Kobayashi, H.; Shibata, K.; Masubuchi, S.; Hirakawa, K.; Ishida, S.; Arakawa, Y.; Machida, T.: Fabrication of single-electron transistor composed of a self-assembled quantum dot and nanogap electrode by atomic force microscope local oxidation. *Appl. Phys. Express* **2010**, *3*, 035001/1-035001/3.

(53) Ihn, T.; Guttinger, J.; Molitor, F.; Schnez, S.; Schurtenberger, E.; Jacobsen, A.; Hellmuller, S.; Frey, T.; Drroer, S.; Stampfer, C.; Ensslin, K.: Graphene single-electron transistors. *Mater. Today (Oxford, U. K.)* **2010**, *13*, 44-50.

(54) Gustafsson, D.; Bauch, T.; Nawaz, S.; Mumtaz, M.; Signorello, G.; Lombardi, F.: Low capacitance HTS junctions for single electron transistors. *Phys. C (Amsterdam, Neth.)* **2010**, *470*, S188-S190.

(55) Paraoanu, G. S.; Halvari, A. M.: Suspended single-electron transistors: fabrication and measurement. *Appl. Phys. Lett.* **2005**, *86*, 093101/1-093101/3.

(56) Saitoh, M.; Hiramoto, T.: Observation of current staircase due to large quantum level spacing in a silicon single-electron transistor with low parasitic series resistance. *J. Appl. Phys.* **2002**, *91*, 6725-6728.

(57) Park, H.; Lim, A. K. L.; Alivisatos, A. P.; Park, J.; McEuen, P. L.: Fabrication of metallic electrodes with nanometer separation by electromigration. *Appl. Phys. Lett.* **1999**, *75*, 301-303.

(58) Ji, L.; Dresselhaus, P. D.; Han, S.; Lin, K.; Zheng, W.; Lukens, J. E.: Fabrication and characterization of single-electron transistors and traps. *J. Vac. Sci. Technol., B* **1994**, *12*, 3619-22.

(59) Fujisawa, T.; Hirayama, Y.; Tarucha, S.: AlGaAs/InGaAs/GaAs single electron transistors fabricated by Ga focused ion beam implantation. *Appl. Phys. Lett.* **1994**, *64*, 2250-2.

(60) Betard, A.; Fischer, R. A.: Metal-Organic Framework Thin Films: From Fundamentals to Applications. *Chem. Rev. (Washington, DC, U. S.)* **2012**, *112*, 1055-1083.

(61) Corma, A.; Garcia, H.; Llabres, i. X. F. X.: Engineering Metal Organic Frameworks for Heterogeneous Catalysis. *Chem. Rev. (Washington, DC, U. S.)* **2010**, *110*, 4606-4655.

(62) Janiak, C.: Engineering coordination polymers towards applications. *Dalton Trans.* **2003**, 2781-2804.

(63) Kohyama, Y.; Murase, T.; Fujita, M.: A self-assembled cage as a non-covalent protective group: regioselectivity control in the nucleophilic substitution of aryl-substituted allylic chlorides. *Chemical Communications* **2012**, *48*, 7811-7813.

(64) Lee, J. Y.; Farha, O. K.; Roberts, J.; Scheidt, K. A.; Nguyen, S. B. T.; Hupp, J. T.: Metal-organic framework materials as catalysts. *Chem. Soc. Rev.* **2009**, *38*, 1450-1459.

(65) Yoshizawa, M.; Klosterman, J. K.; Fujita, M.: Functional Molecular Flasks: New Properties and Reactions within Discrete, Self-Assembled Hosts. *Angew. Chem., Int. Ed.* **2009**, *48*, 3418-3438.

(66) Takezawa, H.; Murase, T.; Fujita, M.: Temporary and Permanent Trapping of the Metastable Twisted Conformer of an Overcrowded Chromic Alkene via Encapsulation. *J. Am. Chem. Soc.* **2012**, *134*, 17420-17423.

(67) Schneider, M. W.; Oppel, I. M.; Mastalerz, M.: Exo-Functionalized Shape-Persistent [2+3] Cage Compounds: Influence of Molecular Rigidity on Formation and Permanent Porosity. *Chem.--Eur. J.* **2012**, *18*, 4156-4160, S4156/1-S4156/20.

(68) Zheng, S.-T.; Wu, T.; Irfanoglu, B.; Zuo, F.; Feng, P.; Bu, X.: Multicomponent Self-Assembly of a Nested Co24@Co48 Metal-Organic Polyhedral Framework. *Angew. Chem., Int. Ed.* **2011**, *50*, 8034-8037.

(69) Sumida, K.; Hill, M. R.; Horike, S.; Dailly, A.; Long, J. R.: Synthesis and Hydrogen Storage Properties of Be12(OH)12(1,3,5-benzenetribenzoate)4. *J. Am. Chem. Soc.* **2009**, *131*, 15120-15121.

(70)   Hunt, J. R.; Doonan, C. J.; LeVangie, J. D.; Cote, A. P.; Yaghi, O. M.: Reticular Synthesis of Covalent Organic Borosilicate Frameworks. *J. Am. Chem. Soc.* **2008**, *130*, 11872-11873.

(71)   Dinca, M.; Long, J. R.: Hydrogen storage in microporous metal-organic frameworks with exposed metal sites. *Angew. Chem., Int. Ed.* **2008**, *47*, 6766-6779.

(72)   El-Kaderi, H. M.; Hunt, J. R.; Mendoza-Cortes, J. L.; Cote, A. P.; Taylor, R. E.; O'Keeffe, M.; Yaghi, O. M.: Designed Synthesis of 3D Covalent Organic Frameworks. *Science (Washington, DC, U. S.)* **2007**, *316*, 268-272.

(73)   Yoshizawa, M.; Nakagawa, J.; Kumazawa, K.; Nagao, M.; Kawano, M.; Ozeki, T.; Fujita, M.: Discrete stacking of large aromatic molecules within organic-pillared coordination cages. *Angew. Chem., Int. Ed.* **2005**, *44*, 1810-1813.

(74)   Sudik, A. C.; Millward, A. R.; Ockwig, N. W.; Cote, A. P.; Kim, J.; Yaghi, O. M.: Design, Synthesis, Structure, and Gas (N2, Ar, CO2, CH4, and H2) Sorption Properties of Porous Metal-Organic Tetrahedral and Heterocuboidal Polyhedra. *J. Am. Chem. Soc.* **2005**, *127*, 7110-7118.

(75)   Rosi, N. L.; Eckert, J.; Eddaoudi, M.; Vodak, D. T.; Kim, J.; O'Keeffe, M.; Yaghi, O. M.: Hydrogen Storage in Microporous Metal-Organic Frameworks. *Science (Washington, DC, U. S.)* **2003**, *300*, 1127-1130.

(76)   Li, H.; Eddaoudi, M.; O'Keeffe, M.; Yaghi, O. M.: Design and synthesis of an exceptionally stable and highly porous metal-organic framework. *Nature* **1999**, *402*, 276-279.

(77)   Fujita, M.; Oguro, D.; Miyazawa, M.; Oka, H.; Yamaguchi, K.; Ogura, K.: Self-assembly of ten molecules into a nanometer-sized organic host frameworks. *Nature (London)* **1995**, *378*, 469-71.

(78)   Kumazawa, K.; Biradha, K.; Kusukawa, T.; Okano, T.; Fujita, M.: Multicomponent assembly of a pyrazine-pillared coordination cage that selectively binds planar guests by intercalation. *Angew. Chem., Int. Ed.* **2003**, *42*, 3909-3913.

(79)   Wang, M.-X.: Nitrogen and Oxygen Bridged Calixaromatics: Synthesis, Structure, Functionalization, and Molecular Recognition. *Acc. Chem. Res.* **2012**, *45*, 182-195.

(80)   Kreno, L. E.; Leong, K.; Farha, O. K.; Allendorf, M.; Van, D. R. P.; Hupp, J. T.: Metal-Organic Framework Materials as Chemical Sensors. *Chem. Rev. (Washington, DC, U. S.)* **2012**, *112*, 1105-1125.

(81)   Wang, M.; Vajpayee, V.; Shanmugaraju, S.; Zheng, Y.-R.; Zhao, Z.; Kim, H.; Mukherjee, P. S.; Chi, K.-W.; Stang, P. J.: Coordination-Driven Self-Assembly of M3L2 Trigonal Cages from Preorganized Metalloligands Incorporating Octahedral Metal Centers and Fluorescent Detection of Nitroaromatics. *Inorg. Chem.* **2011**, *50*, 1506-1512.

(82)   Wanka, L.; Iqbal, K.; Schreiner, P. R.: The Lipophilic Bullet Hits the Targets: Medicinal Chemistry of Adamantane Derivatives. *Chem. Rev. (Washington, DC, U. S.)* **2013**, Ahead of Print.

(83)   Vajpayee, V.; Yang, Y. J.; Kang, S. C.; Kim, H.; Kim, I. S.; Wang, M.; Stang, P. J.; Chi, K.-W.: Hexanuclear self-assembled arene-ruthenium nano-prismatic cages: potential anticancer agents. *Chemical Communications* **2011**, *47*, 5184-5186.

(84)   Anilkumar, P.; Lu, F.; Cao, L.; Luo, P. G.; Liu, J. H.; Sahu, S.; Tackett, K. N., II; Wang, Y.; Sun, Y. P.: Fullerenes for applications in biology and medicine. *Curr. Med. Chem.* **2011**, *18*, 2045-2059.

(85)   Lamoureux, G.; Artavia, G.: Use of the adamantane structure in medicinal chemistry. *Curr. Med. Chem.* **2010**, *17*, 2967-2978.

(86)   Kim, B. Y. S.; Rutka, J. T.; Chan, W. C. W.: Nanomedicine. *N. Engl. J. Med.* **2010**, *363*, 2434-2443.

(87)   Chawla, P.; Chawla, V.; Maheshwari, R.; Saraf, S. A.; Saraf, S. K.: Fullerenes: from carbon to nanomedicine. *Mini-Rev. Med. Chem.* **2010**, *10*, 662-677.

(88)   Mahkam, M.: New terpolymers as hydrogels for oral protein delivery application. *J. Drug Targeting* **2009**, *17*, 29-35.

(89)   Fang, Y.; Murase, T.; Sato, S.; Fujita, M.: Noncovalent Tailoring of the Binding Pocket of Self-Assembled Cages by Remote Bulky Ancillary Groups. *Journal of the American Chemical Society* **2013**, *135*, 613-615.

(90)   Furutani, Y.; Kandori, H.; Kawano, M.; Nakabayashi, K.; Yoshizawa, M.; Fujita, M.: In Situ Spectroscopic, Electrochemical, and Theoretical Studies of the Photoinduced Host-Guest Electron Transfer that Precedes Unusual Host-Mediated Alkane Photooxidation. *J. Am. Chem. Soc.* **2009**, *131*, 4764-4768.

(91)   Yoshizawa, M.; Miyagi, S.; Kawano, M.; Ishiguro, K.; Fujita, M.: Alkane Oxidation via Photochemical Excitation of a Self-Assembled Molecular Cage. *J. Am. Chem. Soc.* **2004**, *126*, 9172-9173.

(92)   Prelog, V.; Seiwerth, R.: New method for the preparation of adamantane. *Ber. Dtsch. Chem. Ges. B* **1941**, *74B*, 1769-72.

(93)   Prelog, V.; Seiwerth, R.: Synthesis of adamantane. *Ber. Dtsch. Chem. Ges. B* **1941**, *74B*, 1644-8.

(94)   Eaton, P. E.; Cole, T. W.: Cubane. *Journal of the American Chemical Society* **1964**, *86*, 3157-3158.

(95)   Maier, G.; Pfriem, S.; Schäfer, U.; Matusch, R.: Tetra-tert-butyltetrahedrane. *Angewandte Chemie International Edition in English* **1978**, *17*, 520-521.

(96)   Ternansky, R. J.; Balogh, D. W.; Paquette, L. A.: Dodecahedrane. *Journal of the American Chemical Society* **1982**, *104*, 4503-4504.

(97)   Paquette, L. A.; Ternansky, R. J.; Balogh, D. W.: A strategy for the synthesis of monosubstituted dodecahedrane and the isolation of an isododecahedrane. *Journal of the American Chemical Society* **1982**, *104*, 4502-4503.

(98)   Ashton, P. R.; Isaacs, N. S.; Kohnke, F. H.; D'Alcontres, G. S.; Stoddart, J. F.: Trinacrene – a Product of Structure-Directed Synthesis. *Angewandte Chemie International Edition in English* **1989**, *28*, 1261-1263.

(99)   Kukula, H.; Veit, S.; Godt, A.: Synthesis of monodisperse oligo(para-phenyleneethynylene)s using orthogonal protecting groups with different polarity for terminal acetylene units. *Eur. J. Org. Chem.* **1999**, 277-286.

(100)   Lavastre, O.; Ollivier, L.; Dixneuf, P.; Sibandhit, S.: Sequential catalytic synthesis of rod-like conjugated polyynes. *Tetrahedron* **1996**, *52*, 5495-504.

(101)   Schumm, J. S.; Pearson, D. L.; Tour, J. M.: Synthesis of linear conjugated oligomers with an iterative divergent/convergent method to the doubling of monomer purity: rapid access to a 128-Å length potentially conductive molecular wire. *Angew. Chem.* **1994**, *106*, 1445-8.

(102)   Grubbs, R. H.; Kratz, D.: Highly unsaturated oligomeric hydrocarbons: α-(phenylethynyl)-ω-phenylpoly [1,2-phenylene(2,1-ethynediyl)]. *Chem. Ber.* **1993**, *126*, 149-57.

(103)   Moore, J. S.: Shape-persistent molecular architectures of nanoscale dimension. *Acc. Chem. Res.* **1997**, *30*, 402-413.

(104)   Xu, Z.; Moore, J. S.: Design and synthesis of a convergent and directional molecular antenna. *Acta Polym.* **1994**, *45*, 83-7.

(105)   Moore, J. S.; Xu, Z.: Synthesis of rigid dendritic macromolecules: enlarging the repeat unit size as a function of generation, permitting growth to continue. *Macromolecules* **1991**, *24*, 5893-4.

(106)   Zhang, J.; Pesak, D. J.; Ludwick, J. L.; Moore, J. S.: Geometrically-Controlled and Site-Specifically-Functionalized Phenylacetylene Macrocycles. *Journal of the American Chemical Society* **1994**, *116*, 4227-4239.

(107)   Zhang, J.; Moore, J. S.: Nanoarchitectures. 6. Liquid Crystals Based on Shape-Persistent Macrocyclic Mesogens. *Journal of the American Chemical Society* **1994**, *116*, 2655-2656.

(108)   Zhang, J.; Moore, J. S.; Xu, Z.; Aguirre, R. A.: Nanoarchitectures. 1. Controlled synthesis of phenylacetylene sequences. *Journal of the American Chemical Society* **1992**, *114*, 2273-2274.

(109)   Moore, J. S.; Zhang, J.: Efficient Synthesis of Nanoscale Macrocyclic Hydrocarbons. *Angewandte Chemie International Edition in English* **1992**, *31*, 922-924.

(110)   Manini, P.; Amrein, W.; Gramlich, V.; Diederich, F.: Expanded cubane: Synthesis of a cage compound with a C56 core by acetylenic scaffolding and gas-phase transformations into fullerenes. *Angew. Chem., Int. Ed.* **2002**, *41*, 4339-4343.

(111)   Tobe, Y.; Nakagawa, N.; Naemura, K.; Wakabayashi, T.; Shida, T.; Achiba, Y.: [16.16.16](1,3,5)Cyclophanetetracosayne (C60H6): A Precursor to C60 Fullerene. *J. Am. Chem. Soc.* **1998**, *120*, 4544-4545.

(112)   Rubin, Y.; Parker, T. C.; Pastor, S. J.; Jalisatgi, S.; Boulle, C.; Wilkins, C. L.: Acetylenic cyclophanes as fullerene precursors: formation of C60H6 and C60 by laser desorption mass spectrometry of C60H6(CO)12. *Angew. Chem., Int. Ed.* **1998**, *37*, 1226-1229.

(113)   Wu, Z.; Moore, J. S.: A freely hinged macrotricycle with a molecular cavity. *Angew. Chem., Int. Ed. Engl.* **1996**, *35*, 297-9.

(114)   Wu, Z.; Lee, S.; Moore, J. S.: Synthesis of three-dimensional nanoscaffolding. *J. Am. Chem. Soc.* **1992**, *114*, 8730-2.

(115)   Whitesides, G. M.; Grzybowski, B.: Self-Assembly at All Scales. *Science* **2002**, *295*, 2418-2421.

(116)   Whitesides, G. M.; Boncheva, M.: Beyond molecules: Self-assembly of mesoscopic and macroscopic components. *Proceedings of the National Academy of Sciences* **2002**, *99*, 4769-4774.

(117)   Ibukuro, F.; Kusukawa, T.; Fujita, M.: A Thermally Switchable Molecular Lock. Guest-Templated Synthesis of a Kinetically Stable Nanosized Cage. *J. Am. Chem. Soc.* **1998**, *120*, 8561-8562.

(118)   Northrop, B. H.; Chercka, D.; Stang, P. J.: Carbon-rich supramolecular metallacycles and metallacages. *Tetrahedron* **2008**, *64*, 11495-11503.

(119)   Kumazawa, K.; Biradha, K.; Kusukawa, T.; Okano, T.; Fujita, M.: Multicomponent Assembly of a Pyrazine-Pillared Coordination Cage That Selectively Binds Planar Guests by Intercalation. *Angewandte Chemie International Edition* **2003**, *42*, 3909-3913.

(120)   Koeberl, M.; Cokoja, M.; Herrmann, W. A.; Kuehn, F. E.: From molecules to materials: Molecular paddle-wheel synthons of macromolecules, cage compounds and metal-organic frameworks. *Dalton Trans.* **2011**, *40*, 6834-6859.

(121)   Jung, H.; Moon, D.; Chun, H.: Non-framework coordination polymers with tunable bimodal porosities based on inter-connected metal-organic polyhedra. *Bull. Korean Chem. Soc.* **2011**, *32*, 2489-2492.

(122)   Alkordi, M. H.; Belof, J. L.; Rivera, E.; Wojtas, L.; Eddaoudi, M.: Insight into the construction of metal-organic polyhedra: metal-organic cubes as a case study. *Chem. Sci.* **2011**, *2*, 1695-1705.

(123)   Farha, O. K.; Hupp, J. T.: Rational Design, Synthesis, Purification, and Activation of Metal-Organic Framework Materials. *Acc. Chem. Res.* **2010**, *43*, 1166-1175.

(124)   Perry, J. J. I. V.; Perman, J. A.; Zaworotko, M. J.: Design and synthesis of metal-organic frameworks using metal-organic polyhedra as supermolecular building blocks. *Chem. Soc. Rev.* **2009**, *38*, 1400-1417.

(125)   Tranchemontagne, D. J.; Ni, Z.; O'Keeffe, M.; Yaghi, O. M.: Reticular chemistry of metal-organic polyhedra. *Angew. Chem., Int. Ed.* **2008**, *47*, 5136-5147.

(126)   Furukawa, H.; Kim, J.; Ockwig, N. W.; O'Keeffe, M.; Yaghi, O. M.: Control of Vertex Geometry, Structure Dimensionality, Functionality, and Pore Metrics in the Reticular Synthesis of Crystalline Metal-Organic Frameworks and Polyhedra. *J. Am. Chem. Soc.* **2008**, *130*, 11650-11661.

(127)   Brant, J. A.; Liu, Y.; Sava, D. F.; Beauchamp, D.; Eddaoudi, M.: Single-metal-ion-based molecular building blocks (MBBs) approach to the design and synthesis of metal-organic assemblies. *J. Mol. Struct.* **2006**, *796*, 160-164.

(128)   Rowsell, J. L. C.; Yaghi, O. M.: Metal-organic frameworks: a new class of porous materials. *Microporous Mesoporous Mater.* **2004**, *73*, 3-14.

(129)   Yaghi, O. M.; O'Keeffe, M.; Ockwig, N. W.; Chae, H. K.; Eddaoudi, M.; Kim, J.: Reticular synthesis and the design of new materials. *Nature* **2003**, *423*, 705-714.

(130)   Kim, J.; Chen, B.; Reineke, T. M.; Li, H.; Eddaoudi, M.; Moler, D. B.; O'Keeffe, M.; Yaghi, O. M.: Assembly of Metal-Organic Frameworks from Large Organic and Inorganic Secondary Building Units: New Examples and Simplifying Principles for Complex Structures. *J. Am. Chem. Soc.* **2001**, *123*, 8239-8247.

(131)   Eddaoudi, M.; Moler, D. B.; Li, H.; Chen, B.; Reineke, T. M.; O'Keeffe, M.; Yaghi, O. M.: Modular Chemistry: Secondary Building Units as a Basis for the Design of Highly Porous and Robust Metal−Organic Carboxylate Frameworks. *Accounts of Chemical Research* **2001**, *34*, 319-330.

(132)   Acharyya, K.; Mukherjee, S.; Mukherjee, P. S.: Molecular Marriage through Partner Preferences in Covalent Cage Formation and Cage-to-Cage Transformation. *J. Am. Chem. Soc.* **2013**, *135*, 554-557.

(133)   Schneider, M. W.; Oppel, I. M.; Ott, H.; Lechner, L. G.; Hauswald, H.-J. S.; Stoll, R.; Mastalerz, M.: Periphery-substituted [4+6] salicylbisimine cage compounds with exceptionally high surface areas: influence of the molecular structure on nitrogen sorption properties. *Chemistry* **2012**, *18*, 836-47.

(134)   Mastalerz, M.: Shape-Persistent Organic Cage Compounds by Dynamic Covalent Bond Formation. *Angew. Chem., Int. Ed.* **2010**, *49*, 5042-5053.

(135)   Uribe-Romo, F. J.; Hunt, J. R.; Furukawa, H.; Kloeck, C.; O'Keeffe, M.; Yaghi, O. M.: A Crystalline Imine-Linked 3-D Porous Covalent Organic Framework. *J. Am. Chem. Soc.* **2009**, *131*, 4570-4571.

(136)   Liu, Y.; Liu, X.; Warmuth, R.: Multicomponent dynamic covalent assembly of a rhombicuboctahedral nanocapsule. *Chem.--Eur. J.* **2007**, *13*, 8953-8959.

(137)   Shomura, R.; Higashibayashi, S.; Sakurai, H.; Matsushita, Y.; Sato, A.; Higuchi, M.: Chiral phenylazomethine cage. *Tetrahedron Lett.* **2012**, *53*, 783-785.

(138)   Belowich, M. E.; Stoddart, J. F.: Dynamic imine chemistry. *Chem. Soc. Rev.* **2012**, *41*, 2003-2024.

(139)   Corbett, P. T.; Leclaire, J.; Vial, L.; West, K. R.; Wietor, J.-L.; Sanders, J. K. M.; Otto, S.: Dynamic Combinatorial Chemistry. *Chem. Rev. (Washington, DC, U. S.)* **2006**, *106*, 3652-3711.

(140)   Lehn, J.-M.: Dynamic combinatorial chemistry and virtual combinatorial libraries. *Chem.--Eur. J.* **1999**, *5*, 2455-2463.

(141)   Scott, L. T.; Boorum, M. M.; McMahon, B. J.; Hagen, S.; Mack, J.; Blank, J.; Wegner, H.; de, M. A.: A rational chemical synthesis of C60. *Science (Washington, DC, U. S.)* **2002**, *295*, 1500-1503.

(142)   Zhang, C.; Chen, C.-F.: Synthesis and Structure of A Triptycene-Based Nanosized Molecular Cage. *J. Org. Chem.* **2007**, *72*, 9339-9341.

(143)   Chinchilla, R.; Najera, C.: Recent advances in Sonogashira reactions. *Chem. Soc. Rev.* **2011**, *40*, 5084-5121.

(144)   Nagy, A.; Novak, Z.; Kotschy, A.: Sequential and domino Sonogashira coupling: Efficient tools for the synthesis of diarylalkynes. *J. Organomet. Chem.* **2005**, *690*, 4453-4461.

(145)   Lam, S. C.-F.; Yam, V. W.-W.; Wong, K. M.-C.; Cheng, E. C.-C.; Zhu, N.: Synthesis and Characterization of Luminescent Rhenium(I)–Platinum(II) Polypyridine Bichromophoric Alkynyl-Bridged Molecular Rods. *Organometallics* **2005**, *24*, 4298-4305.

(146)   Chung, W.-K.; Wong, K. M.-C.; Lam, W. H.; Zhu, X.; Zhu, N.; Kwok, H.-S.; Yam, V. W.-W.: Syntheses, photophysical, electroluminescence and computational studies of rhenium(i) diimine triarylamine-containing alkynyl complexes. *New Journal of Chemistry* **2013**, *37*, 1753-1767.

(147)   Bhattacharya, D.; Chang, C.-H.; Cheng, Y.-H.; Lai, L.-L.; Lu, H.-Y.; Lin, C.-Y.; Lu, K.-L.: Multielectron Redox Chemistry of a Neutral, NIR-Active, Indigo-Pillared ReI-Based Triangular Metalloprism. *Chemistry – A European Journal* **2012**, *18*, 5275-5283.

(148)   Dinolfo, P. H.; Coropceanu, V.; Brédas, J.-L.; Hupp, J. T.: A New Class of Mixed-Valence Systems with Orbitally Degenerate Organic Redox Centers. Examples Based on Hexa-Rhenium Molecular Prisms. *Journal of the American Chemical Society* **2006**, *128*, 12592-12593.

(149)   Sun, S.-S.; Lees, A. J.: Self-Assembly Triangular and Square Rhenium(I) Tricarbonyl Complexes: A Comprehensive Study of Their Preparation, Electrochemistry, Photophysics, Photochemistry, and Host-Guest Properties. *J. Am. Chem. Soc.* **2000**, *122*, 8956-8967.

(150)   Grave, C.; Lentz, D.; Schäfer, A.; Samorì, P.; Rabe, J. P.; Franke, P.; Schlüter, A. D.: Shape-Persistant Macrocycles with Terpyridine Units: Synthesis, Characterization, and Structure in the Crystal. *Journal of the American Chemical Society* **2003**, *125*, 6907-6918.

(151)   St. Fleur, N.; Craig, H. J.; Mayr, A.: Synthesis of alkynyl(tricarbonyl)rhenium complexes containing a lightly coordinated diamine ligand. *Inorg. Chim. Acta* **2009**, *362*, 1571-1576.

(152)   Schmittel, M.; Ammon, H.: A short synthetic route to novel, highly soluble 3,8-dialkyl-4,7-dibromo-1,10-phenanthrolines. *Synlett* **1997**, 1096-1098.

(153)   Shinohara, K. i.; Aoki, T.; Kaneko, T.; Oikawa, E.: Syntheses and enantioselective recognition of chiral poly(phenyleneethynylene)s bearing bulky optically active menthyl groups. *Polymer* **2000**, *42*, 351-355.

(154)   Havens, S. J.; Hergenrother, P. M.: Synthesis of arylacetylenes by the sodium hydride catalyzed cleavage of 4-aryl-2-methyl-3-butyn-2-ols. *J. Org. Chem.* **1985**, *50*, 1763-5.

(155)   Nierengarten, J.-F.; Gu, T.; Hadziioannou, G.; Tsamouras, D.; Krasnikov, V.: A new iterative approach for the synthesis of oligo(phenyleneethynediyl) derivatives and its application for the preparation of fullerene-oligo(phenyleneethynediyl) conjugates as active photovoltaic materials. *Helv. Chim. Acta* **2004**, *87*, 2948-2966.

(156)   Rodriguez, J. G.; Tejedor, J. L.; La, P. T.; Diaz, C.: Synthesis of conjugated 2,7-bis(trimethylsilylethynyl)-(phenylethynyl)nfluoren-9-one and 9-(p-methoxyphenyl)-9-methyl derivatives: optical properties. *Tetrahedron* **2006**, *62*, 3355-3361.

(157)   Khatyr, A.; Ziessel, R.: Synthesis of Soluble Bis-terpyridine Ligands Bearing Ethynylene-Phenylene Spacers. *J. Org. Chem.* **2000**, *65*, 3126-3134.

(158)   Francke, V.; Mangel, T.; Muellen, K.: Synthesis of α,ω-Difunctionalized Oligo- and Poly(p-phenyleneethynylene)s. *Macromolecules* **1998**, *31*, 2447-2453.

(159)   Kovalev, A. I.; Takeuchi, K.; Asai, M.; Ueda, M.; Rusanov, A. L.: Selective cross-coupling of 1-ethynyl-4-iodobenzenes with activated arylacetylenes. *Russ. Chem. Bull.* **2004**, *53*, 1749-1754.

(160)   Li, M.-J.; Liu, X.; Nie, M.-J.; Wu, Z.-Z.; Yi, C.-Q.; Chen, G.-N.: New Rhenium(I) Complexes: Synthesis, Photophysics, Cytotoxicity, and Functionalization of Gold Nanoparticles for Sensing of Esterase. *Organometallics* **2012**, *31*, 4459-4466.

(161)   Odago, M. O.; Hoffman, A. E.; Carpenter, R. L.; Tse, D. C. T.; Sun, S.-S.; Lees, A. J.: Thioamide, urea and thiourea bridged rhenium(I) complexes as luminescent anion receptors. *Inorg. Chim. Acta* **2011**, *374*, 558-565.

(162)   Ng, C.-O.; Lai, S.-W.; Feng, H.; Yiu, S.-M.; Ko, C.-C.: Luminescent rhenium(I) complexes with acetylamino- and trifluoroacetylamino-containing phenanthroline ligands: Anion-sensing study. *Dalton Trans.* **2011**, *40*, 10020-10028.

(163)   Liu, Y.; Li, B.; Cong, Y.; Zhang, L.; Fan, D.; Shi, L.: Optical oxygen sensing materials based on a novel dirhenium(I) complex assembled in mesoporous silica. *J. Lumin.* **2011**, *131*, 781-785.

(164)   Louie, M.-W.; Liu, H.-W.; Lam, M. H.-C.; Lau, T.-C.; Lo, K. K.-W.: Novel Luminescent Tricarbonylrhenium(I) Polypyridine Tyramine-Derived Dipicolylamine Complexes as Sensors for Zinc(II) and Cadmium(II) Ions. *Organometallics* **2009**, *28*, 4297-4307.

(165)   Patrocinio, A. O. T.; Murakami, I. N. Y.: Photoswitches and Luminescent Rigidity Sensors Based on fac-[Re(CO)3(Me4phen)(L)]+. *Inorg. Chem. (Washington, DC, U. S.)* **2008**, *47*, 10851-10857.

(166)   Li, M.-J.; Ko, C.-C.; Duan, G.-P.; Zhu, N.; Yam, V. W.-W.: Functionalized rhenium(I) complexes with crown ether pendants derived from 1,10-phenanthroline: selective sensing for metal ions. *Organometallics* **2007**, *26*, 6091-6098.

(167)   Huynh, L.; Wang, Z.; Yang, J.; Stoeva, V.; Lough, A.; Manners, I.; Winnik, M. A.: Evaluation of Phosphorescent Rhenium and Iridium Complexes in Polythionylphosphazene Films for Oxygen Sensor Applications. *Chem. Mater.* **2005**, *17*, 4765-4773.

(168)   Higgins, B.; DeGraff, B. A.; Demas, J. N.: Luminescent Transition Metal Complexes as Sensors: Structural Effects on pH Response. *Inorg. Chem.* **2005**, *44*, 6662-6669.

(169)   Beer, P. D.; Timoshenko, V.; Maestri, M.; Passaniti, P.; Balzani, V.: Anion recognition and luminescent sensing by new ruthenium(II) and rhenium(I) bipyridyl calix[4]diquinone receptors. *Chem. Commun. (Cambridge)* **1999**, 1755-1756.

(170)   Lees, A. J.: Organometallic complexes as luminescence probes in monitoring thermal and photochemical polymerizations. *Coord. Chem. Rev.* **1998**, *177*, 3-35.

(171)   Zipp, A. P.; Sacksteder, L.; Streich, J.; Cook, A.; Demas, J. N.; DeGraff, B. A.: Luminescence of rhenium(I) complexes with highly sterically hindered α-diimine ligands. *Inorg. Chem.* **1993**, *32*, 5629-32.

(172)   Sacksteder, L.; Demas, J. N.; DeGraff, B. A.: Design of oxygen sensors based on quenching of luminescent metal complexes: Effect of ligand size on heterogeneity. *Anal. Chem.* **1993**, *65*, 3480-3.

(173)   MacQueen, D. B.; Schanze, K. S.: Cation-controlled photophysics in a rhenium(I) fluoroionophore. *J. Am. Chem. Soc.* **1991**, *113*, 6108-10.

(174)   Balasingham, R. G.; Thorp-Greenwood, F. L.; Williams, C. F.; Coogan, M. P.; Pope, S. J. A.: Biologically Compatible, Phosphorescent Dimetallic Rhenium Complexes Linked through Functionalized Alkyl Chains: Syntheses, Spectroscopic Properties, and Applications in Imaging Microscopy. *Inorg. Chem. (Washington, DC, U. S.)* **2012**, *51*, 1419-1426.

(175)   Olmon, E. D.; Hill, M. G.; Barton, J. K.: Using Metal Complex Reduced States to Monitor the Oxidation of DNA. *Inorg. Chem. (Washington, DC, U. S.)* **2011**, *50*, 12034-12044.

(176)   Louie, M.-W.; Fong, T. T.-H.; Lo, K. K.-W.: Luminescent Rhenium(I) Polypyridine Fluorous Complexes as Novel Trifunctional Biological Probes. *Inorg. Chem. (Washington, DC, U. S.)* **2011**, *50*, 9465-9471.

(177)   Lo, K. K.-W.; Zhang, K. Y.; Li, S. P.-Y.: Recent Exploitation of Luminescent Rhenium(I) Tricarbonyl Polypyridine Complexes as Biomolecular and Cellular Probes. *Eur. J. Inorg. Chem.* **2011**, *2011*, 3551-3568.

(178)   Brueckmann, N. E.; Koegel, S.; Hamacher, A.; Kassack, M. U.; Kunz, P. C.: Fluorescent Polylactides with Rhenium(bisimine) Cores for Tumour Diagnostics. *Eur. J. Inorg. Chem.* **2010**, 5063-5068.

(179)   Lo, K. K.-W.; Louie, M.-W.; Sze, K.-S.; Lau, J. S.-Y.: Rhenium(I) Polypyridine Biotin Isothiocyanate Complexes as the First Luminescent Biotinylation Reagents: Synthesis, Photophysical Properties, Biological Labeling, Cytotoxicity, and Imaging Studies. *Inorg. Chem. (Washington, DC, U. S.)* **2008**, *47*, 602-611.

(180)   Dubois, K. D.; Petushkov, A.; Garcia, C. E.; Larsen, S. C.; Li, G.: Adsorption and Photochemical Properties of a Molecular CO2 Reduction Catalyst in Hierarchical Mesoporous ZSM-5: An In Situ FTIR Study. *J. Phys. Chem. Lett.* **2012**, *3*, 486-492.

(181)   Yui, T.; Tamaki, Y.; Sekizawa, K.; Ishitani, O.: Photocatalytic reduction of CO2: from molecules to semiconductors. *Top. Curr. Chem.* **2011**, *303*, 151-184.

(182)   Takeda, H.; Ohashi, M.; Tani, T.; Ishitani, O.; Inagaki, S.: Enhanced Photocatalysis of Rhenium(I) Complex by Light-Harvesting Periodic Mesoporous Organosilica. *Inorg. Chem. (Washington, DC, U. S.)* **2010**, *49*, 4554-4559.

(183)   Takeda, H.; Koike, K.; Inoue, H.; Ishitani, O.: Development of an Efficient Photocatalytic System for CO2 Reduction Using Rhenium(I) Complexes Based on Mechanistic Studies. *J. Am. Chem. Soc.* **2008**, *130*, 2023-2031.

(184)   Sato, S.; Koike, K.; Inoue, H.; Ishitani, O.: Highly efficient supramolecular photocatalysts for CO2 reduction using visible light. *Photochem. Photobiol. Sci.* **2007**, *6*, 454-461.

(185)   Hori, H.; Ishihara, J.; Koike, K.; Takeuchi, K.; Ibusuki, T.; Ishitani, O.: Photocatalytic reduction of carbon dioxide using [fac-Re(bpy)(CO)3(4-Xpy)]+ (Xpy = pyridine derivatives). *J. Photochem. Photobiol., A* **1999**, *120*, 119-124.

(186)   Koike, K.; Hori, H.; Ishizuka, M.; Westwell, J. R.; Takeuchi, K.; Ibusuki, T.; Enjouji, K.; Konno, H.; Sakamoto, K.; Ishitani, O.: Key Process of the Photocatalytic Reduction of CO2 Using [Re(4,4'-X2-bipyridine)(CO)3PR3]+ (X = CH3, H, CF3; PR3 = Phosphorus Ligands): Dark Reaction of the One-Electron-Reduced Complexes with CO2. *Organometallics* **1997**, *16*, 5724-5729.

(187)   Hori, H.; Johnson, F. P. A.; Koike, K.; Ishitani, O.; Ibusuki, T.: Efficient photocatalytic CO2 reduction using [Re(bpy)(CO)3{P(OEt)3}]. *J. Photochem. Photobiol., A* **1996**, *96*, 171-174.

(188)   Hawecker, J.; Lehn, J. M.; Ziessel, R.: Efficient photochemical reduction of carbon dioxide to carbon monoxide by visible light irradiation of systems containing bipyridyl(halo)(tricarbonyl)rhenium or tris(bipyridyl)ruthenium dication-cobalt dication combinations as homogeneous catalysts. *J. Chem. Soc., Chem. Commun.* **1983**, 536-8.

(189)   Jiang, W.; Liu, J.; Li, C.: Photochemical hydrogen evolution catalyzed by trimetallic [Re-Fe] complexes. *Inorg. Chem. Commun.* **2012**, *16*, 81-85.

(190)   Probst, B.; Guttentag, M.; Rodenberg, A.; Hamm, P.; Alberto, R.: Photocatalytic H2 Production from Water with Rhenium and Cobalt Complexes. *Inorg. Chem. (Washington, DC, U. S.)* **2011**, *50*, 3404-3412.

(191)   Wang, H.-Y.; Wang, W.-G.; Si, G.; Wang, F.; Tung, C.-H.; Wu, L.-Z.: Photocatalytic Hydrogen Evolution from Rhenium(I) Complexes to [FeFe] Hydrogenase Mimics in Aqueous SDS Micellar Systems: A Biomimetic Pathway. *Langmuir* **2010**, *26*, 9766-9771.

(192)   Probst, B.; Kolano, C.; Hamm, P.; Alberto, R.: An Efficient Homogeneous Intermolecular Rhenium-Based Photocatalytic System for the Production of H2. *Inorg. Chem. (Washington, DC, U. S.)* **2009**, *48*, 1836-1843.

(193)   Fihri, A.; Artero, V.; Pereira, A.; Fontecave, M.: Efficient H2-producing photocatalytic systems based on cyclometalated iridium- and tricarbonylrhenium-diimine photosensitizers and cobaloxime catalysts. *Dalton Trans.* **2008**, 5567-5569.

(194)   Lam, S.-T.; Wang, G.; Yam, V. W.-W.: Luminescent Metallogels of Alkynylrhenium(I) Tricarbonyl Diimine Complexes. *Organometallics* **2008**, *27*, 4545-4548.

(195)   Lam, S.-T.; Yam, V. W.-W.: Synthesis, characterisation and photophysical study of alkynylrhenium(I) tricarbonyl diimine complexes and their metal-ion coordination-assisted metallogelation properties. *Chem.--Eur. J.* **2010**, *16*, 11588-11593, S11588/1-S11588/5.

(196)   Liu, X.; Xia, H.; Gao, W.; Wu, Q.; Fan, X.; Mu, Y.; Ma, C.: New rhenium(I) complexes with substituted diimine ligands for highly efficient phosphorescent devices fabricated by a solution process. *J. Mater. Chem.* **2012**, *22*, 3485-3492.

(197)   Lundin, N. J.; Blackman, A. G.; Gordon, K. C.; Officer, D. L.: Synthesis and characterization of a multicomponent rhenium(I) complex for application as an OLED dopant. *Angew. Chem., Int. Ed.* **2006**, *45*, 2582-2584.

(198)   Wong, K. M.-C.; Lam, S. C.-F.; Ko, C.-C.; Zhu, N.; Yam, V. W.-W.; Roue, S.; Lapinte, C.; Fathallah, S.; Costuas, K.; Kahlal, S.; Halet, J.-F.: Electroswitchable Photoluminescence Activity: Synthesis, Spectroscopy, Electrochemistry, Photophysics, and X-ray Crystal and Electronic Structures of [Re(bpy)(CO)3(C≡C-C6H4-C≡C)Fe(C5Me5)(dppe)][PF6]n (n = 0, 1). *Inorg. Chem.* **2003**, *42*, 7086-7097.

199

(199)   Yam, V. W.-W.; Lau, V. C.-Y.; Cheung, K.-K.: Synthesis and Photophysics of Luminescent Rhenium(I) Acetylides-Precursors for Organometallic Rigid-Rod Materials. X-ray Crystal Structures of [Re(tBu2bpy)(CO)3(tBuC≡C)] and [Re(tBu2bpy)(CO)3Cl]. *Organometallics* **1995**, *14*, 2749-53.

(200)   Frin, K. P. M.; Zanoni, K. P. S.; Murakami, I. N. Y.: Optomechanical trans-to-cis and cis-to-trans isomerization and unusual photophysical behavior of fac-[Re(CO)3(phen)(CNstpy)]+. *Inorg. Chem. Commun.* **2012**, *20*, 105-107.

(201)   Angelos, S.; Yang, Y.-W.; Khashab, N. M.; Stoddart, J. F.; Zink, J. I.: Dual-Controlled Nanoparticles Exhibiting AND Logic. *J. Am. Chem. Soc.* **2009**, *131*, 11344-11346.

(202)   Ashton, P. R.; Balzani, V.; Kocian, O.; Prodi, L.; Spencer, N.; Stoddart, J. F.: A Light-Fueled "Piston Cylinder" Molecular-Level Machine. *J. Am. Chem. Soc.* **1998**, *120*, 11190-11191.

(203)   Cokoja, M.; Bruckmeier, C.; Rieger, B.; Herrmann, W. A.; Kuehn, F. E.: Transformation of Carbon Dioxide with Homogeneous Transition-Metal Catalysts: A Molecular Solution to a Global Challenge? *Angew. Chem., Int. Ed.* **2011**, *50*, 8510-8537.

(204)   Olah, G. A.: Beyond oil and gas: The methanol economy. *Angew. Chem., Int. Ed.* **2005**, *44*, 2636-2639.

(205)   Olah, G. A.; Goeppert, A.; Prakash, G. K. S.: Chemical Recycling of Carbon Dioxide to Methanol and Dimethyl Ether: From Greenhouse Gas to Renewable, Environmentally Carbon Neutral Fuels and Synthetic Hydrocarbons. *J. Org. Chem.* **2009**, *74*, 487-498.

(206)   Olah, G. A.; Prakash, G. K. S.; Goeppert, A.: Anthropogenic chemical carbon cycle for a sustainable future. *J Am Chem Soc* **2011**, *133*, 12881-98.

(207)   Sakakura, T.; Choi, J.-C.; Yasuda, H.: Transformation of Carbon Dioxide. *Chem. Rev. (Washington, DC, U. S.)* **2007**, *107*, 2365-2387.

(208)   Usubharatana, P.; McMartin, D.; Veawab, A.; Tontiwachwuthikul, P.: Photocatalytic Process for CO2 Emission Reduction from Industrial Flue Gas Streams. *Ind. Eng. Chem. Res.* **2006**, *45*, 2558-2568.

(209)   Fujita, E.; Brunschwig, B. S.: Homogeneous redox catalysis in CO2 fixation. Wiley-VCH Verlag GmbH, 2001; Vol. 4; pp 88-126.

(210)   Wrighton, M.; Morse, D. L.: Nature of the lowest excited state in tricarbonylchloro-1,10-phenanthrolinerhenium(I) and related complexes. *J. Amer. Chem. Soc.* **1974**, *96*, 998-1003.

(211)   Zaman, S.; Smith, K. J.: A Review of Molybdenum Catalysts for Synthesis Gas Conversion to Alcohols: Catalysts, Mechanisms and Kinetics. *Catal. Rev.: Sci. Eng.* **2012**, *54*, 41-132.

(212)   Khodakov, A. Y.; Chu, W.; Fongarland, P.: Advances in the Development of Novel Cobalt Fischer-Tropsch Catalysts for Synthesis of Long-Chain Hydrocarbons and Clean Fuels. *Chem. Rev. (Washington, DC, U. S.)* **2007**, *107*, 1692-1744.

(213)   Petrus, L.; Noordermeer, M. A.: Biomass to biofuels, a chemical perspective. *Green Chem.* **2006**, *8*, 861-867.

(214)   Maitlis, P. M.: Fischer-Tropsch, organometallics, and other friends. *J. Organomet. Chem.* **2004**, *689*, 4366-4374.

(215)   Van, d. L. G. P.; Beenackers, A. A. C. M.: Kinetics and selectivity of the Fischer-Tropsch synthesis: a literature review. *Catal. Rev. - Sci. Eng.* **1999**, *41*, 255-318.

(216)   Maitlis, P. M.; Quyoum, R.; Long, H. C.; Turner, M. L.: Towards a chemical understanding of the Fischer-Tropsch reaction: alkene formation. *Appl. Catal., A* **1999**, *186*, 363-374.

(217)   Kumar, A.; Sun, S.-S.; Lees, A. J.: Photophysics and photochemistry of organometallic rhenium diimine complexes. *Top. Organomet. Chem.* **2010**, *29*, 1-35.

(218)   Long, C.: Photophysics of CO loss from simple metal carbonyl complexes. *Top. Organomet. Chem.* **2010**, *29*, 37-71.

(219)   Vlcek, A., Jr.: Ultrafast excited-state processes in Re(I) carbonyl-diimine complexes: from excitation to photochemistry. *Top. Organomet. Chem.* **2010**, *29*, 73-114.

(220)   Stufkens, D. J.: The remarkable properties of α-diimine rhenium tricarbonyl complexes in their metal-to-ligand charge-transfer (MLCT) excited states. *Comments Inorg. Chem.* **1992**, *13*, 359-85.

(221)   El, N. A.; Consani, C.; Blanco-Rodriguez, A. M.; Lancaster, K. M.; Braem, O.; Cannizzo, A.; Towrie, M.; Clark, I. P.; Zalis, S.; Chergui, M.; Vlcek, A.: Ultrafast Excited-State Dynamics of Rhenium(I) Photosensitizers [Re(Cl)(CO)3(N,N)] and [Re(imidazole)(CO)3(N,N)]+: Diimine Effects. *Inorg. Chem. (Washington, DC, U. S.)* **2011**, *50*, 2932-2943.

(222)   Blanco-Rodriguez, A. M.; Busby, M.; Gradinaru, C.; Crane, B. R.; Di, B. A. J.; Matousek, P.; Towrie, M.; Leigh, B. S.; Richards, J. H.; Vlcek, A., Jr.; Gray, H. B.: Excited-state dynamics of structurally characterized [ReI(CO)3(phen)(HisX)]+ (X = 83, 109) Pseudomonas aeruginosa azurins in aqueous solution. *J. Am. Chem. Soc.* **2006**, *128*, 4365-4370.

(223)   Pomestchenko, I. E.; Polyansky, D. E.; Castellano, F. N.: Influence of a Gold(I)-Acetylide Subunit on the Photophysics of Re(Phen)(CO)3Cl. *Inorg. Chem.* **2005**, *44*, 3412-3421.

(224)   Gabrielsson, A.; Matousek, P.; Towrie, M.; Hartl, F.; Zalis, S.; Vlcek, A., Jr.: Excited States of Nitro-Polypyridine Metal Complexes and Their Ultrafast Decay. Time-Resolved IR Absorption, Spectroelectrochemistry, and TD-DFT Calculations of fac-[Re(Cl)(CO)3(5-Nitro-1,10-phenanthroline)]. *J. Phys. Chem. A* **2005**, *109*, 6147-6153.

(225)   Busby, M.; Matousek, P.; Towrie, M.; Clark, I. P.; Motevalli, M.; Hartl, F.; Vlcek, A., Jr.: Rhenium-to-Benzoylpyridine and Rhenium-to-Bipyridine MLCT Excited States of fac-[Re(Cl)(4-benzoylpyridine)2(CO)3] and fac-[Re(4-benzoylpyridine)(CO)3(bpy)]+: A Time-Resolved Spectroscopic and Spectroelectrochemical Study. *Inorg. Chem.* **2004**, *43*, 4523-4530.

(226)   Dattelbaum, D. M.; Omberg, K. M.; Schoonover, J. R.; Martin, R. L.; Meyer, T. J.: Application of Time-Resolved Infrared Spectroscopy to Electronic Structure in Metal-to-Ligand Charge-Transfer Excited States. *Inorg. Chem.* **2002**, *41*, 6071-6079.

(227)   Kurz, P.; Probst, B.; Spingler, B.; Alberto, R.: Ligand variations in [ReX(diimine)(CO)3] complexes: effects on photocatalytic CO2 reduction. *Eur. J. Inorg. Chem.* **2006**, 2966-2974.

(228)   Yamamoto, Y.; Shiotsuka, M.; Onaka, S.: Luminescent rhenium(I)-gold(I) hetero organometallics linked by ethynylphenanthrolines. *J. Organomet. Chem.* **2004**, *689*, 2905-2911.

(229)   Paolucci, F.; Marcaccio, M.; Paradisi, C.; Roffia, S.; Bignozzi, C. A.; Amatore, C.: Dynamics of the Electrochemical Behavior of Diimine Tricarbonyl Rhenium(I) Complexes in Strictly Aprotic Media. *J. Phys. Chem. B* **1998**, *102*, 4759-4769.

(230)   Chen, Y.; Liu, W.; Jin, J.-S.; Liu, B.; Zou, Z.-G.; Zuo, J.-L.; You, X.-Z.: Rhenium(I) tricarbonyl complexes with bispyridine ligands attached to sulfur-rich core: Syntheses, structures and properties. *J. Organomet. Chem.* **2009**, *694*, 763-770.

(231) Tsubaki, H.; Sugawara, A.; Takeda, H.; Gholamkhass, B.; Koike, K.; Ishitani, O.: Photocatalytic reduction of CO2 using cis,trans-[Re(dmbpy)(CO)2(PR3)(PR'3)]+ (dmbpy = 4,4'-dimethyl-2,2'-bipyridine). *Res. Chem. Intermed.* **2007**, *33*, 37-48.

(232) Baba, A. I.; Shaw, J. R.; Simon, J. A.; Thummel, R. P.; Schmehl, R. H.: The photophysical behavior of d6 complexes having nearly isoenergetic MLCT and ligand localized excited states. *Coord. Chem. Rev.* **1998**, *171*, 43-59.

(233) Shaw, J. R.; Schmehl, R. H.: Photophysical properties of rhenium(I) diimine complexes: observation of room-temperature intraligand phosphorescence. *J. Am. Chem. Soc.* **1991**, *113*, 389-94.

(234) Fredericks, S. M.; Luong, J. C.; Wrighton, M. S.: Multiple emissions from rhenium(I) complexes: intraligand and charge-transfer emission from substituted metal carbonyl cations. *J. Am. Chem. Soc.* **1979**, *101*, 7415-17.

(235) Barigelletti, F.; Ventura, B.; Collin, J.-P.; Kayhanian, R.; Gaviña, P.; Sauvage, J.-P.: Electrochemical and Spectroscopic Properties of Cyclometallated and Non-Cyclometallated Ruthenium(II) Complexes Containing Sterically Hindering Ligands of the Phenanthroline and Terpyridine Families. *European Journal of Inorganic Chemistry* **2000**, *2000*, 113-119.

(236) Si, Z.; Li, X.; Li, X.; Zhang, H.: Synthesis, photophysical properties, and theoretical studies on pyrrole-containing bromo Re(I) complex. *J. Organomet. Chem.* **2009**, *694*, 3742-3748.

(237) Thomas, K. R. J.; Lin, J. T.; Lin, H.-M.; Chang, C.-P.; Chuen, C.-H.: Ruthenium and Rhenium Complexes of Fluorene-Based Bipyridine Ligands: Synthesis, Spectra, and Electrochemistry. *Organometallics* **2001**, *20*, 557-563.

(238) Damrauer, N. H.; Boussie, T. R.; Devenney, M.; McCusker, J. K.: Effects of Intraligand Electron Delocalization, Steric Tuning, and Excited-State Vibronic Coupling on the Photophysics of Aryl-Substituted Bipyridyl Complexes of Ru(II). *J. Am. Chem. Soc.* **1997**, *119*, 8253-8268.

(239) Treadway, J. A.; Loeb, B.; Lopez, R.; Anderson, P. A.; Keene, F. R.; Meyer, T. J.: Effect of Delocalization and Rigidity in the Acceptor Ligand on MLCT Excited-State Decay. *Inorg. Chem.* **1996**, *35*, 2242-6.

(240) Strouse, G. F.; Schoonover, J. R.; Duesing, R.; Boyde, S.; Jones, W. E., Jr.; Meyer, T. J.: Influence Of Electronic Delocalization In Metal-to-Ligand Charge Transfer Excited States. *Inorg. Chem.* **1995**, *34*, 473-87.

(241) Wallace, L.; Rillema, D. P.: Photophysical properties of rhenium(I) tricarbonyl complexes containing alkyl- and aryl-substituted phenanthrolines as ligands. *Inorg. Chem.* **1993**, *32*, 3836-43.

(242) Worl, L. A.; Duesing, R.; Chen, P.; Della, C. L.; Meyer, T. J.: Photophysical properties of polypyridyl carbonyl complexes of rhenium(I). *J. Chem. Soc., Dalton Trans.* **1991**, 849-58.

(243) Englman, R.; Jortner, J.: Energy gap law for radiationless transitions in large molecules. *Mol. Phys.* **1970**, *18*, 145-64.

(244) Alstrum-Acevedo, J. H.; Brennaman, M. K.; Meyer, T. J.: Chemical Approaches to Artificial Photosynthesis. 2. *Inorg. Chem.* **2005**, *44*, 6802-6827.

(245) Agarwal, J.; Sanders, B. C.; Fujita, E.; Schaefer, I. I. I. H. F.; Harrop, T. C.; Muckerman, J. T.: Exploring the intermediates of photochemical CO2 reduction: reaction of Re(dmb)(CO)3 COOH with CO2. *Chem. Commun. (Cambridge, U. K.)* **2012**, *48*, 6797-6799.

(246)   Agarwal, J.; Fujita, E.; Schaefer, H. F.; Muckerman, J. T.: Mechanisms for CO Production from CO2 Using Reduced Rhenium Tricarbonyl Catalysts. *J. Am. Chem. Soc.* **2012**, *134*, 5180-5186.

(247)   Fujita, E.; Muckerman, J. T.: Why Is Re-Re Bond Formation/Cleavage in [Re(bpy)(CO)3]2 Different from That in [Re(CO)5]2? Experimental and Theoretical Studies on the Dimers and Fragments. *Inorg. Chem.* **2004**, *43*, 7636-7647.

(248)   Hayashi, Y.; Kita, S.; Brunschwig, B. S.; Fujita, E.: Involvement of a Binuclear Species with the Re-C(O)O-Re Moiety in CO2 Reduction Catalyzed by Tricarbonyl Rhenium(I) Complexes with Diimine Ligands: Strikingly Slow Formation of the Re-Re and Re-C(O)O-Re Species from Re(dmb)(CO)3S (dmb = 4,4'-Dimethyl-2,2'-bipyridine, S = Solvent). *J. Am. Chem. Soc.* **2003**, *125*, 11976-11987.

(249)   Sullivan, B. P.; Bolinger, C. M.; Conrad, D.; Vining, W. J.; Meyer, T. J.: One- and two-electron pathways in the electrocatalytic reduction of carbon dioxide by fac-(2,2'-bipyridine)tricarbonylchlororhenium. *J. Chem. Soc., Chem. Commun.* **1985**, 1414-16.

(250)   Glazer, E. C.; Magde, D.; Tor, Y.: Ruthenium Complexes That Break the Rules: Structural Features Controlling Dual Emission. *J. Am. Chem. Soc.* **2007**, *129*, 8544-8551.

(251)   Miller, M. T.; Karpishin, T. B.: Phenylethynyl Substituent Effects on the Photophysics and Electrochemistry of [Cu(dpp)2]+ (dpp = 2,9-Diphenyl-1,10-phenanthroline). *Inorg. Chem.* **1999**, *38*, 5246-5249.

(252)   Morse, D. L.; Wrighton, M. S.: Reaction of pentacarbonylmanganese(-I) and rhenium(-I) with metal carbonyl halide derivatives. *J. Organomet. Chem.* **1977**, *125*, 71-7.

(253)   Wagner, J. R.; Hendricker, D. G.: Coordination of manganese(I) and rhenium(I) carbonyls with nitrogen heterocyclic ligands. *J. Inorg. Nucl. Chem.* **1975**, *37*, 1375-9.

(254)   Schmittel, M.; Ammon, H.: A short synthetic route to 4,7-dihalogenated 1,10-phenanthrolines with additional groups in 3,8-position. Soluble precursors for macrocyclic oligophenanthrolines. *Eur. J. Org. Chem.* **1998**, 785-792.

(255)   Schutte, M.; Kemp, G.; Visser, H. G.; Roodt, A.: Tuning the Reactivity in Classic Low-Spin d6 Rhenium(I) Tricarbonyl Radiopharmaceutical Synthon by Selective Bidentate Ligand Variation (L,L'-Bid; L,L'= N,N', N,O, and O,O' Donor Atom Sets) in fac-[Re(CO)3(L,L'-Bid)(MeOH)]n Complexes. *Inorg. Chem. (Washington, DC, U. S.)* **2011**, *50*, 12486-12498.

(256)   Haefelinger, G.; Knapp, W.; Zuschneid, T.; Dietrich, F. P.: Vinyl or isopropenyl substituents as experimental and theoretical probes for diamagnetic anisotropies of aromatic hydrocarbons. *J. Phys. Org. Chem.* **2005**, *18*, 800-817.

(257)   Viglione, R. G.; Zanasi, R.; Lazzeretti, P.: Are Ring Currents Still Useful to Rationalize the Benzene Proton Magnetic Shielding? *Org. Lett.* **2004**, *6*, 2265-2267.

(258)   Klein, A.; Kaim, W.; Waldhor, E.; Hausen, H.-D.: Different orbital occupation by an added single electron in 1,10-phenanthroline and its 3,4,7,8-tetramethyl derivative. Evidence from electron paramagnetic resonance spectroscopy of the anion radicals and of their dimesitylplatinum(II) complexes. X-Ray molecular structure of dimesityl(1,10-phenanthroline)platinum(II). *Journal of the Chemical Society, Perkin Transactions 2* **1995**, 2121-2126.

(259)   Cotton, F. A.; Daniels, L. M.; Lei, P.; Murillo, C. A.; Wang, X.: Di- and trinuclear complexes with the mono- and dianion of 2,6-bis(phenylamino)pyridine: high-field displacement of chemical shifts due to the magnetic anisotropy of quadruple bonds. *Inorg Chem* **2001**, *40*, 2778-84.

(260)   Tan, Z. F.; Liu, C. Y.; Li, Z.; Meng, M.; Weng, N. S.: Abnormally Long-Range Diamagnetic Anisotropy Induced by Cyclic dδ-pπ π Conjugation within a Six-Membered Dimolybdenum/Chalcogen Ring. *Inorg. Chem. (Washington, DC, U. S.)* **2012**, *51*, 2212-2221.

(261)   Cook, M. J.; Lewis, A. P.; McAuliffe, G. S. G.: Luminescent metal complexes. 4 - carbon-13 NMR spectra of the tris chelates of substituted 2,2'-bipyridyls and 1,10-phenanthrolines with ruthenium(II) and osmium(II). *Org. Magn. Reson.* **1984**, *22*, 388-94.

(262)   Smith, T. J., Stevenson, Keith J.: Reference Electrodes. In *Handbook of Electrochemistry*; 1st ed.; Zoski, C. G., Ed.; Elsevier: Kidlington, Oxford OX5 IGB, UK, 2007; pp 73 - 102.

(263)   Swager, T. M.; Gil, C. J.; Wrighton, M. S.: Fluorescence Studies of Poly(p-phenyleneethynylene)s: The Effect of Anthracene Substitution. *J. Phys. Chem.* **1995**, *99*, 4886-93.

(264)   Ziener, U.; Godt, A.: Synthesis and Characterization of Monodisperse Oligo(phenyleneethynylene)s. *J. Org. Chem.* **1997**, *62*, 6137-6143.

(265)   James, P. V.; Yoosaf, K.; Kumar, J.; Thomas, K. G.; Listorti, A.; Accorsi, G.; Armaroli, N.: Tunable photophysical properties of phenyleneethynylene based bipyridine ligands. *Photochem. Photobiol. Sci.* **2009**, *8*, 1432-1440.

(266)   Sudeep, P. K.; James, P. V.; Thomas, K. G.; Kamat, P. V.: Singlet and Triplet Excited-State Interactions and Photochemical Reactivity of Phenyleneethynylene Oligomers. *J. Phys. Chem. A* **2006**, *110*, 5642-5649.

(267)   Matsunaga, Y.; Takechi, K.; Akasaka, T.; Ramesh, A. R.; James, P. V.; Thomas, K. G.; Kamat, P. V.: Excited-State and Photoelectrochemical Behavior of Pyrene-Linked Phenyleneethynylene Oligomer. *J. Phys. Chem. B* **2008**, *112*, 14539-14547.

(268)   Kalyanasundaram, K.: Luminescence and redox reactions of the metal-to-ligand charge-transfer excited state of tricarbonylchloro(polypyridyl)rhenium(I) complexes. *J. Chem. Soc., Faraday Trans. 2* **1986**, *82*, 2401-15.

(269)   Polyansky, D. E.; Danilov, E. O.; Voskresensky, S. V.; Rodgers, M. A. J.; Neckers, D. C.: Delocalization of Free Electron Density through Phenylene-Ethynylene: Structural Changes Studied by Time-Resolved Infrared Spectroscopy. *J. Am. Chem. Soc.* **2005**, *127*, 13452-13453.

(270)   Portenkirchner, E.; Oppelt, K.; Ulbricht, C.; Egbe, D. A. M.; Neugebauer, H.; Knör, G.; Sariciftci, N. S.: Electrocatalytic and photocatalytic reduction of carbon dioxide to carbon monoxide using the alkynyl-substituted rhenium(I) complex (5,5′-bisphenylethynyl-2,2′-bipyridyl)Re(CO)3Cl. *Journal of Organometallic Chemistry* **2012**, *716*, 19-25.

(271)   Hawecker, J.; Lehn, J. M.; Ziessel, R.: Photochemical and electrochemical reduction of carbon dioxide to carbon monoxide mediated by (2,2'-bipyridine)tricarbonylchlororhenium(I) and related complexes as homogeneous catalysts. *Helv. Chim. Acta* **1986**, *69*, 1990-2012.

(272)   Hawecker, J.; Lehn, J.-M.; Ziessel, R.: Electrocatalytic reduction of carbon dioxide mediated by Re(bipy)(CO)3Cl (bipy = 2,2[prime or minute]-bipyridine). *Journal of the Chemical Society, Chemical Communications* **1984**, 328-330.

(273)   Gottlieb, H. E.; Kotlyar, V.; Nudelman, A.: NMR Chemical Shifts of Common Laboratory Solvents as Trace Impurities. *The Journal of Organic Chemistry* **1997**, *62*, 7512-7515.

(274)   Crosby, G. A.; Elfring, W. H.: Excited states of mixed ligand chelates of ruthenium(II) and rhodium(III). *The Journal of Physical Chemistry* **1976**, *80*, 2206-2211.

(275)   Hili, J. C.: Bis-isocyanide rhenium acetylide complexes for the stepwise assembly of molecular cages. 2006.

(276)   Lam, S. C.-F.; Yam, V. W.-W.; Wong, K. M.-C.; Cheng, E. C.-C.; Zhu, N.: Synthesis and Characterization of Luminescent Rhenium(I)-Platinum(II) Polypyridine Bichromophoric Alkynyl-Bridged Molecular Rods. *Organometallics* **2005**, *24*, 4298-4305.

(277)   Dembinski, R.; Bartik, T.; Bartik, B.; Jaeger, M.; Gladysz, J. A.: Toward Metal-Capped One-Dimensional Carbon Allotropes: Wirelike C6-C20 Polyynediyl Chains That Span Two Redox-Active (η5-C5Me5)Re(NO)(PPh3) Endgroups. *J. Am. Chem. Soc.* **2000**, *122*, 810-822.

(278)   Chong, S. H.-F.; Lam, S. C.-F.; Yam, V. W.-W.; Zhu, N.; Cheung, K.-K.; Fathallah, S.; Costuas, K.; Halet, J.-F.: Luminescent Heterometallic Branched Alkynyl Complexes of Rhenium(I)-Palladium(II): Potential Building Blocks for Heterometallic Metallodendrimers. *Organometallics* **2004**, *23*, 4924-4933.

(279)   Yam, V. W.-W.; Wong, K. M.-C.; Chong, S. H.-F.; Lau, V. C.-Y.; Lam, S. C.-F.; Zhang, L.; Cheung, K.-K.: Synthesis, electrochemistry and structural characterization of luminescent rhenium(I) monoynyl complexes and their homo- and hetero-metallic binuclear complexes. *J. Organomet. Chem.* **2003**, *670*, 205-220.

(280)   Wong, K. M.-C.; Lam, S. C.-F.; Ko, C.-C.; Zhu, N.; Yam, V. W.-W.; Roue, S.; Lapinte, C.; Fathallah, S.; Costuas, K.; Kahlal, S.; Halet, J.-F.: Electroswitchable Photoluminescence Activity: Synthesis, Spectroscopy, Electrochemistry, Photophysics, and X-ray Crystal and Electronic Structures of [Re(bpy)(CO)3(C≡C-C6H4-C≡C)Fe(C5Me5)(dppe)][PF6]n (n = 0, 1). *Inorg. Chem.* **2003**, *42*, 7086-7097.

(281)   Yam, V. W.-W.: Luminescent carbon-rich rhenium(i) complexes. *Chem. Commun. (Cambridge, U. K.)* **2001**, 789-796.

(282)   Yam, V. W.-W.; Kam-Wing, L. K.; Man-Chung, W. K.: Luminescent polynuclear metal acetylides. *J. Organomet. Chem.* **1999**, *578*, 3-30.

(283)   Yam, V. W.-W.; Chong, S. H.-F.; Cheung, K.-K.: Synthesis and luminescence behavior of rhenium(I) diynyl complexes. X-Ray crystal structures of [Re(CO)3(tBu2bpy)(C≡C-C≡CH)] and [Re(CO)3(tBu2bpy)(C≡C-C≡CPh)]. *Chem. Commun. (Cambridge)* **1998**, 2121-2122.

(284)   Yam, V. W.-W.; Lau, V. C.-Y.; Cheung, K.-K.: Luminescent Rhenium(I) Carbon Wires: Synthesis, Photophysics, and Electrochemistry. X-ray Crystal Structure of [Re(tBu2bpy)(CO)3(C≡CC≡C)Re(tBu2bpy)(CO)3]. *Organometallics* **1996**, *15*, 1740-4.

(285)   Yam, V. W.-W.; Lau, V. C.-Y.; Cheung, K.-K.: Synthesis and Photophysics of Luminescent Rhenium(I) Acetylides-Precursors for Organometallic Rigid-Rod Materials. X-ray Crystal Structures of [Re(tBu2bpy)(CO)3(tBuC≡C)] and [Re(tBu2bpy)(CO)3Cl]. *Organometallics* **1995**, *14*, 2749-53.

(286)   Bruce, M. I.; Harbourne, D. A.; Waugh, F.; Stone, F. G. A.: Some transition-metal acetylides. *Journal of the Chemical Society A: Inorganic, Physical, Theoretical* **1968**, *0*, 356-359.

(287)   Salah, O. M. A.; Bruce, M. I.: New Group IB metal chemistry. Part 6. Reactions of copper(I) acetylides with chloro([small eta]-cyclopentadienyl)bis(triphenylphosphine)ruthenium and cis-tricarbonylchlorobis(triphenylphosphine)rhenium. *Journal of the Chemical Society, Dalton Transactions* **1975**, *0*, 2311-2315.

(288)   Yam, V. W.-W.; Lau, V. C.-Y.; Cheung, K.-K.: Synthesis and Photophysics of Luminescent Rhenium(I) Acetylides-Precursors for Organometallic Rigid-Rod Materials. X-ray Crystal Structures of [Re(tBu2bpy)(CO)3(tBuC.tplbond.C)] and [Re(tBu2bpy)(CO)3Cl]. *Organometallics* **1995**, *14*, 2749-2753.

(289)   Wong, A.; Gladysz, J. A.: Syntheses and reactions of rhenium vinylidene and acetylide complexes. Unprecedented chirality transfer through a C.tplbond.C triple bond. *Journal of the American Chemical Society* **1982**, *104*, 4948-4950.

(290)   Ramsden, J. A.; Weng, W.; Gladysz, J. A.: Deprotonation of rhenium terminal acetylide complexes (.eta.5-C5R5)Re(NO)(PPh3)(C.tplbond.CH): generation and reactivity of rhenium/lithium C2 complexes. *Organometallics* **1992**, *11*, 3635-3645.

(291)   Appel, M.; Heidrich, J.; Beck, W.: Metallorganische Lewis-Säuren, XXXII1) σ,π-Ethinid- und σ,σ-Ethindid-verbrückte Rheniumcarbonyle, [(OC)5Re(μ-η1,η2-C□CH)Re(CO)5]+ BF–4 und (OC)5Re–C□C–Re(CO)5. *Chemische Berichte* **1987**, *120*, 1087-1089.

(292)   Chong, S. H.-F.; Lam, S. C.-F.; Yam, V. W.-W.; Zhu, N.; Cheung, K.-K.; Fathallah, S.; Costuas, K.; Halet, J.-F.: Luminescent Heterometallic Branched Alkynyl Complexes of Rhenium(I)−Palladium(II): Potential Building Blocks for Heterometallic Metallodendrimers. *Organometallics* **2004**, *23*, 4924-4933.

(293)   Yam, V. W.-W.: Luminescent carbon-rich rhenium() complexes. *Chemical Communications* **2001**, *0*, 789-796.

(294)   Liddle, B. J.; Lindeman, S. V.; Reger, D. L.; Gardinier, J. R.: A Thallium Mediated Route to σ-Arylalkynyl Complexes of Bipyridyltricarbonylrhenium(I). *Inorganic Chemistry* **2007**, *46*, 8484-8486.

(295)   Pearson, R. G.: Hard and soft acids and bases, HSAB, part 1: Fundamental principles. *Journal of Chemical Education* **1968**, *45*, 581.

(296)   Pearson, R. G.: Hard and soft acids and bases, HSAB, part II: Underlying theories. *Journal of Chemical Education* **1968**, *45*, 643.

(297)   Proietti, S. I.; Andemarian, F.; Khairallah, G. N.; Wan, Y. S.; Quach, T.; Tsegay, S.; Williams, C. M.; O'Hair, R. A. J.; Donnelly, P. S.; Williams, S. J.: Copper(I)-catalyzed cycloaddition of silver acetylides and azides: Incorporation of volatile acetylenes into the triazole core. *Org. Biomol. Chem.* **2011**, *9*, 6082-6088.

(298)   Yamamoto, Y.: Silver-Catalyzed Csp-H and Csp-Si Bond Transformations and Related Processes. *Chem. Rev. (Washington, DC, U. S.)* **2008**, *108*, 3199-3222.

(299)   Weibel, J.-M.; Blanc, A.; Pale, P.: Ag-Mediated Reactions: Coupling and Heterocyclization Reactions. *Chem. Rev. (Washington, DC, U. S.)* **2008**, *108*, 3149-3173.

(300)   Halbes-Letinois, U.; Weibel, J.-M.; Pale, P.: The organic chemistry of silver acetylides. *Chem. Soc. Rev.* **2007**, *36*, 759-769.

(301)   Pouwer, R. H.; Williams, C. M.; Raine, A. L.; Harper, J. B.: "One-step" alkynylation of adamantyl iodide with silver(I) acetylides. *Org. Lett.* **2005**, *7*, 1323-1325.

(302)   Carpita, A.; Mannocci, L.; Rossi, R.: Silver(I)-catalyzed protiodesilylation of 1-(trimethylsilyl)-1-alkynes. *Eur. J. Org. Chem.* **2005**, 1859-1864.

(303)   Shahi, S. P.; Koide, K.: Alkynylation: A mild method for the preparation of γ-hydroxy-α,β-acetylenic esters. *Angew. Chem., Int. Ed.* **2004**, *43*, 2525-2527.

(304)   Dillinger, S.; Bertus, P.; Pale, P.: First Evidence for the Use of Organosilver Compounds in Pd-Catalyzed Coupling Reactions; A Mechanistic Rationale for the Pd/Ag-Catalyzed Enyne Synthesis? *Org. Lett.* **2001**, *3*, 1661-1664.

(305)   Agawa, T.; Miller, S. I.: Reaction of silver acetylide with acylpyridinium salts: N-benzoyl-2-phenylethynyl-1,2-dihydropyridine. *J. Am. Chem. Soc.* **1961**, *83*, 449-53.

(306)   Davis, R. B.; Scheiber, D. H.: The preparation of acetylenic ketones using soluble silver acetylides. *J. Am. Chem. Soc.* **1956**, *78*, 1675-8.

(307)   Zhao, L.; Mak, T. C. W.: Silver(I) 1,3-Butadiynediide and Two Related Silver(I) Double Salts Containing the C42- Dianion. *J. Am. Chem. Soc.* **2004**, *126*, 6852-6853.

(308)   Brasse, C.; Raithby, P. R.; Rennie, M.-A.; Russell, C. A.; Steiner, A.; Wright, D. S.: Structural Variation in Silver Acetylide Complexes: Syntheses and x-ray Structure Determinations of [Ph3PAgC≡CPh]4·3.5THF and [Me3PAgC≡CSiMe3]∞. *Organometallics* **1996**, *15*, 639-44.

(309)   Mitsudo, K.; Shiraga, T.; Mizukawa, J.-i.; Suga, S.; Tanaka, H.: Electrochemical generation of silver acetylides from terminal alkynes with a Ag anode and integration into sequential Pd-catalyzed coupling with arylboronic acids. *Chem. Commun. (Cambridge, U. K.)* **2010**, *46*, 9256-9258.

(310)   Viterisi, A.; Orsini, A.; Weibel, J.-M.; Pale, P.: A mild access to silver acetylides from trimethylsilyl acetylenes. *Tetrahedron Lett.* **2006**, *47*, 2779-2781.

(311)   Letinois-Halbes, U.; Pale, P.; Berger, S.: Ag NMR as a Tool for Mechanistic Studies of Ag-Catalyzed Reactions: Evidence for in Situ Formation of Alkyn-1-yl Silver from Alkynes and Silver Salts. *J. Org. Chem.* **2005**, *70*, 9185-9190.

(312)   Teo, B. K.; Xu, Y. H.; Zhong, B. Y.; He, Y. K.; Chen, H. Y.; Qian, W.; Deng, Y. J.; Zou, Y. H.: A Comparative Study of Third-Order Nonlinear Optical Properties of Silver Phenylacetylide and Related Compounds via Ultrafast Optical Kerr Effect Measurements. *Inorganic Chemistry* **2001**, *40*, 6794-6801.

(313)   Davis, R. B.; Scheiber, D. H.: The Preparation of Acetylenic Ketones Using Soluble Silver Acetylides. *Journal of the American Chemical Society* **1956**, *78*, 1675-1678.

(314)   Xu, X.-N.; Wang, L.; Wang, G.-T.; Lin, J.-B.; Li, G.-Y.; Jiang, X.-K.; Li, Z.-T.: Hydrogen-Bonding-Mediated Dynamic Covalent Synthesis of Macrocycles and Capsules: New Receptors for Aliphatic Ammonium Ions and the Formation of Pseudo[3]rotaxanes. *Chem.--Eur. J.* **2009**, *15*, 5763-5774, S5763/1-S5763/10.

(315)   Schmittel, M.; Kalsani, V.; Michel, C.; Mal, P.; Ammon, H.; Jäckel, F.; Rabe, J. P.: Towards Nanotubular Structures with Large Voids: Dynamic Heteroleptic Oligophenanthroline Metallonanoscaffolds and their Solution-State Properties. *Chemistry – A European Journal* **2007**, *13*, 6223-6237.

(316)   Cheng, X.; Heyen, A. V.; Mamdouh, W.; Uji-i, H.; De, S. F.; Hoeger, S.; De, F. S.: Synthesis and Adsorption of Shape-Persistent Macrocycles Containing Polycyclic Aromatic Hydrocarbons in the Rigid Framework. *Langmuir* **2007**, *23*, 1281-1286.

(317)   Couet, J.; Biesalski, M.: Conjugating self-assembling rigid rings to flexible polymer coils for the design of organic nanotubes. *Soft Matter* **2006**, *2*, 1005-1014.

(318)   Kalsani, V.; Ammon, H.; Jaeckel, F.; Rabe, J. P.; Schmittel, M.: Synthesis and self-assembly of a rigid exotopic bisphenanthroline macrocycle: Surface patterning and a supramolecular nanobasket. *Chem.--Eur. J.* **2004**, *10*, 5481-5492.

(319)   Hoeger, S.: Shape-persistent macrocycles: from molecules to materials. *Chem.--Eur. J.* **2004**, *10*, 1320-1329.

(320)   Matsui, K.; Segawa, Y.; Itami, K.: Synthesis and Properties of Cycloparaphenylene-2,5-pyridylidene: A Nitrogen-Containing Carbon Nanoring. *Org. Lett.* **2012**, *14*, 1888-1891.

(321)   Leu, W. C. W.; Fritz, A. E.; Digianantonio, K. M.; Hartley, C. S.: Push-Pull Macrocycles: Donor-Acceptor Compounds with Paired Linearly Conjugated or Cross-Conjugated Pathways. *J. Org. Chem.* **2012**, *77*, 2285-2298.

(322)   Abe, H.; Chida, Y.; Kurokawa, H.; Inouye, M.: Selective Binding of D2h-Symmetrical, Acetylene-Linked Pyridine/Pyridone Macrocycles to Maltoside. *J. Org. Chem.* **2011**, *76*, 3366-3371.

(323)   Qin, B.; Ren, C.; Ye, R.; Sun, C.; Chiad, K.; Chen, X.; Li, Z.; Xue, F.; Su, H.; Chass, G. A.; Zeng, H.: Persistently Folded Circular Aromatic Amide Pentamers Containing Modularly Tunable Cation-Binding Cavities with High Ion Selectivity. *J. Am. Chem. Soc.* **2010**, *132*, 9564-9566.

(324)   Jiang, J.; MacLachlan, M. J.: Unsymmetrical Triangular Schiff Base Macrocycles with Cone Conformations. *Org. Lett.* **2010**, *12*, 1020-1023.

(325)   Sanford, A. R.; Yuan, L.; Feng, W.; Yamato, K.; Flowers, R. A.; Gong, B.: Cyclic aromatic oligoamides as highly selective receptors for the guanidinium ion. *Chemical Communications* **2005**, 4720-4722.

(326)   Kawase, T.; Tanaka, K.; Seirai, Y.; Shiono, N.; Oda, M.: Complexation of Carbon Nanorings with Fullerenes: Supramolecular Dynamics and Structural Tuning for a Fullerene Sensor. *Angewandte Chemie International Edition* **2003**, *42*, 5597-5600.

(327)   Baxter, P. N. W.: Synthesis and fluorescence ion-sensory properties of the first dehydropyridoannulene-type cyclophane with enforced exotopic metal ion binding sites. *Chem.--Eur. J.* **2003**, *9*, 2531-2541.

(328)   Chen, P.; Jäkle, F.: Highly Luminescent, Electron-Deficient Bora-cyclophanes. *Journal of the American Chemical Society* **2011**, *133*, 20142-20145.

(329)   Zhu, Y.-Y.; Li, C.; Li, G.-Y.; Jiang, X.-K.; Li, Z.-T.: Hydrogen-Bonded Aryl Amide Macrocycles: Synthesis, Single-Crystal Structures, and Stacking Interactions with Fullerenes and Coronene. *J. Org. Chem.* **2008**, *73*, 1745-1751.

(330)   Nakamura, Y.; Aratani, N.; Osuka, A.: Cyclic porphyrin arrays as artificial photosynthetic antenna: synthesis and excitation energy transfer. *Chemical Society Reviews* **2007**, *36*, 831-845.

(331)   Zhao, T.; Liu, Z.; Song, Y.; Xu, W.; Zhang, D.; Zhu, D.: Novel Diethynylcarbazole Macrocycles: Synthesis and Optoelectronic Properties. *J. Org. Chem.* **2006**, *71*, 7422-7432.

(332)   Sun, S.-S.; Lees, A. J.: Synthesis and Photophysical Properties of Dinuclear Organometallic Rhenium(I) Diimine Complexes Linked by Pyridine-Containing Macrocyclic Phenylacetylene Ligands. *Organometallics* **2001**, *20*, 2353-2358.

(333)   Nakao, K.; Nishimura, M.; Tamachi, T.; Kuwatani, Y.; Miyasaka, H.; Nishinaga, T.; Iyoda, M.: Giant Macrocycles Composed of Thiophene, Acetylene, and Ethylene Building Blocks. *J. Am. Chem. Soc.* **2006**, *128*, 16740-16747.

(334)   Gross, D. E.; Zang, L.; Moore, J. S.: Arylene-ethynylene macrocycles: privileged shape-persistent building blocks for organic materials. *Pure Appl. Chem.* **2012**, *84*, 869-878.

(335)   Iyoda, M.; Yamakawa, J.; Rahman, M. J.: Conjugated Macrocycles: Concepts and Applications. *Angew. Chem., Int. Ed.* **2011**, *50*, 10522-10553.

(336)   Hoeger, S.: Shape-persistent rings and wheels. *Pure Appl. Chem.* **2010**, *82*, 821-830.

(337)   Diederich, F.; Kivala, M.: All-Carbon Scaffolds by Rational Design. *Adv. Mater. (Weinheim, Ger.)* **2010**, *22*, 803-812.

(338)   Tykwinski, R. R.; Gholami, M.; Eisler, S.; Zhao, Y.; Melin, F.; Echegoyen, L.: Expanded radialenes: modular synthesis and properties of cross-conjugated enyne macrocycles. *Pure Appl. Chem.* **2008**, *80*, 621-637.

(339)   Zhang, W.; Moore, J. S.: Shape-persistent macrocycles: structures and synthetic approaches from arylene and ethynylene building blocks. *Angew. Chem., Int. Ed.* **2006**, *45*, 4416-4439.

(340)   Hoeger, S.: Shape-persistent phenylene-acetylene macrocycles: Large rings-low yield? *Angew. Chem., Int. Ed.* **2005**, *44*, 3806-3808.

(341)   Zhao, D.; Moore, J. S.: Shape-persistent arylene ethynylene macrocycles: syntheses and supramolecular chemistry. *Chem. Commun. (Cambridge, U. K.)* **2003**, 807-818.

(342)   Grave, C.; Schluter, A. D.: Shape-persistent, nano-sized macrocycles. *Eur. J. Org. Chem.* **2002**, 3075-3098.

(343)   Hoger, S.: Highly efficient methods for the preparation of shape-persistent macrocyclics. *J. Polym. Sci., Part A: Polym. Chem.* **1999**, *37*, 2685-2698.

(344)   Sisco, S. W.; Moore, J. S.: Directional Cyclooligomers via Alkyne Metathesis. *Journal of the American Chemical Society* **2012**, *134*, 9114-9117.

(345)   Zhang, W.; Moore, J. S.: Alkyne metathesis: catalysts and synthetic applications. *Adv. Synth. Catal.* **2007**, *349*, 93-120.

(346)   Zhang, W.; Moore, J. S.: Arylene Ethynylene Macrocycles Prepared by Precipitation-Driven Alkyne Metathesis. *J. Am. Chem. Soc.* **2004**, *126*, 12796.

(347)   Ge, P.-H.; Fu, W.; Herrmann, W. A.; Herdtweck, E.; Campana, C.; Adams, R. D.; Bunz, U. H. F.: Structural characterization of a cyclohexameric meta-phenyleneethynylene made by alkyne metathesis with in situ catalysts. *Angew. Chem., Int. Ed.* **2000**, *39*, 3607-3610.

(348)   Guieu, S.; Crane, A. K.; MacLachlan, M. J.: Campestarenes: novel shape-persistent Schiff base macrocycles with 5-fold symmetry. *Chem. Commun. (Cambridge, U. K.)* **2011**, *47*, 1169-1171.

(349)   Shopsowitz, K. E.; Edwards, D.; Gallant, A. J.; MacLachlan, M. J.: Highly substituted Schiff base macrocycles via hexasubstituted benzene: a convenient double Duff formylation of catechol derivatives. *Tetrahedron* **2009**, *65*, 8113-8119.

(350)   Korich, A. L.; Hughes, T. S.: Arylene Imine Macrocycles of C3h and C3 Symmetry from Reductive Imination of Nitroformylarenes. *Organic Letters* **2008**, *10*, 5405-5408.

(351)   Fastrez, J.: Macrocyclization versus polymerization in polycondensation reactions under high-dilution conditions: a theoretical study. *J. Phys. Chem.* **1989**, *93*, 2635-42.

(352)   Ercolani, G.; Mandolini, L.; Mencarelli, P.: Kinetic treatment of irreversible cyclooligomerization of bifunctional chains and its relevance to the synthesis of many-membered rings. *Macromolecules* **1988**, *21*, 1241-6.

(353)   Brouard, M.: *Reaction Dynamics*; Oxford University Press Inc.: New York, 1998.

(354)   Datar, A.; Gross, D. E.; Balakrishnan, K.; Yang, X.; Moore, J. S.; Zang, L.: Ultrafine nanofibers fabricated from an arylene-ethynylene macrocyclic molecule using surface assisted self-assembly. *Chem. Commun. (Cambridge, U. K.)* **2012**, *48*, 8904-8906.

(355)   Feng, W.; Yamato, K.; Yang, L.; Ferguson, J. S.; Zhong, L.; Zou, S.; Yuan, L.; Zeng, X. C.; Gong, B.: Efficient Kinetic Macrocyclization. *J. Am. Chem. Soc.* **2009**, *131*, 2629-2637.

(356)   Seo, S. H.; Jones, T. V.; Seyler, H.; Peters, J. O.; Kim, T. H.; Chang, J. Y.; Tew, G. N.: Liquid Crystalline Order from ortho-Phenylene Ethynylene Macrocycles. *J. Am. Chem. Soc.* **2006**, *128*, 9264-9265.

(357)   Nomoto, A.; Sonoda, M.; Yamaguchi, Y.; Ichikawa, T.; Hirose, K.; Tobe, Y.: A Clue to Elusive Macrocycles: Unusually Facile, Spontaneous Polymerization of a Hexagonal Diethynylbenzene Macrocycle. *J. Org. Chem.* **2006**, *71*, 401-404.

(358)   Liu, Y.; Qin, B.; Zeng, H.: $POCl_3$-mediated H-bonding-directed one-pot synthesis of macrocyclic pentamers, strained hexamers and highly strained heptamers. *SCIENCE CHINA Chemistry* **2012**, *55*, 55-63.

(359)   Norouzi-Arasi, H.; Pisula, W.; Mavrinskiy, A.; Feng, X.; Müllen, K.: Synthesis and Self-Assembly of Macrocyclic Mesogens Based on 1,10-Phenanthroline. *Chemistry – An Asian Journal* **2011**, *6*, 367-371.

(360)   Yuan, L.; Feng, W.; Yamato, K.; Sanford, A. R.; Xu, D.; Guo, H.; Gong, B.: Highly Efficient, One-Step Macrocyclizations Assisted by the Folding and Preorganization of Precursor Oligomers. *Journal of the American Chemical Society* **2004**, *126*, 11120-11121.

(361)   Wettach, H.; Hoeger, S.; Chaudhuri, D.; Lupton, J. M.; Liu, F.; Lupton, E. M.; Tretiak, S.; Wang, G.; Li, M.; De, F. S.; Fischer, S.; Foerster, S.: Synthesis and properties of a triphenylene-butadiynylene macrocycle. *J. Mater. Chem.* **2011**, *21*, 1404-1415.

(362)   Kaleta, J. i.; Mazal, C.: A Triangular Macrocycle Altering Planar and Bulky Sections in Its Molecular Backbone. *Organic Letters* **2011**, *13*, 1326-1329.

(363)   Chen, S.; Yan, Q.; Li, T.; Zhao, D.: Arylene Ethynylene Macrocycles with Intramolecular π-π Stacking. *Org. Lett.* **2010**, *12*, 4784-4787.

(364)   Opris, D. M.; Franke, P.; Schlueter, A. D.: Shape-persistent macrocycles with bipyridine units: progress in accessibility and widening of applicability. *Eur. J. Org. Chem.* **2005**, 822-837.

(365)   Lehmann, U.; Schluter, A. D.: A shape-persistent macrocycle with two opposing 2,2':6',2''-terpyridine units. *Eur. J. Org. Chem.* **2000**, 3483-3487.

(366)   Staab, H. A.; Neunhoeffer, K.: [2.2.2.2.2.2]Metacyclophane-1,9,17,25,33,41-hexayne from m-iodophenylacetylene by sixfold Stephens-Castro coupling. *Synthesis* **1974**, 424.

(367)   Shortell, D. B.; Palmer, L. C.; Tour, J. M.: Solid-phase approaches toward cyclic oligomers. *Tetrahedron* **2001**, *57*, 9055-9065.

(368)   Höger, S.; Meckenstock, A.-D.; Pellen, H.: High-Yield Macrocyclization via Glaser Coupling of Temporary Covalent Templated Bisacetylenes. *The Journal of Organic Chemistry* **1997**, *62*, 4556-4557.

(369)   Fischer, M.; Höger, S.: Synthesis of a shape-persistent macrocycle with intraannular carboxylic acid groups. *Tetrahedron* **2003**, *59*, 9441-9446.

(370)   Schmittel, M.; Ammon, H.: Preparation of a rigid macrocycle with two exotopic phenanthroline binding sites. *Synlett* **1999**, 750-752.

Appendix Chapter 1

Figure AC1. 1: ^{1}H NMR (300 MHz, CDCl₃) of 1,4-dihexyl-2-triisopropylsilylethynyl-4-trimethylsilylethynylbenzene (**47**).
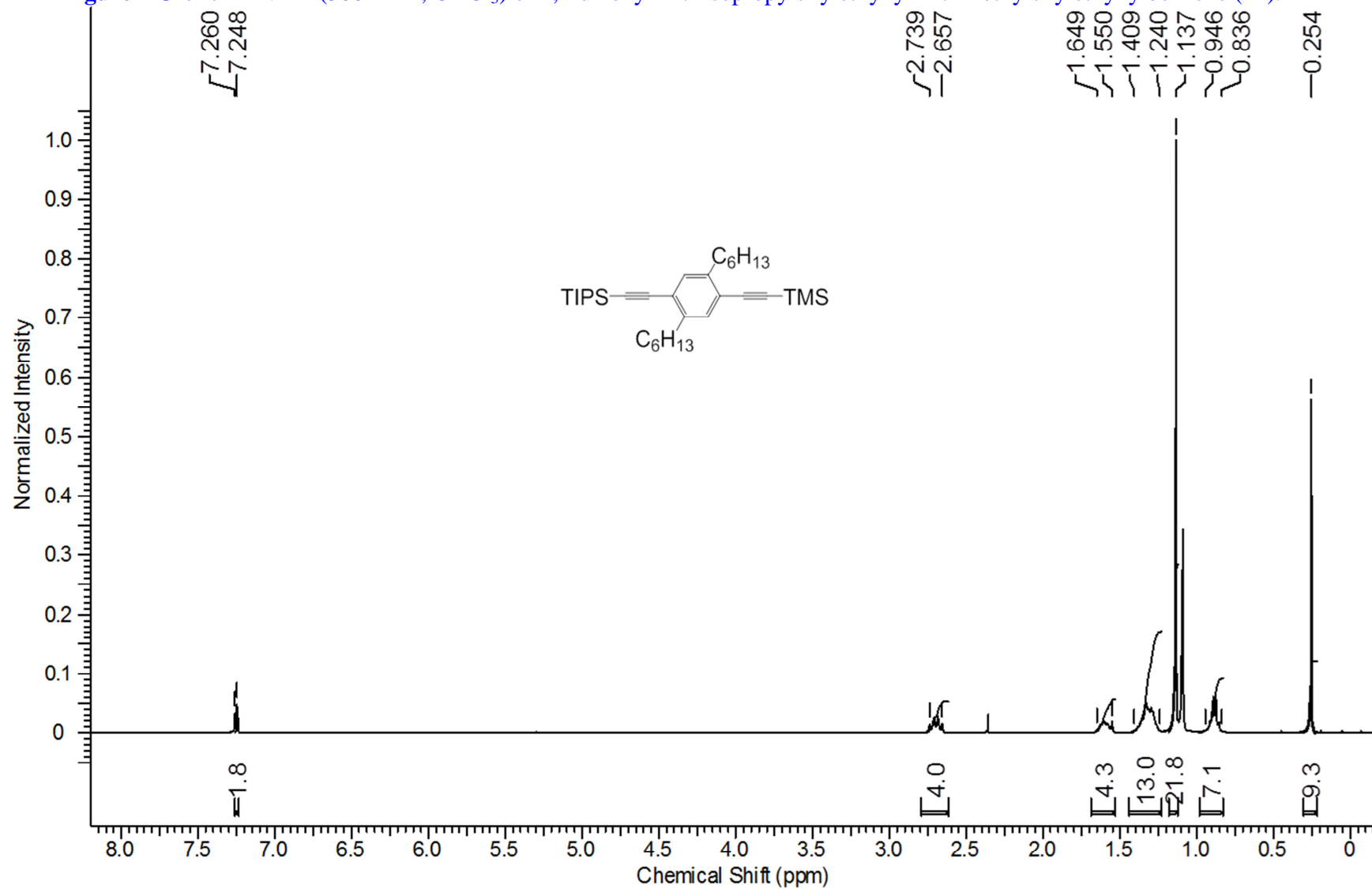
Figure AC1. 2: ^{13}C NMR (400 MHz, CDCl$_3$) of 1,4-dihexyl-2-triisopropylsilylethynyl-4-trimethylsilylethynylbenzene (**47**).
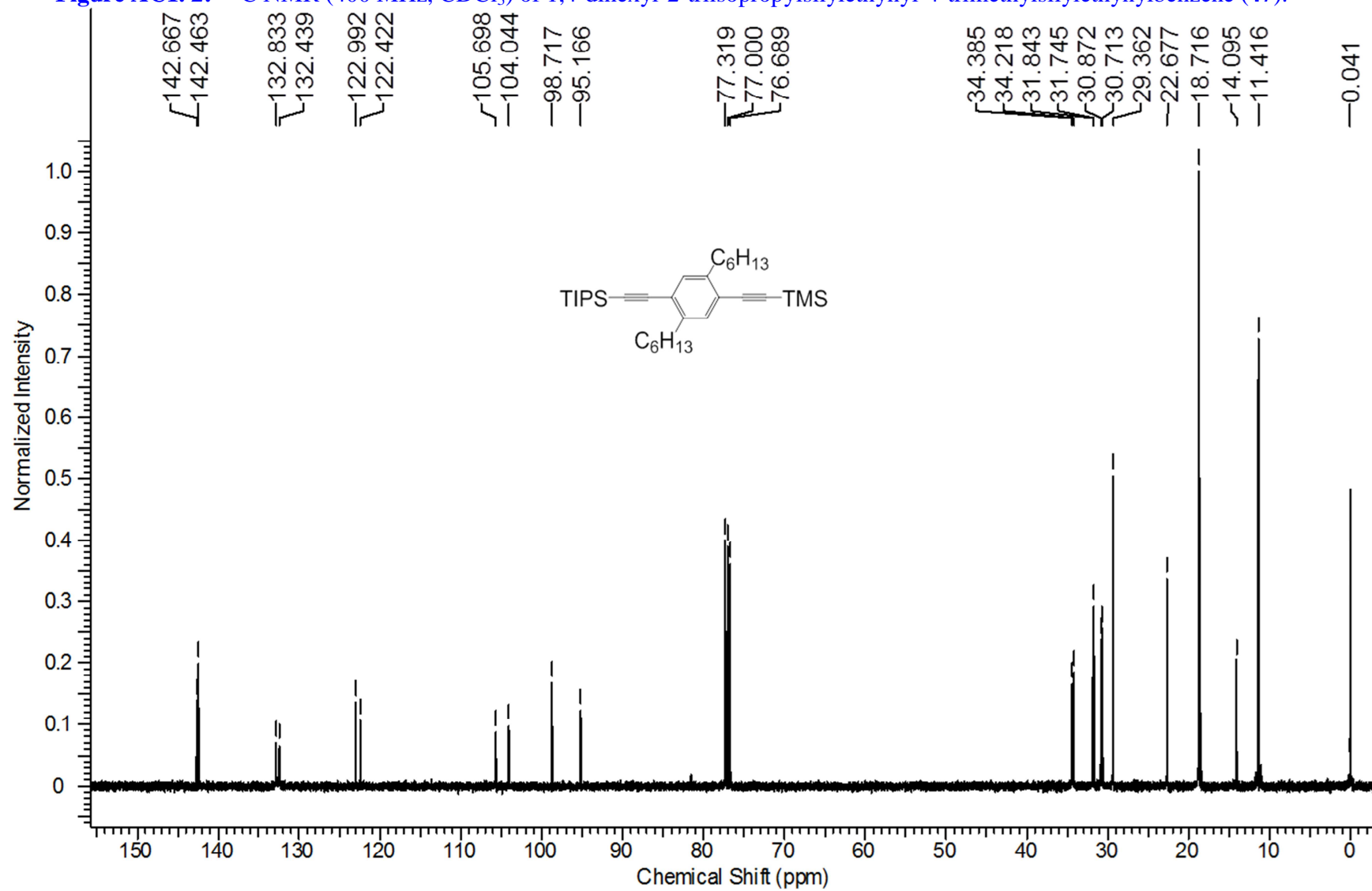
Figure AC1. 3: ^{1}H NMR (300 MHz, CDCl$_3$) of 4-(4-iodo-2,5-dihexylphenyl)-2-methyl-3-butyn-2-ol (**45**).
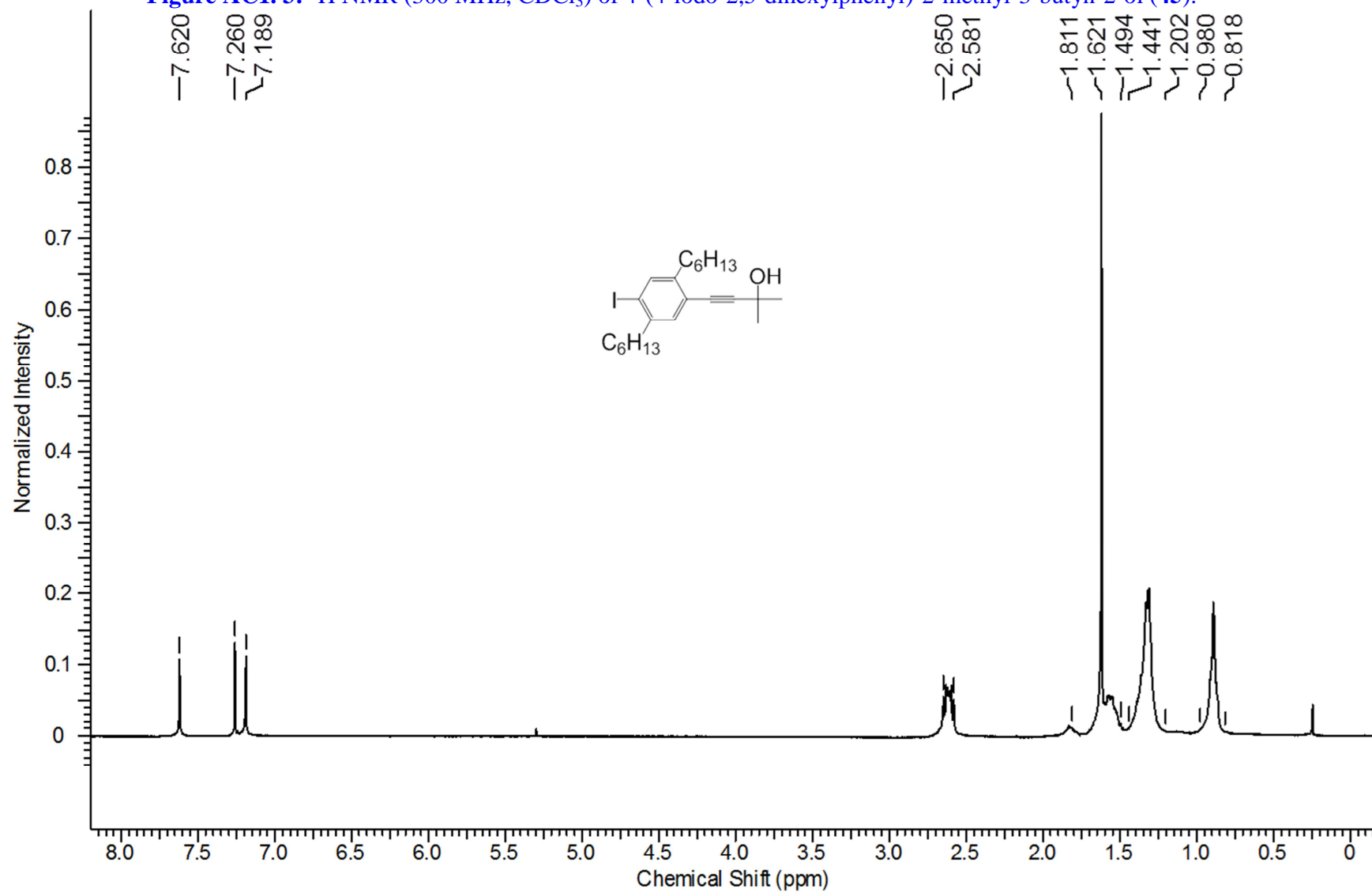
Figure AC1. 4: ^{13}C NMR (400 MHz, CDCl$_3$) of 4-(4-iodo-2,5-dihexylphenyl)-2-methyl-3-butyn-2-ol (**45**).

215
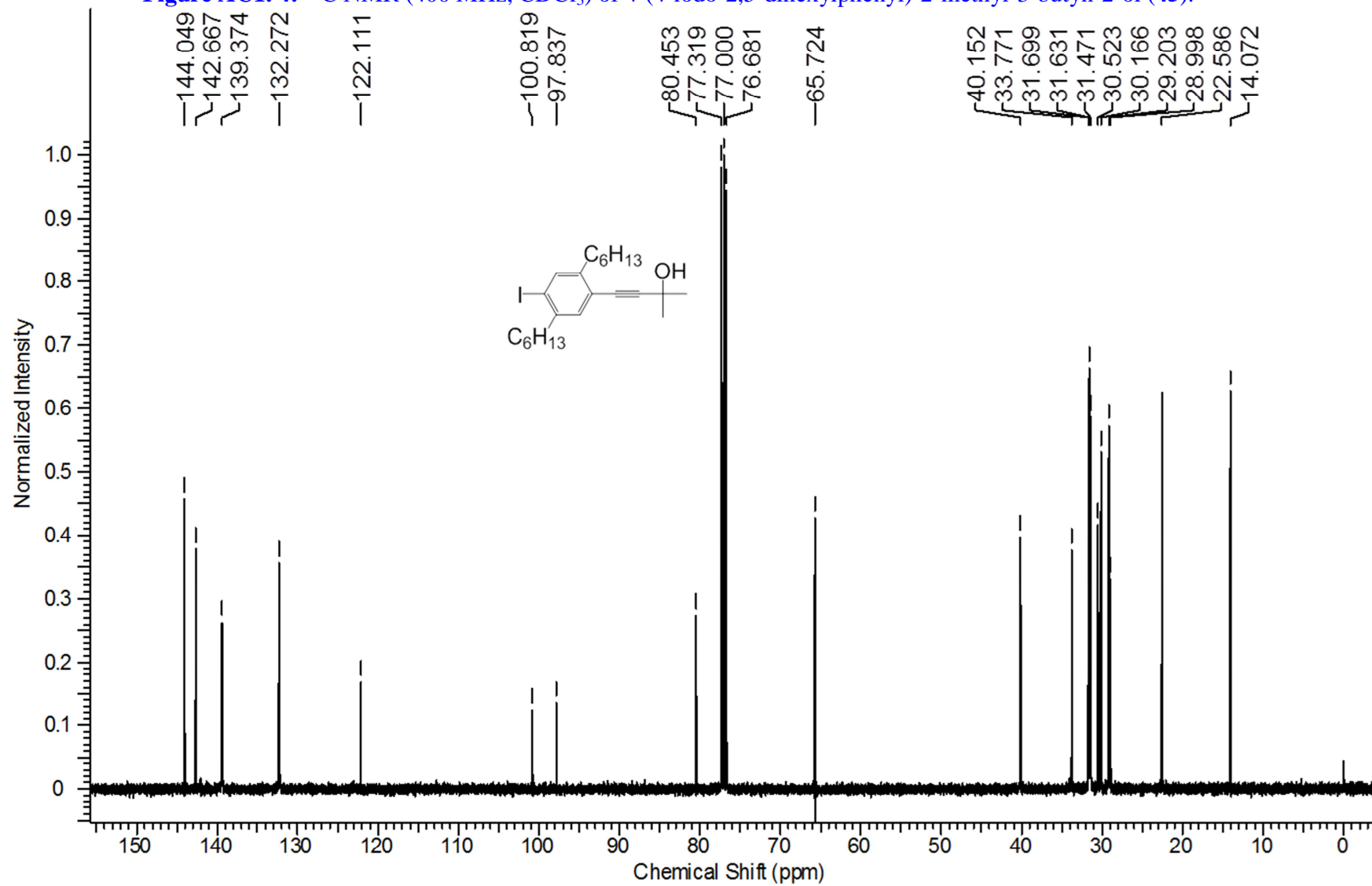
Figure AC1. 5: ^{1}H NMR (400 MHz, CDCl$_3$) of 4-(4-trimethylsilylethynyl-2,5-dihexylphenyl)-2-methyl-3-butyn-2-ol (**46**).
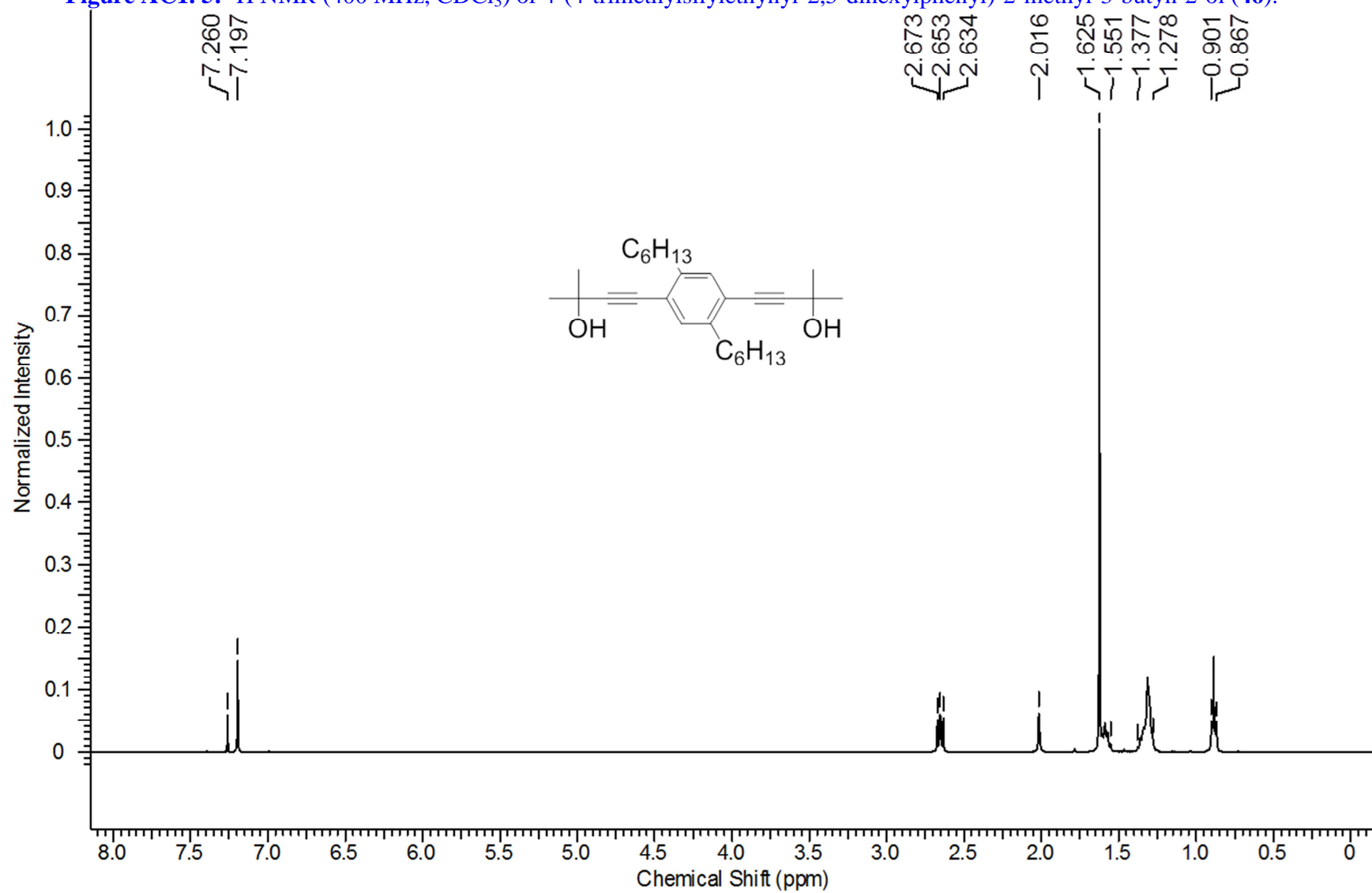
217
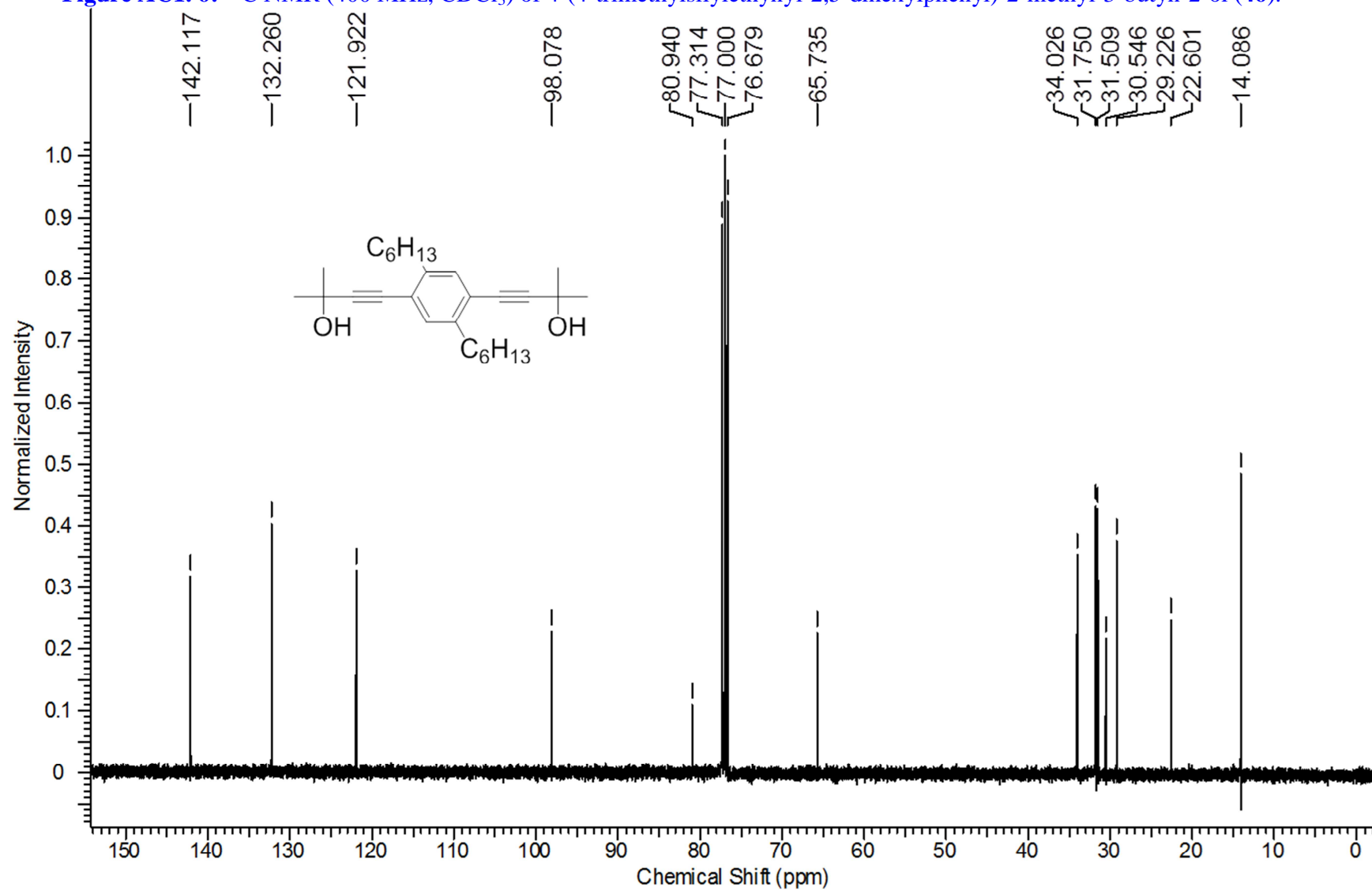
Figure AC1. 7: ^{1}H NMR (300 MHz, CDCl$_3$) of 4-(4-trimethylsilylethynyl-2,5-dihexylphenyl)-2-methyl-3-butyn-2-ol (**48**).
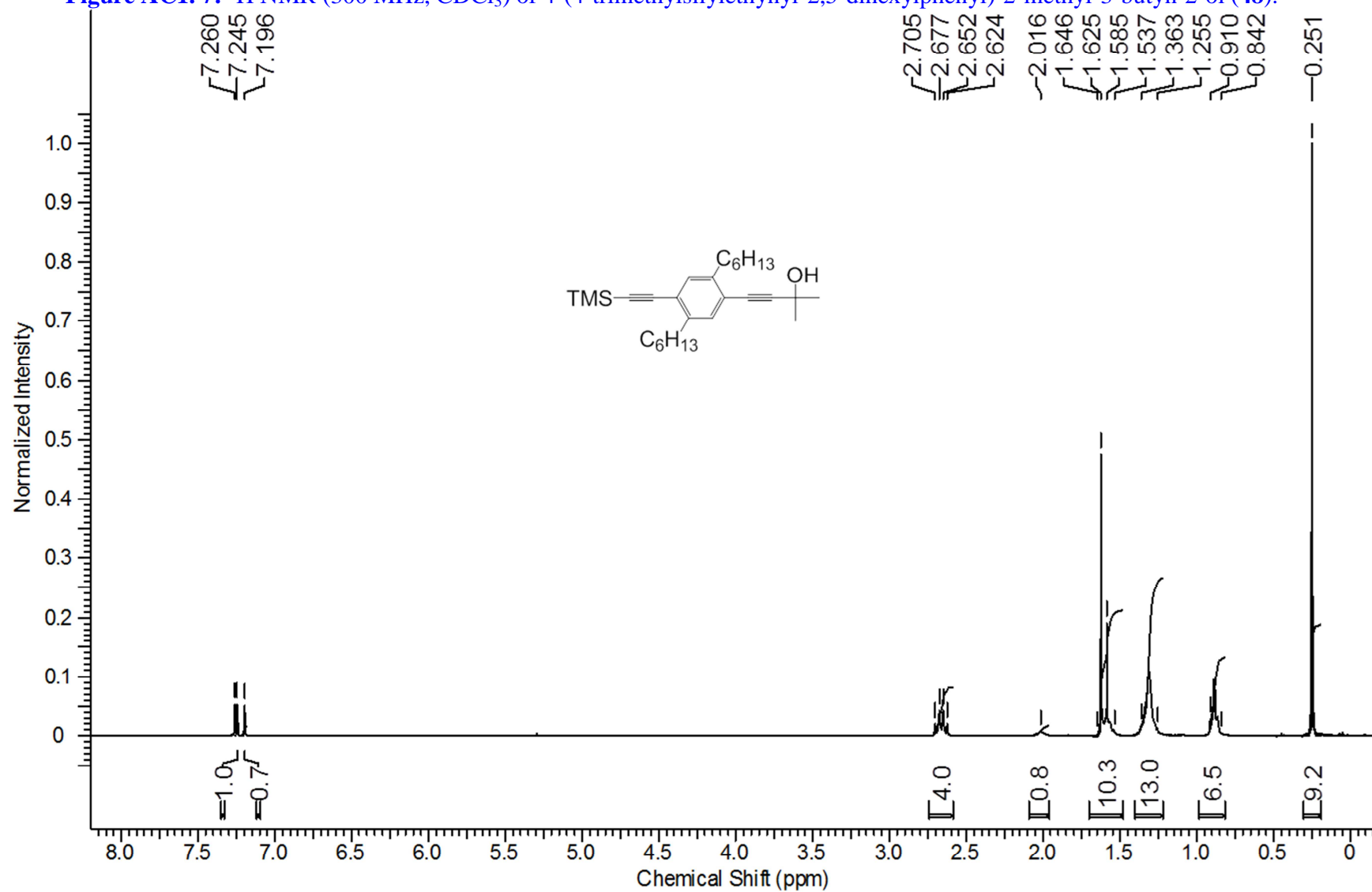
Figure AC1. 8: ^{13}C NMR (400 MHz, CDCl$_3$) of 4-(4-trimethylsilylethynyl-2,5-dihexylphenyl)-2-methyl-3-butyn-2-ol (**48**).

142.690
142.060
132.454
132.249
122.377
122.111
103.900
98.732
98.216
80.999
77.319
77.000
76.681
65.724
34.097
34.029
31.752
31.707
31.502
30.553
29.240
22.601
14.079
-0.042
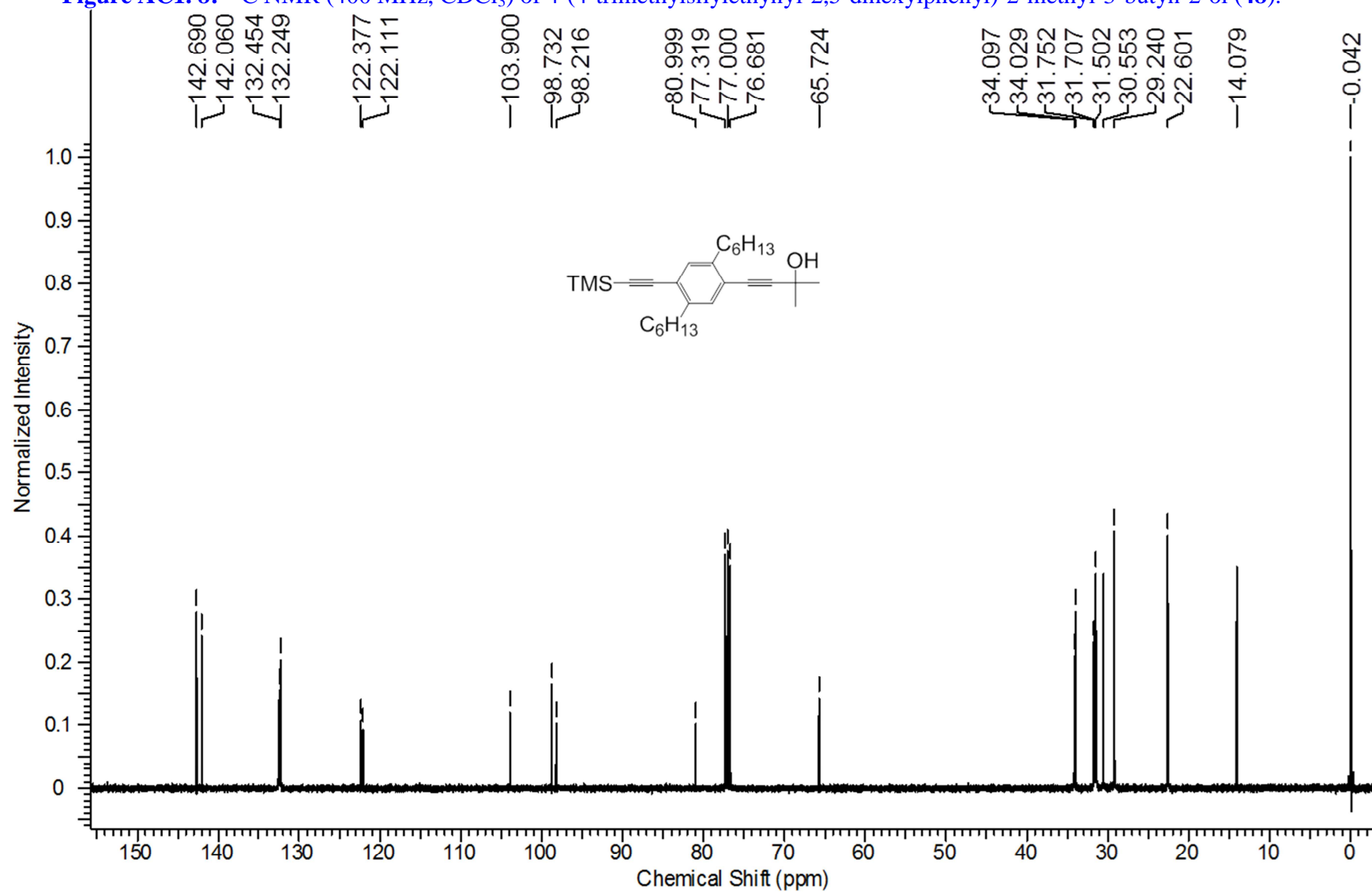
Figure AC1. 9: ^{1}H NMR (300 MHz, CDCl$_3$) of 4-(4-triisopropylsilylethynyl-2,5-dihexylphenyl)-2-methyl-3-butyn-2-ol (**49**).
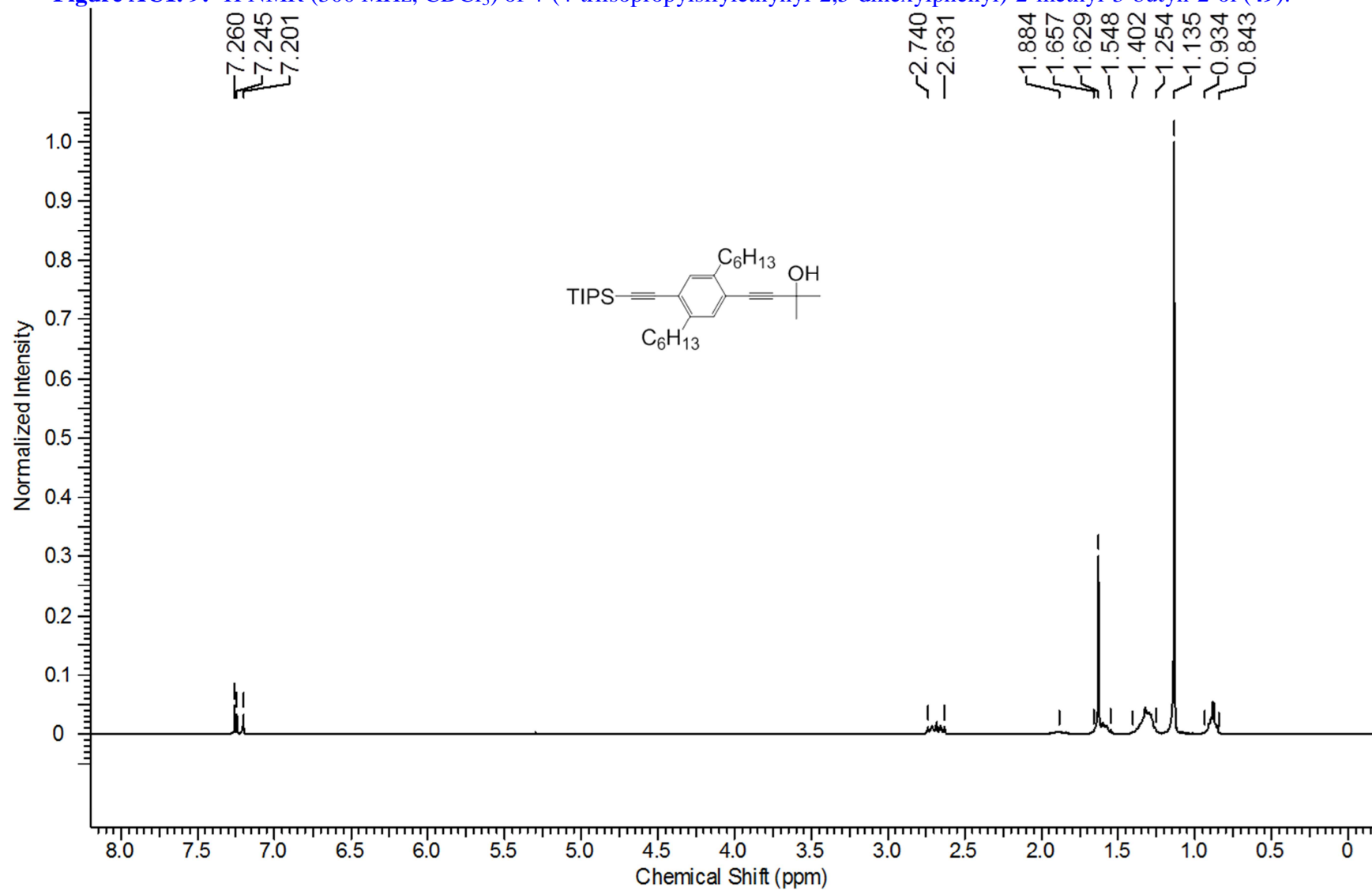
Figure AC1. 10: ^{13}C NMR (400 MHz, CDCl$_3$) of 4-(4-triisopropylsilylethynyl-2,5-dihexylphenyl)-2-methyl-3-butyn-2-ol (**49**)
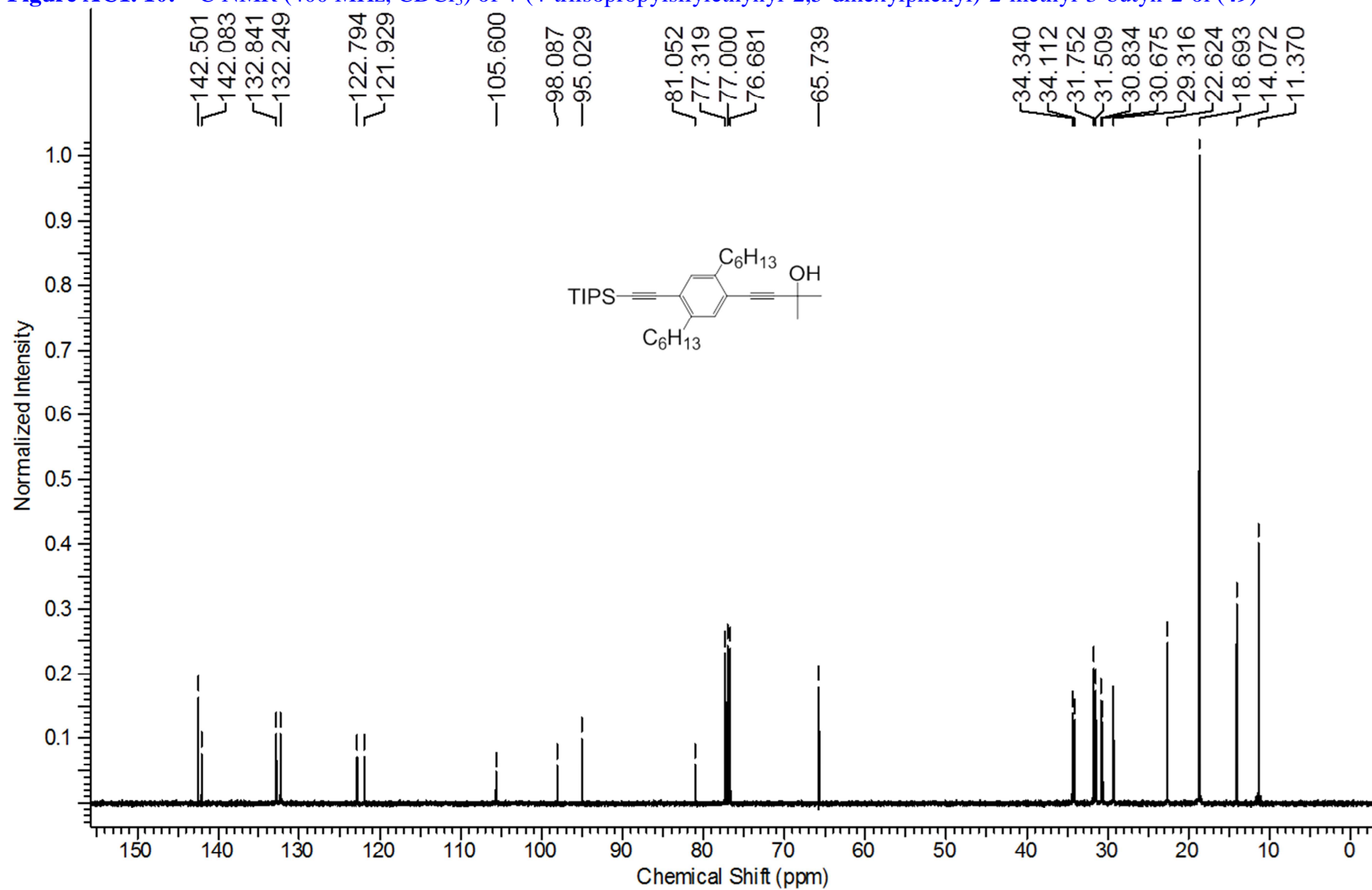
Figure AC1. 11: ^{1}H NMR (300 MHz, CDCl$_3$) of 4-(4-ethynyl-2,5-dihexylphenyl)-2-methyl-3-butyn-2-ol (**28**).
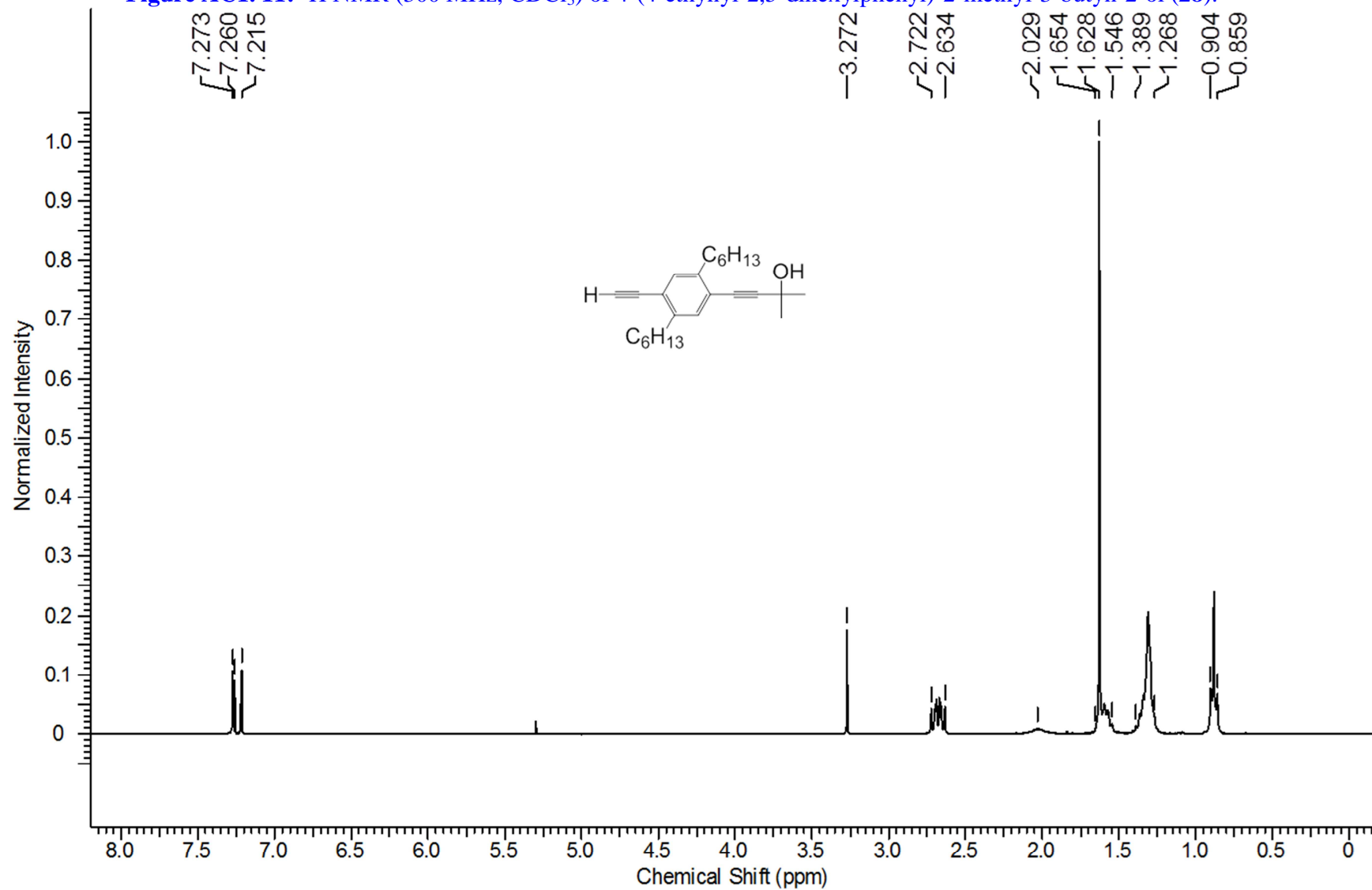
Figure AC1. 12: ^{13}C NMR (400 MHz, CDCl$_3$) of 4-(4-ethynyl-2,5-dihexylphenyl)-2-methyl-3-butyn-2-ol (**28**).
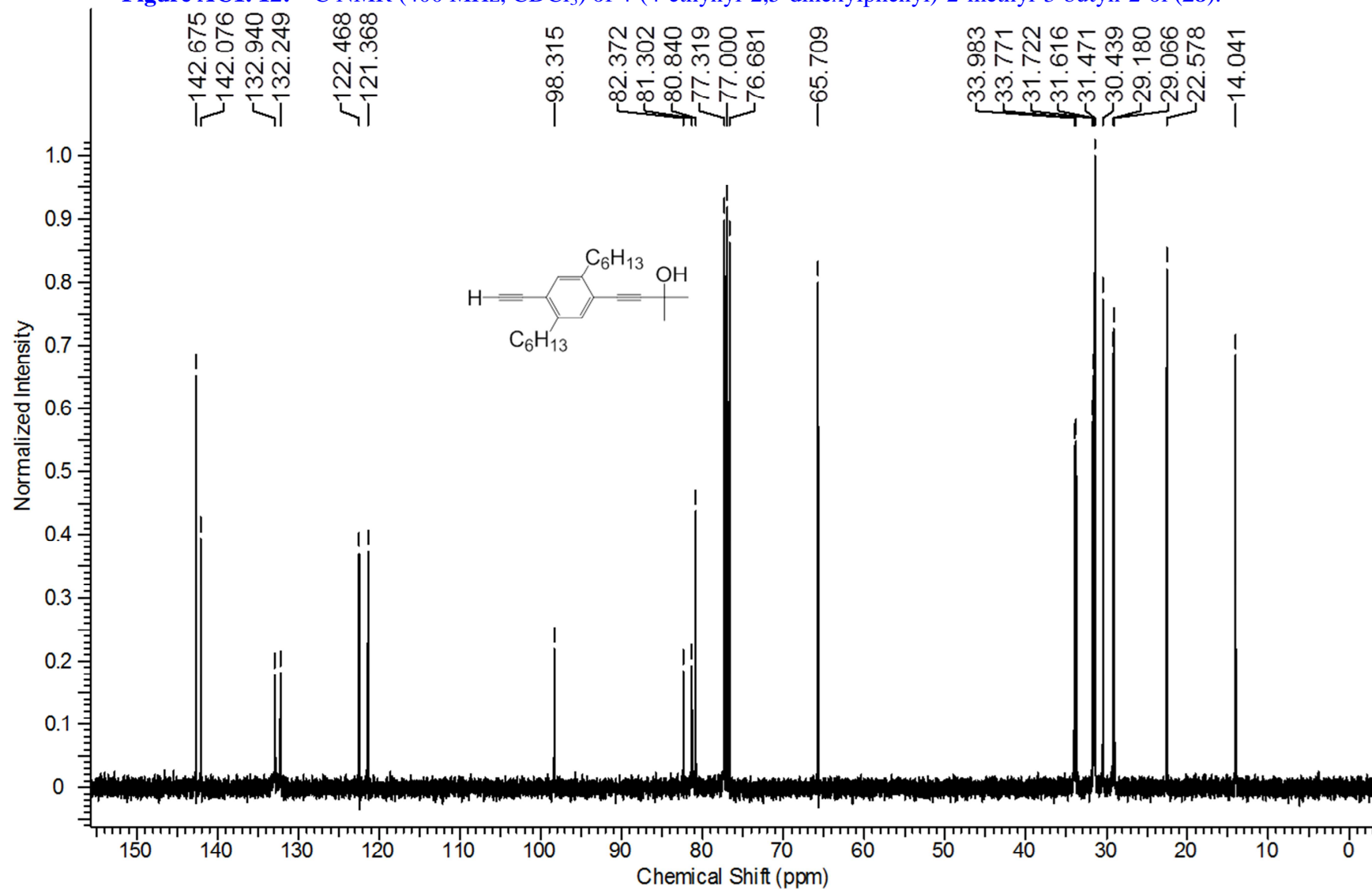
Figure AC1. 13: ^{1}H NMR (300 MHz, CDCl$_3$) of 1-ethynyl-2,5-dihexyl-4-trimethylsilylethynylbenzene (**26**).
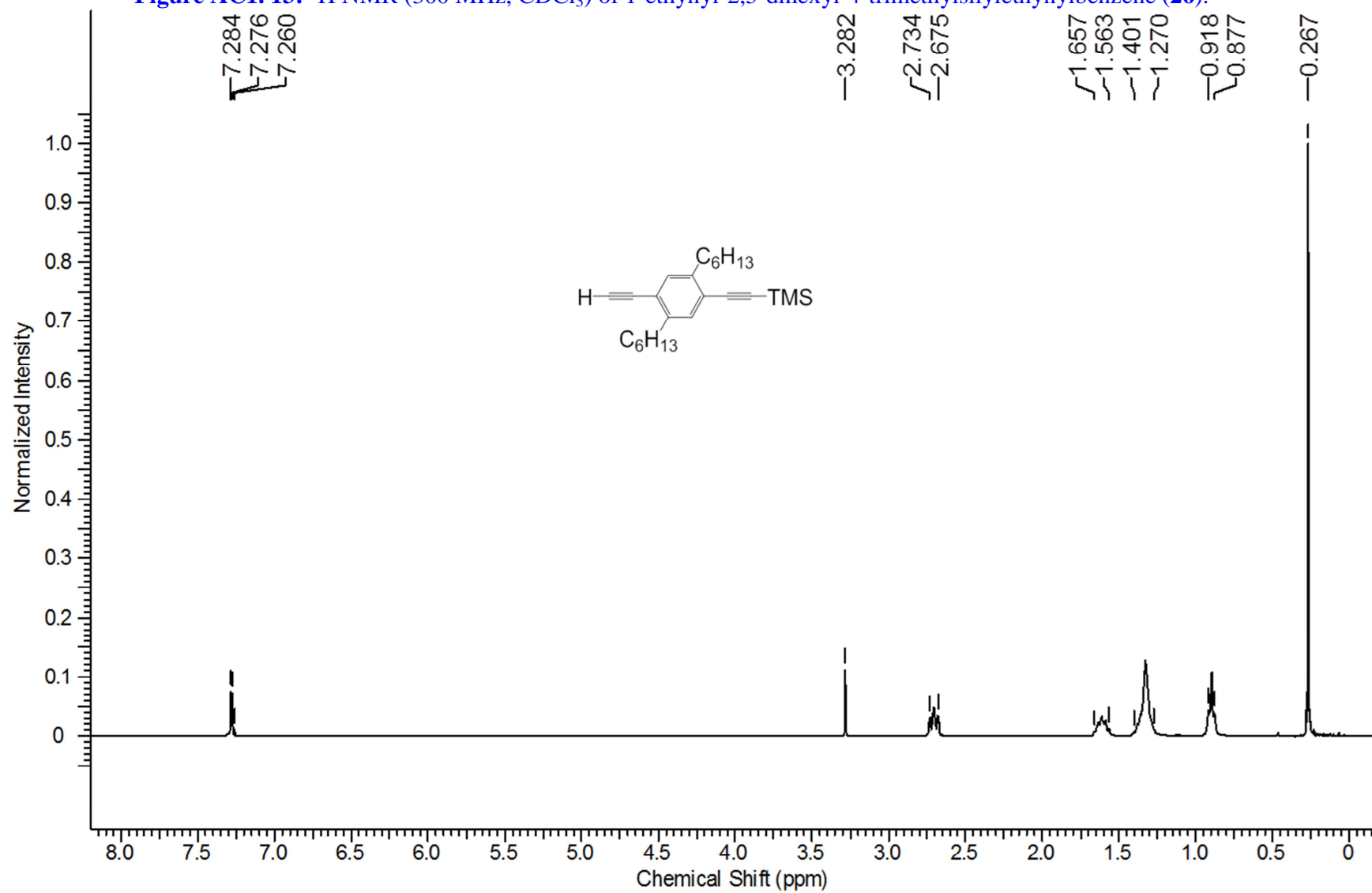
Figure AC1. 14: ^{13}C NMR (400 MHz, CDCl$_3$) of 1-ethynyl-2,5-dihexyl-4-trimethylsilylethynylbenzene (**26**).
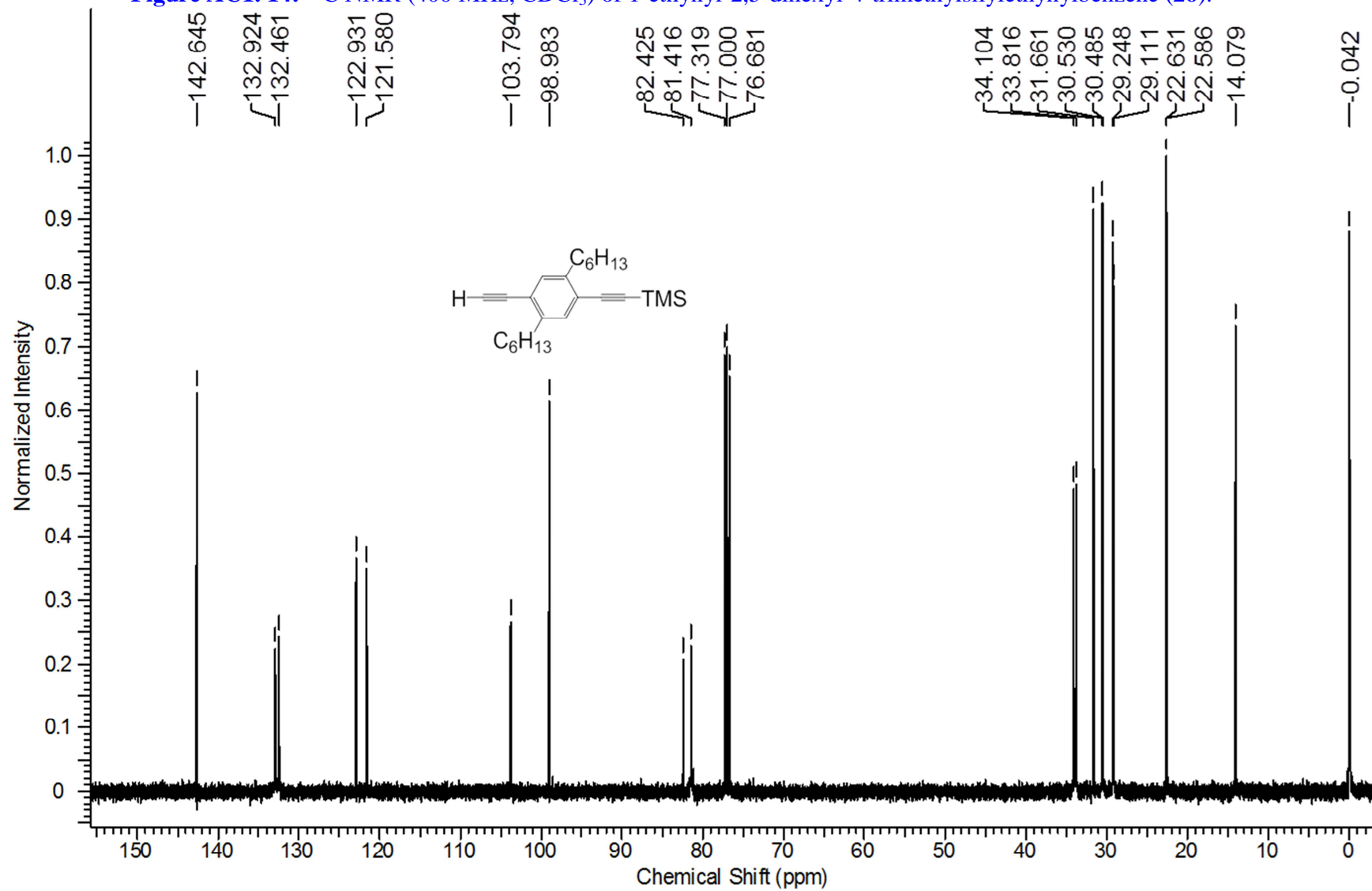
142.645

132.924
132.461

122.931
121.580

103.794

98.983

82.425
81.416
77.319
77.000
76.681

34.104
33.816
31.661
30.530
30.485
29.248
29.111
22.631
22.586

14.079

-0.042

Structure drawn: H—≡—benzene ring with C$_6$H$_{13}$ substituents—≡—TMS
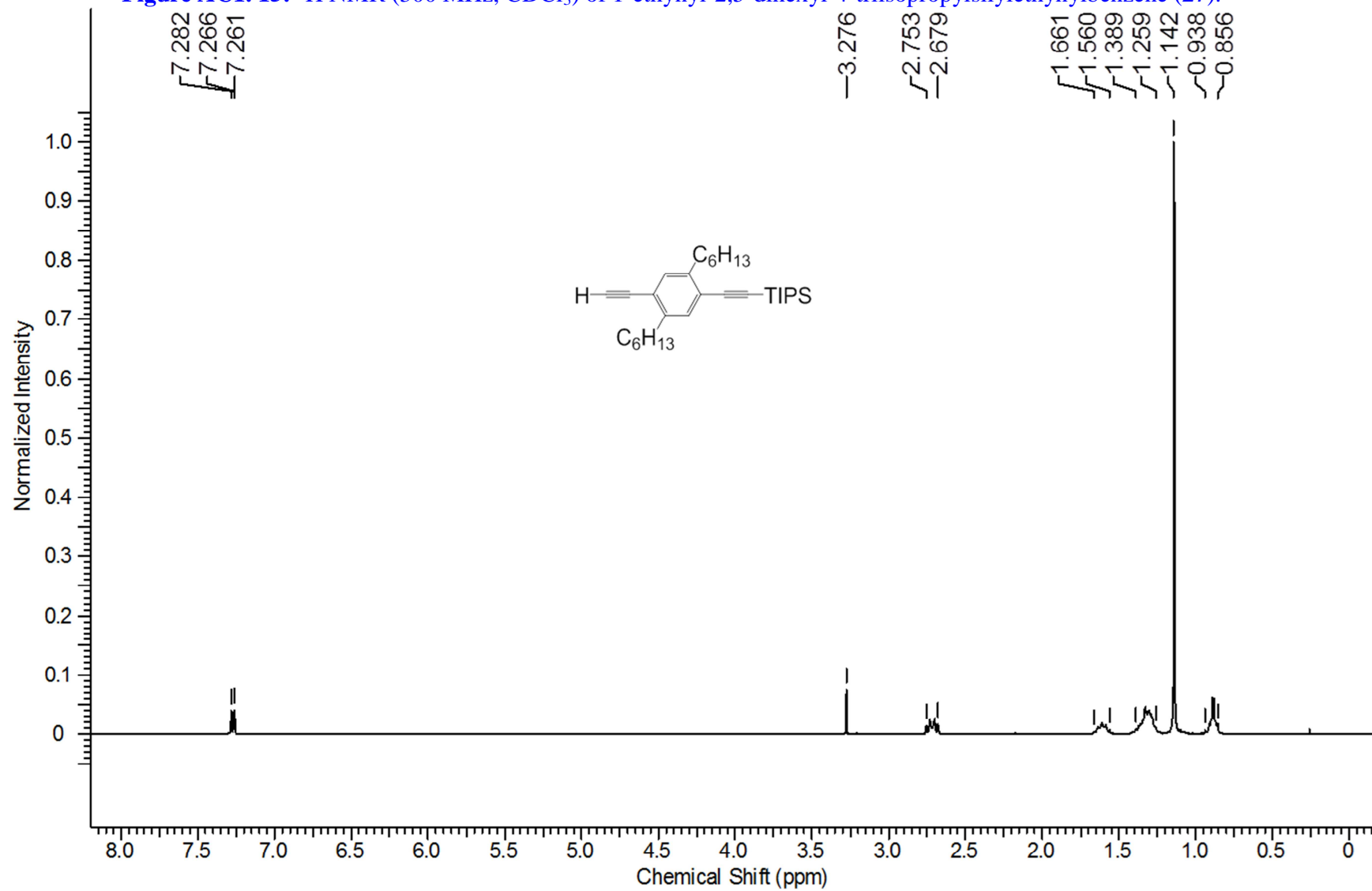
Figure AC1. 16: ^{13}C NMR (400 MHz, CDCl$_3$) of 1-ethynyl-2,5-dihexyl-4-triisopropylsilylethynylbenzene (**27**).
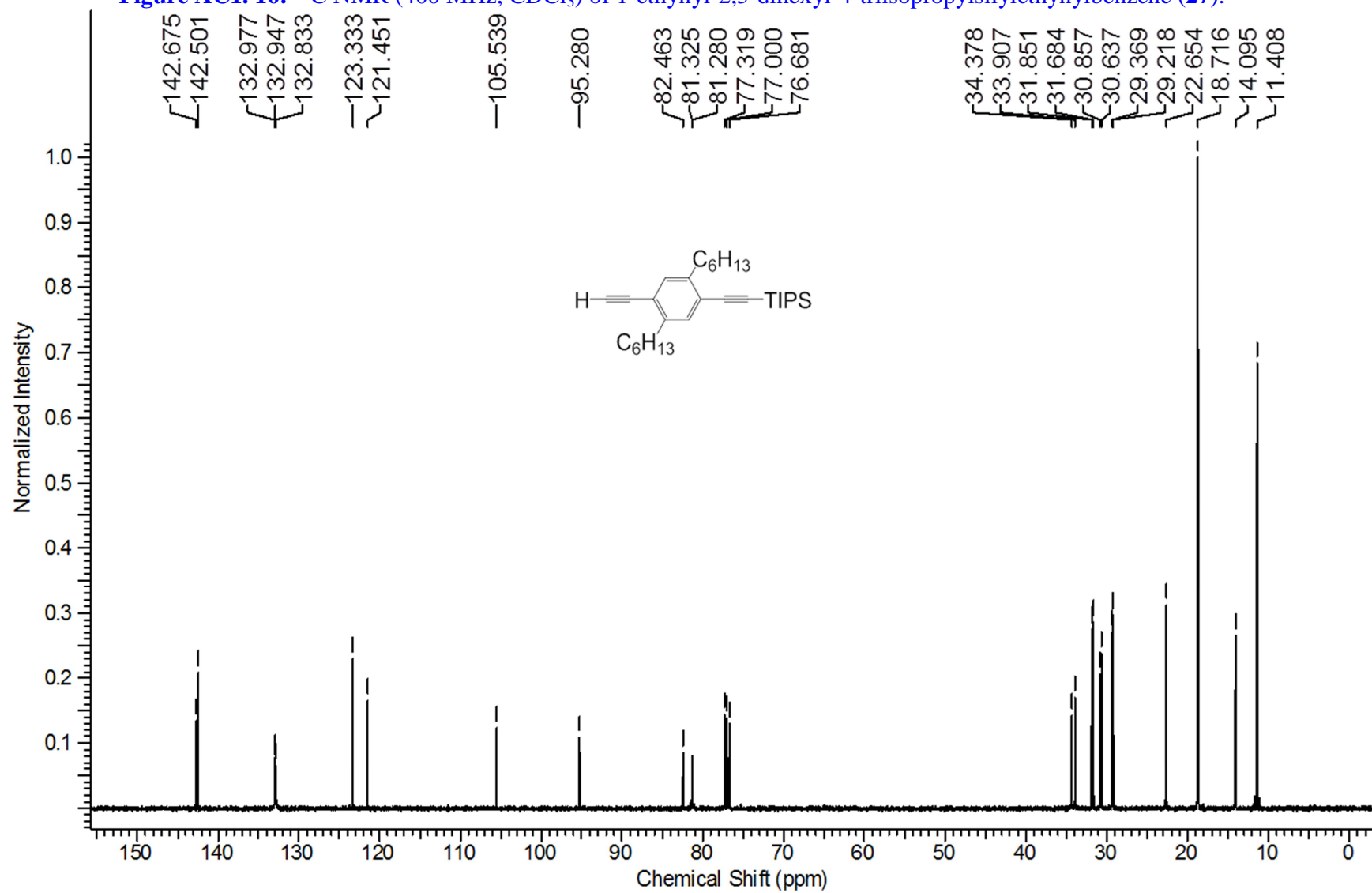
Appendix Chapter 2

Figure AC2. 1: ^{1}H NMR (300 MHz, CDCl$_3$) **53**.
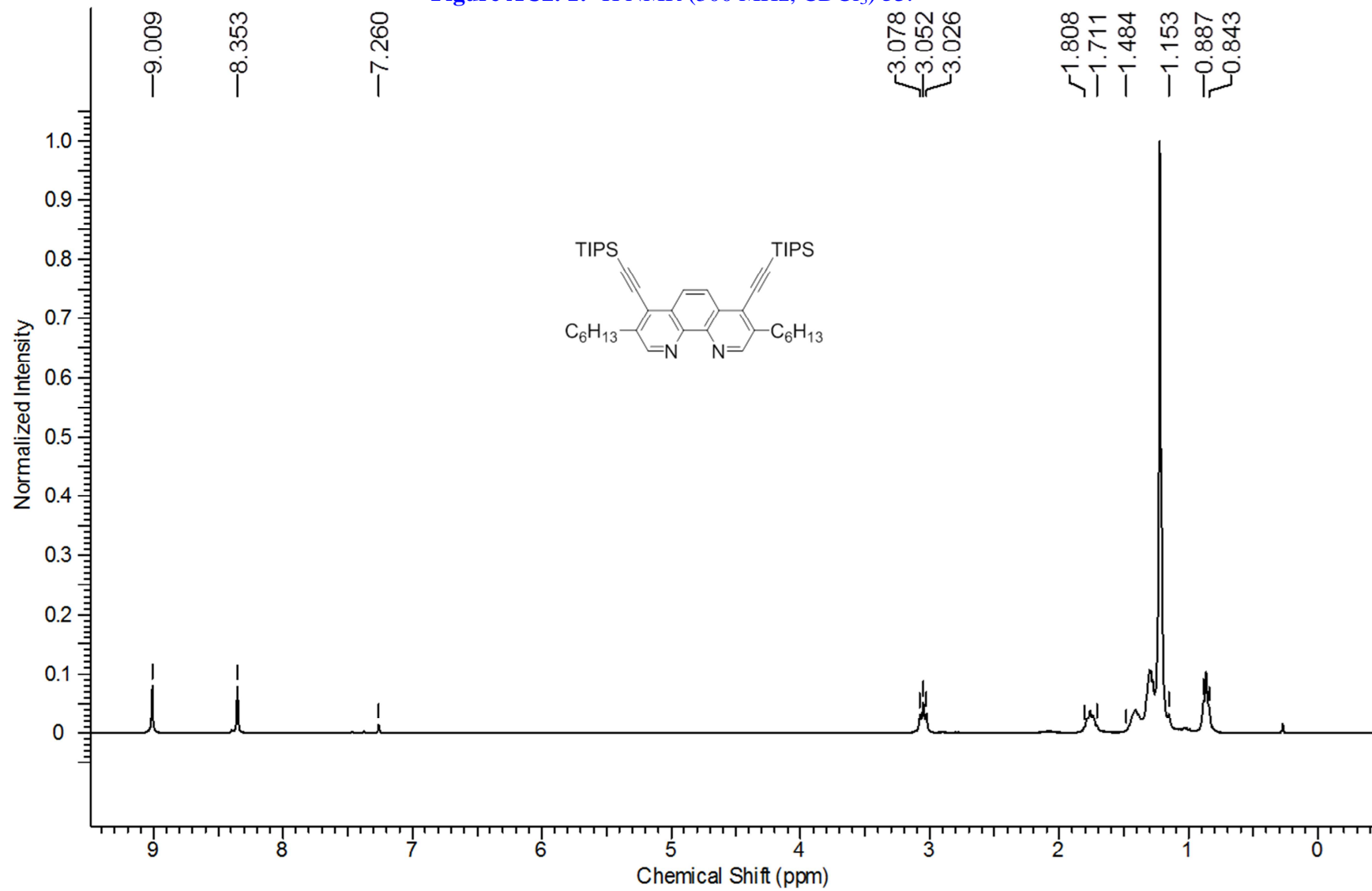
Figure AC2. 2: ^{13}C NMR (400 MHz, CDCl$_3$) **53**.
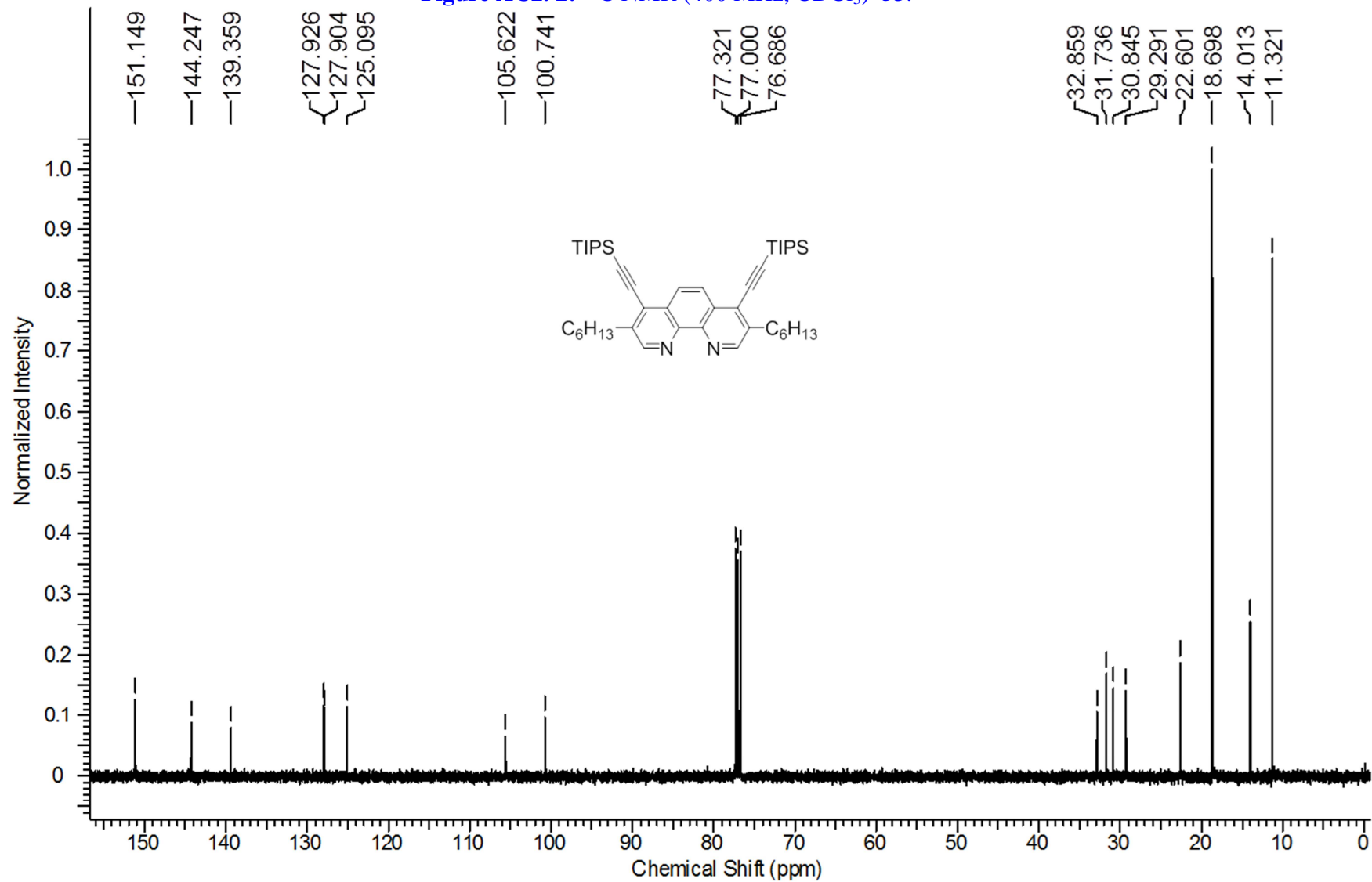
Figure AC2. 3: ^{1}H NMR (300 MHz, CDCl$_3$) **55**.
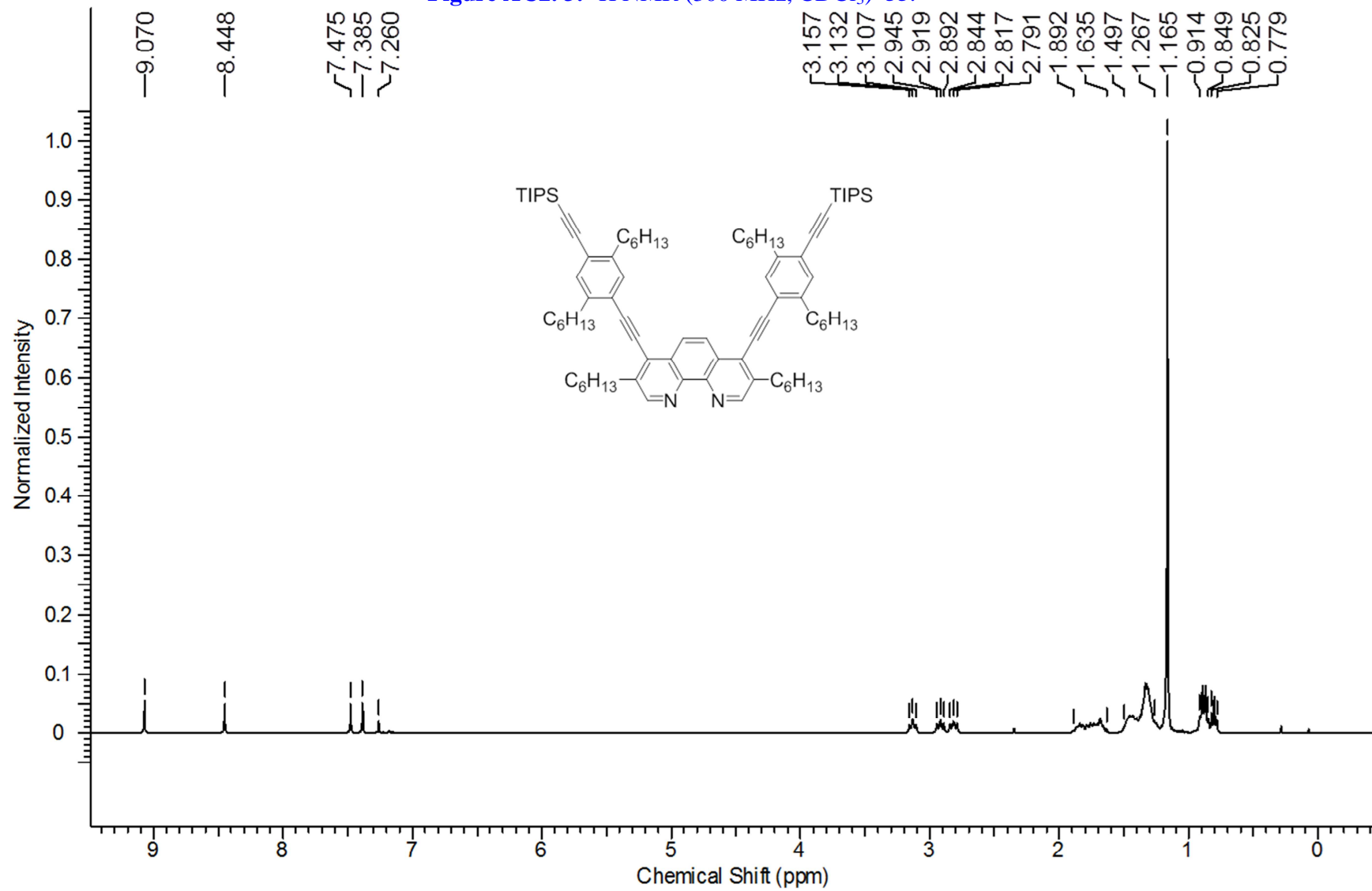
Figure AC2. 4: ^{13}C NMR (400 MHz, CDCl$_3$) **55**.

232
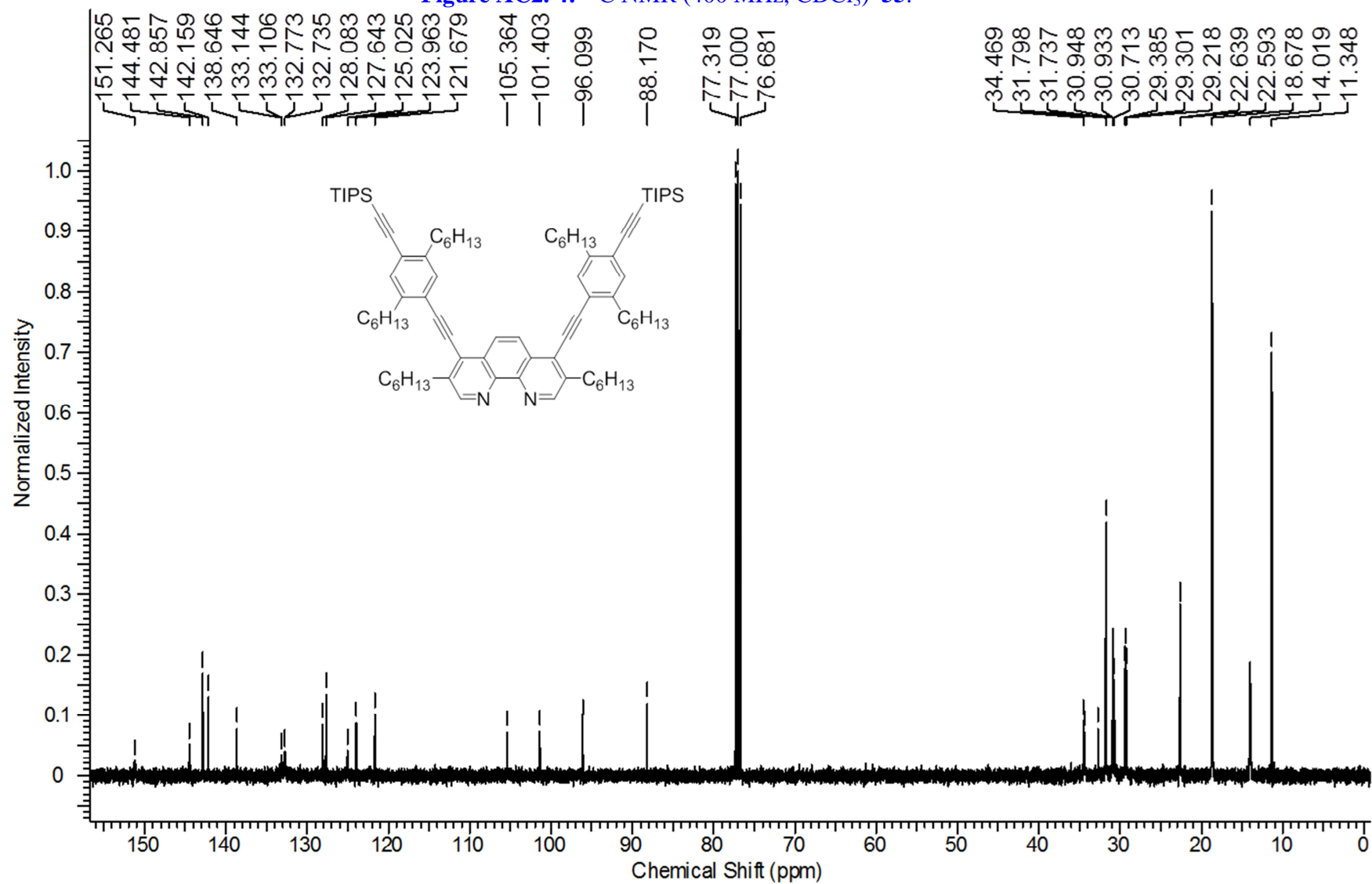
Figure AC2. 5: ^{1}H NMR (400 MHz, CDCl$_3$) **50**.
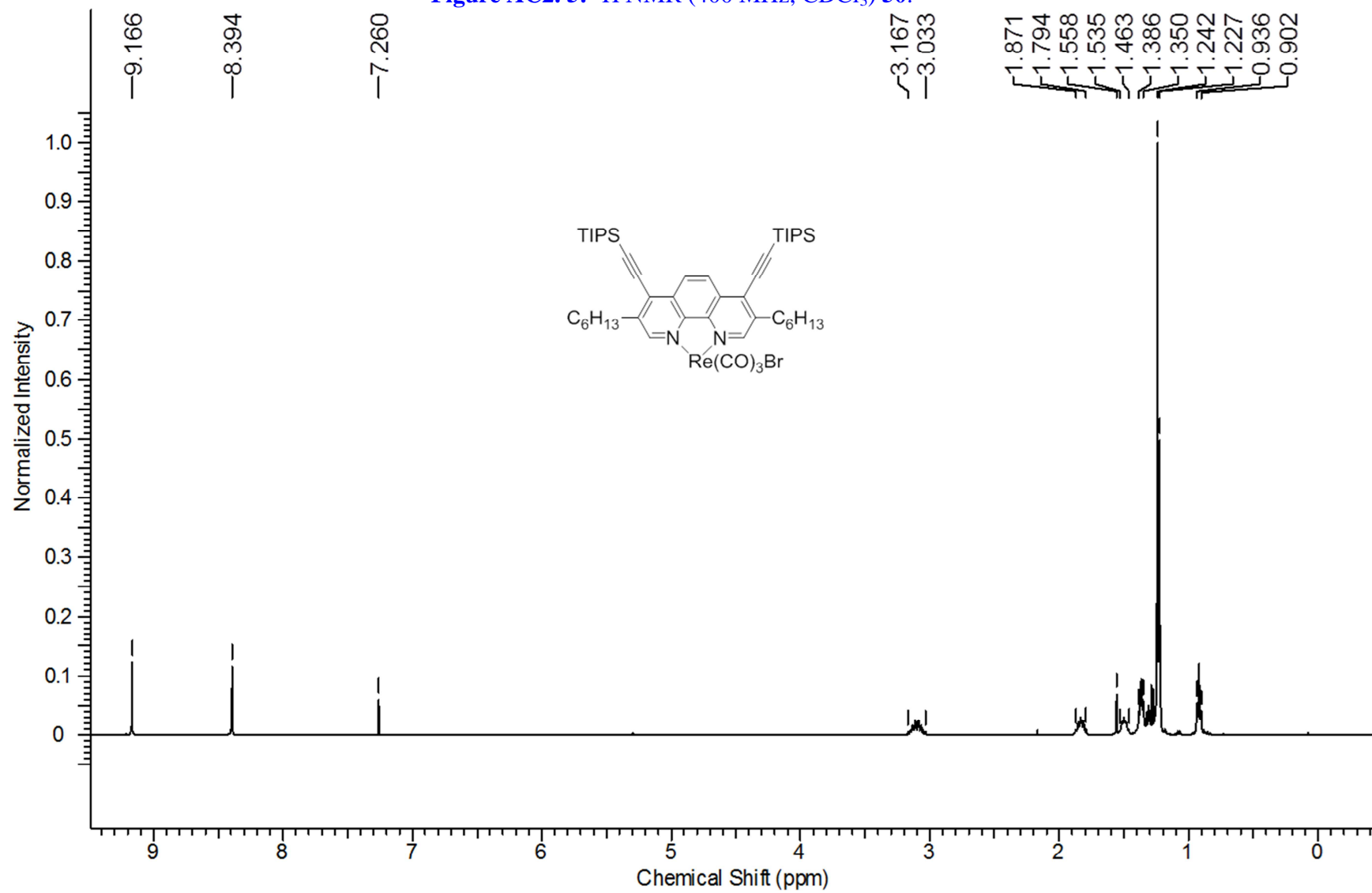
Figure AC2. 6: ^{13}C NMR (400 MHz, CDCl$_3$) **50**.
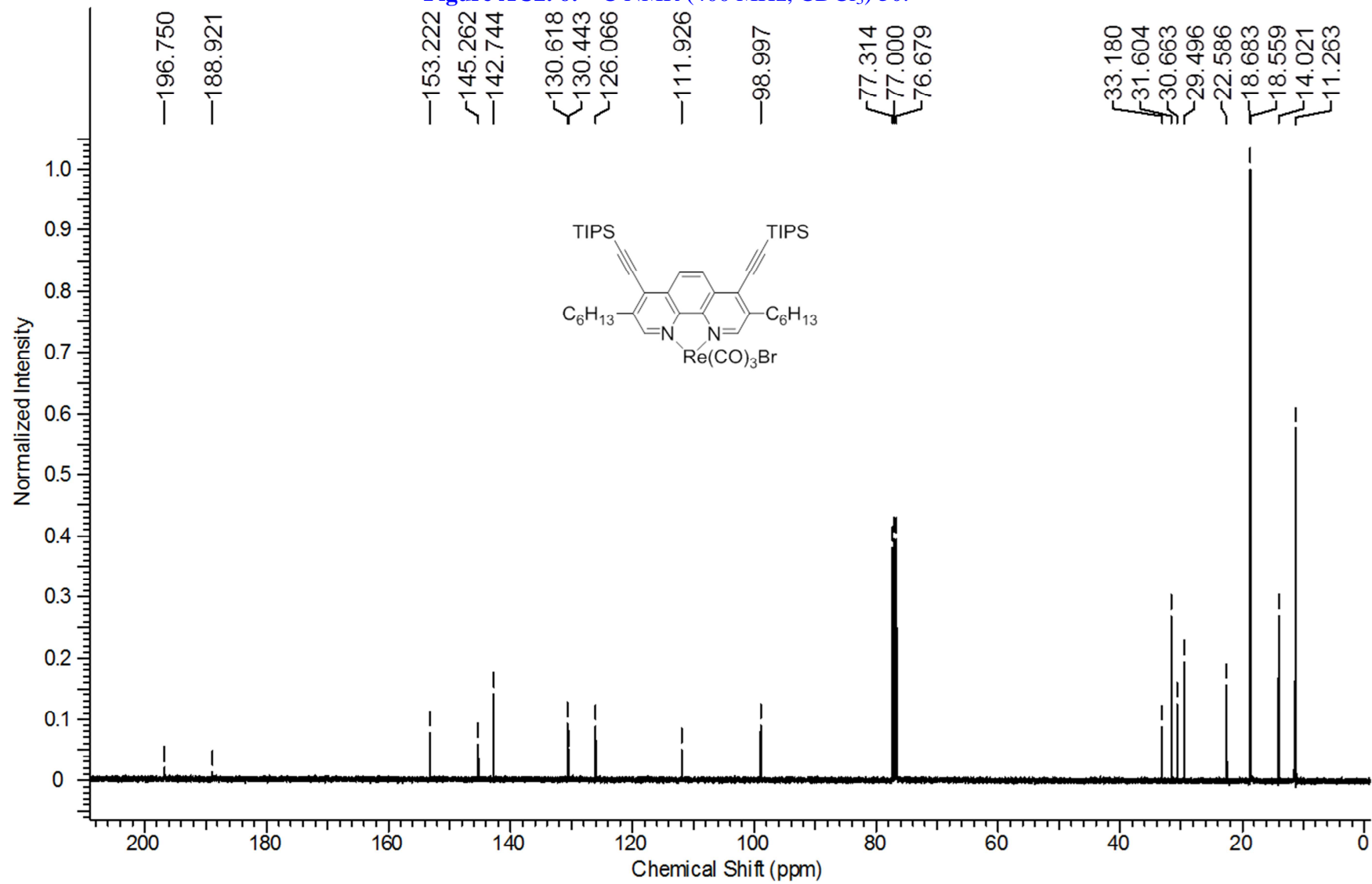
Figure AC2. 7: ^{1}H NMR (400 MHz, CDCl$_3$) **50(I)**.
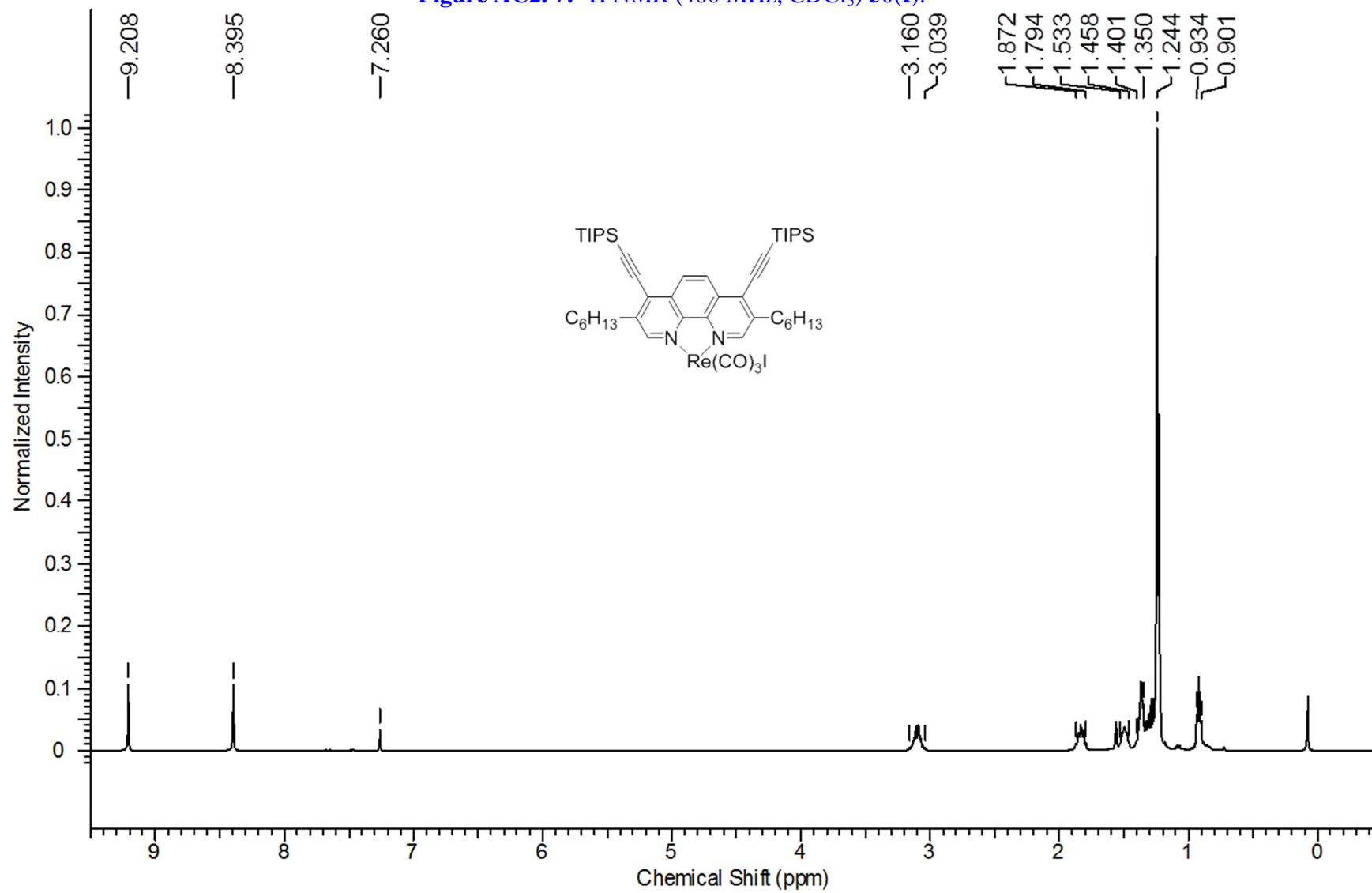
Figure AC2. 8: ^{13}C NMR (400 MHz, CDCl$_3$) **50(I)**.
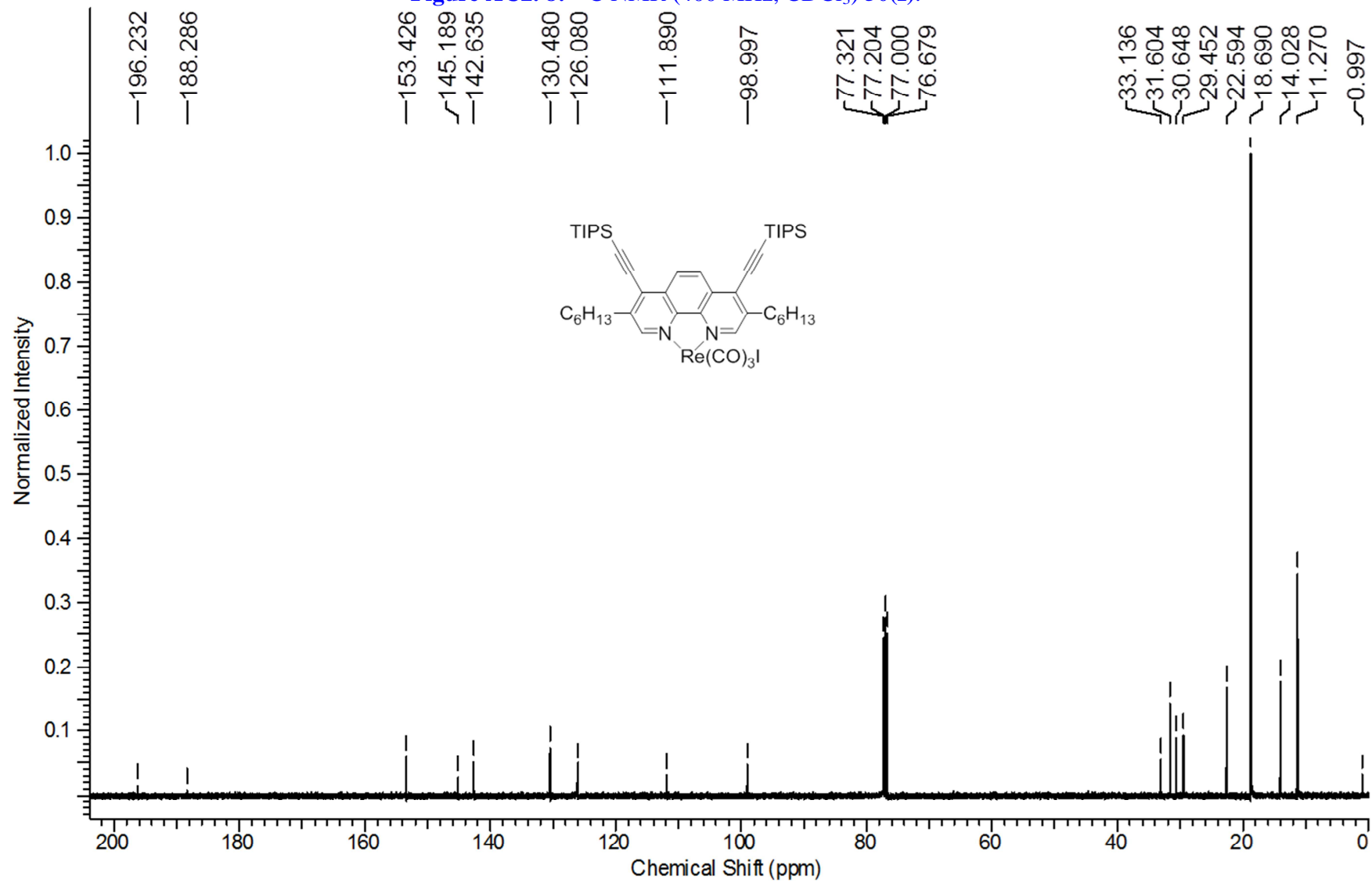
Figure AC2. 9: ^{1}H NMR (400 MHz, CDCl$_3$) **51**.
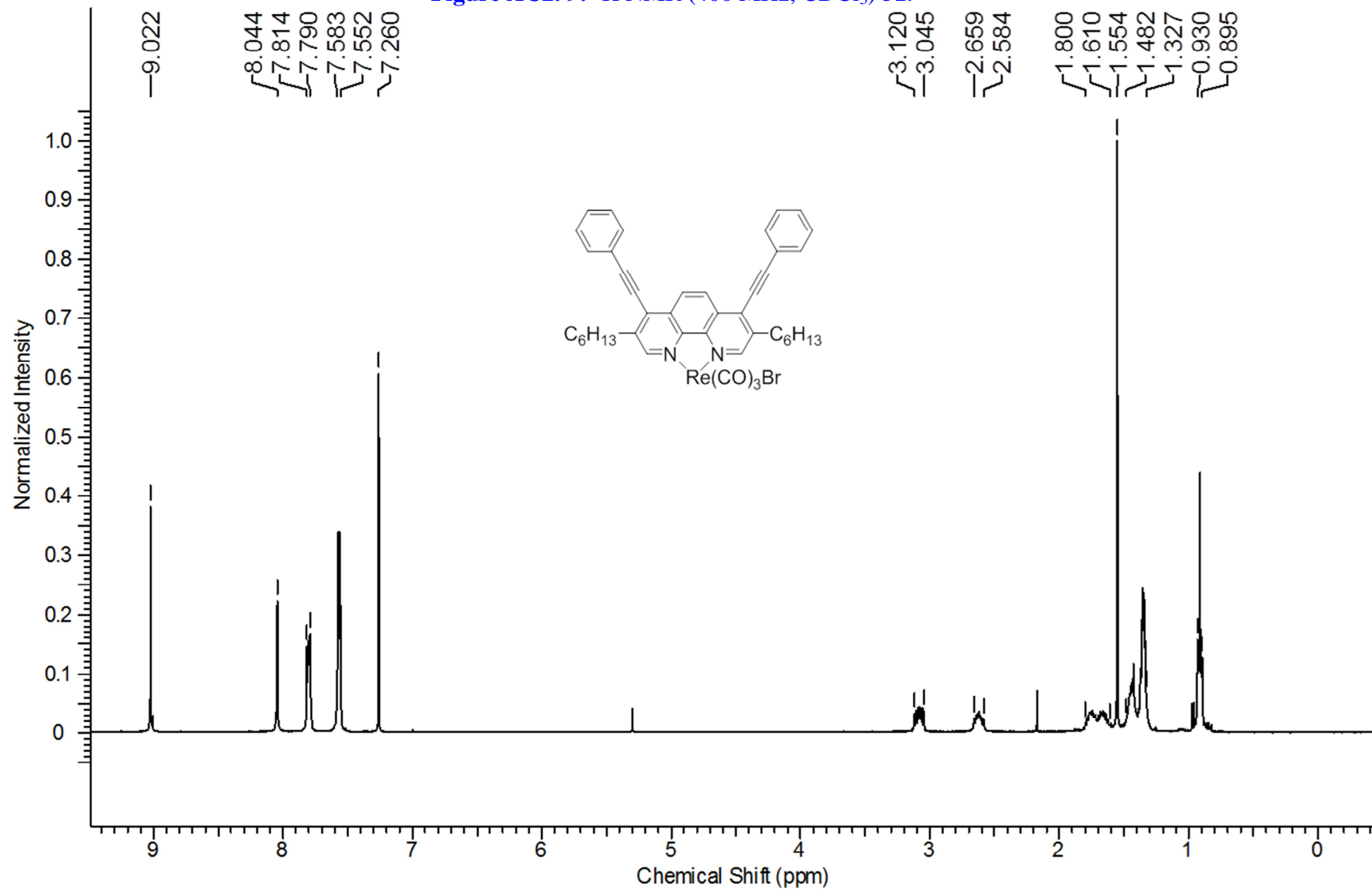
Figure AC2. 10: ^{13}C NMR (400 MHz, CDCl$_3$) **51**.

Figure AC2. 11: ^{1}H NMR (400 MHz, CDCl$_3$) **52**.
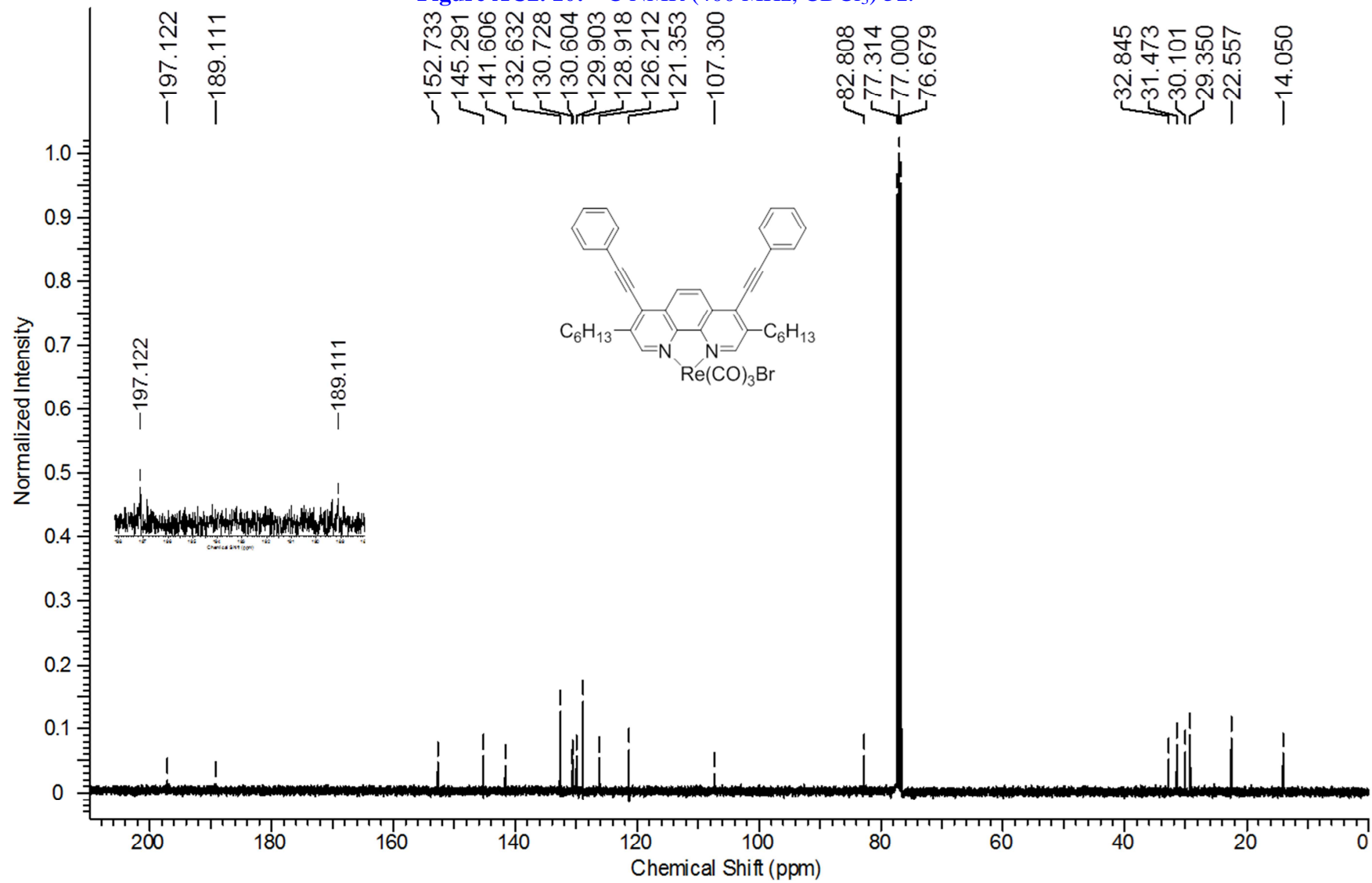
Figure AC2. 12: ^{13}C NMR (400 MHz, CDCl$_3$) **52**.

240
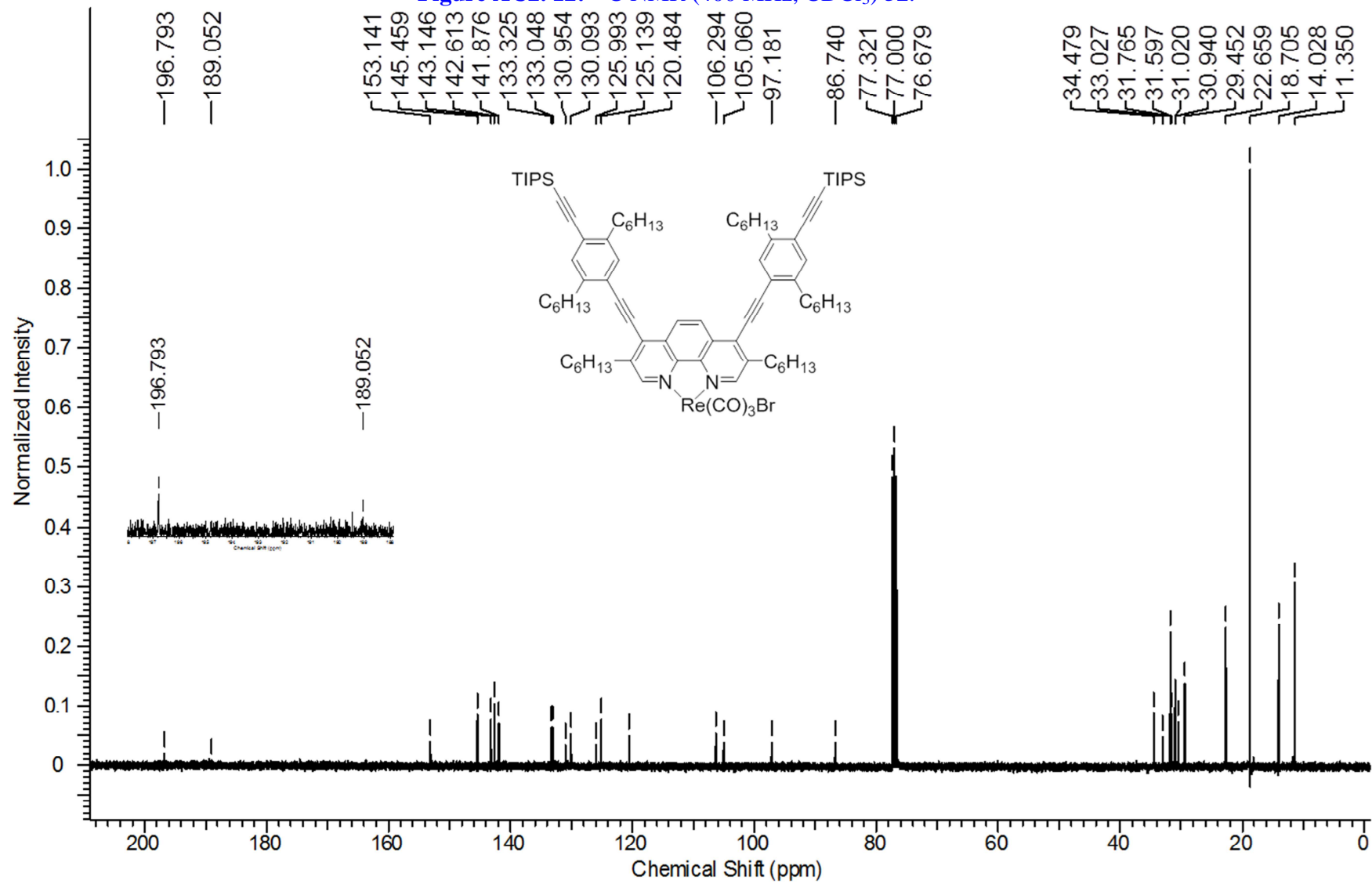
Figure AC2. 13: ^{1}H NMR (400 MHz, CDCl$_3$) **52(I)**.
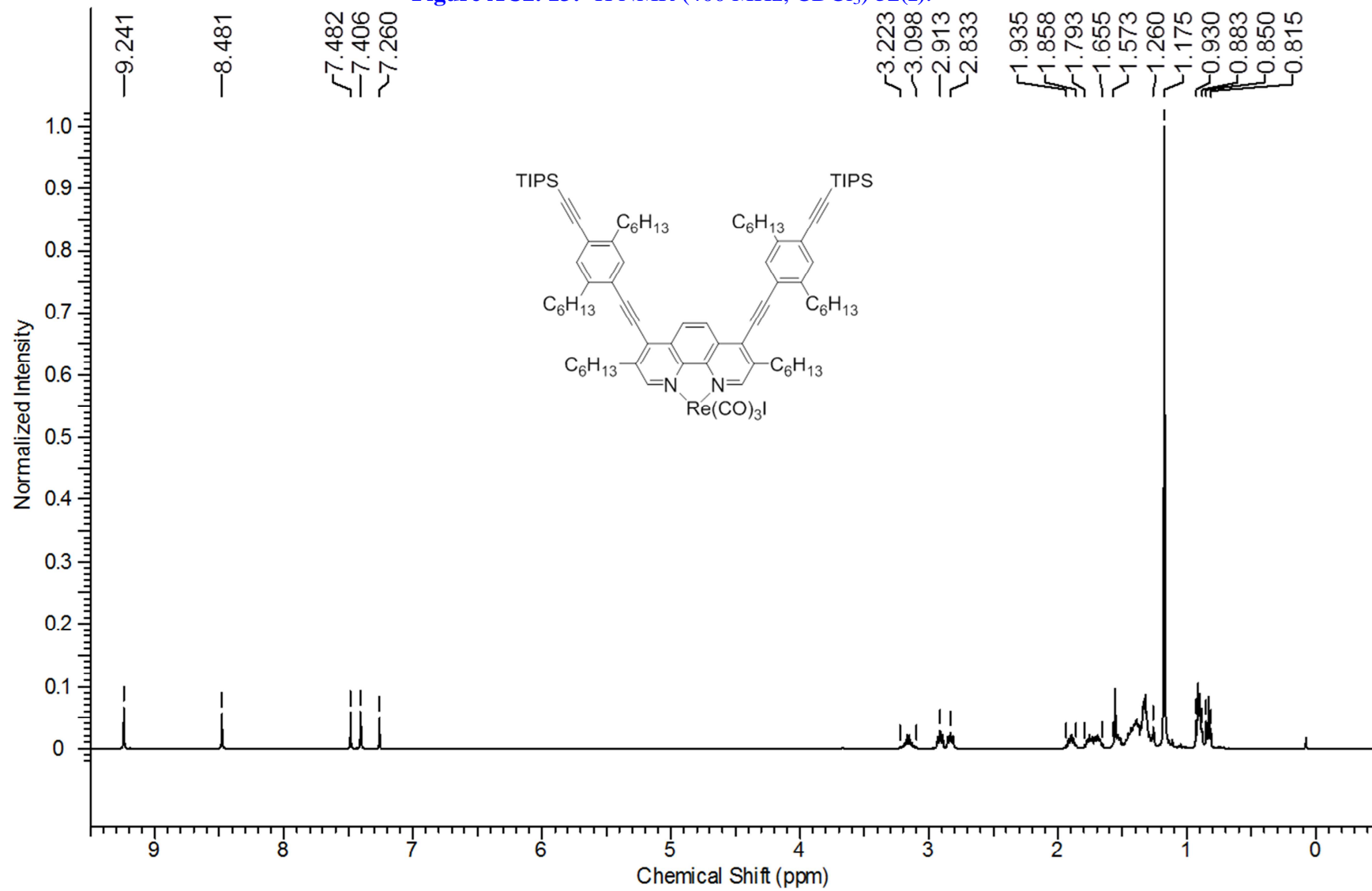
Figure AC2. 14: ^{13}C NMR (400 MHz, CDCl$_3$) **52(I).**

9.209
9.104
8.518
8.495
8.412
8.389
7.477
7.411
7.260
3.235
3.030
2.914
2.835
1.938
1.658
1.583
1.298
1.176
0.961
0.870

243
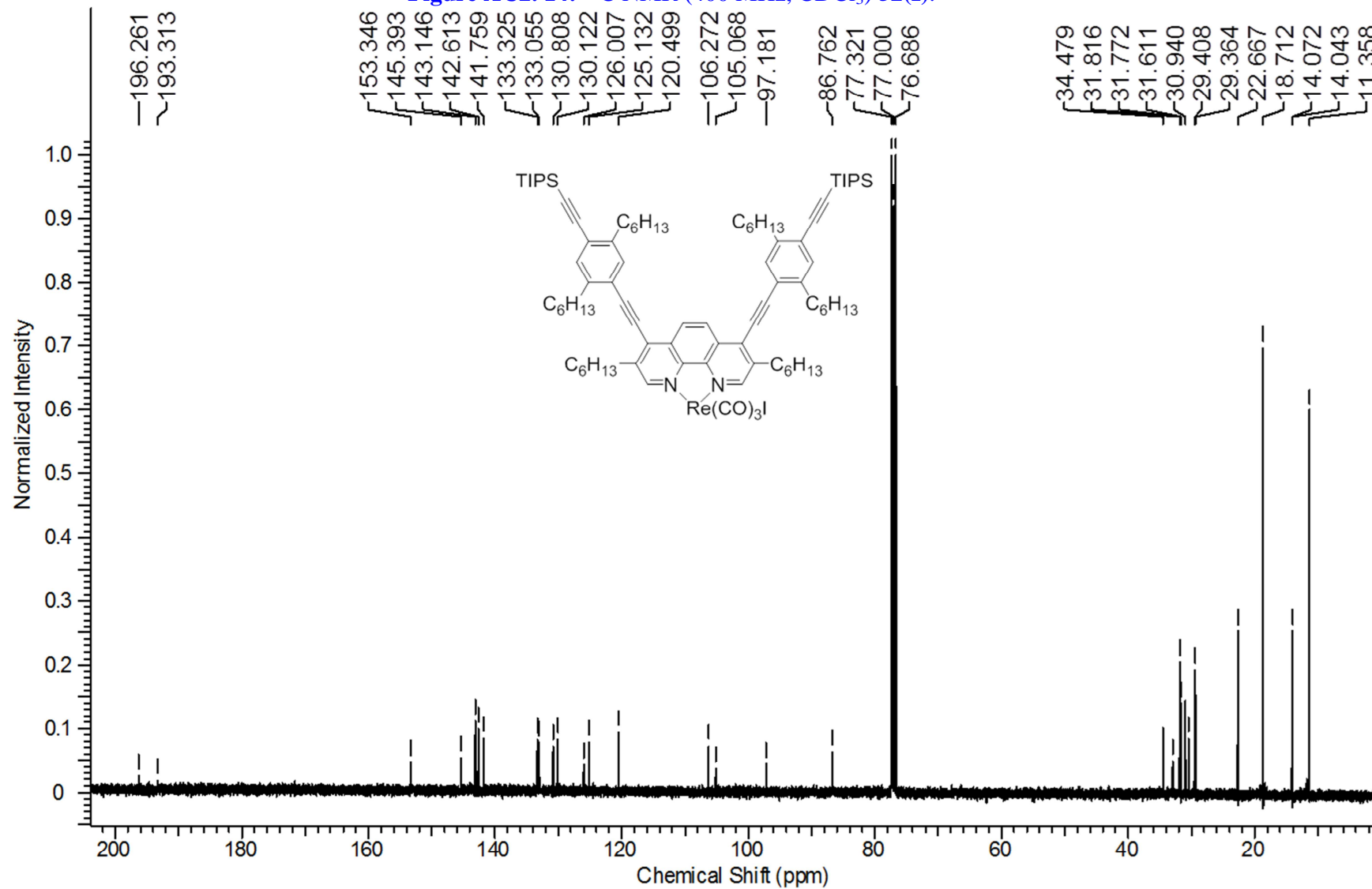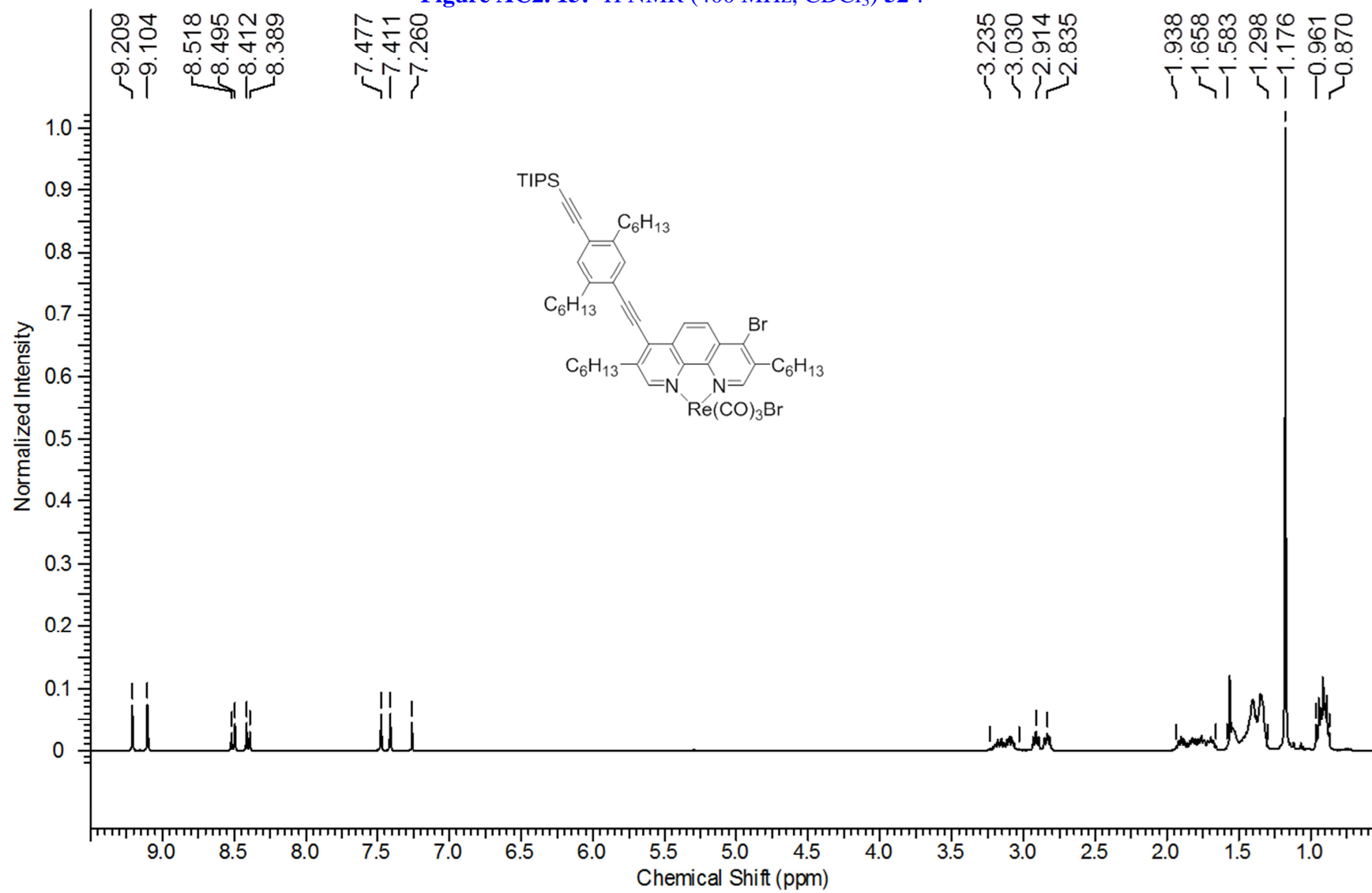
Figure AC2. 16: ^{13}C NMR (400 MHz, CDCl$_3$) **52'**.
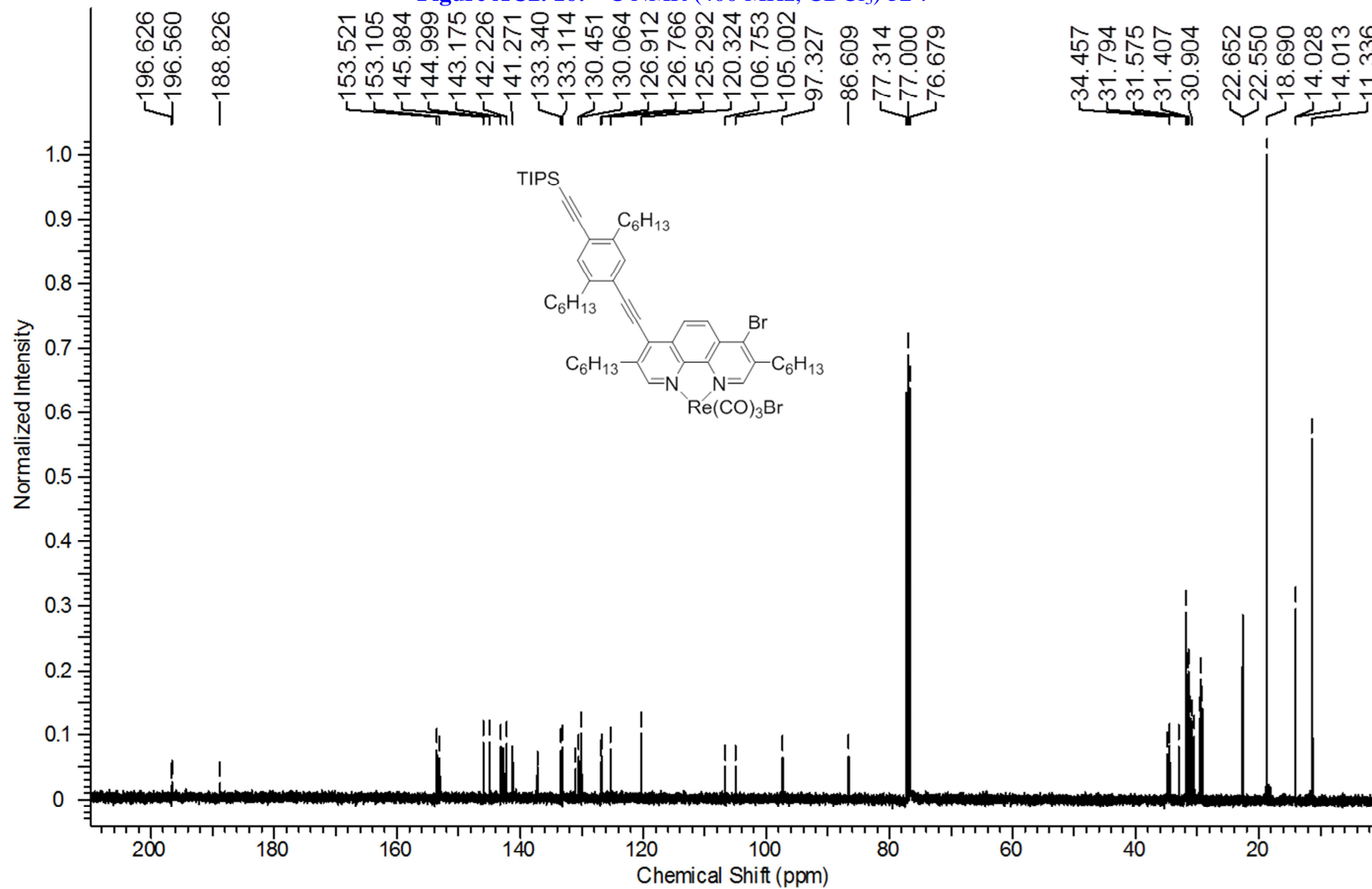
Figure AC2. 17: ^{13}C NMR-APT (400 MHz, CDCl$_3$) **54**.
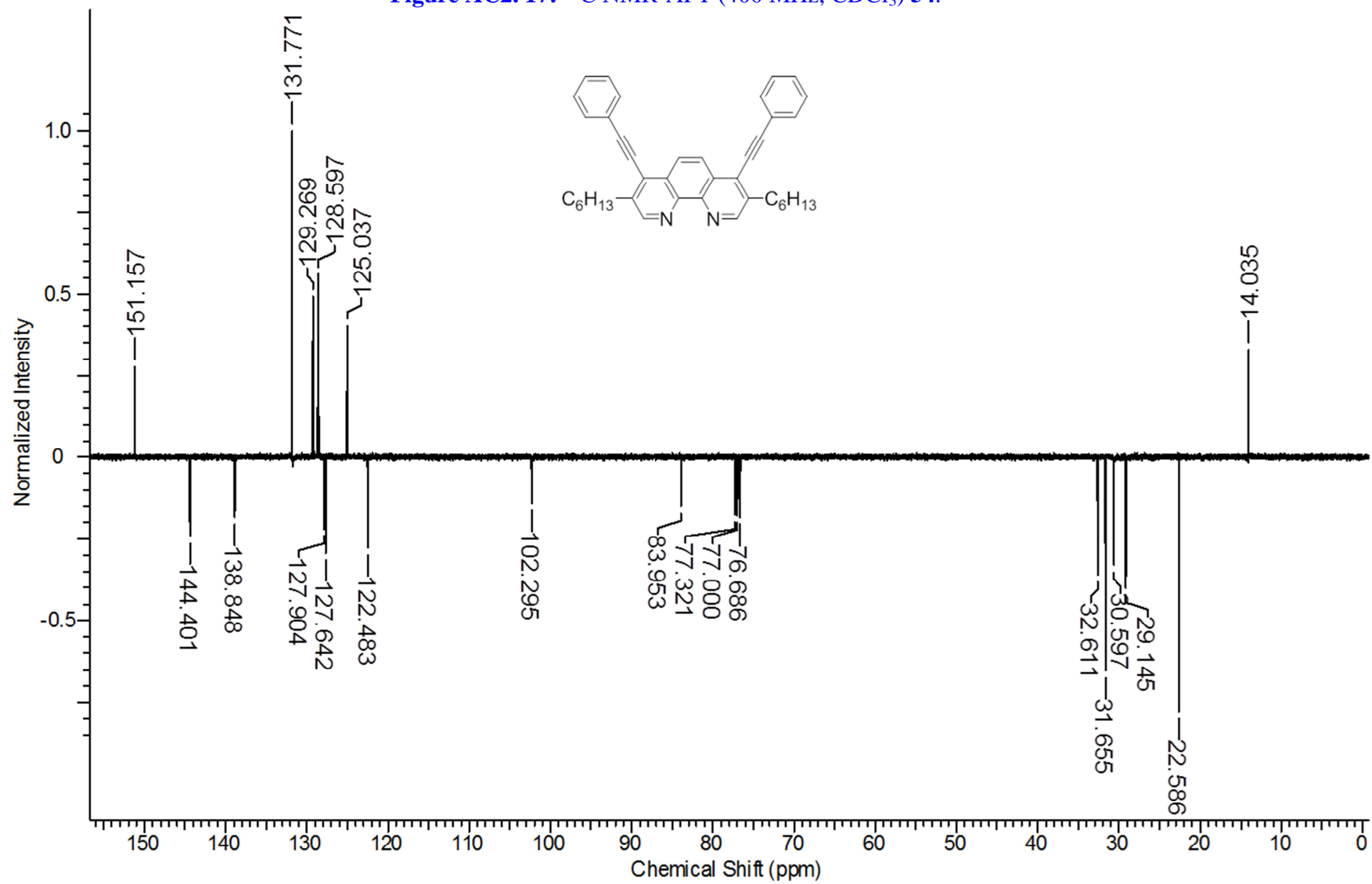
Figure AC2. 18: ^{13}C NMR-APT (400 MHz, CDCl$_3$) **55**.
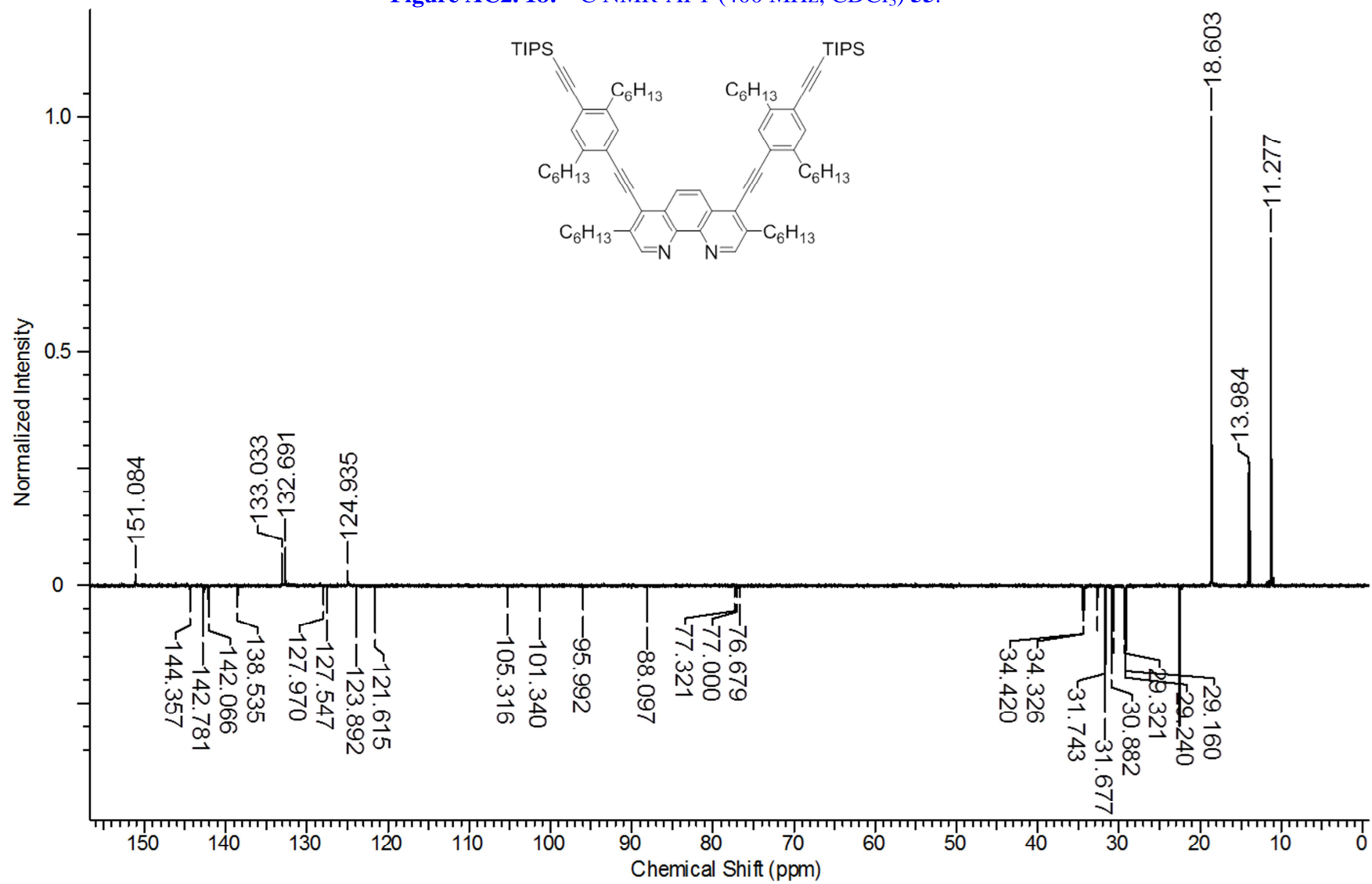
Figure AC2. 19: ^{13}C NMR-APT (400 MHz, CDCl$_3$) **51**.
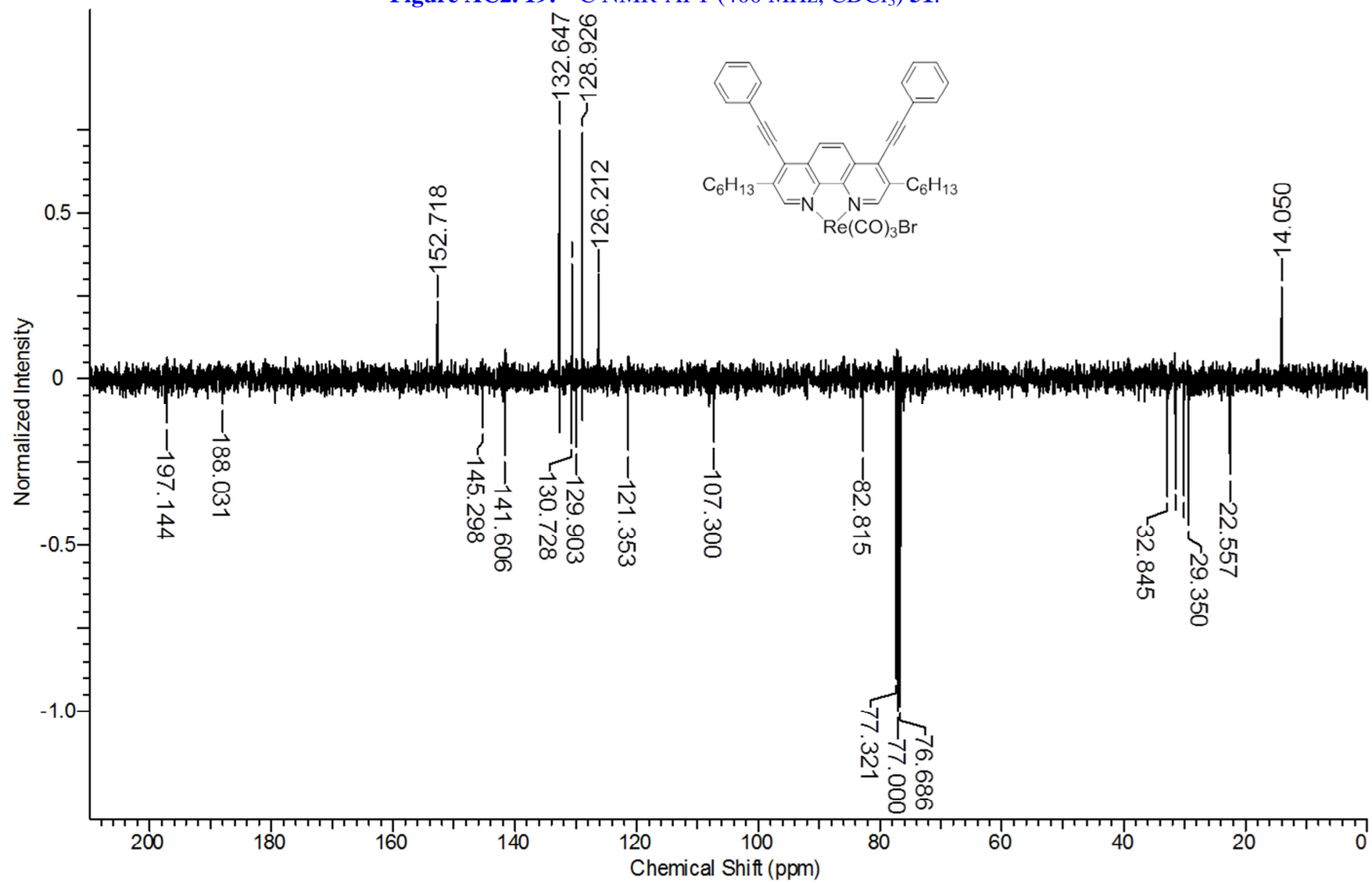
Figure AC2. 20: ^{13}C NMR-APT (400 MHz, CDCl$_3$) **52**.
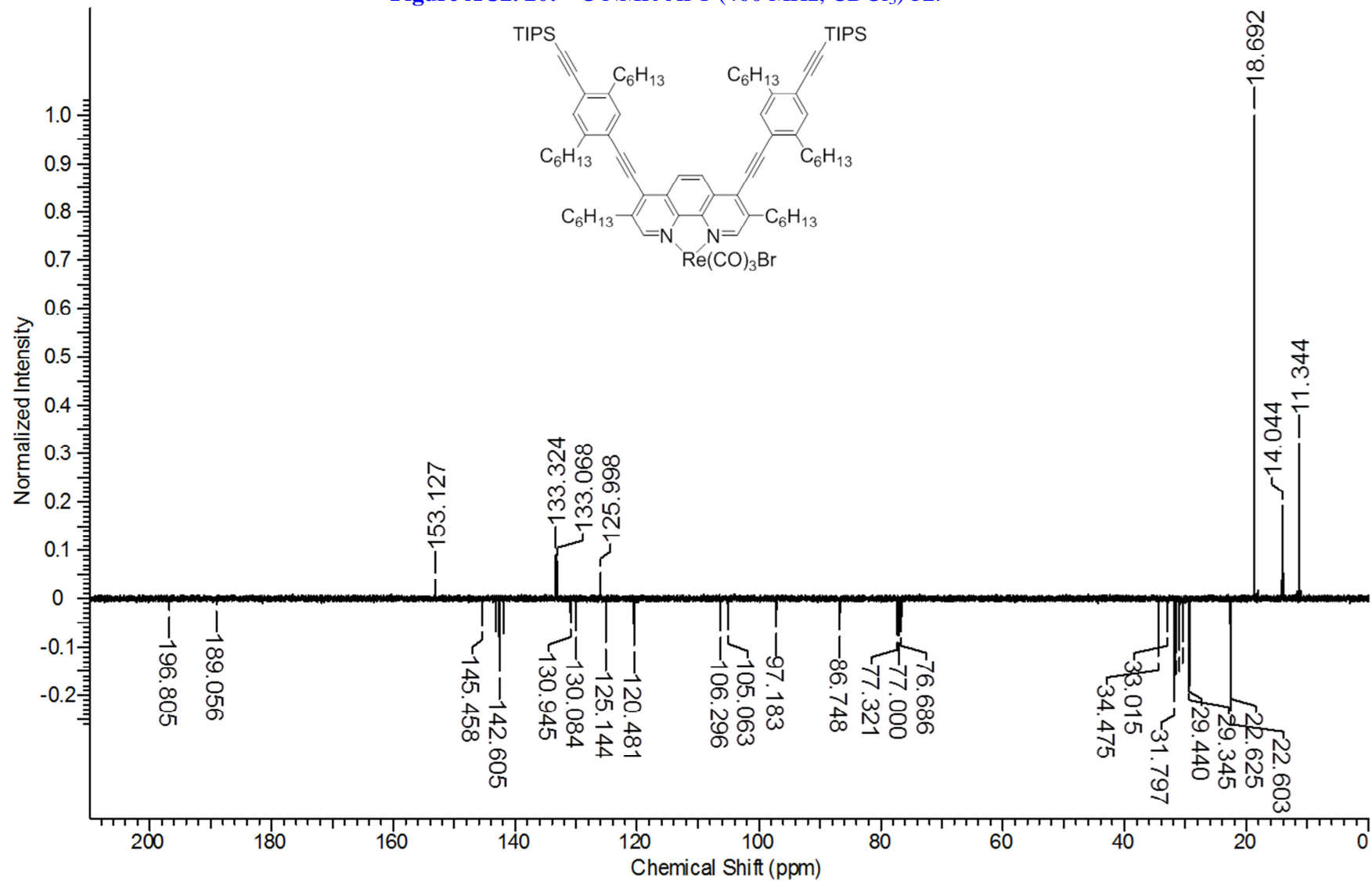
Figure AC2. 21: ^{1}H NMR-COSY (400 MHz, CDCl₃) **51**.
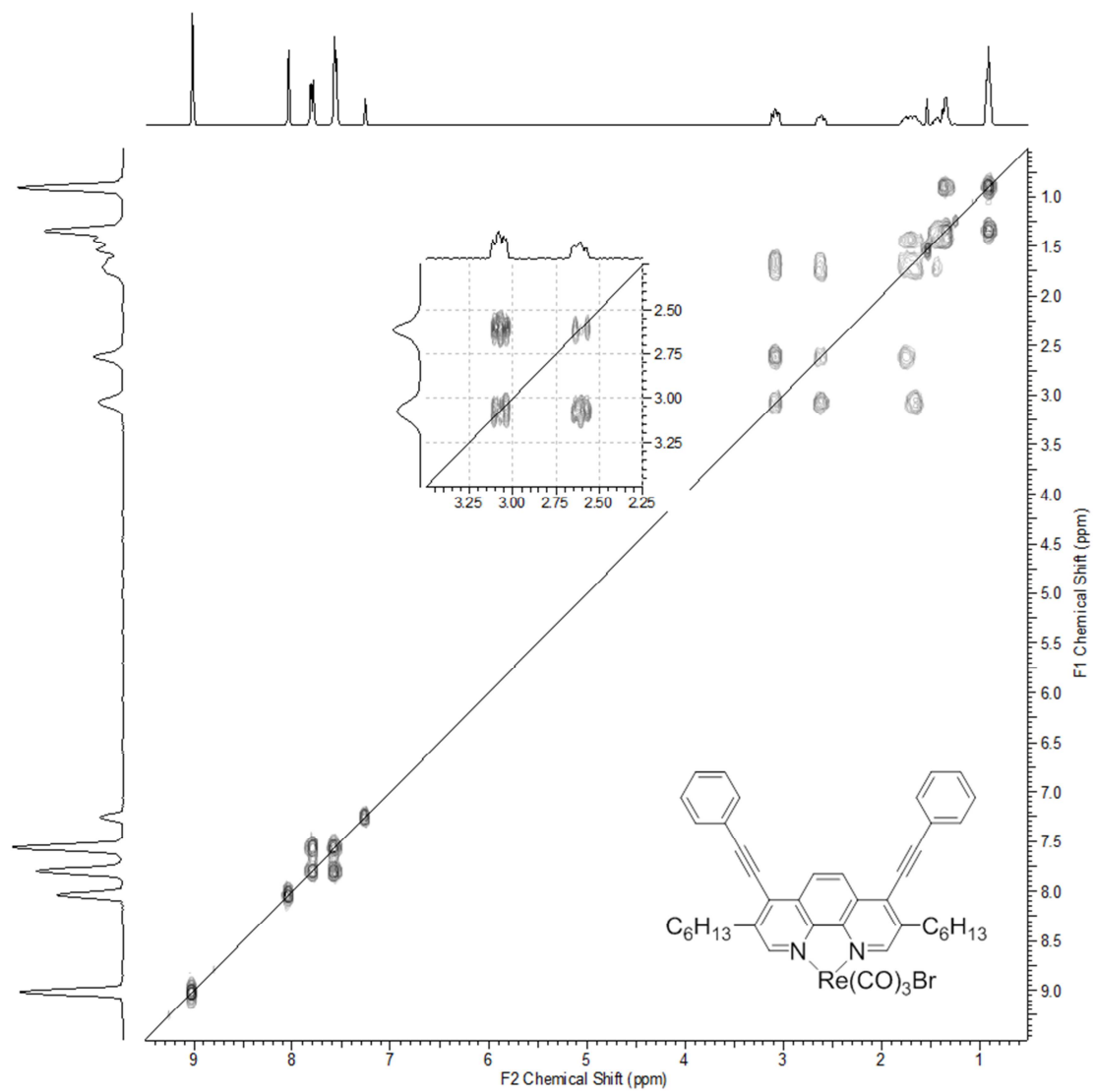
Appendix Chapter 4

Figure AC4. 1: ^{1}H NMR (300 MHz, CDCl$_3$) of Compound **112**.

Figure AC4. 2: ^{13}C NMR (400 MHz, CDCl$_3$) of Compound **112**.

Figure AC4. 3: ^{1}H NMR (300 MHz, CDCl$_3$) of Compound **114**.
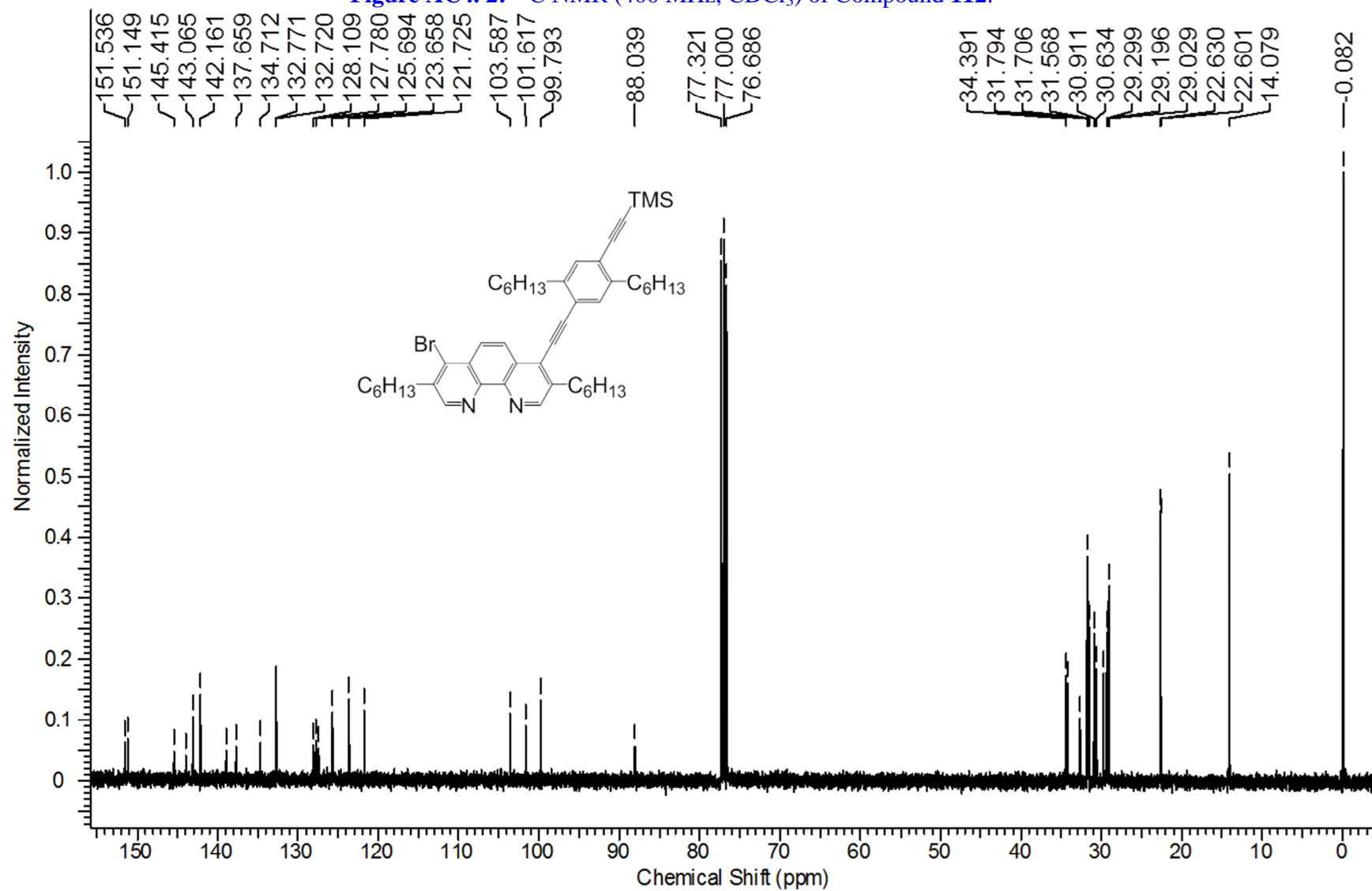
Figure AC4. 4: ^{13}C NMR (400 MHz, CDCl$_3$) of Compound **114**.
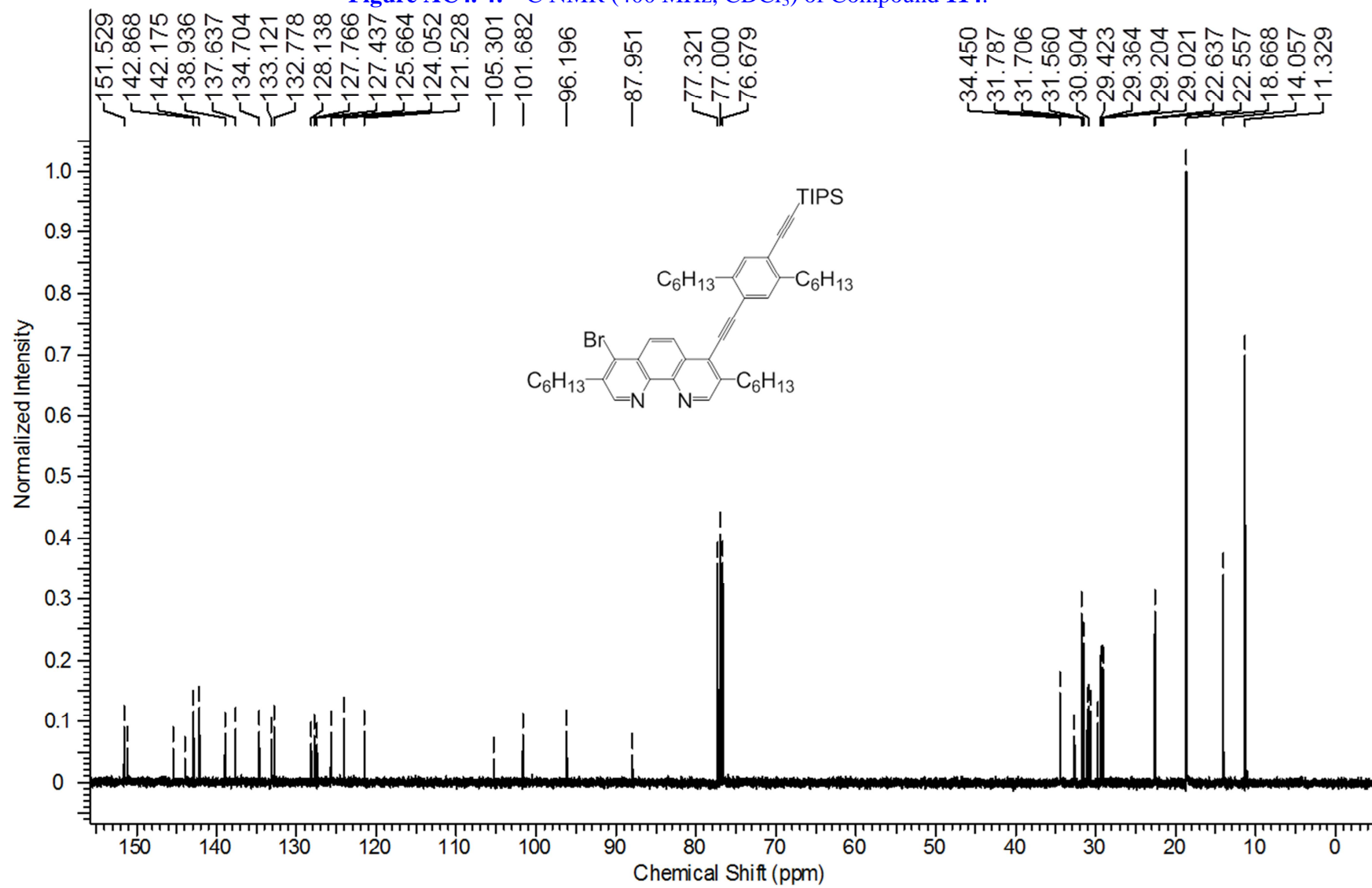
Figure AC4. 5: ^{1}H NMR (300 MHz, CDCl$_3$) of Compound **115**.

255

Figure AC4. 6: ^{13}C NMR (400 MHz, CDCl$_3$) of Compound **115**.

Figure AC4. 7: ^{1}H NMR (300 MHz, CDCl$_3$) of Compound **116**.

257
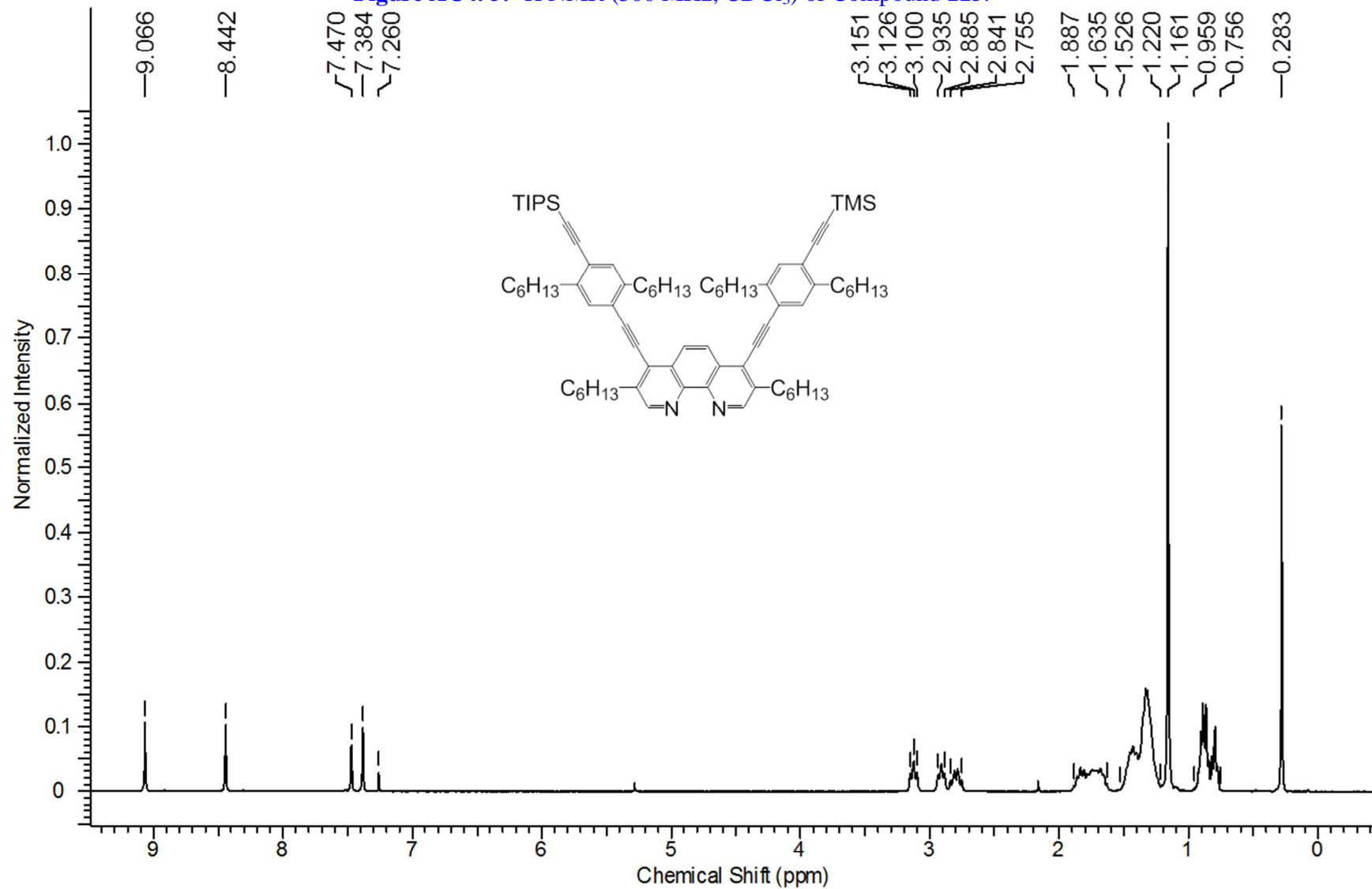
Figure AC4. 8: ^{13}C NMR (400 MHz, CDCl$_3$) of Compound **116**.
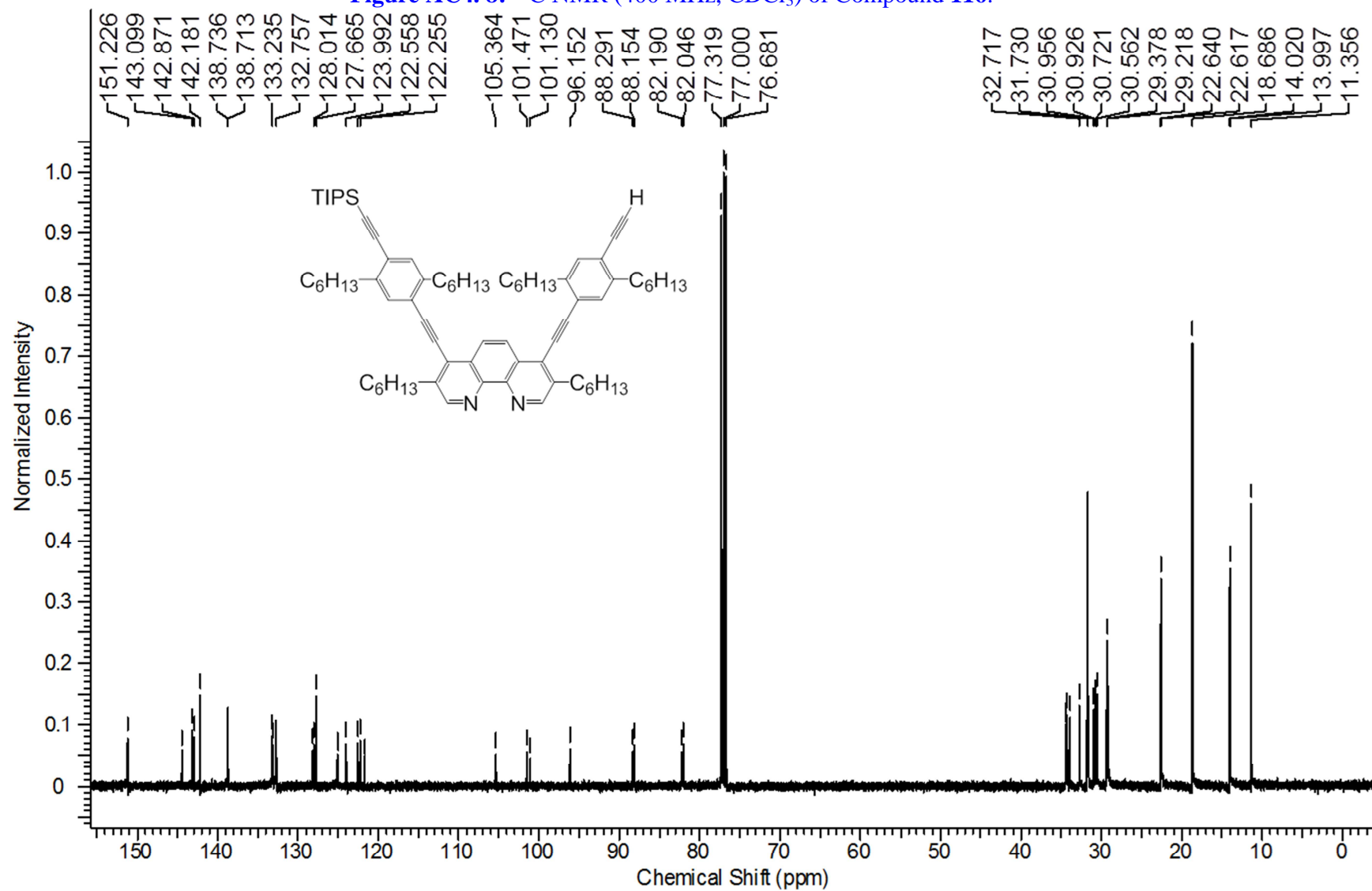
Figure AC4. 9: ^{1}H NMR (300 MHz, CDCl$_3$) of Compound **117**.

Figure AC4. 10: ^{13}C NMR (400 MHz, CDCl$_3$) of Compound **117**.
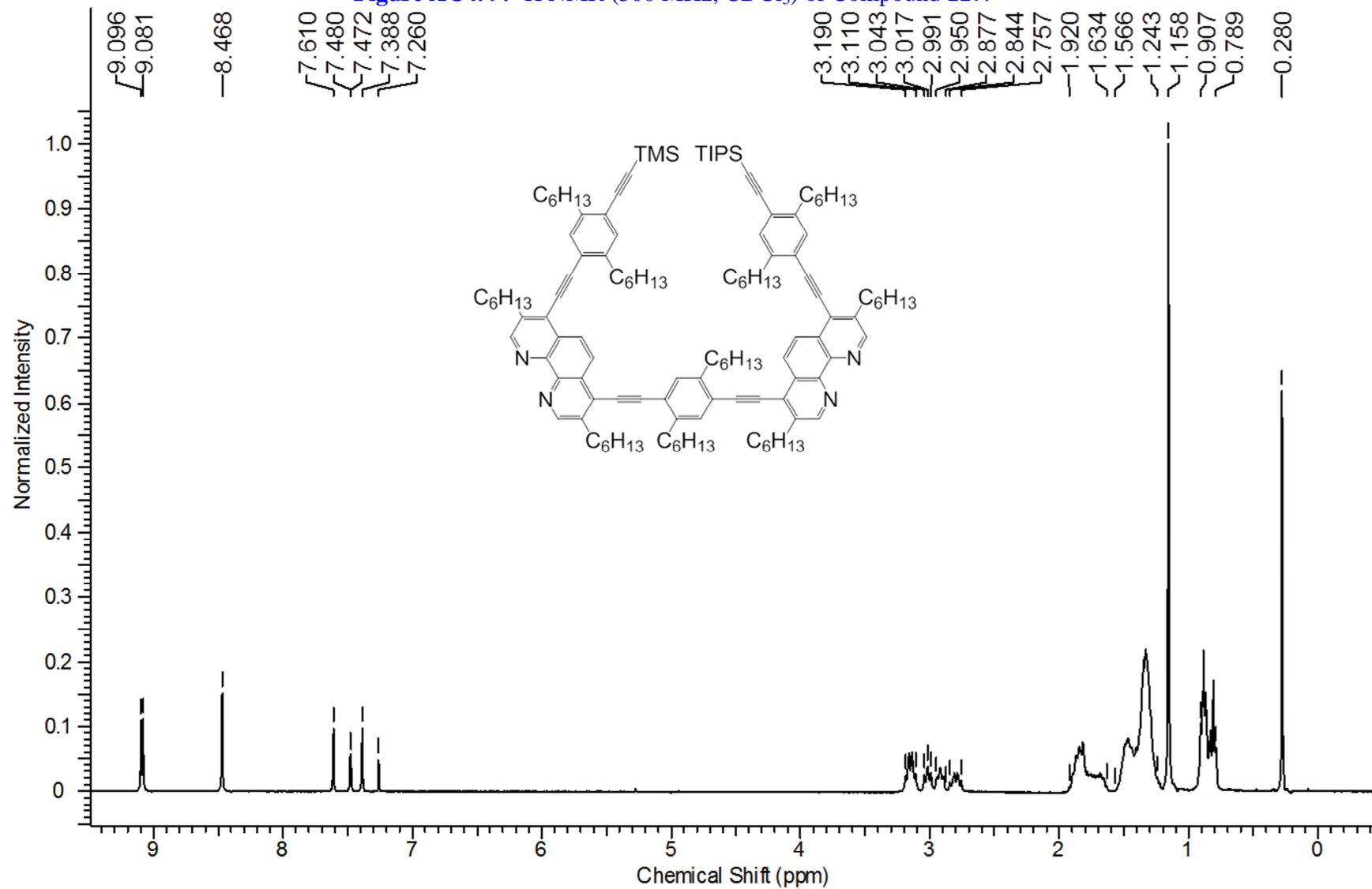
Figure AC4. 11: ^{1}H NMR (300 MHz, CDCl$_3$) of Compound 118.
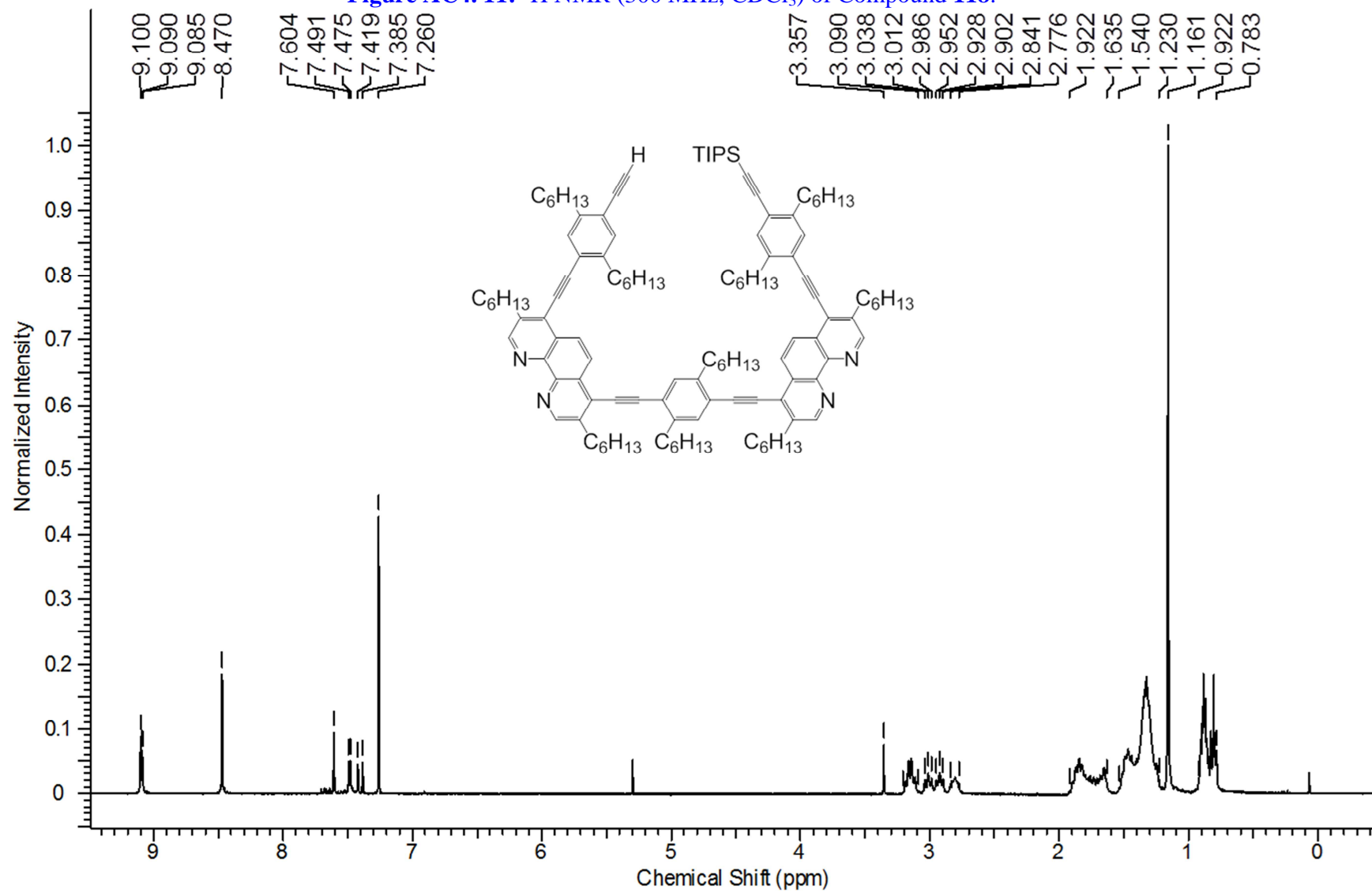
Figure AC4. 12: ^{13}C NMR (400 MHz, CDCl$_3$) of Compound **118**.
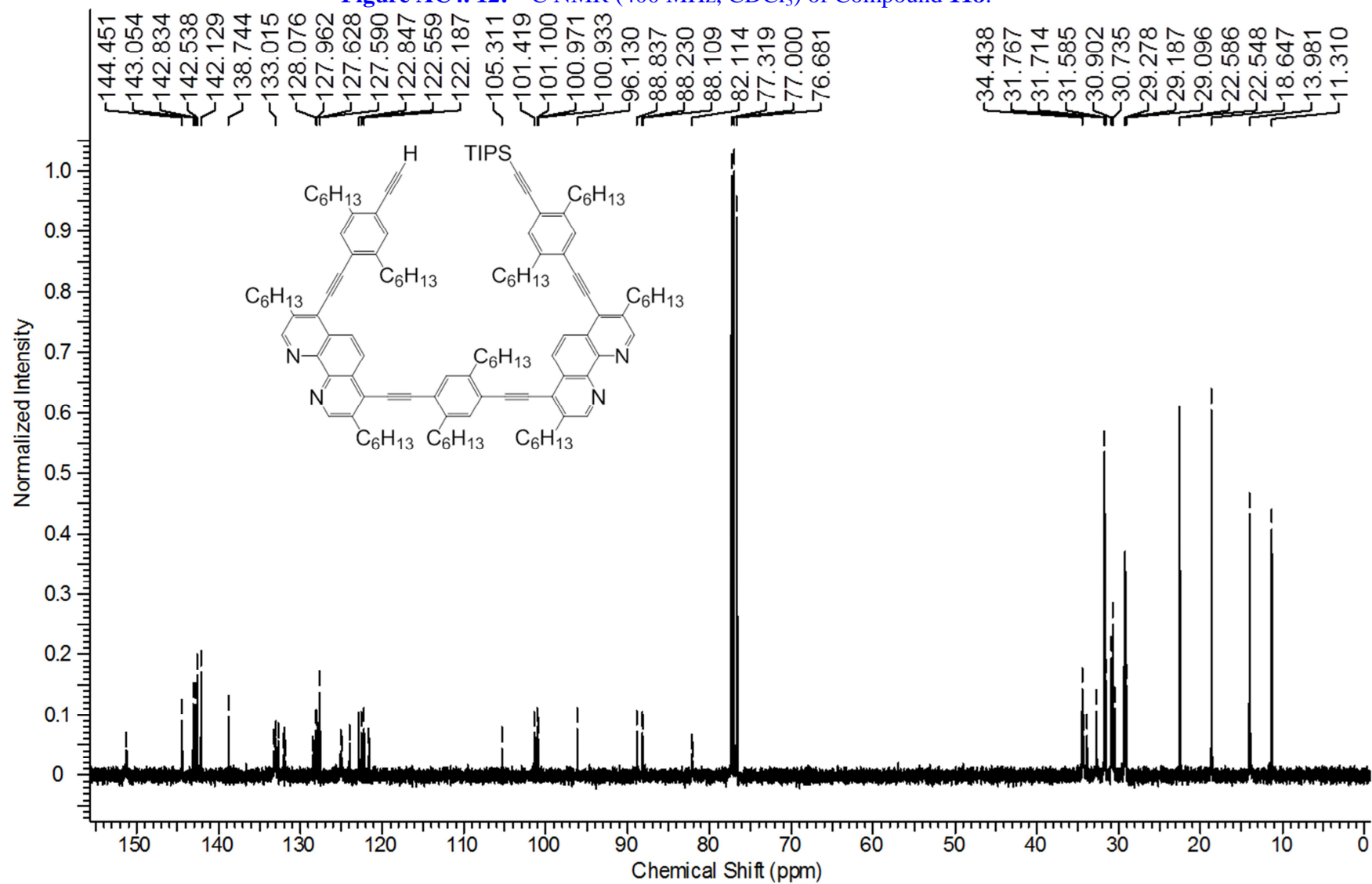
Figure AC4. 13: ^{1}H NMR (400 MHz, CDCl$_3$) of Compound **119**.
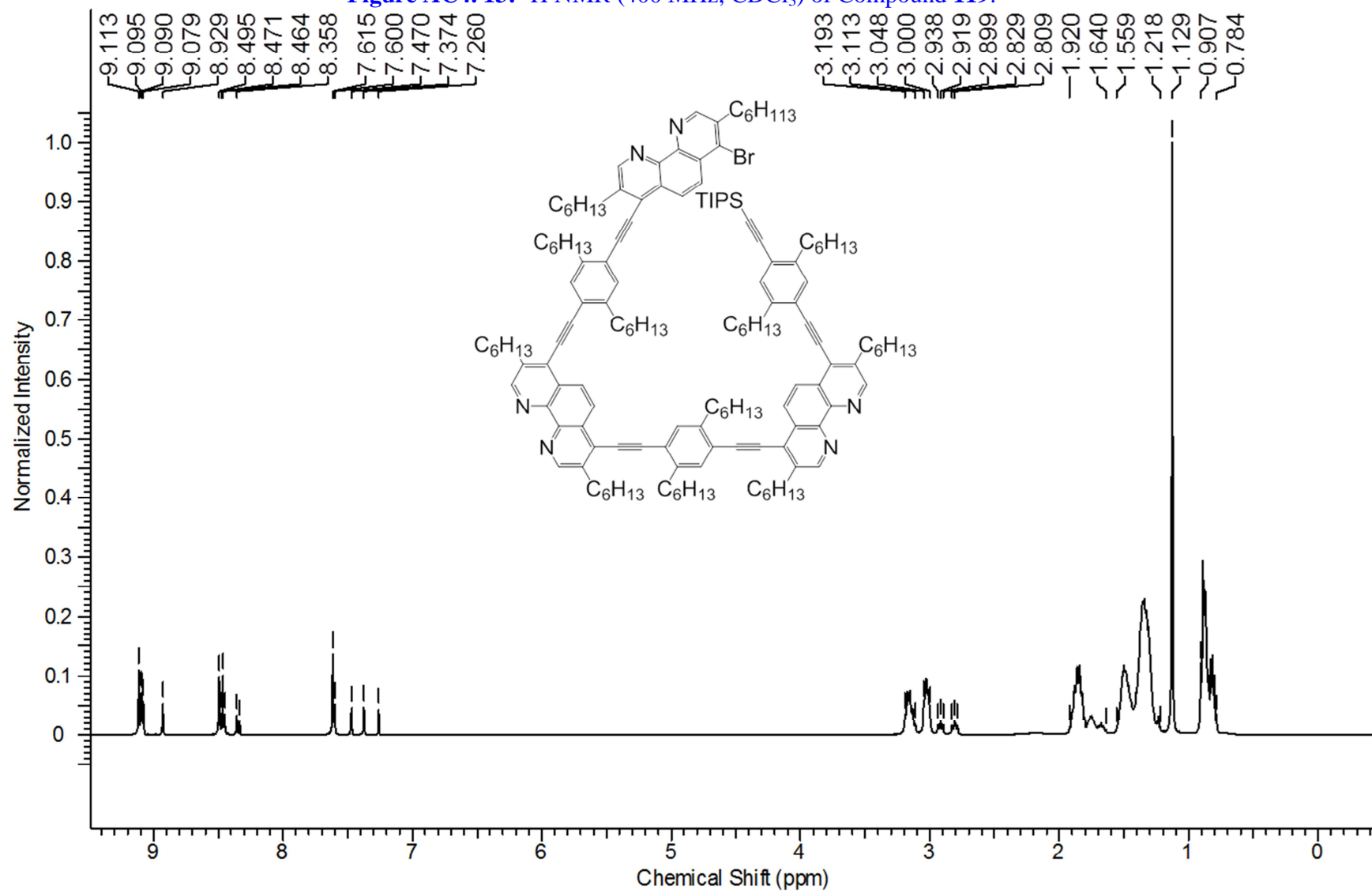
Figure AC4. 14: ^{13}C NMR (400 MHz, CDCl$_3$) of Compound **119**.
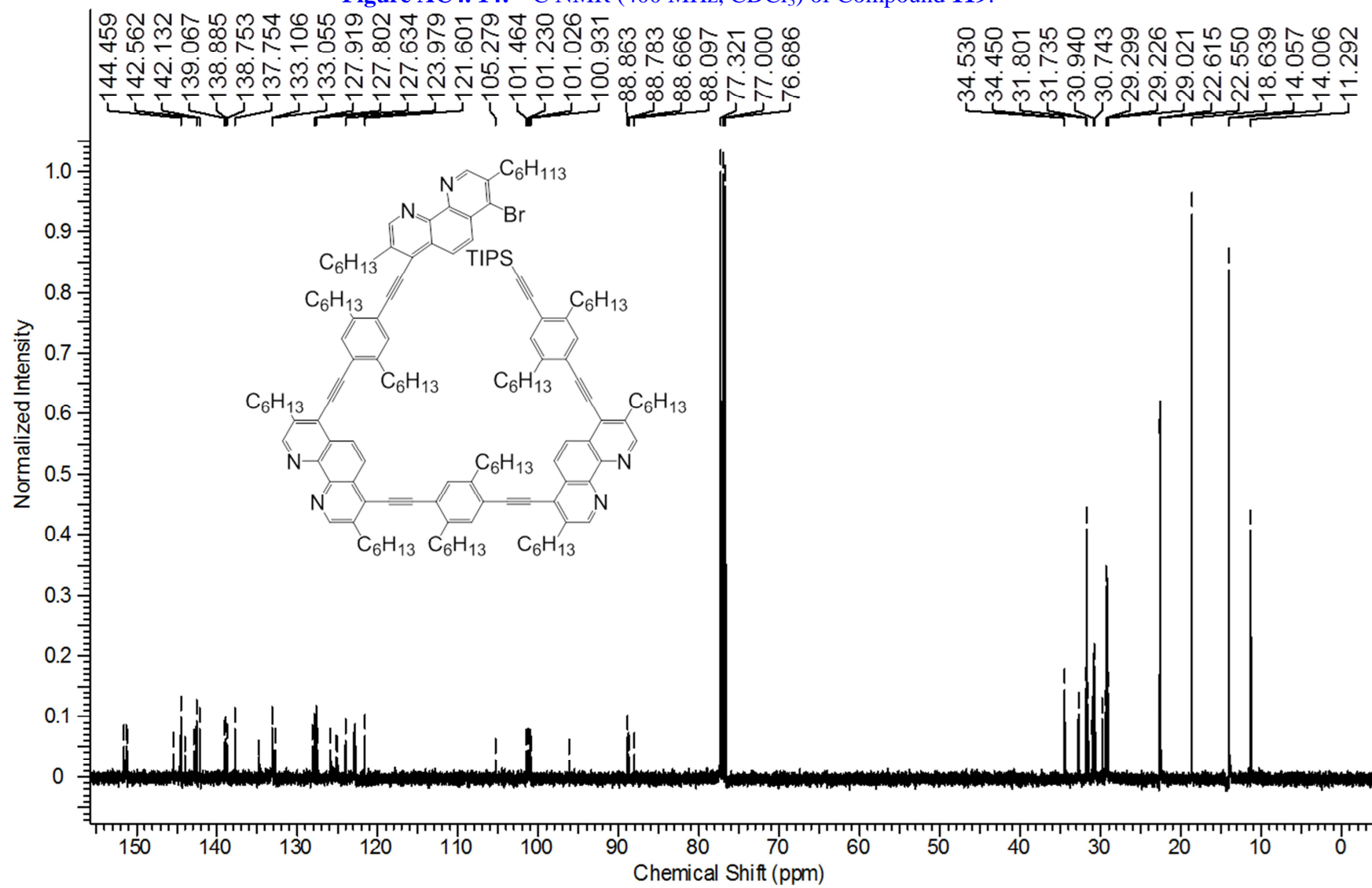
Figure AC4. 15: ^{1}H NMR (300 MHz, CDCl$_3$) of Compound **120**.
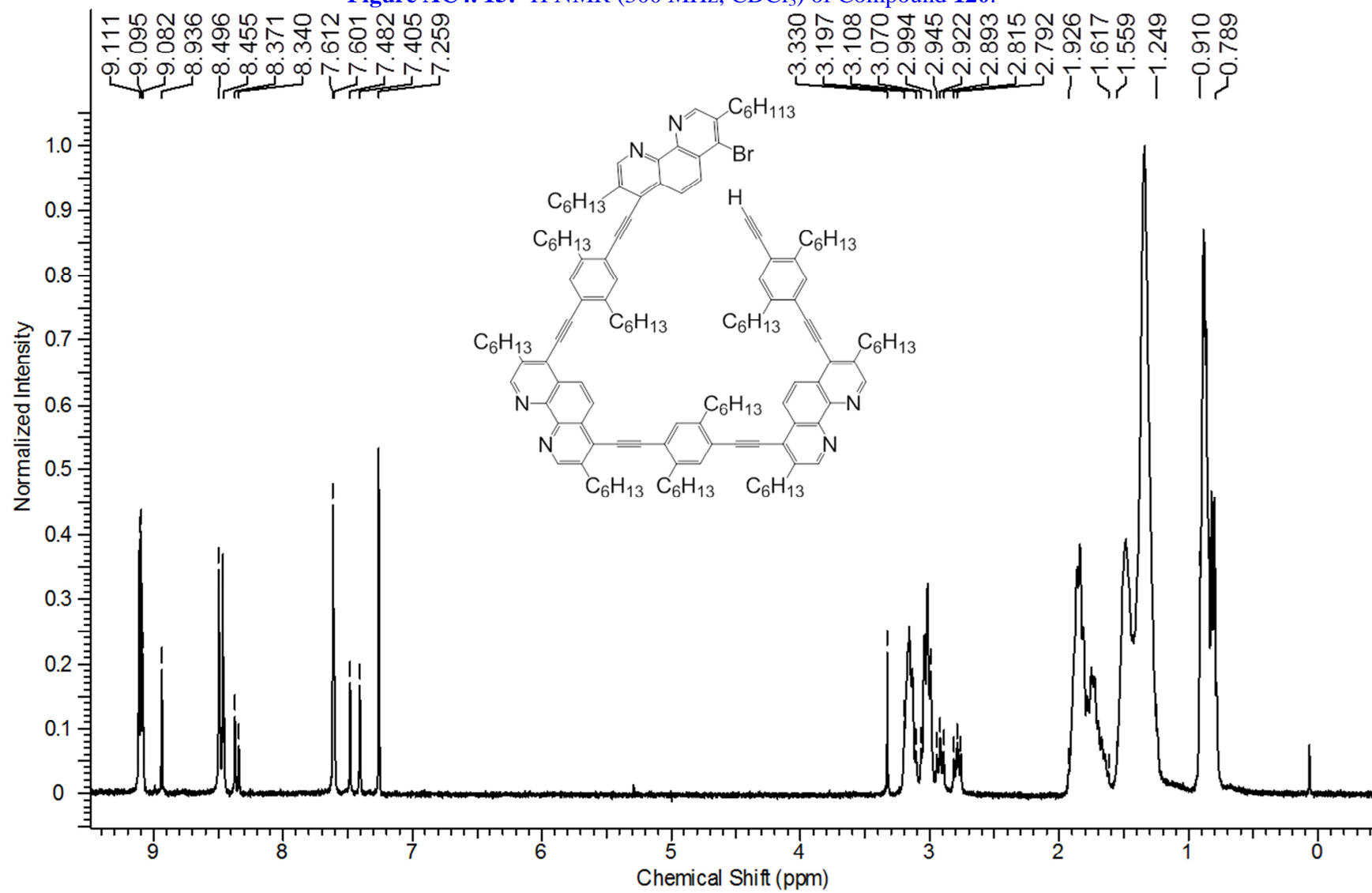
Figure AC4. 16: ^{13}C NMR (300 MHz, CDCl$_3$) of Compound **120**.
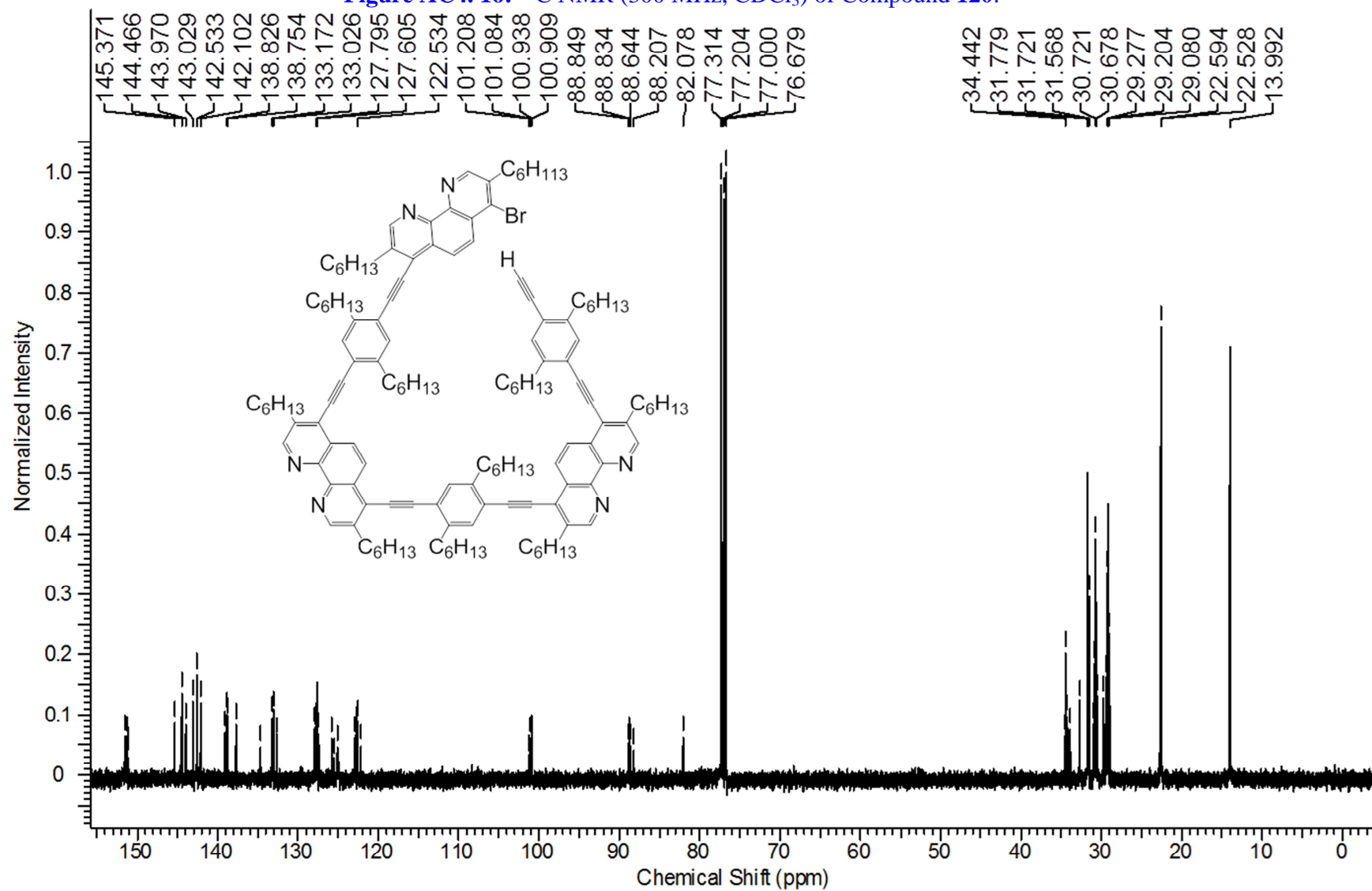
Figure AC4. 17: ^{1}H NMR (300 MHz, CDCl$_3$) of Compound **32**.
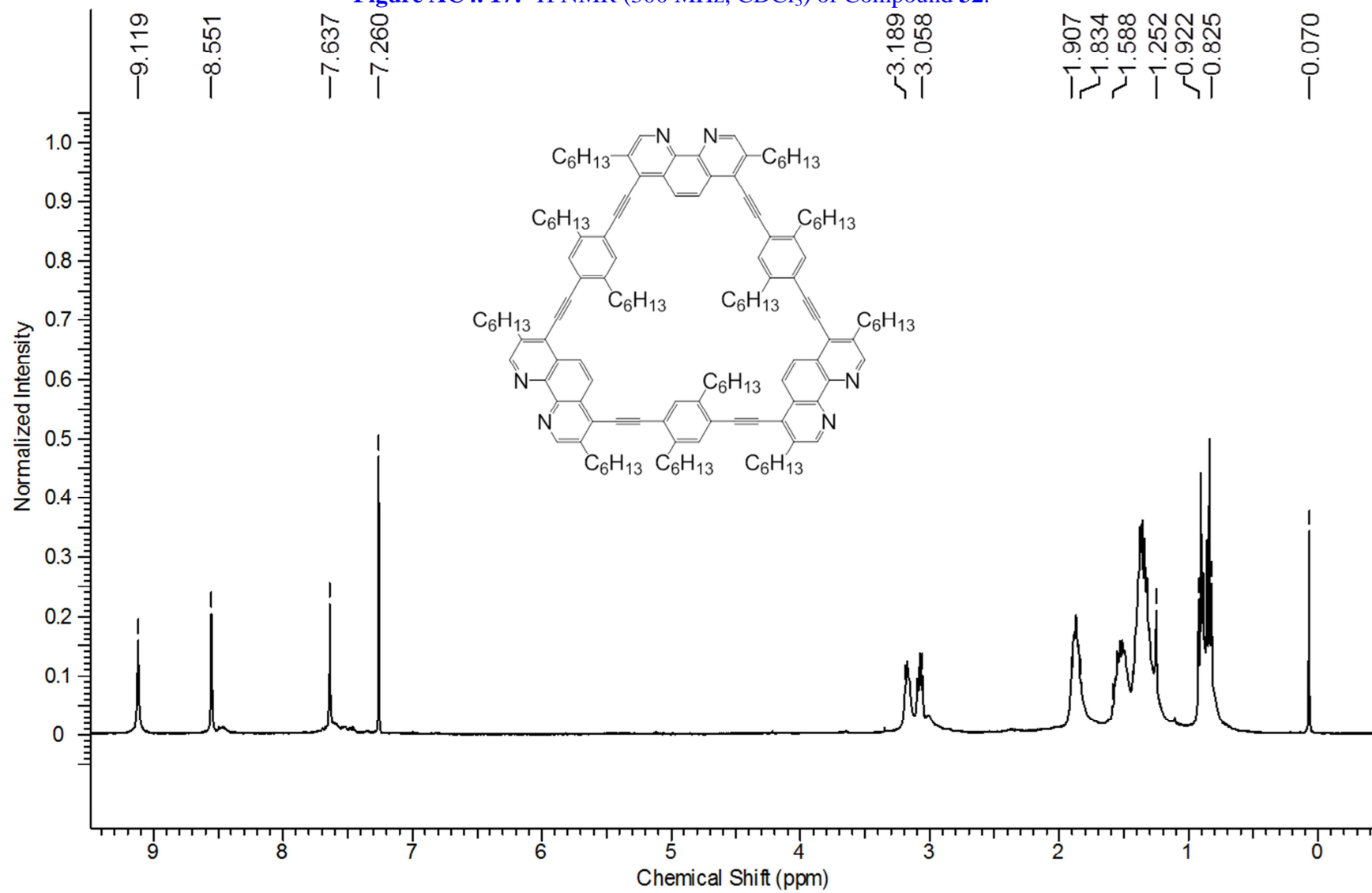
Figure AC4. 18: ^{13}C NMR (400 MHz, CDCl$_3$) of Compound **32**.
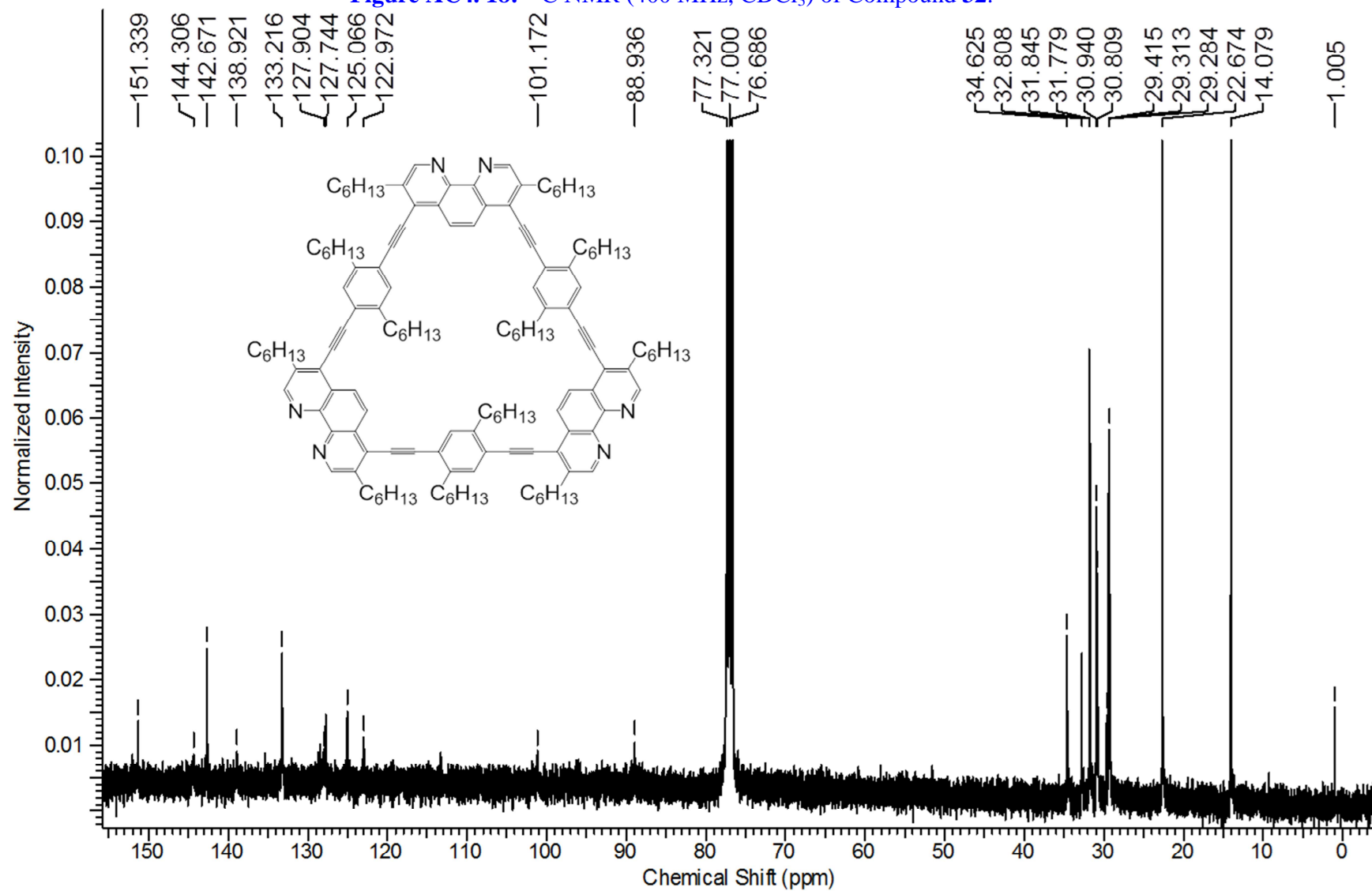
Figure AC4. 19: ^{1}H NMR (300 MHz, CDCl$_3$) of Compound 122.
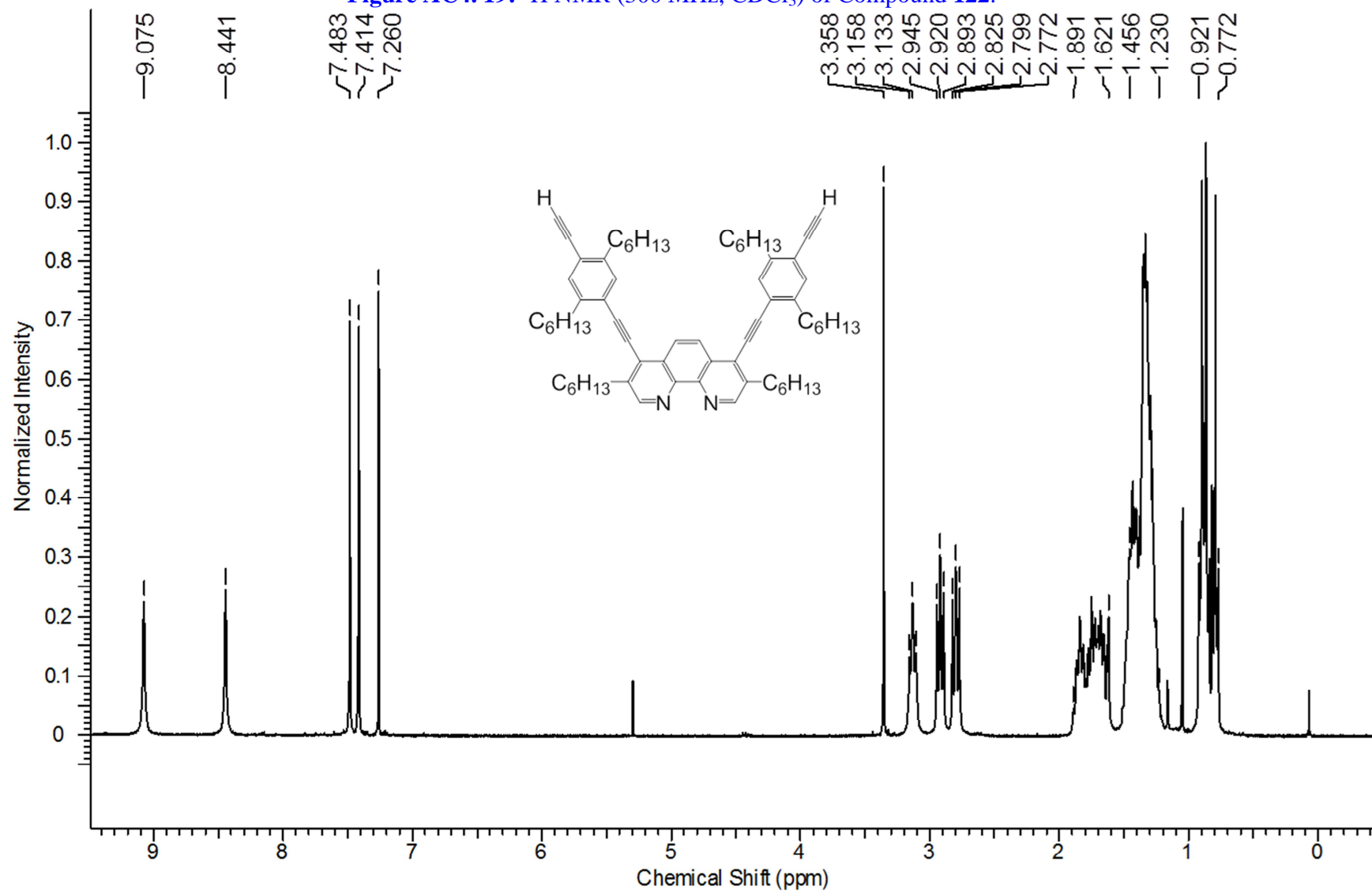
Figure AC4. 20: ^{13}C NMR (400 MHz, CDCl$_3$) of Compound **122**.
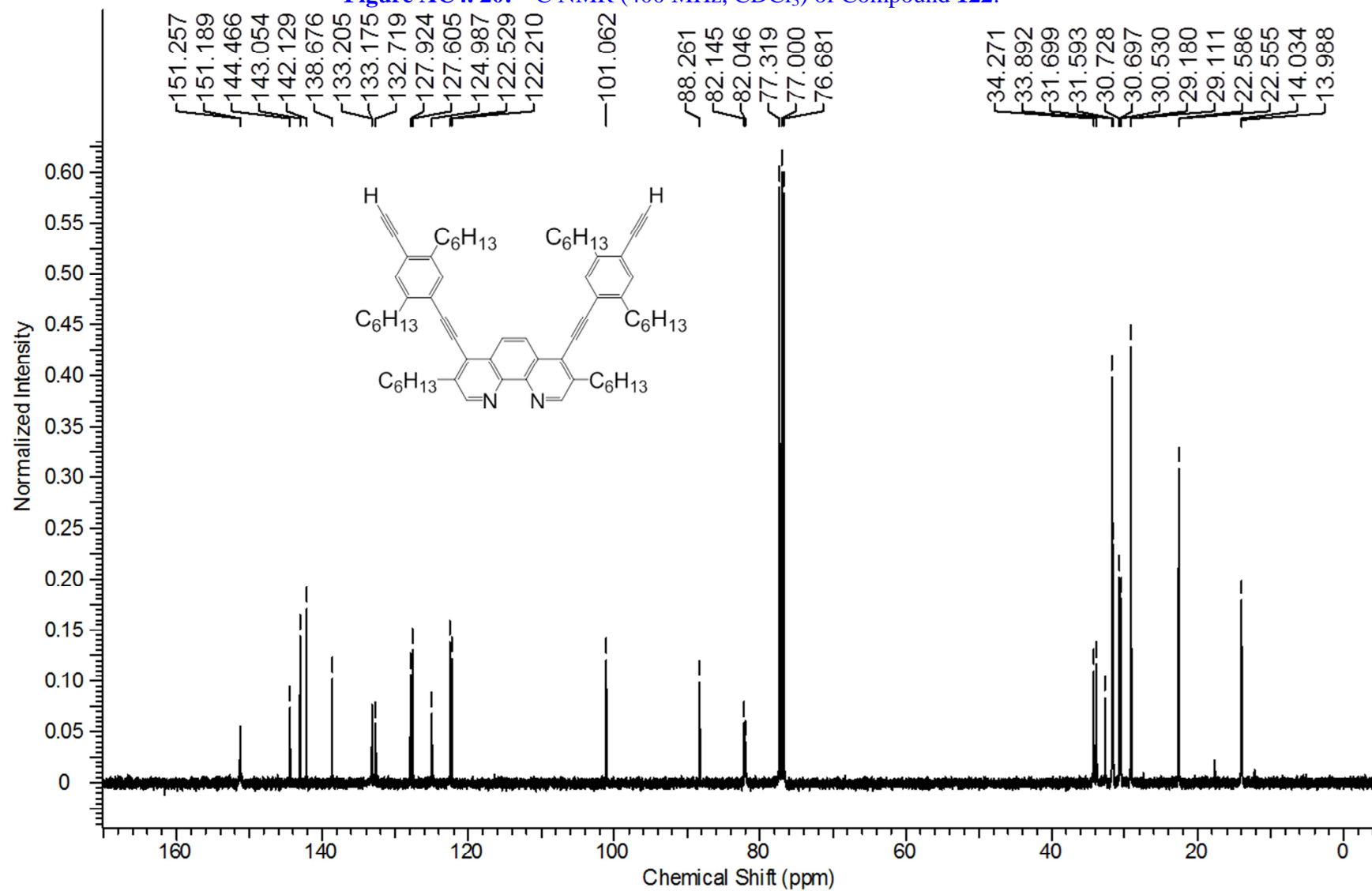
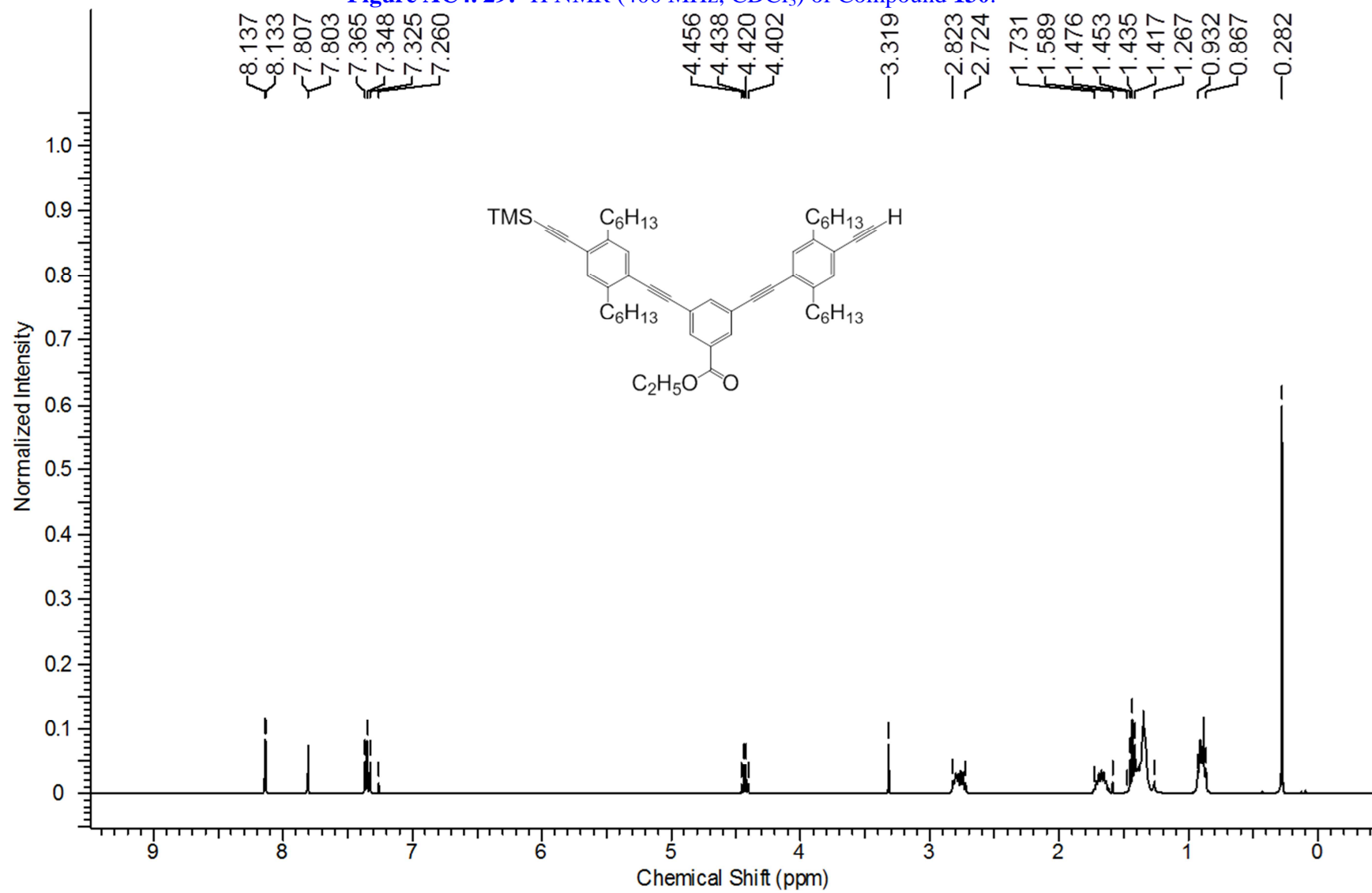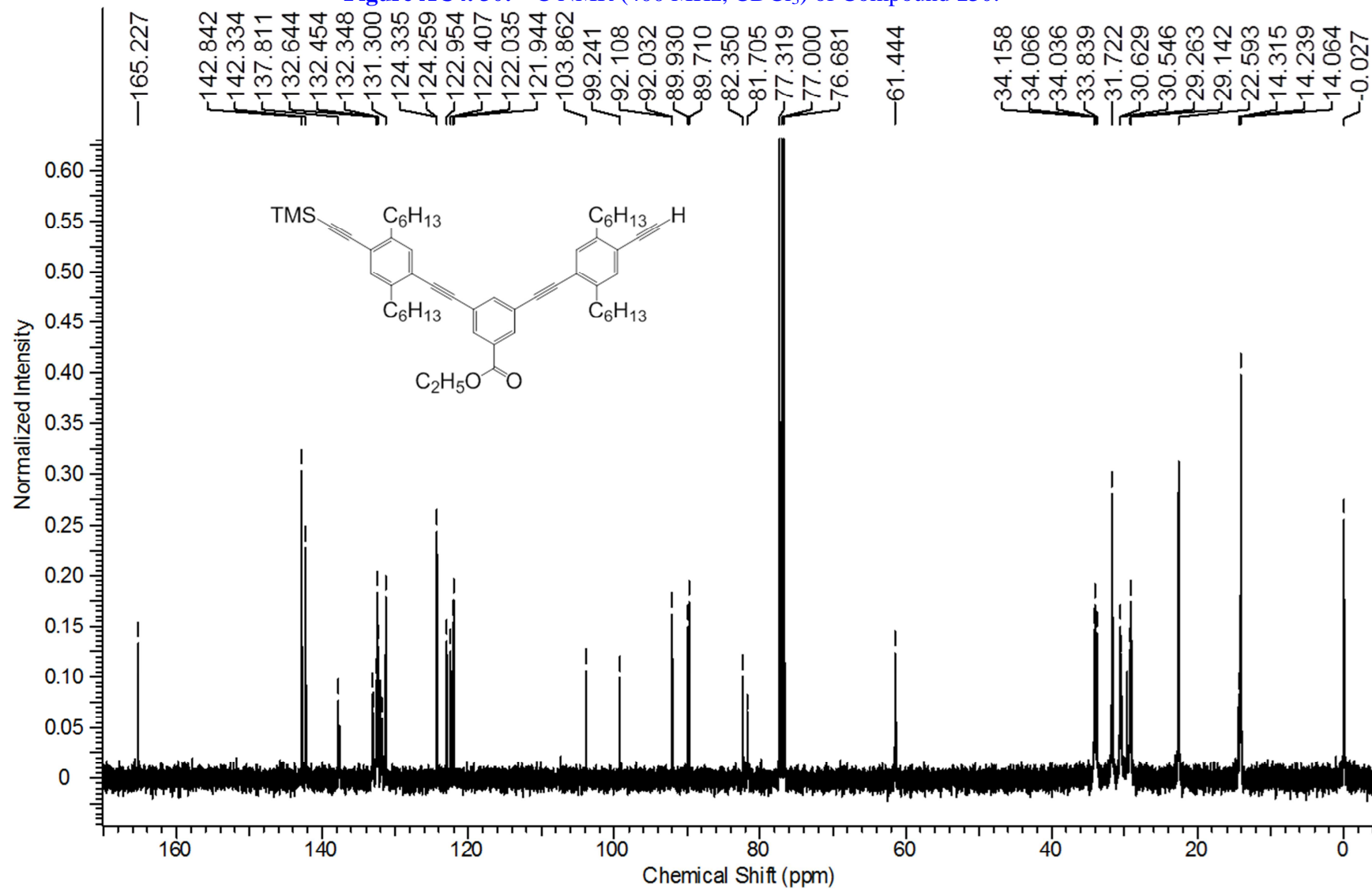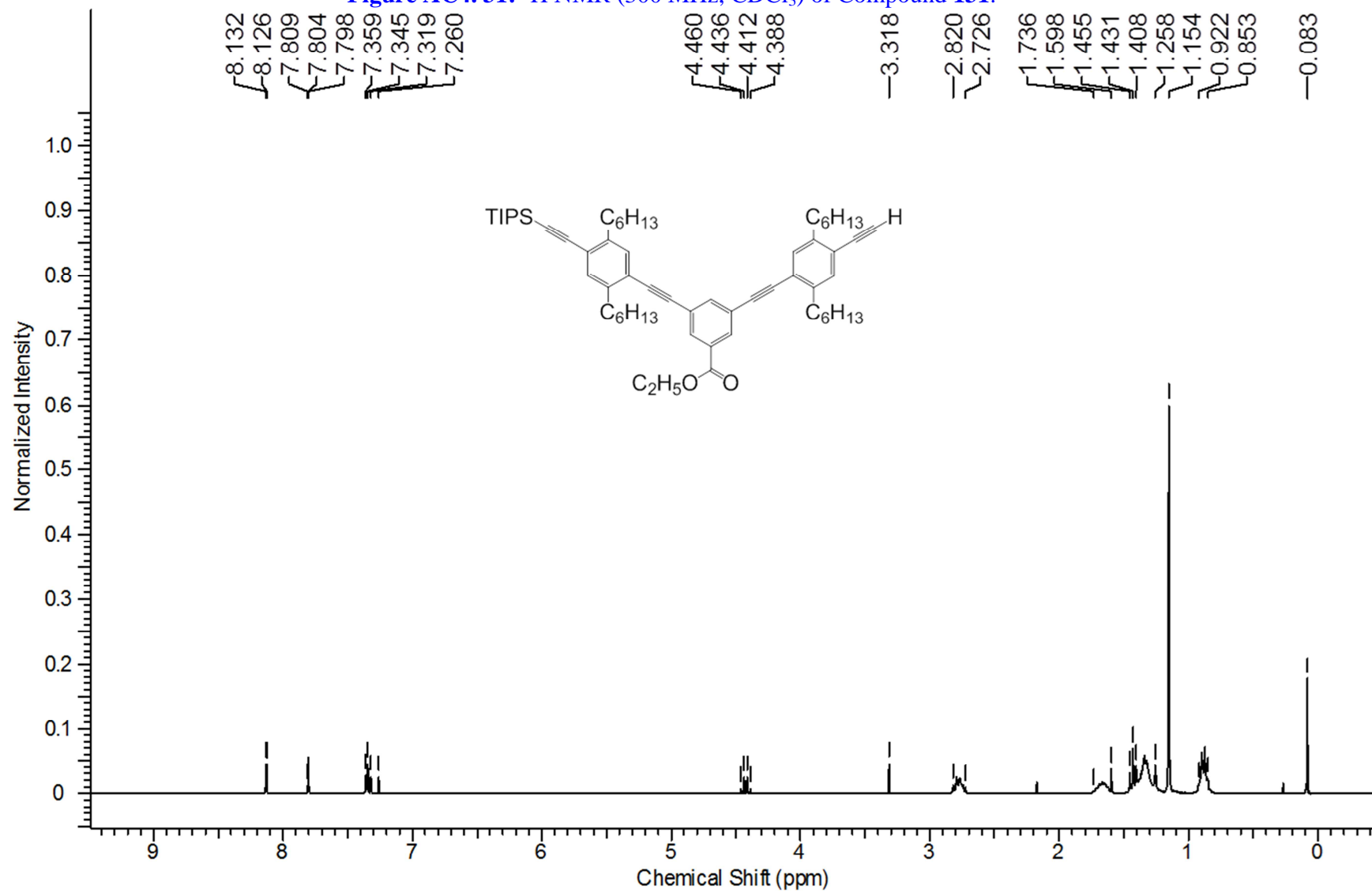Figure AC4. 21: ^{1}H NMR (300 MHz, CDCl$_3$) of Compound 125.
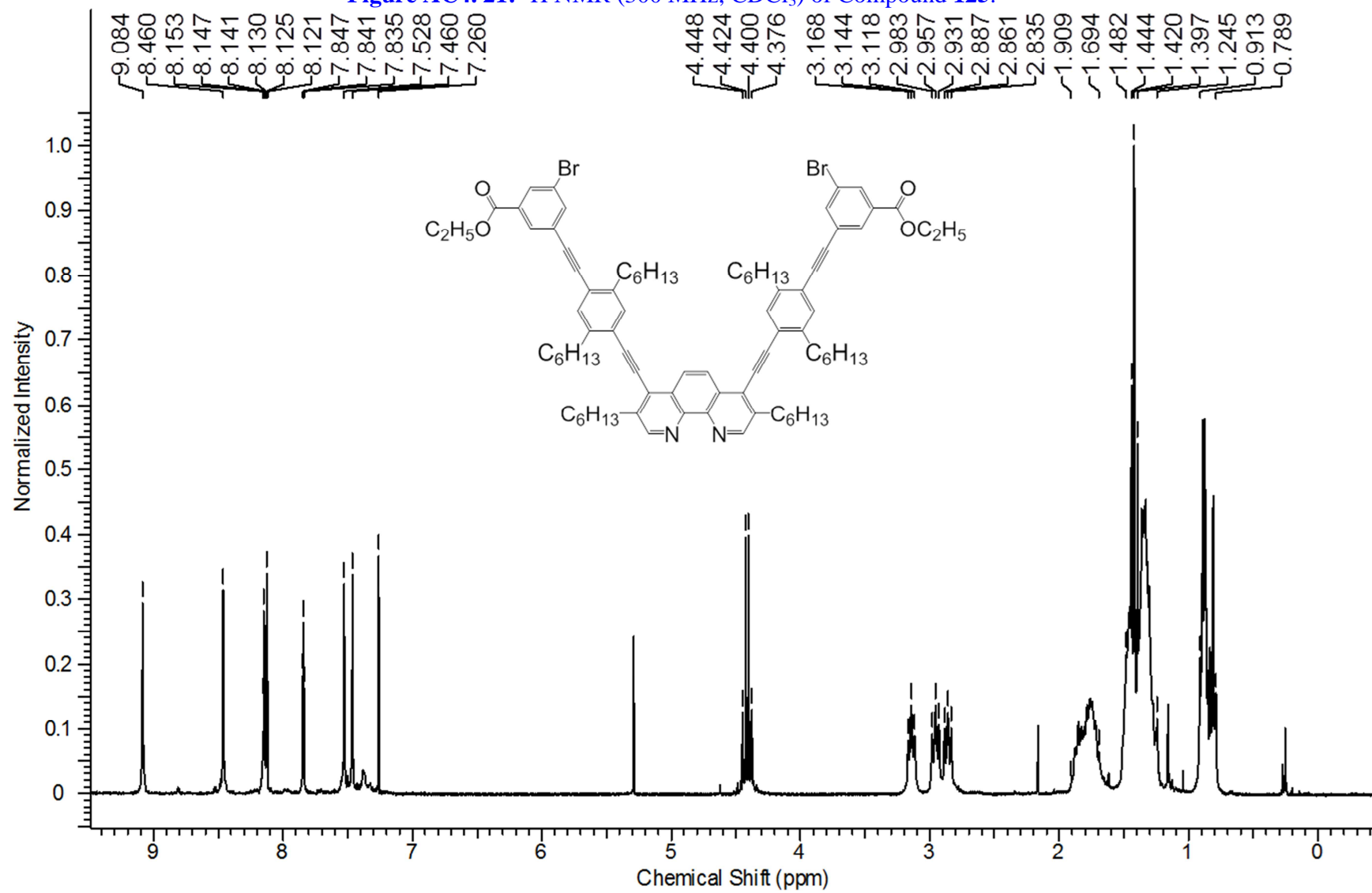
Figure AC4. 22: ^{13}C NMR (300 MHz, CDCl$_3$) of Compound **125**.
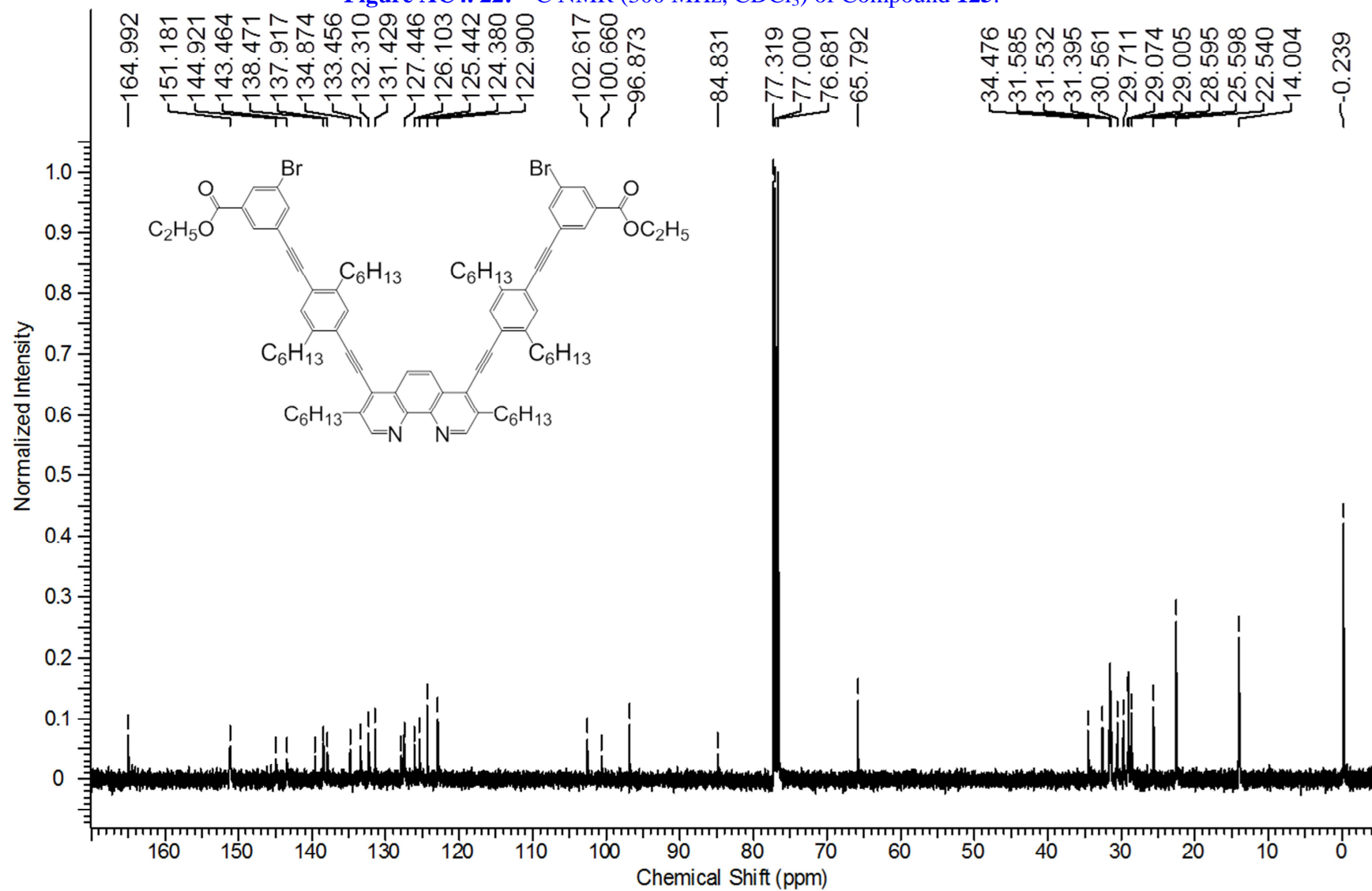
Figure AC4. 23: ^{1}H NMR (300 MHz, CDCl$_3$) of Compound **126**.
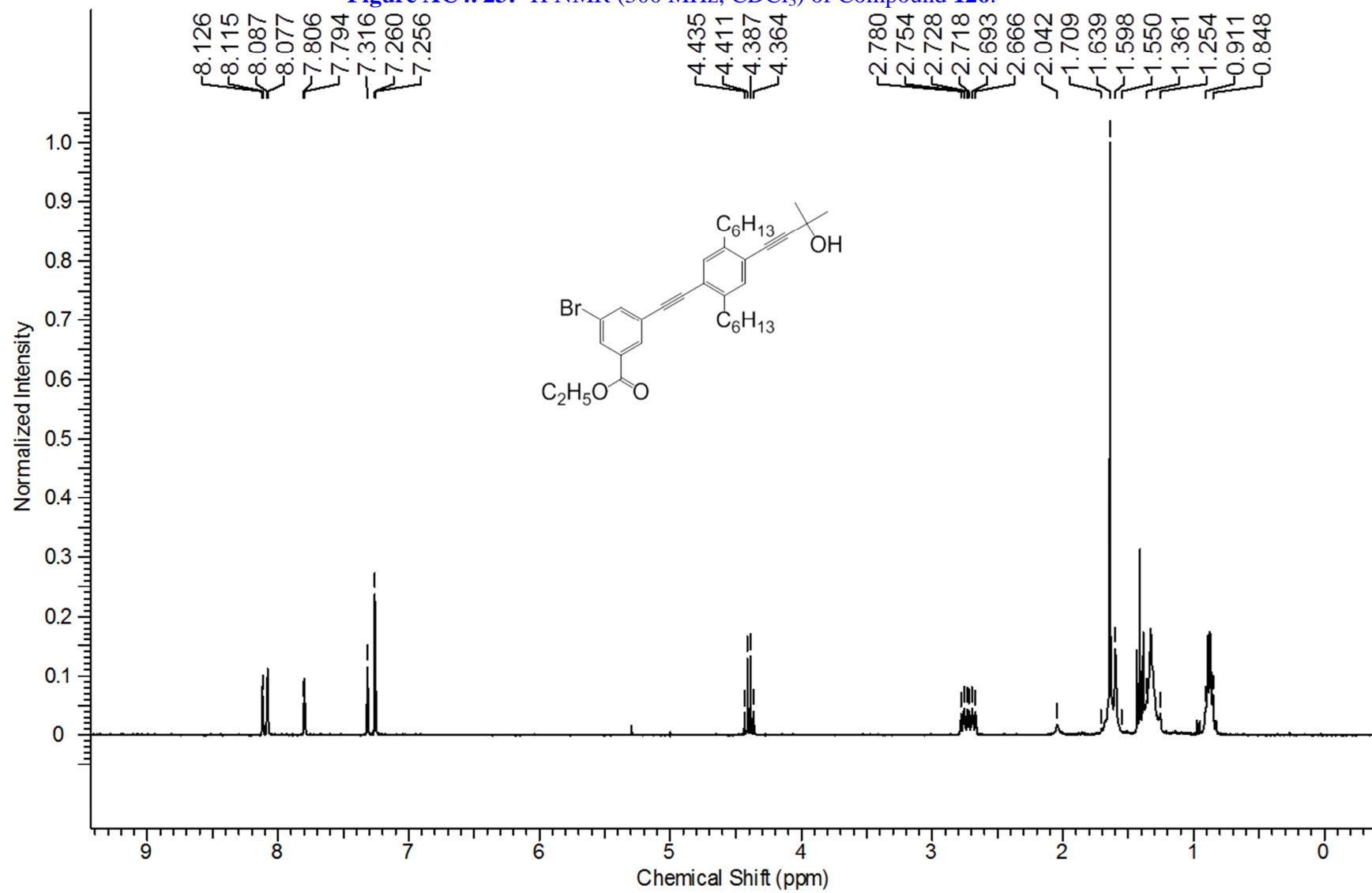
Figure AC4. 24: ^{13}C NMR (400 MHz, CDCl$_3$) of Compound **126**.
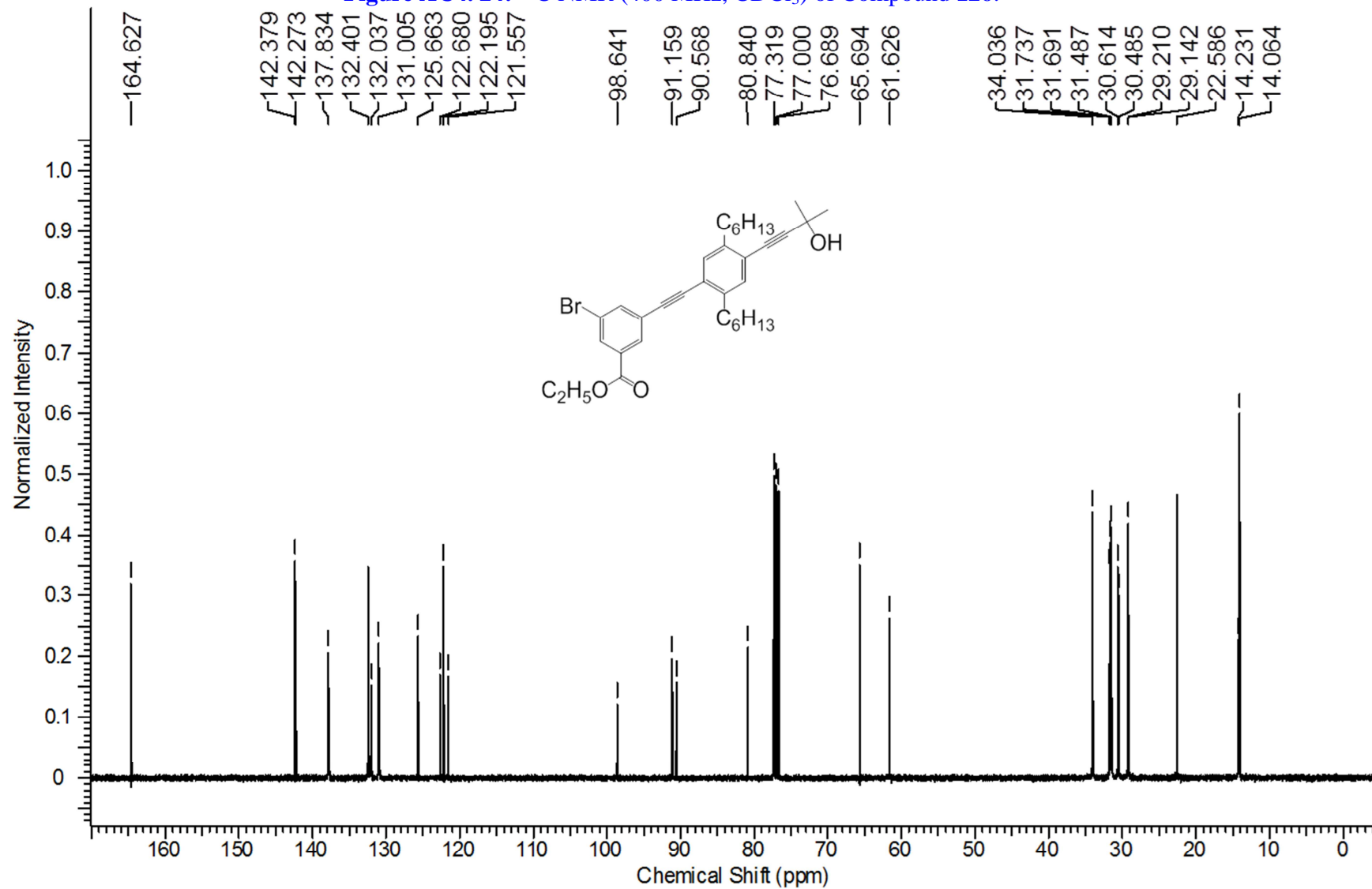
Figure AC4. 25: ^{1}H NMR (300 MHz, CDCl$_3$) of Compound **128**.
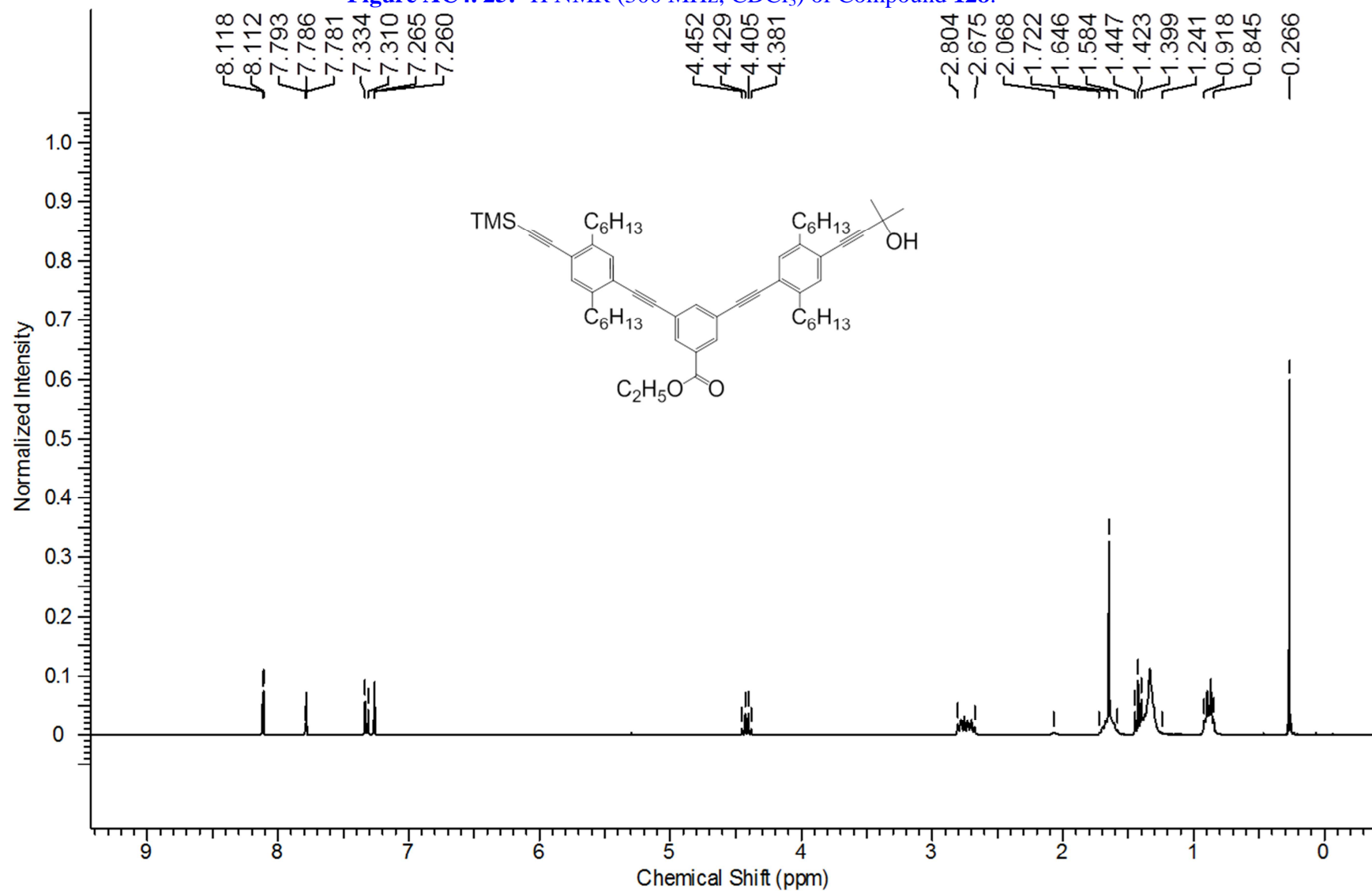
Figure AC4. 26: ^{13}C NMR (400 MHz, CDCl$_3$) of Compound **128**.
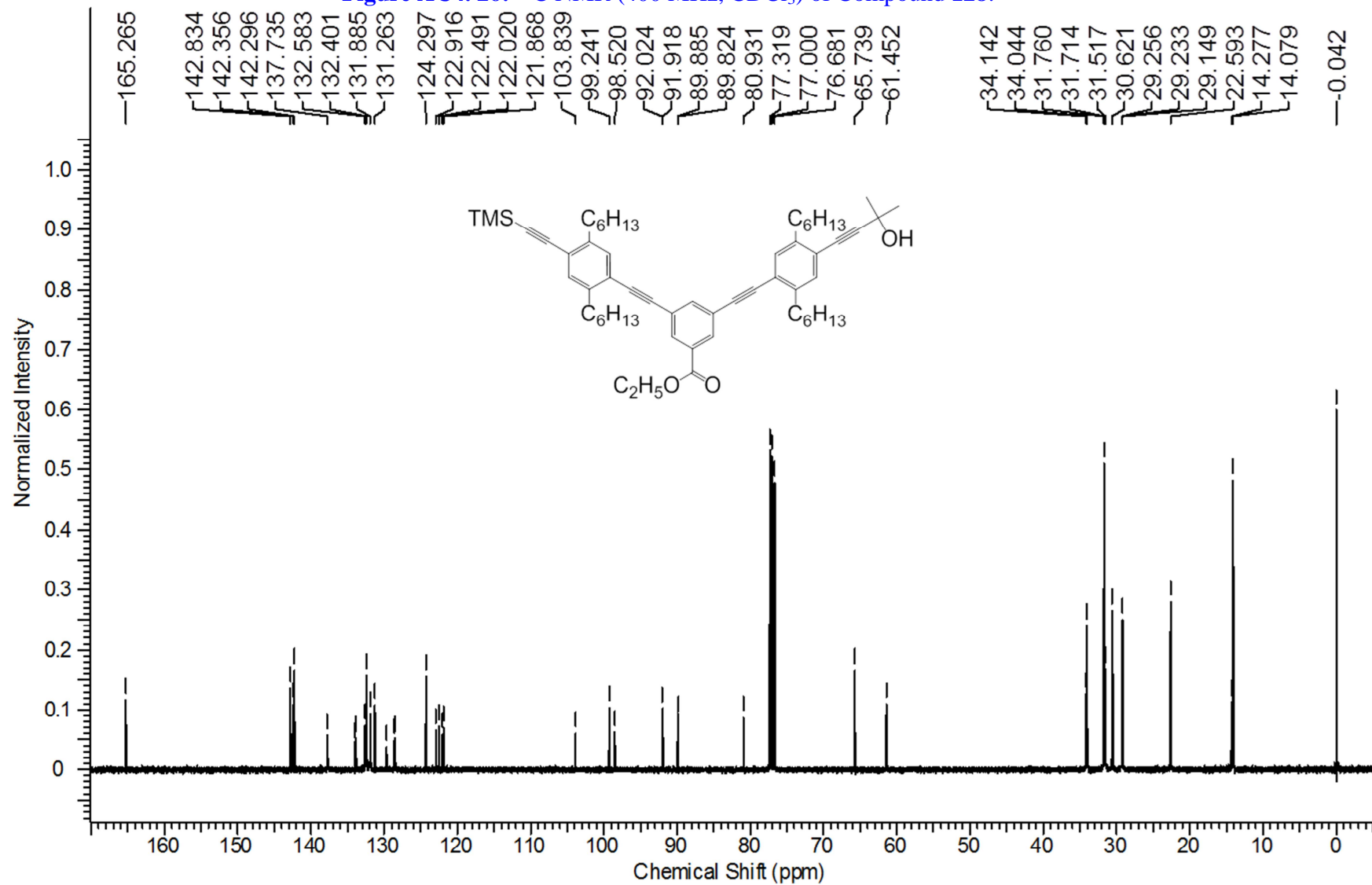
Figure AC4. 27: ^{1}H NMR (300 MHz, CDCl$_3$) of Compound **129**.
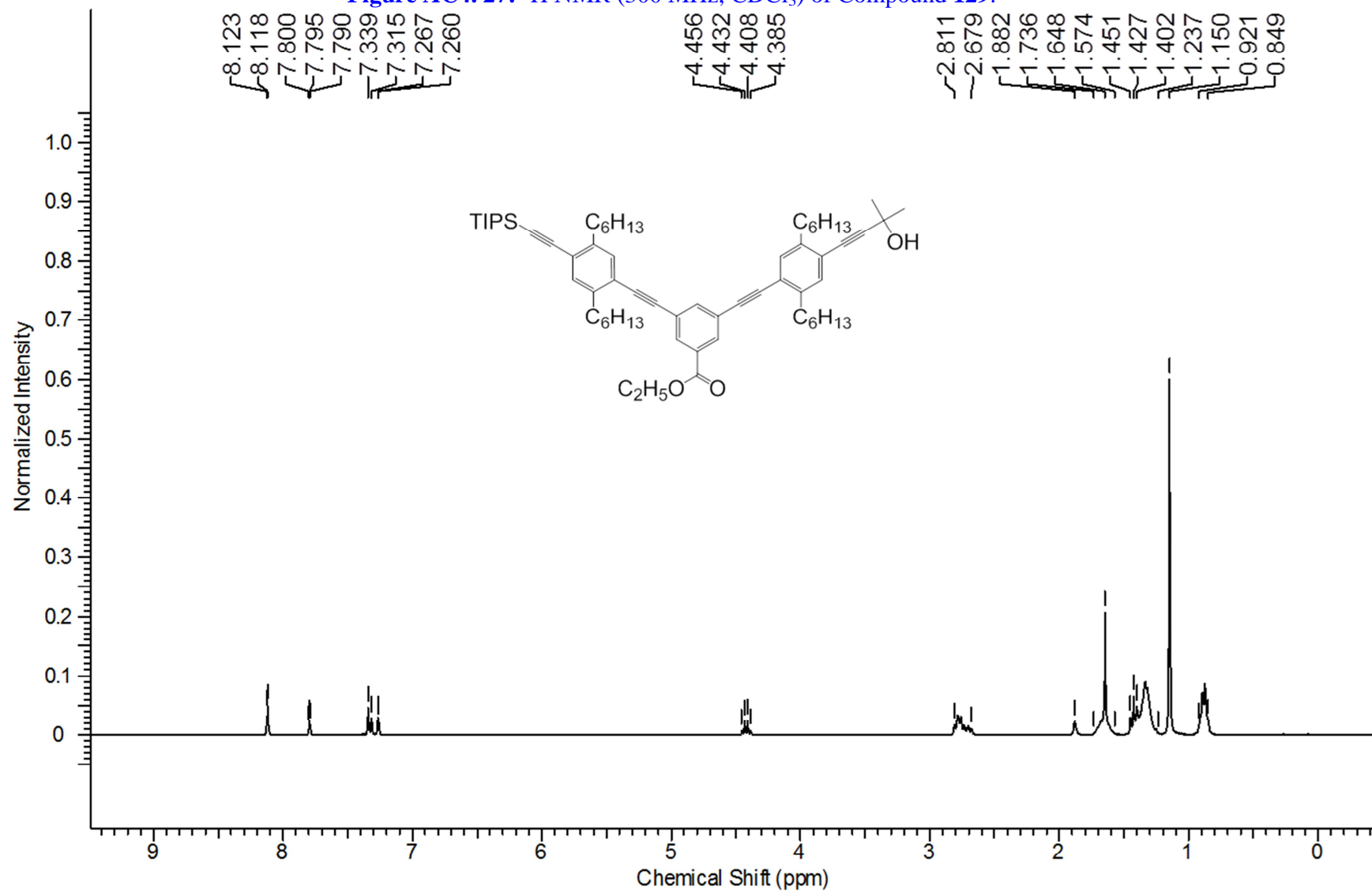
Figure AC4. 28: ^{13}C NMR (400 MHz, CDCl$_3$) of Compound **129**.
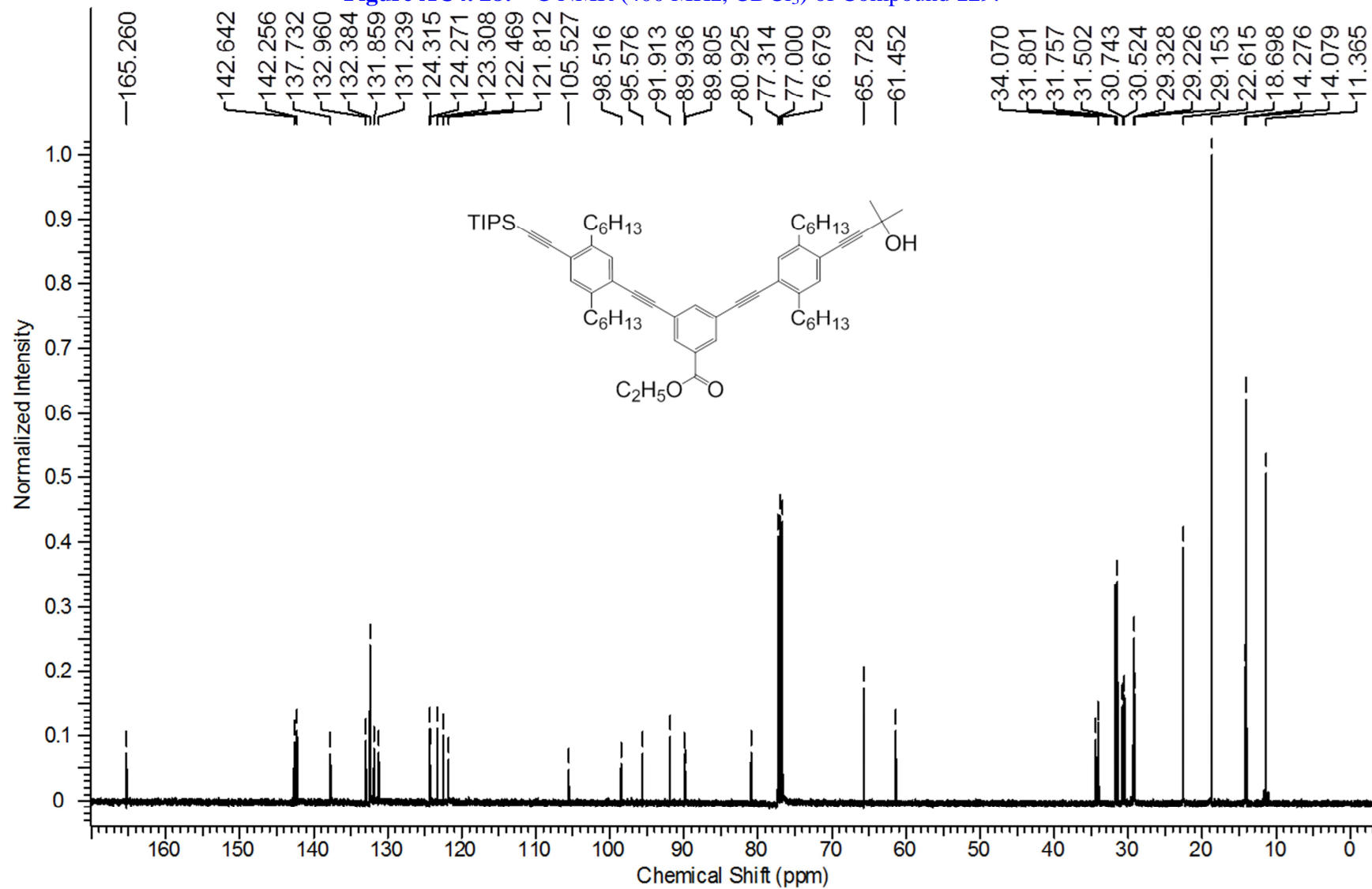
Figure AC4. 29: ^{1}H NMR (400 MHz, CDCl$_3$) of Compound **130**.

Figure AC4. 30: ^{13}C NMR (400 MHz, CDCl$_3$) of Compound **130**.

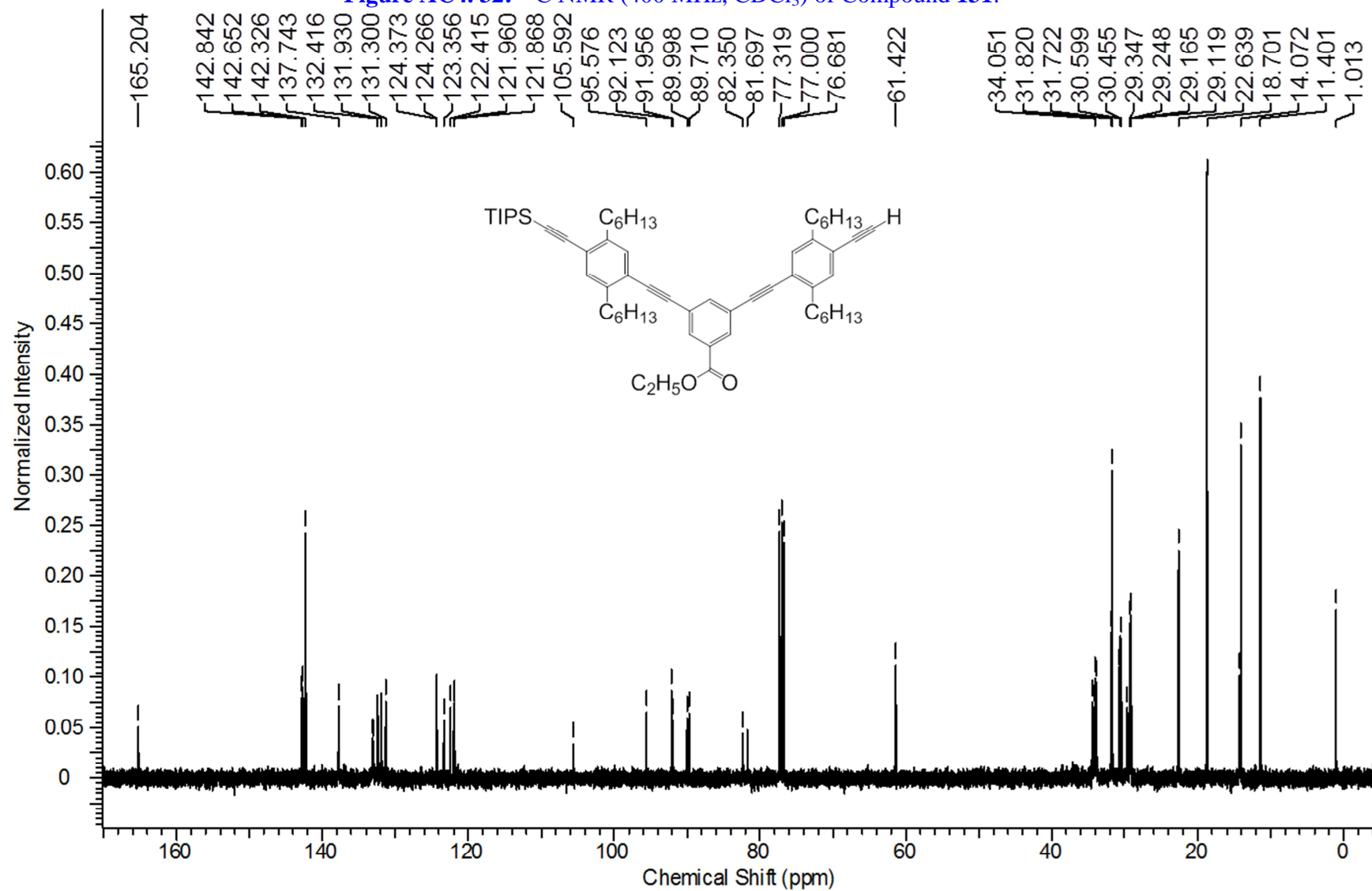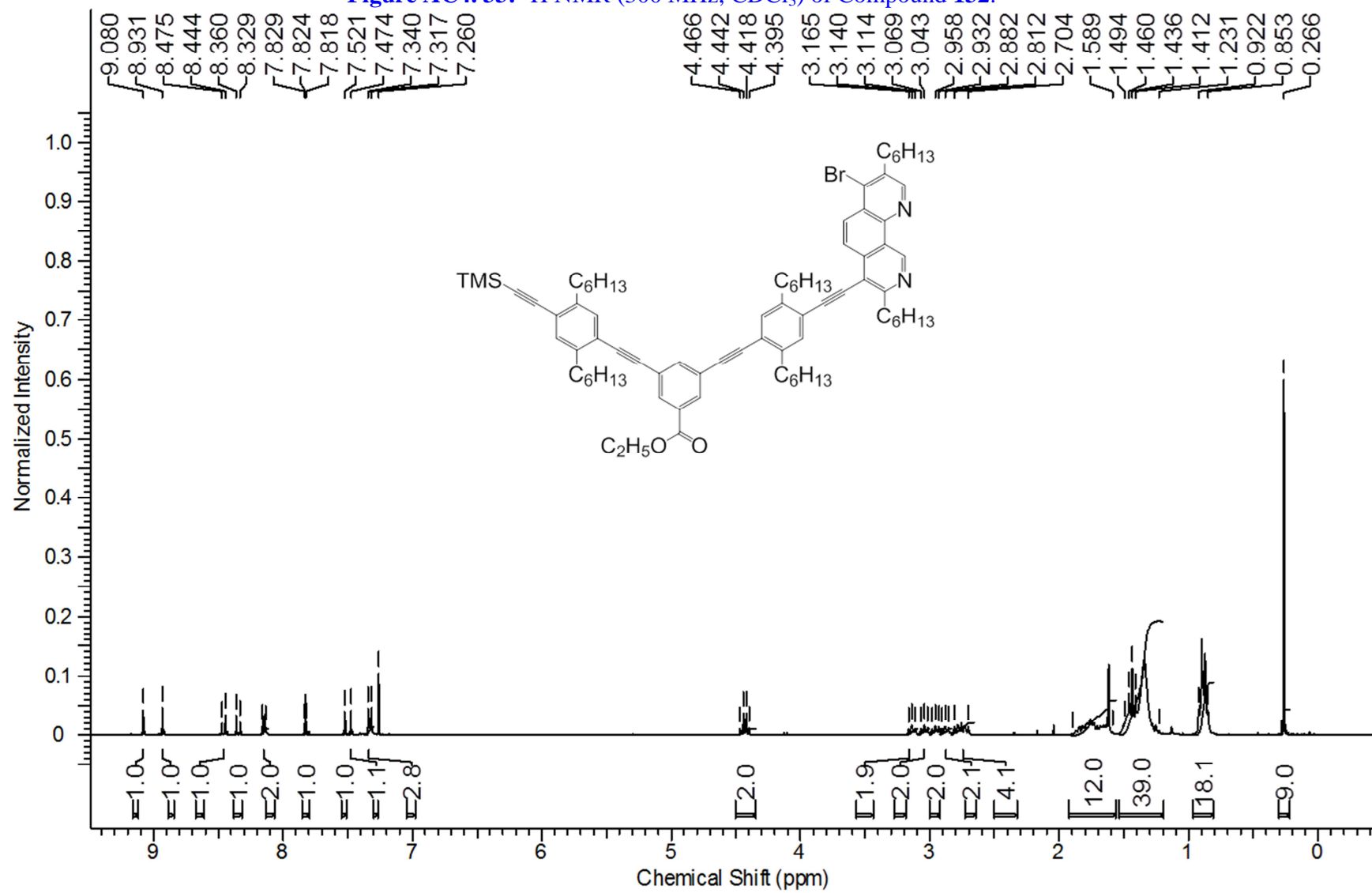**Figure AC4. 33:** ^{1}H NMR (300 MHz, CDCl$_{3}$) of Compound **132**.

Figure AC4. 34: ^{13}C NMR (400 MHz, CDCl$_3$) of Compound **132**.